CEX-68.3

LEVEL 4

AEC Category: HEALTH AND SAFETY

CEX-68.3

CIVIL EFFECTS STUDY

NUCLEAR WEAPONS EFFECTS TESTS OF BLAST TYPE SHELTERS

A Documentary Compendium of Test Reports

Issuance Date: June 1969

CIVIL EFFECTS TEST OPERATIONS
U.S. ATOMIC ENERGY COMMISSION

Printed in USA. Price $3.00. Available from the Clearinghouse for Federal Scientific and Technical Information, National Bureau of Standards, U. S. Department of Commerce, Springfield, Virginia 22151.

USAEC Division of Technical Information Extension, Oak Ridge, Tennessee

NUCLEAR WEAPONS EFFECTS TESTS OF BLAST TYPE SHELTERS

A Documentary Compendium of Test Reports

Compiled and Edited by CHRISTIAN BECK

Approved by: L. J. DEAL, Chief
Civil Effects Branch

Civil Effects Branch, Division of Biology and Medicine
U. S. Atomic Energy Commission, Washington
June 1969

NOTICE

PREFACE

A large number of experiments to test the response of various structures to nuclear effects were conducted at the Nevada and Pacific test sites during the 1950's. The results of the tests were published in Weapons Test (WT) Reports, but these received only limited distribution. A review of the reports reveals a wealth of information regarding blast shelters designed to resist the initial effects of nuclear explosions. This report presents as a series of summaries the results of interest. These summaries were prepared to make the results of applicable field experiments available to a larger professional audience with the practicing engineer specifically in mind. In general, the order of presentation follows the chronological order of the tests.

Data have been extracted from the original WT Reports to give the reader an understanding of the significant elements of the test projects. Where appropriate, reference is made to the need to modify or update test findings to ensure that design information will be compatible with high-yield nuclear weapons effects. Structures tested were in most cases exposed to the effects of relatively low-yield nuclear explosions. An independent evaluation of various aspects of the test results has been added.

Users of these summaries should have at hand the latest revised edition (1964) of *The Effects of Nuclear Weapons* (ENW), which affords much applicable information.

Since the completion of the field testing and the compilation of data, as summarized here, a large number of studies, in some instances supported by laboratory experiments, have added considerable up-to-date knowledge to blast-shelter design. Some of the study reports covering this work, as well as other technical publications offering helpful guidelines in detail design of such structures, are listed in the bibliography. A number of other similarly applicable publications are listed in the bibliography.

Christian Beck

Washington, D. C.
January 1969

ACKNOWLEDGMENTS

The author wishes to express his gratitude for the pioneering efforts of the late Prof. H. L. Bowman in getting the results of blast-shelter tests summarized and assembled in a single, accessible document. In early 1965, Professor Bowman, then Consultant to the Civil Effects Branch (CEB), Division of Biology and Medicine (DBM), U. S. Atomic Energy Commission (USAEC), expressed the urgent need for such a publication. This need was further recognized and actively pursued by L. J. Deal, Chief of CEB.

The author is particularly grateful for the valuable assistance and advice of W. T. Armstrong (CEB) during the preparation of the manuscript.

Further acknowledgment is made to W. W. Schroebel (CEB) for valuable editorial assistance; to Juanita Wines (CEB) for expert typing of the numerous preliminary drafts of the summaries; and to Marian C. Fox and Mary N. Hill of the Editorial Branch, AEC Division of Technical Information Extension, Oak Ridge, for their meticulous final editing of the summary manuscripts.

Valuable comments regarding the content of the publication were given by Jack R. Kelso of the Defense Atomic Support Agency, U. S. Department of Defense; L. J. Vortman of the Sandia Corporation, Albuquerque, N. Mex.; and Dr. C. S. White, I. G. Bowen, and D. Richmond of the Lovelace Foundation, Albuquerque, N. Mex.

CONTENTS

SUMMARY 1

FCDA FAMILY SHELTER EVALUATION

(Report WT-359, Operation Buster, Project 9.1a, same title, by Archie P. Flynn, Federal Civil Defense Administration, Washington, D. C., March 1952.)

OBJECTIVES AND SCOPE OF TESTS

The project was designed to determine the effects of atomic explosions on small civil defense shelters for family use. Information was desired on the degree of protection provided by various shelters of simple design, including resistance to blast pressure, the reaction of earth cover, protection against radiation, and effect of the orientation of the structure with respect to Ground Zero (GZ). The test shelters were exposed to Baker, Charlie, and Dog shots (ref. ENW, p. 672). Twenty-nine shelters were built along an arc approximately 1200 ft from the air-burst shots of yields in the low kiloton range.

TEST STRUCTURES, TEST CONDITIONS, AND INSTRUMENTATION

Eighteen of the structures were covered-trench wood-sheathing shelters, type A (Figs. 1 and 2), placed both below and partly above the natural grade; five were metal-arch shelters, type B, of which only one was completed for the tests (Fig. 3); four were wood-arch shelters, type C (Fig. 4); and two were basement lean-to shelters, type D (Fig. 5). Details of design and orientation toward GZ are summarized in Tables 1 to 4.

With the exception of the wood-arch shelters, the designs were typical of those under consideration for recommendation to the public. In addition, several reduced-strength structures were tested, not to determine their degree of protection but to develop technical data for design purposes.

When moved, soil at the test site lacked cohesive properties; consequently much of the earth cover on the shelters was removed by the first shot. Since a change in test operations prevented the planned restoration of structures and replacement of cover after each blast, this reaction materially influenced test results. Effects of the first explosion (Baker shot) added considerably to the damage normally resulting from the succeeding shots (Charlie and Dog shots) and cumulative damage was all that could be appraised. This limited the use of test data from the second and third explosions in evaluating the protection afforded by the shelters.

Only limited instrumentation, mostly by improvised methods, of the test structures was available. It consisted of gamma film badges for radiation measurements, simple improvised devices to measure deflection, and a limited number of land-mine fuses for determining pressures inside the shelters.

RESULTS

Peak overpressures, thermal radiation, and gamma readings at the shelter structures were mostly based on actual recorded data. Average values of these readings are summarized in Table 5. The pressures for Dog shot had to be estimated, and the gamma-radiation values were considered subject to revision.

Test structures were severely damaged by the three shots, but considerable useful data were obtained. Below-grade covered-trench shelters provided protection against Baker shot and withstood the three explosions. Partly above-grade covered-trench shelters provided less protection against blast and gamma radiation. The only completed metal-arch shelter failed before sufficient data could be obtained, but the metal-arch trench shelters set in concrete footing reacted well. The tests indicated that this type of shelter could, with minor modifications in design, provide good protection. Wood-arch shelters survived the first explosion but collapsed in the second. The wood arch, as designed, proved unsuitable as a substitute for the metal arch. Because of the inadequacy of the test structures, no information was obtained on the reaction of basement lean-to shelters.

Results showed that structures were less severely damaged when they were protected by even a small amount of earth cover. This was particularly evident where entrance structures were poorly protected. When covered, they survived. It appeared that, if earth cover were below natural grade, the entrance would not be greatly affected by blast. Thus lowering the grade level of shelters would add considerably to their safety. The removal of great amounts of earth cover by successive explosions, with subsequent loss of the benefits of earth arch action, partially accounts for the relatively poor resistance of arch-type shelters.

All structure entrances were considerably weaker than the shelters proper. Entrances to the arch-type shelters collapsed completely on Baker shot. On the next two shots, practically all above-grade entrance construction was demolished and blown away. Gamma-radiation readings showed that entrance areas could not be used for shelter purposes. They did, however, effectively block off thermal radiation, and there was no indication that material was disturbed within the shelters. Debris thrown toward the shelters was trapped in entrances and would not have injured occupants. It did block the access to many of the shelters, however, and escape would have been hazardous.

The end and front sections of the covered-trench shelters showed a tendency to fail where they were joined to the roof sections. Since these parts were tied together only by wall studs toenailed to the roof joists, failure was particularly severe where the spacing was increased.

Various sections of the metal-arch shelter showed a tendency to pull apart. They should be joined more securely. End sections partly gave way in Baker shot because of failure of supporting stakes. Since this occurred also in one of the wood-arch shelters, it was attributed not to faulty construction but to design.

Orientation toward GZ of the covered-trench shelters had a major effect on their protective value only where the front faced the explosion. Radiation doses within such a shelter were considerably higher than in shelters facing in other directions. Greater damage to the entrance apparently was the probable cause.

Scorching of parts of the entrance panels not directly exposed to the blast indicated the possibility of heat reflection of some magnitude. However, even in the shelter where the entrance side faced the blast, there was no evidence of heat entering the shelter proper. Hence, entrances would provide protection against thermal radiation even if facing the blast.

Total gamma radiation from test shots, as shown in Table 6. was sufficiently large that even the 3 ft of earth cover did not provide desired protection. Since the blast preceded the gamma radiation, only a portion of the earth cover was effective. This may have slightly increased radiation doses within the shelters.

Table 1—SHELTER TEST STRUCTURES, TYPE A, COVERED-TRENCH

Shelter No.	Orientation	Earth cover	Roof joists	Studs	Wood sheathing
		Group I, Below Grade, Basic Design			
A-1	Back to GZ	3 ft	2 X 6 @ 3¾ in.	2 X 4 @ 16 in.	1 X 6
A-2	Back to GZ	2 ft	2 X 6 @ 3¾ in.	2 X 4 @ 16 in.	1 X 6
A-3	Long side to GZ	2 ft	2 X 6 @ 3¾ in.	2 X 4 @ 16 in.	1 X 6
A-4	Front to GZ	3 ft	2 X 6 @ 3¾ in.	2 X 4 @ 16 in.	1 X 6
		Group II, Below Grade, Lightened Frame			
A-5	Back to GZ	3 ft	2 X 4 @ 24 in.	2 X 4 @ 24 in.	1 X 6
A-6	Back to GZ	2 ft	2 X 4 @ 24 in.	2 X 4 @ 16 in.	1 X 6
A-7	Back to GZ	3 ft	2 X 4 @ 16 in.	2 X 4 @ 16 in.	1 X 6
A-8	Back to GZ	2 ft	2 X 4 @ 16 in.	2 X 4 @ 16 in.	1 X 6
A-13	Back to GZ	3 ft	2 X 4 @ 8 in.	2 X 4 @ 8 in.	1 X 6
A-14	Back to GZ	2 ft	2 X 4 @ 8 in.	2 X 4 @ 8 in.	1 X 6
A-15	Back to GZ	3 ft	2 X 6 @ 5 in.	2 X 4 @ 12 in.	1 X 6
A-16	Back to GZ	2 ft	2 X 6 @ 5 in.	2 X 4 @ 12 in.	1 X 6
		Group III, Semi-buried, Lightened Frame			Wood roof*
A-9	Back to GZ	2 ft	2 X 4 @ 8 in.	2 X 4 @ 8 in.	1 X 6
A-10	Back to GZ	3 ft	2 X 4 @ 8 in.	2 X 4 @ 8 in.	1 X 6
A-11	Back to GZ	2 ft	2 X 4 @ 16 in.	2 X 4 @ 16 in.	1 X 6
A-12	Back to GZ	3 ft	2 X 4 @ 16 in.	2 X 4 @ 16 in.	1 X 6
A-17	Back to GZ	3 ft	2 X 6 @ 5 in.	2 X 4 @ 12 in.	1 X 6
A-18	Back to GZ	2 ft	2 X 6 @ 5 in.	2 X 4 @ 12 in.	1 X 6

*Chicken-wire-and-tar-paper sides.

Table 2—SHELTER TEST STRUCTURES, TYPE B, METAL-ARCH

Shelter	Orientation	Earth cover	Roof arch	Walls
		Group I, Below Grade, Basic Design		
B-1	Back to GZ	3 ft	12-Gauge	Concrete block
		Group II, Arch on Concrete Footing, Shelter Not Completed		
B-2	Back to GZ	2 ft	12-Gauge	Concrete footing
B-3	Back to GZ	2 ft	16-Gauge	Concrete footing
B-4	Back to GZ	3 ft	16-Gauge	Concrete footing
B-5	Back to GZ	3 ft	12-Gauge	Concrete footing

Table 3—SHELTER TEST STRUCTURES, TYPE C, WOOD-ARCH, ABOVE GRADE

Shelter	Orientation	Earth cover	Roof arch	Walls
C-1	Back to GZ	2 ft	2 X 4 @ 8 in.	Concrete block
C-2	Back to GZ	3 ft	2 X 4 @ 8 in.	Concrete block
C-3	Back to GZ	2 ft	2 X 4 @ 16 in.	Concrete block
C-4	Back to GZ	3 ft	2 X 4 @ 16 in.	Concrete block

Table 4—SHELTER TEST STRUCTURES, TYPE D, BASEMENT LEAN-TO

Shelter	Orientation	Foundation wall	Lean-to const. 1-in. sheathing	Type of fastening
D-1	Wall to GZ	Conc. block	2 X 6 @ 5 in.	Bottom bolted Top toenailed
D-2	Wall to GZ	Conc. block	2 X 6 @ 5 in.	Bottom bolted Top free

Table 5—BASIC EFFECTS DATA FOR SHELTER STRUCTURES

Shot	Peak side-on pressure, psi	Thermal radiation, cal/cm^2	Gamma radiation, r
Baker	8.0	41	9,600
Charlie	14.9	114	29,800
Dog	14.7	155	50,700

Table 6—TOTAL GAMMA RADIATION IN COVERED-TRENCH SHELTERS, AVERAGE READINGS (IN r) FOR BAKER SHOT

	Earth cover, 2 ft		Earth cover, 3 ft	
Shelters	Shelter area	Entrance area	Shelter area	Entrance area
Below grade	173	246	151	198
Partly above grade	290	430	206	320

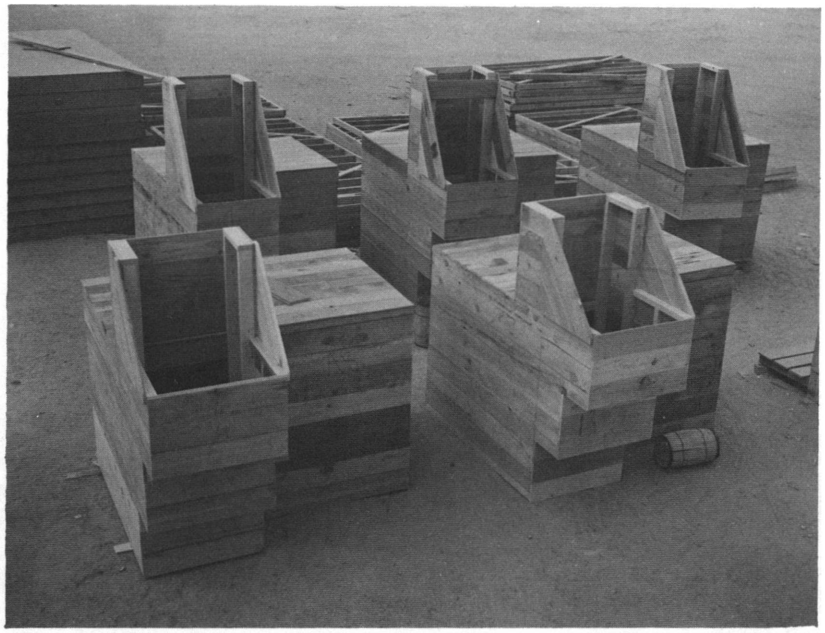

Fig. 1—Prefabricated structures for covered-trench shelters (carpentry yard).

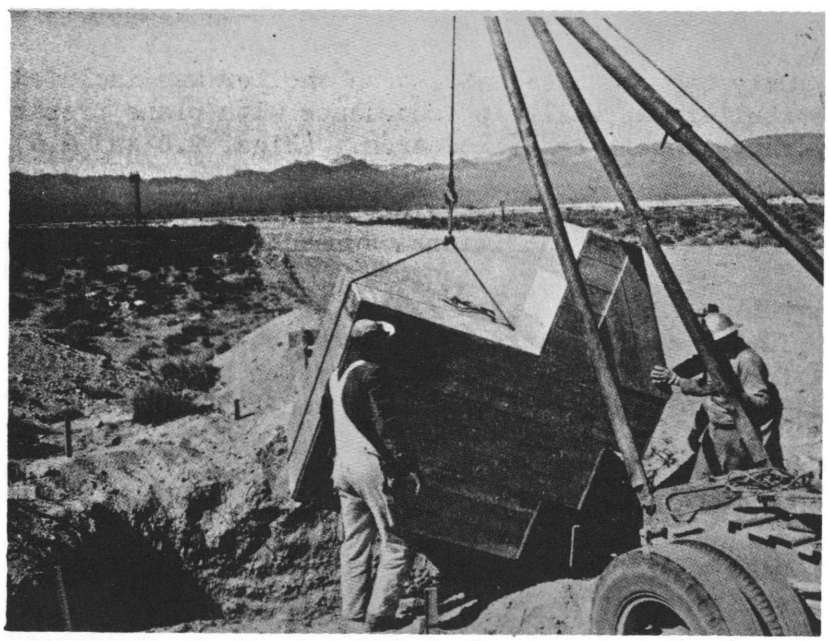

Fig. 2—Placing structure in position for shelter A-1

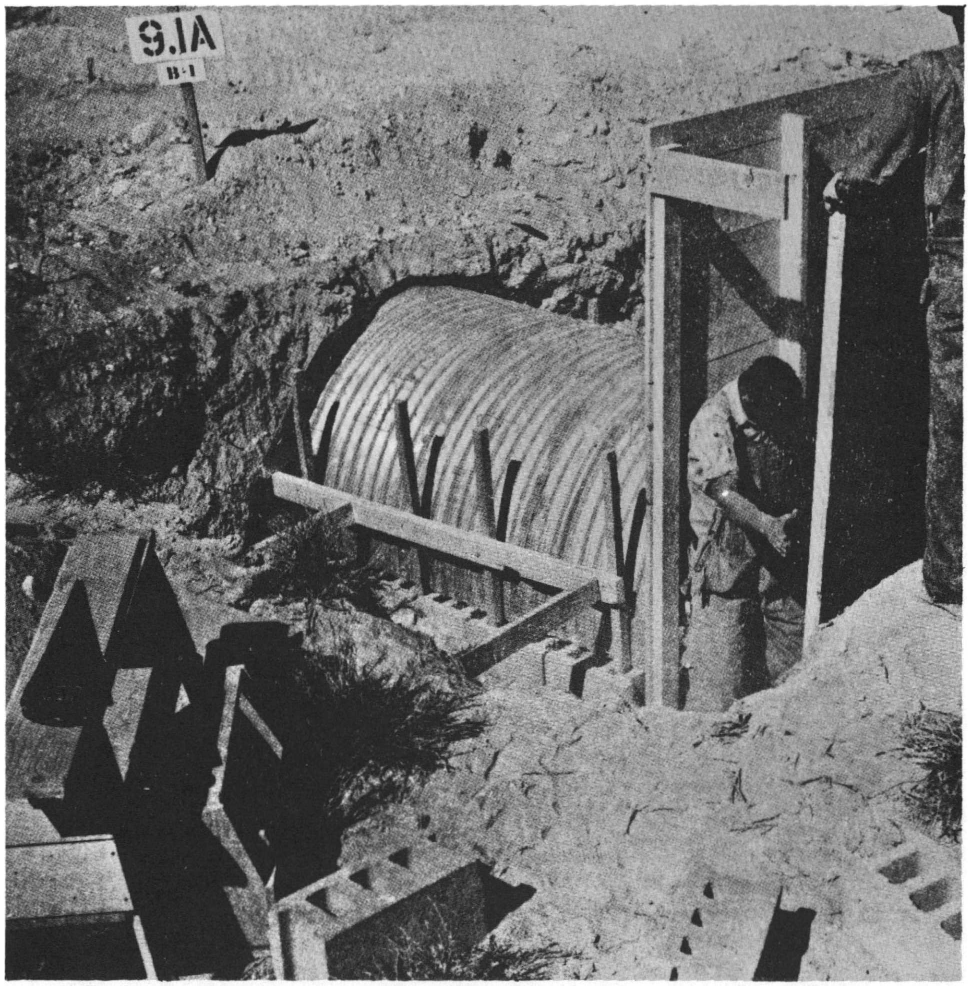

Fig. 3—Metal-arch shelter B-1 under construction.

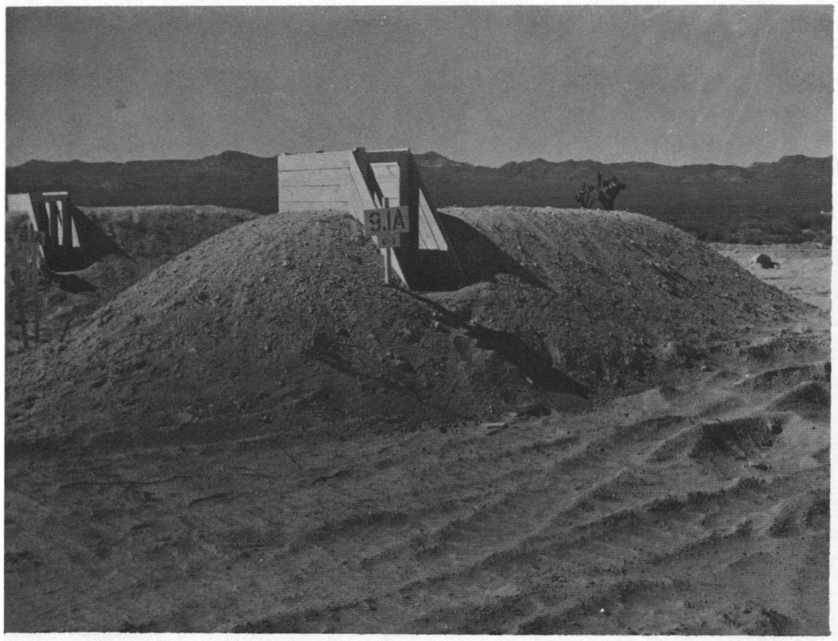

Fig. 4—Shelter C-1 completed.

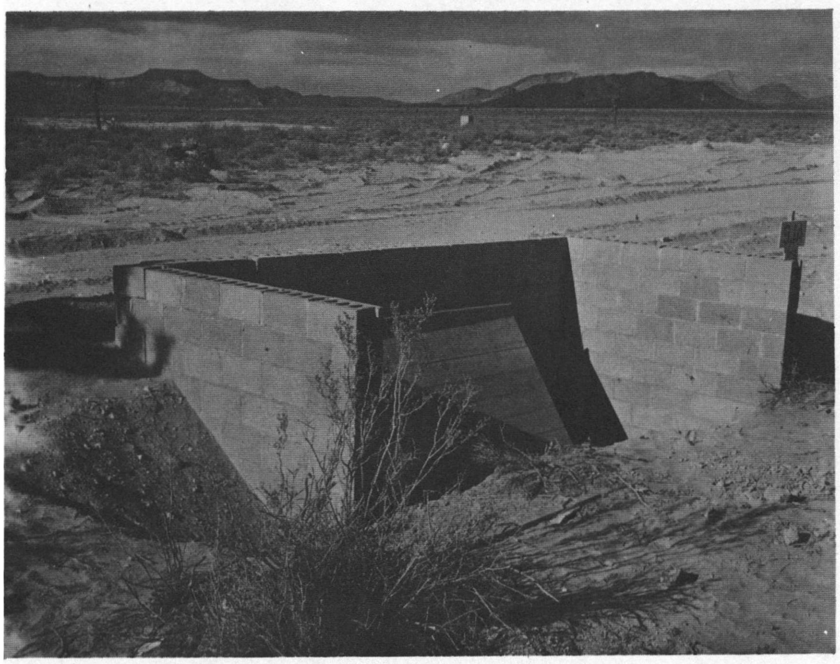

Fig. 5—Structure for test of basement lean-to shelter.

SUMMARY 2

AEC COMMUNAL SHELTER EVALUATION

(Report WT-360, Operation Buster, Project 9.1b, same title, by Robert L. Corsbie, U. S. Atomic Energy Commission, Washington, D. C., March 1952.)

OBJECTIVES AND SCOPE

The objectives of the tests were to determine the blast, radiation, and thermal effects of several atomic bomb explosions on an open communal-type shelter as a function of distance and orientation; to evaluate the cumulative effects on the structure without structural repair between explosions; and to compare the effectiveness of the different designs and materials used in the construction of the shelter against the explosion hazards.

The test shelter was a 48-ft combination concrete-pipe and steel-pipe structure placed underground with the principal axis perpendicular to the radius toward Ground Zero (GZ). Double-ramp entrances, normal to the axis of the shelter, were provided at each end. The approximate overall dimensions were 57 ft long by 40 ft and 44 ft wide at the steel and concrete ramps, respectively.

The test structure was instrumented to provide comparable data on overpressures, deflections, and displacements inside the steel and concrete pipes. Film badges were distributed along the axis of the shelter and in the open ramps in exposed locations to measure gamma radiation. Burlap bags filled with a mixture of earth and sawdust were placed along the floor of the shelter to indicate the magnitude and direction of dynamic overpressures.

The structure was subjected to air-burst shots Baker, Charlie, Dog, and Easy (ref. ENW, p. 672) at 889, 972, 800, and 3590 ft, respectively. Easy shot was too far away to provide significant data.

TEST STRUCTURE AND TEST CONDITIONS

The test structure (Figs. 1 and 2) was comprised of two types of pipe joined together. One end consisted of a section of three 8-ft lengths (24 ft) of 7¾-in.-thick standard centrifugally spun reinforced-concrete pipe 90 in. in inside diameter. A poured-in-place reinforced-concrete double ramp provided entrance to this end of the structure (Fig. 3). Joined to the concrete section was a section of four 6-ft lengths (24 ft) of 10-gauge corrugated Multi-Plate steel pipe 90 in. in inside diameter. Entrance to this end of the structure was provided by a double ramp constructed of 10- and 12-gauge corrugated metal sheet and of structural steel beams (Fig. 4). The completed structure (48 ft, exclusive of ramps) was designed to shelter 48 persons. Over the concrete and metal pipe sections were placed 3 ft and 3 ft 8 in. of earth,

respectively, mounded about 2 ft above normal grade over the principal axis of the pipe and sloped at about 1 in 10.

The soil at the shelter location was predominantly of silt-sized particles. It had a very low moisture content and was difficult to compact. The test operations did not permit the replacement of the earth cover removed by each explosion nor the removal of any soil that had flowed or blown down the ramps and into the open ends of the shelter.

The shelter was designed to withstand the overpressure equivalent to that from a nominal (20-kt) air burst at a distance of 2000 ft from GZ (~30 psi) and to attenuate gamma radiation from such a detonation to the order of 100 r integrated dose, a level that would produce few, if any, casualties.

RESULTS

Blast Pressures

Peak air pressures measured by pressure–time gauges at ground level located at the same distance from the detonation as the shelter are given in Table 1 together with the pressure measured by indenter gauges inside the structure (Fig. 5).

The pressures shown in Table 1 are considered reasonable. That the indenter-gauge pressures are considerably higher than the surface peak pressures is credited to a reflection process resulting from almost simultaneous entrance of air shock waves into the open ends of the shelter and the resultant collision and reflection near the center of the tubular structure. The free-flowing soil after Charlie shot effected a reduction of approximately 30% in the clear opening of the entrances.

Downward deflections and displacements are given in Table 2. The locations of gauges are shown in Fig. 5. Upward movements were not recorded.

Nuclear Effects

Film badges placed in exposed locations outside the shelter showed gamma-radiation doses at ground level of 13,000, 35,000, 70,000, and 2150 r following Baker, Charlie, Dog, and Easy shots, respectively.

Average gamma radiation inside the shelter for the various shots is shown in Table 3.

Thermal Effects

Thermal measurements were not included in the instrumentation of this project; however, measurements at the same distance from the detonation but on a different azimuth showed thermal energy of 60, 160, 220, and 50 cal/cm^2 for Baker, Charlie, Dog, and Easy shots, respectively. The most pronounced evidence of thermal intensity was present from Dog shot at 220 cal/cm^2. These effects included additional overall surface spalling; bubbled soil plastered while in a molten state against structural steel shapes with surfaces normal to GZ; areas blackened by Charlie shot enlarged and more noticeable; and considerable charring of exposed concrete and metal surfaces.

Physical Damage

The overpressures measured at ground level were lower than had been expected. Therefore, the pipe structures were not subjected to blast loadings that had been estimated to produce heavy to severe damage. Structural damage would in no case have imperiled the lives of shelter occupants. Cumulative damage caused by the series of shots is summarized in the following:

1. Dog shot completed the leveling of the site, removing the mounded earth cover and lowering the structure in relation to ground level. Large quantities of soil had seeped and drifted into the ramps and shelter entrances. Only 50 to 60% of each pipe end remained a clear opening.

2. The four concrete-beam struts that tied the ramp retaining walls together at ground level suffered heavy damage; however, the structural value of the walls was not seriously impaired.

3. Baker and Charlie shots lessened the structural stability of the metal ramp and breached the metal-sheet retaining wall. Therefore, the ramp did not have consistent structural strength to resist the blast effects of Dog shot. Under the impact of the blast loadings, the section collapsed during Dog shot (Fig. 6).

4. A slight crimping occurred above the center line of the first and second metal sections from the south end, and a few bolts were loosened.

5. The light to moderate damage to the concrete-pipe section caused by Baker and Charlie shots was not significantly intensified by the subsequent detonations. The center part of the three-section concrete-pipe end of the structure was offset ½ in., and the joints between pipe sections were widened to ¼ in. at the ceiling and 2 in. at the floor. Ceiling cracks opened to a maximum of ⅛ in. and additional hairline cracks appeared.

Structural damage caused by Charlie shot, the first detonation of any consequence, showed the following: A considerable amount of the mounded earth cover was removed, and large quantities of soil flowed down the ramps and sloped into the pipe ends, reducing the clear-opening area by 20 to 30%.

No damage was observed in the metal-pipe sections; however, structural members in the metal ramp suffered considerable damage and deformation. Light to moderate damage was observed in the concrete pipe; many cracks and considerable spalling were apparent in parts of the concrete ramp.

The displacements of the 50-lb earth-and-sawdust-filled burlap bags (simulated dummies) tested under Charlie and Dog shots, as well as their orientations after overturning, indicated the behavior of the reflected pressures. After Charlie shot the dummies were found in the following positions, reading from the steel (south) end to the concrete (north) end (Fig. 7):

Dummy 1, 14 ft from center, moved 18 in. south toward the opening, on its side with top to south.

Dummy 2, 7 ft from center, position unchanged, on its side with top to south.

Dummy 3, on center, position unchanged, on its side with top to south.

Dummy 4, 7 ft from center, moved 6 in. north toward the opening, on its side with top open end to north.

Dummy 5, 14 ft from center, moved 10 in. north, bag broken, with top to north.

For other shelter and ramp orientations, the shock fronts would collide nearer an end, rather than near the center as was the case here, and would therefore have a larger potential for producing greater effects.

DISCUSSION

This project was of particular interest because it was one of the very few test projects involving an open shelter without the protective features of blast doors. The few advantages of an open shelter, such as easy access and certain cost savings in structural items and mechanical equipment, are more than offset by the disadvantages so clearly demonstrated by the tests, which include the high blast overpressure and the dynamic pressure effects on any shelter occupants.

The large quantities of soil blown into the shelter ends by the blast may be attributed to the relatively loose soil conditions at the test site. The successive losses of earth cover during each detonation may also to a great extent be blamed on this particular soil condition. Better protected openings to the shelter body would help to reduce the rather high radiation doses received near the ends of the shelter and modify to some degree the peak pressures inside the shelter.

Table 1—PRESSURE MEASUREMENTS

Shot	Peak overpressure, psi	Indenter-gauge measurements, psi					
		A	B	C	D	E	F
Baker	9	13.0	18.8	32.0	39.9	38.3	23.8
Charlie	24	16.8	28.7	34.7	54.7	40.4	†
Dog	25*	†	24.4	37.0	40.5	†	†
Easy	6	†	9.6	11.3	11.2	†	†

*Estimated.

†Gauges buried under soil in ramp entrances, hence not read.

Table 2—DEFLECTIONS AND DISPLACEMENTS

Shot	Concrete pipe		Steel pipe	
	Maximum, in.	Permanent, in.	Maximum, in.	Permanent, in.
Baker	1.24	0.56	1.14	0.44
Charlie	0.68	0.00	0.74	0.16
Dog	2.10	0.93	2.72	0.60
Easy	0.62	0.07	1.20	0.37
		Total 1.56		Total 1.57

Table 3—AVERAGE GAMMA RADIATION INSIDE SHELTER

Shot	Metal section		Center, r	Concrete section	
	21 ft from center, r	15 ft from center, r		15 ft from center, r	21 ft from center, r
Baker	388 (est.)	343	73	343	388 (est.)
Charlie	830 (est.)	710	260	530	830 (est.)
Dog	880	735	375	320	Not available

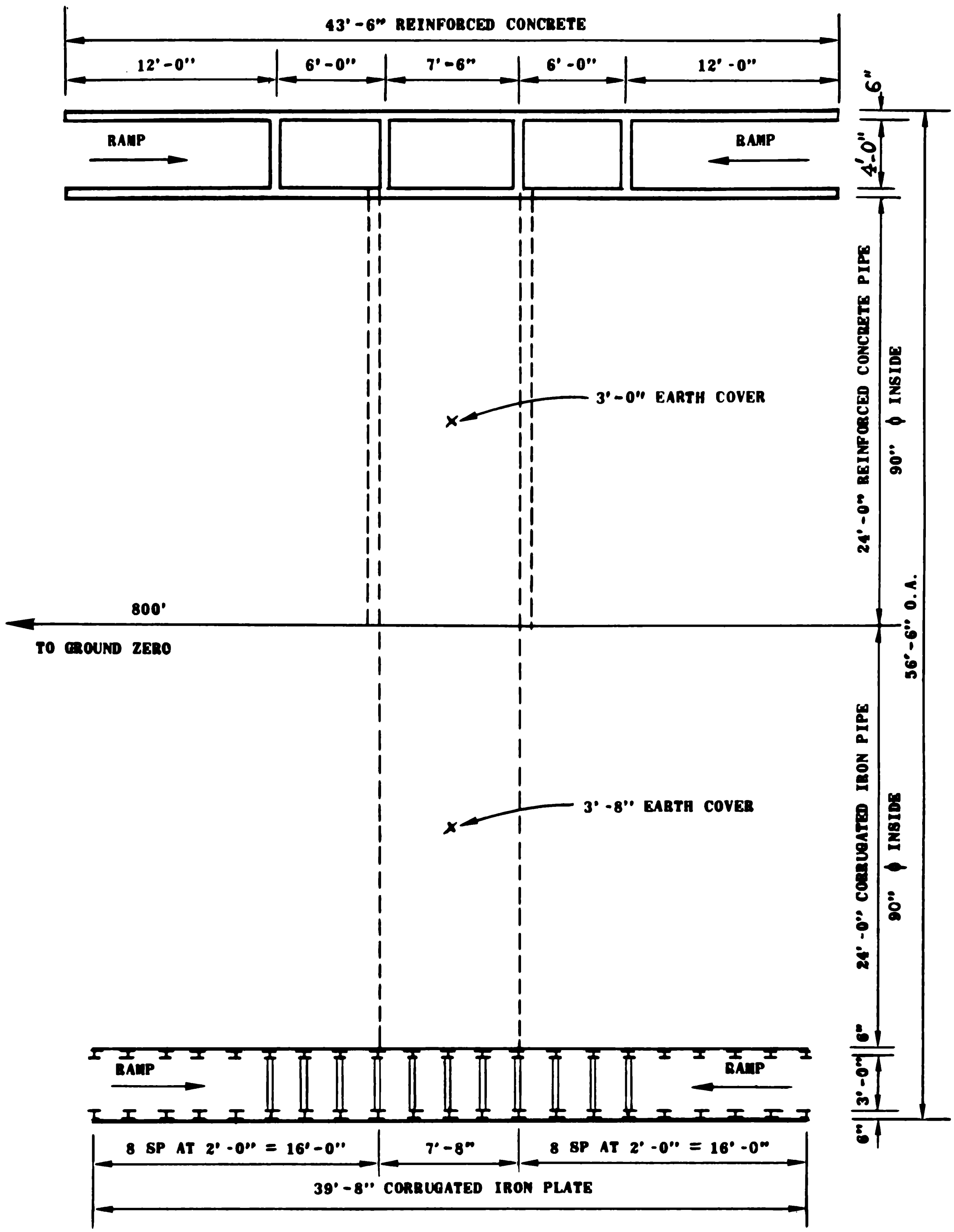

Fig. 1—Shelter plan at ground level.

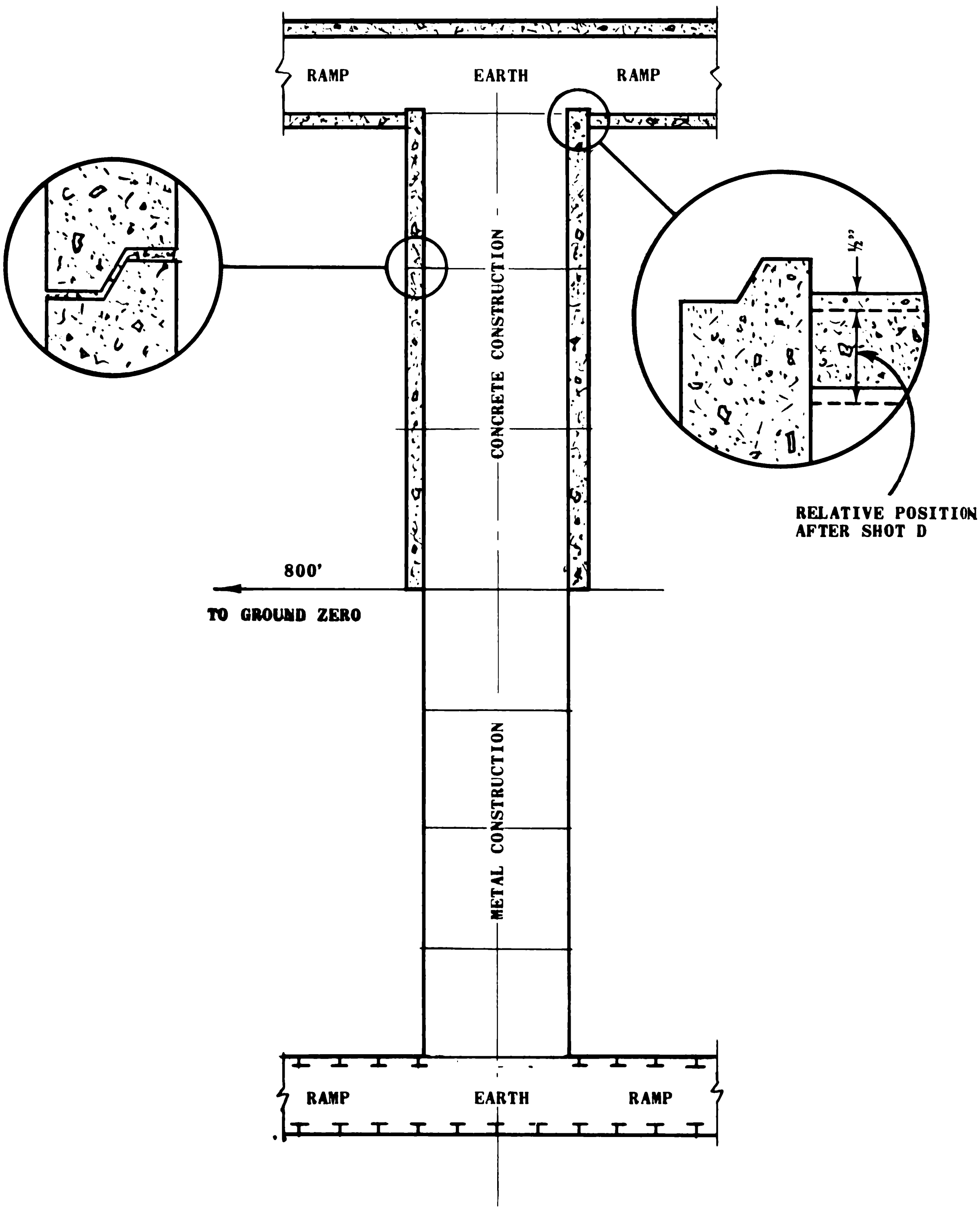

Fig. 2—Shelter plan at horizontal center line of pipe.

Fig. 3—Completed concrete ramp entrance before placing earth cover.

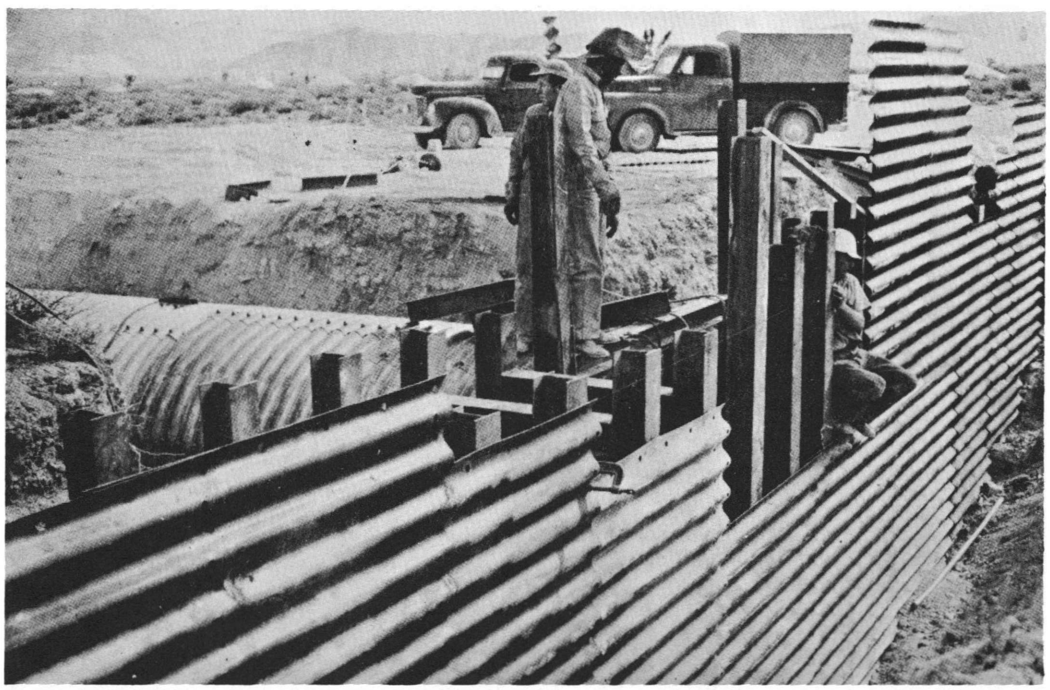

Fig. 4—Erecting steel Multi-Plate ramp entrance.

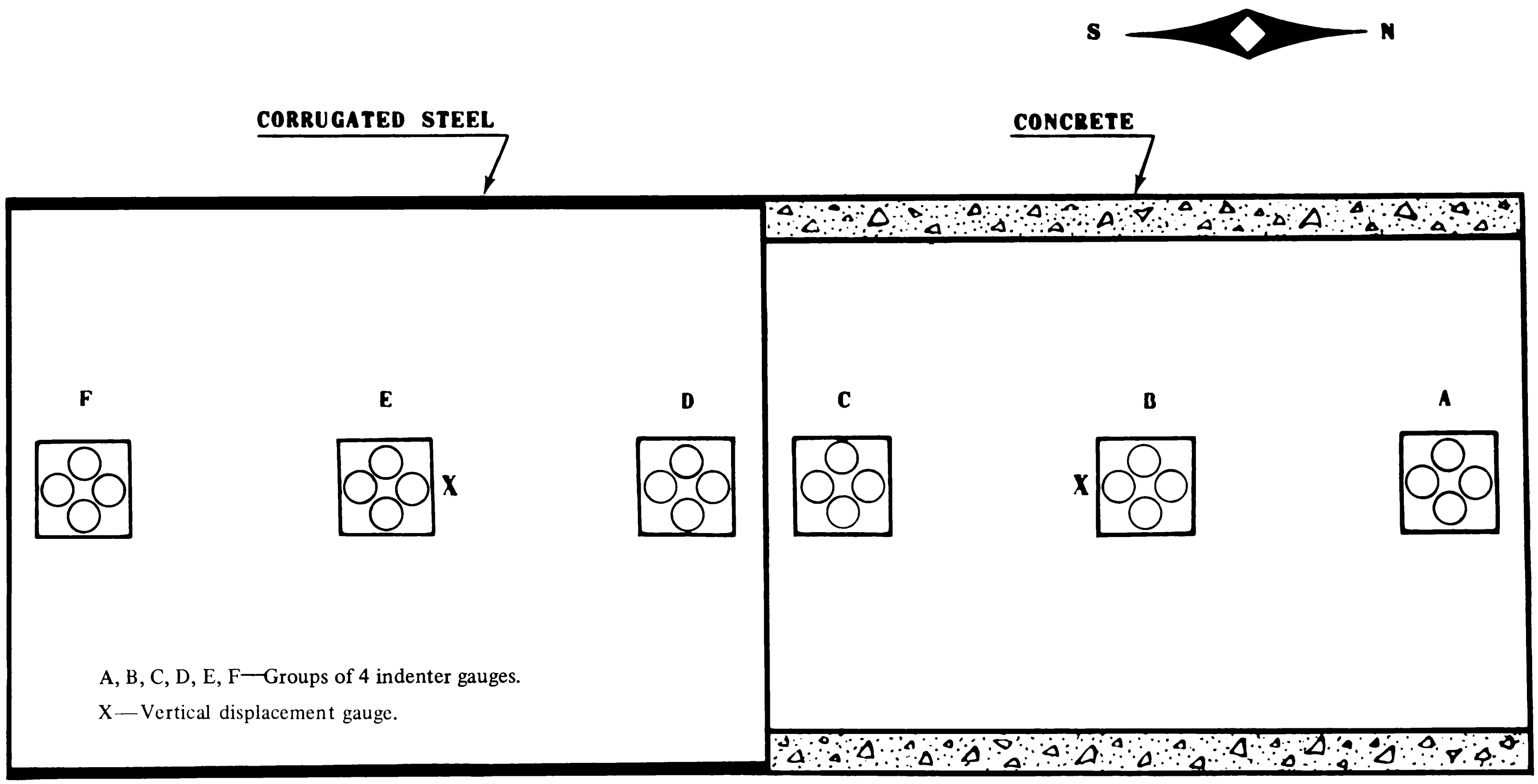

Fig. 5—Top view of shelter showing gauge positions.

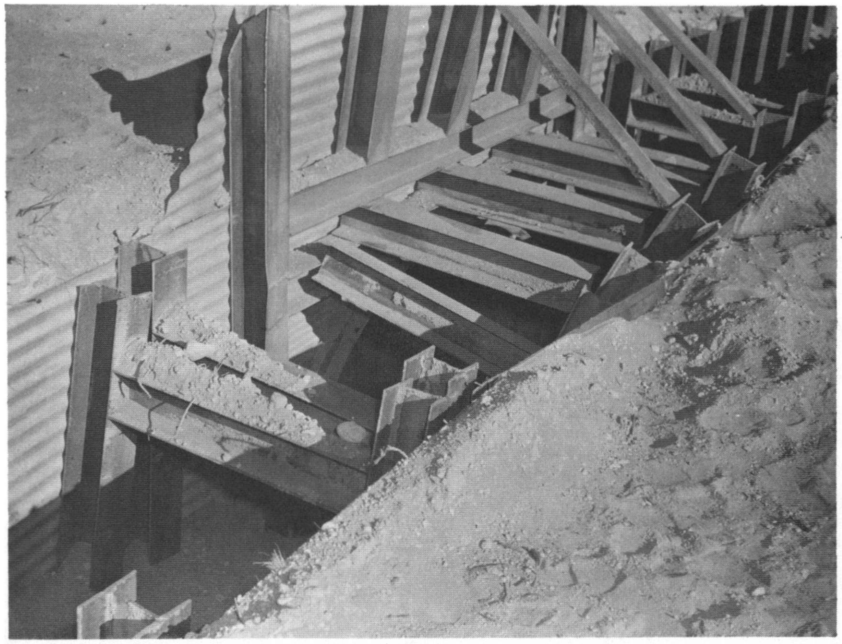

Fig. 6—Close-up view showing collapse of steel ramp wall after Dog shot.

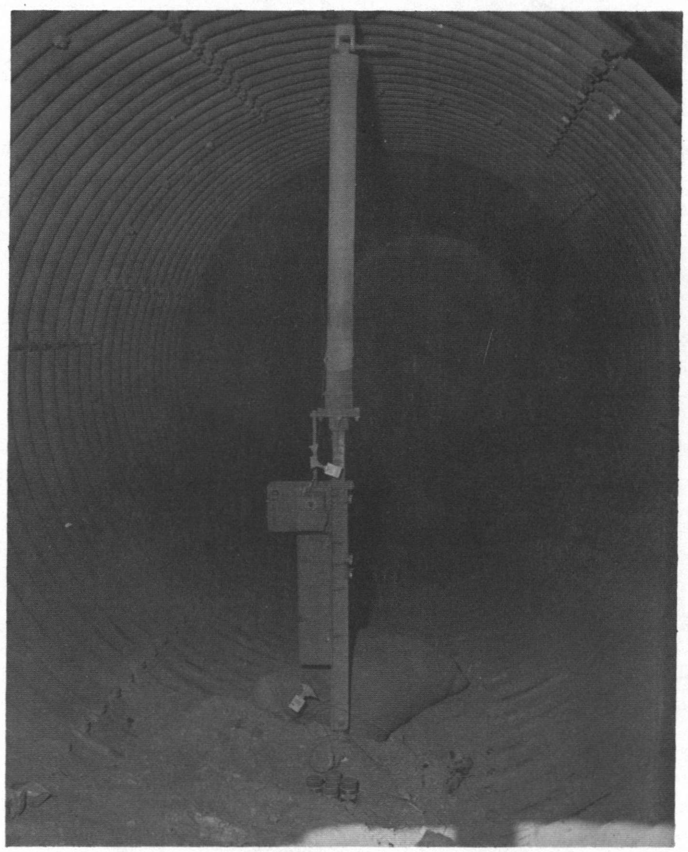

Fig. 7—General interior view facing north, showing instrumentation, dummies, and debris after Charlie shot.

SUMMARY 3

HASTY TYPE AIR RAID SHELTERS

(Report WT-560, Operation Tumbler, AFSWP Project, same title, by Albert E. Murdock, Capt., USAF, Sandia Base, Albuquerque, N. Mex., February 1953.)

OBJECTIVES AND SCOPE

Trench shelters that can be constructed rapidly with ordinary ditching machinery were tested to determine the relative protection afforded by such shelters when covered with earth spoil and when uncovered. Shelters were placed at various distances from Ground Zero (GZ) and instrumented with film badges to measure the value of nuclear radiation. Clothed dummies were used to indicate the effects of blast and thermal radiation.

The objectives of the test were to determine:

1. The highest peak overpressure in which survival of personnel using either the covered or uncovered shelter might reasonably be expected
2. The type of failure that might occur involving the material of the walls or the top cover of the shelter
3. If variation in the depth of the main trench is a major factor in survival probability, especially as it pertains to blast effects
4. If the shape of the earth-spoil overlay is an important factor in protection against blast.

The effects of the shot 4 air burst were expected to be similar to those of a nominal (20 kt) weapon. Peak overpressures expected at positions 1, 2, 3, and 4 were 40, 19, 8, and 4 psi, respectively, at approximate distances of 750, 1675, 2900, and 5100 ft from the anticipated GZ of shot 4. Orientation of all the shelters was such that the blast wave front struck against the long dimension of the shelters thus producing maximum blast effect.

TEST STRUCTURES, INSTRUMENTATION, AND TEST CONDITIONS

Figure 1 shows the typical trench design. The main portion of the trench was dug approximately 25 to 30 ft long and 24 to 26 in. wide for both the covered and uncovered shelters. The arms forming the entrances varied from 8 to 11 ft in length and were dug to a depth of 2 ft at their outer edge and sloped to the level of the floor of the main trench. One series of trenches was dug to a depth of 5 ft and another series to 6 ft. At position 2 the earth overlay at the covered shelter was made narrow and quite peaked so that its depth at the middle portion was approximately 26 in.

The cover for covered shelters was constructed of 2-in. wood planking overlapping the sides of the main trench by at least 2 ft and overlaid with the spoil taken from the trench.

Dummies of varying heights and configurations, weighing between 150 and 200 lb, were used to determine the effects of blast. The dummies were placed in positions that would be taken by personnel using such a shelter during an actual attack.

The gamma-radiation effect on personnel was measured by film badges placed 4 ft 6 in. from each entrance and 1½, 3, and 4 ft from the floor of the covered shelters. Uncovered trenches also had film badges at 4 ft 6 in. from entrances, but they were placed only at the 3-ft level from the floor. Outside, at positions 2 and 3, film badges were placed 4 ft above the surface of the ground.

Only estimates of thermal levels were made; these estimates were based upon visual observations of the clothing of the dummies and of the undersurface of the wood portions exposed to thermal radiation.

Soil conditions before shot 4 were as follows:

Positions 1 and 4: The soil structure at these locations was made up of finely granulated soil with occlusions of small rocks and rock fragments. Such soil structure was not suitable for the type of shelters constructed. Both the covered and uncovered shelters showed signs of erosion before the test shot.

Positions 2 and 3: Soil structure at these positions consisted of hard caliche with a thin overlay of 4 to 10 in. of finely granulated soil. This soil was expected to form a very hard, rock-like material for the walls of the shelter. Some soil erosion due to heavy rains was noted; however, the surface soil was nearly dry at the time of shot 4.

RESULTS

Tables 1, 2, and 3 summarize the measurements of prompt-gamma and residual-gamma radiation and blast and thermal effects. More detailed descriptions of the results follow.

Shelters at position 1 (68-psi overpressure at surface): Only a depression in the earth following the outline of the uncovered shelter remained after the shot (Fig. 2).

The covered shelter collapsed entirely. Portions of the wood showed signs of severe charring. Figure 3 shows the filled-in rear entrance and part of the charred wood covering of the shelter. On the basis of the charring of the wood ceiling inside the shelter, it was assumed that occupants of such a shelter under similar conditions would receive severe third-degree burns over all areas of exposed skin and also burns of a lesser degree over covered portions of the body. The total prompt-gamma dose was probably 7000 to 11,000 r. Film badges could not be recovered since collapse of the shelter was total. It is doubtful if any survivors could be expected in a similar shelter subjected to similar atomic effects conditions.

Shelters at position 2 (18.5-psi peak overpressure at surface): The damage to the uncovered shelter area damaged previously by shot 3 was only slightly extended; however, it contributed to the cave-in of the rear wall and the filling of the main trench with debris. Dummies had been tipped over. No charring of the dummies took place (possibly because they were wet) even though portions of wood frames on which film badges were placed facing GZ did show signs of charring. Personnel in this shelter would have received from 2000 to 3000 r of gamma radiation, and no survivors could be expected.

Where the walls of the covered shelter had been undercut, the walls gave way. Dirt from the overlay of soil had spilled into the entrance, as shown in Fig. 4. Several of the 2- by 12-in. wood members cracked, but only three boards showed signs of failure. Depth of the earth overlay had decreased from 26 to 9 in.

The dummy nearest the front entrance was approximately in the same position as before the shot. No signs of charring of the dummies or wood ceiling of the shelter could be found; therefore it was concluded that the thermal level within the covered shelter was below 8 cal/cm^2, which could cause only slight to moderate burns to exposed skin. Prompt-gamma dose was between 1400 and 2200 r.

Position 3 (8.8-psi peak overpressure at surface): Little blast effect was shown in the uncovered shelter; only a small amount of debris was blown into the shelter. Dummies were in the same locations as originally placed, but they were tipped over. There was no sign of charring on the dummies and only slight charring of the wooden frames holding film badges. Thermal radiation would have probably produced only first- and second-degree burns to exposed skin and probably no burning of unexposed skin. Prompt-gamma dose was 600 to 800 r as measured at 3 ft from the shelter floor.

In the covered shelter little blast effect was found. Dummies were in the same position as before the shot except that some were tipped. The height of the earth mound was only slightly altered. No dummies or interior wood surfaces were charred. Exposed skin would have sustained only very light burns. The prompt-gamma dose was 52 to 175 r according to the film badges recovered. It is highly probable that there would be survivors in a shelter of this type under similar atomic conditions. The level of residual-gamma radiation was sufficiently low that rescue work could be carried on for an extended period. The residual-gamma level was 0.9 r/hr 1 hr after the shot and less than 0.16 r/hr 24 hr later.

Position 4 (3.9-psi peak overpressure at surface): The walls of the uncovered shelter trench collapsed at 7 ft from the rear entrance to almost the front entrance, principally owing to the poor soil structure at this location. The trench filled with soil to within 2 ft 10 in. of the top. The sides at this point were widened to 3 ft 8 in. Dummies uncovered showed no signs of charring or displacement. Recovered film badges showed a prompt-gamma dose between 13 and 14 r.

In the covered shelter the main trench was filled to within 2 ft 7 in. of the top and was widened to 3 ft 8 in. for its entire length. The rear entrance was widened to approximately 36 in., as shown in Fig. 5. The dummies had not been displaced, and there was no evidence of charring. Recovered film badges showed a prompt-gamma dose of from 1.2 to 5 r. Had the sides of this shelter been revetted, as would be necessary with loose soil, all personnel would have survived.

CONCLUSIONS

The covered trench, as expected, affords greater protection against radiation than the uncovered trench; however, as far as the blast and thermal effects are concerned, the advantage of the covered trench is surprisingly small.

Soil structure is a major factor in determining how well the shelter walls will withstand the effect of a blast. At position 2 where the soil structure was fairly good, the shelter withstood an 18.5-psi overpressure, but at position 4 where the soil structure was poor, the sides of the shelter gave way under only a 3.9-psi overpressure.

Planking of 2-in. thickness will apparently withstand peak overpressures in excess of 15 psi but not 20 psi.

The depth of the trench apparently does not affect the probability of survival although it affects the total gamma dose received by the occupants. It is recommended that a 6-ft depth be used to accommodate tall occupants.

The earth mound over the wood cover should be broad and flat. The peaked mound of the covered shelter at position 2 was greatly reduced, and the flat, low mound formed by the spoil from the uncovered shelter at that position was only slightly altered by the blast.

Total thermal-radiation data estimated from observations of clothed dummies and charred wood are inadequate and certainly not of any great reliability.

DISCUSSION

The results of this test should be of considerable interest in case of an emergency situation with few or no resources available for more substantial shelter construction. Even though the magnitude of the effects (overpressure vs. time, thermal and nuclear radiation, etc.) is different for small nuclear weapons than it is for the large thermonuclear weapons now available and the physical environment (terrain, soil structure, etc.) is not typical of most populated areas, the data obtained from this test should be useful in evaluating the protection afforded by such emergency, or hasty type, shelters.

Table 1—PROMPT-GAMMA DATA SHEET IN ROENTGENS

	Position 1	2	3	4
Distance from GZ, ft	625	1,550	2,725	4,925
Intensity on surface, r	77,000*	18,000*	3,030	183
Covered shelter:				
Standing position,	11,000†	2,200(F)‡	160(F)‡	4(F)‡
4 ft from shelter floor		2,200(B)‡	175(B)‡	5(B)‡
Kneeling position	10,000†	2,200(F)‡	80(F)‡	2.3(F)‡
3 ft from shelter floor		2,200(B)‡	100(B)‡	2.5(B)‡
Sitting position,	7,000	1,430	52(F)‡	1.2(F)‡
18 in. from shelter floor			65(B)‡	
Uncovered shelter:				
Kneeling position,	14,000†		600(F)‡	13(F)‡
3 ft from shelter floor		2,700(B)‡	800(B)‡	14(B)‡

*Estimated from values measured at position 3.
†Estimated from values measured in shelters at position 3.
‡(F) Measured near front entrance; (B) measured near rear entrance.

Table 2—POST-SHOT GAMMA-RADIATION LEVELS (r/hr)

	H + 1 hr	H + 24 hr	H + 48 hr	H + 72 hr
Position 1 (625 ft)	100	10	1	0.8
Position 2 (1550 ft)	4.5	2	0.3	0.1
Position 3 (2725 ft)	0.9	0.165	0.05	0.02
Position 4 (4925 ft)	0.01	0.005	Background	Background

Table 3—BLAST AND THERMAL DATA

Position	Distance from GZ, ft	Peak overpressure at surface, psi	Damage sustained: Covered	Damage sustained: Uncovered	Thermal level at surface, cal/cm^2
1	625	68	Complete collapse	Complete	350
2	1550	18.5	Moderate to severe	Moderate to severe	145
3	2725	8.8	Slight	Moderate	60
4	4925	3.9	Severe*	Severe*	20

*Caused by poor soil structure and lack of revetment.

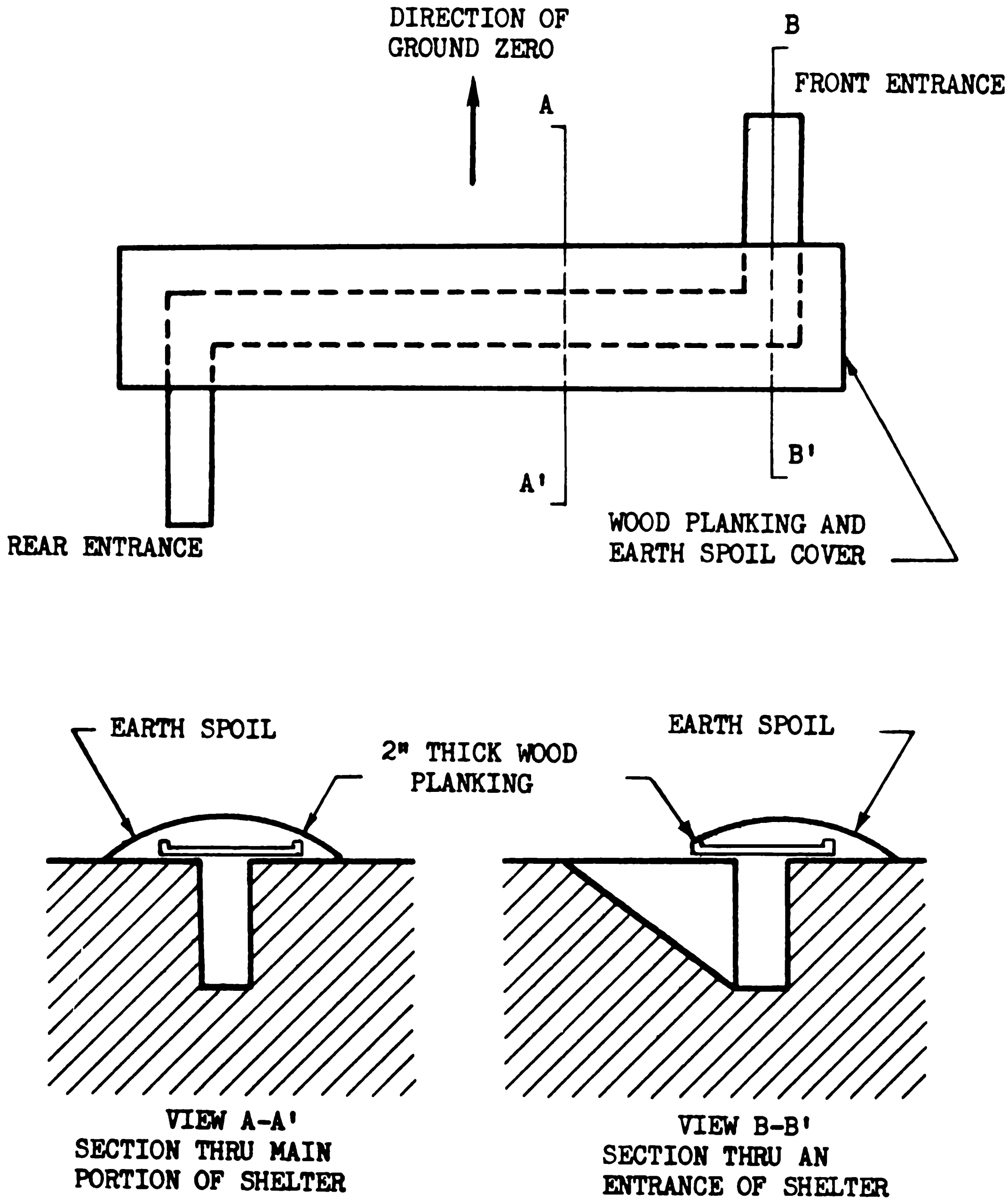

Fig. 1—Diagram of covered shelter.

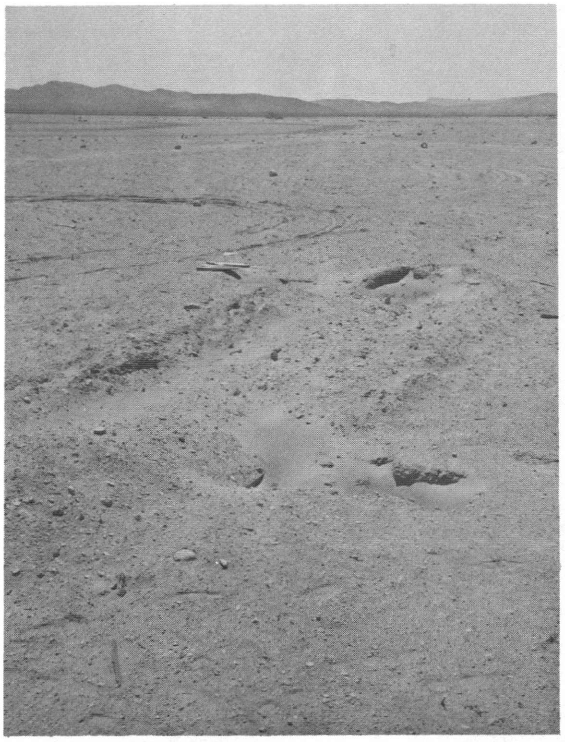

Fig. 2—Uncovered shelter remains at position 1.

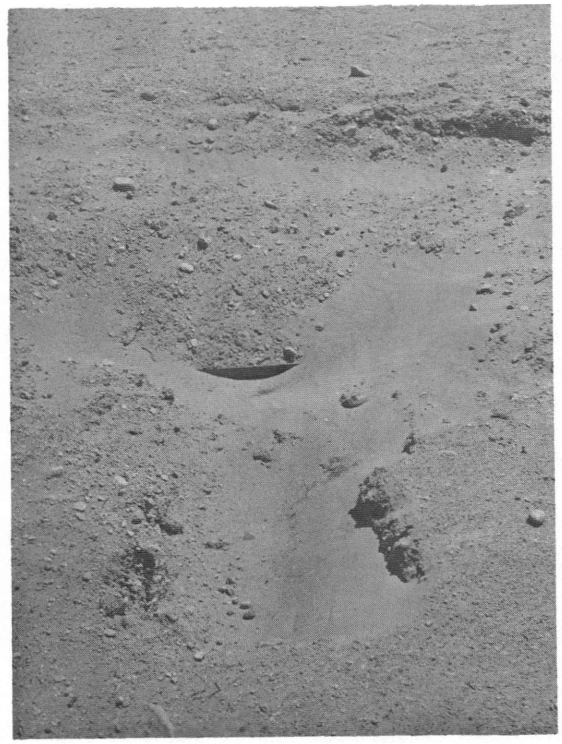

Fig. 3—Filled-in rear entrance at position 1.

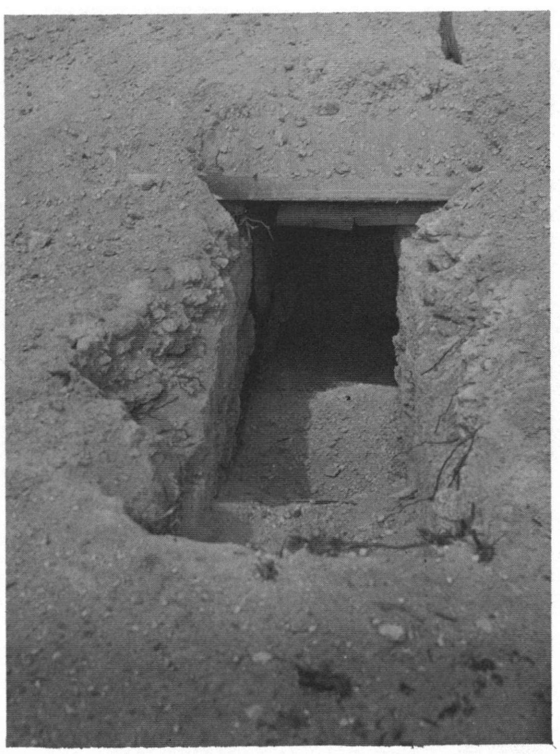

Fig. 4—Front entrance to covered shelter at position 2.

Fig. 5—Rear entrance at position 4.

SUMMARY 4

AIR BLAST EFFECTS ON ENTRANCES AND AIR INTAKES OF UNDERGROUND INSTALLATIONS

(Report WT-726, Operation Upshot-Knothole, Project 3.7, same title, by G. K. Sinnamon, W. J. Austin, and N. M. Newmark, University of Illinois, Feb. 1, 1955.)

OBJECTIVES AND SCOPE

This shelter project was designed to obtain under field conditions in an atomic blast data on various devices suitable for air intakes and ventilation ducts and data on the performance of entranceways of two simple designs. These data were to be compared with similar data obtained in shock-tube tests of small-scale models. The structure in which the devices were installed was subjected to blast from two shots: shot 9 that produced on the ground surface at the location of the structure an overpressure of about 20 psi and shot 10 that produced an overpressure of about 110 psi. The primary objective was to test those parts of a shelter which appear most vulnerable to air blast, i.e., ducts and ventilating equipment that bring in the air supply and the doors and entranceways for the shelter structure.

TEST STRUCTURE AND EQUIPMENT

Figures 1 to 6 show the below-grade test structure with gauge locations; orientation of the structure relative to Ground Zero (GZ); and schematic diagrams of the ventilation equipment tested. All equipment was contained in the two separated halves of the single structure located about 2 ft below the surface of the ground. Entrance to each half of the structure was provided through a different type of entranceway and corridor. There was at one end a T entranceway with two stairways and at the other end a single stairway leading into a corridor that had a number of turns and baffles.

The location of the blast door in each corridor entranceway was determined by two primary conditions: (1) the door should not be exposed to the direct effect of the shock wave and (2) it should be placed so that it would not be hurled into the structure in the event of failure. Tight closure of the doors was necessary also to isolate the large test chambers of the shelter so that an independent pressure measurement could be obtained.

The ventilating ducts tested led either into one of two main chambers or into smaller auxiliary chambers. These vents were of six different designs: a Swedish rock grille, a muffler design, a simple T duct, a 180°-bend duct, and two additional T ducts, one which led directly to a set of Chemical Corps filters

between the T and the chamber and the other which led from the T intake to an antiblast valve and then through a set of Chemical Corps filters into the chamber.

Instrumentation consisted of 34 channels of air-blast measurements, of which 8 were in the individual ducts, 10 were in the test chambers to which the ducts led, 15 were in the entranceways, and 1 was used to obtain the overpressure on the ground surface.

RESULTS

In the first test, which was intended to produce an overpressure of about 20 psi, the shock wave had a regular shape of about the order of magnitude expected. (See Figs. 7 to 10 and Table 1.) Good records of pressures in the various entranceways, chambers, and ducts were obtained in this shot. No damage was observed either in the structure or in the ventilating elements and ducts, with the exception of minor damage to ventilating fans that were mounted on the ducts leading to the large chamber. The fans were removed before the second shot.

In the second test the ground blast pressure was of the order of twice the 65-psi overpressure expected, and the pressure pulse was of a highly irregular shape. Only 6 pressure–time records out of a total of 36 were obtained for this shot. All the ventilating ducts failed with the exception of the rock grille. Only the data from the rock grille could be correlated with data from the previous shot. There were also major cracks in the entranceways.

It is notable that in this series of tests the Swedish rock grille was not a particularly efficient throttling device. The internal pressure permitted for shot 9 by the rock grille in the small plenum chamber was 11.2 psi; however, that which reached the chamber through the 180° bend was only 8.2 psi, and that which reached the chamber through the muffler was only 5.2 psi. However, the rock grille led into its chamber through a pipe with a diameter twice that of the other items. Thus this may have permitted much less throttling than was obtained with the other devices. The test in this respect was not completely fair for the rock grille.

The test data concerning the entranceways show roughly the following characteristics: After some "clearing" time the pressures in the entranceway passages appear to be the same as those outside the structure in the general area. The records indicate the passage of the shock through the corridor to the farthest point, a reflection, and a return passage to the entrance. Because of the various interferences, the maximum reflected pressure is of an order of magnitude of twice the peak outside pressure that enters in the first place. The reflection coefficient would normally be much higher than this for the pressures considered, but apparently interferences and other factors confine the value to this order of magnitude. For shot 9 (20-psi pressure), the maximum pressures recorded in the entranceways were of the order of 30 to 40 psi. No values can be given for shot 10 (110 psi) since all the entranceway instrumentation ceased to function.

The results of the entranceway tests, discussed above, are not considered sufficiently conclusive to serve as a general basis for design.

Figures 7 to 10 show typical pressure–time curves for the vents. The curves show that all the vents appreciably lengthened the rise time in the plenum chambers and in some cases reduced the maximum pressure by a large factor. An initial peak or spike, however, occurred in the pressure records for the ducts. The most probable values determined from the pressure curves are summarized in Table 1. These pressures compare with the maximum pressure of 20.3 psi recorded on ground surface at the shelter structure.

The high blast pressure (110 psi maximum) experienced in shot 10 caused considerable damage to the vents. Four of the steel ducts were torn off just above the ground level, i.e., the two ducts above the Chemical Corps filter units, the muffler vent, and the duct with the 180° bend. The failure in each case was in or adjacent to a weld. The two T-shaped intake vents were severely bent at ground level, and the two T-shaped exhaust vents were bent slightly.

The concrete boxes of the Swedish rock grilles were heavily cracked above the ground surface on the face toward GZ and on the two sides.

Table 1—MAXIMUM VENT PRESSURES, SHOT 9

Vent	Gauge		Pressure, psi	
	Location	Number	Initial peak	Maximum*
		Small plenum		
T-shaped intake	Duct	19F	10.4	7.5
	Chamber	19R		7.8
180°-bend intake	Duct	19G	11.4	7.6
	Chamber	19S		8.2
Swedish rock grille	Duct	19C	2.2	9.7
	Chamber	19O		11.2
Muffler	Duct	19B	4.7	5.0
	Chamber	19N		5.2
Filters	Duct	19E	0.8	2.6
	Chamber	19Q		2.3
Antiblast valve and filters	Duct	19D	0.4	0.3
	Chamber	19P		0.3
		Large plenum		
T-shaped intake	Duct	19H	21.1	
	Chamber	19L		3.9
	Chamber	19M		4.2
Swedish rock grille	Duct	19A	10.9	
	Chamber	19K		2.0
	Chamber	19J		2.5

*These pressures were determined from smoothed pressure–time curves and consequently may be slightly less than the peak values shown on Figs. 7 to 10.

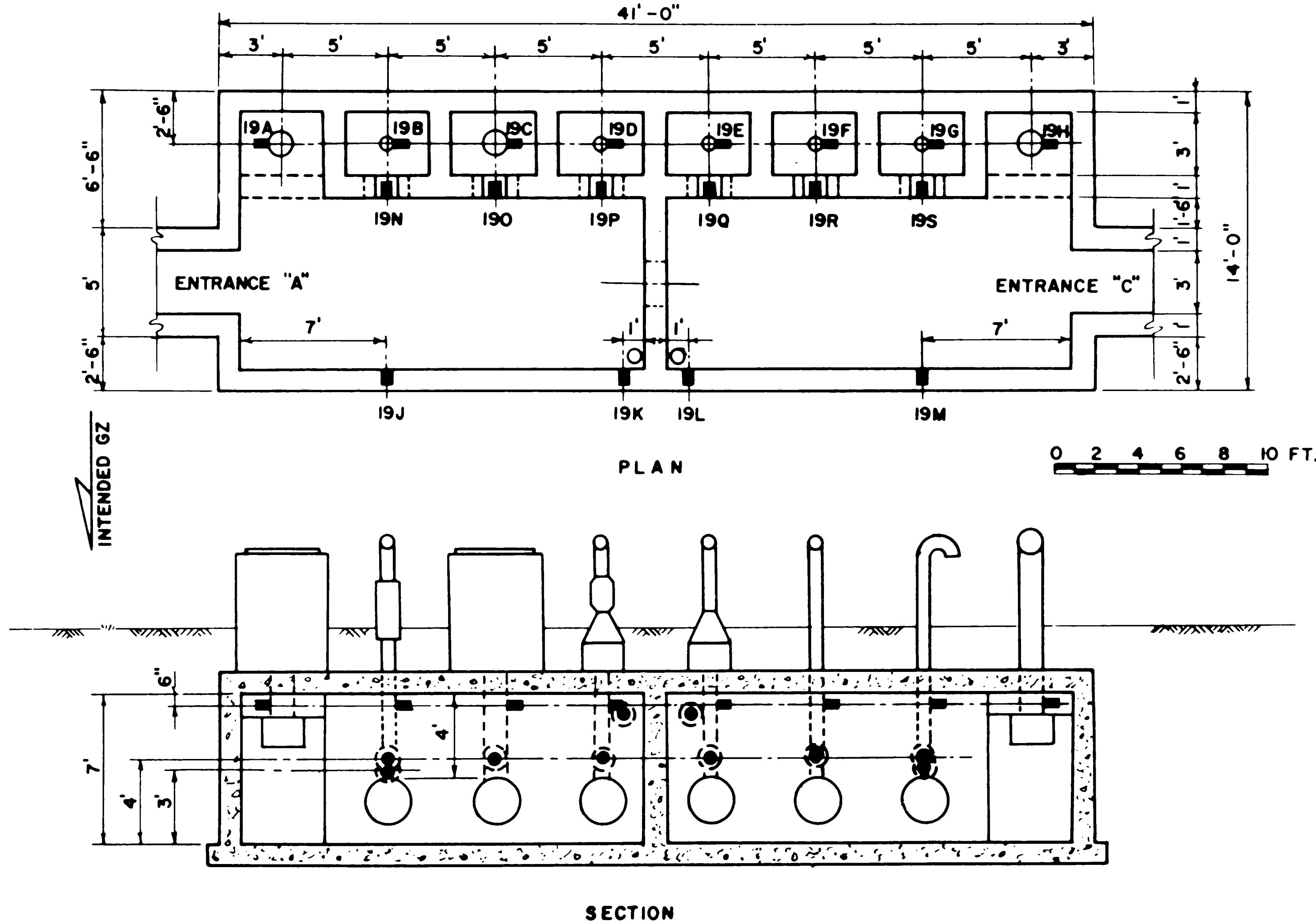

Fig. 1—Gauge locations for vents and plenum chambers.

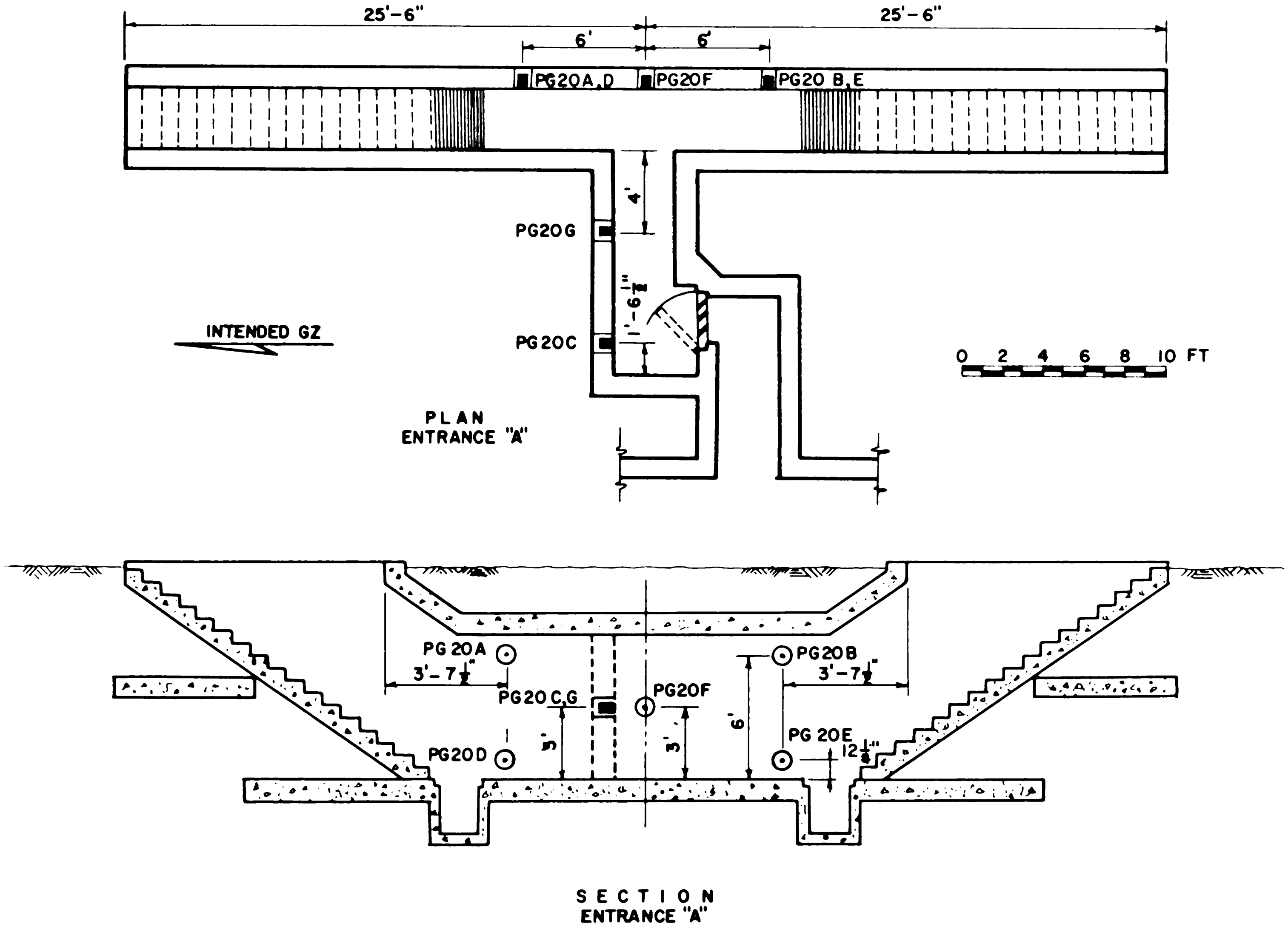

Fig. 2—Gauge locations for entranceway A.

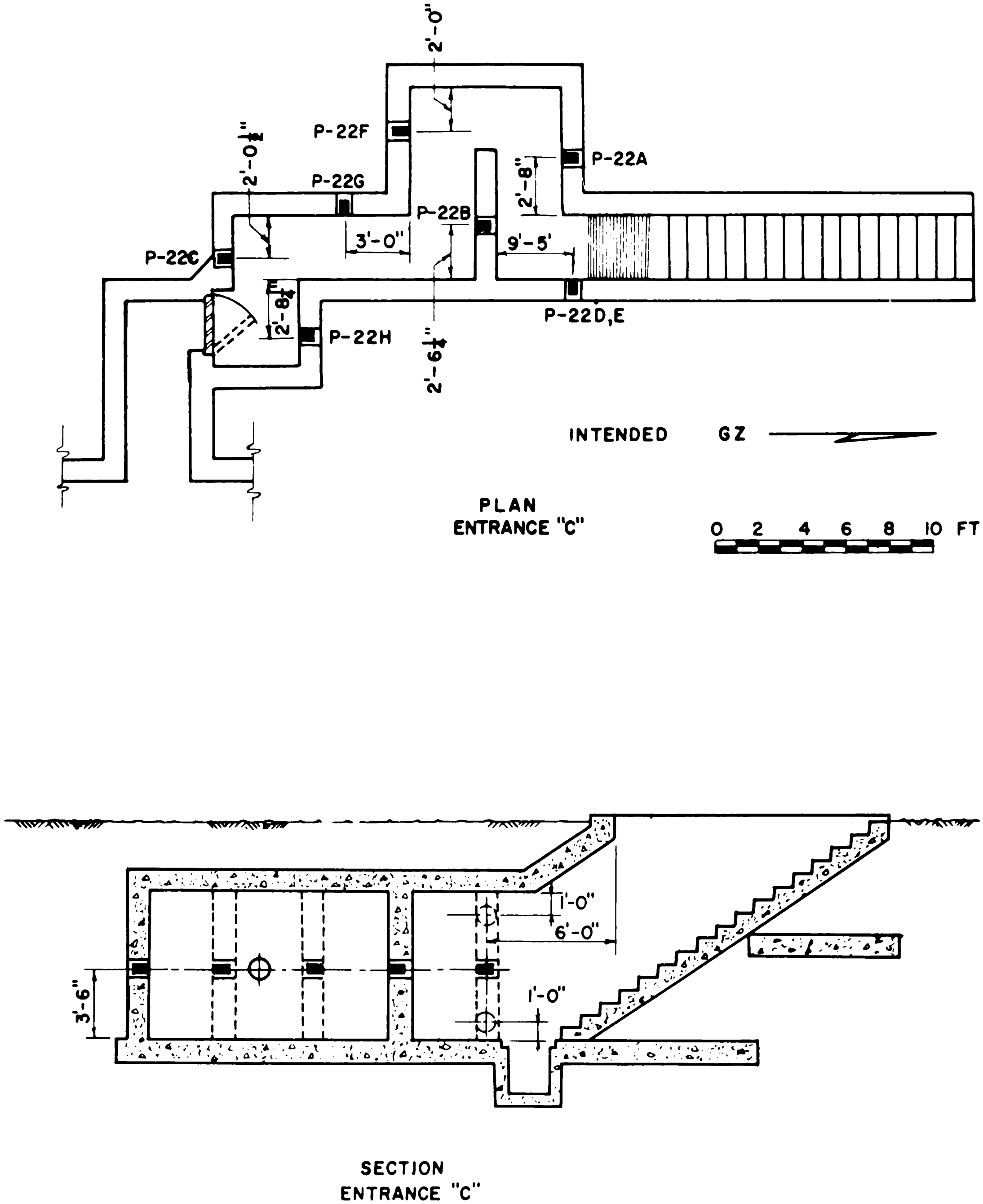

Fig. 3—Gauge locations for entranceway C.

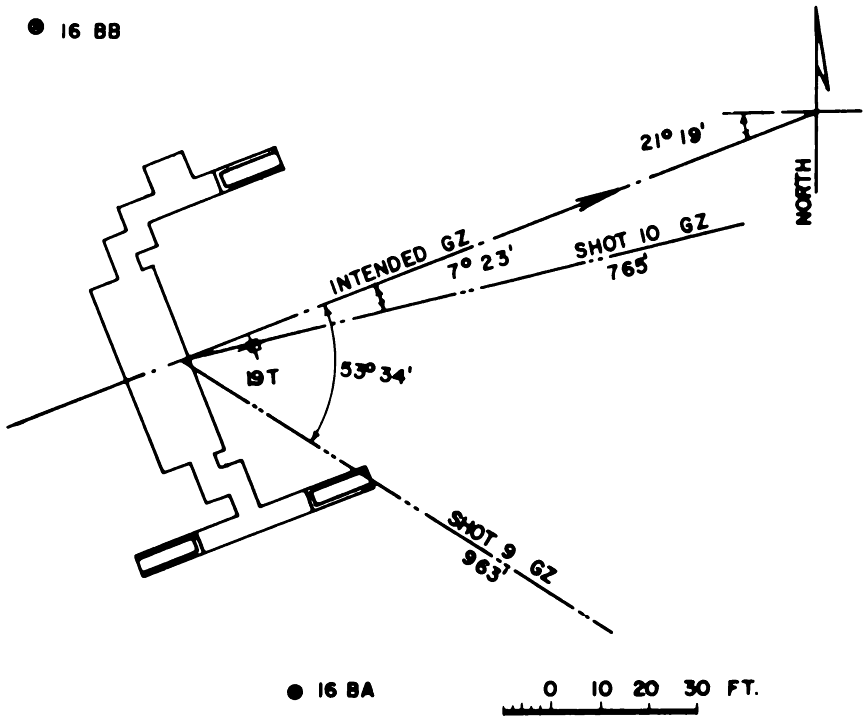

PLAN

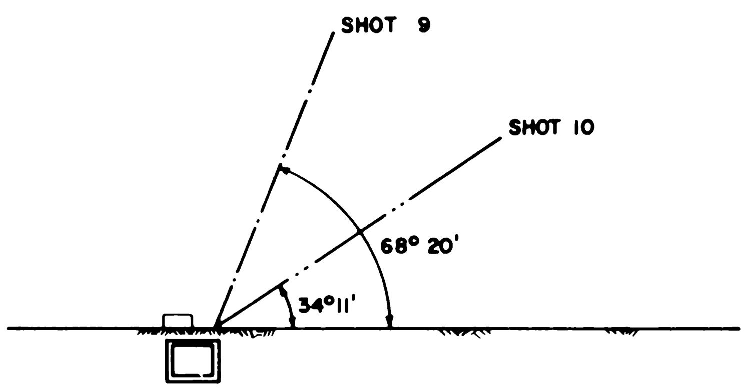

ANGLE OF INCLINATION

Fig. 4—Orientation of structure.

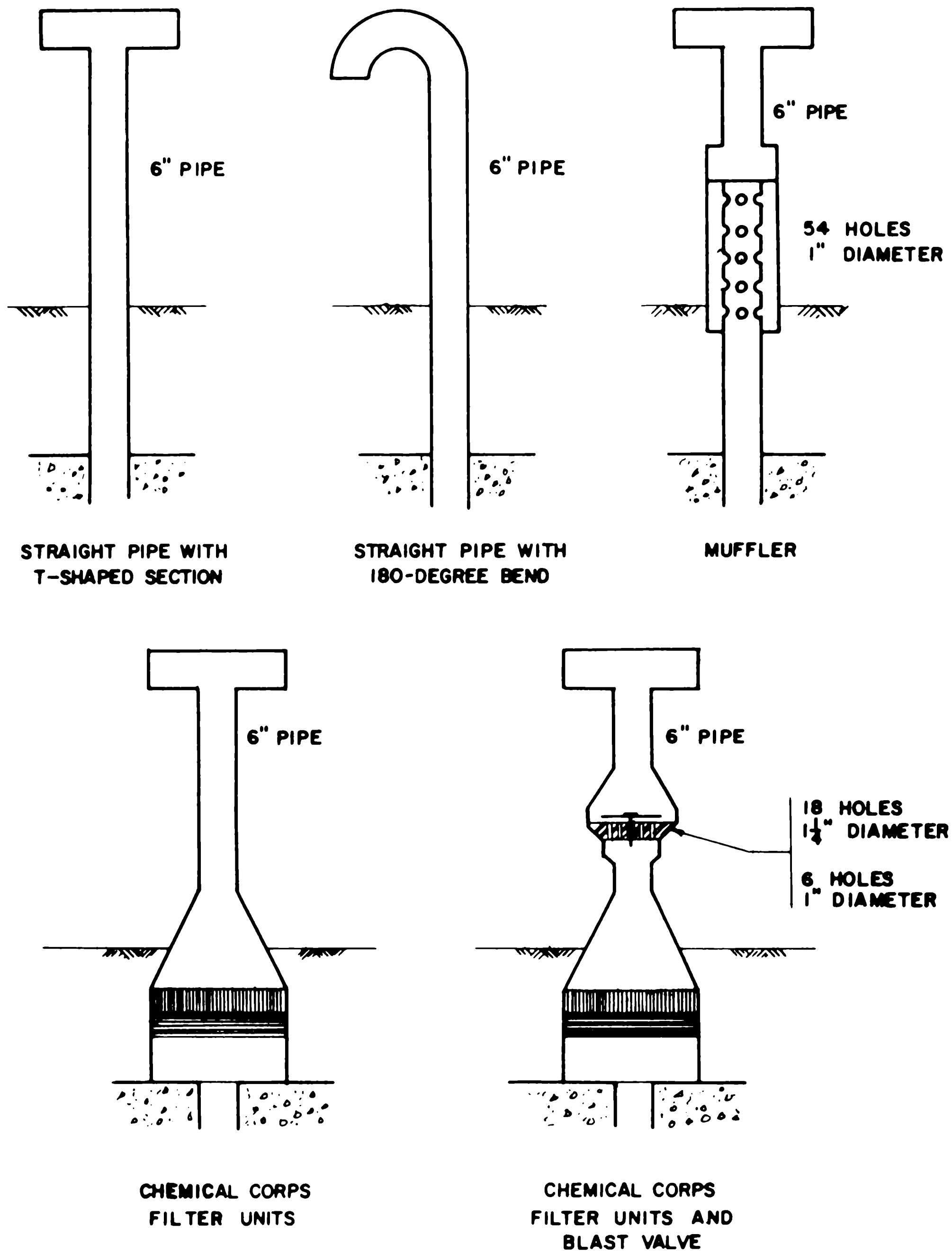

Fig. 5—Schematic diagrams of vents.

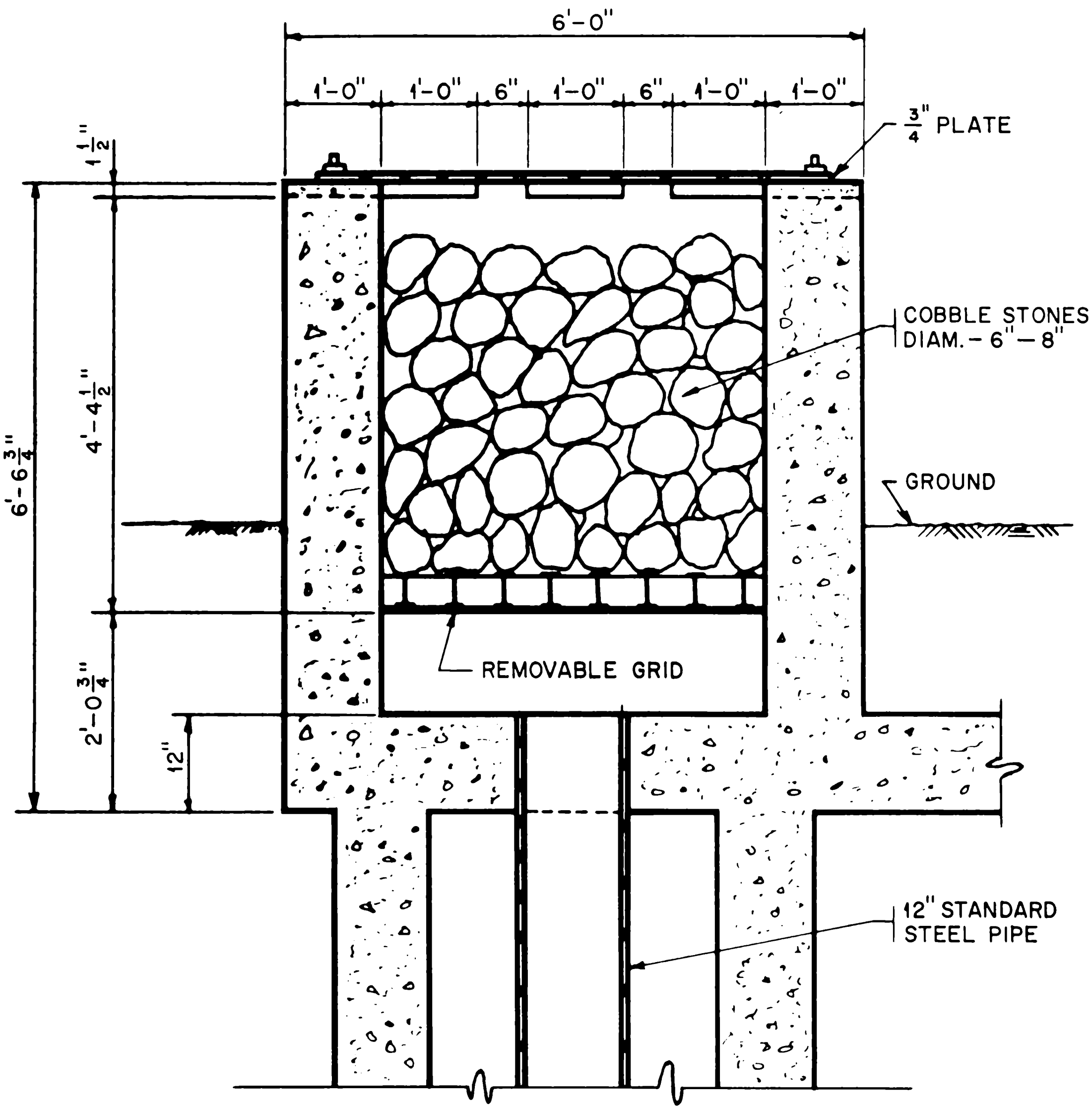

Fig. 6—Cross section of Swedish rock grille.

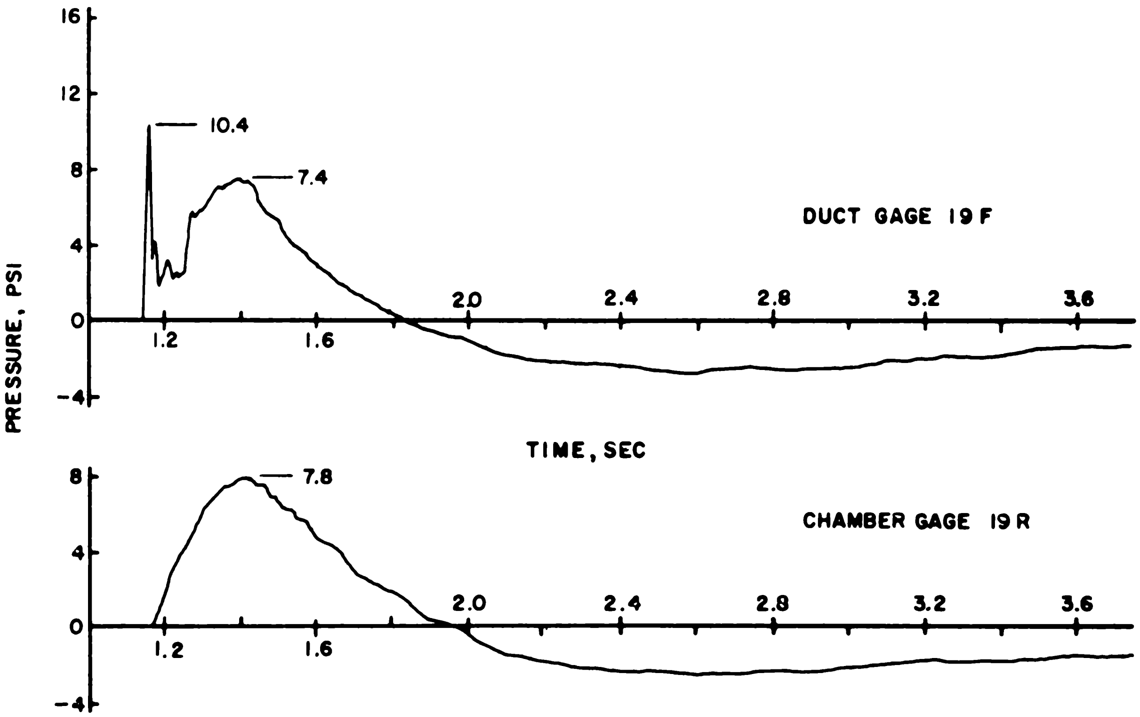

Fig. 7—Pressure–time curves for T-shaped vent, shot 9.

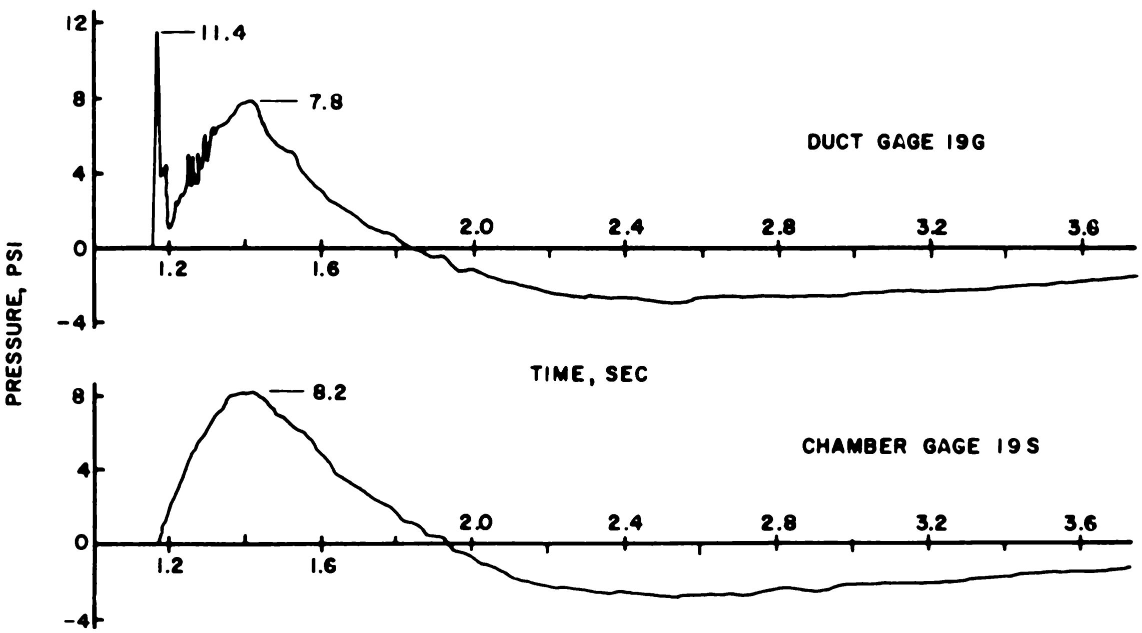

Fig. 8—Pressure–time curves for 180°-bend vent, shot 9.

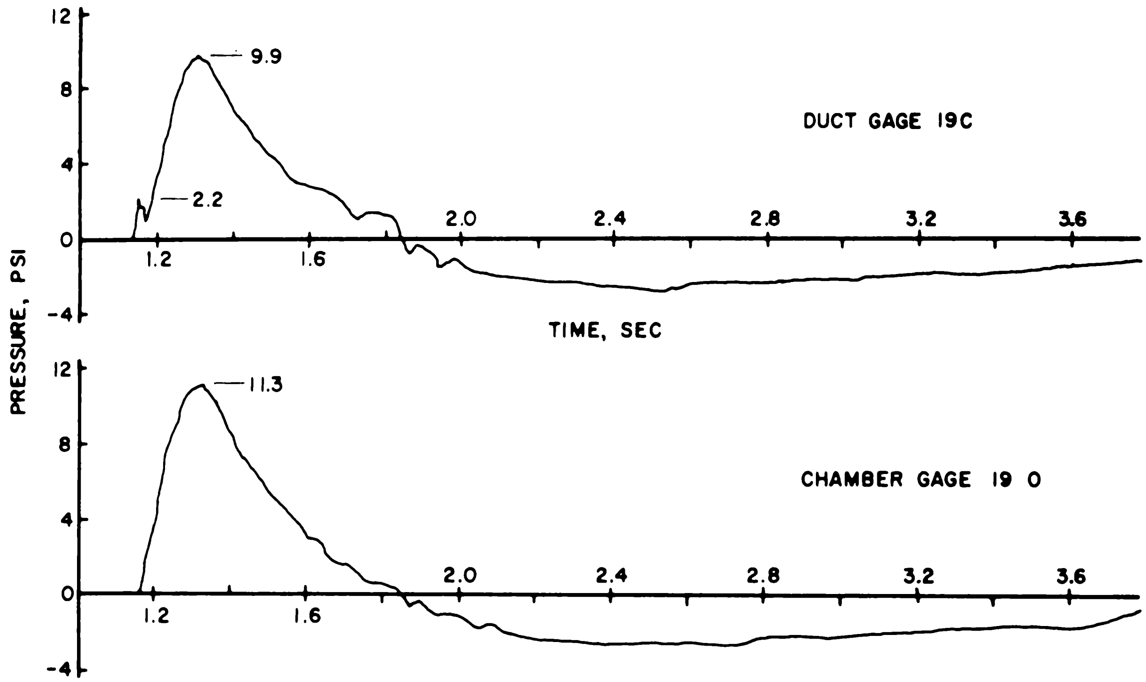

Fig. 9—Pressure–time curves for Swedish rock grille, shot 9.

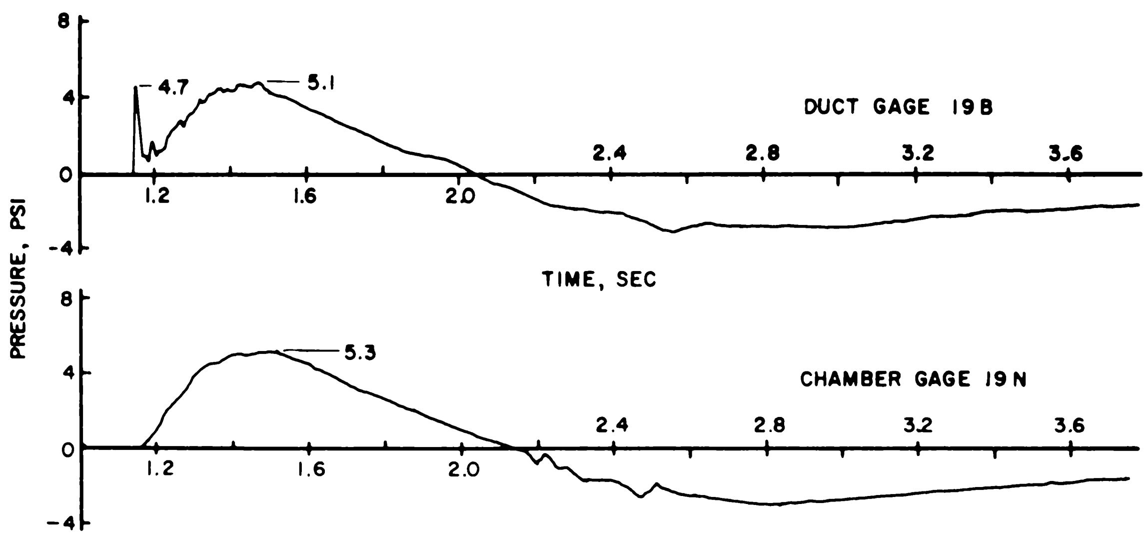

Fig. 10—Pressure–time curves for muffler, shot 9.

SUMMARY 5

AIR BLAST EFFECTS ON UNDERGROUND STRUCTURES

(Report WT-727, Operation Upshot-Knothole, Project 3.8, same title, by N. M. Newmark and G. K. Sinnamon, University of Illinois, Urbana, Ill., January 1954.)

OBJECTIVES AND SCOPE

The specific objectives of this project were: (1) to investigate the nature of the forces, initiated by a burst of an atomic bomb, transmitted through the earth to underground structures; (2) to determine the variation of these forces with the depth of transmission through the earth and with the flexibility of the structural elements subjected to the forces; and (3) to study the response of simple structural elements of different stiffnesses subjected to the transmitted dynamic forces.

The structures were primarily reinforced-concrete boxes having a large number of simply supported steel beam strips forming the roof. Three structures were included in the program, having earth cover over the beam strips of 1 ft, 4 ft, and 8 ft for structures 3.8a, 3.8b, and 3.8c, respectively, and each of the structures had a number of individual beam strips, with several strips of each of three different degrees of flexibility. All of the beam strips had the same span, namely 8 ft.

The structures were tested in two shots, the first (shot 9) producing an overpressure of about 15 psi, and the second (shot 10) about 63 psi.

TEST STRUCTURES, INSTRUMENTATION, AND SOIL CONDITIONS

The structures were designed on the basis of an expected pressure of 60 psi. Figure 1 shows the location of the test structures, 3.8a, b, and c relative to the two shots. Table 1 and Figs. 2 to 6 show details and arrangement of the beam strips as well as of the supporting concrete test chambers.

The instrumentation consisted of: (1) the transient measurement of pressures, strains, deflections, and accelerations with electronic equipment; (2) the measurement of permanent strains in the beam strips with mechanical strain gauges; and (3) the measurement of permanent deflections of the beam strips and relative motion of the structures with a precise surveyor's level. Most of the electronic instrumentation was performed by the Ballistic Research Laboratories as a part of Project 3.28.1. For location of gauges, see Figs. 6 and 7.

The soil in the Frenchman Flat area where the three test structures were constructed is a tan silt with a trace of clay. In its natural state this soil is very friable. The excavation for the three structures was done carefully so that the base slabs could be poured directly onto the undisturbed soil. The excavated material

was used for backfilling after the structures were completed. This material was thoroughly mixed to the proper water content by spreading, sprinkling, and windrowing until it was at a uniform moisture content approximately equal to the plastic limit of the material. The backfill, placed in layers of about 4 in. loose thickness, was generally compacted by pneumatic hand tampers.

RESULTS

Visible Results

There was little evidence of any effect whatsoever from shot 9 at about 15 psi except for a small amount of cracking of the surface of the fill over the structures and other similar surface disturbances in the soil.

After shot 10 it was almost immediately evident that structure 3.8a had been subjected to considerable motion within the soil. The roof covering had apparently been raised several inches and had fallen back into place. There was, however, no visible effect on the structure and no visible evidence of any appreciable permanent strain in the beam strips, even in structure 3.8a. The deeper structures showed no evidence even of relative motion and no indication of any serious overstress.

Transient Effects

In shot 9 only some of the instrumented channels produced records; however, even these records are not very useful because of unsatisfactory gauge settings. In shot 10 excellent dynamic records were obtained on a majority of the instrument channels. The pressures on the ground surface are shown in Figs. 8 and 9 for shots 9 and 10, respectively.

The pressures recorded by the gauges at various depths in free earth are shown in Fig. 10. The traces illustrate a reduction in intensity of pressure and a marked reduction in the duration of the positive phase of the pressures with depth below the surface.

All the pressures measured at the various points on the beam surfaces of the three structures at different depths had, in general, the same major characteristics, and these were similar to the pressures at the ground surface. Pressure–time diagrams for the quarter points of the P-beam strips, which are typical of all the other records, are shown for each of the depths in Fig. 11.

The pressures on the bottom of the structures measured by the gauges embedded in the floor also were similar to the pressures measured at the ground surface except for a difference in magnitude. The base pressure curve obtained for structure 3.8b is shown in Fig. 12. It is noted that the magnitude of the pressure on the base was about three-quarters of the pressure on the ground surface.

The horizontal pressures on the vertical walls at the ends of the test chambers were measured at a number of points. The general nature of the measurements is indicated by the typical curve plotted in Fig. 13 for structure 3.8a.

Acceleration measurements were made on all the structures so that the motion of the structure as a whole could be determined. In order to obtain a measure of the maximum velocity and displacement of the concrete test chambers, integrations were performed on the acceleration records originally obtained. The results are shown in Table 2.

CONCLUSIONS AND DISCUSSION

Analysis of the test data indicates the following:

1. In well-compacted silty subsoil of the type at the test site, there is no effective attenuation of a pressure pulse applied at the surface with depth through the subsoil when the pressure is transmitted to a structure in the soil. The transient as well as the permanent strains and deformations of the beam strips were of about the same order of magnitude at all three depths and showed only a slight decrease for the 8-ft depth compared with the others. This indicates that for deflections of less than 0.5% of the span and for

depth of cover less than the span length, the dynamic "arching" phenomenon is negligible and the beneficial effect of added cover is primarily that attributable to the added mass of such cover.

2. For underground structures having a net density less than that of the displaced soil, the overall accelerations of the structure act to reduce the influence of the pressures applied to the top of the structure. The influence, however, is not large and may be neglected in design.

3. The lateral pressures exerted on vertical faces of a buried structure, which are produced by pressures applied at the top surface of the soil, are of the order of magnitude of 15% of the vertical pressures on the surface for well-compacted silty soils of the type at the test site.

4. The pressures exerted upward on the base or floor slab of buried structures are of the same order of magnitude as the pressures on the roof. A base pressure about three-fourths of the roof pressure appears to be sufficient for design purposes unless the duration of stress is extremely long.

Theoretical considerations indicate that these conclusions are not unreasonable for other types of soil, except that the horizontal pressures might be larger in other soils. It is also reasonable to expect that the conclusions are conservative for larger deflections approaching more nearly the collapse limit.

Table 1—DIMENSIONS AND PROPERTIES OF BEAM STRIPS

	Beam strip type		
	P	M	E
Rolled sections used, each side	Two 7[9.8	8I23	15I50
Width of ½-in. plate, in.	21.25	20.25	23.25
Total width supported, in.	22	21	24
Total moment of inertia, $in.^4$	162.0	232.8	1462
Distance to neutral axis			
Top flange, in.	2.19	2.67	5.79
Bottom flange, in.	5.31	5.83	9.71
Max. stress (100-psi load), ksi†	83.1*	60.6*	18.4
Max. deflection (100-psi load)			
Neglecting shear, in.	0.501	0.333	0.0605
Including shear, in.	0.542	0.366	0.0764
Equiv. dead load			
1-ft cover, psi	1.1	1.1	1.3
4-ft cover, psi	3.4	3.4	3.6
8-ft cover, psi	6.5	6.5	6.7
Dead-load stress			
1-ft cover, ksi	0.9	0.7	0.23
4-ft cover, ksi	2.8	2.1	0.66
8-ft cover, ksi	5.4	4.0	1.23
Dead-load deflection			
1-ft cover, in.	0.0058	0.0041	0.0010
4-ft cover, in.	0.0184	0.0125	0.0027
8-ft cover, in.	0.0352	0.0239	0.0051
Fundamental period (T)			
Steel section only, msec	11	11	5
1-ft cover, msec	21	18	9
4-ft cover, msec	38	32	15
8-ft cover, msec	53	44	20

*Assuming linear elastic action.

†The abbreviation ksi is the standard notation for kips (kilopounds) per square inch, or 1000 lb/sq in.

Table 2—BASE PRESSURES AND PEAK ACCELERATIONS FOR TEST CHAMBERS

	Structure		
	3.8a	3.8b	3.8c
Peak air pressure at ground, shot 10, psi	63	63	63
Max. pressure top of beams			
Av.* for shot 10, psi	62	61	63
Pressure corr. to max. reactions			
Av. for shot 10, psi	69	85	72
Peak base pressure, shot 10, psi	24	47	
Approx. max. acceleration			
From ground pressure, including earth mass and structure mass, g	7.5	2.1	
From beam pressure and structure mass only, g	8.6	3.1	
From reactions and structure mass only, g	10.1	8.6	
Max. measured acceleration, g	7.6	6–10†	1.0
Max. acceleration in obsolete record, g	8.3	5.9	
Calc. max. velocity, ft/sec	4	3	
Calc. max. displacement, in.	2.1	2.5	

*Average for all values not beyond calibration range.

†Peak greater than 10 g on rerun, but nearly 6 g on original record.

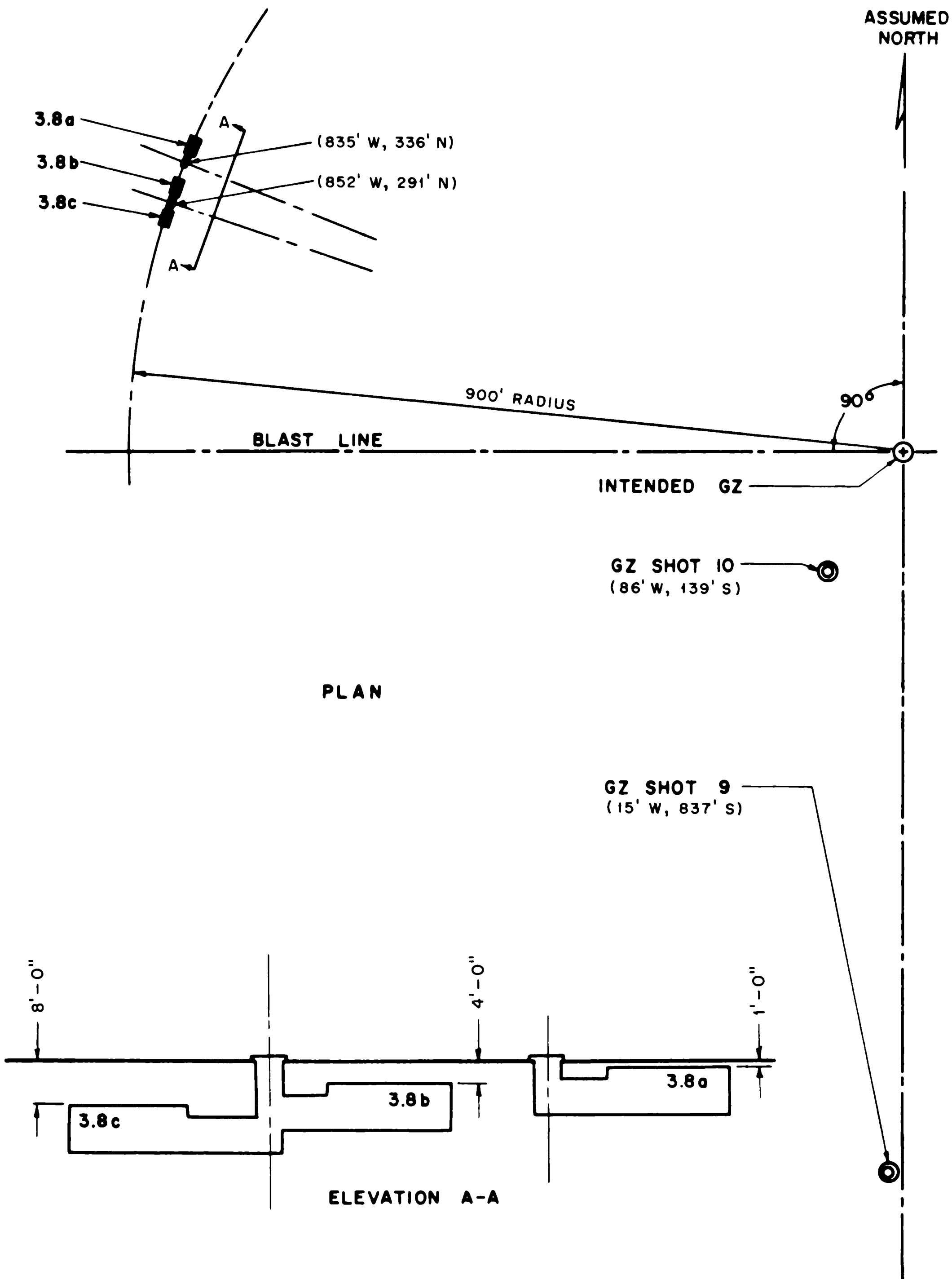

Fig. 1—Location of structures.

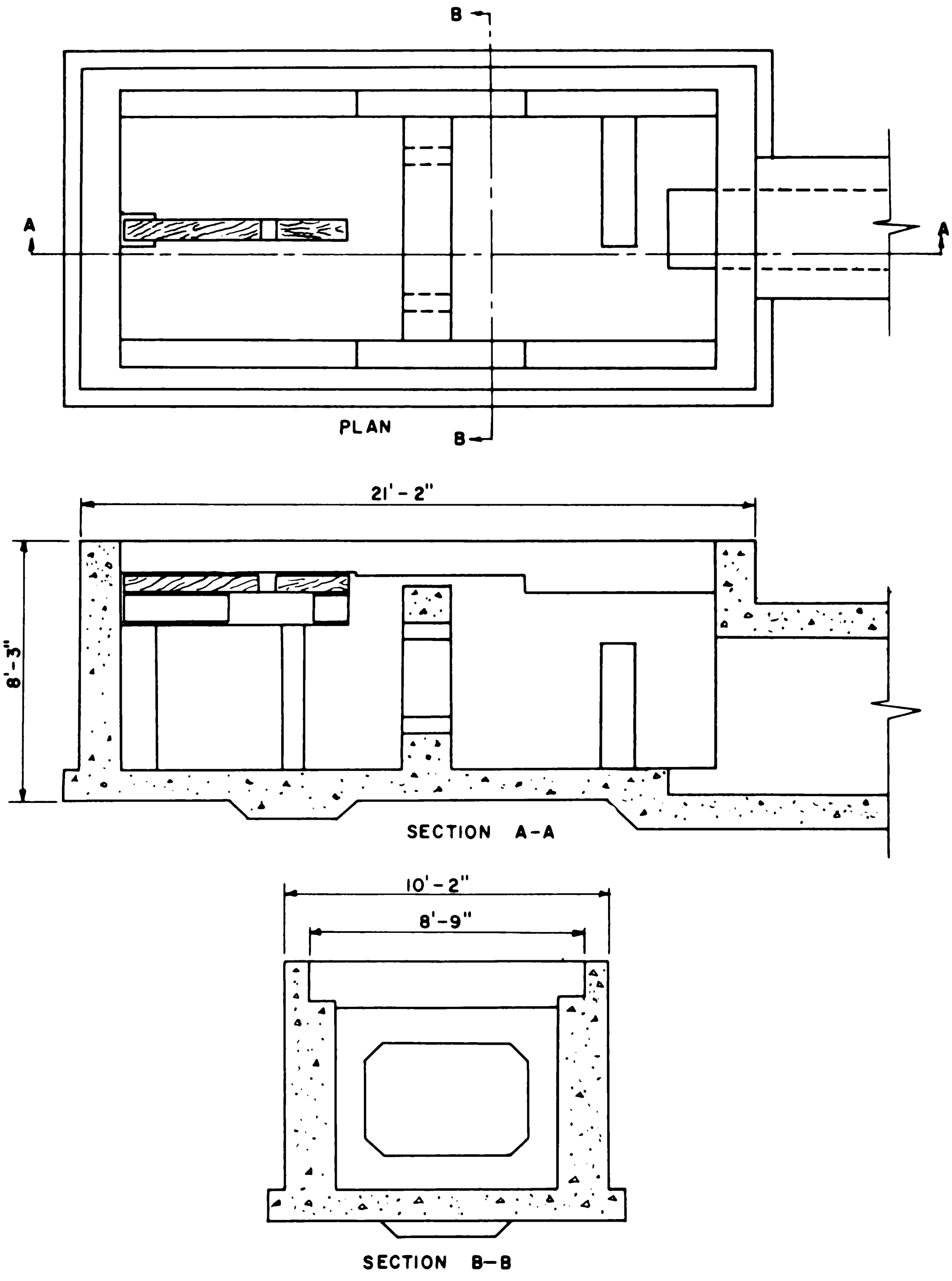

Fig. 2—Concrete test chambers.

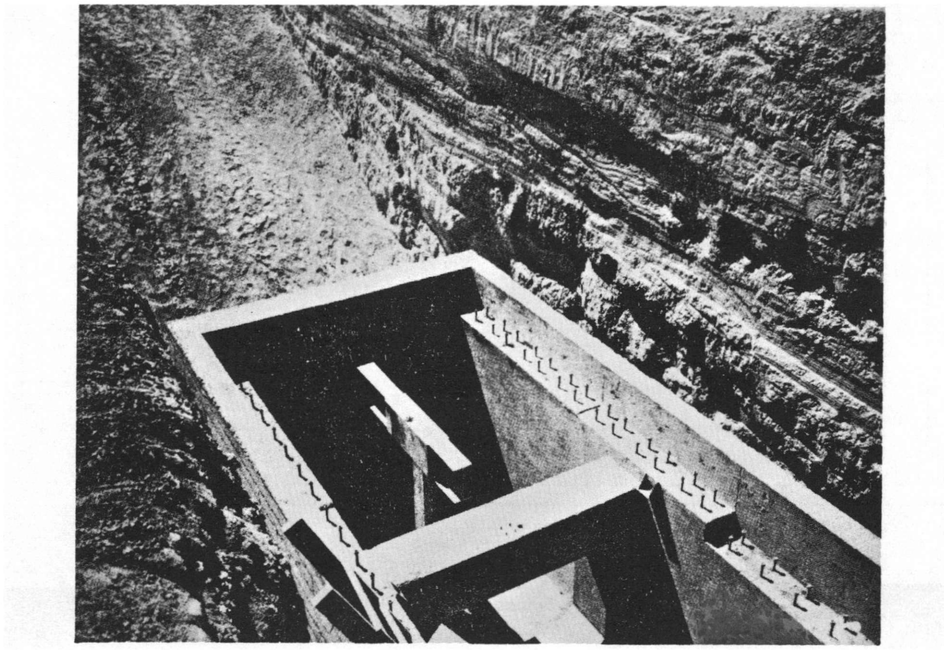

Fig. 3—Structure 3.8c during construction.

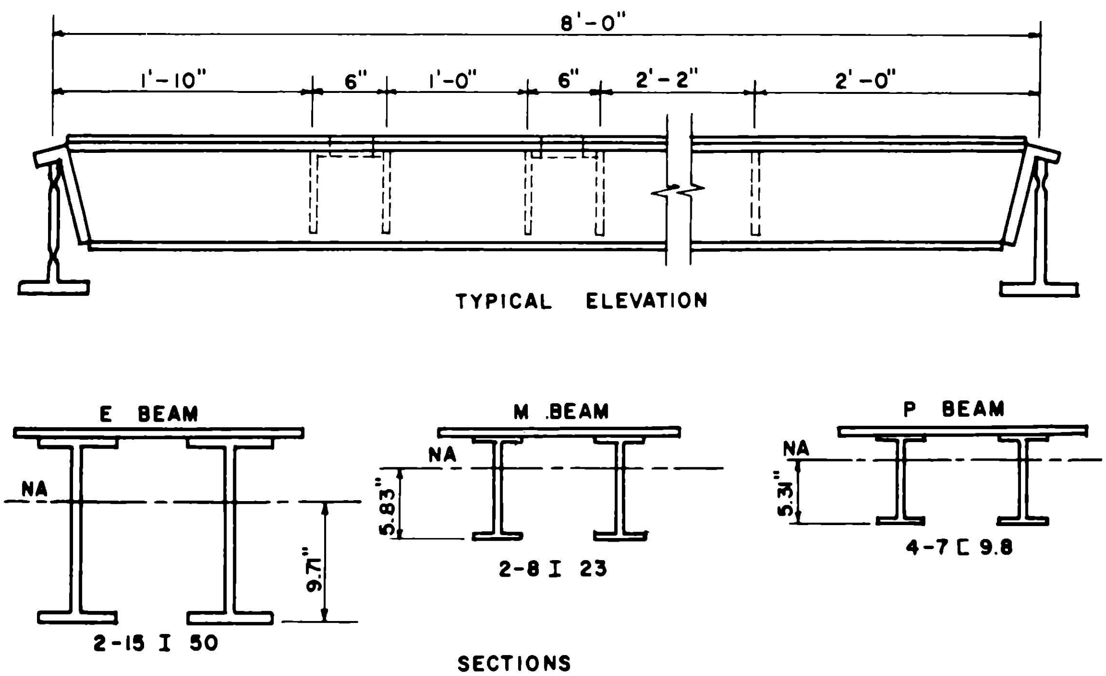

Fig. 4—Elevation and sections of beam strips.

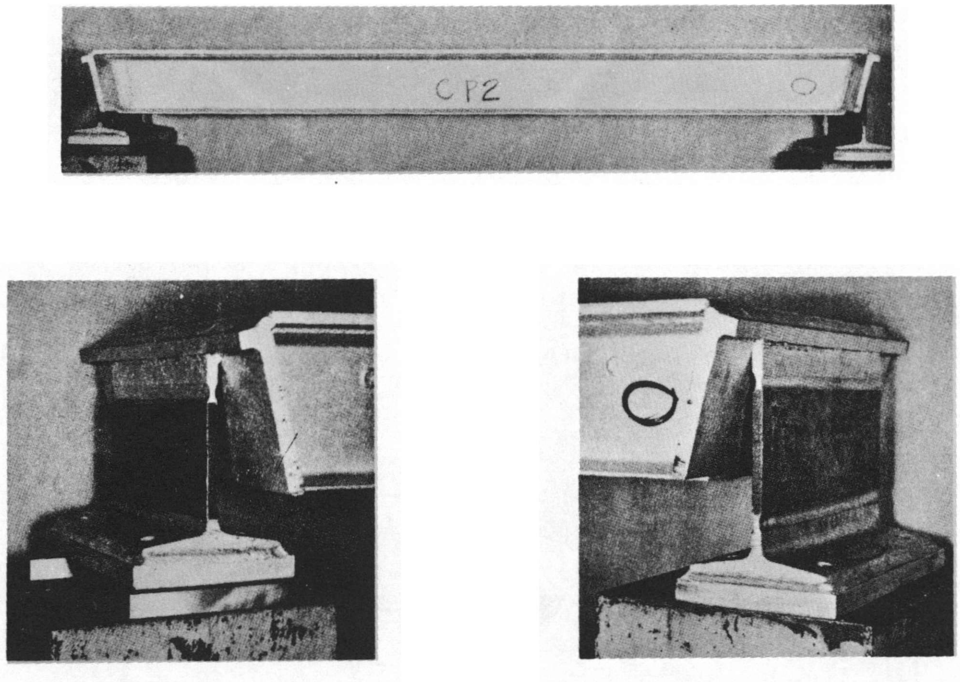

Fixed Shoe

Expansion Shoe

Fig. 5—Beam strip CP2 and supporting shoes.

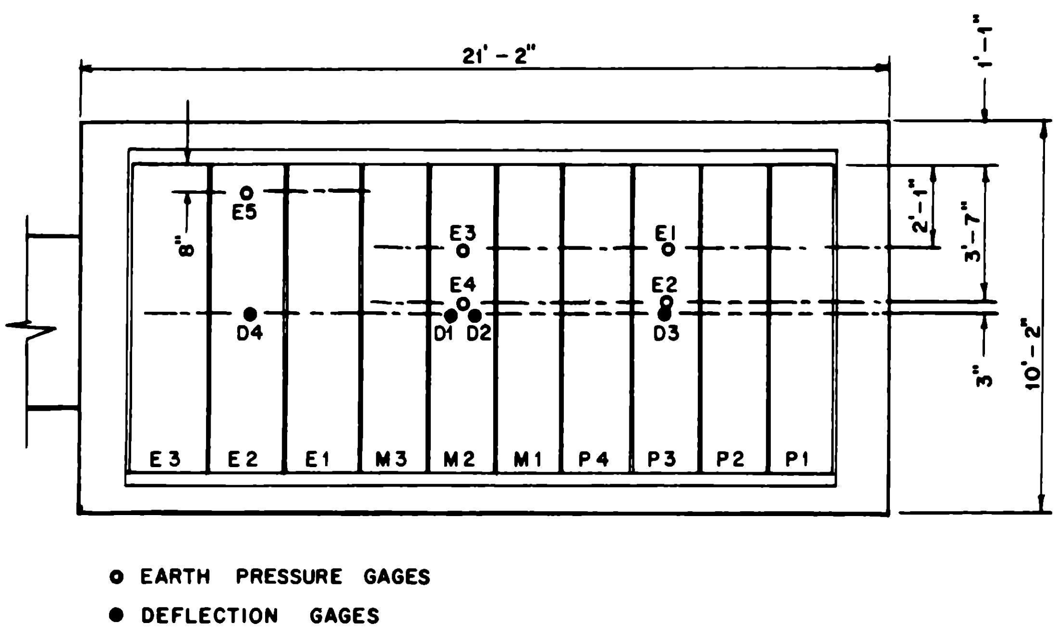

Fig. 6—Arrangement of beam strips in roof and location of gauges.

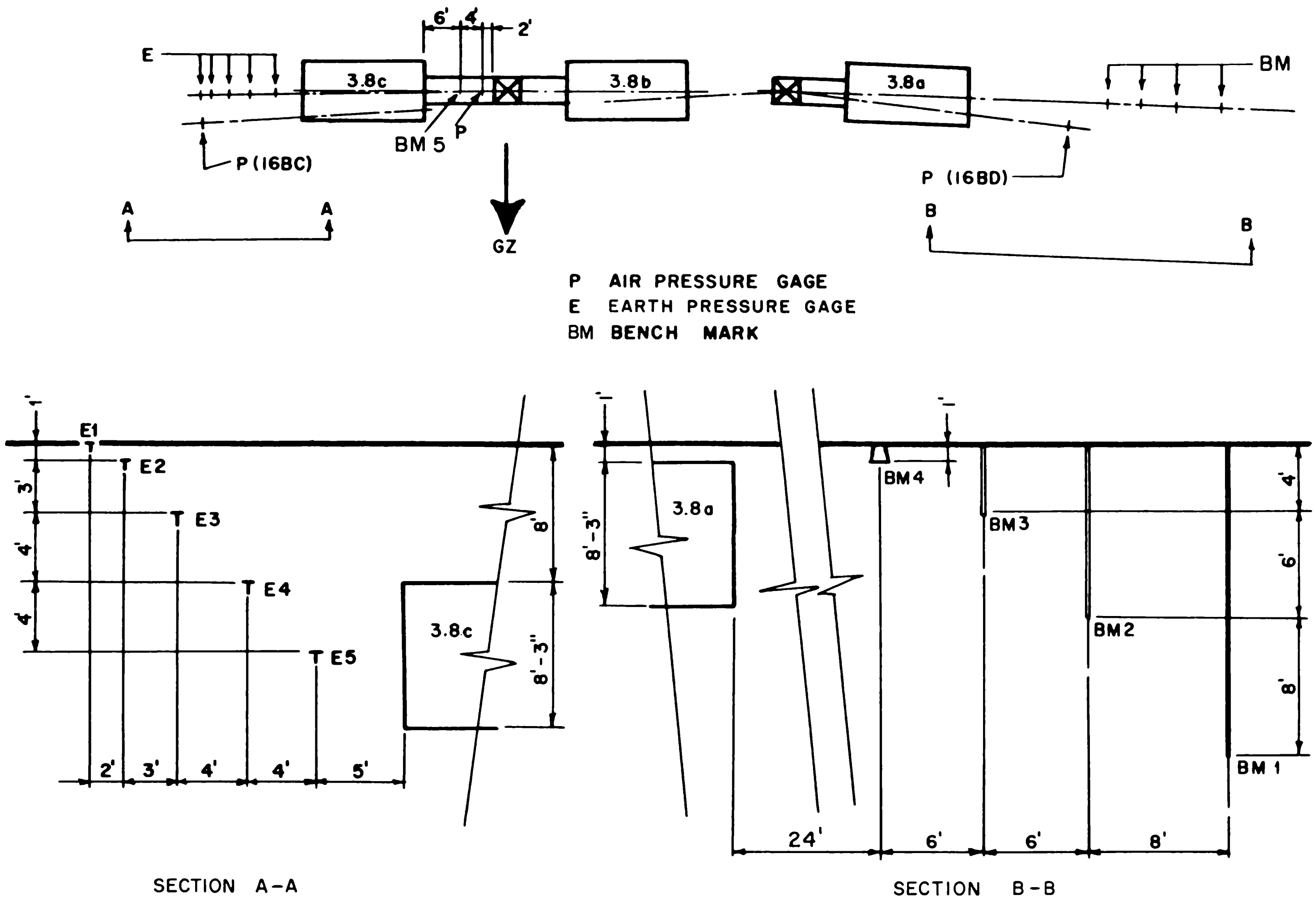

Fig. 7—Location of earth-pressure gauges and bench marks.

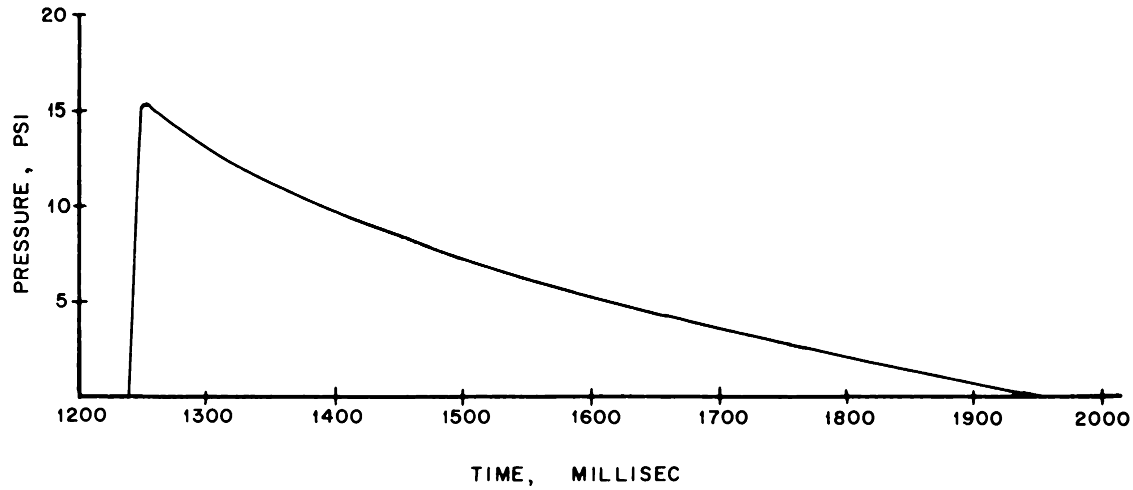

Fig. 8—Pressure on ground surface, shot 9.

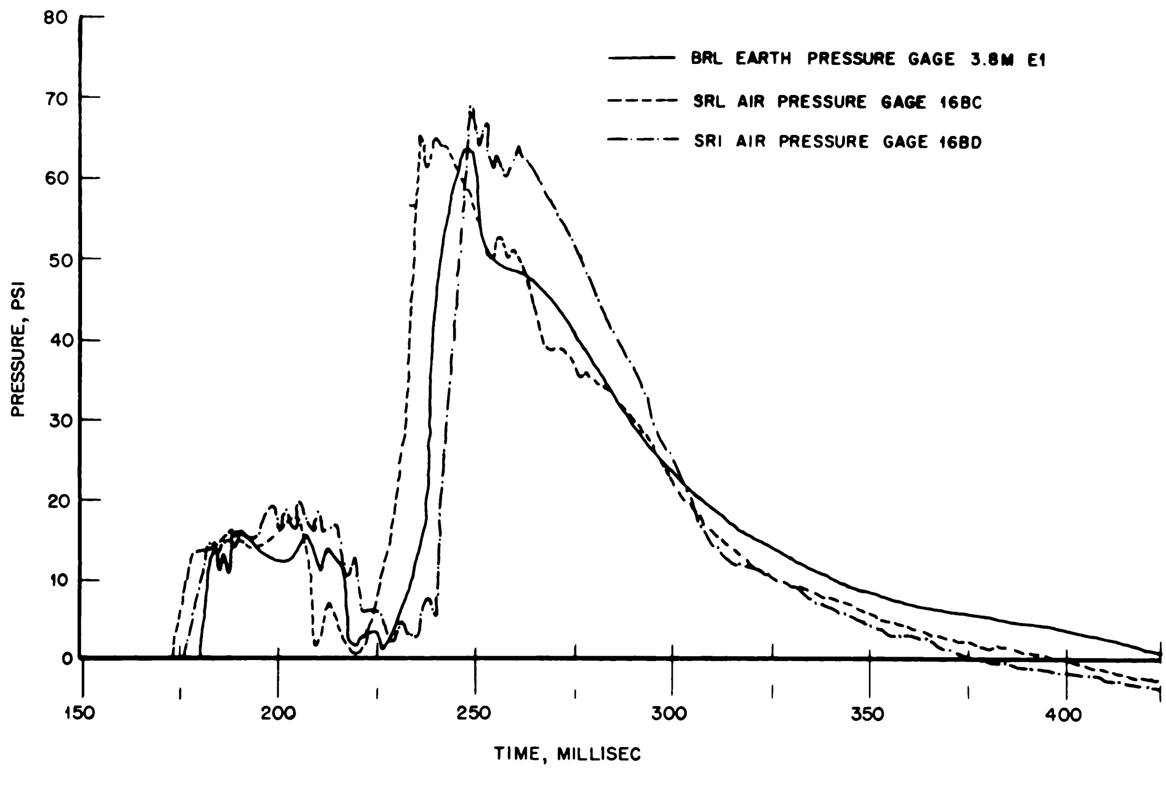

Fig. 9—Pressure on ground surface, shot 10.

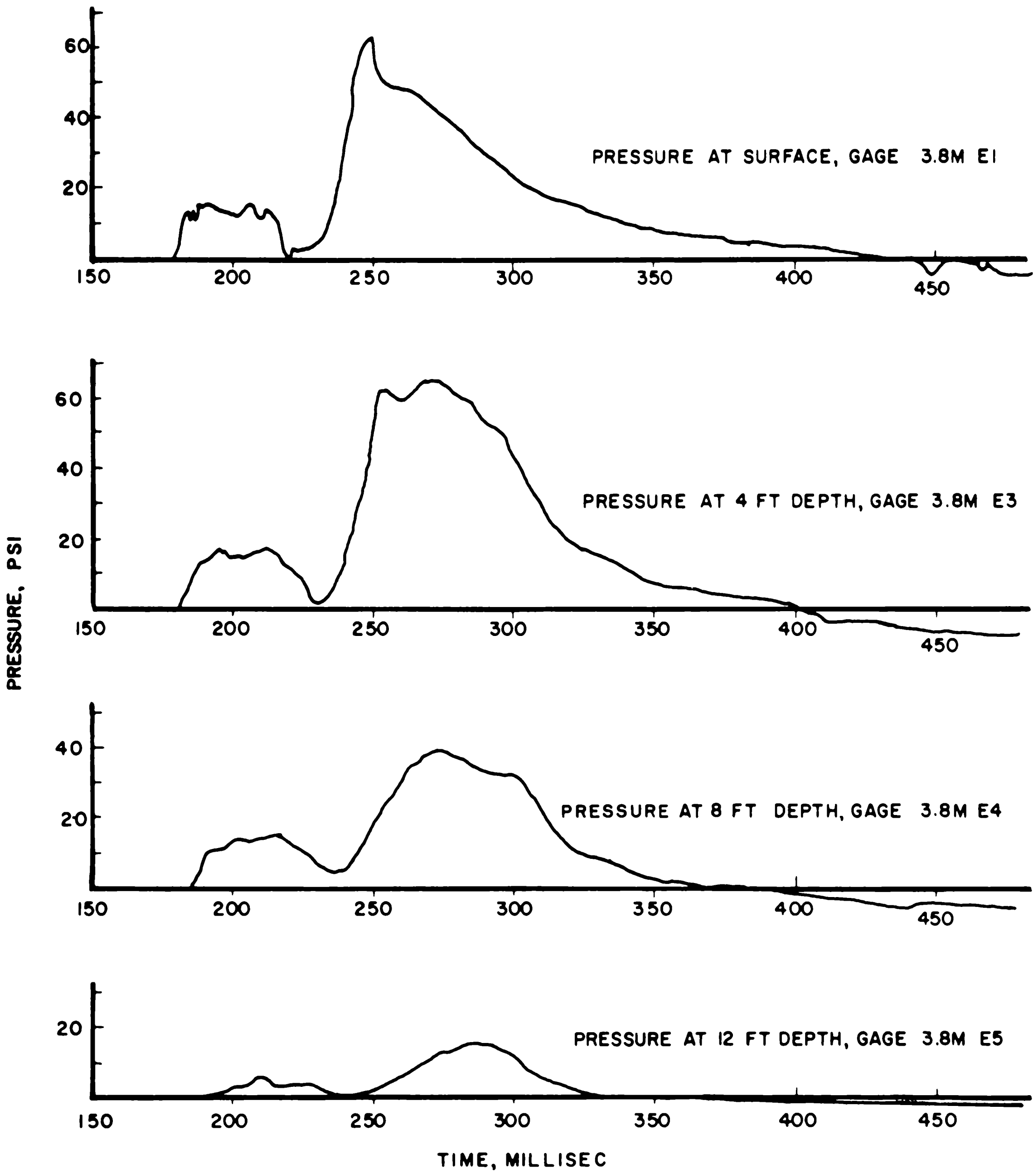

Fig. 10—Pressures in free earth.

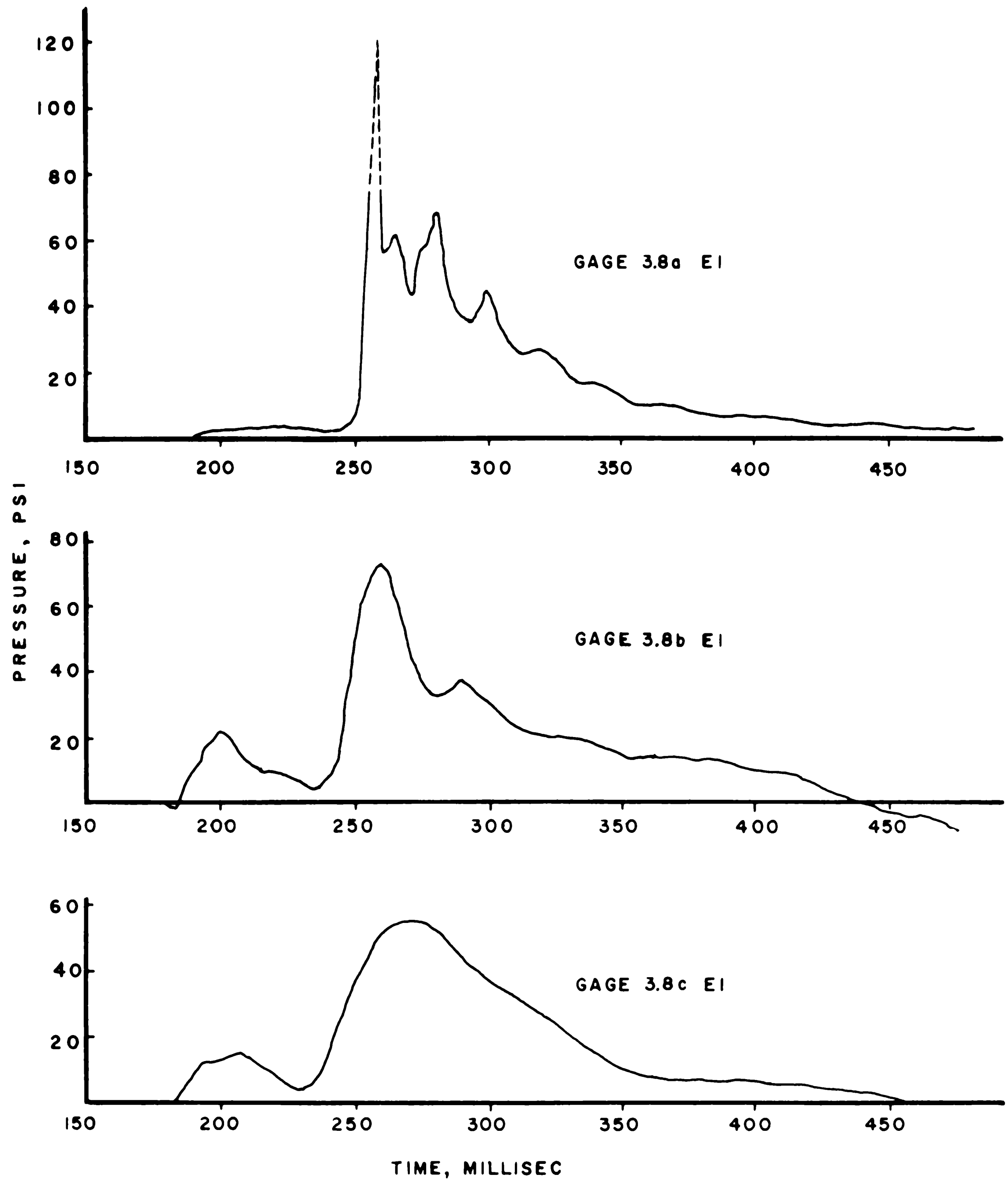

Fig. 11—Pressures on beam strips at quarter point of P beams.

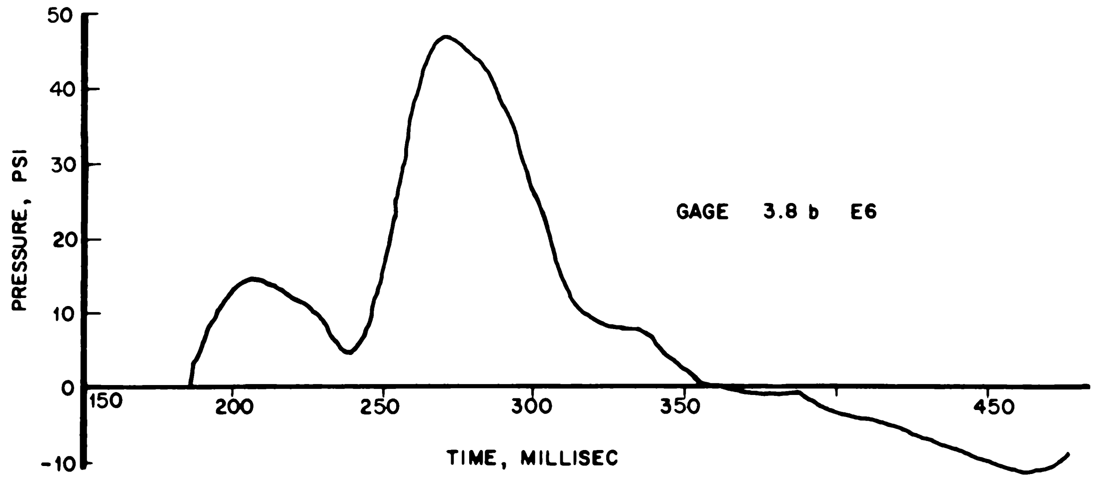

Fig. 12—Base pressure on structure 3.8b.

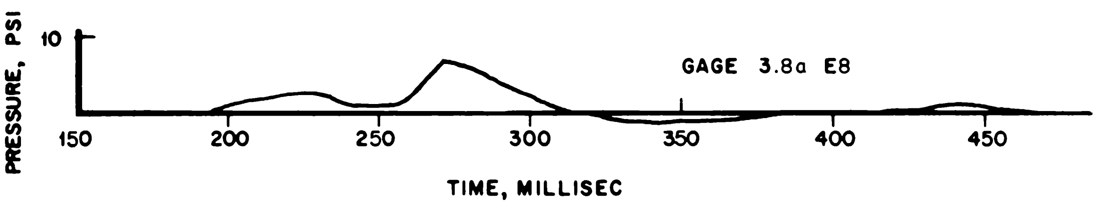

Fig. 13—Side pressure on structure 3.8a.

SUMMARY 6

NAVY STRUCTURES

(Report WT-729, Operation Upshot-Knothole, Projects 3.11-3.16, same title, by R. M. Longmire, LTJG, CEC, USN, and L. D. Mills, LTJG, CEC, USNR, May 1955.)

GENERAL

Subject report WT-729 covers the description and results of atomic tests (U-K shots 9 and 10) on several structural types, including earth-covered, as well as more conventional type buildings, for resistance to blast and thermal and gamma radiation. Table 1 lists the structures involved in all the test projects and includes data on ground ranges, peak pressures, and positive durations for both shots. The following summary is concerned only with the tests of those structures of particular interest in shelter design and construction specifically covered under Projects 3.13 and 3.15.

OBJECTIVES AND SCOPE

The objectives of this experiment were:

1. To evaluate the effectiveness of earth cover in protecting aboveground buildings against air blast. Of particular interest were a precast gable structure (3.13a) and a corrugated steel-arch ammunition magazine (3.15).
2. To determine the adequacy of these two structures as personnel shelters.
3. To gain information leading toward the optimum design of earth-covered structures.
4. To develop an analytical method for predicting the response of earth-covered structures.

TEST STRUCTURES AND INSTRUMENTATION

Figure 1 gives design details for structure 3.13a with inside dimensions of 22 by 48 ft. The main framing consisted of 12 pairs of precast concrete panels with wedge-shaped edge beams bolted together along the edge beams, at the crown of the building, and to the foundation. The interior was subdivided into three main sections by two precast concrete partitions. Exterior doors consisted of a $\frac{1}{4}$-in. steel plate stiffened by tees and angles.

The roof of the structure was covered with earth to a depth of 3 ft. Figure 2 shows the earth-covered structure with the 6-ft tunnel entrance and corrugated-pipe tunnels leading to inlets and outlets.

Structure 3.15 (Fig. 3) was a 25- by 48-ft steel-arch personnel shelter. The barrel of this structure was an Armco Multi-Plate arch composed of curved corrugated and punched sheets that were bolted together to

form a semicircular arch roof. The foundation consisted of a 1-ft-wide by 2-ft-deep wall footing of reinforced concrete.

An Armco Multi-Plate pipe 84 in. in diameter was bolted to the front wall of the structure to form an entrance tunnel.

Instrumentation included SR-4 strain gauges, BRL deflection gauges, Wiancko-Carlson gauges for earth-pressure measurements, and self-recording air-pressure gauges.

RESULTS

Both structures exhibited completely elastic response to shot 9, and only minor permanent deflections were noted. The entrances to both structures were damaged during this shot; the door of structure 3.15 was ripped from its frame and projected about 24 ft into the structure. Maximum side-on overpressure was about 10.8 psi at both structures; however, neither 3.13a nor 3.15 was oriented exactly normal to the blast line.

In shot 10 the maximum side-on overpressure was about 8.1 psi at both structures, and the structures in this case were approximately normal to the blast line. The structures again showed almost completely elastic response with slight permanent damage occurring to 3.13a.

Conclusions concerning the blast effects on structure 3.15 were that:

1. The steel-arch building remained in operational condition and would, except for the doorframe following shot 9, have provided satisfactory protection during these two shots.
2. In a region where the side-on overpressure in the open plain was 11 psi, the steel in the arch barrel, with 3 ft of earth cover above the crown, remained within the elastic range.
3. The end wall with no entrance tunnel sustained serious deflection and possibly represents the weakest component of the structure.
4. The end wall with the entrance tunnel did not sustain serious deflection; it was therefore concluded that an entrance tunnel adequately connected to an end wall serves as a completely satisfactory reinforcement to the end wall.
5. The blast pressure at the structure entrance door was approximately the same as the side-on blast pressure in the open.
6. The doorframe as originally designed failed to withstand a pressure of 11 psi.
7. The permanent deflection of the building produced by the earth cover alone is crown up, haunches in.

It was concluded for structure 3.13 that:

1. The precast concrete gable building (3.13a), when covered with earth to a 3-ft depth, remained in operational condition and would have provided satisfactory protection during the two shots.
2. The main building remained within the elastic range. The primary mode of deflection appeared to be crown down, haunches out. Small cracks were observed in the end panels and the associated vertical beams.
3. In a region where the side-on pressure in the open was 8 psi, this building with no earth cover (3.13b) remained essentially within the elastic range, but the primary mode of deflection was windward, haunches in, crown up. Larger cracks were apparent in the end panels and vertical beams.

In particular, regarding the benefit of earth cover, it was estimated that with no earth cover structure 3.15 would collapse under a blast pressure of the order of 3 to 6 psi, but, with 3 ft over the crown, it would probably withstand more than 35 psi before collapse occurred.

Regarding structure 3.13a it seemed clear in a general way that earth cover was beneficial. This was evident in the fact that the postshot survey indicated wider cracks in the end walls after 8 psi on shot 10 without earth cover than were produced by 11 psi on shot 9 with earth cover. In general, the benefit of the earth cover on this type of building is reduced because the framing design is much more rigid and consequently less flexible than the structure 3.15 design.

Table 1—GROUND RANGES, PEAK PRESSURE, AND POSITIVE DURATIONS FOR SHOTS 9 AND 10 (ACTUAL VALUES)

		Shot 9			Shot 10		
Structure	Description	Ground range, ft	Peak pressure, psi	Positive duration, sec	Ground range, ft	Peak pressure, psi	Positive duration, sec
3.11a	Reinforced 40- X 100-ft steel warehouse	12,000	1.6	1.15	12,000	1.0	1.08
3.11b	Plain 40- X 100-ft steel warehouse	20,000	1.0	1.4	20,000	1.0	1.15
3.12a	Panel-over-brick protection	4,900	6.4	0.95	4,900*	3.3	0.88
3.12b	Precast-panel test	7,600*	3.4	1.05	7,600*	1.5	1.00
3.12c	Precast-panel test	9,300*	2.5	1.10	9,300*	1.2	1.03
3.13a	Gable shelter, covered	2,700	10.8	0.82	2,300	9.6	0.62
3.13b	Gable shelter, uncovered	4,900	6.4	0.95	4,900	3.3	0.88
3.13c	Torque-tube panel	2,250*	10.8	0.77	2,250	8.6	0.61
3.14	40- X 120-ft precast warehouse (Frame only)	6,500	4.4	1.03	6,500	2.0	0.95
3.15	Corrugated-steel shelter, covered	2,700	10.8	0.82	2,300	8.6	0.62
3.16a	Window and glazing test	7,600	3.4	1.05	7,600	1.5	1.00
3.16b	Window and glazing test	12,500	1.5	1.17	12,500*	1.0	1.09
3.16c	Window and glazing test	20,000	1.0	1.4	20,000*	1.0	1.15

*These values are estimates.

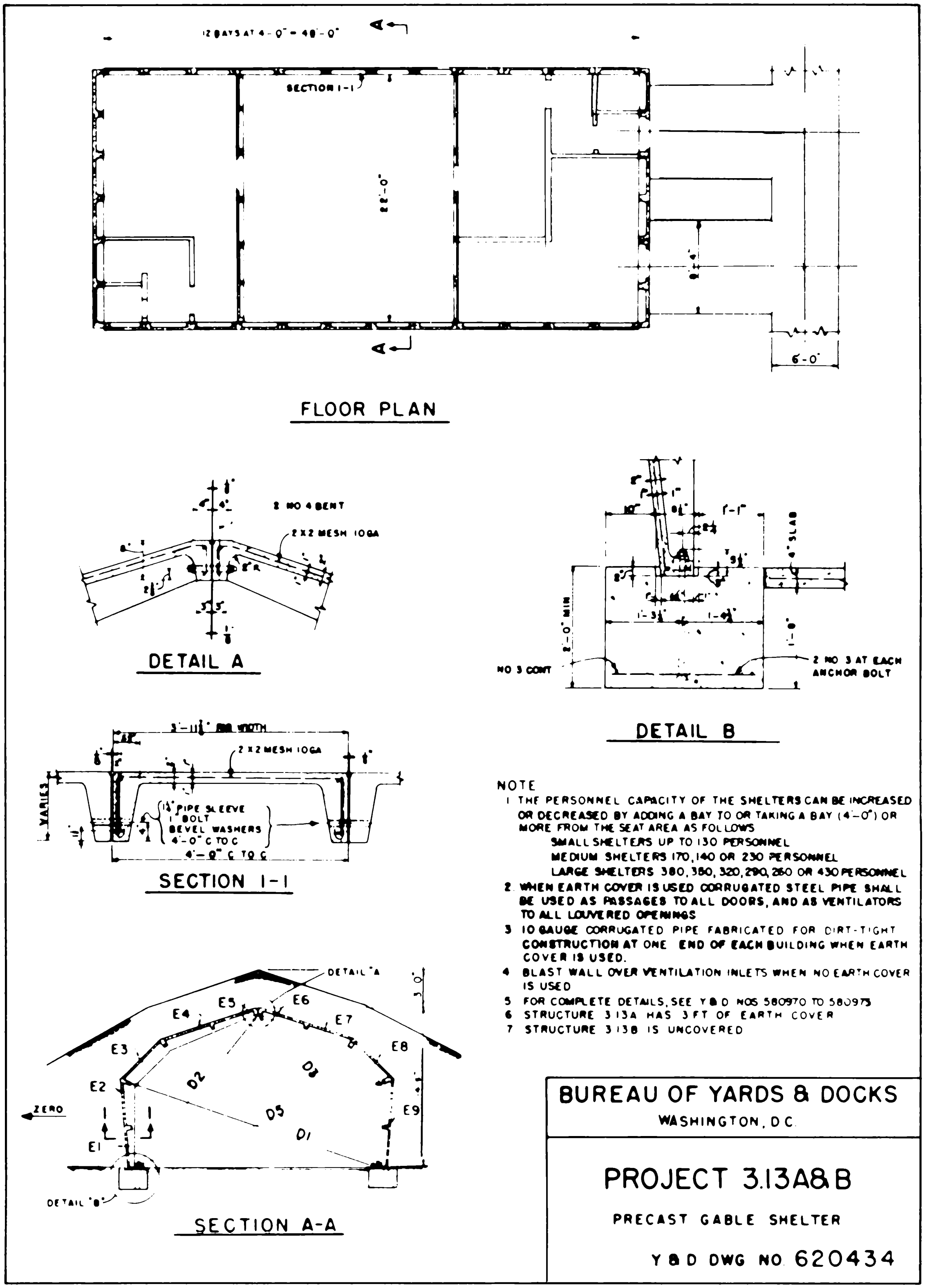

Fig. 1—Details of design, structure 3.13.

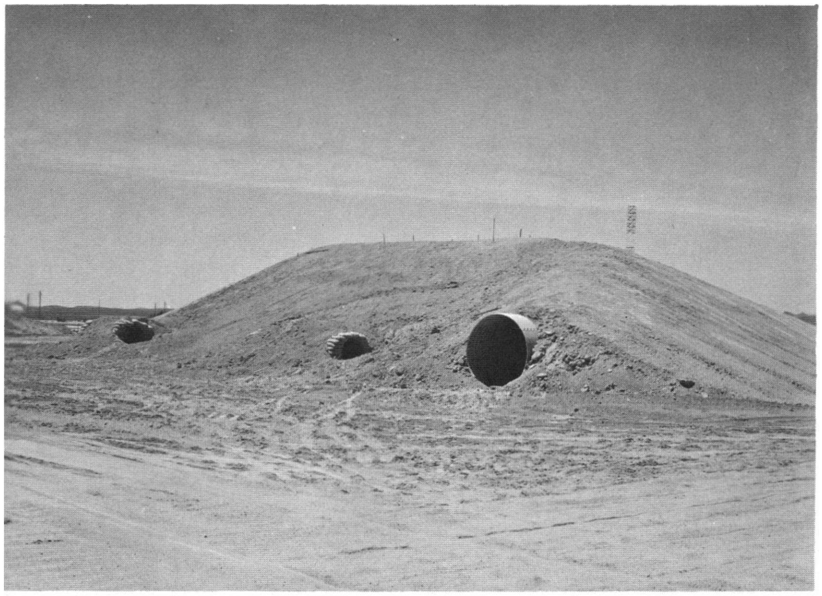

Fig. 2—Substitute 6-ft tunnel entrance, structure 3.13a. Note entrances to 2-ft corrugated-pipe tunnels leading to air inlets and outlets.

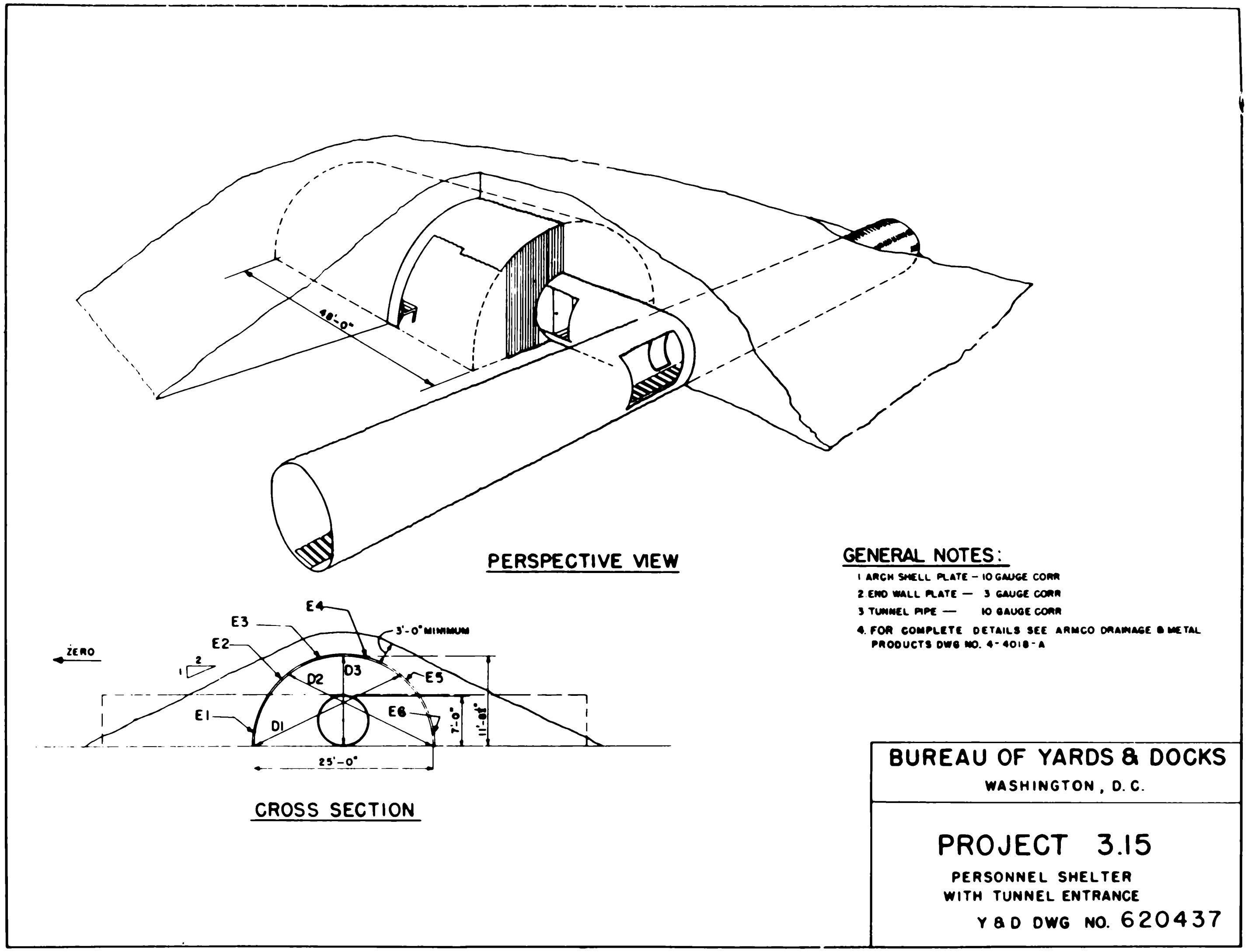

Fig. 3—Details of design, structure 3.15.

SUMMARY 7

EFFECTS OF OVERPRESSURES IN GROUP SHELTERS ON ANIMALS AND DUMMIES

(Report WT-798, Operation Upshot-Knothole, Project 23.15, Part 1, same title, by J. E. Roberts et al., Lovelace Foundation, Albuquerque, N. Mex., September 1953.)

OBJECTIVE

Project 23.15 was conducted to study biological hazards of overpressure and displacement in shelters with open entrances.

SHELTER DESIGN AND EXPERIMENTAL METHOD

Three communal type underground shelters, designated 601, 602, and AEC Communal (ref. Summary 2), were involved in the tests. Dogs and anthropometric dummies, variously positioned in the shelters, were subjected to three detonations, namely shots 1, 8, and 11. Figures 1 and 2 show details of shelters 601 and 602 and positioning of the test specimens. They were subjected to shot 1 (16 kt) and shot 8 (32 kt), both on 300-ft towers. The AEC Communal Shelter was involved in shot 11 (61 kt) at 1334 ft height of burst.

In shelter 601 an open ramp led down into a roofed entranceway, which, in turn, opened at a right angle into a blast trap. These components of the structure were of poured concrete. Opening at a right angle from the blast trap was the shelter proper, constructed of prefabricated reinforced-concrete culvert-pipe sections, 90 in. in inside diameter, with a poured concrete floor. Benches were built along each side of the interior. An emergency escape hatch with ventilation duct was provided in the far end of the shelter, shown in the plan view (Fig. 1) as a rectangular projection.

In anticipation of possible blast hazards, shelter 602 was designed to reduce the peak overpressure attained within the structure and to reduce the rate of rise of the overpressure. The basic construction remained the same as that of shelter 601 except that three sections of steel culvert replaced the first three reinforced-concrete sections. Of special interest were the double ramp and the blast trap that was revised to contain a baffle.

The AEC Communal Shelter had already been structurally tested by Project 9.1b, Operation Buster. Design and construction details are contained in Summary 2. The entire length of the second concrete-pipe section was filled with sandbags, leaving the first concrete-pipe section open at a right angle to the ramp in its entire cross-sectional area as the effective shelter area used in the Project 23.15 experiment.

The orientations of the animals within the shelters were maintained by special restraining harness. Figure 3 shows dummies in shelter 601.

RESULTS

Physical Data

Maximum recorded overpressures and their durations for shots 1 and 8 are shown in Figs. 1 and 2.

Although for this test the effects of shots 1 and 8 were of primary concern, shot 11 afforded opportunity to obtain overpressure data on four animals. For this shot the overpressure outside the shelter was approximately 35 psi. Two peak pressure gauges in the floor recorded 37 and 38 psi; a gauge at the bottom of the ramps recorded 40 psi. A gauge located in the bulkhead recorded a doubtful peak of 100 psi.

Shot 1 Animals: The time between detonation and recovery was 4.5 hr. Animal D-15 was found whining and presumably in pain by an advance party and was chloroformed. Dog D-14 had labored respiration and appeared to be in shock. All animals were subdued and lethargic. One-third of them (D-1, D-3, D-7, D-8, D-14) exhibited some degree of ataxia. In D-1, D-7, and D-8, ataxia persisted for more than 24 hr (until autopsy).

Shot 8 Animals: Dog D-3 was found disarranged in the harness and bleeding from nose and mouth. D-2 was slightly singed. All animals except D-3 were lively and displayed normal reaction patterns. No clinical evidences attributable to blast damage were found. Electrocardiograms recorded during the shot were normal.

Shot 11 Animals: Recovery was 11 hr after detonation. The dogs were lethargic and displayed stupefied responses. All animals were markedly displaced; they had been burned, three severely. After eating and drinking, two dogs vomited several times, but the other two refused food and water. The eyes of Dog C-1 were injured; the lids were held in a squint, and there was a profuse mucoid discharge.

Displacement of Dummies in Shelter 601

Shot 1: The sitting dummy was displaced 4 ft along the bench. Physical evidence within the shelter indicated violent displacement of the standing dummy; one of the ¼-in. eyebolts to which a restraining cable had been attached was bent open into an S-shape.

Shot 8: The standing dummy, although jarred off-balance, appeared to merely topple over from force of gravity. No final linear displacement was observed for the sitting dummy although the high-speed pictures indicated a 4.8-in. sway downstream and a 7.2-in. sway upstream, with return to original position.

CONCLUSIONS

Biological damage appeared to be related to the rate of rise of the overpressure and the air drag as well as to the maximum overpressure. Extrapolation of these data from dog to man is not explicitly possible. The data might hold, in a general way, for an adult man; if, however, infants and children are to be considered, the values might be grossly in error.

The general problem of the protection from the effects of overpressures afforded by these types of shelter requires consideration of present and anticipated weapon yields and also of the location and orientation of the shelters with respect to probable air-burst sites. Such considerations greatly extend the complexity of the problem; indeed, they may prompt the contention that with respect to overpressure and displacement injuries, the protective features of these structures are doubtful.

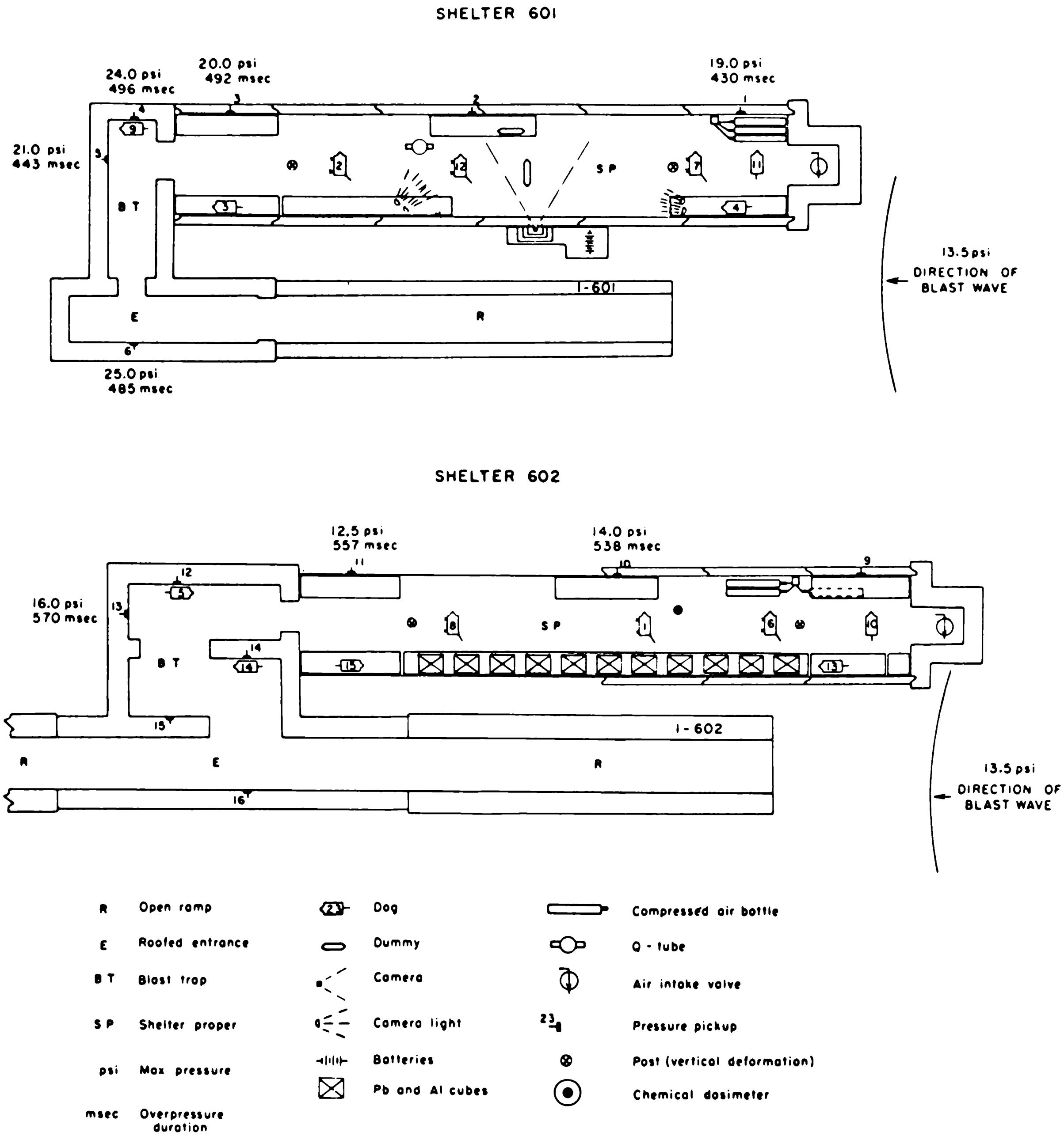

Fig. 1—Plan view of shelters 601 and 602 and contents as used on shot 1. Maximum recorded overpressures and their durations are also shown.

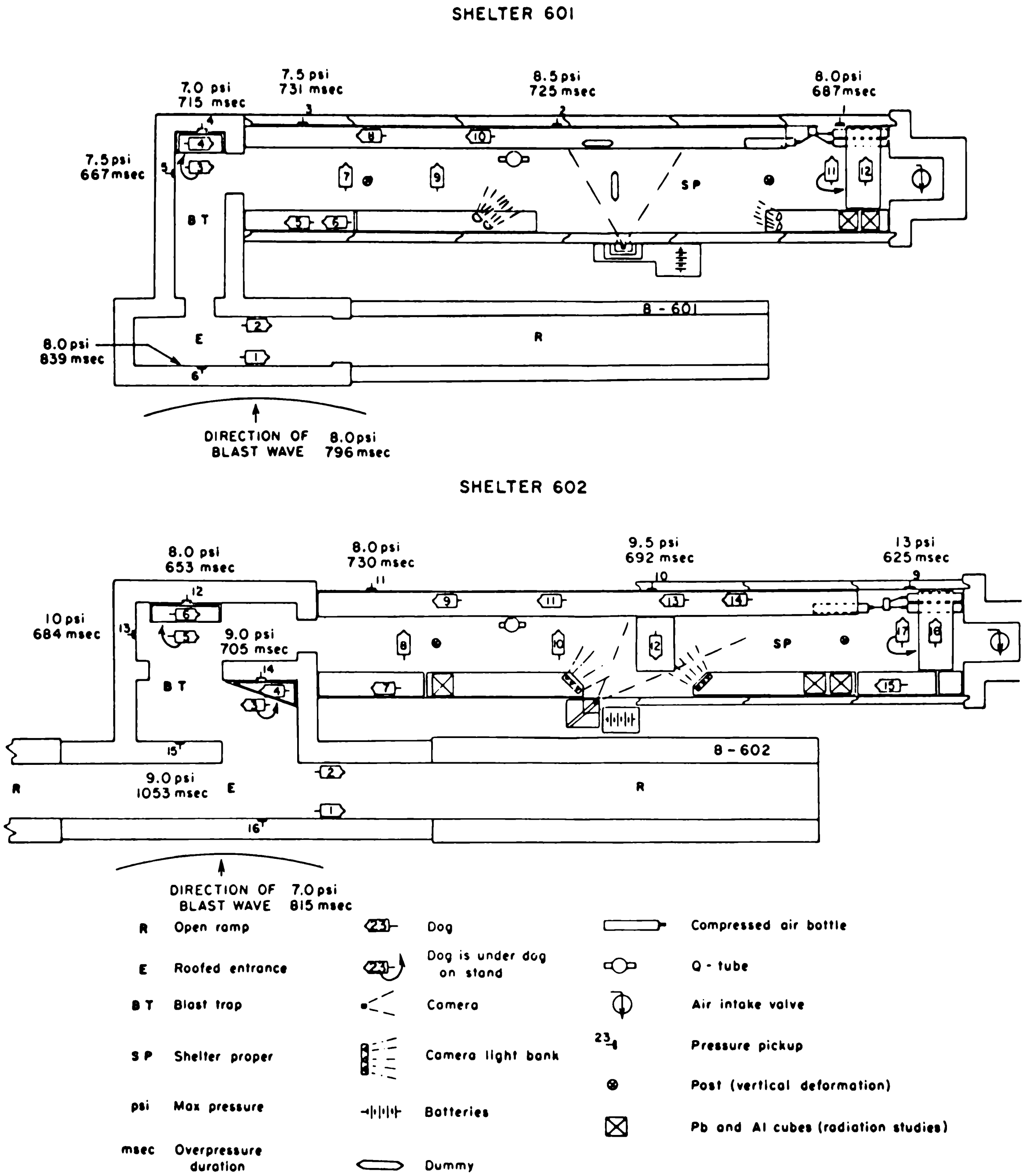

Fig. 2—Plan view of shelters 601 and 602 and contents as used on shot 8. Maximum recorded overpressures and their durations are also shown.

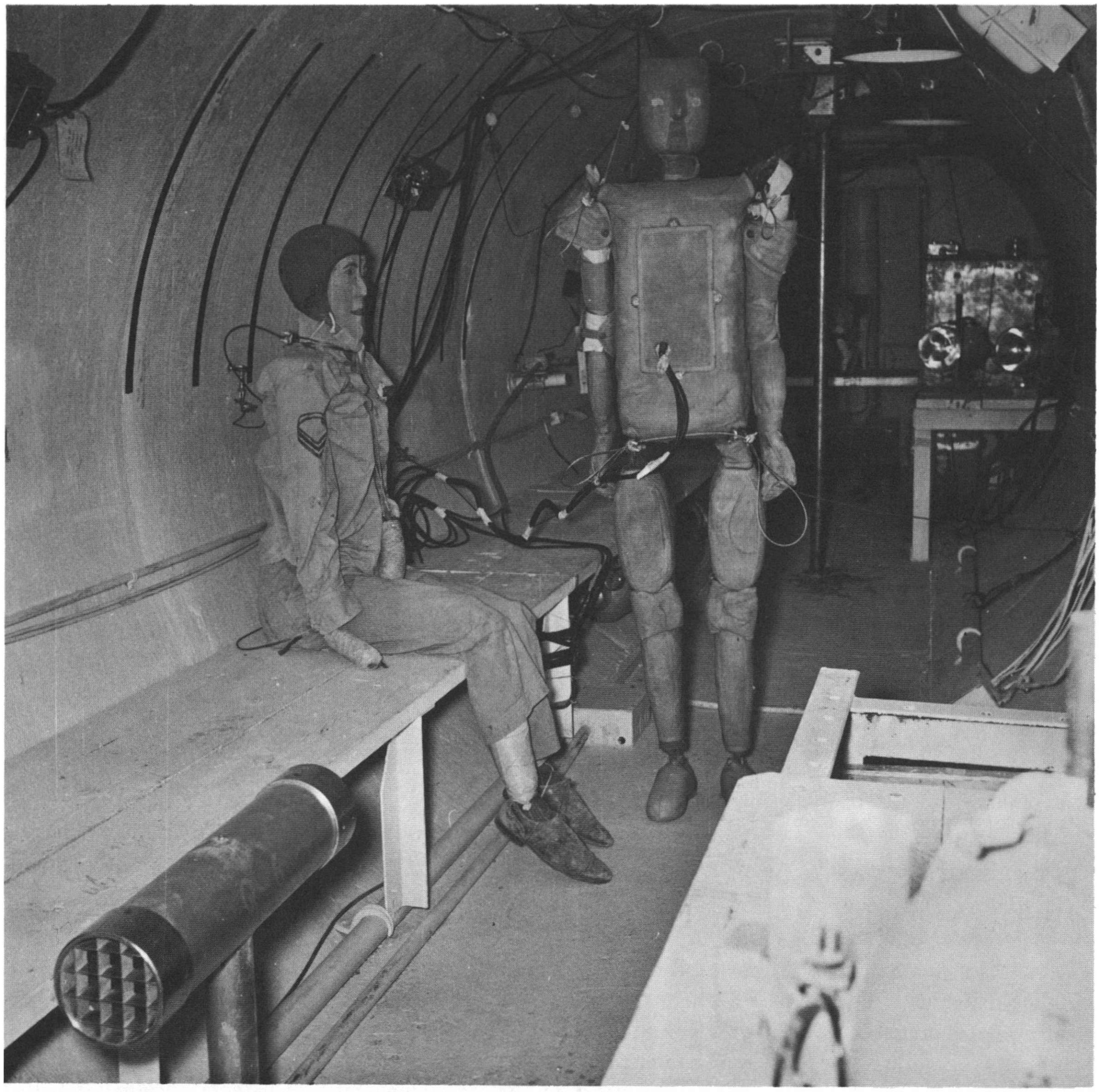

Fig. 3—Dummies in shelter 601. In the left foreground is the drag gauge. The dummy positioning and restraining methods are shown. Accelerometer leads extend from a cavity in the standing dummy.

SUMMARY 8

EFFECTS OF AN ATOMIC EXPLOSION ON UNDERGROUND AND BASEMENT TYPES OF HOME SHELTERS

(Report WT-801, Operation Upshot-Knothole, Project 21.1, same title, by Joseph B. Byrnes, Federal Civil Defense Administration, Washington, D. C., October 1953.)

OBJECTIVES

Eight outdoor and four indoor home shelters located at various distances from Ground Zero (GZ) (Fig. 1) were exposed to a 16.4-kt atomic device exploded from a 300-ft tower. The purpose of the test was to check the adequacy of the shelters, as proposed by the Federal Civil Defense Administration, for protection against gamma radiation and thermal and blast effects.

TEST STRUCTURES AND EQUIPMENT

The test results of Operation Buster 9.1a, Family Shelter Evaluation (see Summary 1), showed weaknesses in the entrances. Since wood has a comparatively short life in many parts of the United States, building materials of a more permanent nature were used. The earth-covered trench was redesigned to have reinforced concrete-block walls and a wood and concrete roof. New types of shelter added were the basement corner room, the block-wall basement exit, and the concrete pipe. The lean-to designed for FCDA by Lehigh University Institute of Research was modified for attachment to a basement wall. The Lehigh design for a reinforced-concrete basement exit was selected as the most blast-resistant.

Figure 1 shows the location and orientation of test structures relative to GZ, as well as detail sections of the various shelter types. Figure 2 shows, in perspective, details of the wooden lean-tos located at 3500 and 7500 ft from GZ. Figure 3, taken before the blast, shows the occupied lean-to at 7500 ft. Details of the other test structures are given in Figs. 4 to 8.

No funds were available for instrumentation; consequently it was necessary to improvise in an effort to determine thermal and blast effects. Gamma-radiation film badges were placed in all the shelters. Locations of badges are shown in Fig. 1.

Temperature-recording treated-paper strips were mounted in some of the shelters. Cubes of ordinary household paraffin and swatches of olive drab nylon cloth were placed at various locations in the structures for low thermal measurements (cal/cm^2/sec).

Attempts were made to measure permanent deflection of the concrete roof slabs in the reinforced-concrete basement exit, in the covered trench at 1450 ft, and in the covered trenches at 1800 ft. A solid Monel wire, 0.020 in. in diameter, was used as a reference line for measuring deflection. The center point of the span on the bottom of the slab directly over the wire was marked. A steel scale graduated to $\frac{1}{64}$ in. was used to measure vertical distances from the center points to the wire. Mannequins were placed in most of the structures.

RESULTS

Peak overpressures at the various locations had been calculated, for use in the design of the shelters, to be approximately 48, 31, 20, 5.6, and 1.5 psi at distances of 1230, 1450, 1800, 3500, and 7500 ft, respectively. Actual pressures, however, were found to be much lower, as indicated by the test pressures of 23, 15, and 10 psi recorded at distances of 1230, 1450, and 1800 ft, respectively.

Details of the blast effects are briefly described in the following:

1. Reinforced-concrete basement exit 1230 ft from GZ (Fig. 4): The roof slab showed no cracks and no permanent deflection. Between the concrete steps and left entrance wall there was a $\frac{1}{16}$-in. separation, which extended from the grade to the shelter floor. No other damage to the structure was observed. Inside the shelter the leg of the bench near the entrance was removed by the blast. The child mannequin, although thrown to the floor and partially covered with sand, was undamaged. The adult dummy had separated at the waist when the wood dowel used to connect the upper and lower parts was broken.
2. Earth-covered trench shelters at 1450 and 1800 ft from GZ (Fig. 5): In each shelter an 84-lb mannequin was not moved or damaged by the blast. No damage to the shelter was evident. The roof slabs showed no cracks and had no permanent deflection at midspan.
3. Wood-covered trench shelter with open shaft entrance at 1800 ft from GZ (Fig. 6): A break in one of the longitudinal block walls about midway between the end wall and the entrance was attributed to faulty construction. The roof joists suffered no damage; the experimental shaft entrance, however, was considerably damaged.
4. Earth-covered trench shelter with closed shaft entrance (Fig. 7), block-wall basement exit structure, and concrete-pipe shelter with closed shaft entrance: All were 1800 ft from GZ and suffered no significant interior or exterior damage.
5. Wooden lean-to shelter (Fig. 2) and basement corner-room shelter (Fig. 8): At both 3500 and 7500 ft from GZ, there was no damage to structures or mannequins (Figs. 3 and 9) except for minor damage in the basement corner room at 3500 ft. One basement roof joist cracked under the debris load of the collapsed house above.

Another earth-covered trench shelter located at 3500 ft from GZ was undamaged, and no movement of, or damage to, a 37-lb mannequin was observed.

High residual radiation levels remained in the area for two days, and most of the film badges placed to measure initial gamma radiation were collected as late as 78 hr after the blast. Very little penetration was expected because of the relatively large mass of earth between the explosion and the interior of the shelters and the low incident angle caused by the 300-ft-altitude burst. Fluctuations in readings, probably due to the shifting of sand under the action of wind, made it impossible to differentiate between the amounts of initial and residual radiation to which the badges had been exposed. Total doses recorded by the badges are shown in Fig. 1.

None of the temperature-recording paper strips in the shelters showed discoloration. This indicated that, if there was any rise in temperature, it did not reach 94°F, the lowest temperature the strips were designed to record.

CONCLUSIONS

Although the adequacy of protection afforded by the shelters at full design pressures could not be determined because the actual pressures were about one-half the design value, the test showed nevertheless that the designs appeared to be structurally satisfactory at the pressures recorded. There was some evidence that pressure inside the shelters, because no doors were provided, might cause injury to occupants and that their safety might depend upon the orientation of the entrances.

The amount of thermal energy entering the shelters even at close range probably would not have caused skin burns to human occupants.

Since in an atomic attack the majority of residences, and consequently the home shelters, in the area might not be in the high-pressure regions, the information was considered to be of real value to Civil Defense.

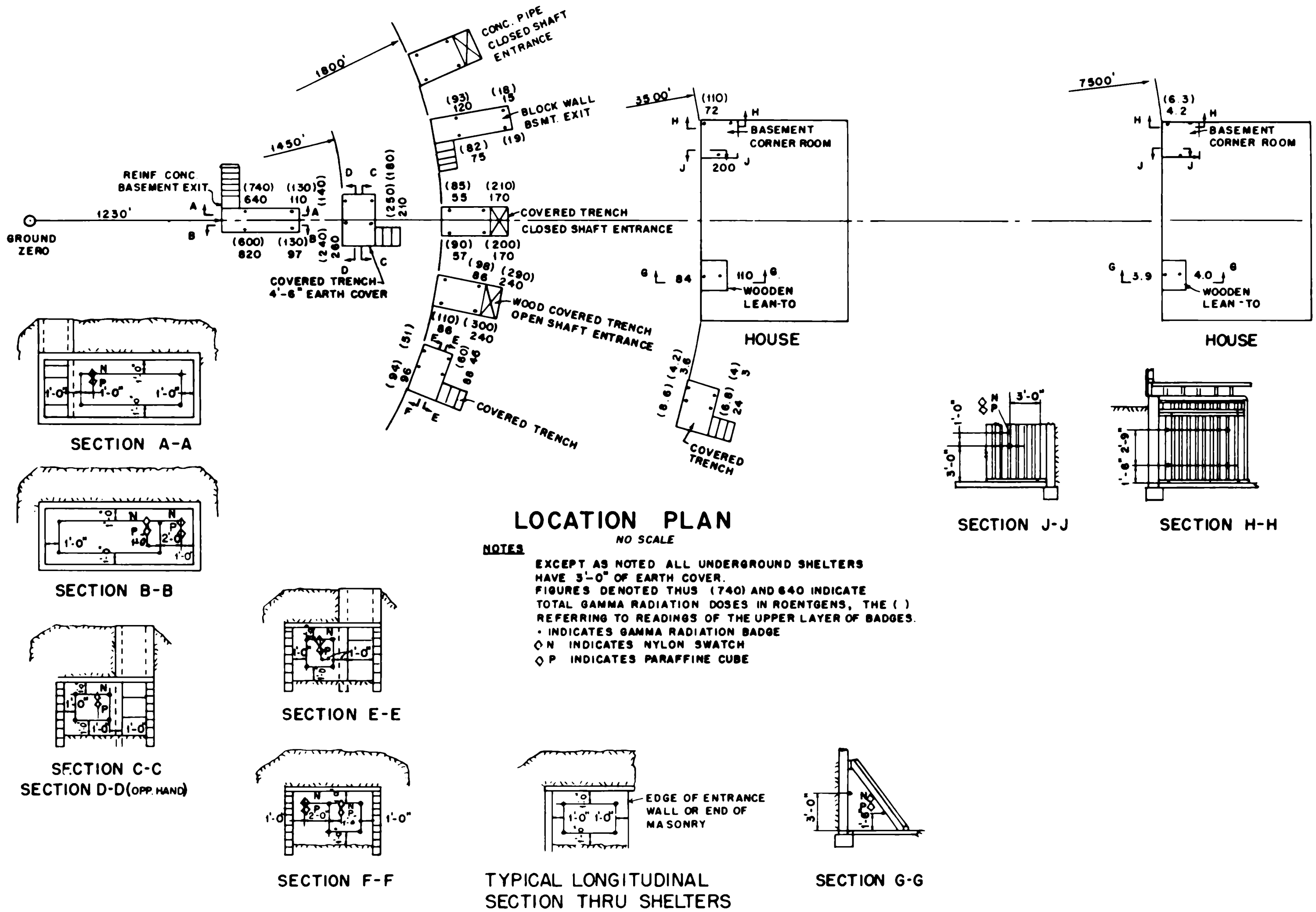

Fig. 1—Location plan of test structures.

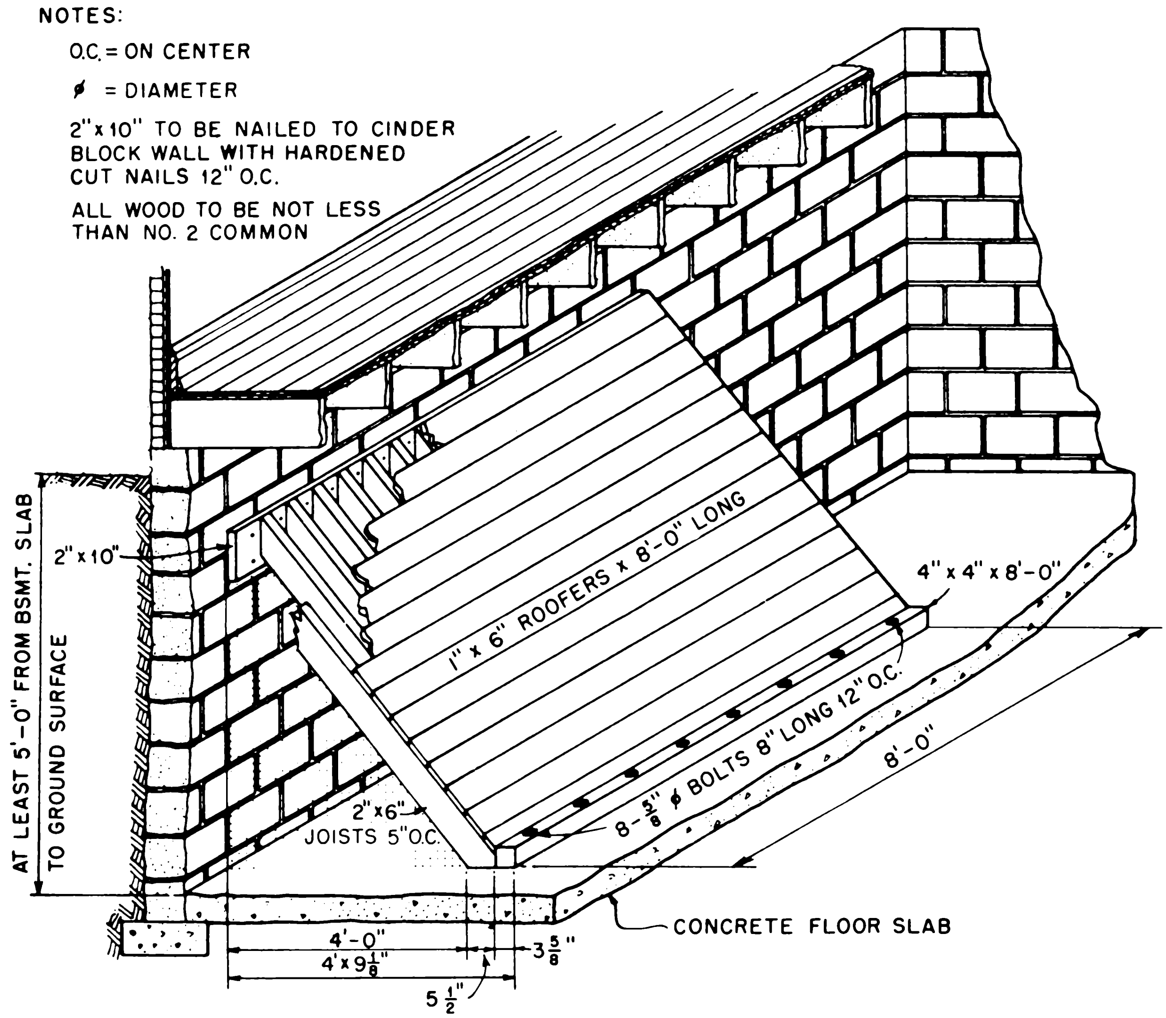

Fig. 2—Wooden lean-to tested at 3500 and 7500 ft.

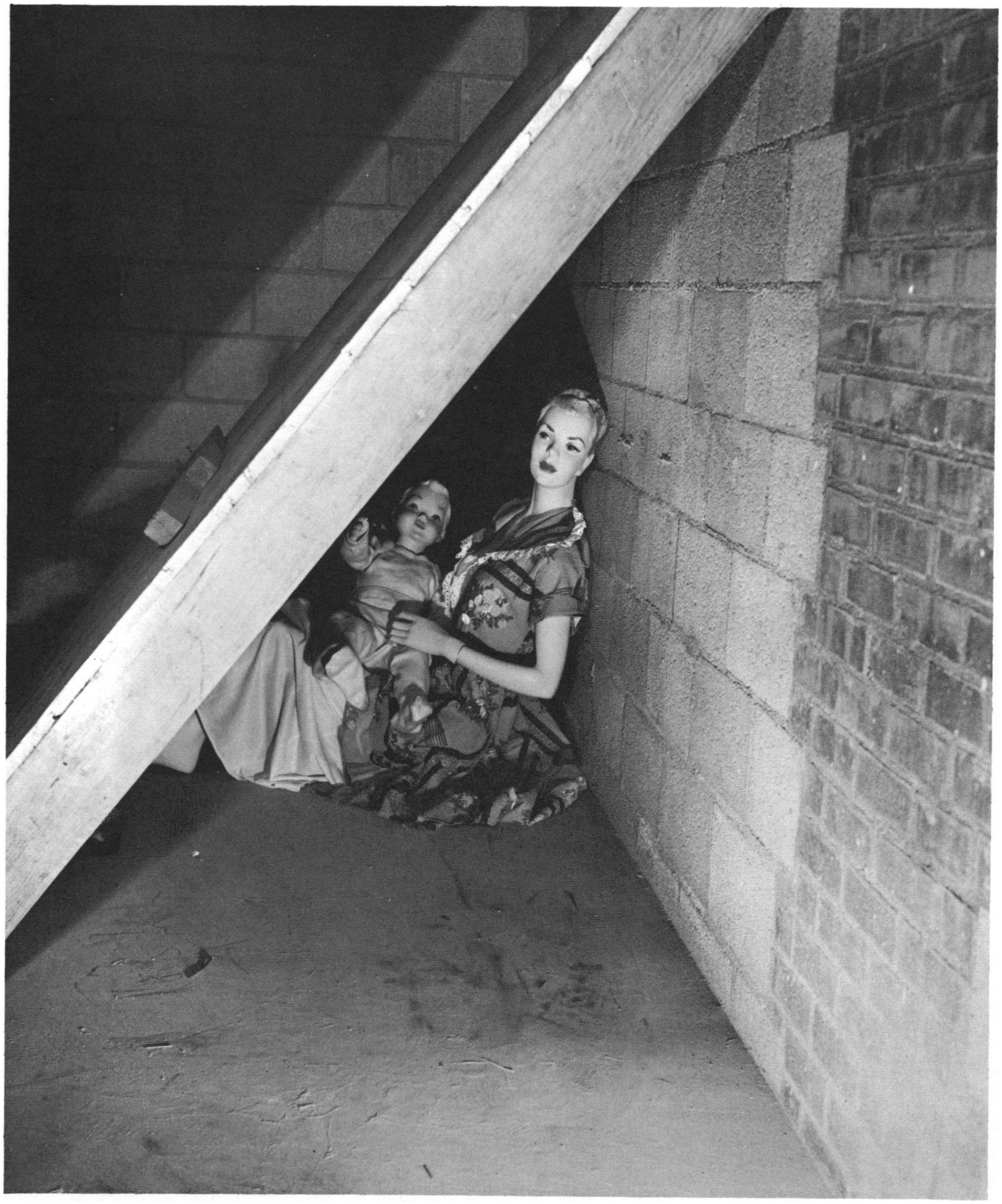

Fig. 3—Lean-to at 7500 ft before blast.

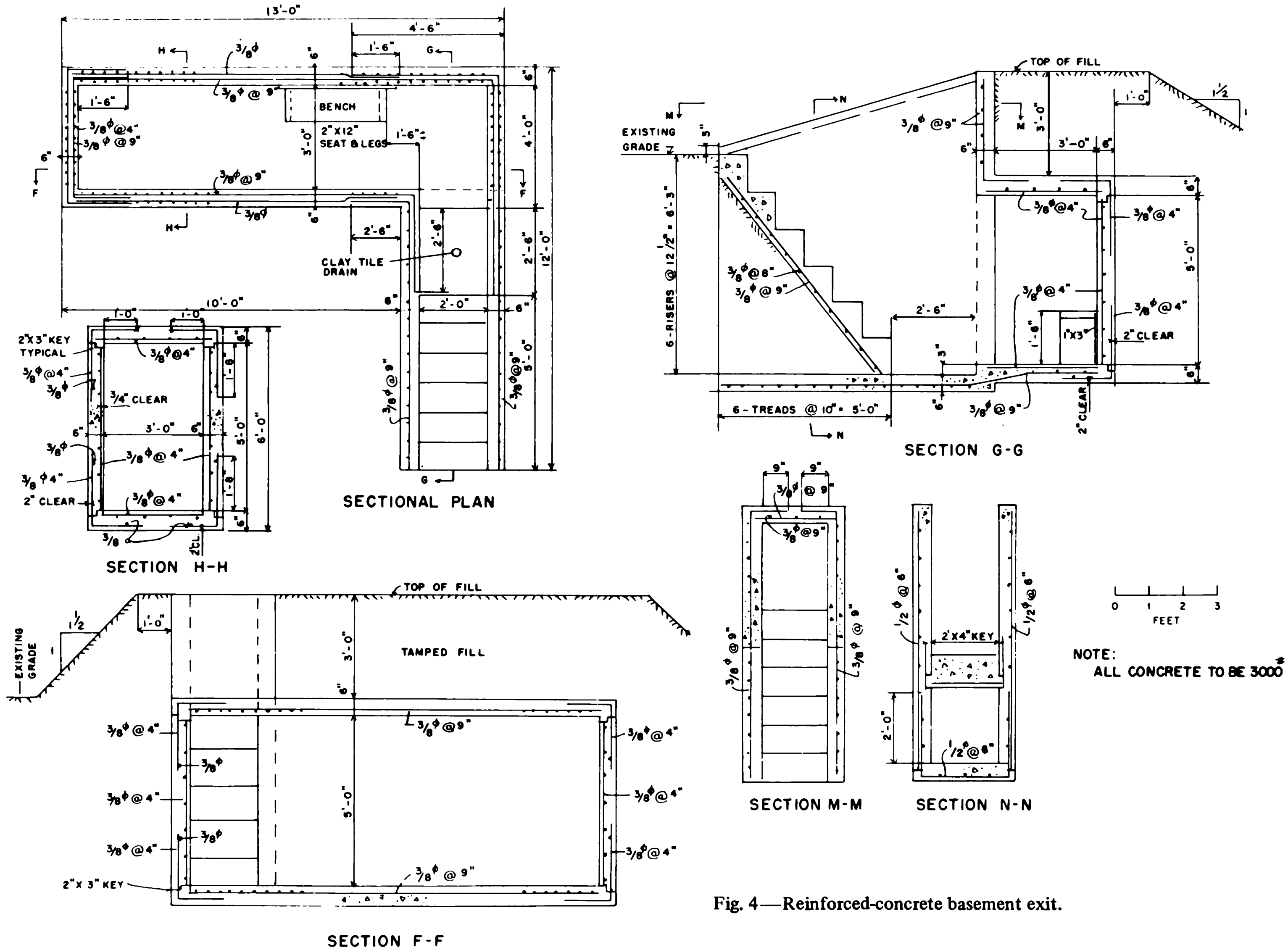

Fig. 4—Reinforced-concrete basement exit.

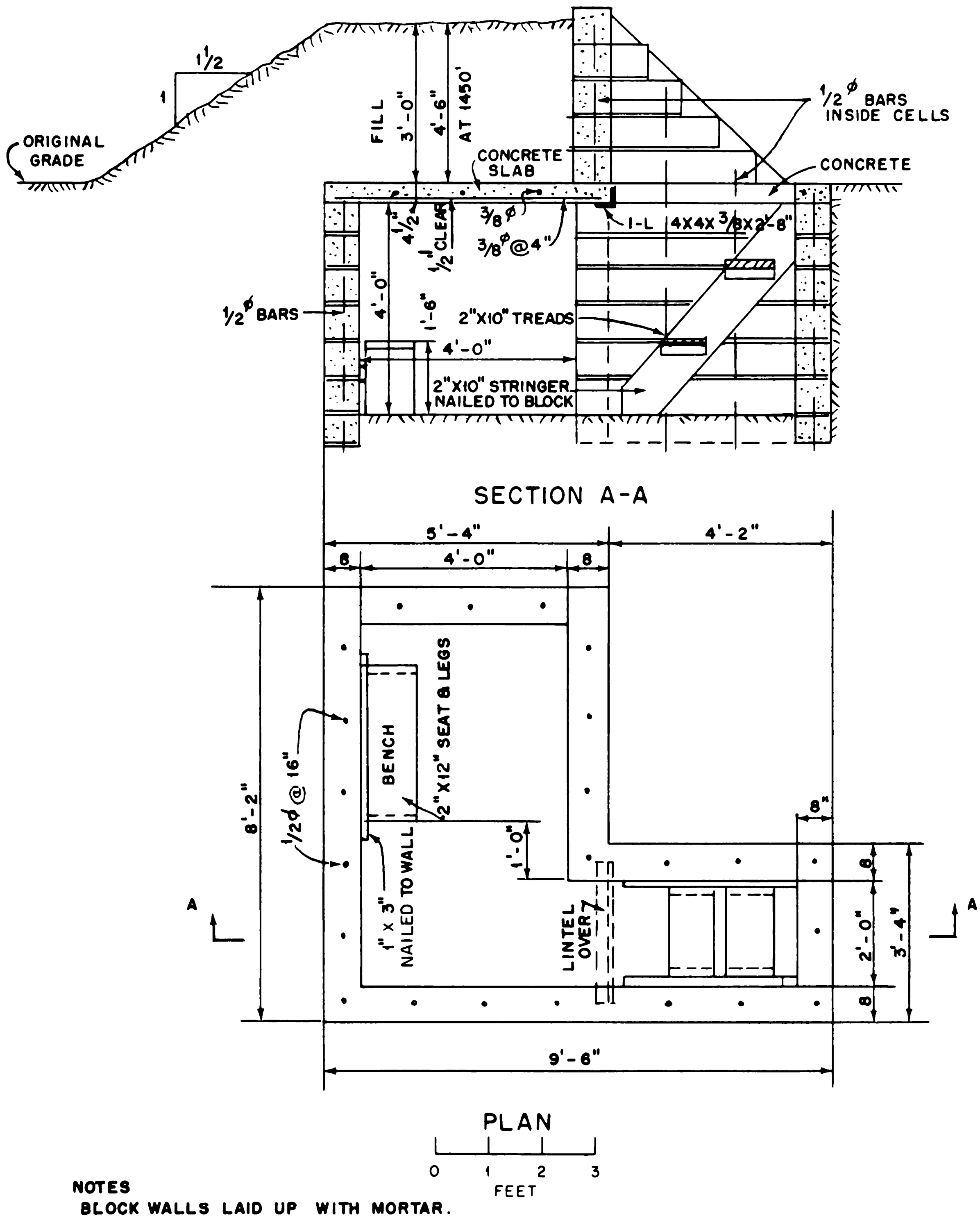

NOTES

BLOCK WALLS LAID UP WITH MORTAR.
FILL CELLS OF ALL BLOCKS WITH CONCRETE.
USE 3000# CONCRETE IN ROOF SLAB.
SLAB REINFORCING BARS TO BE STRAIGHT STANDARD A-305 OR ORDINARY DEFORMED WITH HOOKED ENDS.

Fig. 5—Earth-covered trench placed at 1450, 1800, and 3500 ft.

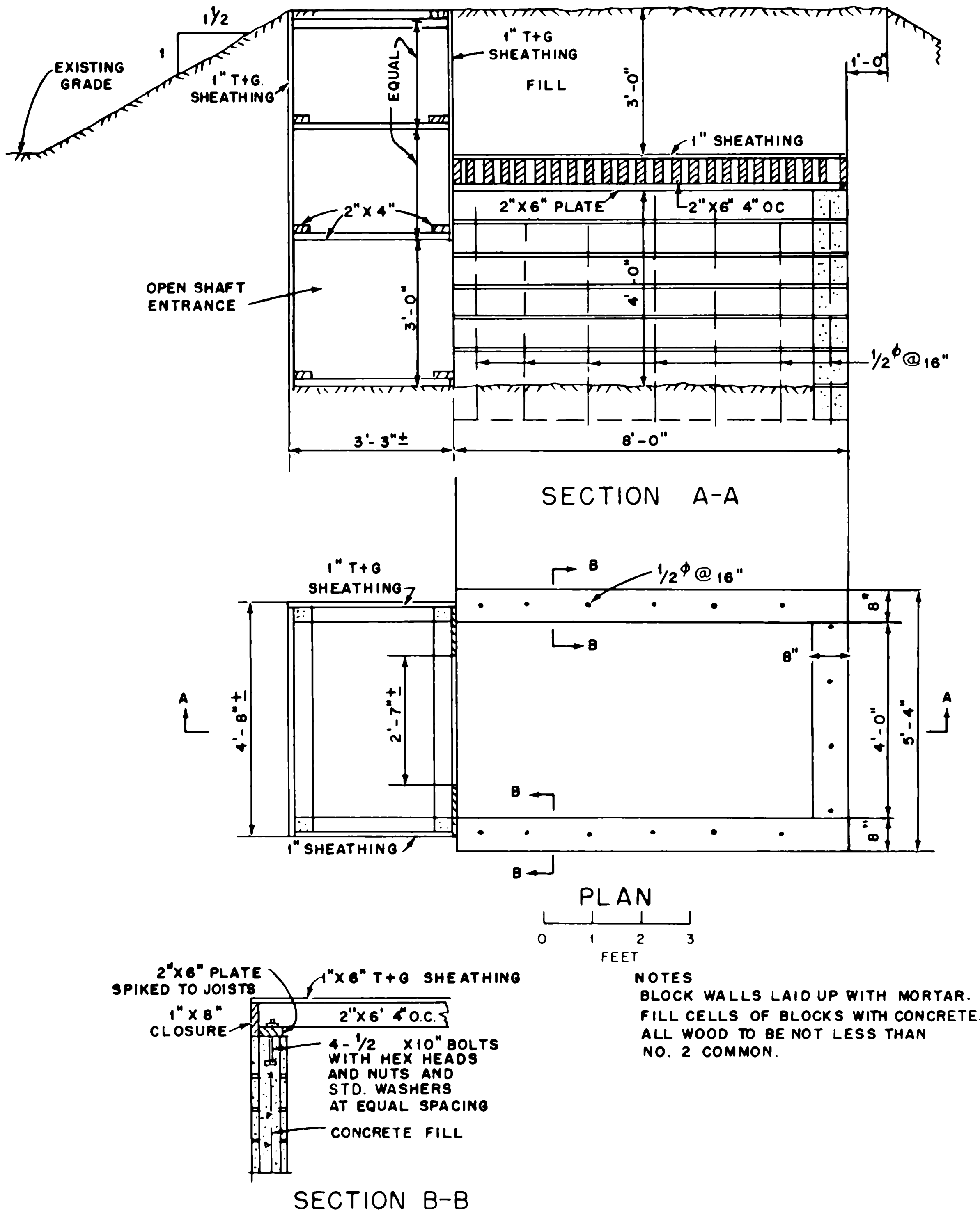

Fig. 6—Wood-covered trench.

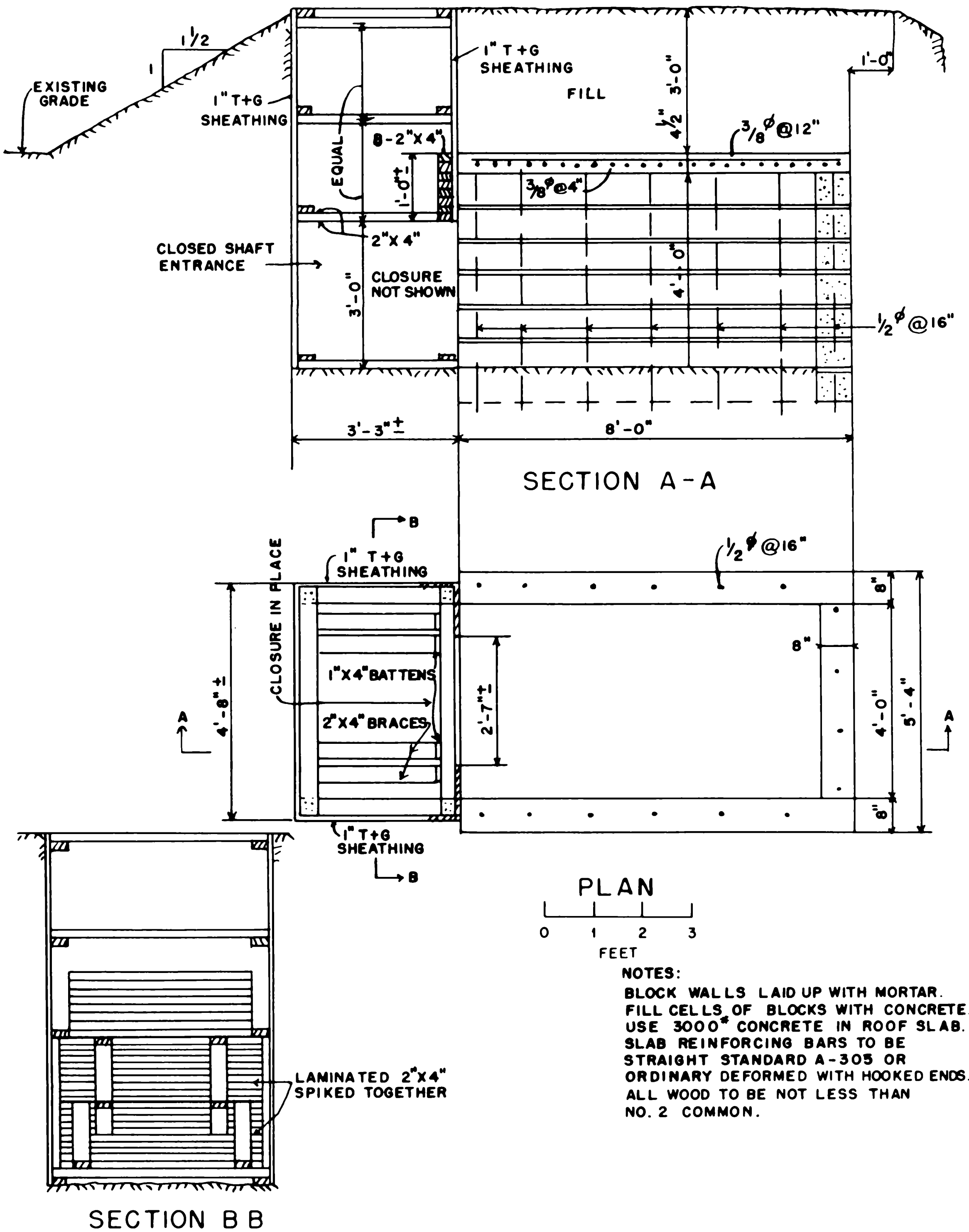

Fig. 7—Earth-covered trench with closed shaft entrance.

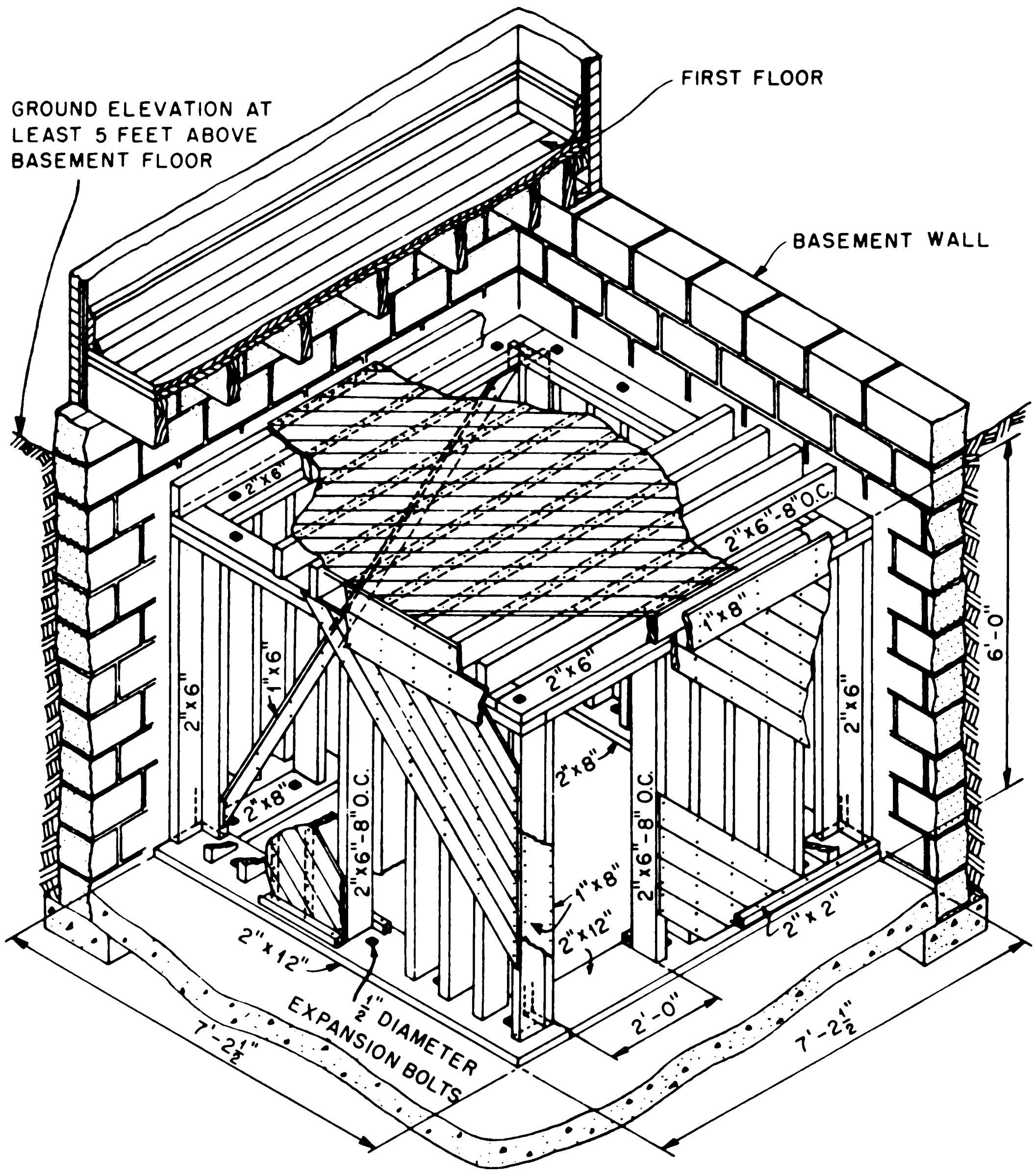

Fig. 8—Basement corner room tested at 3500 and 7500 ft. All wood to be not less than No. 2 common. Roof to be prefabricated and erected as a unit.

Fig. 9—Basement corner room (at 7500 ft) after blast.

SUMMARY 9

BEHAVIOR OF UNDERGROUND STRUCTURES SUBJECTED TO AN UNDERGROUND EXPLOSION

(Report WT-1126, Operation Teapot, Project 3.3.2, same title, by G. K. Sinnamon et al., University of Illinois, Urbana, Ill., Oct. 11, 1957.)

OBJECTIVES AND SCOPE

The objectives of this project were to obtain information regarding the loads applied to buried structures by an underground explosion and the response of the structures to these loads.

Two buried reinforced-concrete four-walled structures without floors and roofs were tested, one at 200 ft (designated 3.3.2-a-1) and the other at 250 ft (designated 3.3.2-a-2), with a 1.2-kt device (shot 7) detonated underground at a depth of 67 ft. The structures were instrumented to give transient load and response data. Provisions were made to obtain data on permanent displacements and strain.

The results of this project were to be correlated with previous test results of similar nature that had been obtained with relatively small high-explosive charges at Dugway, Utah, and also from the Jangle underground atomic shot.

TEST STRUCTURES, TEST CONDITIONS, AND INSTRUMENTATION

Excavation for the structures was done so that the surrounding soil would be disturbed only a minimum amount. Each box-type test structure (Figs. 1 and 2) was cast in place in an open cut that was backfilled subsequently so that the top of the box was 3 ft 9 in. below the original ground level. The open cut had been made as small as possible, with nearly vertical sides. The excavated material used in the backfill was dampened and placed in approximately 6-in. layers.

The outside dimensions of the boxes were 12 ft 6 in. square by 8 ft 10 in. high. The front, facing Ground Zero (GZ), and rear walls were 24 in. thick, and the side walls were 12½ in. thick. The walls were reinforced with both tension and compression steel at 0.6% for the main steel in the front and rear walls. The average compressive strength of the concrete was approximately 3700 psi.

For the resistance of the front wall, the calculations using the ultimate theory of reinforced concrete were based on the following assumptions: (1) The dynamic yield point of the reinforcing bars was 20% higher than the experimentally determined static value (see Fig. 3), and (2) the dynamic strength of the concrete was 20% higher than the experimentally determined static value. These originally determined

assumptions were found later not to be valid. The strain rate was not as high as expected. The resistances of the front and rear walls were recomputed for use in the posttest analysis on the basis of the measured static properties of the materials.

Instrumentation measurements were taken before, during, and after the explosion. The transient instrumentation consisted of six earth-stress gauges, six accelerometers, and four displacement gauges, located as shown in Fig. 4. The predicted peak values for these gauges and the measured values for comparison are summarized in Table 1.

The measurements of permanent effects included survey-point readings to determine the rigid-body motion of the structures and the relative displacements of the front, side, and rear walls with respect to the original shape. The locations of the survey points are shown in Fig. 5. Provisions were made also to measure the permanent strain in the main reinforcing bars of the front and rear walls, located as shown in Fig. 5.

RESULTS

The test shot (7) was fired on Mar. 23, 1955. Aerial observation soon after the blast disclosed that test structures were completely covered by throw-out from the crater. The apparent crater radius measured at ground elevation was 146 ft, and the crater depth was 90 ft. Primarily because of radiological hazard, posttest examination of the boxes was not conducted until October 1955.

Permanent motion of the ground surface, as obtained under another project (Project 1.7), is shown graphically in Fig. 6. Permanent displacements of structures and sand columns, also obtained under another project (Project 1.6), are indicated in Fig. 7.

Measurement of transient effects in the medium was carried out by Project 1.7. The medium acceleration and earth stress measured at 10-ft depths are given in Figs. 8 and 9, respectively.

Peak values of the transient measurements are listed in Table 1.

Upon removal of the earth cover, which was approximately 10.5 ft over 3.3.2-a-1 and 9.0 ft over 3.3.2-a-2, careful inspection of the interior surfaces of the boxes was made. No sign of distress was apparent, and the absence of damage was confirmed by measurements of permanent distortions.

The boxes moved away from GZ essentially along a radial line horizontally and upward vertically, and they were tilted backward as shown in Fig. 7. The results obtained from the survey points and from the permanent strain measurements are presented in Tables 2 and 3. The results indicate that the permanent deformation of the boxes was negligible.

CONCLUSIONS

The results of this test are of interest in determining the effects of an underground nuclear explosion on a buried blast shelter. The following applicable conclusions were reached:

1. Structures with strength comparable to the 3.3.2 boxes will not be damaged when located at distances equal to or greater than 1.3 crater radius.

2. To suffer structural damage, a structure probably has to be located close to the edge of or within the crater.

3. If the structure is not within or near the crater, problems not related to the strength of the structure are likely to predominate. Some of these are: loss of air supply because of the smothering of intakes by earth throw-out; damage to service (electric, water, sanitary) pipes and conduits caused by large differences in earth motion over large distances; and sealing of entranceways and escape tunnels by throw-out and large earth movements.

4. Because of the lack of relative motion between a structure and the soil in its immediate vicinity, any appurtenances to a structure, such as entranceways and ventilation ducts, and electric, water, and sanitary conduits, probably will suffer only minor damage at their juncture with the structure.

5. Such a structure will move essentially with the soil and will be subjected to accelerations essentially equal to those of the surrounding medium.

6. For buried high-explosive charges, the structure may be subjected to severe accelerations; as the size of the charge increases for scaled ranges, however, the accelerations will decrease since accelerations scale as the reciprocal of the cube root of the charge weight. This indicates that for large-size buried explosions accelerations of the structure will not be too severe.

7. Because of the long rise time, the structure should be designed to withstand the pressure of the medium applied statically.

Table 1—MEASUREMENTS AND PREDICTED RESULTS

Gauge	Gauge	Location	Measured peak	Predicted peak
Structure acceleration	EA1	3.3.2-a-1 Front wall	4.3 g*	190 g
	EA2	Rear wall	6.4 g*	95 g
	EA3	Side wall	7.2 g†	11.5 g
	EA4	3.3.2-a-2 Front wall	1.7 g*	60 g
	EA5	Rear wall	3.3 g*	30 g
	EA6	Side wall	1.9 g†	2.5 g
Structure pressure	EP1	3.3.2-a-1 Front wall	33 psi	510 psi
	EP2	Rear wall	42 psi	250 psi
	EP3	3.3.2-a-2 Front wall	53 psi	165 psi
	EP4	Front wall	50 psi	165 psi
	EP5	Rear wall	30 psi	80 psi
	EP6	Side wall	18 psi	55 psi
Deflection	ED1	3.3.2-a-1 Front wall	0.144 in.	>3.5 in.
	ED2	Rear wall	0.133 in.	>3.5 in.
	ED3	3.3.2-a-2 Front wall	0.171 in.	<3.5 in.
	ED4	Rear wall	0.201 in.	<3.5 in.
Medium stress	71CH10	200-ft range 10-ft depth	125 psi	170 psi
	72CH10	250-ft range 10-ft depth	41.5 psi	55 psi
Medium acceleration	71H10	200-ft range 10-ft depth	10 g	11.5 g
	72H10	250-ft range 10-ft depth	2.25 g	2.5 g

*The electronic record had a very small amplitude trace. Because of this, the values are not reliable.

†Acceleration is radial from GZ.

Table 2—SURVEY MEASUREMENTS

Structure	Bolt*	Elevation, ft		Vertical displacement, ft	Horizontal displacement, ft	
		Original	Final		Radial	Tangential
3.3.2-a-1	A1	86.16	89.14	1.98		
	A7	87.14	89.05	1.91		
	A15	87.18	88.46	1.28		
	A9	87.17	88.37	1.20		
	A4				3.83	0.07†
	A12				3.83	0
3.3.2-a-2	A1	87.95	88.08	0.13		
	A7	87.94	‡			
	A15	87.96	87.99	0.04		
	A9	87.94	87.94	0		
	A4				0.50	0.07†
	A12				0.50	0.10†

*For bolt locations see Fig. 5.

†Toward the east.

‡Bolt sheared off during test.

Table 3—SUMMARY OF PERMANENT STRAINS

Structure	Front wall: Gauge line*	Front wall: Strain,† in./in.	Rear wall: Gauge line*	Rear wall: Strain,† in./in.
3.3.2-a-1	B 1	−0.0008	B 1	−0.0001
	2	+0.0002	2	0
	3	−0.0001	3	−0.0001
	4	+0.0008	4	−0.0003
	5	−0.0005	5	−0.0002
	6	+0.0001	6	−0.0002
	7	+0.0007	7	−0.0003
	C 1	−0.0004	C 1	−0.0003
	2	+0.0001	2	−0.0001
	3	0	3	−0.0010
	4	−0.0002	4	−0.0002
	5	−0.0001	5	−0.0014
	6	−0.0001	6	−0.0005
	7	0	7	−0.0002
	D 1	0	D 1	−0.0012
	2	−0.0003	2	−0.0005
	3	+0.0002	3	−0.0005
	4	+0.0002	4	+0.0001
	5	+0.0003	5	0
	6	+0.0002	6	0
	7	−0.0004	7	−0.0003
3.3.2-a-2	B 1	+0.0001	B 1	0
	2	+0.0001	2	−0.0002
	3	0	3	−0.0002
	4	−0.0004	4	−0.0004
	5	0	5	−0.0004
	6	−0.0003	6	−0.0004
	7	−0.0005	7	−0.0006
	C 1	−0.0001	C 1	−0.0002
	2	−0.0004	2	−0.0003
	3	+0.0002	3	−0.0002
	4	0	4	0
	5	+0.0005	5	+0.0002
	6	−0.0001	6	−0.0001
	7	+0.0004	7	−0.0001
	D 1	−0.0004	D 1	+0.0008
	2	−0.0004	2	−0.0002
	3	−0.0003	3	+0.0005
	4	+0.0001	4	+0.0003
	5	−0.0004	5	−0.0002
	6	−0.0001	6	−0.0001
	7	−0.0007	7	+0.0002

*For location of strain-gauge lines see Fig. 5.

† + indicates tension and − indicates compression.

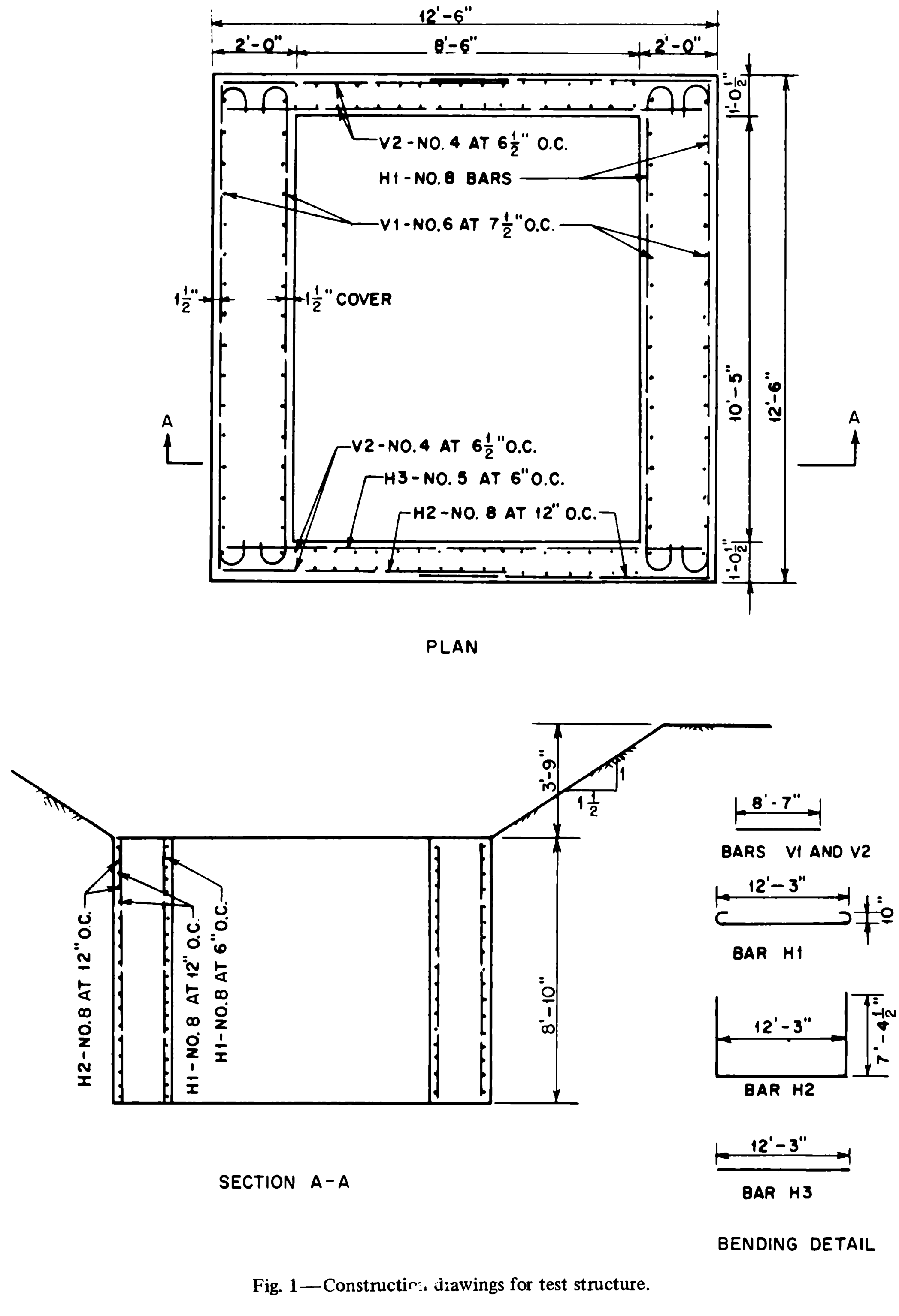

Fig. 1—Construction drawings for test structure.

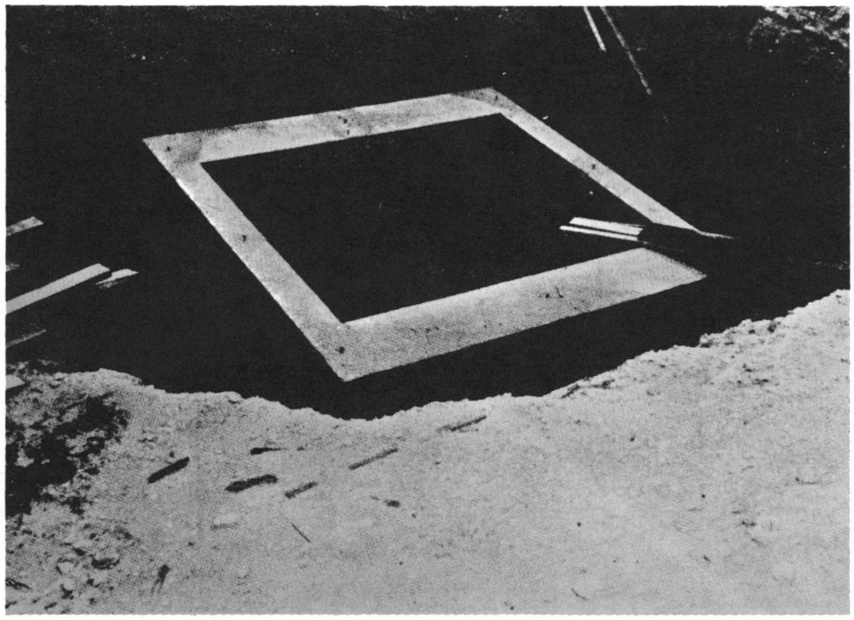

Fig. 2—Completed test structure 3.3.2-a-2.

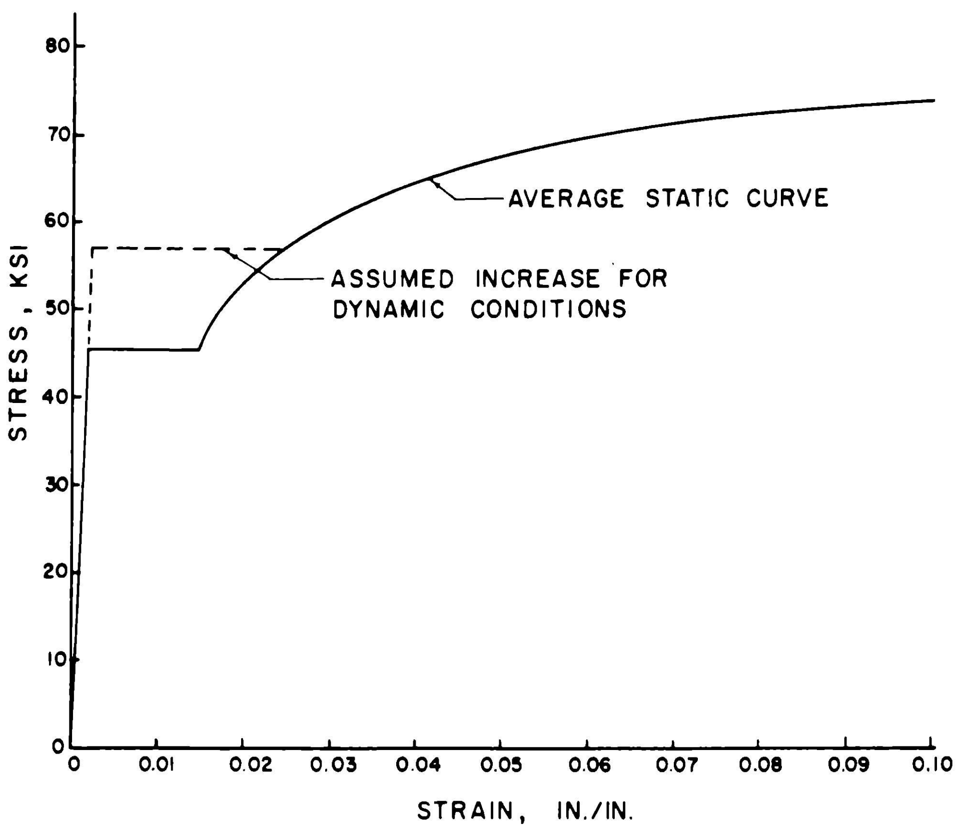

Fig. 3—Average stress–strain curve for reinforcing bars.

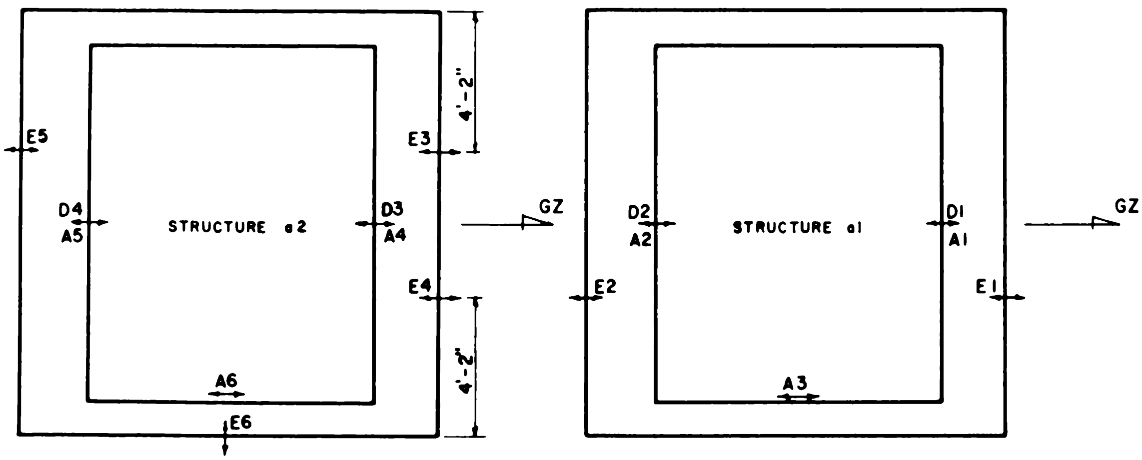

A = ACCELEROMETER
D = DISPLACEMENT GAGE
E = EARTH PRESSURE GAGE

ALL EARTH PRESSURE GAGES MOUNTED 59" FROM TOP. ALL OTHERS MOUNTED AT MID-HEIGHT, 53" FROM TOP.

Fig. 4—Instrument locations.

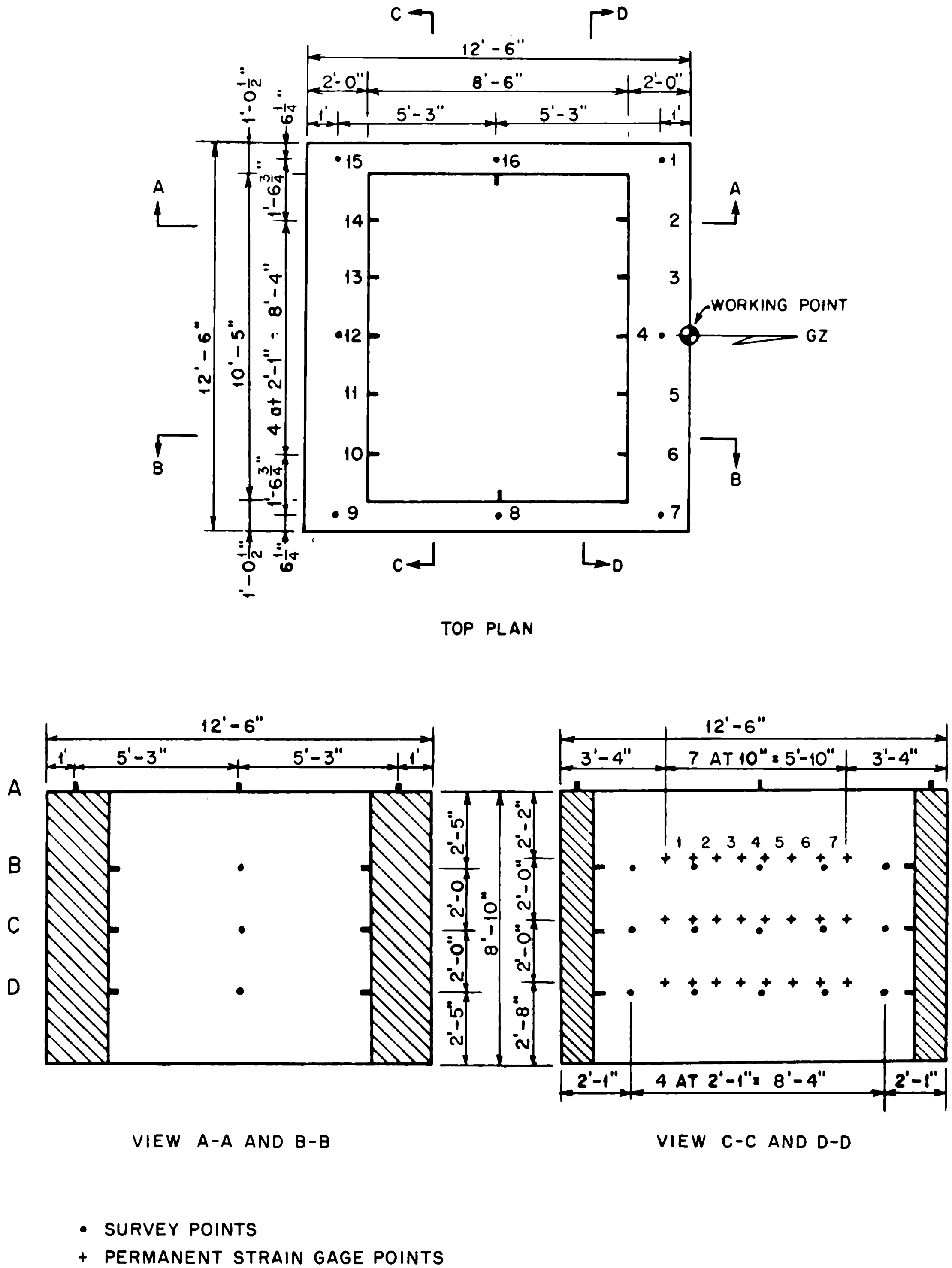

Fig. 5—Location of survey points and of permanent strain-gauge points.

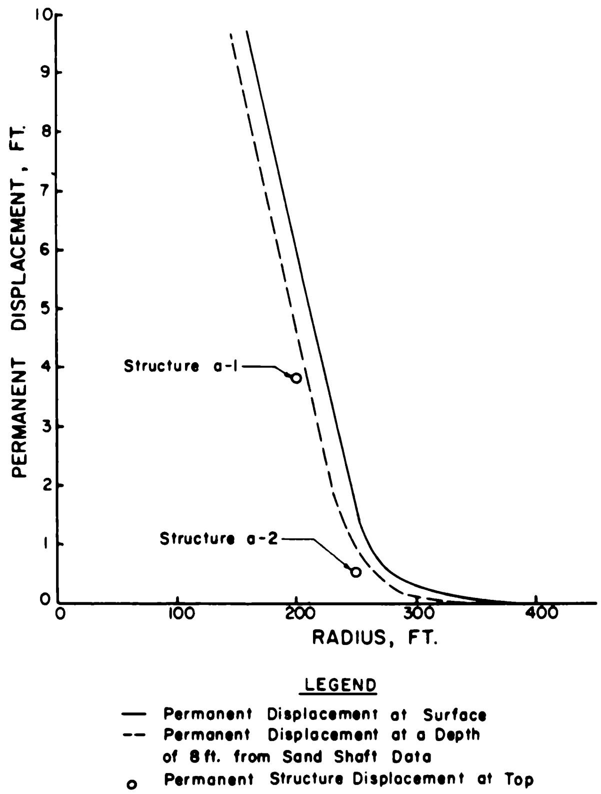

Fig. 6—Permanent displacement vs. distance.

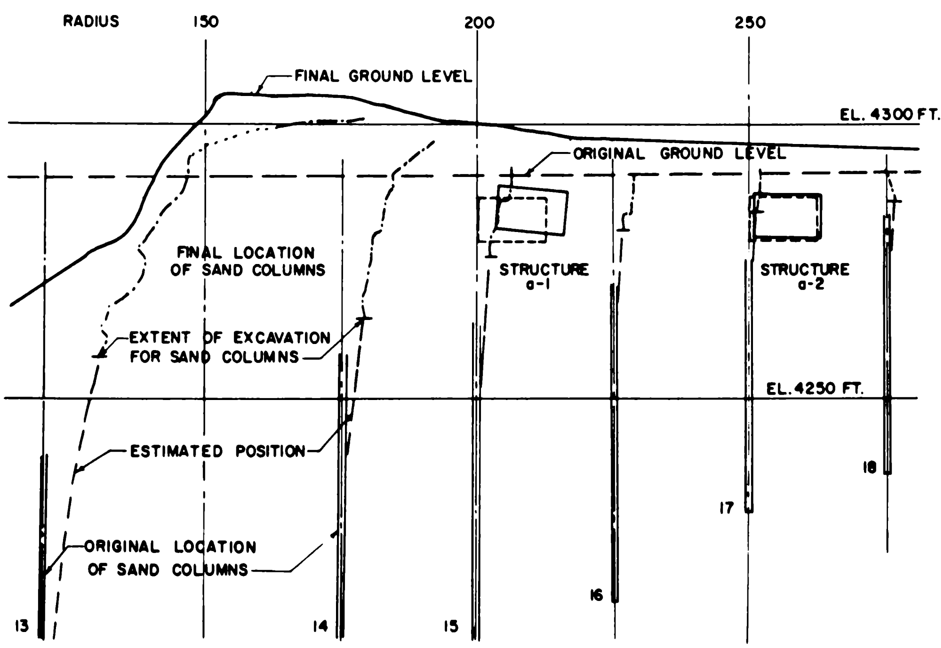

Fig. 7—Permanent displacements of structures and sand columns.

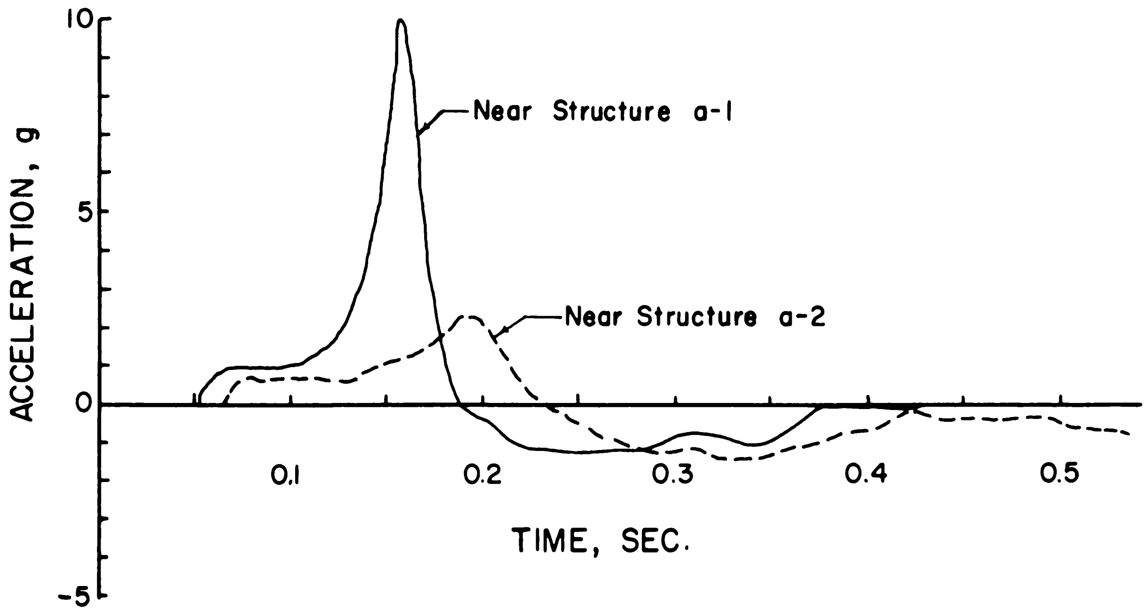

Fig. 8—Medium acceleration vs. time.

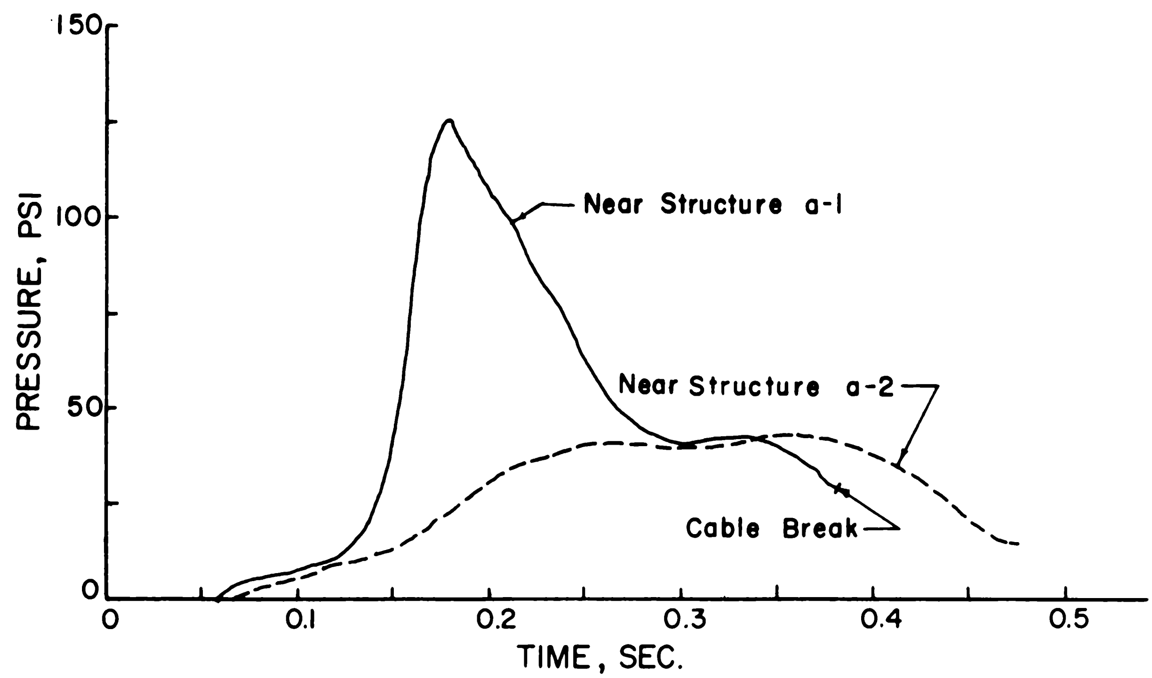

Fig. 9—Medium stress vs. time.

SUMMARY 10

AIR BLAST EFFECTS ON UNDERGROUND STRUCTURES

(Report WT-1127, Operation Teapot, Project 3.4, same title, by R. E. Woodring, G. K. Sinnamon, and N. M. Newmark, University of Illinois, Urbana, Ill., Aug. 20, 1957.)

OBJECTIVES AND SCOPE

The general purpose of this project was to obtain the necessary basic data from which to develop criteria for the economical and efficient design of underground protection from air-blast forces.

The test was an extension of the first two tests of the series conducted in Operation Upshot-Knothole (U-K) Project 3.8 (see Summary 5) and used the same structures that had been subjected to 15- and 63-psi surface overpressures from U-K shots 9 and 10, respectively. In this test three structures (3.4a, 3.4b, and 3.4c) were subjected to Teapot-Met shot (ref. ENW, p. 674), with a ground surface pressure of about 90 psi.

The specific objectives of the test were essentially the same as in the U-K tests. Because in the U-K tests only small permanent deflections occurred in the so-called "plastic" beams (the plastic beams were intended to be considerably weaker than the others), the plastic beams in this test were intentionally weakened by cutting material from their lower flanges.

TEST STRUCTURES AND INSTRUMENTATION

The structures tested in this project were the ones tested in U-K Project 3.8 except for the modifications of plastic beams as illustrated in Fig. 1 and Table 1. Structure locations are shown in Fig. 2. For details on concrete test chambers, beam strips, soil conditions, etc., see Summary 5.

Again, as in U-K Project 3.8, the installation and operation of the gauges and recorders for this project were performed by the Ballistic Research Laboratories.

RESULTS

Visible Results

It was evident that structure 3.4a had been subjected to considerable motion within the soil during the test. The soil above the structure apparently had risen several inches and had fallen back into place. There was no indication of any structural failure. Some permanent deflections on the plastic beams and negligible deflections on the other beams were observed.

Examination of the soil above structures 3.4b and 3.4c did not indicate soil action similar to that described above for structure 3.4a; in the interiors of these two structures there were no visible permanent deflections or disturbance of the roof beams.

Survey Measurements

The permanent deflection of the center of each beam with respect to its ends is tabulated in Table 2. Beams 1P1, 4P1, and 8P1 typically refer to beam P1, located in structures 3.4a, 3.4b, and 3.4c, respectively. Survey measurements of the displacements of the structures relative to bench marks 1, 2, 3, and 4, at depths of 20, 12, and 4 ft, and at ground surface, respectively, are given in Table 3. Bench mark GKS is on top of the entrance to structure 3.4a, and bench marks 1A, 1B, 10B, and 1C are located in the three test structures. These data indicate that the overall permanent displacement of the structures was negligible.

Permanent Strains

A summary of permanent-strain data is given in Table 4. It appears that only the permanent strains measured on beams 1P3 and 1M2 in structure 3.4a are of any significance.

Transient Measurements

Locations and designations of all the gauges typical for each structure are shown in Fig. 3.

Transient deflection records for structure 3.4a are shown in Fig. 4; vertical acceleration records for the same structure are shown in Fig. 5.

Maximum dynamic strain measured at the center of the beam strips is listed in Table 5.

The average air pressure at ground surface measured approximately 90 psi, i.e., close to expected value.

CONCLUSIONS AND DISCUSSION

The results of this test in many ways confirm the conclusions reached in the U-K Project 3.8 tests.

In silty, well-cemented soils there seems to be some slight effective attenuation of pressure transmitted to a buried structure, depending upon the depth of cover over the structure and the flexibility of the structure. There is a change in shape of the pressure–time curve, particularly in the rise time, which appears to be primarily a modification of the initial shape. This change results in a reduction in peak pressure transmitted through the soil from the surface to the buried structure below. This reduction, however, would be materially less for a very long pressure pulse, as would be the case in a very high yield detonation, than for a short one. For a structure buried no more than the span of the structure, it would be unwise and probably unsafe to assume that there is any real attenuation in force or structural response in the case of a large nuclear device in the megaton range, even though some of the free-earth test data indicate considerable attenuation for devices in the kiloton range.

The stiffness of the structure relative to the stiffness of the soil has a definite effect on the pressure transmitted to the structure. Where the structure is quite stiff, there is possibly a reflection of the pressure, but, where the structure is flexible, there appears to be a reduction in response corresponding to a probable reduction in pressure acting on the surface of the structure.

The stiffness of the soil has a definite bearing upon the behavior of the buried structure. In the U-K Project 3.8 tests the backfill was newly placed and probably only added to the mass of the beam strips. In this test, however, the soil had hardened and was quite stiff. The response of the flexible beam strips in the two deeper structures under the hardened soil was less than the response of the flexible beam strips in the shallowest structure under the newly placed soil. The response of the more rigid beam strips nevertheless did not decrease with depth of cover.

Table 1—DIMENSIONS AND PROPERTIES OF BEAM STRIPS

Quantity	Beam strip type: E	M	P: Original	P: Modified
Rolled sections used, each side	15I50	8I23	Two 7[9.8	Two 7[9.8
Width of ½-in. plate, in.	23.25	20.25	21.25	21.25
Total width supported, in.	24	21	22	22
Total moment of inertia, $in.^4$	1462	232.8	162.0	134.2
Distance to neutral axis, in.				
Top flange	5.79	2.67	2.19	1.95
Bottom flange	9.71	5.83	5.31	5.55
Max. stress, 100-psi load, ksi*	18.4	60.6	83.1	104.9
Max. defl., 100-psi load, in.				
Neglecting shear	0.0605	0.333	0.501	0.557
Including shear	0.0752	0.365	0.541	0.601
Equiv. dead load, psi				
1-ft cover	1.3	1.1	1.1	1.1
4-ft cover	3.6	3.4	3.4	3.4
8-ft cover	6.7	6.5	6.5	6.5
Dead-load stress, ksi				
1-ft cover	0.23	0.7	0.9	1.1
4-ft cover	0.66	2.1	2.8	3.6
8-ft cover	1.23	4.0	5.4	6.8
Dead-load defl., in.				
1-ft cover	0.0009	0.0040	0.0058	0.0064
4-ft cover	0.0027	0.0125	0.0184	0.0204
8-ft cover	0.0051	0.0238	0.0352	0.0391
Fundamental period T, msec†				
Steel section only	5	9	11	12
1-ft cover	9	17	21	22
4-ft cover	15	31	39	39
8-ft cover	21	42	53	55

*Linear elastic action was assumed.
†Fundamental period was based on flexural stiffness.

Table 2—SUMMARY OF PERMANENT DEFLECTIONS

Beam	Permanent deflection, in.: Survey	Electronic record	Beam	Permanent deflection, in.: Survey	Electronic record
1P1	0.14		4M2	0.04	Negligible
1P2	0.88		4M3	0.02	
1P3	1.28	1.2	4E1	0.06	
1P4	0.80		4E2	0	0.003
1M1	0.23		4E3	0	
1M2	0.12	0.33	8P1	0.04	
1M3	0.10		8P2	0.04	
1E1	0.11		8P3	0.04	Negligible
1E2	0	0.01	8P4	0.03	
1E3	0.04		8M1	0.03	
4P1	0.04		8M2	0.03	Negligible
4P2	0.03		8M3	0	
4P3	0.09	Negligible	8E1	0.02	
4P4	0.03		8E2	0	0.02
4M1	0.01		8E3	0.02	

Table 3—PERMANENT VERTICAL DISPLACEMENTS FROM BENCH MARKS

Bench mark	Elevation, ft		Change, ft
	Pretest	Posttest	(pretest–posttest)
BM 1	−18.28*	−18.28	
BM 2	−10.28	−10.26	−0.02
BM 3	−4.27	−4.27	0
BM 4	+0.05	+0.03	+0.02
BM GKS	+0.04	+0.03	+0.01
BM 1A	−6.34	−6.35	+0.01
BM 1B	−9.14	−9.12	−0.02
BM 10B	−7.34	−7.34	0
BM 1C	−12.84	−12.83	−0.01
BM 1†	−18.30	−18.28	−0.02

*Elevation assumed from U-K Project 3.8.
†Reading used to check the set of levels.

Table 4—SUMMARY OF PERMANENT STRAIN MEASUREMENTS

Beam	Permanent strain, in./in.				
	Whittemore gauge		Direct-reading gauge		Scratch gauge far beam
	Far beam*	Near beam	Far beam	Near beam	
1P1	+0.0005	+0.0065	−0.001	+0.003	
1P2	+0.0146	+0.0216	+0.019	+0.023	
1P3	Beyond range	Beyond range	+0.039	+0.039	+0.0278
1P4	+0.0221	+0.0169	+0.025	+0.018	
1M1	+0.0038	+0.0020	+0.004	+0.003	
1M2	+0.0008	+0.0072	+0.005	+0.010	+0.00135
1M3	+0.0013	+0.0002	+0.003	+0.001	
1E1	0	−0.0001	+0.0005	+0.0005	
1E2	0	+0.0001	+0.0005	+0.001	0
1E3	0	+0.0002	+0.0005	+0.0005	
4P1	+0.0003	+0.0003	+0.0015	+0.0020	
4P2	+0.0002	+0.0001	+0.0005	0	
4P3	−0.0003	+0.0005	+0.0035	+0.0020	0
4P4	+0.0002	+1.0001	−0.0015	+0.0005	
4M1	+0.0002	+0.0004	0	−0.0005	
4M2	+0.0004	0	0	+0.0005	0
4M3	0	0	+0.0005	+0.0005	
4E1	+0.0001	−0.0001	+0.0005	+0.0010	
4E2	+0.0001	−0.0001	+0.0010	−0.0005	0
4E3	−0.0001	+0.0001	−0.0005	−0.0010	
8P1	+0.0001	+0.0002	+0.0010	+0.0035	
8P2	+0.0004	+0.0002	+0.0015	+0.0015	
8P3	+0.0003	+0.0011	+0.0020	+0.0005	0
8P4	−0.0003	+0.0003	+0.0015	+0.0010	
8M1	+0.0002	+0.0001	+0.0010	+0.0035	
8M2	0	−0.0002	+0.0010	+0.0005	0
8M3	+0.0001	+0.0001	+0.0010	+0.0005	
8E1	−0.0002	−0.0001	+0.0005	+0.0015	
8E2	−0.0002	−0.0004	0	−0.0010	0
8E3	−0.0001	−0.0001	0	+0.0005	

*The designation far beam refers to the I-section in a beam strip farther from the structure entrance; near beam refers to the one closer to the entrance.

Table 5—SUMMARY OF DYNAMIC-STRAIN MEASUREMENTS

Beam	Dynamic strain, in./in. Scratch gauge First peak	Scratch gauge Second peak	Calculated from electronic deflection records* First peak	Calculated from electronic deflection records* Second peak	$\left(\frac{\text{Measured strain}}{\text{Computed strain}}\right)$† First peak	$\left(\frac{\text{Measured strain}}{\text{Computed strain}}\right)$† Second peak
1P3	+0.0044	+0.0308	Not elastic	Not elastic		
1M2	+0.0007	+0.0029	Not elastic	Not elastic		
1E2	+0.0003	+0.0005	+0.0007	+0.0008	0.429	0.625
4P1	+0.0006	+0.0007				
4P2	Poor record	Poor record				
4P3	+0.0011	+0.0021	+0.0027	+0.0038	0.408	0.553
4P4	+0.0014	+0.0021				
4M1	+0.0009	+0.0016				
4M2	+0.0009	+0.0015	+0.0015	+0.0022	0.600	0.682
4M3	+0.0006	+0.0008				
4E1	+0.0005	+0.0008				
4E2	+0.0003	+0.0004	+0.0006	+0.0008	0.500	0.500
4E3	+0.0002	+0.0004				
8P1	+0.0008	+0.0014				
8P2	+0.0009	+0.0015				
8P3	+0.0009	+0.0016	+0.0018	+0.0027	0.500	0.593
8P4	+0.0009	+0.0015				
8M1	+0.0009	+0.0015				
8M2	+0.0008	+0.0013	+0.0014	+0.0021	0.572	0.618
8M3	+0.0006	+0.0009				
8E1	+0.0004	+0.0009				
8E2	+0.0003	+0.0006	+0.0006	+0.0010	0.500	0.600
8E3	Poor record	Poor record				

*Calculations were based on the assumption of elastic behavior and uniformly distributed load.
†Strain measured by scratch gauge divided by strain computed from electronic records.

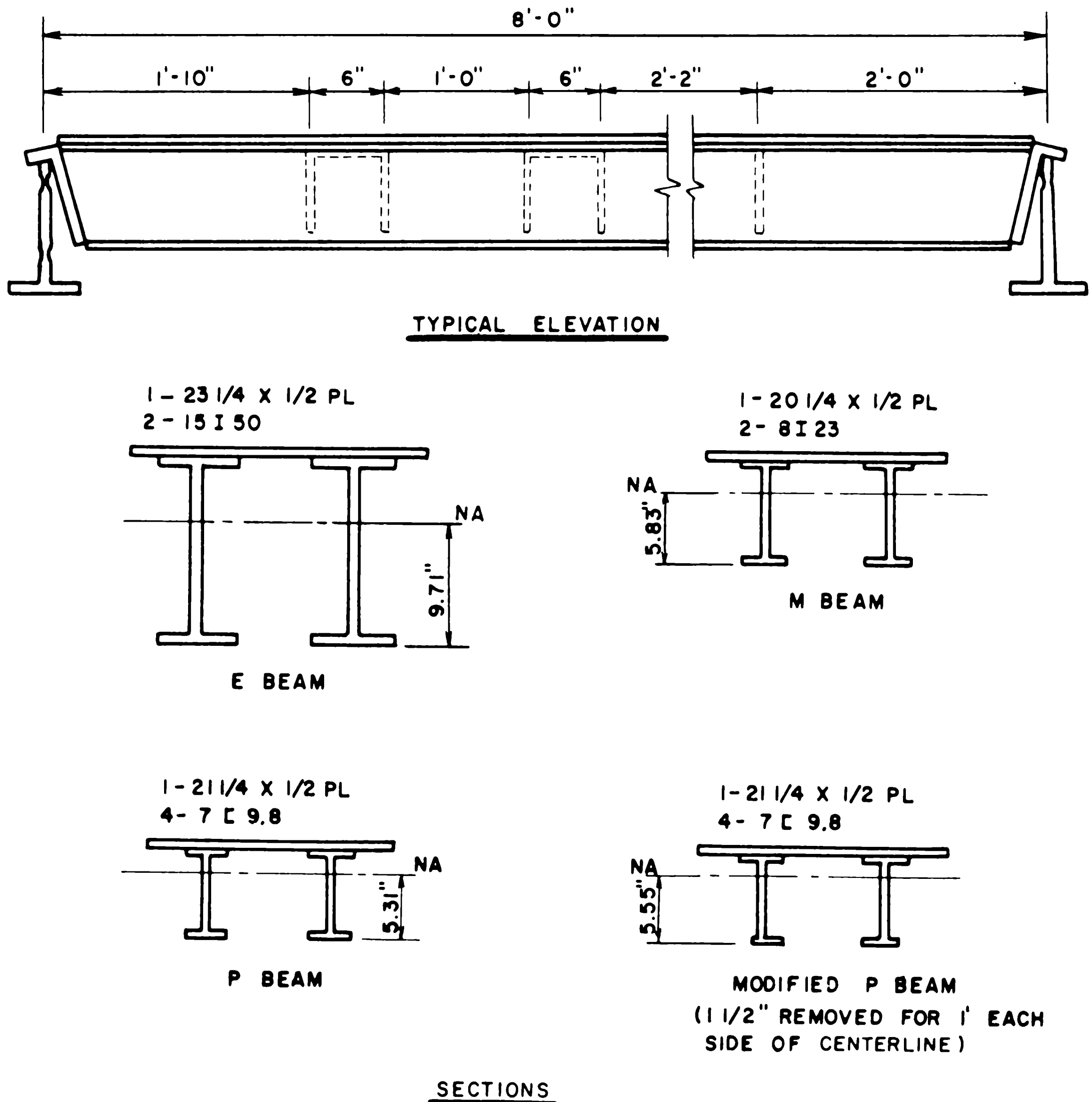

Fig. 1—Elevation and sections of beam strips.

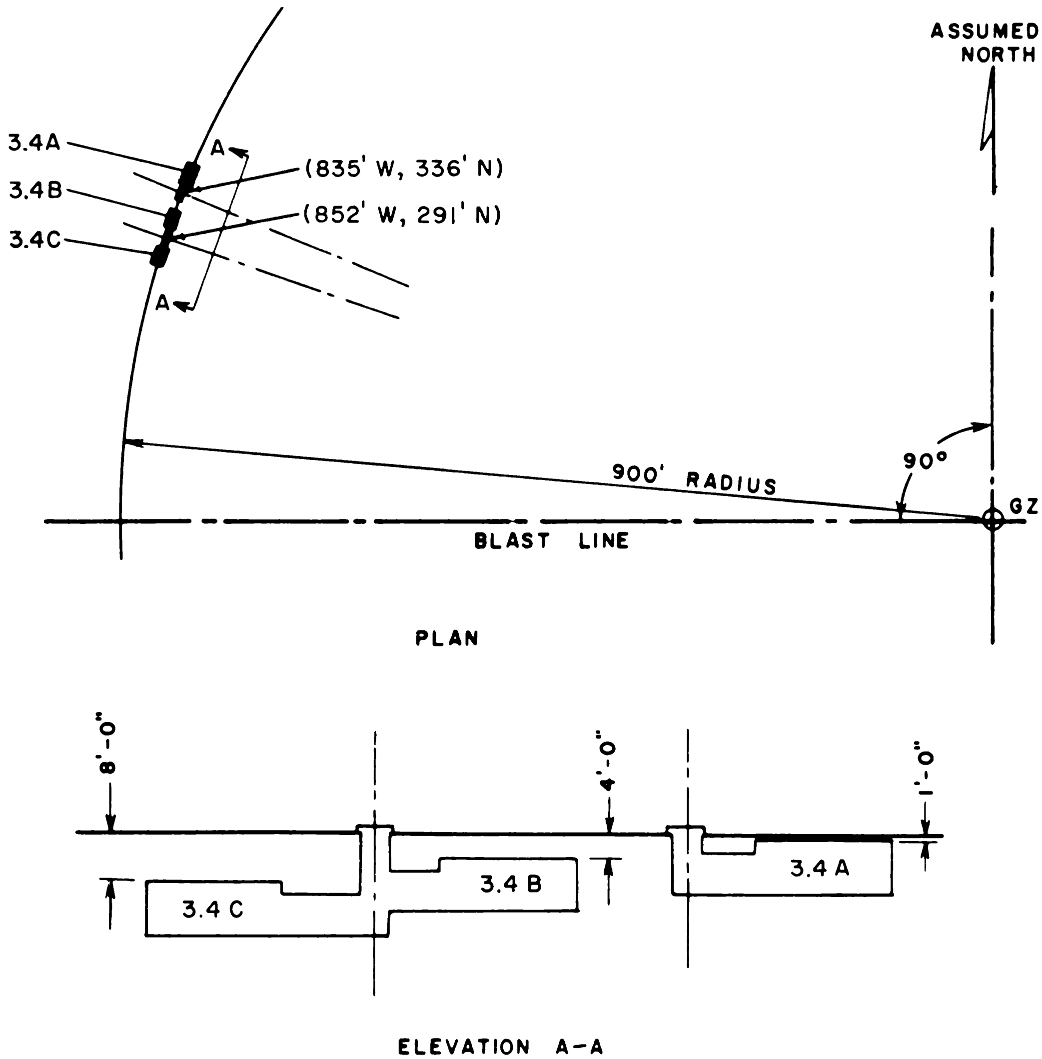

Fig. 2—Location of structures.

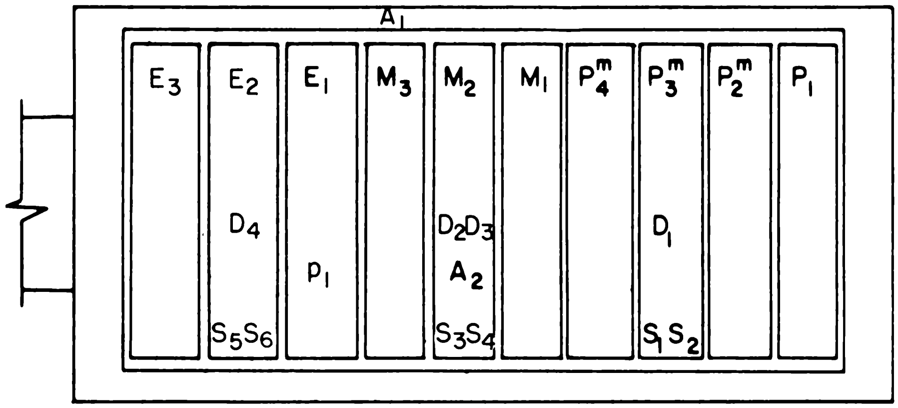

LEGEND

A	accelerometer	p	pressure gage
D	deflection gage	P^m	modified plastic beam strip
E	elastic beam strip	P	unmodified plastic beam strip
M	intermediate beam strip	S	strain gage

Fig. 3—Location of electronic gauges in structure.

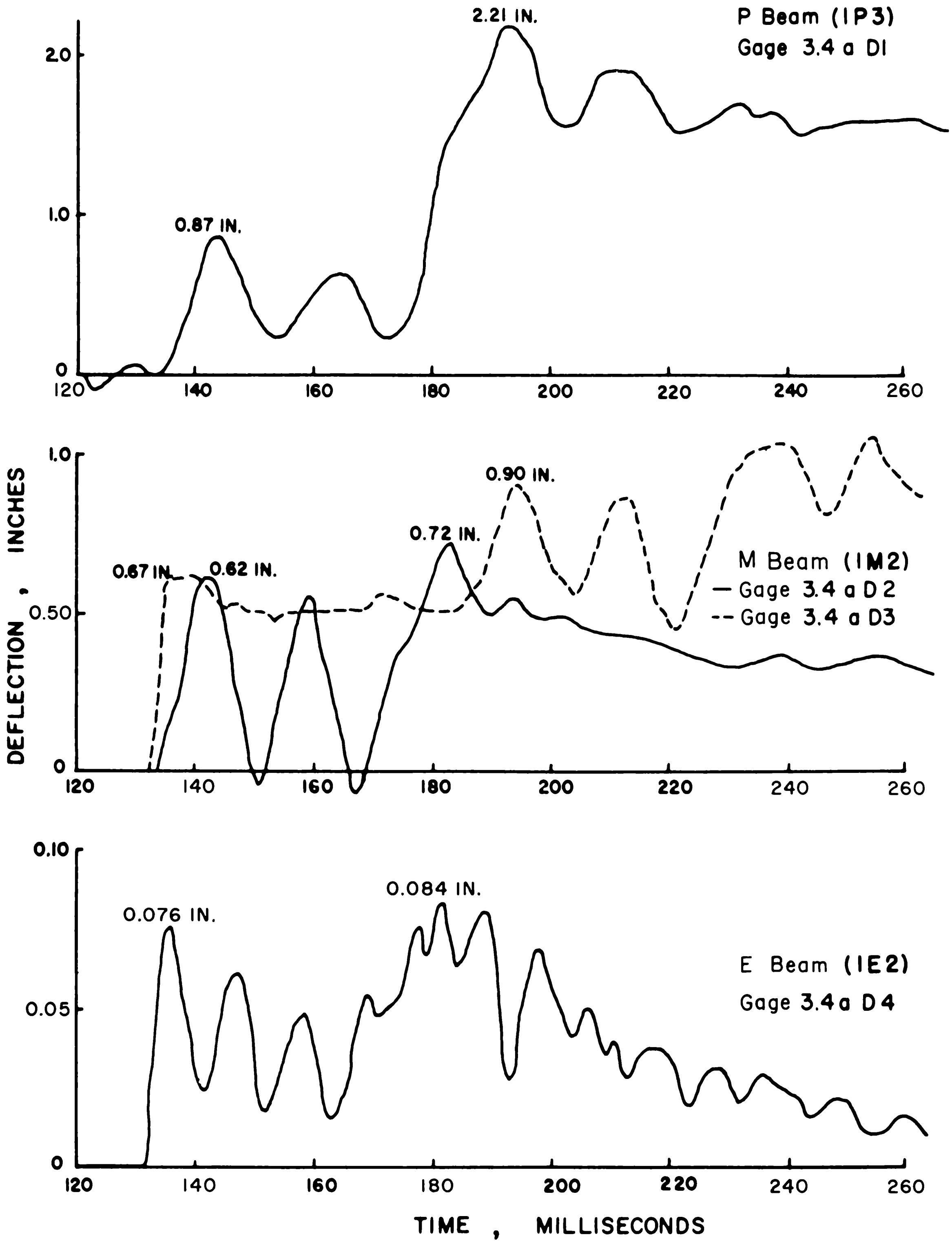

Fig. 4—Deflection records for structure 3.4a.

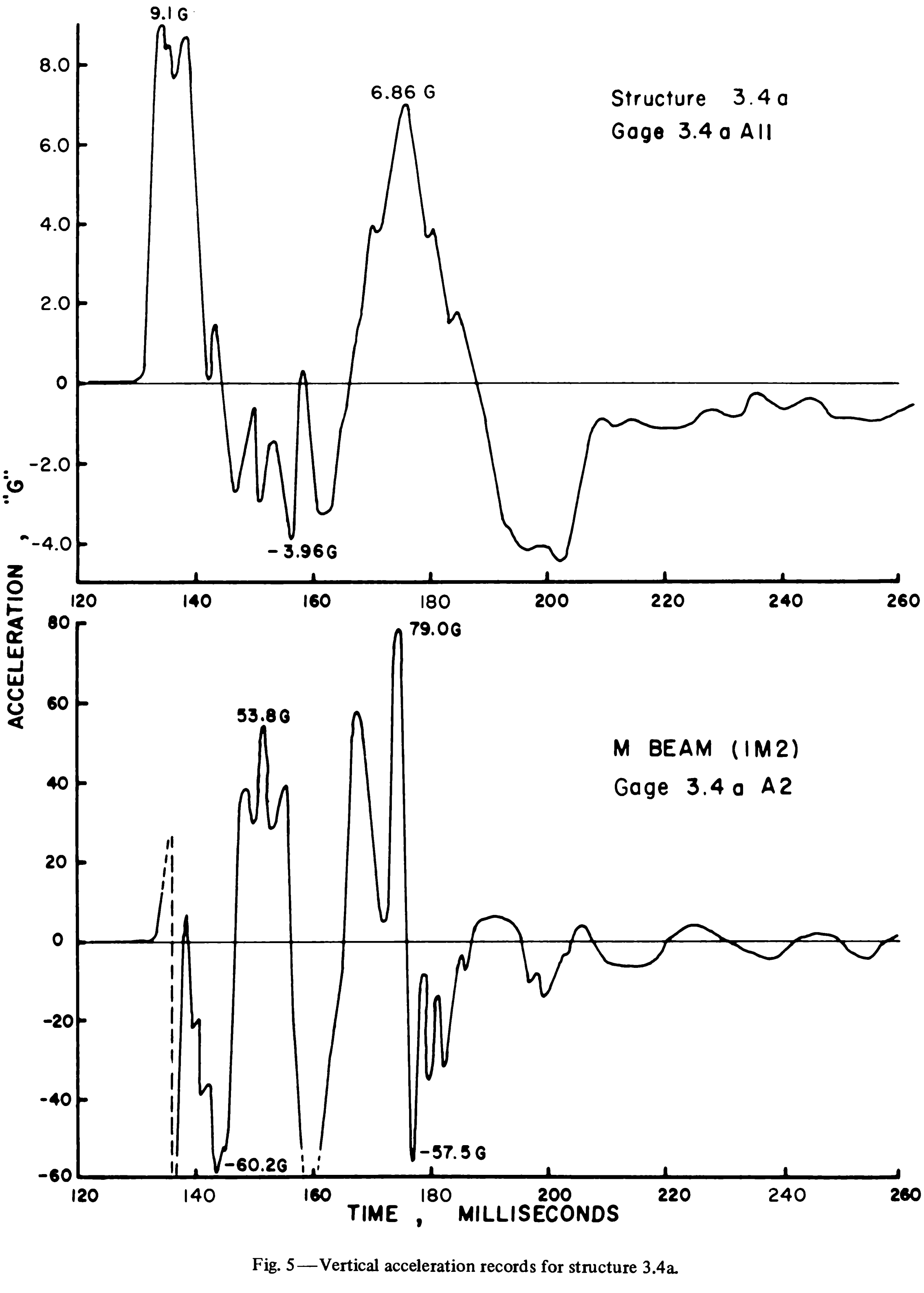

Fig. 5—Vertical acceleration records for structure 3.4a.

SUMMARY 11

EVALUATION OF EARTH COVER AS PROTECTION TO ABOVEGROUND STRUCTURES

(Report WT-1128, Operation TEAPOT, Project 3.6; same title, by R. B. Vaile, Jr., and L. D. Mills, LTJG, USN; Bureau of Yards and Docks, Department of the Navy, Washington, D. C., December 1956.)

OBJECTIVES AND SCOPE

The primary objectives of this project were to determine the degree of protection that earth cover offers to aboveground structures and, particularly, to test the adequacy of a corrugated steel-arch ammunition magazine modified as a personnel shelter, building 3.6. Both the blast resistance and the radiation resistance of such structures were objectives of the test.

Since the arch-type building is weakest against forces transverse to its longitudinal axis, the building was oriented so that the side of the building faced Ground Zero (GZ).

Building U-K 3.15, constructed for Upshot-Knothole Project 3.15, was also tested; it was located at a distance from Teapot shot 12-Met (ref. ENW, p. 674) where both the radiation and the blast load were expected to be in the range of interest but not as high as at the location of the main structure, building 3.6.

Models were added to this experiment with the primary objective of determining, if possible, the relation between model and prototype performances.

Table 1 shows the locations of buildings and models.

TEST STRUCTURES AND INSTRUMENTATION

The main structure, building 3.6, was a 25-by-48-ft steel-arch ammunition shelter (Figs. 1 and 2). The barrel of the structure was an 8-gauge Multi-Plate steel arch composed of curved, corrugated sheets bolted together to form a semicircular arched roof. The foundation was a 1-ft-wide by 2-ft-deep wall footing of reinforced concrete. A blast-resistant door and bulkhead were designed especially for this test with sufficient strength so that their performance would not interfere with the evaluation of the building as a whole.

Building U-K 3.15 was similar to building 3.6 in that it also was a 25-by-48-ft steel arch, but the barrel was of a lighter gauge, i.e., 10-gauge Multi-Plate (see Summary 5). For this test the earth cover was shaped differently so that its horizontal top was tangent to the arch barrel at the crown. (See Figure 7.) The fill for the earth cover was placed in layers not over 6 in. thick; it was compacted by a sheepsfoot roller to a

height of 8 ft. The fill above the structure was dampened by a sprinkler during placement. Several times after placement and before the shot, it was wet down to settle the surface level further.

In addition to the two full-scale structures, three steel and three aluminum models were used, scaled to approximately one-fourth the size of building 3.6. The properties of the models compared to those of the prototype are shown in Table 2. Figure 3 is a photograph of one of the models without earth cover.

Four deflection gauges were used to determine the shape and movement of the center section of the barrel arch of building 3.6. An SR-4 resistance-wire strain gauge was placed to measure total compressive strain at the crown.

Nine self-recording Ballistic Research Laboratories air-pressure gauges were placed on the earth berm: three on the windward slope, three on top, and three on the leeward slope. In addition, two remote-recording airblast gauges were placed on the earth berm, one on the windward face and one on the leeward face.

Scratch gauges were placed around the inside of the arch of each building, including the models, to measure both permanent and maximum deflection. Radiation measurements were made in buildings 3.6 and 3.15 only.

RESULTS

The maximum dynamic pressures produced by the Met shot at the close-in ranges of most interest to this project exceeded the predicted values by something more than 60%. Figure 4 shows the blast measurements at 1500 ft. The peak dynamic pressure of 160 psi at a 10-ft height can be assumed to be equivalent to a wind velocity of about 3000 mph. The main structure, building 3.6, collapsed under these forces (Figs. 5 and 6); there is, however, support for the belief that it would have withstood the predicted values successfully.

Radiation measurements inside building 3.6 indicated a total gamma dose somewhat above the lethal dose and a neutron dose less than the lethal value (Fig. 7).

The performance of the models was in accord with predictions. Of the three steel models that were intended to collapse at the same external pressures as building 3.6, the two at 1400 and 1500 ft, which received pressures similar to or larger than those applied to building 3.6, collapsed. The third, at 2000 ft, which received roughly one-third the pressure applied to building 3.6, remained standing. Of the three aluminum models that were expected to fail under pressures roughly one-fourth of those that would produce failure in building 3.6, the one at 2000 ft did fail; those at 2500 and 3000 ft, however, remained standing (see Tables 3 and 4). Building U-K 3.15 withstood forces 15% of those received by building 3.6 with trivial deflections.

Figure 7 shows the measured radiation doses at buildings U-K 3.15 and 3.6. Comparison of the radiation measurements in these buildings demonstrates the value of the 3 ft of earth cover above the crown of building 3.6.

CONCLUSIONS

The physical results of this test, particularly the pressures measured on the windward slope compared with the free-field measurements, together with the fact that building 3.6 collapsed, demonstrate that a structure of this type and shape is, from a blast-damage standpoint, primarily a drag-type or a dynamic-pressure (q) sensitive rather than an overpressure (p) sensitive target. Drag forces will be reduced by reducing the height of the earth berm until these forces become zero for complete burial of the structure. Resistance to both q and p forces would be enhanced by increasing the gauge of the corrugated steel, increasing the depth of corrugation, decreasing the span of the arch, stabilizing the soil used for cover, and widening the earth berm.

The protection against radiation afforded by building 3.6 was inadequate to assure survival of occupants, just as the building's resistance to blast was inadequate to assure survival under the test conditions.

It was concluded that if this building had been placed 10% farther away from GZ it would have been operational after the test as far as blast is concerned. (The q forces would have been reduced about 17%.) However, the radiation at a 10% increased distance would still have been above the lethal dose; in fact, the structure would have to be moved to a radius of some 2100 ft before the radiation dose inside would have been reduced to the order of 200 rem.

It was also concluded that static tests of models would be valuable in approaching an optimum design of shelters at a minimum cost.

Table 1—LOCATIONS OF BUILDINGS AND MODELS

Unit	Material	Radius from GZ, ft
Building 3.6	Steel	1500
Model 1	Steel	1400
Model 2	Steel	1500
Model 3	Steel	2000
Model 4	Aluminum	2000
Model 5	Aluminum	2500
Model 6	Aluminum	3000
Building U-K 3.15	Steel	2300

Table 2—STRUCTURAL PROPERTIES OF BUILDING 3.6 AND MODELS

	Building 3.6	Steel models			Aluminum models		
Property	Magnitude	Magnitude	Actual ratio	Desired ratio	Magnitude	Actual ratio	Desired ratio
Arch diameter, ft	25	6.25	1/4	1/4	6.25	1/4	1/4
E, psi	30×10^6	30×10^6	1	1	11×10^6	1/2.74	1/4
I, $in.^4$/ft*	0.922	0.0210	1/44	1/64	0.0172	1/54	1/64
I/C, cu in./ft*	0.958	0.0801	1/12	1/16	0.0656	1/15	1/16
Section area (A), sq in./ft*	2.38	0.639	1/3.7	1/4	0.523	1/4.5	1/4
Yield strength(Sy), kips/sq in.	32.9	35.1	1.07	1	11.85	1/2.8	1/4
Ultimate strength, kips/sq in.	45.5	43.5	0.955	1	16.7	1/2.7	1/4
1/IE	3.62×10^{-8}	1.59×10^{-6}	44	64	5.29×10^{-6}	146	256
$\frac{(\text{Size ratio})^4}{\text{IE}}$†	3.62×10^{-8}	0.621×10^{-8}	1/5.9	1/4	2.07×10^{-8}	0.57	1
A Sy‡	78.4	22.4	1/3.5	1/4	6.19	1/19	1/16
(I/C)Sy§	31.5	2.82	1/11	1/16	0.779	1/40	1/64

*Per foot of barrel length.

†Deflection (below yield) for a given psi loading varies approximately as $(\text{size ratio})^4$/IE.

‡Direct load capacity at failure varies as A Sy.

§Bending capacity at failure varies as (I/C)Sy.

Table 3—PERFORMANCE OF MODELS

Model	Ground range, ft	Maximum dynamic pressure (q),* psi	Maximum side-on pressure (p),* psi	p + 0.25q	Movement of crown, in.		
					Permanent	Maximum excursion	
						Up†	Down‡
1 steel	1400	200	35	85	Collapsed		
2 steel	1500	180	30	75	Collapsed		
3 steel	2000	64	19	35	5.4	$4\frac{1}{8}$	$4\frac{3}{16}$
4 aluminum	2000	64	19	35	Collapsed		
5 aluminum	2500	14	9	13	1.3	$2\frac{1}{16}$	$\frac{15}{16}$
6 aluminum	3000	2	8	9	0.6	$\frac{5}{8}$	$\frac{9}{16}$

*Blast-line pressures at 3-ft height.
†At 45°, up and away from GZ.
‡At 45°, down and away from GZ.

Table 4—MEASURED MODEL DEFLECTIONS

Model	q, psi	Measured deflection, in.	Model ratio		Equivalent values for prototype	
			Pressure	Deflection	q, psi	Deflection, in.,
1 steel	200	Collapsed	1	1/0.17	200	Collapsed
2 steel	180	Collapsed	1	1/0.17	180	Collapsed
3 steel	64	4.12	1	1/0.17	64	24
4 aluminum	64	Collapsed	4	4/0.57	256	Collapsed
5 aluminum	14	2.1	4	4/0.57	56	15
6 aluminum	2	0.625	4	4/0.57	8	4.4

Fig. 1—Building 3.6 without earth cover.

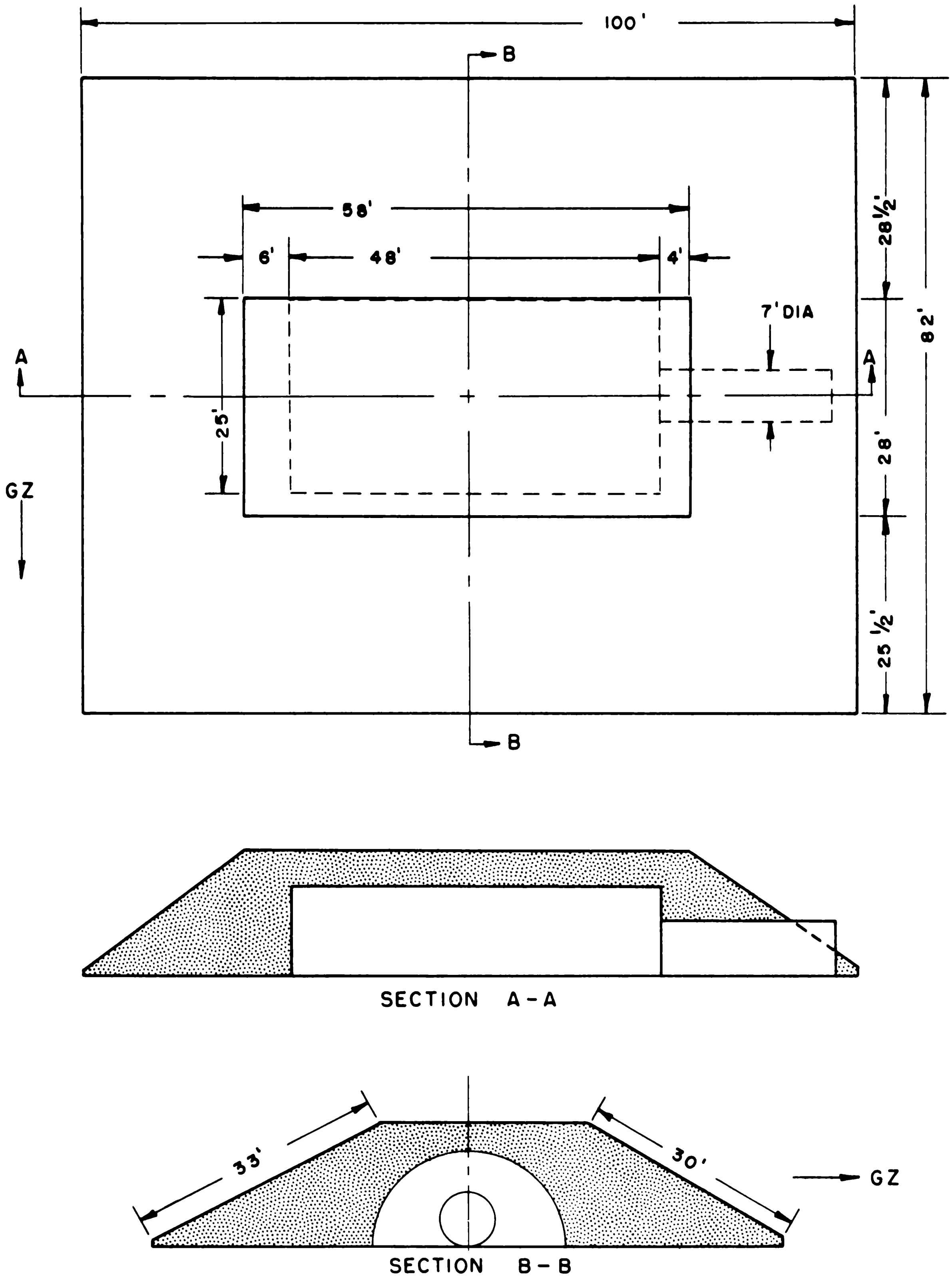

Fig. 2—Plan and profile of earth cover, building 3.6.

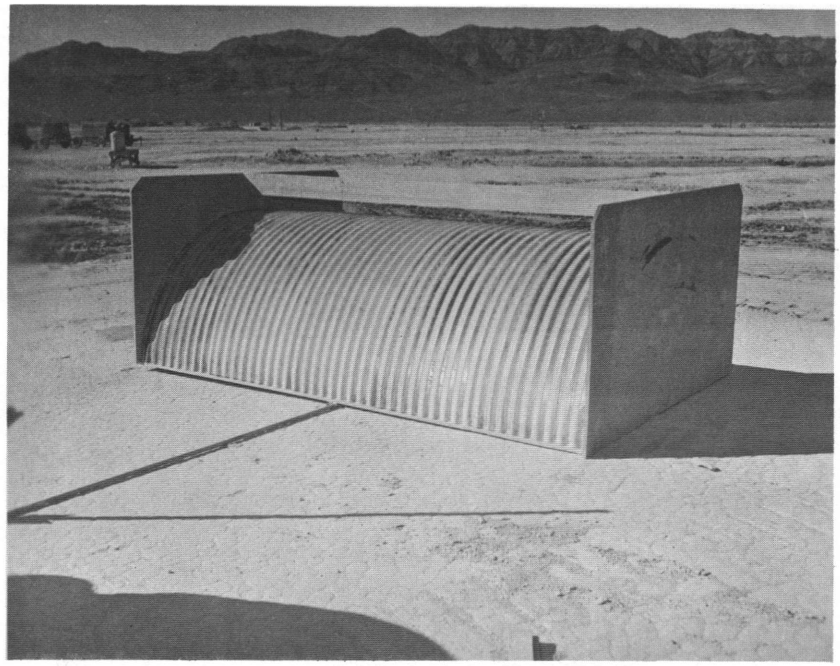

Fig. 3—Model without earth cover.

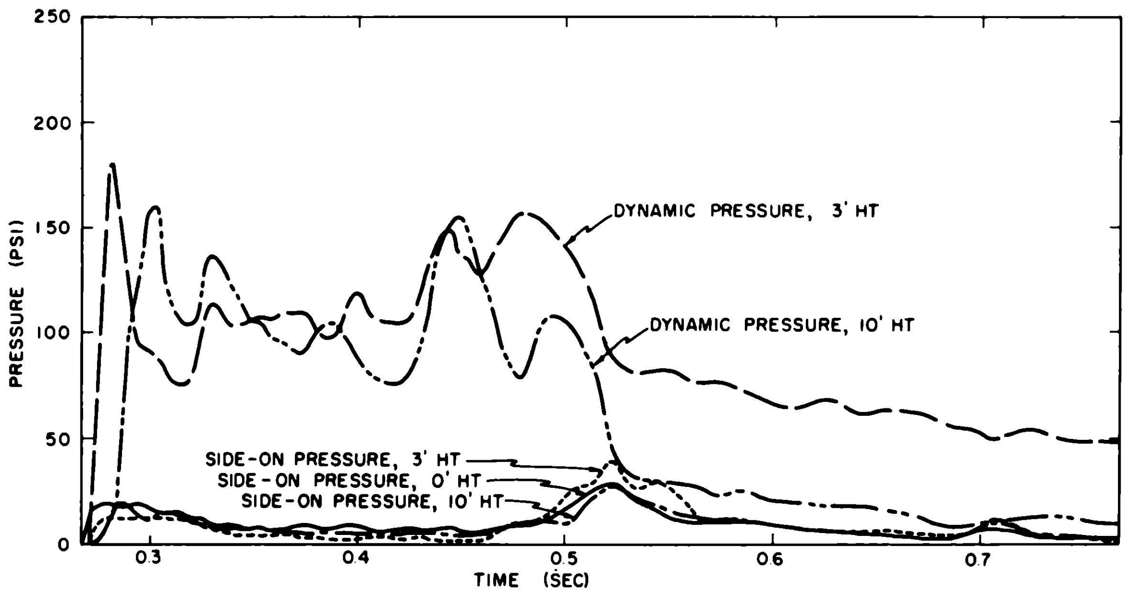

Fig. 4—Pressure–time, desert line, 1500 ft.

Fig. 5—Interior of building 3.6 after shot.

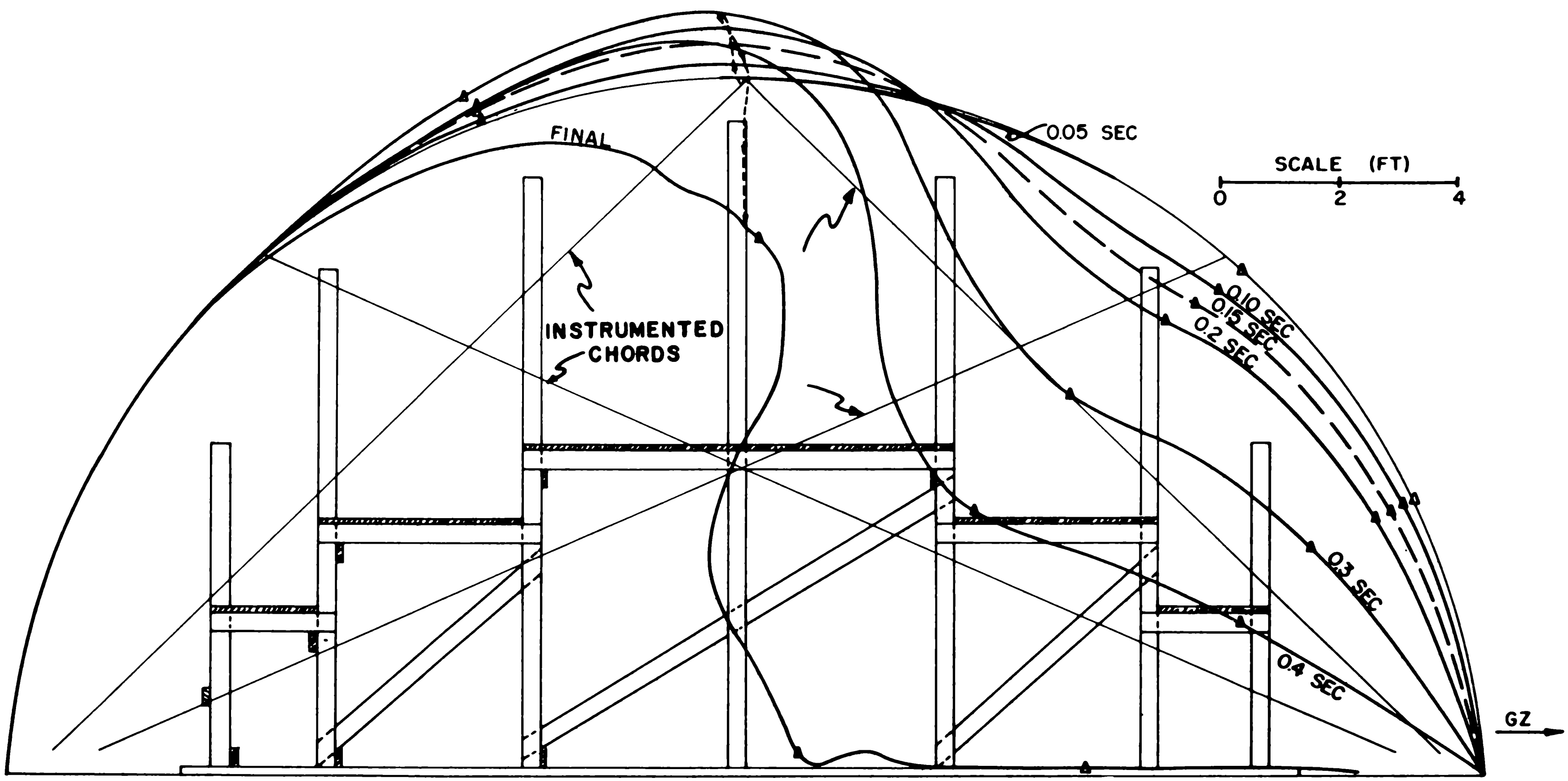

Fig. 6—Profile at various times, building 3.6.

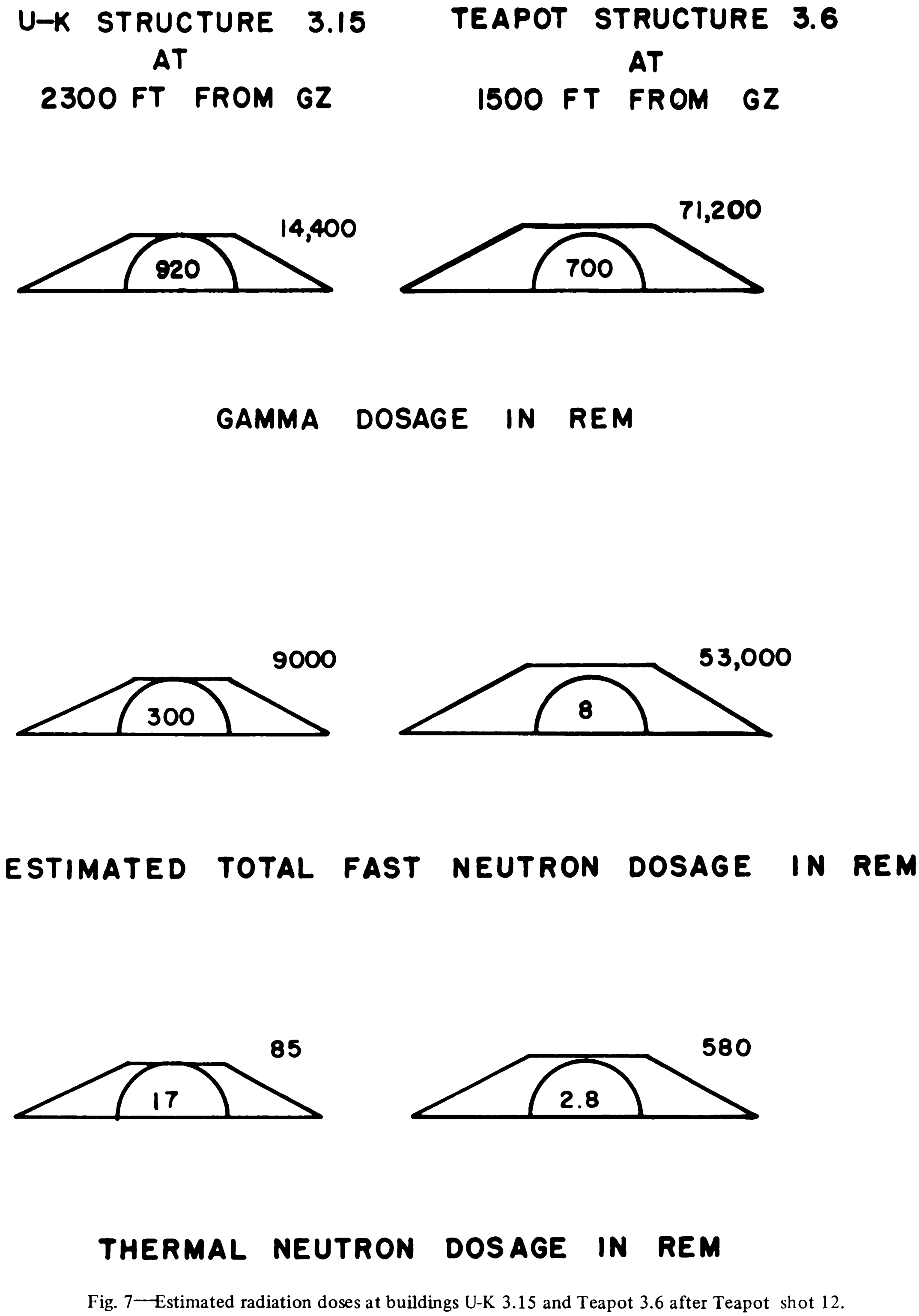

Fig. 7—Estimated radiation doses at buildings U-K 3.15 and Teapot 3.6 after Teapot shot 12.

SUMMARY 12

EFFECTS OF AN ATOMIC EXPLOSION ON GROUP AND FAMILY TYPE SHELTERS

(Report WT-1161, Operation TEAPOT, Projects 34.1 and 34.3, same title, by L. J. Vortman, Sandia Corp., Albuquerque, N. Mex. Technical Associates: Harold Birnbaum and Edward Laing, Ammann & Whitney, Consulting Engineers; Frank G. Ort and Ralph V. Schumacher, Army Chemical Center; and Craig C. Hudson, Sandia Corp., Jan. 21, 1957.)

OBJECTIVES AND SCOPE

The primary purpose of Projects 34.1 and 34.3 was to evaluate shelter designs proposed by the Federal Civil Defense Administration for protection against nuclear and thermal radiation and blast effects. The effectiveness of two types of protective ventilation for buried shelters was also to be evaluated.

Figures 1 and 2 show locations of test structures for Apple I shot and Apple II shot (ref. ENW, p. 674), respectively, and Table 1 gives a summary of the shelters tested. They included two underground shelters (50-man capacity each), one closed (structural, type a) and one open (biomedical, type b), exposed to Apple I shot and two of the same types of underground shelters exposed to Apple II shot; three basement-exit shelters exposed to Apple I shot and four exposed to Apple II shot. Exposed to Apple II shot only were groups of three aboveground utility-type shelters (one of masonry blocks, one of precast reinforced concrete, and one of poured-in-place reinforced concrete); two reinforced-concrete bathroom shelters in rambler-type houses; three types of basement shelter constructed in two frame houses; and two types of basement shelter constructed in two brick houses.

Figures 3 to 20 show details of the test structures. In some cases gauge locations within the shelters are shown.

Instrumentation (Table 1) consisted of Wiancko pressure gauges, q tubes, temperature- and noise-metering devices, gamma-radiation film dosimeters, and neutron detectors. No measurements of structural behavior were made. For demonstration purposes, mannequins were placed in some shelters for Apple II shot.

The effectiveness of two methods of protective ventilation for buried shelters was evaluated by the Army Chemical Corps. The first method (pressurized shelter) used a motor blower with filter units to provide a continuous supply of filtered air and to maintain a positive pressure of purified air within the structure.

The second method (diffusion shelter) for providing the desired protective ventilation depends on a filter medium known as "diffusion board." It is similar to ordinary wallboards, such as Celotex, except that activated charcoal has been added to the wet pulp makeup. This kind of board, when used to form the walls of a protective enclosure, serves as a reactive diffusion barrier.

RESULTS

Structural Damage

UNDERGROUND PERSONNEL SHELTERS (STRUCTURAL AND BIOMEDICAL). *Shot Apple I (Stations 4–34.3 a-1 and b-1 at 1050 ft).* Neither shelter suffered any visible damage at the peak incident pressure of 47 psi. An appreciable amount of dirt and missiles littered the stairwells. The concrete sliding door, as well as the Navy-type door and escape hatch in structural shelter 4–34.3 a-1, was undamaged. The biomedical shelter 4–34.3 b-1 suffered some slight damage to the door and the doorframe.

Blast force distorted the vents projecting from the ground, leaving them bent away from Ground Zero (GZ) at an angle of about 30°.

Shot Apple II (Stations 1–34.3 a-2 and b-2 at 1050 ft). Neither shelter suffered structural damage at 92 psi, but dirt and missiles littered the stairwells. The blast tore off the vent tees at the junction of the tee and the vertical pipe.

In the structural shelter (1–34.3 a-2), the Army Chemical Corps ventilation equipment suffered no discernible damage. Two wheels of the sliding door were destroyed, and the retaining wall around the concrete door was damaged.

In the biomedical shelter (1–34.3 b-2), the peak unbalanced pressure between the chambers was proportionately less than in the Apple I shelter, and the reinforced doorframes in the partition wall sustained no plastic deformation from this unbalanced pressure.

BASEMENT-EXIT SHELTERS. *Shot Apple I (Stations 4–34.1 b-1, b-2, b-3 at 1350 ft).* The closed, partially closed, and open shelters suffered moderate, serious, and severe damage, respectively, caused by an excess of interior over exterior pressure on the walls. Retaining walls failed, exposing reinforcing steel in some places. Shelter walls cracked from tension in the closed and partially closed shelters; in the open shelter the walls either separated from the roof and floor or were badly cracked. Doors on the closed and partially closed shelters failed, indicating that a stronger rebound device would be required. All shelters were littered with dirt and missiles.

Shot Apple II (Stations 1–34.1 c-1, c-2, d-1, d-2). Closed shelters at 1270 ft sustained severe structural damage. All doors blew off in the positive phase, and rebound locks and retaining walls failed under a pressure of 45 psi. Interior walls were cracked and had outward deformations caused by an unbalance of interior over exterior pressure.

Closed shelters at 1470 ft suffered little interior damage, but all doors and retaining walls failed, apparently during the negative phase.

Damage to open shelters at 1270 and 1470 ft was severe and moderate, respectively. From each structure some earth cover was blown away, and vent pipes were either blown away or bent.

UTILITY-TYPE SHELTERS. *Shot Apple II (Stations 1–34.1 e,f,g at 2250 ft).* The masonry shelter disintegrated. The poured-in-place reinforced-concrete shelter remained intact. It was displaced and came to rest on its side 50 ft from its original position. The precast reinforced-concrete shelter failed severely. Door fastenings failed on the poured-in-place structure, and the doors on the precast shelter blew away.

Shot Apple II (Stations 1–34.1 h, i, j at 2750 ft). These three shelters remained in place under slightly more than 10 psi, the design pressure, and suffered no discernible damage. Outer doors were intact, but each interior door was blown off its hinges.

Shot Apple II (Stations 1–34.1 k, l, m at 3750 ft). These shelters suffered no structural damage. Inner doors, however, failed at the hinges and latches at this distance. The bolts latching the outer door of shelter 34.1 m were badly deformed.

INDOOR FAMILY-TYPE SHELTERS. *Shot Apple II (at 4700, 5500, 7800, and 10,500 ft). Basement lean-to shelters* in the brick and the wood-frame houses, at up to 5-psi overpressure, suffered no damage. Despite the fact that the houses at the closer ranges were virtually destroyed, the first-floor framing system did not fail, and there was no debris load in the basement.

Basement corner-room shelters in the same houses as the lean-to shelters were undamaged. The reinforced-concrete basement shelters in the wood-frame houses at 5500 and 7800 ft remained intact.

Reinforced-concrete bathroom shelters in the one-story rambler houses at 4700 and 10,500 ft suffered no damage although the house at 4700 ft was totally destroyed and the shelter was subjected to a pressure of 5 psi.

Radiation

Table 2 gives the radiation summary. The closed underground group personnel shelters provided satisfactory protection from radiation. These shelters had been designed to reduce radiation to at least 25 r. The basement shelters and the utility-type shelters did not provide satisfactory radiation protection, and the reinforced-concrete bathroom shelter at 4700 ft was also unsatisfactory.

Thermal Effects

Temperatures inside the open biomedical shelter were less than had been predicted. Although this shelter would not ordinarily be used as an open shelter, it has shown that occupants of an open similarly designed shelter at this distance would sustain some burns.

Biological Effects

See Summary 13, "Biological Effects of Pressure Phenomena Occurring Inside Protective Shelters Following a Nuclear Detonation;" see also Summary 14, "The Effects of Noise in Blast-Resistant Shelters."

Protective Ventilation

Pressurized Shelter. The 92-psi peak overpressure encountered during the test did not adversely affect the efficiency of the protective ventilation.

Diffusion Shelter. Under the 47-psi shock-wave loading at the shelter location, the protective characteristics of the shelter and its air-filtration system were not impaired by the test detonation.

Table 1—SUMMARY OF SHELTERS TESTED

Project	Structure	Station	Shot	Distance, ft	Desired over-pressure, psi	Actual over-pressure, psi	Gauges
34.1a	Basement lean-to-shelters						
	Brick house	31.1 a-1	Apple II	4,700	5	4.85–5.1	1 pressure
	Brick house	31.1 a-2	Apple II	10,500	1.7		
	Frame house	31.1 b-1	Apple II	5,500	4		
	Frame house	31.1 b-2	Apple II	7,800	2.5		
34.1a	Basement corner-room shelters						
	Brick house	31.1 a-1	Apple II	4,700	5		
	Brick house	31.1 a-2	Apple II	10,500	1.7		
	Frame house	31.1 b-1	Apple II	5,500	4	3.75	1 pressure
	Frame house	31.1 b-2	Apple II	7,800	2.5		
34.1a	Basement reinforced-concrete shelters						
	Frame house	31.1 b-1	Apple II	5,500	4		
	Frame house	31.1 b-2	Apple II	7,800	2.5		
34.1a	Reinforced-concrete bathroom shelters						
	Rambler house	31.1 c-1	Apple II	4,700	5	4.85–5.1	1 pressure
	Rambler house	31.1 c-2	Apple II	10,500	1.7		
34.1b	Masonry utility-	34.1 g	Apple II	2,250	13	11.7	
	type shelters	34.1 j	Apple II	2,750	10	11.6	
		34.1 m	Apple II	3,750	7	7.8	
34.1b	Reinforced-concrete	34.1 f	Apple II	2,250	13	11.7	1 pressure
	utility-type shelters	34.1 i	Apple II	2,750	10	11.6	1 pressure
	(poured-in-place)	34.1 l	Apple II	3,750	7	7.8	1 pressure
34.1b	Reinforced-concrete	34.1 e	Apple II	2,250	13	11.7	
	utility-type	34.1 h	Apple II	2,750	10	11.6	
	shelters (precast)	34.1 k	Apple II	3,750	7	7.8	
34.1b	Basement exit shelters						
	Closed	34.1 b-1	Apple I	1,350	45	17.3	2 pressure
	Partly open	34.1 b-2	Apple I	1,350	45	17.3	2 pressure
	Open	34.1 b-3	Apple I	1,350	45	17.3	2 pressure
	Closed	34.1 c-1	Apple II	1,270	55	44.4	1 pressure
	Open	34.1 c-2	Apple II	1,270	55	44.4	1 pressure
	Closed	34.1 d-1	Apple II	1,470	35		1 pressure
	Open	34.1 d-2	Apple II	1,470	35		1 pressure
34.3	Group shelters						
	Structural	34.3 a-1	Apple I	1,050	100	47	3 pressure, 1 noise
	Biomedical	34.3 b-1	Apple I	1,050	100	47	12 pressure, 1 noise, 2 temperature, 1 dynamic pressure
	Structural	34.3 a-2	Apple II	1,050	100	91.9	3 pressure, 1 noise, 1 acceleration
	Biomedical	34.3 b-2	Apple II	1,050	100	91.9	12 pressure, 1 noise, 2 temperature, 1 dynamic pressure
34.3	Blast line		Apple I	1,050	100	47	1 pressure
			Apple I	1,350	45	17.3	1 pressure
			Apple II	1,050	100	91.9	1 pressure
				1,270	55	44.4	1 pressure
				1,470	35		1 pressure
				2,250	13	11.7	1 pressure
				2,750	10	11.6	1 pressure
				3,750	7	7.8	1 pressure
				4,700	5	4.85–5.1	3 pressure
				10,500	1.7	1.7–2.1	3 pressure
				15,000	1	1.26	1 pressure

Table 2—RADIATION SUMMARY

Shelter	Ground distance, ft	Neutrons/cm^2 Incident Fast	Neutrons/cm^2 Incident Thermal	Neutrons/cm^2 Local Fast	Neutrons/cm^2 Local Thermal	Rep Upper limit	Rep Lower limit	Rem Upper limit	Rem Lower limit	Average gamma inside, r	Total exposure Upper limit, r	Total exposure Lower limit, r	Sick, % Lower	Sick, % Upper	Dead, % Lower	Dead, % Upper
APPLE I																
Underground group																
4–34.3 a-1	1,050	2.87×10^{11}	1.33×10^{8}	1.72×10^{8}		68		109		0.4	109			7	0	0
4–34.3 b-1 (fast-fill)	1,050			7.18×10^{8} (entrance)		285		456		14	470			75		15
4–34.3 b-1 (slow-fill)	1,050									130	586			85		30
Basement-exit																
4–34.1 b-1	1,350	1.39×10^{11}	5.9×10^{12}	$5.9 \times 10^{9\,a}$	$7.3 \times 10^{11\,a}$	2,300	1,800	3,680	2,880	84	3,764	2,964	100	100	100	100
4–34.1 b-2	1,350			$9 \times 10^{9\,a}$	$9.7 \times 10^{11\,a}$	3,500	2,400	5,600	3,840	194	5,794	4,034	100	100	100	100
4–34.1 b-3	1,350			$1.2 \times 10^{10\,a}$	$1.24 \times 10^{12\,a}$	4,700	3,100	7,520	4,960	226	7,746	5,186	100	100	100	100
APPLE II																
Underground group																
1–34.3 a-2	1,050	1.53×10^{12}	3×10^{13}	4.01×10^{8}		160		256		1.57	258		0	45		0
				2.94×10^{7}	2.33×10^{8}	12	<1	19	<1		20.5	2	0	0	0	0
				$<2 \times 10^{6}$	$7.75–8.85 \times 10^{6}$	<1	2	<1	3		2	5	0	0	0	0
1–34.3 b-2 (fast-fill)	1,050			1.62×10^{9}	1.03×10^{11}	650	260	1,040	416	50	1,090	466	75	100	15	100
1–34.3 b-2 (slow-fill)	1,050			5.03×10^{9}	8.56×10^{11}	2,000	2,100	3,200	3,360	460	3,660	3,820	100	100	100	100
Basement-exit																
1–34.1 c-1	1,270	7.6×10^{11}	1.6×10^{13}	3.76×10^{10}	2×10^{12}	15,000	4,900	24,000	7,840	377	24,377	8,217	100	100	100	100
1–34.1 c-2	1,270			5.43×10^{10}	$3.4 \times 10^{12\,b}$	22,000	8,300	35,200	13,300	600	35,800	13,900	100	100	100	100
1–34.1 d-1	1,470	5.2×10^{11}	9.6×10^{12}	1.92×10^{10}	1.18×10^{12}	7,500	2,900	12,000	4,640	229	12,229	4,869	100	100	100	100
1–34.1 d-2	1,470			5.72×10^{10}	2.02×10^{12}	25,000	4,900	40,000	7,840	388	40,388	8,228	100	100	100	100
Utility-type																
1–34.1 e (precast)	2,250	8.8×10^{10}	1.5×10^{12}	$1.55 \times 10^{10\,c}$	$1.51 \times 10^{12\,c}$	6,000	3,700	9,600	5,920	2,650	12,250	8,570	100	100	100	100
1–34.1 f (poured)	2,250			$1.55 \times 10^{10\,c}$	$1.51 \times 10^{12\,c}$	6,000	3,700	9,600	5,920	2,388	11,988	8,308	100	100	100	100
1–34.1 g (masonry)	2,250			1.55×10^{10}	1.51×10^{12}	6,000	3,700	9,600	5,920	7,250[d]	12,020	8,340	100	100	100	100
1–34.1 h (precast)	2,750	3.1×10^{10}	5.1×10^{11}	$5.45 \times 10^{9\,c}$	$5.1 \times 10^{11\,c}$	2,300	1,250	3,680	2,000	1,205	4,885	3,205	100	100	100	100
1–34.1 i (poured)	2,750			$5.45 \times 10^{9\,c}$	$5.1 \times 10^{11\,c}$	2,300	1,250	3,680	2,000	1,075	4,755	3,075	100	100	100	100
1–34.1 j (masonry)	2,750			$5.45 \times 10^{9\,c}$	$5.1 \times 10^{11\,c}$	2,300	1,250	3,680	2,000	1,179	4,859	3,179	100	100	100	100
1–34.1 k (precast)	3,750	4.4×10^{9}	6.9×10^{10}	$7.75 \times 10^{8\,c}$	$6.9 \times 10^{10\,c}$	300	175	480	280	277	757	557	85	95	25	60
1–34.1 l (poured)	3,750			$7.75 \times 10^{8\,c}$	$6.9 \times 10^{10\,c}$	300	175	480	280	275	755	555	85	95	25	60
1–34.1 m (masonry)	3,750			$7.75 \times 10^{8\,c}$	$6.9 \times 10^{10\,c}$	300	175	480	280	226	706	506	80	90	20	50
Bathroom	4,700	8.8×10^{8}	1.1×10^{10}			<350	<25[e]	<560	<40	51	<611	<91	<5	85	0	35
(reinforced concrete)	10,500	1.0×10^{5}	5.8×10^{5}			<1	<1[e]	<1	<1	0.24	<1	<1	0	0	0	0
Basement room	5,500	2.4×10^{8}	2.7×10^{9}			<95	<7[e]	<152	<11	1.77	<154	<13	0	20	0	0
(reinforced concrete)	7,800	6.2×10^{6}	5.2×10^{7}			<2.5	<1[e]	<4	<1	0.20	<4	<1	0	0	0	0
Basement corner room	4,700	8.8×10^{8}	1.1×10^{10}			<350	<25[e]	<560	<40	28	<588	<68	0	85	0	30
	5,500	2.4×10^{8}	2.7×10^{9}			<95	<7[e]	<152	<11	21	<173	<32	0	25	0	0
	7,800	6.2×10^{6}	5.2×10^{7}			<2.5	<1[e]	<4	<1	1.22	<5	<2	0	0	0	0
	10,500	1.0×10^{5}	5.8×10^{5}			<1	<1[e]	<1	<1	0.13	<1	<1	0	0	0	0
Basement lean-to	4,700	8.8×10^{8}	1.1×10^{10}			<350	<25[e]	<560	<40	6.7	<567	<47	0	85	0	30
	5,500	2.4×10^{8}	2.7×10^{9}			<95	<7[e]	<152	<11	2.48	<155	<14	0	20	0	0
	7,800	6.2×10^{6}	5.2×10^{7}			<2.5	<1[e]	<4	<1	0.67	<4	<1	0	0	0	0
	10,500	1.0×10^{5}	5.8×10^{5}			<1	<1[e]	<1	<1	>0.10	<1	<1	0	0	0	0

[a]Estimated as same or intermediate percentage of incident neutron flux as measured in Apple II.
[b]Estimated as same percentage of incident neutron flux as station 1–34.1 d-2.
[c]Estimated as same percentage of incident neutron flux as measured for station 1–34.1 g.
[d]Average of only two dosimeters, both of which read high because of relatively long postshot contact with the ground; 2420 r used for calculations in table.
[e]Based on unadjusted values of estimated external radiation; probably overestimates interior neutron effect by two to four times.

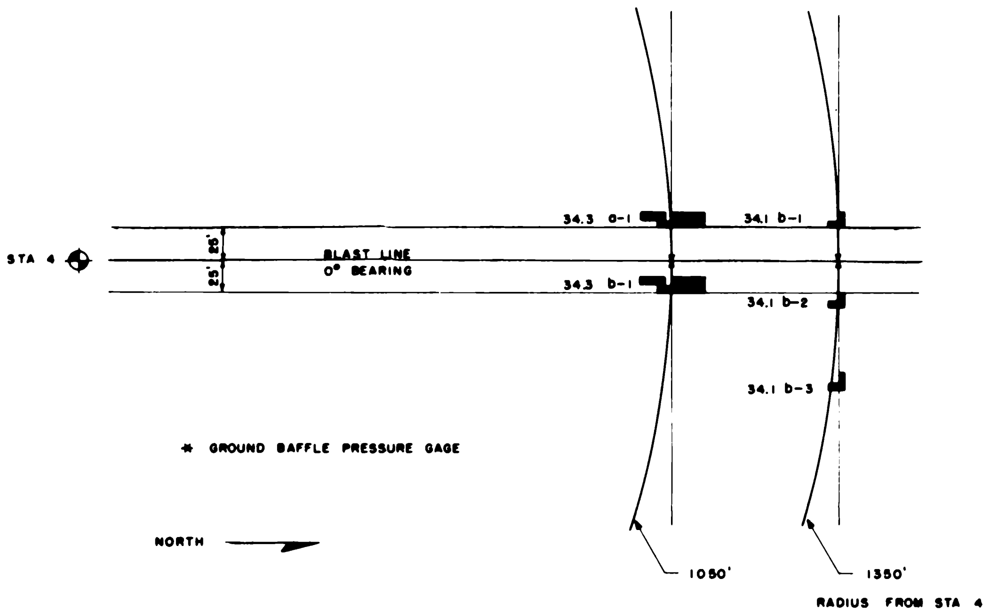

Fig. 1—Location of test structures for Apple I shot.

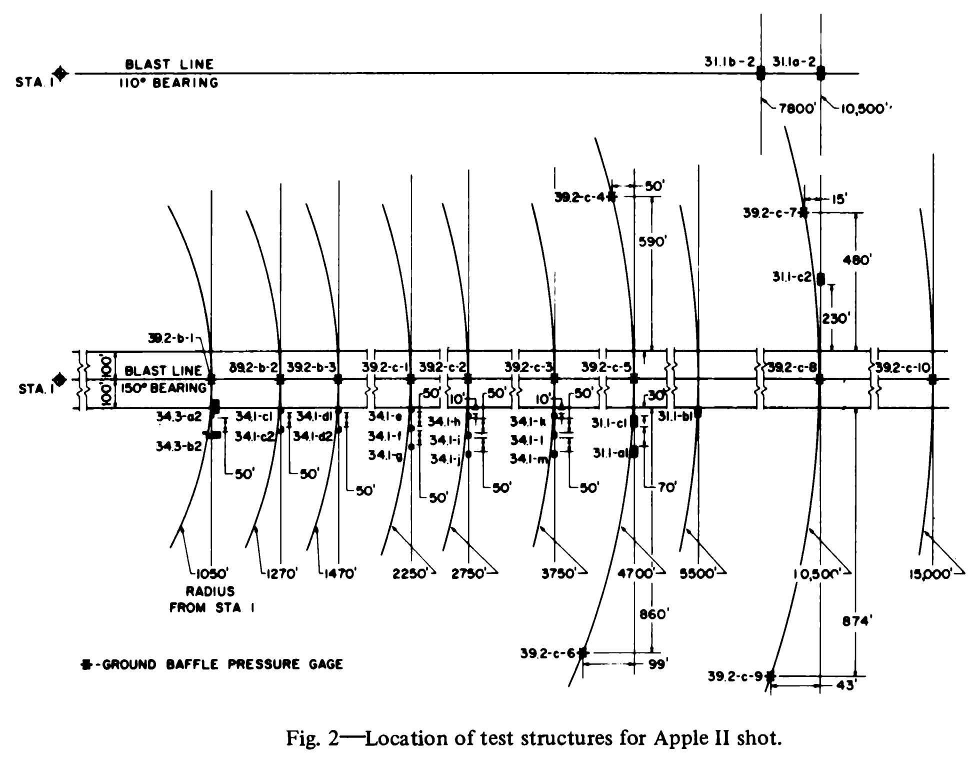

Fig. 2—Location of test structures for Apple II shot.

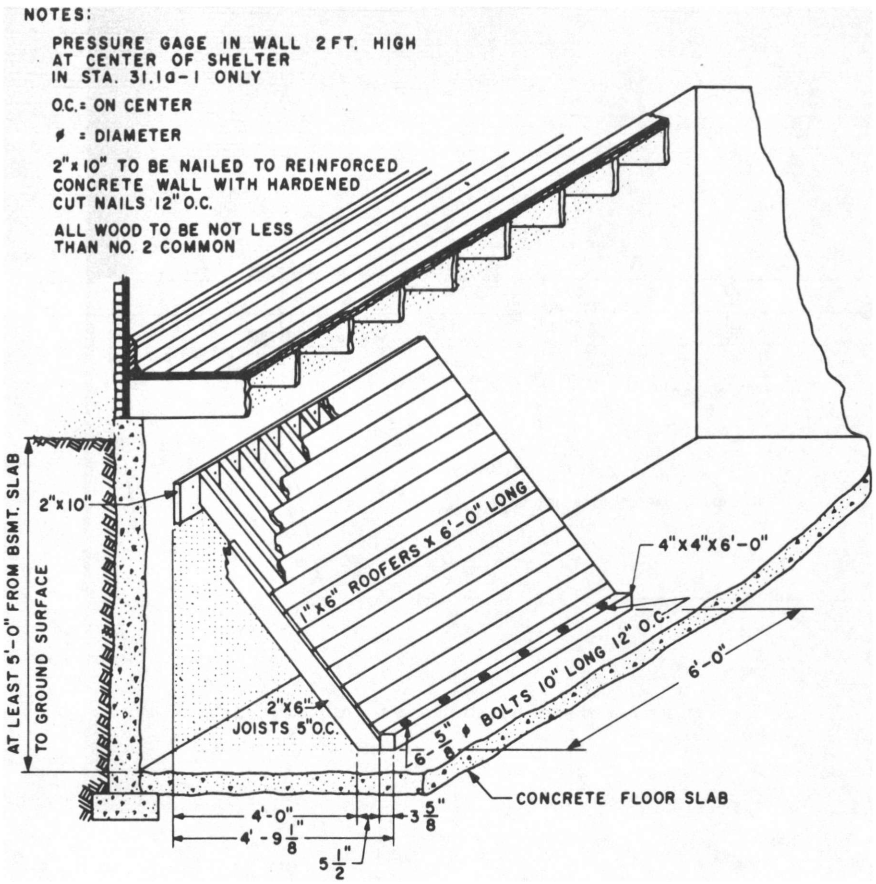

Fig. 3—Sketch of basement lean-to shelter.

Fig. 4—Basement lean-to shelter.

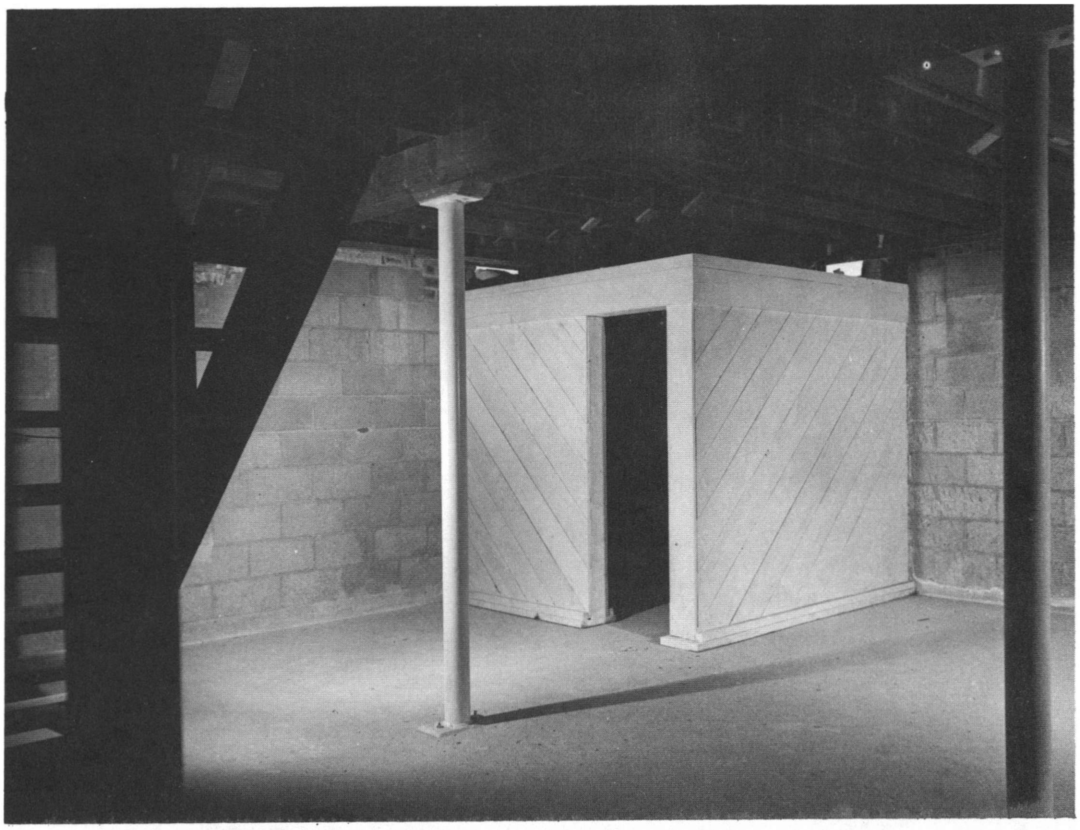

Fig. 5—Basement corner-room shelter.

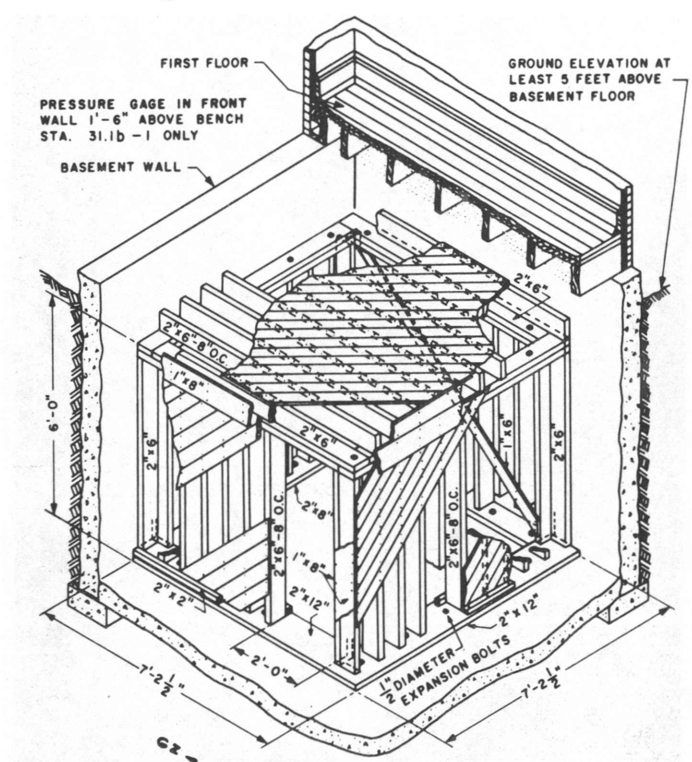

Fig. 6—Sketch of basement corner-room shelter.

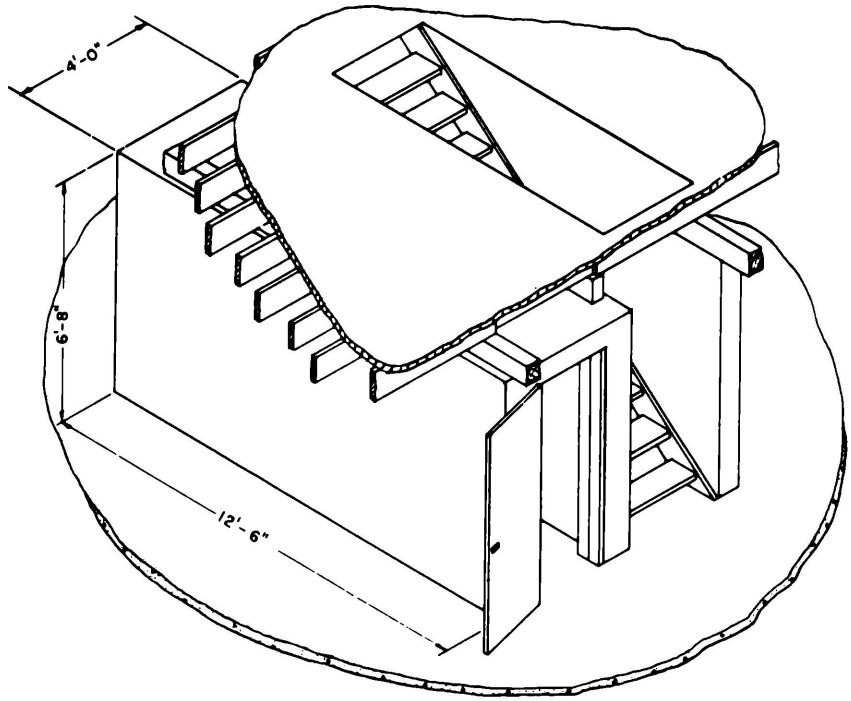

Fig. 7—Sketch of basement concrete-room shelter.

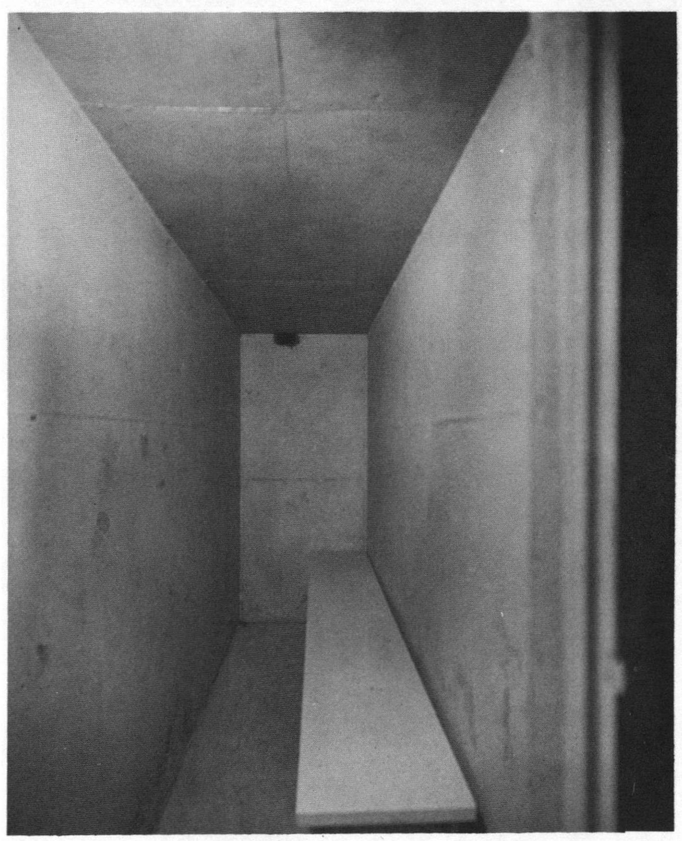

Fig. 8—Interior of basement concrete-room shelter.

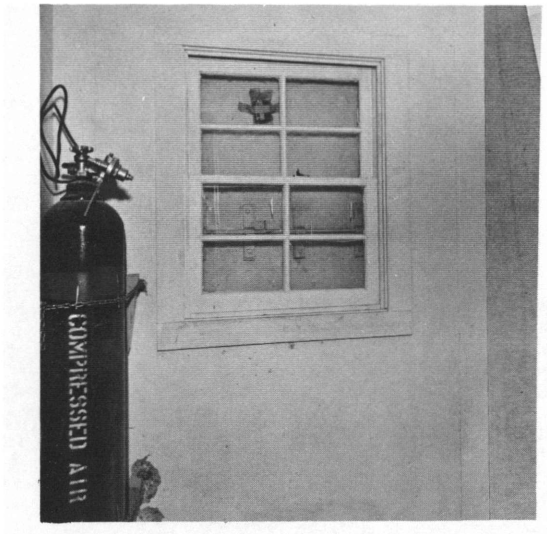

Fig. 9—Interior of concrete bathroom shelter showing window detail.

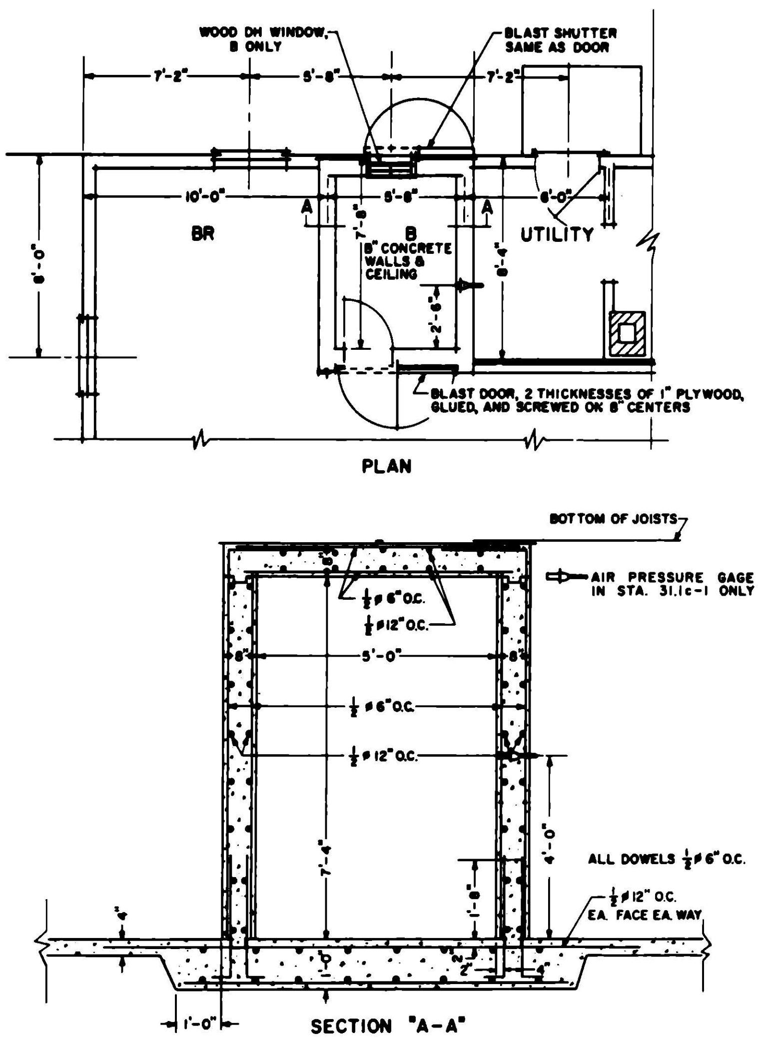

Fig. 10—Plan and section of concrete bathroom shelter.

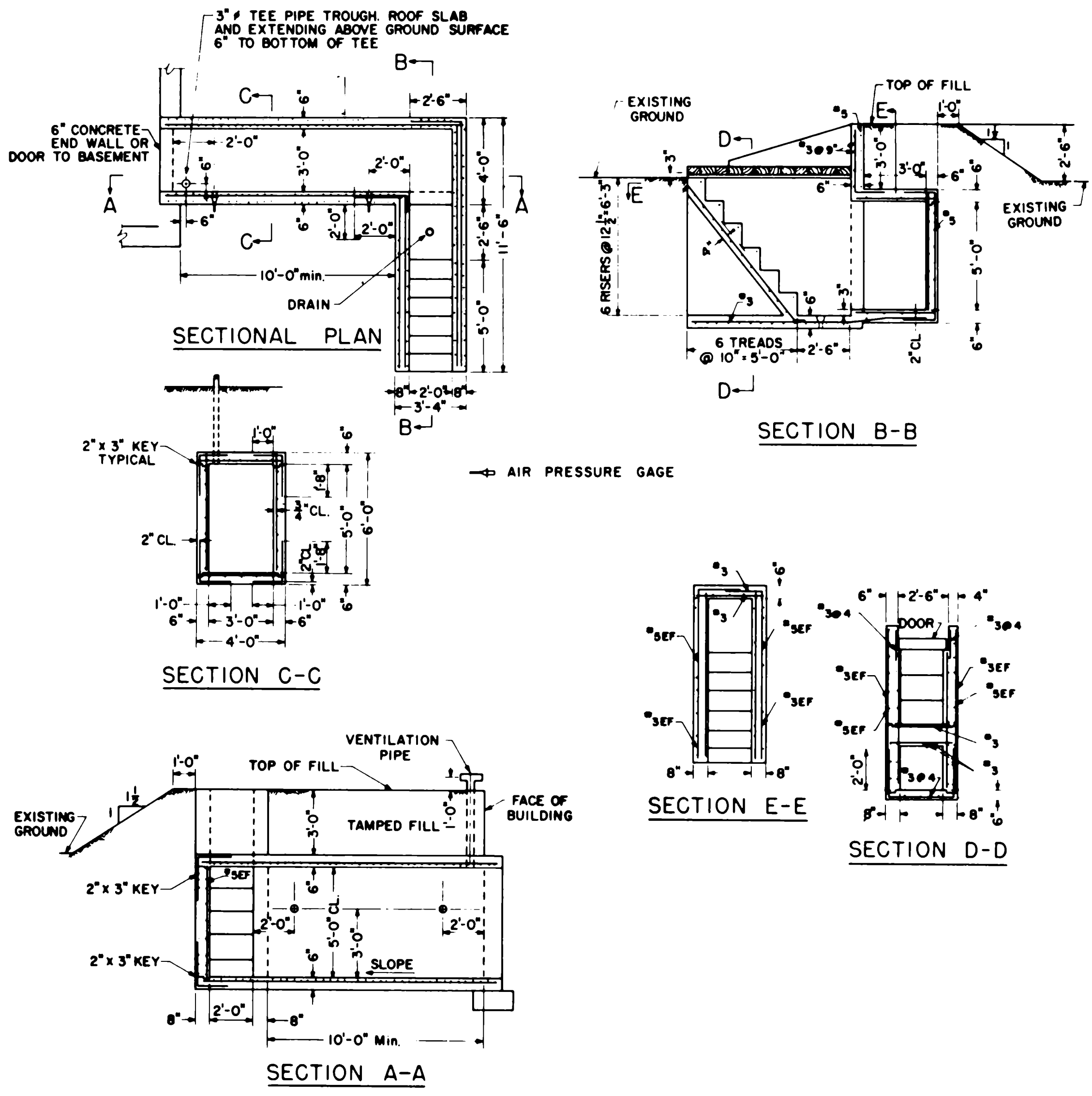

Fig. 11—Details of basement-exit shelter, stations 4–34.1 b, 1–34.1 c, and 1–34.1 d.

Fig. 12—Exterior of basement-exit shelter, stations 4–34.1 b, 1–34.1 c, and 1–34.1 d.

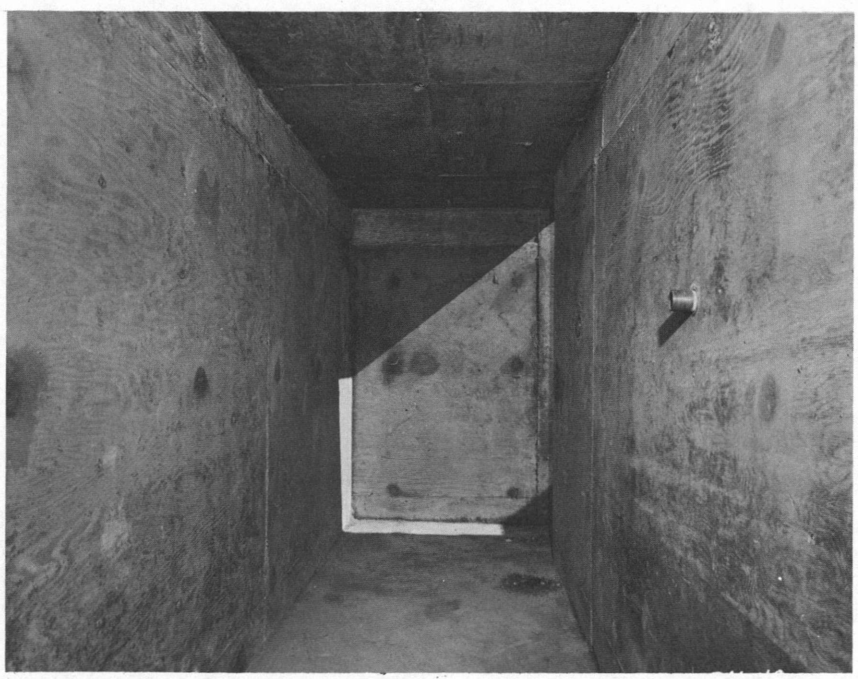

Fig. 13—Interior of basement-exit shelter, stations 4–34.1 b, 1–34.1 c, and 1–34.1 d.

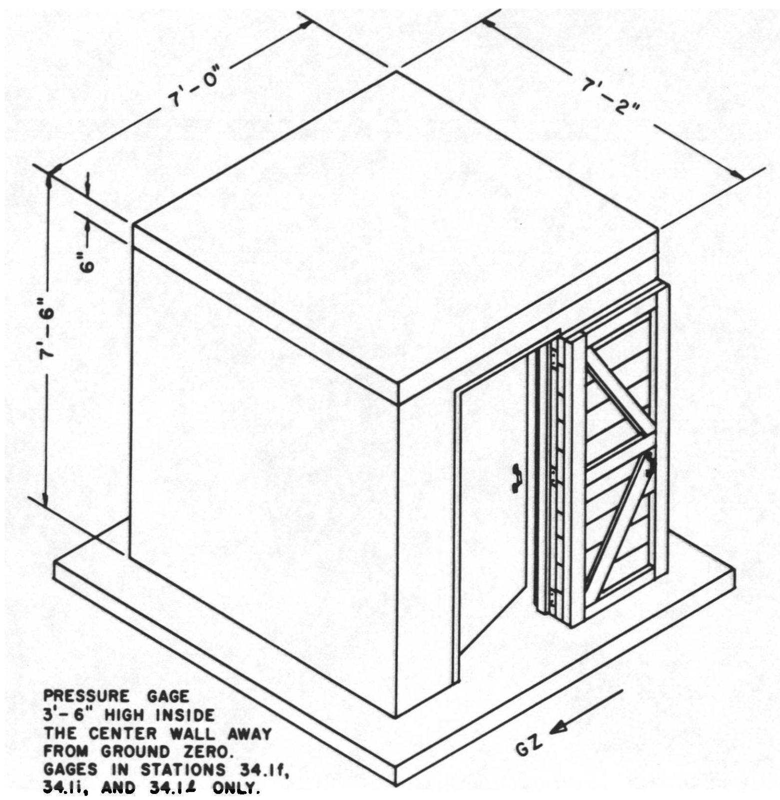

Fig. 14—Sketch of utility-type shelter, stations 1–34.1 e to m.

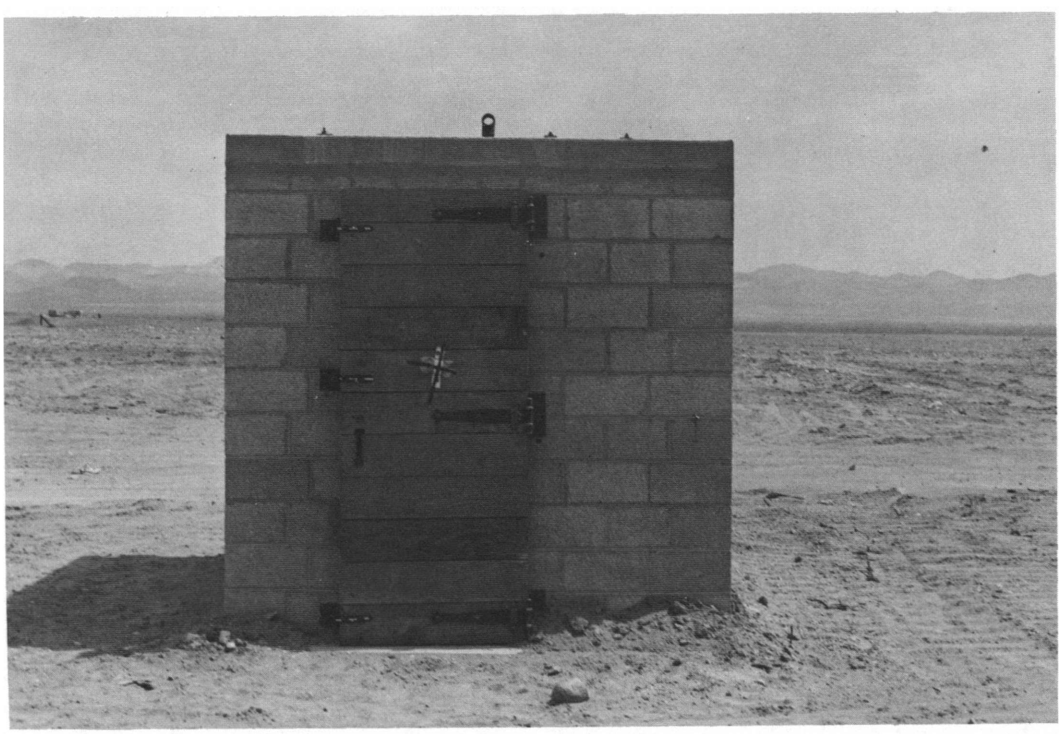

Fig. 15—Exterior of masonry utility-type shelter, stations 1–34.1 g, j, and m.

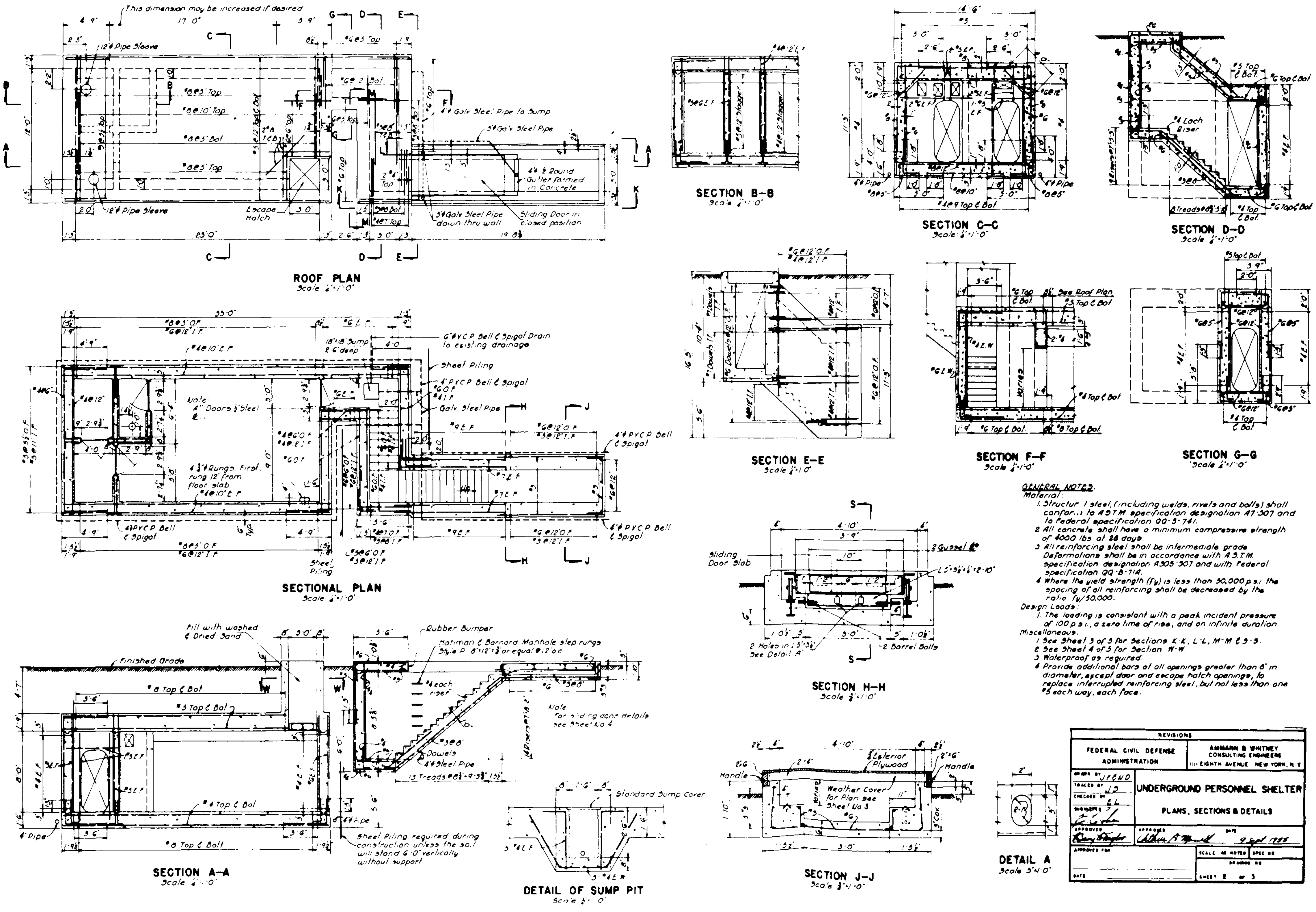

Fig. 16—Plans, sections, and details, underground personnel shelter.

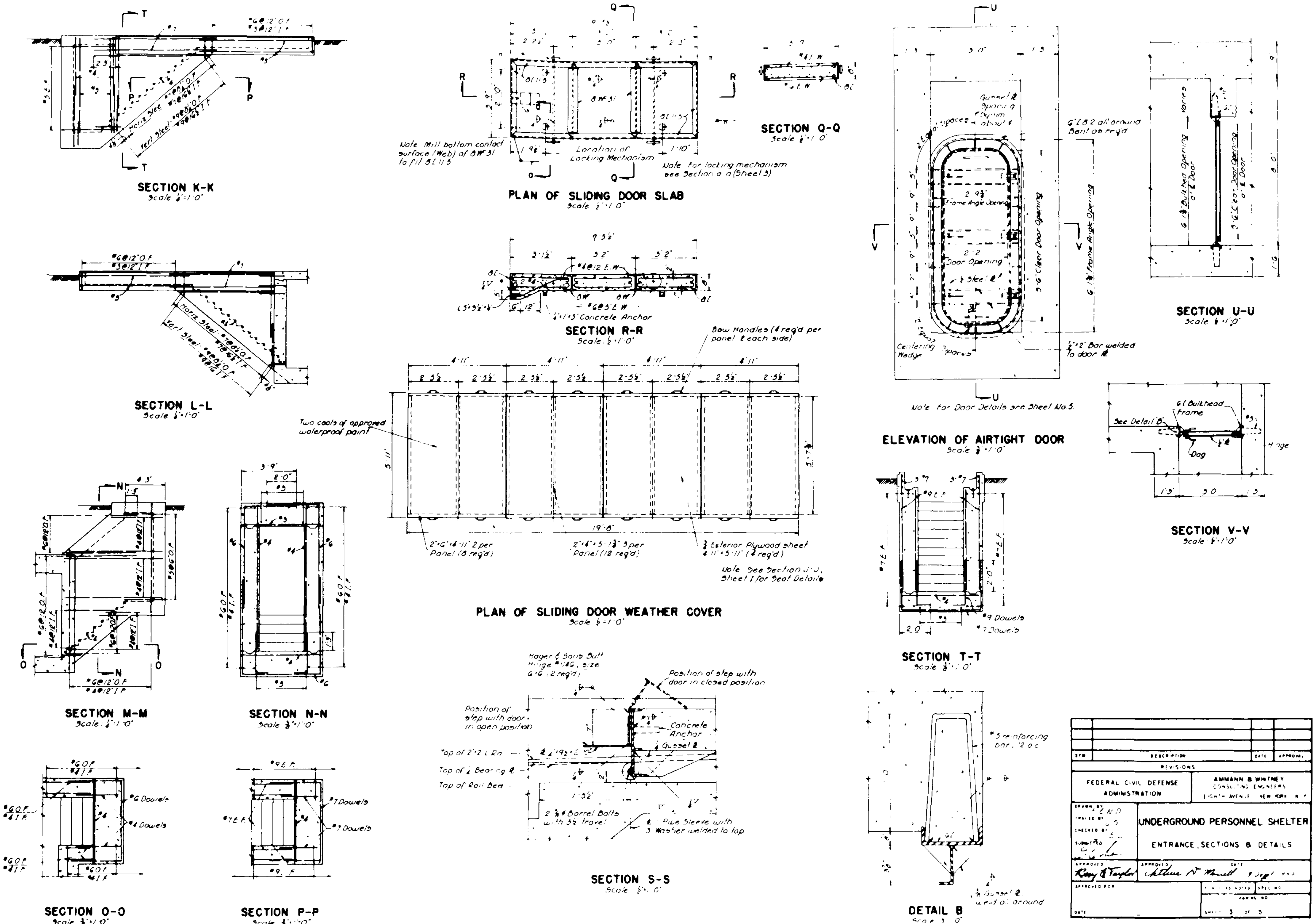

Fig. 17—Entrance details, underground personnel shelter.

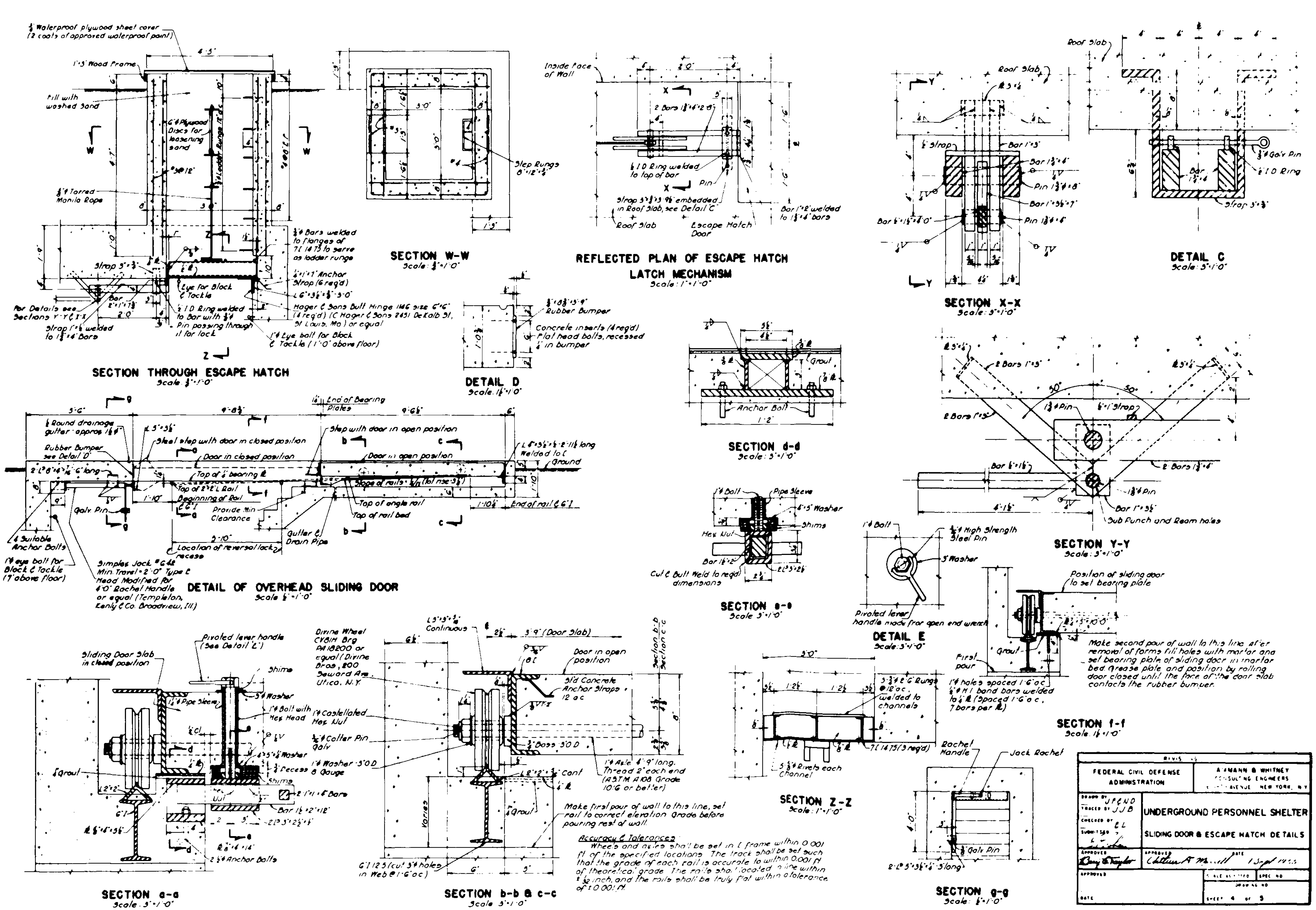

Fig. 18—Sliding-door and escape-hatch details, underground personnel shelter.

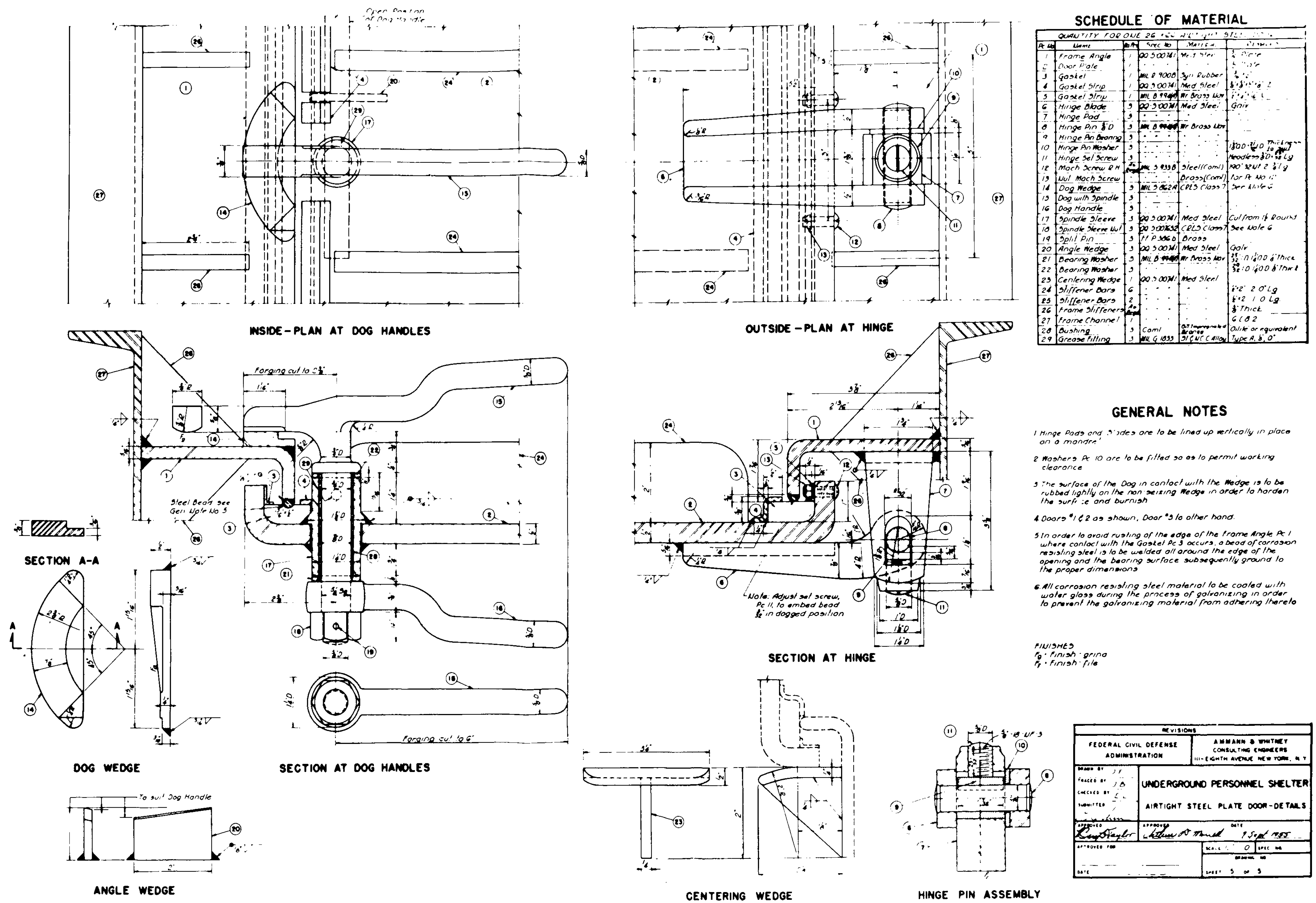

Fig. 19—Airtight steel-plate door details, underground personnel shelter.

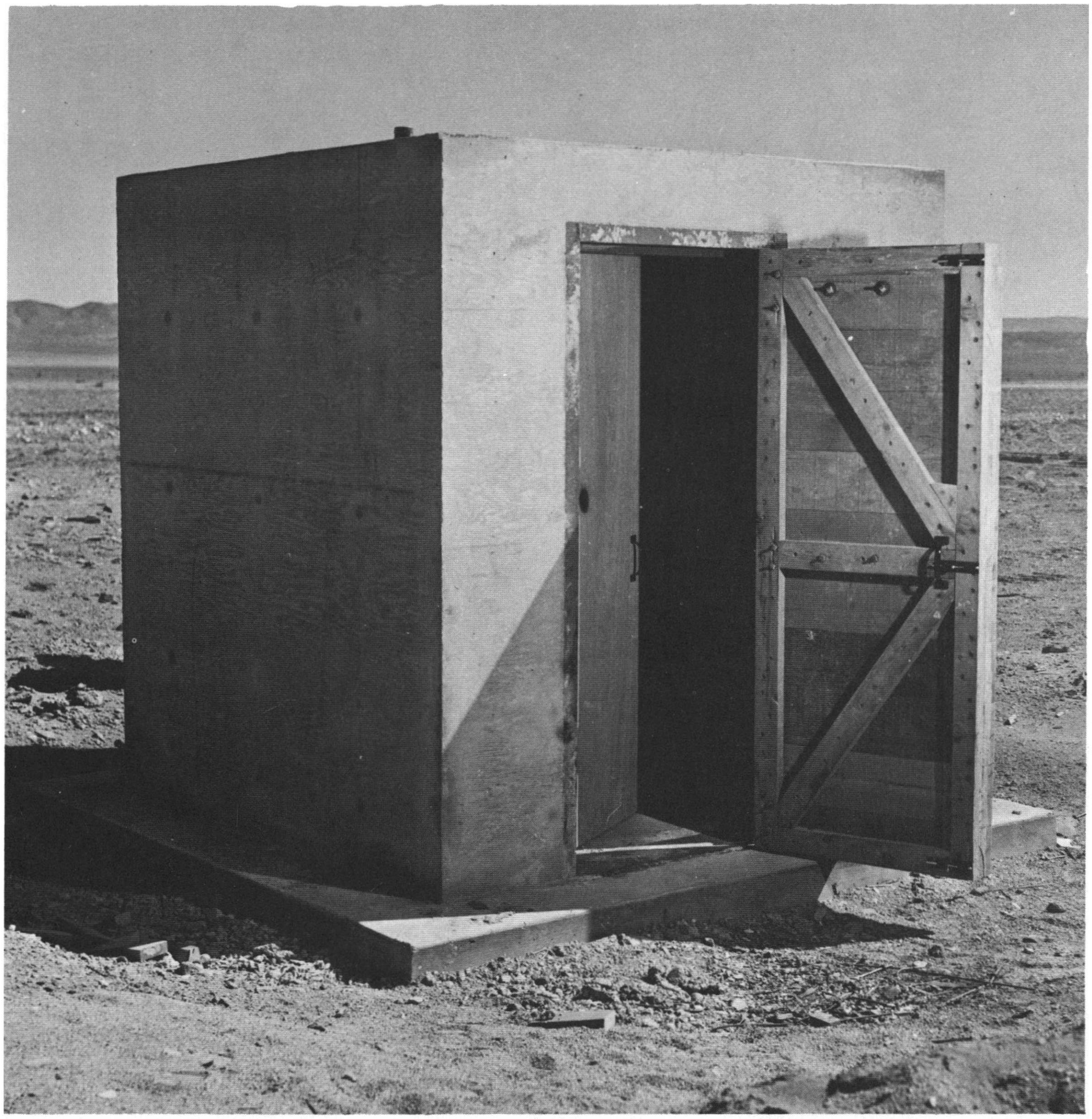

Fig. 20—Exterior of reinforced-concrete utility-type shelter, stations 1–34.1 f, i, and l.

SUMMARY 13

BIOLOGICAL EFFECTS OF PRESSURE PHENOMENA OCCURRING INSIDE PROTECTIVE SHELTERS FOLLOWING A NUCLEAR DETONATION

(Report WT-1179, Operation Teapot, Project 33.1, same title, by C. S. White, et al., Lovelace Foundation for Medical Education and Research, Albuquerque, N. Mex., October 1956.)

OBJECTIVES

The purpose of the experiments was to assess the biological effects of blast by exposing animals to metered variations in pressures produced by nuclear explosions.

EXPERIMENTAL METHOD

In the combined work of the several experiments during two shots (designated Series I and Series II), six types of shelters were used. Summary 12 describes the structural tests and gives information on design, construction, orientation with respect to Ground Zero (GZ), and physical results. Table 1 lists the shelters in the biological experiments and their designations for identification in Summary 12.

The nuclear detonation for the Series I experiments at the Nevada Test Site was the Apple I shot, a 14-kt device exploded on a 500-ft tower. For the Series II experiments, the detonation Apple II, a 29-kt device, was exploded on a 500-ft tower.

One hundred twenty animals were placed in the group shelter and basement-exit shelters for Series I, and 157 animals were placed in shelters for Series II.

RESULTS

Table 2 summarizes the pressure environments and related pathology; it is arranged in the order of increasing overpressures as measured inside the shelters.

DISCUSSION AND CONCLUSIONS

Although these experiments were concerned with the biological effects of blast-produced variations in the environment, the shelter problem also includes thermal and nuclear radiation effects. A satisfactory shelter should provide a total environment that is safe and acceptable for human occupancy. Some of the experimental animals definitely exhibited radiation damage and some were burned.

Concerning the blast, this study demonstrated that the geometry and design of an open shelter, or of a closed shelter in which the entryway fails, may intensify or minimize internal pressure–time phenomena compared with those occurring outside a structure and that displacement due to the dynamic pressure may be more damaging than the overpressure.

Table 1—SHELTERS IN WHICH EXPERIMENTAL ANIMALS WERE EXPOSED

Type of shelter	Interior dimensions, ft	Series I No. of shelters and identification	Series II No. of shelters and identification	Distance from GZ, ft	Overpressure, psi Outside shelter	Overpressure, psi Inside shelter
Group shelter, concrete, underground	12 X 25 X 8; partitioned into two 12 X 12 X 8 chambers	1 34.3 b-1		1050	47	Slow-fill* 6.7 av. Fast-fill* 33.8 av.
Group shelter, concrete, underground	12 X 25 X 8, partitioned into two 12 X 12 X 8 chambers		1 34.3 b-2	1050	91.9	Slow-fill* 22.0 av. Fast-fill* 66.6 av.
Basement-exit shelter, concrete, underground	3 X 12.66 X 5	3 34.1 b-1 (closed)		1350	17.3	12.5 av.
		34.1 b-2 (half-open)†		1350	17.3	42.8 av.
		34.1 b-3 (open)‡		1350	17.3	40.9 av.
Basement-exit shelter, concrete, underground	3 X 12.66 X 5		4 34.1 c-1 (closed)	1270	44.4	71.6
			34.1 c-2 (open)‡	1270	44.4	85.8
			34.1 d-1 (closed)	1470		18.5
			34.1 d-2 (open)‡	1470		53.0 est.
Utility shelter, concrete, aboveground	6 X 6 X 7		3 34.1 f	2250	11.7	Shelter displaced
			34.1 i	2750	11.6	4.3
			34.1 l	3750	7.8	2.6
Bathroom shelter, concrete, aboveground in one-story wood-frame rambler house	7 X 5 X 7.33		1 31.1 c-1	4700	5.1	1.3
Lean-to-shelter, wood, in basement of 2-story brick house	6 X 4 X 5		1 31.1 a-1	4700	5.1	4.6
Corner shelter, wood, in basement of 2-story wood-frame house	6 X 6 X 6		1 31.1 b-1	5500	4.0	3.7

*Both chambers of both group shelters were used as open shelters, the fast-fill chambers by removing the shelter door, the slow-fill chambers by having an open circular escape hatch 19 in. in diameter for Series I and 36 in. in diameter for Series II.

†Entryway half-open.

‡Entryway open.

Table 2—SUMMARY OF PRESSURE ENVIRONMENT AND RELATED PATHOLOGY

Experimental Series	Shelter	Gauge designation	Distance from Ground Zero, ft	Max. internal over-press., psi	Time, msec: Arrival to peak press.	Time, msec: Over-press. duration	Max. internal neg. press., psi	Time to max. neg. press., msec	No. of animals	Animal designation and location	Gross pathology
II	Bathroom	Bath	4700	1.3	419.8	1346.4	−0.77	2338.3	2 dogs	Bath-A	None
										Bath-B	
II	Utility-37	U-37	3750	2.6	276.4	739.8	−1.5	2057.9	2 dogs	U-37-A	
										U-37-B	None
II	Basement corner room	Cor	5500	3.7	131.6	1232.0	−0.67	2501.9	2 dogs	Cor-A	None
										Cor-B	
II	Utility-27	U-27	2750	4.3	265.3	860.8	−1.4	1958.0	2 dogs	U-27-A	
										U-27-B	None
II	Basement lean-to	Lt	4700	4.6	90.0	1051.1	−0.73	2361.9	2 dogs	Lt-A	1 of 4 eardrums ruptured (25%)
										Lt-B	
II	Utility-22	U-22	2250	(Shelter displaced)					2 dogs	U-22-A	Minor lung hemorrhage; left frontal sinus hemorrhage
										U-22-B	Dead of strangulation; subendocardial petechiae; frontal sinus hemorrhage, bilateral
I	Group slow-fill chamber	A-9		6.7	206.3	637.3	−2.7	1050.8	10 dogs	A-9-A to A-12-A	None
		A-10		2.05*	61.0	(Gauge read to 76 msec after arrival)			23 rabbits	Ceiling racks 1, 3, 6, 9, 10; Nos. 21, 23, 26 on table	1 of 5 had minor lung hemorrhage (petechiae); 11 of 24 usable eardrums ruptured (26%)
		A-11		5.14*	120.0	(Gauge read to 491.7 msec after arrival)					
		A-12		4.14*	67.7	(Gauge read to 164.7 msec after arrival					
			Average	6.7	206.3	(Questionable data not included)			24 guinea pigs	Ceiling racks 2, 5, 8, 12; Nos. 22, 24, 25, 27 on table	1 of 5 had minor lung hemorrhage (petechiae); 13 of 28 usable eardrums ruptured (46%)
									27 rats	Ceiling racks 4, 7, 11; Nos. 28, 34 on table	1 of 5 had minor lung hemorrhage (petechiae); 3 of 8 usable eardrums ruptured (38%)

(Table continued on p. 124.)

Table 2—(Continued)

Experimental Series	Shelter	Gauge designation	Distance from Ground Zero, ft	Max. internal over-press., psi	Time, msec: Arrival to peak press.	Time, msec: Over-press. duration	Max. internal neg. press., psi	Time to max. neg. press., msec	No. of animals	Animal designation and location	Gross pathology
									20 mice	Ceiling racks 1, 3, 6, 9, 10	3 of 5 had minor lung hemorrhage (petechiae)
											Sample of 5 animals of each species sacrificed immediately except for mice (all sacrificed)
I	Basement exit, closed	B-1-A		11.5	153.5	(No crossover)			2 dogs	B-1-A	None
		B-1-B		13.5	57.0	735.8	−1.4	1225.7		B-1-B	
			Average	12.5	105.3						
II	Basement exit, closed	B-D-1	1470	18.5	56.9	685.1	−1.9	1286.5	2 dogs	B-D-1	2 of 4 usable eardrums ruptured (50%)
										B-D-1-0	
II	Group slow-fill chamber	Z-9	1050	22.3	130.8	563.3	−3.3	1465.3	10 dogs	Z-9-A to Z-12-B	1 minor lung hemorrhage; 2 hemorrhagic spleens (subcapsular); 1 mucosal tear of urinary bladder; 8 of 12 usable eardrums ruptured (40%)
		Z-10		21.5	139.3	568.1	−2.8	1451.0			
		Z-11		22.8	121.2	567.8	−3.3	1518.0			
		Z-12		21.4	111.8	569.8	−2.7	1492.6			
			Average	22.0	125.8	567.3					
									23 rabbits	Ceiling racks 1, 3, 6, 9, 10; Nos. 21, 23, 31 on table	1 severe lung hemorrhage; 3 minor lung hemorrhages; 18 of 25 usable eardrums ruptured (72%)
									22 guinea pigs	Ceiling racks 2, 5, 8, 12; Nos. 22, 23 on table	1 of 22 expired; 1 severe lung hemorrhage; 4 moderate lung hemorrhages (1 dead); 5 minor lung hemorrhages; 29 of 32 usable eardrums ruptured (91%)

									30 rats	Ceiling racks 4, 7, 11; Nos. 24, 30, BI, BII, BIII on table	3 minor lung hemorrhages; 6 of 8 usable eardrums ruptured (75%)
									20 mice	Ceiling racks 1, 3, 6, 9, 10, 13, 14	17 of 20 expired (85%); 5 severe, 9 moderate, 2 minor lung hemorrhages; 1 pulmonary congestion; 1 subcapsular hemorrhage at liver; 1 had petechiae in mediastinal fat; 1 had petechiae in meninges; 3 survivors, no pathology
I	Group fast-fill chamber	A-1		26.6	85.0	371.3	−2.5	388.0	10 dogs	A-1 to A-8-B	1 displaced — mediastinal and lung hemorrhages, brachial plexis injury, bilateral conjunctivitis; 2 subcapsular splenic hemorrhages; 10 of 20 usable eardrums ruptured (50%)
		A-2		15.5*	21.7	(Gauge read to 20.4 msec after arrival)					
		A-3		35.0	45.3	324.1	−6.4	1460.4			
		A-4		36.3	74.0	626.3	−2.4	896.8			
		A-5		34.1*	73.5	(Gauge read to 75.5 msec after arrival)					
		A-6		36.9	68.1	328.2	−4.4	468.3			
		A-7		34.2*	62.3	(Gauge read to 66.2 msec after arrival)					
		A-8		34.4	73.4	591.9	−2.7	684.6			
			Average	33.8	69.2	448.3	(Questionable values not included)				
		Q-A		12.25	(Read from smoothed curves)						
I	Basement exit, open	B-3-A		38.6	35.5	(Gauge read to 47.5 msec after arrival)			2 dogs	B-3-A	2 of 4 usable eardrums ruptured (50%)
		B-3-B		43.1	5.5	(Gauge read to 28.9 msec after arrival)				B-3-B	
			Average	40.9	20.5						

(Table continued on p. 126.)

Table 2—(Continued)

Experimental Series	Shelter	Gauge designation	Distance from Ground Zero, ft	Max. internal over-press., psi	Time, msec: Arrival to peak press.	Time, msec: Over-press. duration	Max. internal neg. press., psi	Time to max. neg. press., msec	No. of animals	Animal designation and location	Gross pathology
I	Basement exit, half open	B-2-A		38.6	36.6	443.6	−2.9	836.6	2 dogs	B-2-A	Splenic hemorrhage; hemorrhage, right frontal sinus;
		B-2-B		47.0	21.5	(Gauge read to 38.6 msec after arrival)				B-2-B	2 of 4 usable eardrums ruptured (50%)
			Average	42.8	29.1						
II	Basement exit, open	B-D-2	1470	53.0†	5.0†	(Gauges failed)			2 dogs	D-2	Minor lung hemorrhage; mucosal tear of urinary bladder; frontal sinus hemorrhage, bilateral
										D-2-0	Severe lung hemorrhage; 3 of 4 usable eardrums ruptured (75%)
									2 rabbits	15-a, f	1 of 2 usable eardrums ruptured (50%)
									2 guinea pigs	15-b, c	1 minor lung hemorrhage; 2 of 2 usable eardrums ruptured (100%)
									2 rats	15-c, d	None
II	Group fast-fill chamber	Z-1	1050	63.9	108.8	562.0	−3.9	1647.2	10 dogs	Z-1 to Z-8-B	1 fatality due to violent impact (Z-1); 2 others nonfatally displaced (Z-2 and Z-8-B); otherwise: 4 minor lung hemorrhages (Z-½, Z-3, Z-6, Z-8-B); 2 hemorrhagic spleens (Z-½, Z-8-B); 1 pneumothorax (Z-7); 1 had subendocardial petechiae (Z-½); 1 had mesenteric petechiae (Z-8-A); 1 leg fracture (Z-8-B); 10 of 12 usable eardrums ruptured (83%)
		Z-2		64.9	107.4	518.5	−6.0	1835.3			
		Z-3		73.2	90.1	572.3	−4.6	617.1			
		Z-4		67.2	102.5	565.6	−2.2	1172.1			
		Z-5		65.5	91.9	555.1	−5.2	1064.4			
		Z-6		63.6	95.6	546.3	−3.0	682.3			
		Z-7		68.0	96.1	569.0	−2.9	1340.9			
		Z-8		66.5	101.2	556.1	−3.2	1178.0			
			Average	66.6	99.2	555.6					
		Q-Z		12.7	2.2	(Read from smoothed curves)					

									4 rabbits	13-c, d 14-c, d	1 minor lung hemorrhage; 4 of 5 usable eardrums ruptured (80%)
									4 guinea pigs	13-b, e 14-b, e	2 minor lung hemorrhages; 5 of 5 usable eardrums ruptured (100%)
									4 rats	13-a, f 14-a, f	2 minor lung hemorrhages; eardrums not usable
									4 mice	13-g, h 14-g, h	1 fatality — moderate lung hemorrhage; 1 minor lung hemorrhage among 3 survivors
II	Basement exit, closed	B-C-1	1270	71.6	110.9	567.1	−2.9	1571.3	2 dogs	C-1 C-1-0	Mucosal tear, urinary bladder; left frontal sinus hemorrhage; 3 of 3 usable eardrums ruptured (100%)
II	Basement exit, open	B-C-2	1270	85.8	4.0	569.5	−3.3	1131.0	2 dogs	C-2	Moderate lung hemorrhage; splenic hemorrhage; mucosal tear, urinary bladder; subendocardial petechiae; frontal sinus hemorrhage, bilateral
										C-2-0	Moderate lung hemorrhage; left extradural hemorrhage; subendocardial petechiae; frontal sinus hemorrhage, bilateral; 4 of 4 usable eardrums ruptured (100%)

* Questionable data.
† Estimated value.

SUMMARY 14

THE EFFECTS OF NOISE IN BLAST-RESISTANT SHELTERS

(Report WT-1180, Operation Teapot, Project 33.2, same title, by F. G. Hirsch, Joan Longhurst, D. R. McGiboney, and H. H. Sander, Sandia Corporation, Albuquerque, N. Mex., May 1956.)

OBJECTIVES

The primary objective of this study was to determine the effects on rats of noise from a nuclear explosion. A secondary objective was to study the effects of a nuclear explosion on the learning process of rats.

EXPERIMENTAL METHOD

Two nuclear detonations were used for the experiment, and two shelters were used for each detonation. The reinforced-concrete shelters were basically of identical construction, and all were located about 5 ft underground. For each shot, one shelter, 12 by 25 by 8 ft, was closed. The other shelter was divided by a concrete wall into two chambers of identical size, 12 by 12 by 8 ft. Both chambers were used as open shelters, one chamber by removing the shelter door, the other chamber by having open an escape hatch with a circular opening adjusted to 19 in. in diameter for the first shot and to 36 in. in diameter for the second shot. The chamber with the escape hatch is referred to as the slow-fill side. Design and construction details of the shelters are contained in Summary 12. Shelter designations are as follows:

34.3 a-1	Closed	Shot 1
34.3 b-1	Open, partitioned	
34.3 a-2	Closed	Shot 2
34.3 b-2	Open, partitioned	

One hundred seven albino rats were subjects for the study. Some of them were trained and some untrained, some surgically deafened and some not deafened. All shelters were 1050 ft from Ground Zero (GZ). The yield of the first shot was 14 kt and that of the second shot, 29 kt. Both were on 500-ft towers.

RESULTS

First Shot

Incident overpressure outside the shelters was 47 psi.

No useful data concerning noise were obtained from shot 1 although it can be said that the parameter of noise was not found to be of significance.

The animals exposed to shot 1 were untrained; all developed radiation sickness. Although they did learn a discrimination problem postshot, all animals failed to meet the learning criterion. There was no difference in the degree of inability to learn of animals in the closed shelter compared with those in the open shelter. No difference in learning ability was observed between deafened and nondeafened rats. All the unexposed control animals learned the discrimination problem in a normal way.

Second Shot

Incident overpressure outside the shelters was 92 psi.

The measured noise intensity in the slow-fill side of the open shelter was 181 db. The duration of this peak was 35 msec. Measured noise intensity in the closed shelter was 173 db with a duration of 128 msec.

Measured overpressure in the slow-fill chamber was 37 psi; there was no measured overpressure in the closed shelter.

Although a high air-temperature flux of 340 to 360°C was measured in the slow-fill chamber, its duration was too brief to account for the type of burns sustained by the animals. All the rats were burned to some degree, some severely.

The animals when recovered from the open shelter appeared to be fatigued and showed little interest in food and drink. The animals from the closed shelter, by contrast, appeared normal; they were alert, thirsty, and hungry. All rats were made to perform the discrimination test in which they had been trained, beginning with the first animal 14 hr after exposure and concluding with the last exposed animal 19 hr after exposure. No differences in retention in the trained rats were found to exist between the deafened and nondeafened animals, the open-shelter and the closed-shelter groups, nor the exposed and unexposed groups.

The untrained animals in the slow-fill chamber began to sicken and die the fourth day after exposure. These deaths all resulted from ionizing radiation. Thus the results of the effects on learning of the explosion experience were limited to those untrained animals that had been housed in the closed shelter. These animals showed no differences, qualitative or quantitative, in their ability to learn.

CONCLUSIONS

It was concluded that noise as such is not a parameter of importance in bomb-shelter design considerations.

Animals that have been thoroughly trained will not have their learning disturbed by the experience of living through a nuclear explosion while housed in adequate or inadequate (within the limits of this study's design) bomb shelters.

On the other hand, animals that have not been trained will have difficulty in learning new things unless they are housed in adequate shelters.

SUMMARY 15

BLAST LOADING AND RESPONSE OF UNDERGROUND CONCRETE-ARCH PROTECTIVE STRUCTURES

(Report WT-1420, Operation Plumbbob, Project 3.1, same title, by W. J. Flathau, Project Officer, R. A. Breckenridge, and C. K. Wiehle, U.S. Army Engineer Waterways Experiment Station, Corps of Engineers, Vicksburg, Miss., and U.S. Naval Civil Engineering Laboratory, Port Hueneme, Calif., June 1959.)

OBJECTIVES AND SCOPE

The purpose of this project was to evaluate the effects of a nuclear airburst on buried reinforced-concrete arch structures located in the high overpressure region. Since these were to be considered as protective personnel structures, they were evaluated for resistance to blast, radiation, and missile hazards.

Four structures, with the top of the arch crown 4 ft below ground surface, were positioned at three different overpressure ranges for Priscilla shot (ref. ENW, p. 675), a 36.6-kt 700-ft-high burst. All four arches were semicircular in cross section, with an inside span of 16 ft and an arch thickness of 8 in. Three of the structures were 20 ft long; the fourth was 32 ft long. A 20-ft structure was placed at each of the predicted ground-surface air overpressure levels of 50, 100, and 200 psi; the 32-ft-long structure was placed at the 50-psi level. The general location and the shot geometry for the structures are shown in Fig. 1. Figure 2 shows the plan and cross sections of a typical structure.

The four structures were instrumented for measurements of air overpressures, earth pressures, deflections, accelerations, strains, radiation, and missile hazards. Figures 3 and 4 give the instrumentation layouts for structures 3.1a, b, and c, and for structure 3.1n, respectively.

CONSTRUCTION DETAILS

The average concrete compressive strength of the four structures at the time of the Priscilla shot was approximately 4500 psi. Reinforcing-steel properties averaged approximately 50,000 and 74,000 psi for yield and ultimate strength, respectively.

The soil in the test area was uniform in appearance and texture; it was generally classified as clayey silt. The compressibility of the compacted backfill was about equal to that of the natural undisturbed soil when compared by means of similar tests, shown in Table 1. The compressive modulus for the compacted backfill as determined by the Soniscope test was lower than that for the natural soil, possibly as a result of test conditions.

RESULTS

At their various locations the four structures received actual air overpressures of 56, 124, and 199 psi. Suffering only minor damage, they remained structurally serviceable. The structure at the 199-psi pressure level exhibited obvious cracking of the floor slab and minor tension cracking of the arch intrados; however, even though the damage was slight, the peak floor-slab acceleration of 13.4 g might have been physiologically hazardous to personnel.

In general, the buried concrete arches effectively resisted the blast effects from the nuclear detonation. It was observed that the earth loading around the arch surface was not uniform, and that the arch itself underwent appreciable bending. The passive pressure exerted by the soil on the arch surface aided in developing the transmission of the compressive load. The peak transient earth pressures on structure 3.1b (Fig. 5) show that in several instances the earth pressure exceeded the ground-surface air overpressure. Even though the values of pressure were recorded to the nearest 1 psi, some of the values could not be accurately determined because either the range of the calibration or the range of the amplifying equipment was exceeded.

The peak transient radial deflections of the arch with respect to the center of the floor slab for structures 3.1a, b, and c are shown in Fig. 6. The permanent deflection of the crown with respect to the spring line for structures 3.1a, b, and c is compared in Fig. 7, which clearly illustrates the influence of the end walls in restraining arch deflection.

The peak transient accelerations of the floor slabs are shown in Fig. 8. The largest acceleration was a 13.4 g at the spring line of structure 3.1c. The acceleration had a duration of approximately 25 msec.

Strain vs. time records were taken for structure 3.1n only. The largest recorded concrete strain was 575 μin./in. at the crown of the extrados. The largest recorded steel strain, 1000 μin./in. in tension, was in the top steel in the center of the floor slab.

The total radiation dose within structure 3.1a (Fig. 9) shows that the entranceway admitted the major portion of the radiation dose into the structure. Although designed to exclude air overpressure only, the entranceway could easily be modified to greatly reduce the amount of radiation transmitted through it to the structure interior.

No missiles (concrete fragments) were found in the missile traps that had been provided in the structures.

The damage survey, a visual inspection of the interior of the structures, revealed minor damage in the form of small hairline cracks in the floor and in the arch intrados in structures 3.1a and n, small-to-medium cracks (up to $\frac{1}{16}$ in.) in structure 3.1b, and a large number of cracks (up to $\frac{3}{16}$ in. in the floor slab) in structure 3.1c (Fig. 10).

CONCLUSIONS AND RECOMMENDATIONS

The 3.1-type of structure proved to be an adequate shelter for resisting air overpressure of up to 200 psi and showed that an underground reinforced-concrete arch affords excellent protection against nuclear-blast effects. It was indicated, however, that a reasonable design method for underground arches cannot be developed until more is known about the dynamic properties of soil–structure combinations. In this case it was observed that the earth pressure around the relatively stiff arches was nonuniform and slightly asymmetric. This condition, therefore, caused the arch to undergo appreciable bending.

Displacement of the 3.1 structures as a whole, as well as the relative deflection of the crown, is directly proportional to the overpressure, and during the transient loading the structure moved at approximately the same rate and magnitude as the free-field surrounding soil.

The end walls affected arch action for a distance of about $1\frac{1}{2}$ times the arch radius.

Strain-gauge measurements indicated that the largest moments and thrusts occurred near the spring line; this, therefore, would be the probable location of any failure.

The simple type of entranceway used for the structures sealed out the air pressure, but, as predicted, it did not provide adequate radiation protection for personnel.

At high pressure levels (greater than 100 psi), floor slabs that were monolithic with the arch received relatively high magnitude loads and accelerations; this may make it necessary to use shock-mounted flooring to reduce possible adverse physiological effects.

It was recommended that the use of footings be investigated for arch-type structures. The floor slab, poured separately, could then be made much thinner and joined to the footing with some type of flexible water seal. This method of connection would most likely reduce the induced acceleration to the floor slab caused by the air-induced ground shock.

The entranceway should be modified to reduce the radiation admitted to the interior of the structure. This could be accomplished in several ways, e.g., by baffle walls or a 90° horizontal turn in the entranceway.

It was also recommended that simple models be tested in the laboratory to complement future full-scale tests.

Table 1—COMPARISON OF COMPRESSIBILITY CHARACTERISTIC OF NATURAL SOIL WITH COMPACTED BACKFILL

	Natural soil, psi			Compacted backfill, psi		
	Ranged			Ranged		
	From	To	Average	From	To	Average
Modulus of deformation (consolidated tests at applied stress = 50 psi)	2,410	6,080	4,130	3,200	6,950	5,300
Modulus of compression (triaxial tests)	1,500	12,000	6,450	3,850	14,000	7,600
Compressive modulus (Soniscope tests)	223,580	734,050	506,000	130,440	146,340	135,800

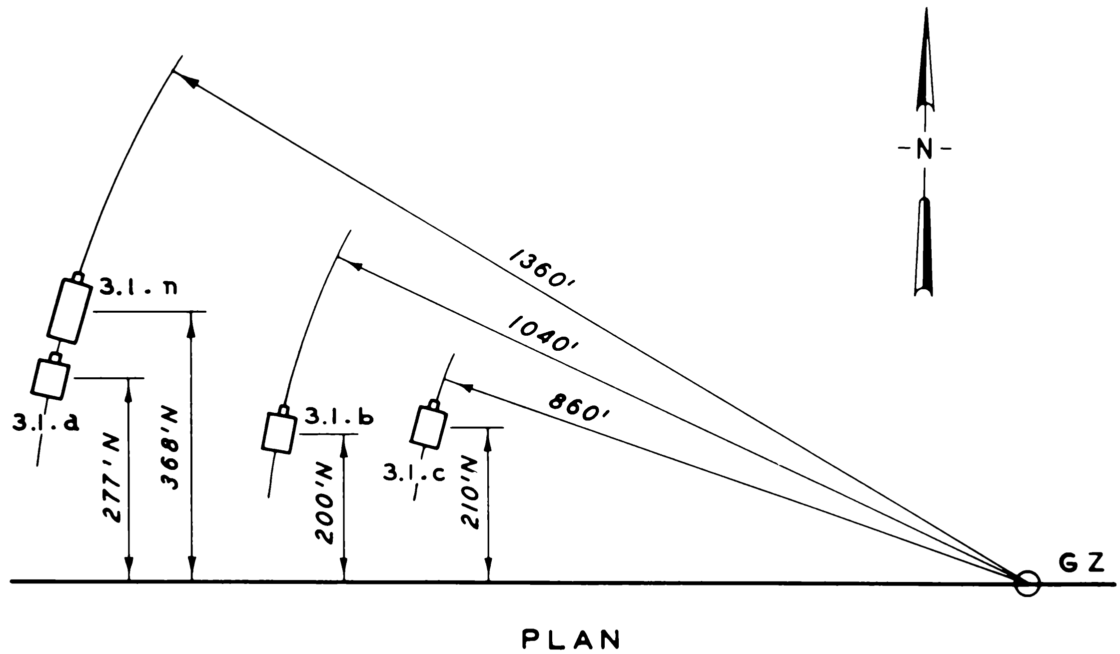

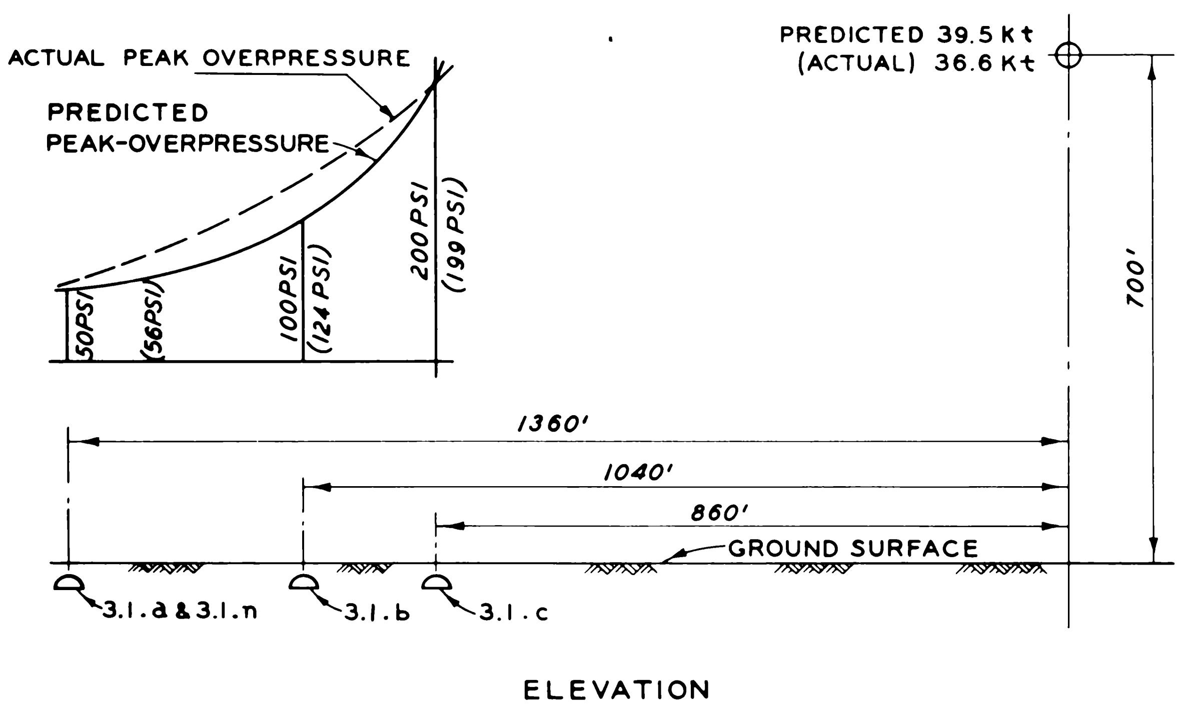

Fig. 1—Project plot plan.

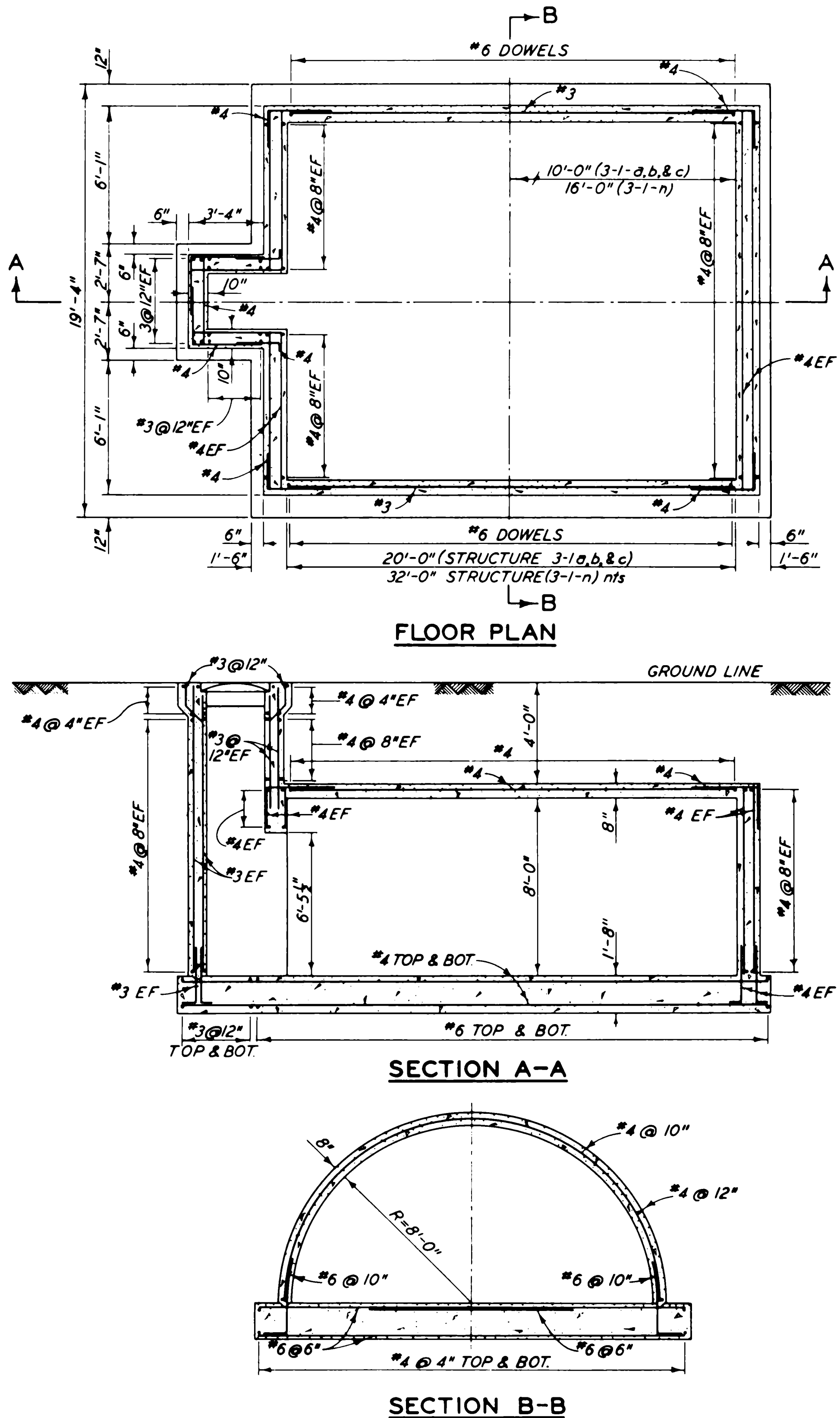

Fig. 2—Plan and elevations of typical structure.

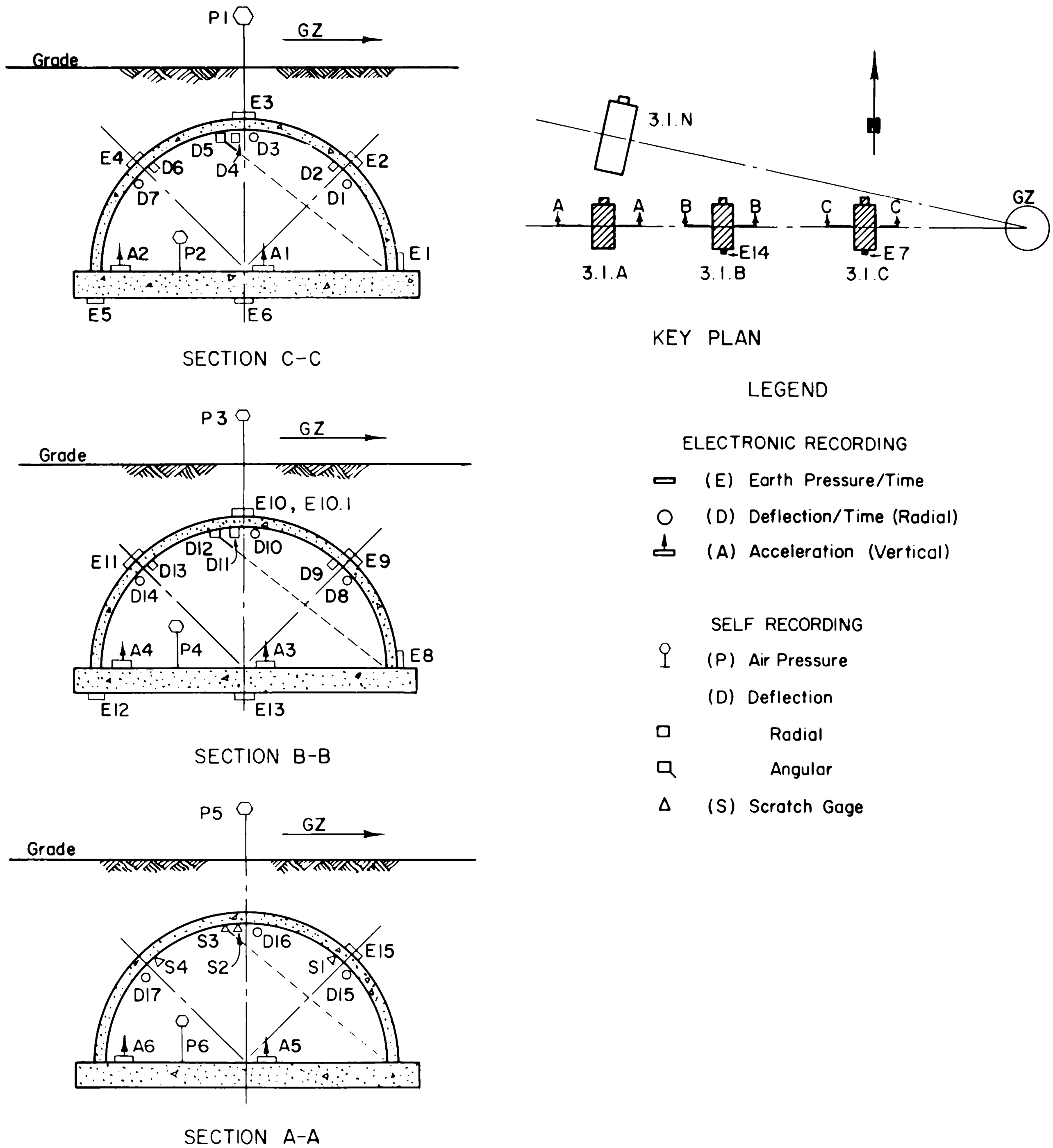

Fig. 3—Instrumentation layout, structures 3.1a, b, and c.

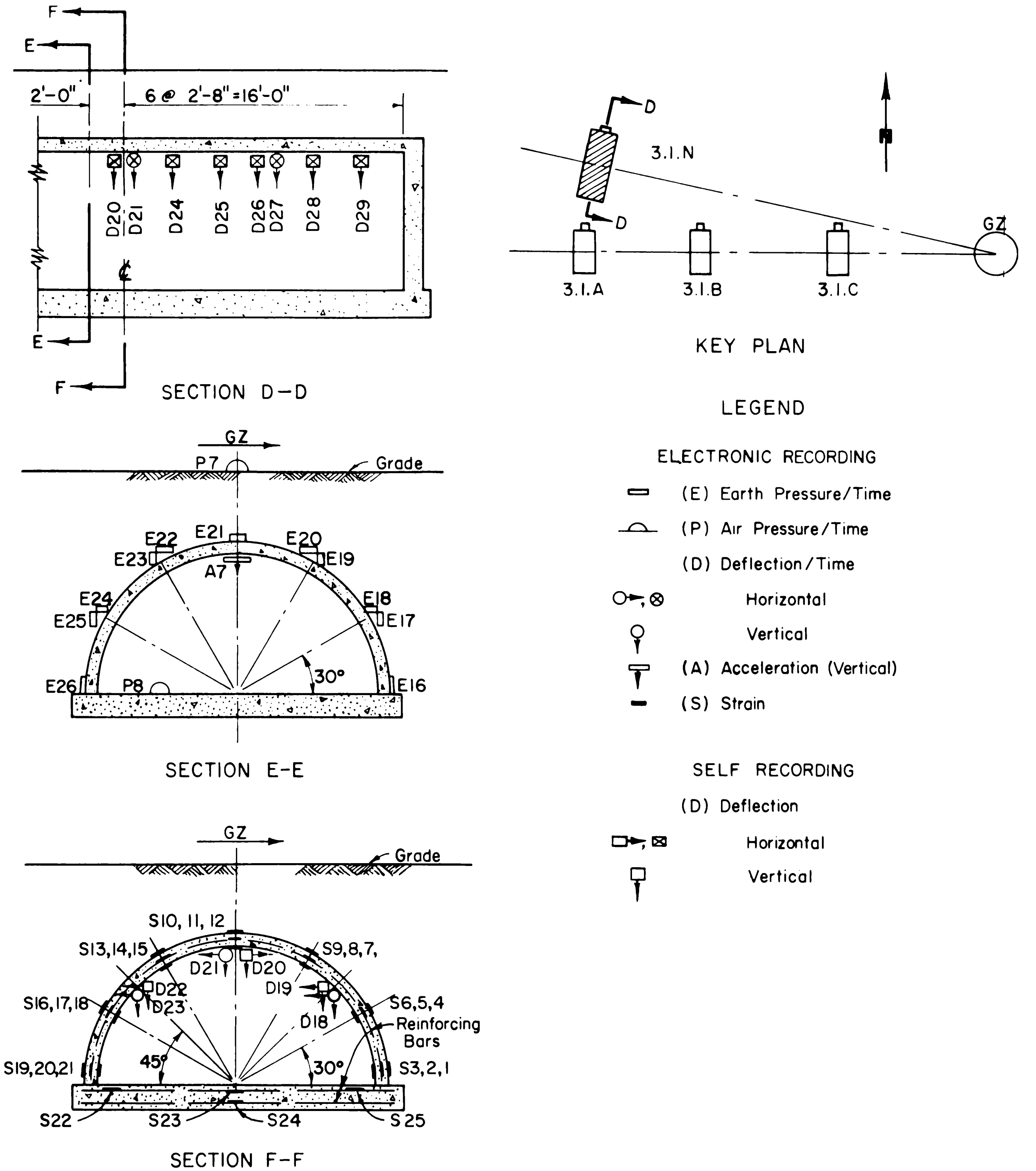

Fig. 4—Instrumentation layout, structure 3.1n.

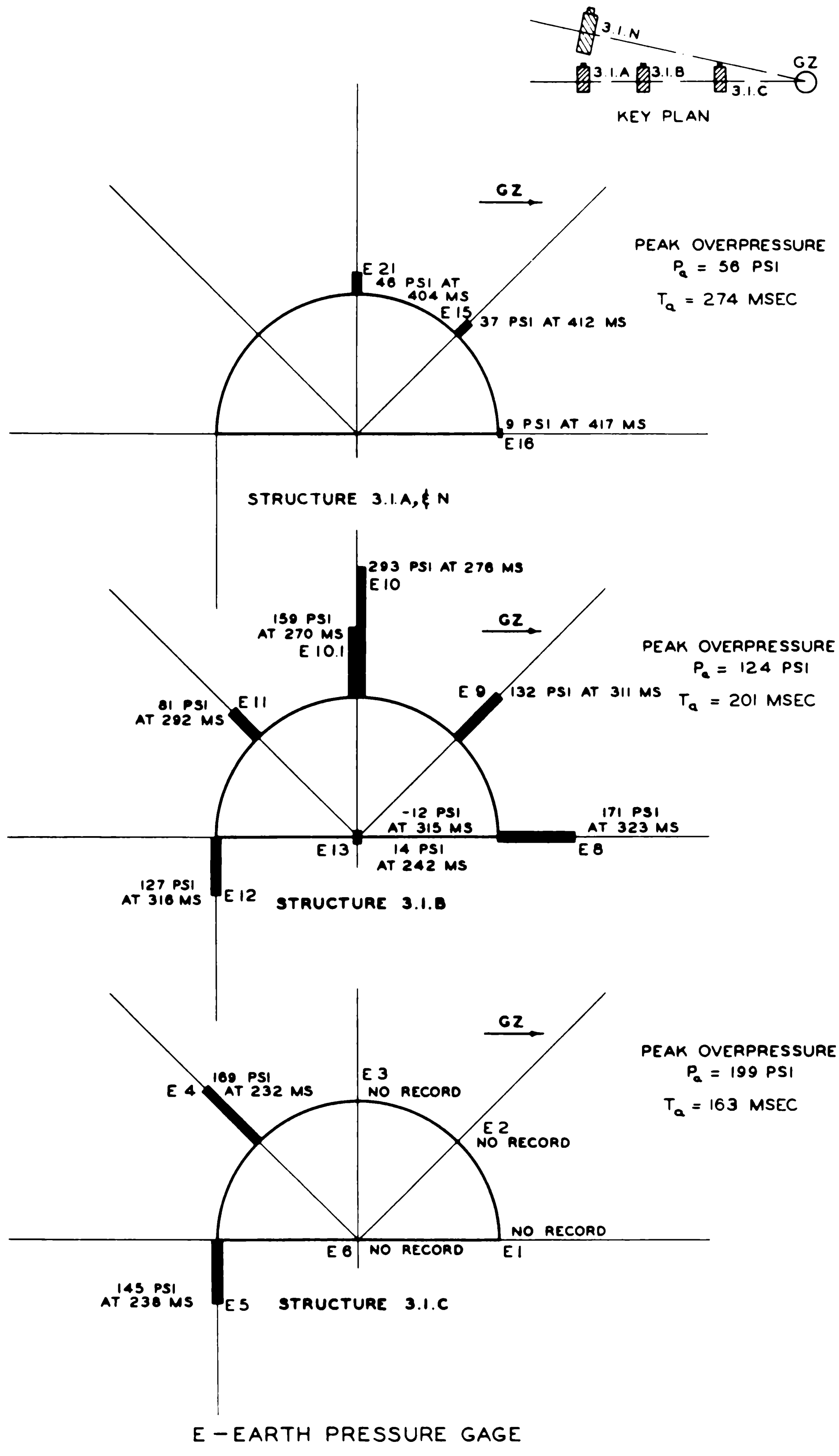

Fig. 5—Peak transient earth pressure, structures 3.1a, b, c, and n.

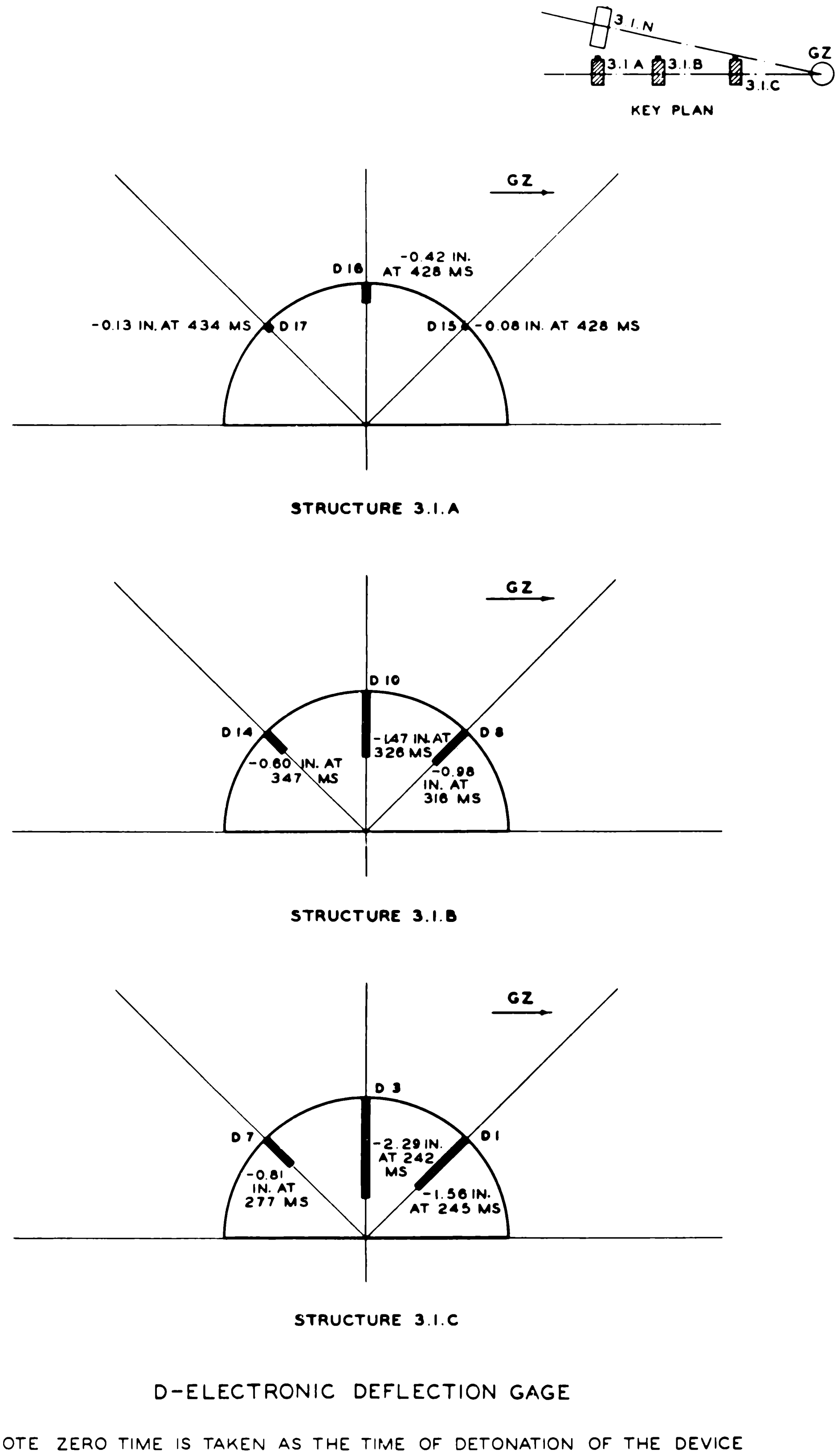

Fig. 6—Peak transient deflection with respect to the center of the floor slab, structures 3.1a, b, and c.

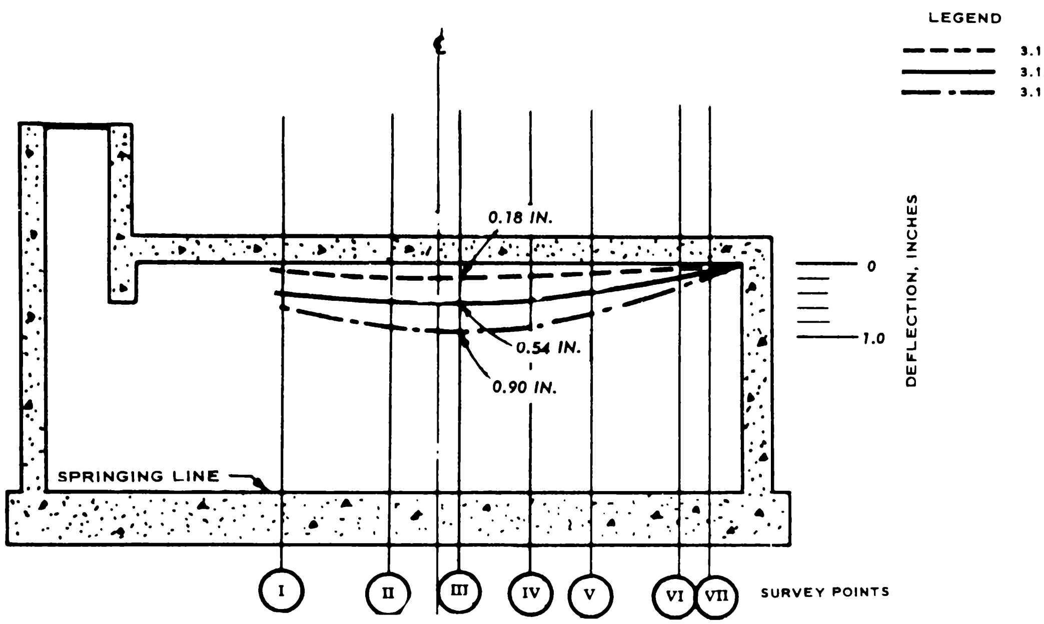

Fig. 7—Permanent crown deflection with respect to the spring line of the arch, structures 3.1a, b, and c.

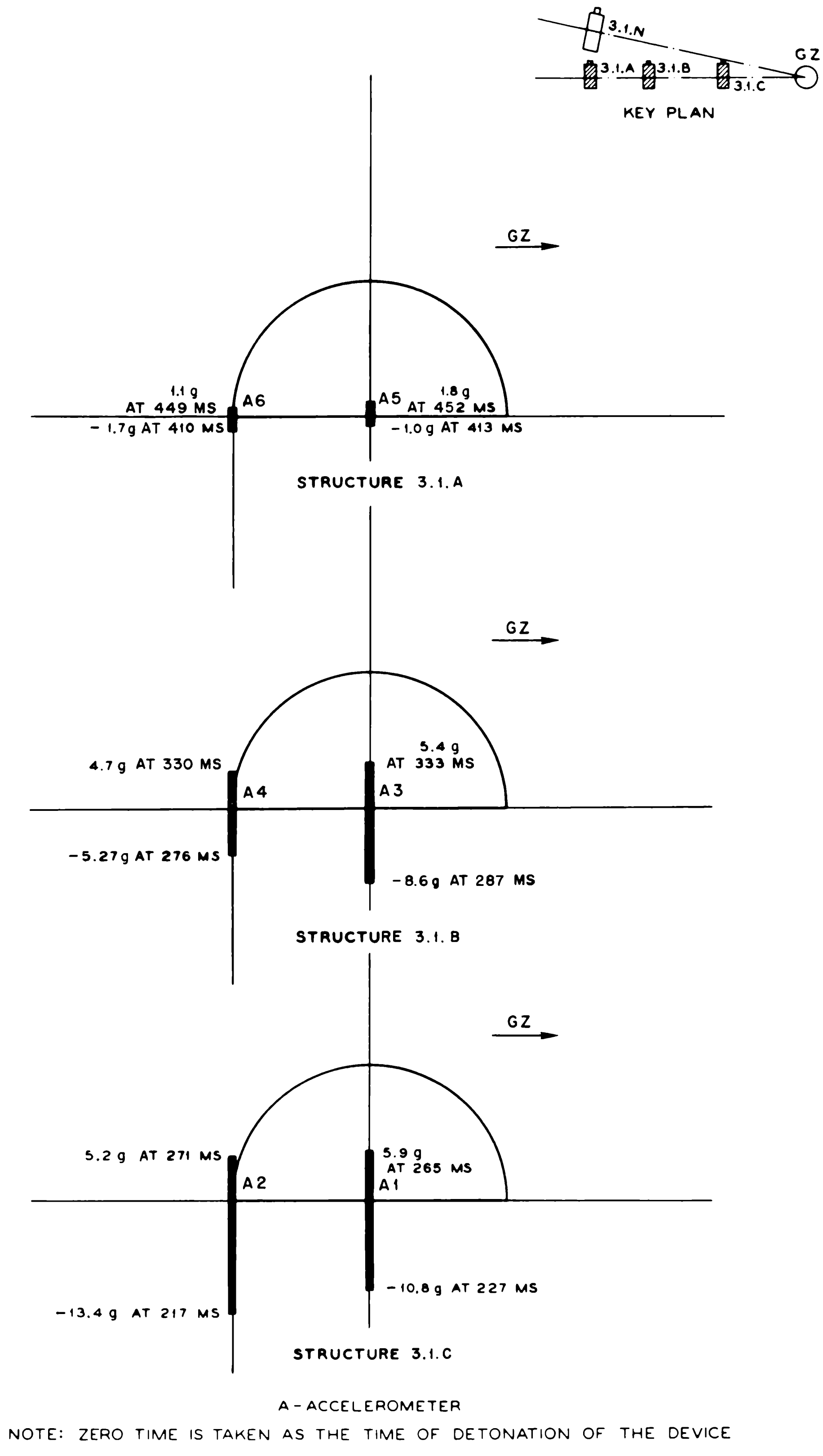

Fig. 8—Peak transient acceleration, structures 3.1a, b, and c.

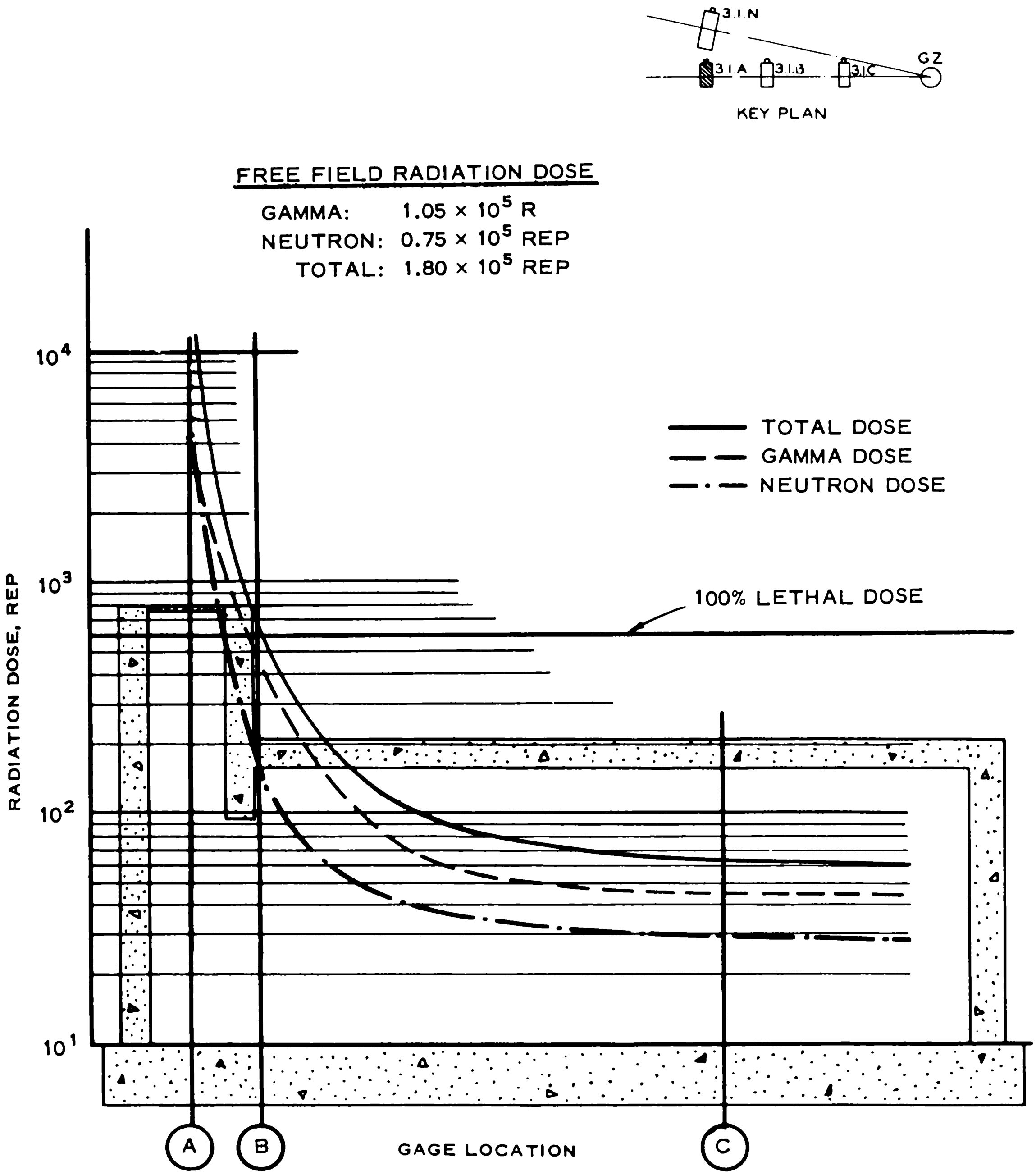

Fig. 9—Total nuclear radiation dose profile, structure 3.1a.

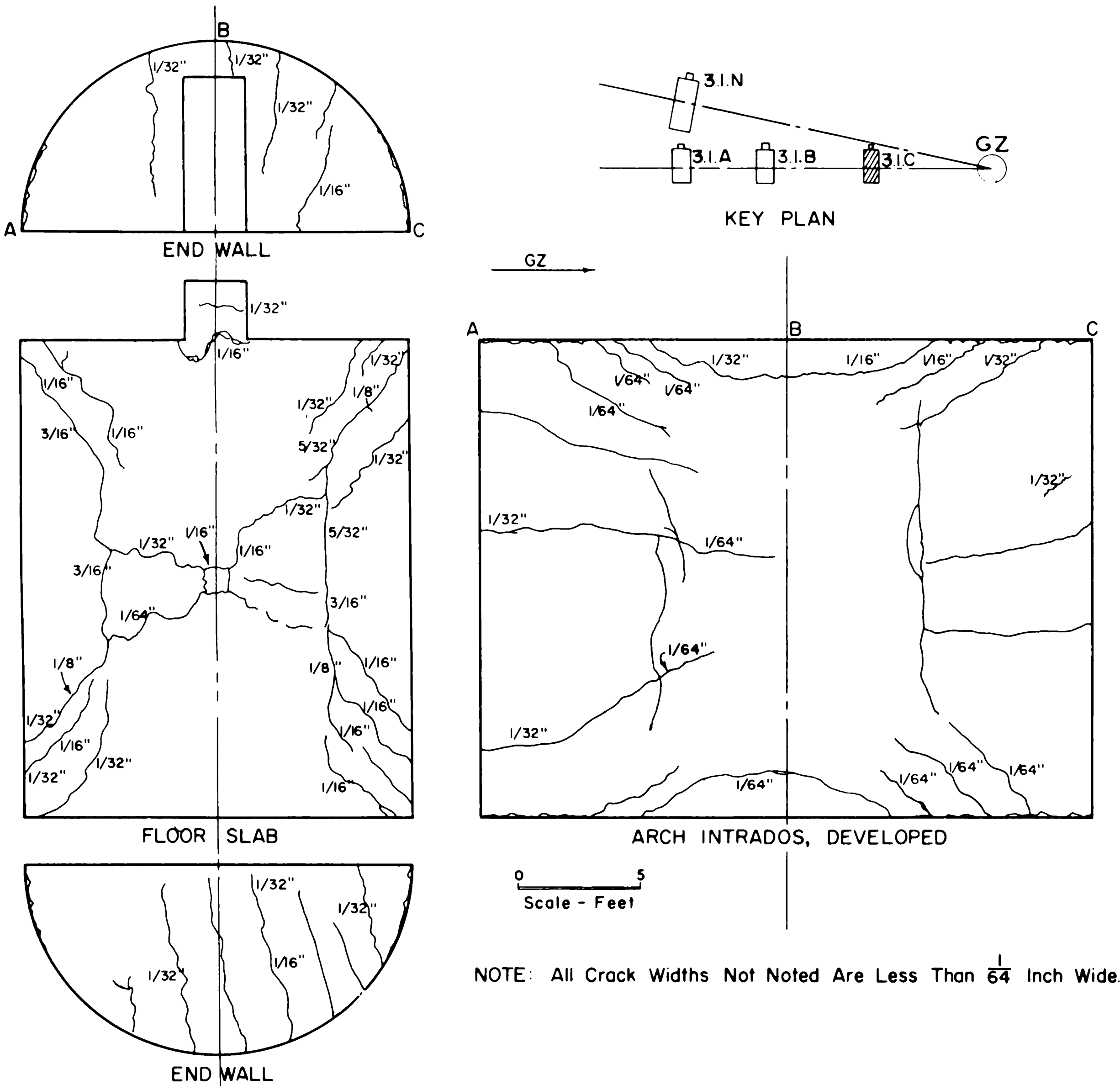

Fig. 10—Postshot crack survey, structure 3.1c.

SUMMARY 16

EVALUATION OF BURIED CONDUITS AS PERSONNEL SHELTERS

(Report WT-1421, Operation Plumbbob, Project 3.2, same title, by G. H. Albright, LTJG, CEC, USNR, Project Officer, J. C. LeDoux, LCDR, CEC, USNR, and R. A. Mitchell, LTJG, CEC, USNR, Bureau of Yards and Docks, Washington, D. C., and U.S. Naval Civil Engineering Laboratory, Port Hueneme, Calif., July 14, 1960.)

OBJECTIVES AND SCOPE

The general purpose of this project was to obtain the information necessary to develop criteria for the selection of standard conduit sections for economical and practical use as buried shelters to protect personnel from the effects of nuclear radiation and air blast in the relatively high pressure region.

Twelve large-diameter commercially available steel and concrete conduits of various shapes were tested in the 60- to 149-psi overpressure region of Priscilla shot (ref. ENW, page 675).

Measurements were made of free-field overpressure at the ground surface above the structures, pressure inside the structures, acceleration and deflection of each structure, dust inside each structure, fragmentary missiles inside the concrete structures, and gamma and neutron radiation dose inside each structure.

TEST STRUCTURES AND INSTRUMENTATION

Table 1 and Fig. 1 show the arrangement of the structures at the test site as well as distances from and orientation toward Ground Zero (GZ). A brief description of the test conduits is given in Table 2. Conduits 3.2a, b, c, f, g, k, and m in Table 2 consisted of curved and flat 10-gauge corrugated-steel sections assembled into 20-ft-long cattle-pass shapes, according to details shown in Figs. 2 and 3.

Conduits 3.2d and h in Table 2 were standard 10-gauge corrugated-steel 8-ft-diameter 20-ft-long test sections. (See Figs. 4 and 5.)

The conduits designated 3.2e, j, and l in Table 2 were standard concrete sewer pipe (Figs. 6 and 7).

For this test particular attention was given to those effects defined as environmental hazards to personnel inside closed underground conduits; these are, specifically, acceleration effects, internal pressure effects, missile hazards, and (in concrete conduits) dust hazards.

Structural instrumentation is summarized in Table 3 and the locations of instruments in the conduits are shown in Fig. 8. For nuclear radiation shielding measurements, gamma film packets and chemical neutron dosimeters were placed in all 12 conduits, and neutron threshold devices were placed in conduit 3.2f.

RESULTS

It was observed that

1. The corrugated-steel cattle-pass conduit with 7.5 ft of earth cover withstood a peak overpressure of 149 psi.
2. The corrugated-steel cattle-pass conduit with 5 ft of earth cover withstood a peak overpressure of 126 psi.
3. The corrugated-steel circular conduit with 7.5 ft of earth cover withstood a peak overpressure of 126 psi.
4. The precast-concrete circular conduit with 7.5 ft of earth cover withstood a peak overpressure of 126 psi.
5. All conduits tested provided adequate protection against nuclear radiation.

Structural measurements, including pressure data, are given in Table 4. Peak downward accelerations of 5 and 8 g, with durations of about 50 msec, were measured at the conduit floor. An upward acceleration of smaller peak magnitude followed the initial downward acceleration.

Peak-pressure gauges indicated overpressures of up to 3.7 psi inside the conduit sections, which may have been caused by a leakage between the individual wood members of the bulkhead; they were included only to provide an economical end closure for the test section.

Measurements of missiles and dust in the concrete conduits in which missile traps were installed indicated that occupants of these shelters would have suffered no real harm. The dust might have been annoying to personnel and might have interfered with certain operations.

Neither direct thermal radiation nor nuclear radiation from fallout were of significance; consequently the radiation of interest consisted of initial gamma and neutron radiation. These are summarized in Table 5.

It was concluded that all types of conduits tested in this project will provide adequate protection, in at least a 100-psi region and comparable radiations, for conditions of loading, soil, dimensions, etc. similar to those in this test.

Table 1—ARRANGEMENT OF CONDUITS AT TEST SITE, PRISCILLA SHOT*

Station	Conduit	Range from GZ to center of structure, ft	Slant range, yd	Angle of sight, deg	Topographic coordinates		Predicted theoretical overpressure at earth surface, psi
					North	East	
9016.01	3.2a	970	399	36	746,889.76	715,271.52	125
9016.02	3.2f	1040	418	34	746,819.76	715,130.58	100
9016.03	3.2c	1040	418	34	746,868.75	715,164.73	100
9016.04	3.2b	1040	418	34	746,915.74	715,201.66	100
9016.05	3.2g	1150	449	31	746,525.82	714,884.17	75
9016.06	3.2m	1360	510	27	746,686.76	714,712.71	50
9016.07	3.2k	1360	510	27	746,957.70	714,839.35	50
9017.01	3.2e	1040	418	34	747,003.73	715,284.11	100
9017.02	3.2j	1150	449	31	746,677.78	714,933.14	75
9017.03	3.2l	1360	510	27	747,007.69	714,871.34	50
9018.01	3.2d	1040	418	34	746,961.73	715,242.36	100
9018.02	3.2h	1150	449	31	746,602.80	714,906.06	75

*Yield, 37 kt; height of detonation, 700 ft.

Table 2—DESCRIPTION OF TEST CONDUITS

Conduit	Nominal depth of earth cover, ft	Type of structure	Material	Internal width, ft	in.	Internal height, ft	in.
3.2a	7.5	Steel cattle pass	Corrugated steel	5	10	7	8
3.2b	10.0	Steel cattle pass	Corrugated steel	5	10	7	8
3.2c	7.5	Steel cattle pass	Corrugated steel	5	10	7	8
3.2d	7.5	Steel circular	Corrugated steel	8		8	
3.2e	7.5	Concrete circular	Precast concrete	8		8	
3.2f	5.0	Steel cattle pass	Corrugated steel	5	10	7	8
3.2g	7.5	Steel cattle pass	Corrugated steel	5	10	7	8
3.2h	7.5	Steel circular	Corrugated steel	8		8	
3.2j	7.5	Concrete circular	Precast concrete	8		8	
3.2k	7.5	Steel cattle pass	Corrugated steel	5	10	7	8
3.2l	7.5	Concrete circular	Precast concrete	8		8	
3.2m	5.0	Steel cattle pass	Corrugated steel	5	10	7	8

Table 3—STRUCTURE INSTRUMENTATION SCHEDULE

Number	Type	Location
12	Deflection gauge (scratch)	One in each of 12 conduits (at top)
4	Self-recording pressure–time gauge (on earth surface)	Conduit 3.2a (125 psi) Conduit 3.2b,c (100 psi) Conduit 3.2h,g (75 psi) Conduit 3.2l (50 psi)
12	Peak internal-pressure gauge	One in each of 12 conduits
12	Peak accelerometer (vertical component)	One in each of 12 conduits
4	Electronic dynamic accelerometer (vertical component)	One in conduit 3.2a (125 psi) One in conduit 3.2f (100 psi) One in conduit 3.2g (75 psi) One in conduit 3.2l (50 psi)

Table 4—STRUCTURAL MEASUREMENTS

Conduit	Station	Nominal depth of earth cover, ft	Peak over-pressure at earth surface, psi	Positive duration of pressure pulse, sec	Peak internal pressure, psi	Peak downward acceleration of bottom conduit, g	Maximum vertical deflection from scratch gauges,* in.	Residual vertical deflection from scratch gauges,* in.	Change in internal height from D + 9 days survey,* in.	Change in internal height from D + 113 days survey,* in.	Change in internal width from D + 9 days survey,* in.	Gross movement of conduit bottom relative to reference point from D + 9 days survey,* in.
3.2a‡	9016.01	7.5	149	0.232	3.7	8.0	−16/16†	−8/16	−16/16	−28/16	−7/16	−5/8
3.2b‡	9016.04	10.0	126	0.206	No record	<5	−17/16	−9/16−	−10/16	−12/16	−5/16	+7/8
3.2c‡	9016.03	7.5	126	0.206	2.0	<5	−14/16†	−4/16	−2/16	−2/16	−6/16	−1 1/2
3.2d§	9018.01	7.5	126		3.0	No record	−12/16†	−8/16	−20/16	−18/16	0	−5/8
3.2e¶	9017.01	7.5	126		3.0	<5	−10/16	−5/16	−20/16	−20/16	+8/16	−1 1/2
3.2f‡	9016.02	5.0	126		3.0	5.0	−16/16	−8/16	−10/16	−10/16	−4/16	+1/8
3.2g‡	9016.05	7.5	100	0.333	2.0	5.0	−10/16	−3/16	−4/16	−4/16	0	−3/4
3.2h§	9018.02	7.5	100	0.333	1.3	<5	−14/16	−8/16	−10/16	−10/16	+4/16	0
3.2j¶	9017.02	7.5	100		3.0	<5	−5/16	−2/16	−12/16	−12/16	0	−1 1/4
3.2k‡	9016.07	7.5	60		1.0	<10	−6/16	+1/16	−2/16	−2/16	−3/16	−1
3.2l¶	9017.03	7.5	60	0.361	1.5	<10	−5/16	−1/16	−10/16	−12/16	+2/16	−1 5/8
3.2m‡	9016.06	5.0	60		1.7	<5	−4/16	+1/16	−14/16	−2/16	−1/16	−1 1/4

*+ Indicates upward deflection, or increase in height or width; − indicates downward deflection, or reduction in height or width.
†Incomplete record.
‡Steel cattle pass.
§Steel circular.
¶Concrete circular.

Table 5—NUCLEAR RADIATION MEASUREMENTS

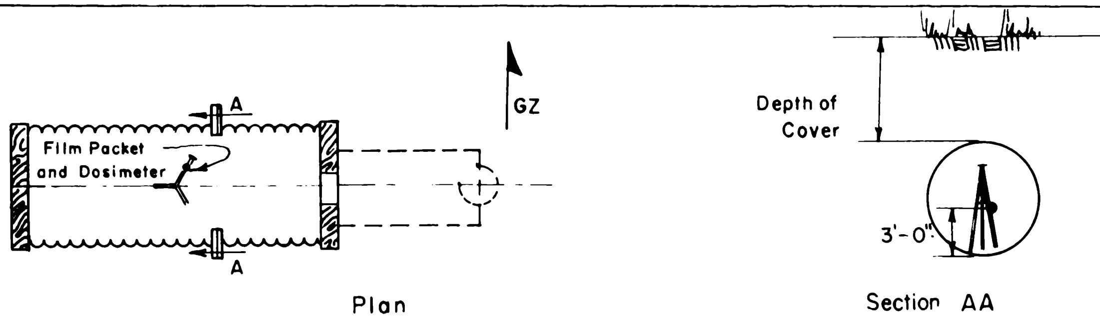

Conduit	Depth of earth cover, ft	Free-field measurements		Measurements inside conduits			
				Gamma dose, r		Neutron dose, rep	
		Gamma dose, r	Neutron dose, rep	Film packet	Chemical dosimeter	Foil method	Chemical dosimeter
3.2a	7.5	2.35×10^5	1.42×10^5	0.2	<5	*	<10
3.2b	10.0	1.89×10^5	1.62×10^5	0	<5	*	<10
3.2c	7.5	1.89×10^5	1.62×10^5	0	<5	*	<10
3.2d	7.5	1.89×10^5	1.62×10^5	0	<5	*	<10
3.2e	7.5	1.89×10^5	1.62×10^5	0	<5	*	<10
3.2f	5.0	1.89×10^5	1.62×10^5	7.7	<5	<25	<10
3.2g	7.5	1.35×10^5	1.24×10^5	0	<50†	*	<50†
3.2h	7.5	1.35×10^5	1.24×10^5	0	<5	*	<10
3.2j	7.5	1.35×10^5	1.24×10^5	0	<5	*	<10
3.2k	7.5	1.02×10^5	7.65×10^4	0	<5	*	<10
3.2l	7.5	1.02×10^5	7.65×10^4	0	<5	*	<10
3.2m	5.0	1.02×10^5	7.65×10^4	1.3	<5	*	<10

*Not instrumented.
†High-range dosimeter accidentally installed.

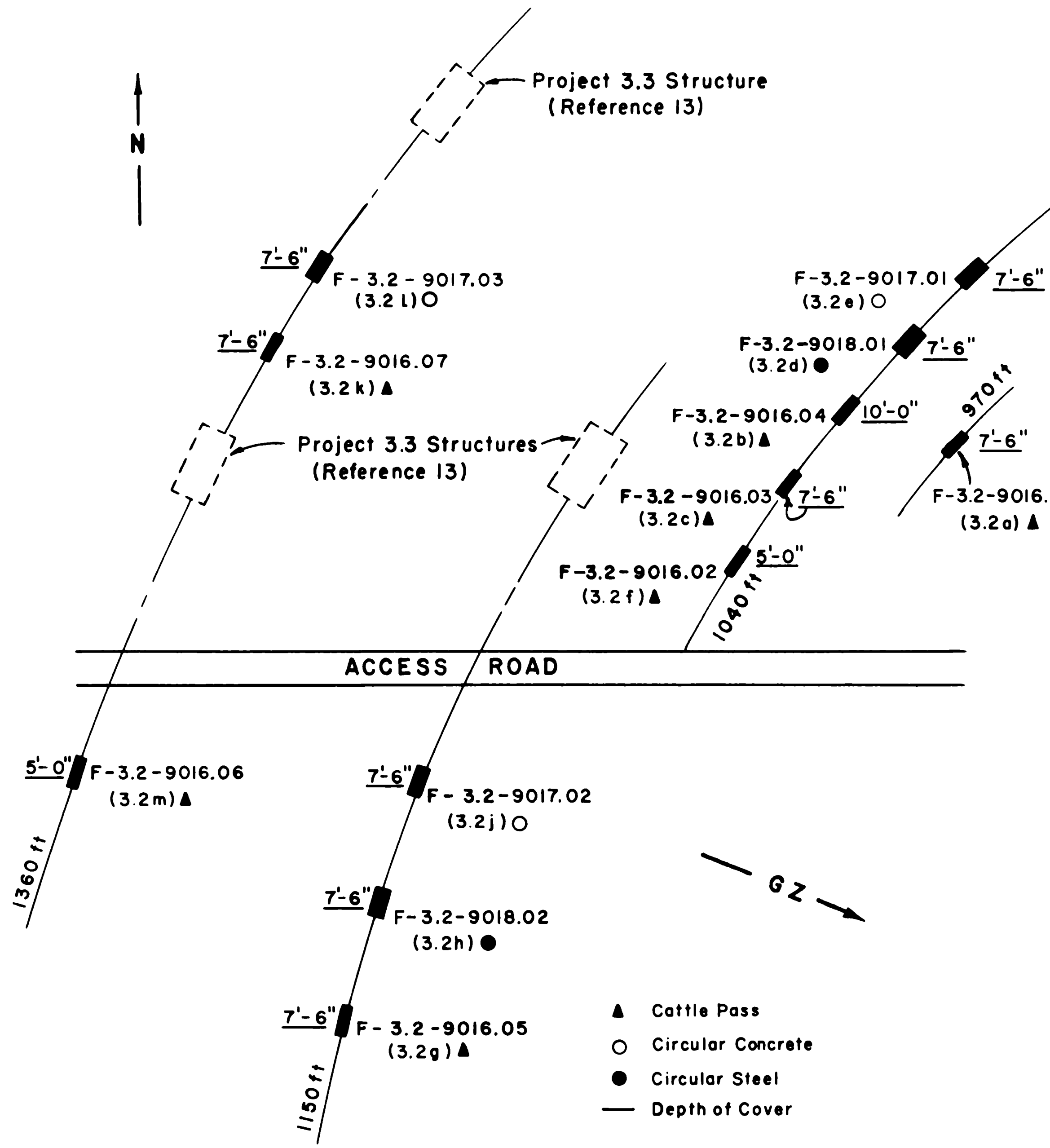

Fig. 1—Plot plan, Project 3.2.

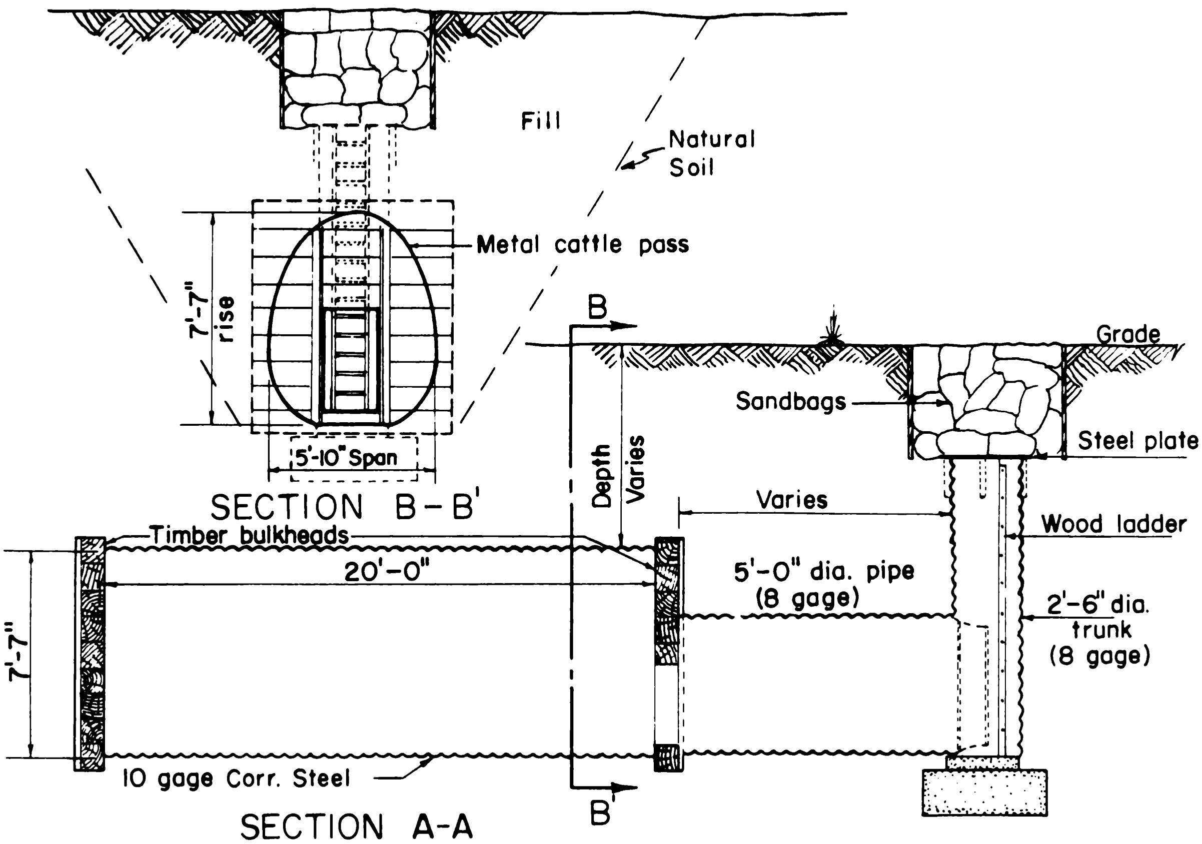

Fig. 2—Cattle-pass test section and access passage.

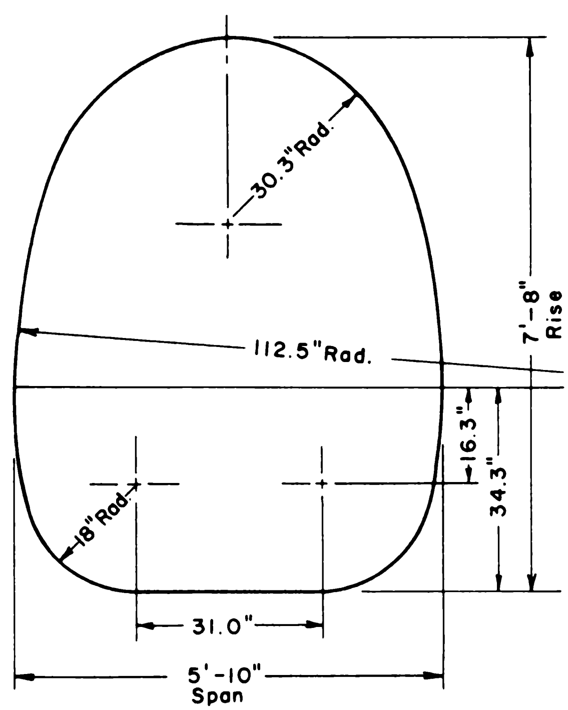

Fig. 3—Shape of assembled cattle-pass section.

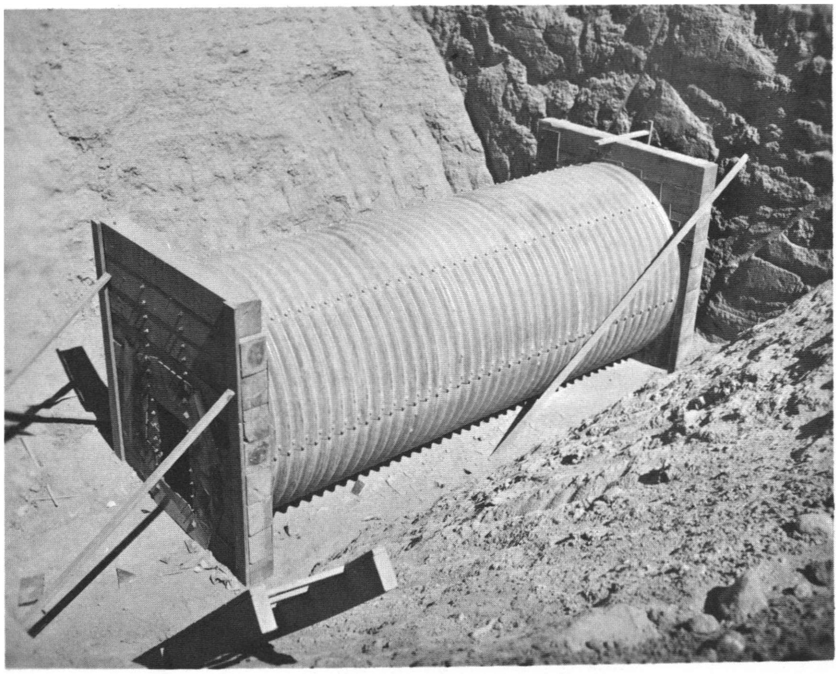

Fig. 4—Exterior view of circular steel conduit before installation of access passage.

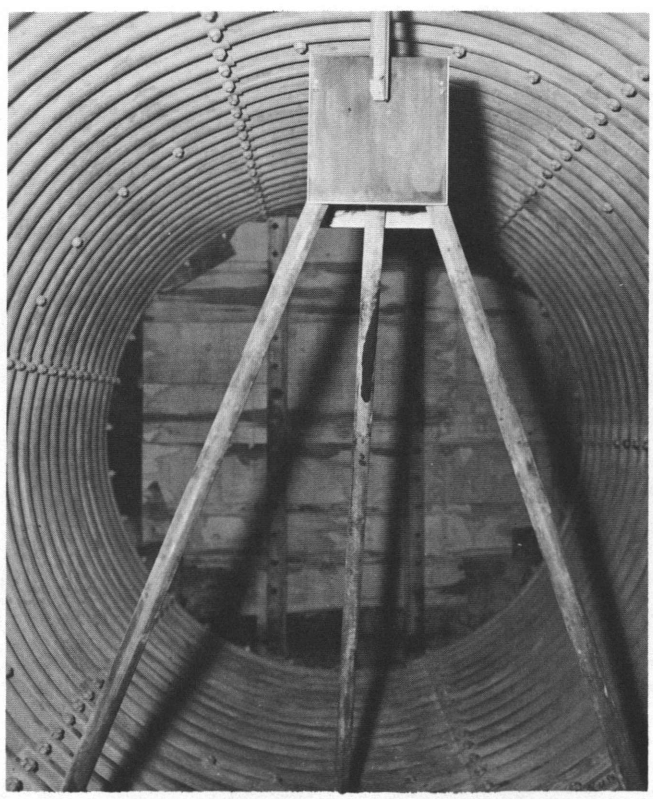

Fig. 5—Interior view of typical circular steel conduit.

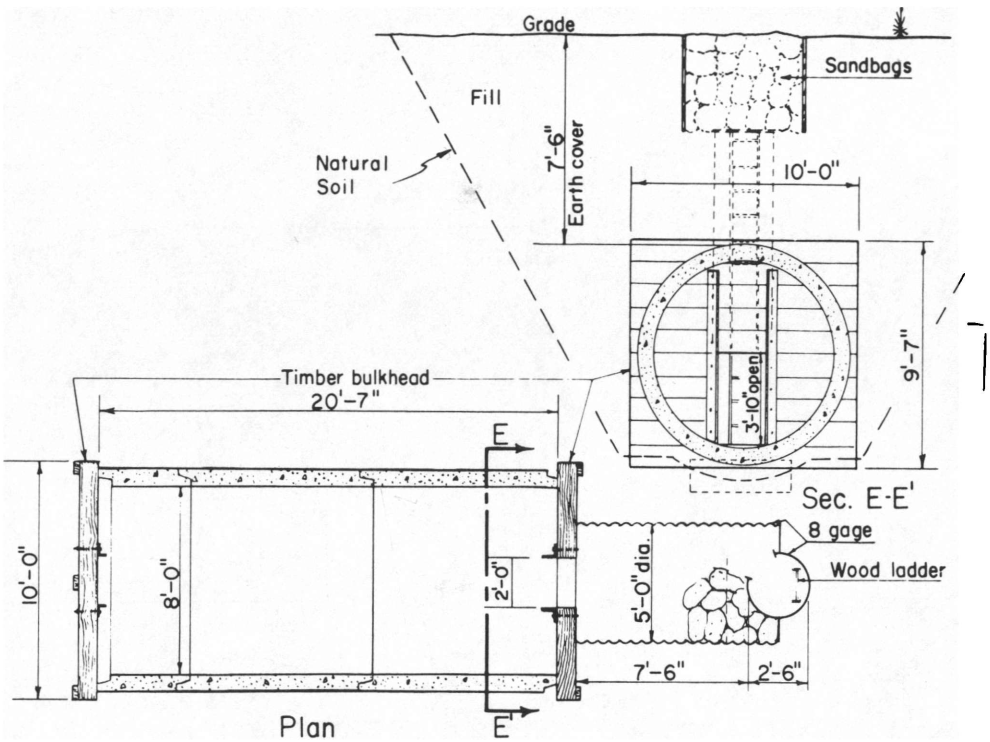

Fig. 6—Concrete conduit section and access passage.

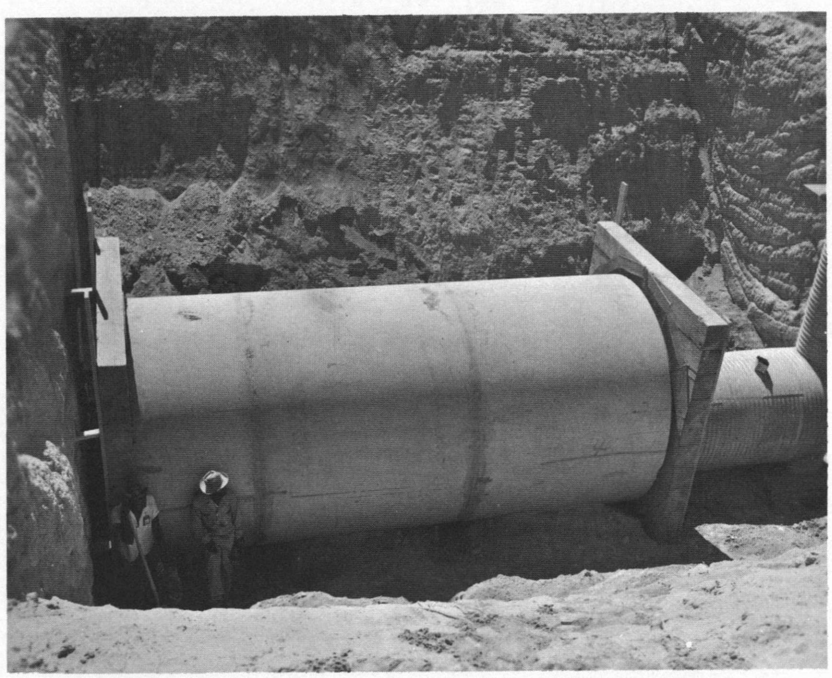

Fig. 7—Exterior view of typical circular concrete conduit before backfilling.

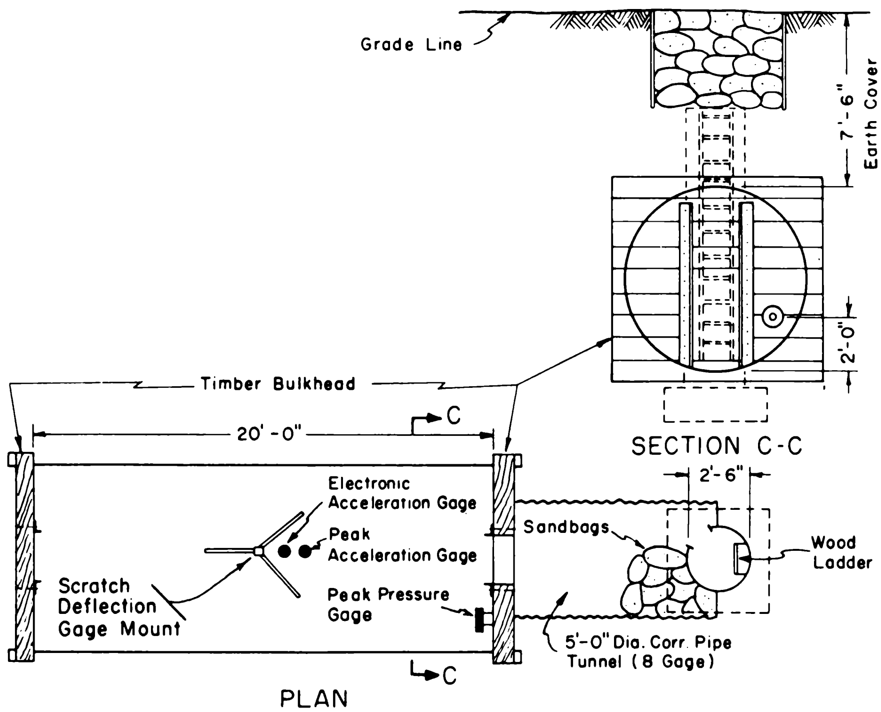

Fig. 8—Typical gauge locations inside test section.

SUMMARY 17

EVALUATION OF BURIED CORRUGATED-STEEL ARCH STRUCTURES AND ASSOCIATED COMPONENTS

(Report WT-1422, Operation Plumbbob, Project 3.3, same title, by G. H. Albright, LTJG, CEC, USNR, Project Officer, E. J. Beck, J. C. LeDoux, LCDR, CEC, USN, and R. A. Mitchell, LTJG, CEC, USNR, Bureau of Yards and Docks, Navy Department, Washington, D. C., and U. S. Naval Civil Engineering Laboratory, Port Hueneme, Calif., Feb. 28, 1961.)

OBJECTIVES AND SCOPE

The test was concentrated on three basic components of a personnel shelter: the shelter structure, the blast closure valve, and the electric power source. The objectives were: (1) to determine the degree of protection from blast and radiation afforded by earth-covered corrugated-steel arch structures; (2) to determine the capabilities of a blast closure valve under blast conditions; and (3) to determine the suitability of open pits for the protection of power generators against blast.

Two types of 25-ft-diameter 48-ft-long arch structures, the E19R1 blast closure valve, and two types of pit enclosure for power generators were tested during shot Priscilla (ref. ENW, p. 675). Figure 1 shows the layout of structures, blast closure valve plenum, and generator pits at the test site. Table 1 gives the range of structures from Ground Zero (GZ) and the predicted theoretical overpressures at the structures.

Because of the differences in structural character, aspects of interest, etc., the test data for the three specimen types are considered separately.

TEST OF CORRUGATED-STEEL ARCH STRUCTURES

Description of Structures

The arch-type structures were modified prefabricated ammunition-storage magazines, as shown in Figs. 2 and 3, 4 and 5, and 6 and 7 for structures 3.3a, b, and c, respectively. The curved sections were of 10-gauge corrugated-steel plates (Table 2). Steel arch ribs were added in structures 3.3a and c only. The end bulkheads on all structures were reinforced by a tieback-and-deadman arrangement (Fig. 8). Standard 8-gauge rear bulkheads were used in structure 3.3b, but 3-gauge end bulkheads were used for structures 3.3a and c (Table 2).

The same configuration was used for each of the entrances to the three test shelters. This consisted of a horizontal, 8-gauge corrugated-steel tube, 7 ft in diameter, with a vertical access trunk of 8-gauge corrugated steel, 3 ft 6 in. in diameter, resting on a concrete pad. At the ground surface, a submarine-type circular hatch served as a blast door.

On the basis of the results of previous tests, as summarized in Table 3 (Summaries 6 and 11), the earth configuration was further modified to reduce the dynamic-pressure sensitivity for this test. This configuration was based upon a balanced cut-and-cover procedure, with the berm extending along the earth surface to the intersection of an approximate 45° line from the base of the structure. With the modified earth cover, it was estimated that the structure would withstand approximately a 50-psi side-on overpressure at the earth surface.

The earth backfilling operations followed conventional construction practices. A gravelly, silty sand from an off-site gravel pit was used rather than the silt of the dry lake bed at the site.

Results

The more significant structural survey and other instrumentation data are shown in Tables 4 and 5. It is doubtful that the internal pressure shown as high as 2.7 psi actually existed; however, the cause of the suspected error was not known.

In each structure there was a tendency for the circumferential length of the structure to reduce because of the slipping of corrugated plates at the horizontal seams. No sheared bolts, however, were observed. Structure 3.3a experienced the greatest amount of movement at each seam, particularly near the spring line, i.e., approximately ⅛ to ⅜ in. The slipping of joints in structures 3.3 b and c was approximately 0 to ⅛ in.

There was minor physical damage to interior partitions, airlocks, and doors, by slight racking. On initial postshot entry, however, all interior doors opened without forcing. There was no noticeable physical damage to the plumbing and electrical systems in structure 3.3c. The lights in structure 3.3c were operated postshot with power from one of the pit-enclosed generators. No repairs were necessary to the system.

The end walls in all three structures were in excellent condition postshot. Entrances and hatch arrangements suffered no significant damage except for a slight buckling of the ladder uprights, which were compressed by the entrance trunk as it deformed slightly.

For this project, thermal radiation was not of significance. The residual nuclear radiation was very small compared to the initial nuclear radiation; consequently the radiation of interest consisted of prompt-gamma and neutron radiation. The gamma and neutron doses are summarized in Table 6.

Discussion

The test results indicate the structural suitability of the arch structures for use as personnel shelters if used under conditions identical to those of this test. The structures tested had a certain inherent strength owing to their form and their material characteristics. A significant part of their strength was due, however, to the passive resistance of the soil developed by deformation of the flexible arch into the soil backfill.

The relatively large average residual footing displacements (1½ and 2$\frac{7}{16}$ in.) indicate a general downward movement of the arch. It is likely that this movement caused a reduction in the peak soil pressure acting on the arch.

The reflected-pressure and the dynamic-pressure effects would likely be reduced by streamlining the earth berm. The same amount of cover material could be placed with a flat 14:1 slope extending out from the crest over the arch crown.

Project 3.2 of Operation Hardtack (Summary 31) tested two earth-covered, 25-ft-span, corrugated-steel, 180° arch structures; one (structure 3.2a) was subjected to a 90-psi overpressure from a kiloton-range detonation and the other (structure 3.2b) was subjected to 78 psi from a megaton-range detonation. It was reported that "since the two arch shells were identical and the confining earthworks were almost identical, the fact that structure 3.2b suffered complete collapse at 78 psi (long-duration loading), and structure 3.2a sustained extensive localized damage without complete collapse at 90 psi (short-duration loading) is significant." These two Hardtack structures were similar to Plumbbob structure

3.3b, which withstood a 60-psi overpressure, but the soil type and earth-cover configuration were quite different. Therefore a direct comparison of results of the Hardtack 3.2 and Plumbbob 3.3 projects is not warranted.

Peak vertical acceleration of the floor slab of each structure was less than 3 g. Had the floor slab not been isolated from the metal arch, the accelerations would probably have been greater.

Under the test conditions it is unlikely that shelter occupants would have suffered any harm from dust inside the shelter.

The following general conclusions, based on the particular conditions of this test and within the accuracy of the overpressure measurements can be made:

1. The steel-arch structure without arch ribs withstood a peak overpressure of 60 psi.
2. The steel-arch structure with arch ribs withstood a peak overpressure of 100 psi.
3. All three structures tested provided adequate protection against nuclear radiation.
4. No significant physical damage occurred to the plumbing and electrical fixtures installed in the ribbed arch structure at the 60-psi overpressure range.

TEST OF BLAST CLOSURE VALVE

Background and Description

Included in a typical shelter design for atomic, biological, and chemical warfare are provisions for forced ventilation. Such a ventilating system, using a protective-collector filter system, is extremely vulnerable to air-blast pressure entering through the ductwork. A blast closure valve is necessary to prevent damage to both the filter system and the shelter contents.

In this project, to avoid possible failure of the other tests in the structure if the valve malfunctioned, the ventilating ducts were sealed. The valve was attached to a separate plenum (Figs. 9 and 10). This valve, developed by the Army Chemical Center, was rated at 600 cfm. The test plenum contained approximately 215 cu ft, or far less than the shelter proper; this would affect the interpretation of the results. Had the chamber in which the valve was located been larger, the pressure rise would have been less.

A view of the completed air-intake ducting and plenum access hatch is shown in Fig. 11 and schematic details of the valve mechanism are given in Fig. 12.

Results

The peak overpressure observed at earth surface was 60 psi. The duration of the positive phase was 345 msec. The peak internal pressures in the plenum were 0.32 psi (positive) and 1.20 psi (negative).

The blast valve appears to be adequate in sealing against the positive pressures to 60 psi for 345 msec. It is certain that this valve cannot be expected to seal effectively against negative pressures since by virtue of its basic design it can function properly in only the positive direction. However, if the expected maximum pressure is within the design tolerances of the collective protective filter, the expansion chamber need be designed only for the positive phase. Under the test conditions the pressures were within the limits that the filters could tolerate, or cause rupture of the eardrum to humans.

PIT ENCLOSURES FOR EMERGENCY POWER GENERATORS

Background and Description

Because of the noise, vibration, and heat from an engine-driven generator set, the set must be installed in an enclosure separate from the personnel shelter. The tests described here are of a first design of a partially enclosed pit shelter for generator sets; the principal design criteria were to protect the units from high drag loading and missiles. The pit shelter was not designed to provide a suitable environment for storage, maintenance, or operation of a generator set.

The pits were slightly larger in plan than the test generator sets. They were constructed to resist deformation under the test conditions but were not covered except for a metal grille (Figs. 13 and 14).

One 15-kva and one 5-kva unit were placed in separate pits adjacent to each of the underground structures 3.3a, b, and c. Structure 3.3a was located in the 100-psig overpressure region, 3.3b and c were in the 60-psig overpressure region. In each case the long side of the pit was oriented toward GZ parallel to the shock front. This is the preferred orientation because it minimizes the time for pressure buildup as the pressure wave passes over the pit.

Results

The damage sustained by individual components of the six portable generator sets is tabulated in Table 7. Neither of the two units at the 100-psig range was operable and only one of the four at the 60-psi range was immediately usable. Any of the six units could have been repaired with a moderate expenditure of shop time under favorable conditions. The degree of fallout contamination would be a factor in determining when these repairs could be made.

All generator units were displaced upon their foundations, but it is not clear whether this resulted from reflected pressures from the pit walls or from ground accelerations. In any event, they could have been used without remounting. The evidence points to ground accelerations as the cause because there was no evidence of high horizontal forces on the sheet metal such as would be required to dislodge a heavy engine.

In an evaluation of the results, the fact that there was a lack of flying debris, flammable materials, and the like, which might be sources of damage in a typical residential or industrial location, should be considered. On the other hand, the loose condition of the surface soil of the test site probably produced much heavier dust loading and contamination than would be experienced in a typical residential location.

Discussion

Because the damage was patently too high, the pit design is not considered practicable for a standby power source for shelters. For the less demanding case of a facility in which the requirement for some repair before use is tolerable, protection was nearly adequate at even 100-psig overpressure.

Compared to the gasoline types, diesel engines have characteristics that make them much more desirable as standby emergency generators for shelters; however, they are more expensive. In diesel engines the generally heavy construction, internal governors, heavy cast radiator tanks and crankcase pans, etc., might obviate the necessity for modifications. Furthermore, diesel engines do not have carburetors and usually do not have external governor linkages. Reduced fire hazard from spilled or leaking diesel fuel, compared with gasoline, would be a distinct advantage.

Even though all the generators suffered damage, and the application is, in general, not considered satisfactory, damage was light compared with what would have been predicted for unshielded units at the same locations.

Table 1—ARRANGEMENT OF STRUCTURES, PRISCILLA SHOT*

Structure	Station number	Range from GZ to center of structure, ft	Slant range, yd	Angle of sight, deg	Topographic coordinates	Predicted theoretical overpressure at earth surface, psi
3.3a	9019.01	1150	449	31	N 746,877.74 E 715,037.10	75
3.3c	9019.02	1360	510	27	N 746,881.72 E 714,796.31	50
3.3b	9019.03	1360	510	27	N 747,111.67 E 714,948.56	50

*Yield, 36.6 kt; height of burst, 700 ft.

Table 2—PROPERTIES OF CORRUGATED-STEEL PLATES

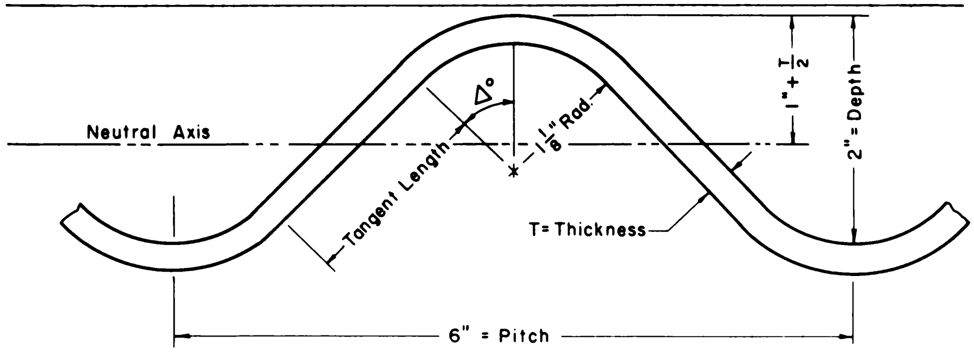

Properties	3 Gage	8 Gage	10 Gage
Thickness T, in	0.2451	0.1644	0.1345
Tangent length, in	1.7377	1.8283	1.8606
Angle Δ, deg	45 deg 47 min	45 deg 00 min	44 deg 44 min
Moment of inertia, in^4 *	1.756	1.153	0.937
Area of section, in^2 *	3.658	2.449	2.003
Section modulus, in^3 *	1.564	1.066	0.878
Radius of gyration, in	0.693	0.686	0.684

* Per ft of horizontal protection.

Table 3—SUMMARY OF CORRUGATED-STEEL STRUCTURE TESTS

Operation and shot	Surface structure	Exposure condition	Overpressure, psi	Dynamic pressure, psi	Damage
Upshot-Knothole, shot 9	3.15	3-ft earth cover on sides of arch (lake-bed silt)	10.8	Not recorded	Elastic response; door projected into structure
Upshot-Knothole, shot 10	3.15	3-ft earth cover on sides of arch (lake-bed silt)	8.1	Not recorded	Elastic response; no significant damage
Teapot, shot 12	3.15	3-ft earth cover on sides of arch (lake-bed silt); crown awash	13.0	33.0	No significant damage
Teapot, shot 12	3.6	3-ft earth cover (granular material); moderately wide earth berm	30.0	150.0	Side of arch toward GZ collapsed; not operational; 50 to 100% personnel casualties estimated

Table 4—INSTRUMENTATION OF STRUCTURES

Number	Type	Structure	Position in structure
4,4	Deflection gauge (scratch)	3.3a, 3.3c	Crown (steel plate) Crown (ribs) Quarter points (ribs)
3	Deflection gauge (scratch)	3.3b	Crown (steel plate) Quarter points (steel plate)
3	Self-recording pressure–time gauge	3.3a, 3.3b 3.3c	Original earth surface Center of earth berm
3	Peak internal-pressure gauge	3.3a, 3.3b, 3.3c	Interior
2	Self-recording accelerometer (vertical component)	3.3a, 3.3c	Floor (center)
1	Peak accelerometer (vertical component)	3.3b	Crown (steel plate)
3	Electronic dynamic accelerometer (vertical component)	3.3a, 3.3b, 3.3c	Center of floor

Table 5—STRUCTURAL MEASUREMENTS

	Structure		
	3.3a	3.3c	3.3b
Station number	9019.01	9019.02	9019.03
Type of structure	Ribbed	Ribbed	Not ribbed
Nominal depth of earth cover, ft	5	5	5
Peak overpressure at earth surface, psi	100	60	60
Positive duration of pressure pulse, msec	333		361
Dynamic pressure, psi*	310	200	200
Peak internal pressure, psi	2.7	0	1.0
Peak vertical acceleration of floor, g	<3	<3	<3
Average displacement of footings at mid-length relative to floor slab, in.	$2\frac{7}{16}$	$1\frac{1}{2}$	$1\frac{1}{2}$
Maximum deflection of arch rib at crown relative to floor slab, in.	$4\frac{1}{8}$	$3\frac{1}{16}$	
Residual deflection of arch rib at crown relative to floor slab, in.	2	$1\frac{13}{16}$	
Maximum deflection of corrugated-steel arch at crown relative to floor slab, in.	$5\frac{5}{16}$	$3\frac{5}{8}$	4
Residual deflection of corrugated-steel arch at crown relative to floor slab, in.	$3\frac{5}{16}$	$2\frac{1}{8}$	$2\frac{3}{4}$
Ratio: maximum deflection of corrugated-steel arch at crown relative to floor span, %	1.76	1.20	1.33
Ratio: residual deflection of corrugated-steel arch at crown relative to floor span, %	1.10	0.71	0.92

*From preliminary composite dynamic pressure curve for height of 3 ft.

Table 6—RADIATION MEASUREMENTS

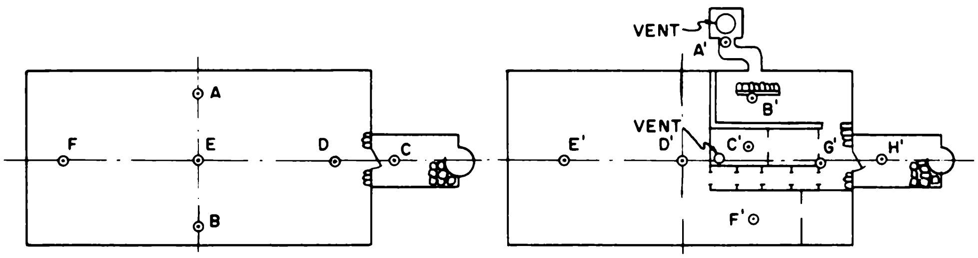

Structure	Location	Gamma Dose, r: Foil Method	Gamma Dose, r: Chemical Dosimeter	Neutron Dose, rep: Foil Method	Neutron Dose, rep: Chemical Dosimeter
3.3a	A	*	< 5	†	< 10
	B	*	< 5	†	< 10
	C	*	64	†	64
	D	16.2	24	†	14
	E	*	10	< 25	44
	F	7.4	36	†	*
3.3b	A	1.2	< 5	†	< 10
	B	2.3	< 5	†	< 10
	C	94	94	†	< 10
3.3c	A′	90	88	†	140
	B′	1.05	< 5	†	< 10
	C′	5.0	< 5	†	< 10
	D′	4.5	< 5	< 25	< 10
	E′	4.0	< 5	< 25	< 10
	F′	3.0	< 5	†	< 10
	G′	15.0	27.5	†	20
	H′	97	117	†	< 10

* Lost in processing. † Not instrumented.

Table 7—TABULATION OF GENERATOR DAMAGE

All estimates of repair time are based on operations in a shop.

Part Name	Adjacent to Structure 3.3a: 5-kva Damage	Repair	Time	15-kva Damage	Repair	Time	Adjacent to Structure 3.3b: 5-kva Damage *	Repair	15-kva Damage	Repair	Time	Adjacent to Structure 3.3c: 5-kva Damage	Repair	Time	15-kva Damage	Repair	Time	Type of Load
			hr			hr					hr			hr			hr	
Radiator:																		
Top tank	Dished in			Dished in			Dished in	No				Dished in	No					Pressure/drag
Fan shroud	Bent	Yes	1/2	Bent	No										Bent	Yes	1/6	Drag
Front guard	Bent	No					Bent	No	Damaged	No		Bent	No		Bent	No		Drag
Top hose	Scorched	No		Loose	Yes													Drag
Bottom hose				Loose	Yes													Drag
Overflow line							Broken	No				Flattened	No					Missile
Fill cap				Torn off	Yes	3			Missing	No					Missing	No		Drag
Carburetor:																		
Body				Sheared mount	Yes	1												Drag
Float												Bent and cracked	Yes	1/4				Pressure
Float lever †	Damaged	Yes	1/2															Pressure
Air cleaner	Bent	No					Loose	No	Loose	No		Bent	Yes	1/6				Drag
Automatic choke															Inoperative	No ‡		Drag
Sediment bowl				Missing	Yes	1/4						Dirt	Yes	1/2	Missing	Yes	1/6	Drag
Sediment bowl housing															Bent	Yes	1/4	Drag
Fuel supply system:																		
Supply line				Flattened	Yes	1/4			Flattened	Yes	1/3							Pressure
Tank	Leaky	Yes	1/6 §	Leaking	Yes	1			Bottom bent	No		Bent, dirty	No	1/12	Dirty	No		Pressure
Tank filter and cap												Missing	No		Bent	No		Drag
Instruments:																		
Gage glass (s)	Broken	No		Broken	No		Broken	No	Broken	No		Broken	No					Pressure
Panel light	Missing	No										Bulb broken	No					
Temperature shutdown (safety)							Line broken	No ¶										Drag
Wiring:																		
Generator ground	Loose	Yes	1/12															Drag
Ammeter, generator				Blown out	Yes	1/2												Pressure
Terminal block				Cracked	No				Cracked	No								Drag
Governor:																		
Control rod	Bent	Yes	1/6						Bent, slightly	Yes	1/12	Bent	Yes		Bent	Yes	1/12	Drag
Spring adjustment lever									Broken	Yes	1/4				Broken, bolt sheared	Yes	1/2	Drag
Housing, generator:				Severe damage	No				Slight	No					Bent, broken hinge	No		Drag
Electrical panel door	Bent	No					Damaged	No	Bent	No		Bent	No		Bent	No		Drag
Electrical panel housing							Damaged	No				Bent	No					Drag
Tool box															Severe	No		Pressure
Crankcase:																No		Pressure
Oil drain pipe				Severe damage	Yes	2												
Breather pipe				Sheared	Yes	1/2									Missing	No		Drag

* Fully operable at end of test. † Solder after first start. ‡ Alternate: manual operation. § Install portable tank. ¶ Depends upon mode of operation.

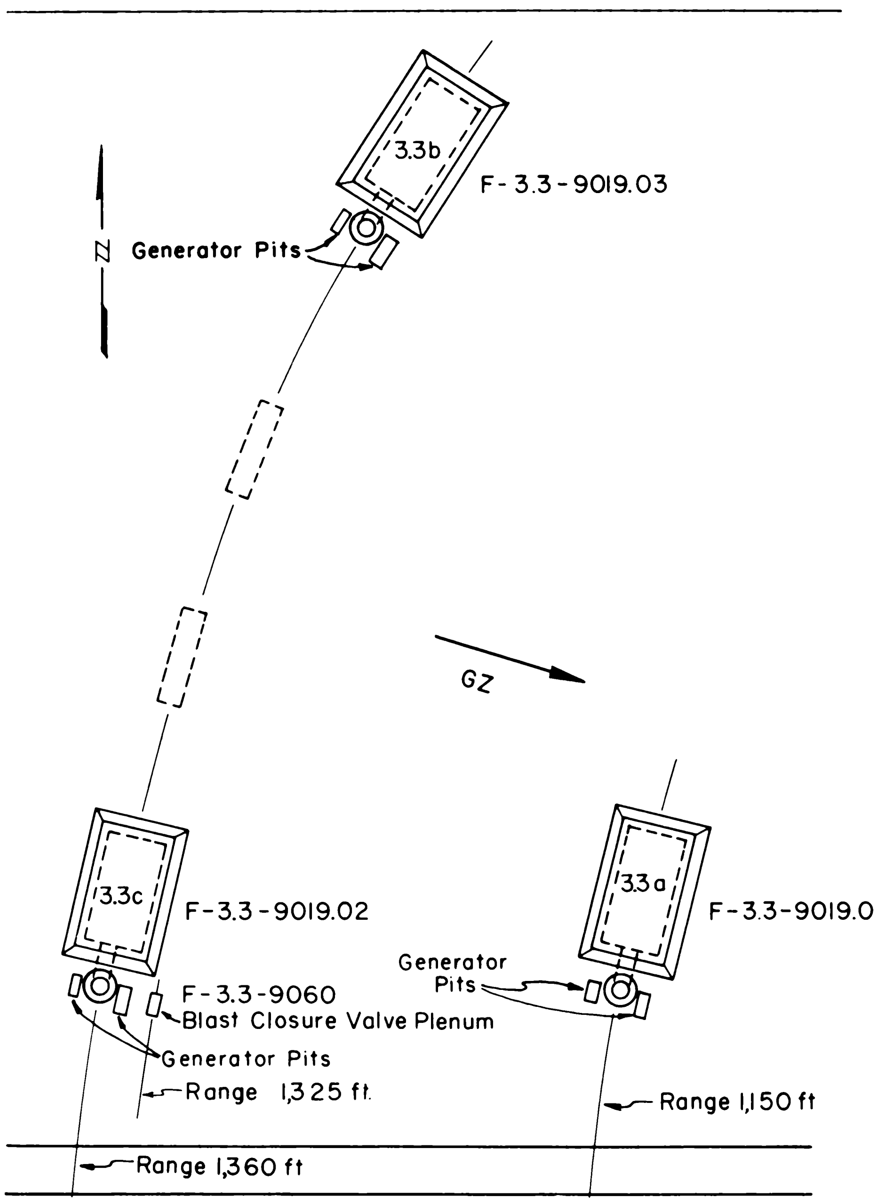

Fig. 1—Plot plan of test structures.

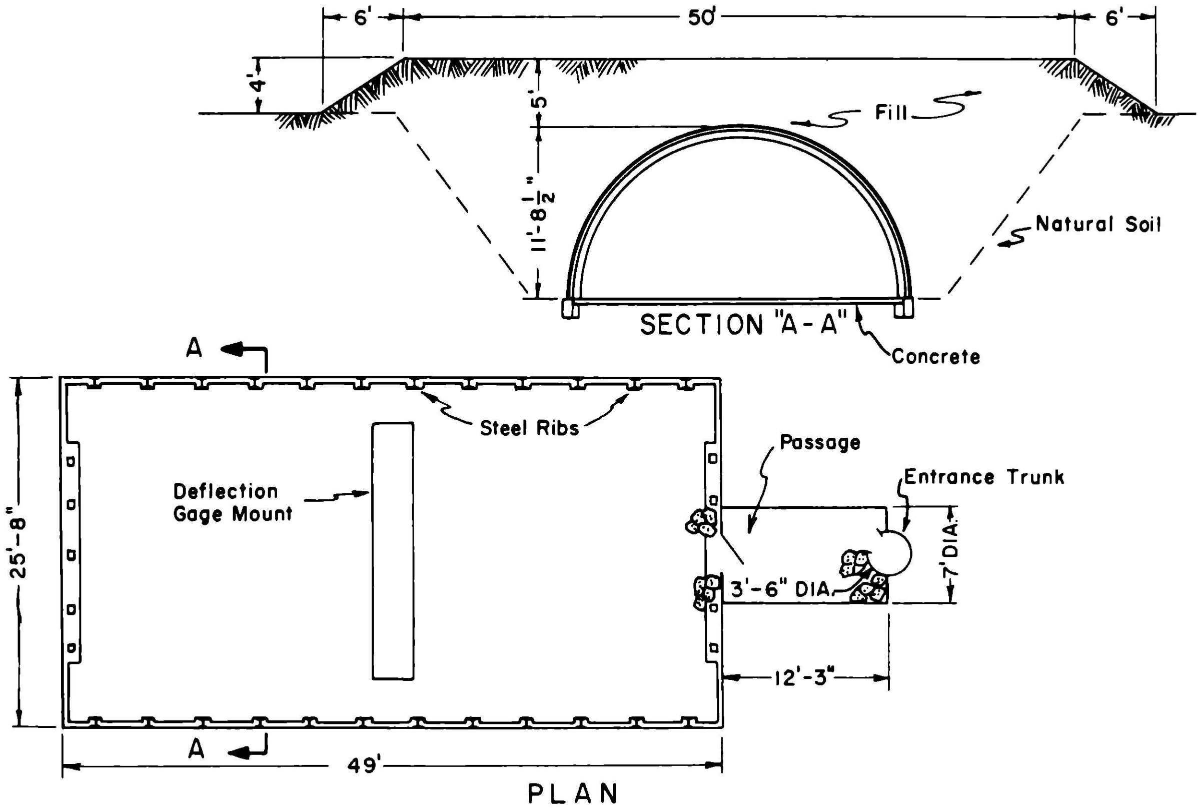

Fig. 2—Plan and section of structure 3.3a.

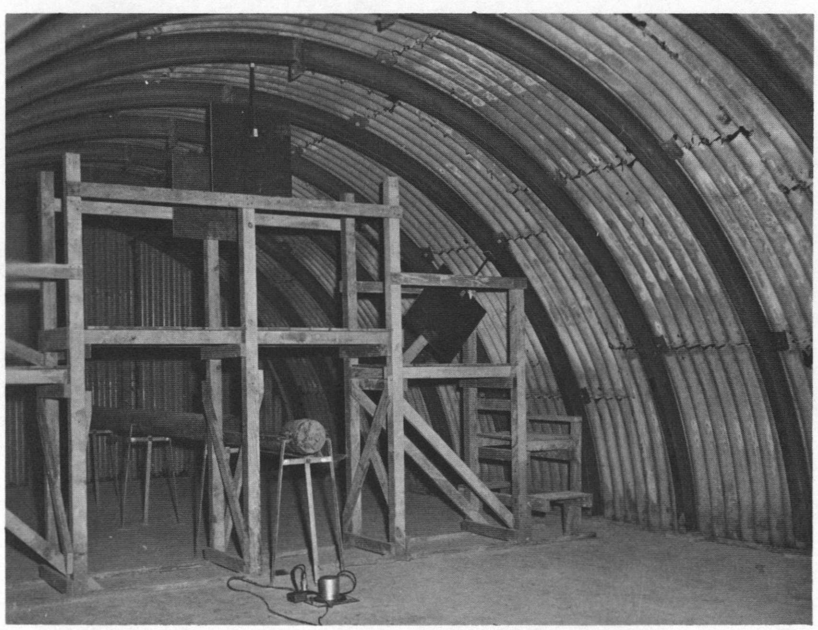

Fig. 3—Interior view, structure 3.3a.

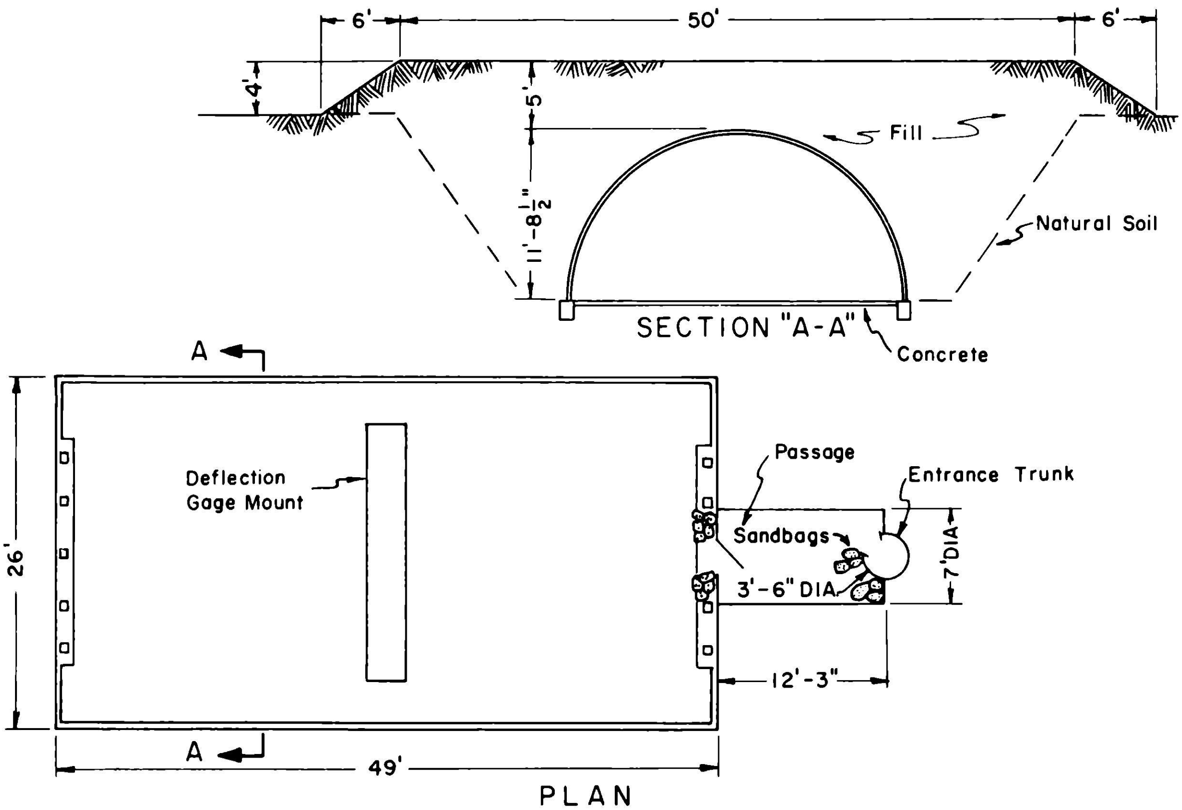

Fig. 4—Plan and section of structure 3.3b.

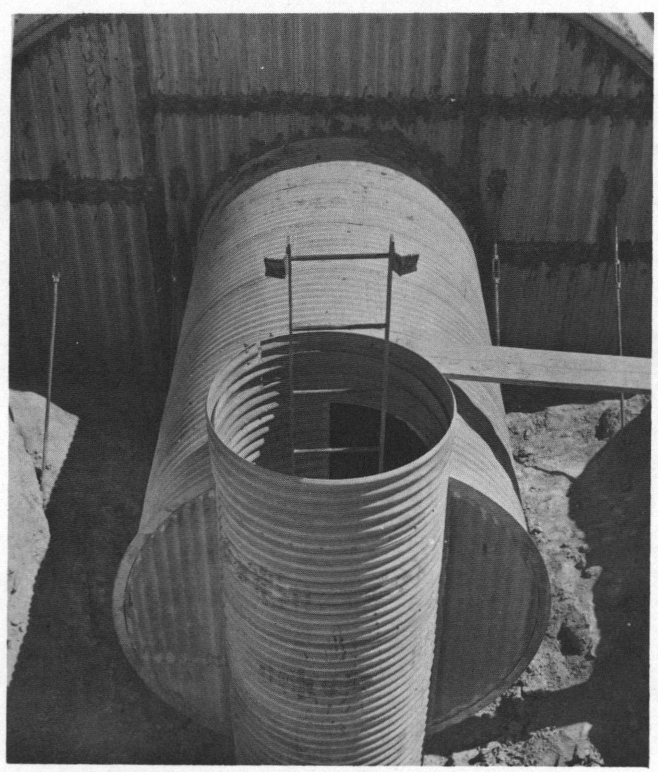

Fig. 5—Access entrance during construction of structure 3.3b.

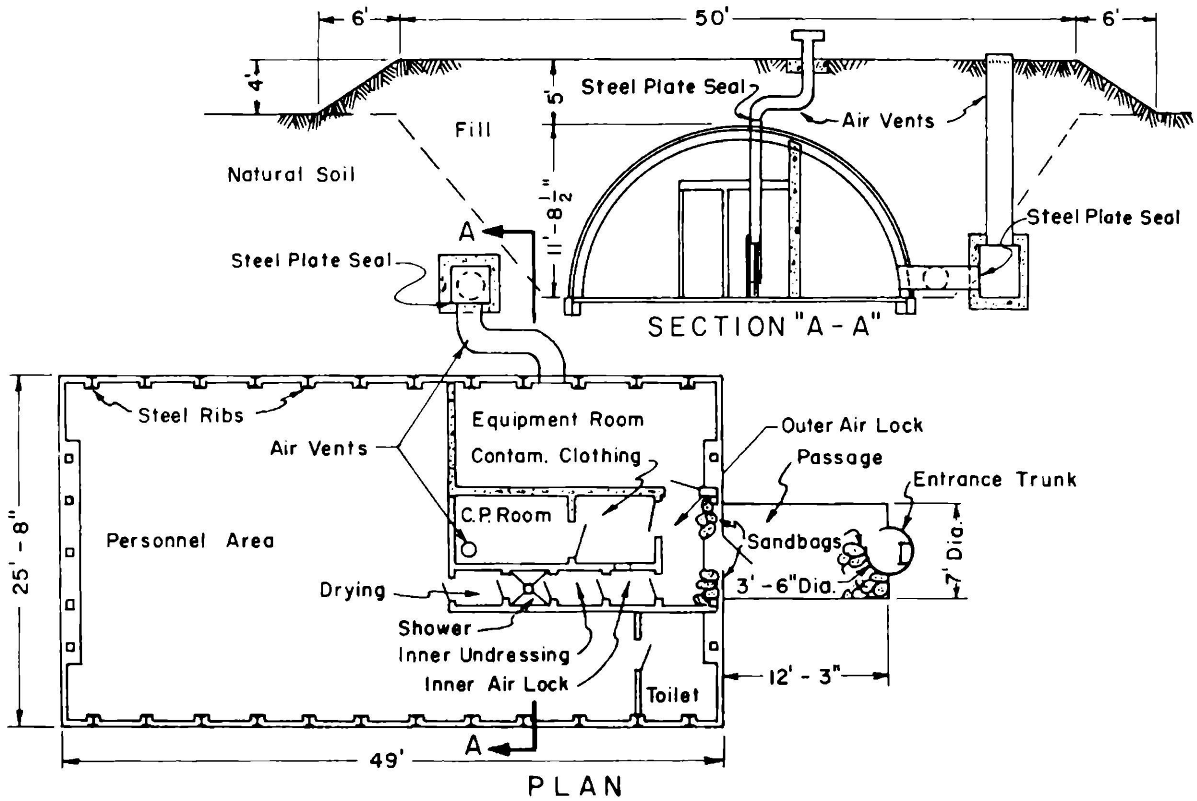

Fig. 6—Plan and section of structure 3.3c.

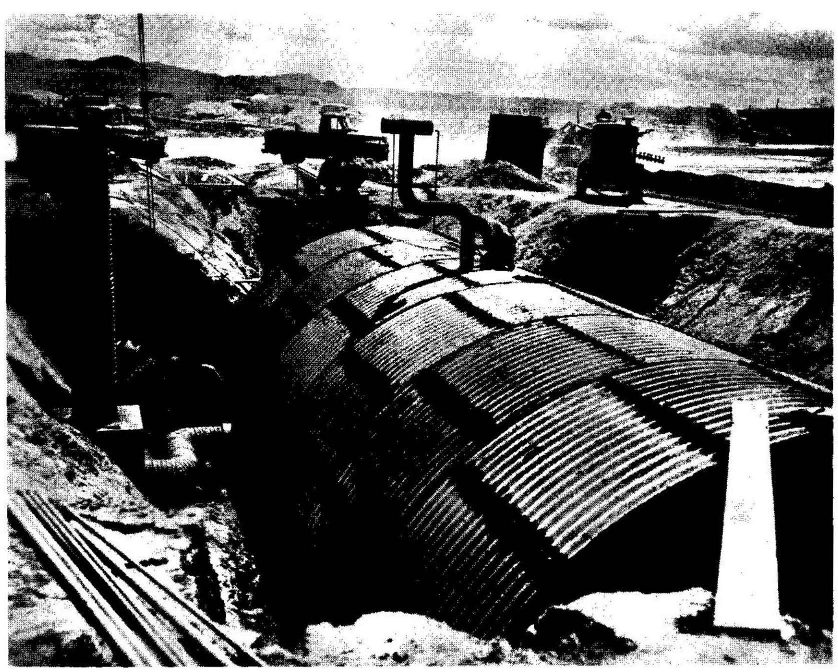

Fig. 7—Overall view before backfilling, structure 3.3c.

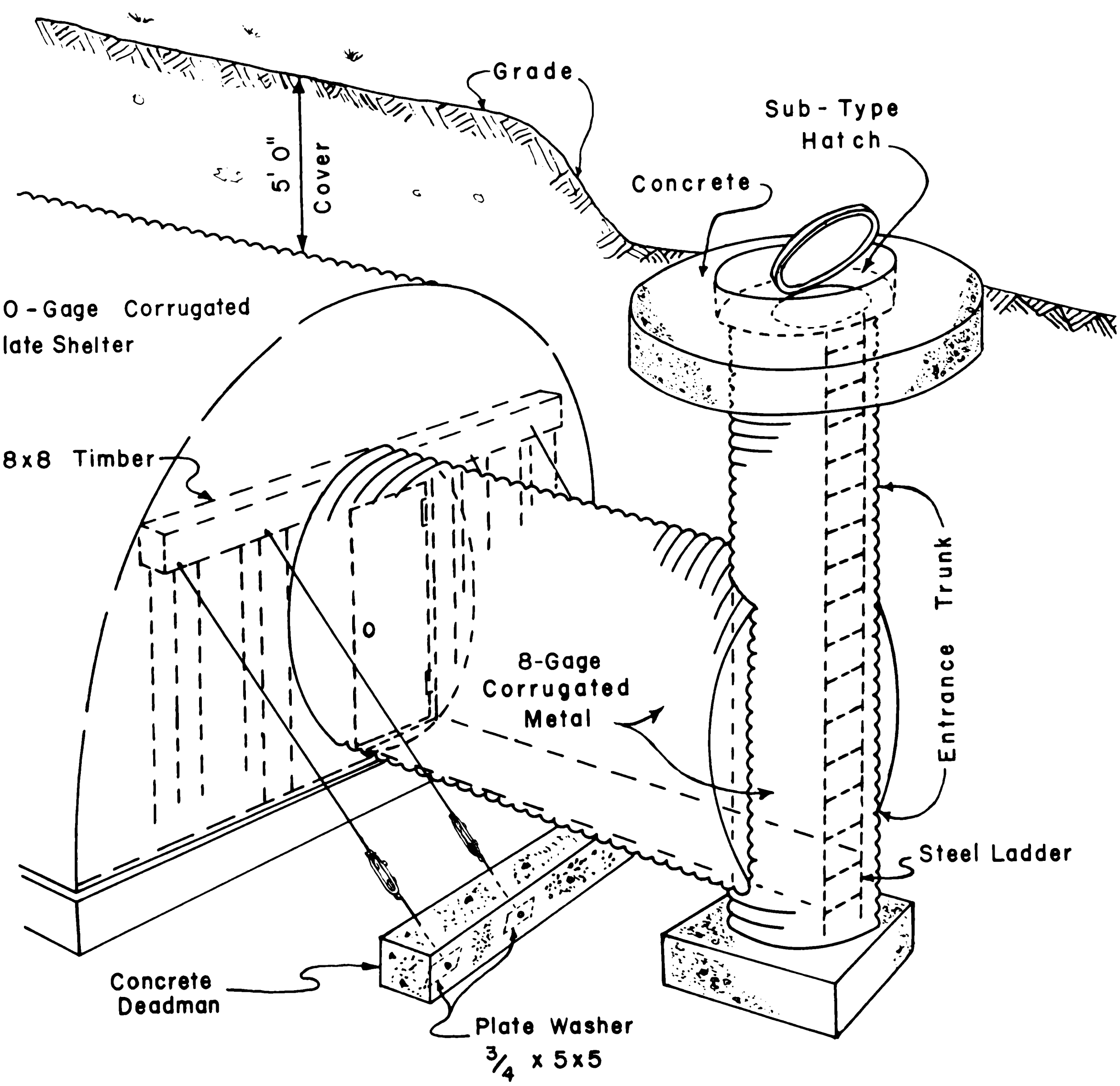

Fig. 8—Sketch of shelter entrance.

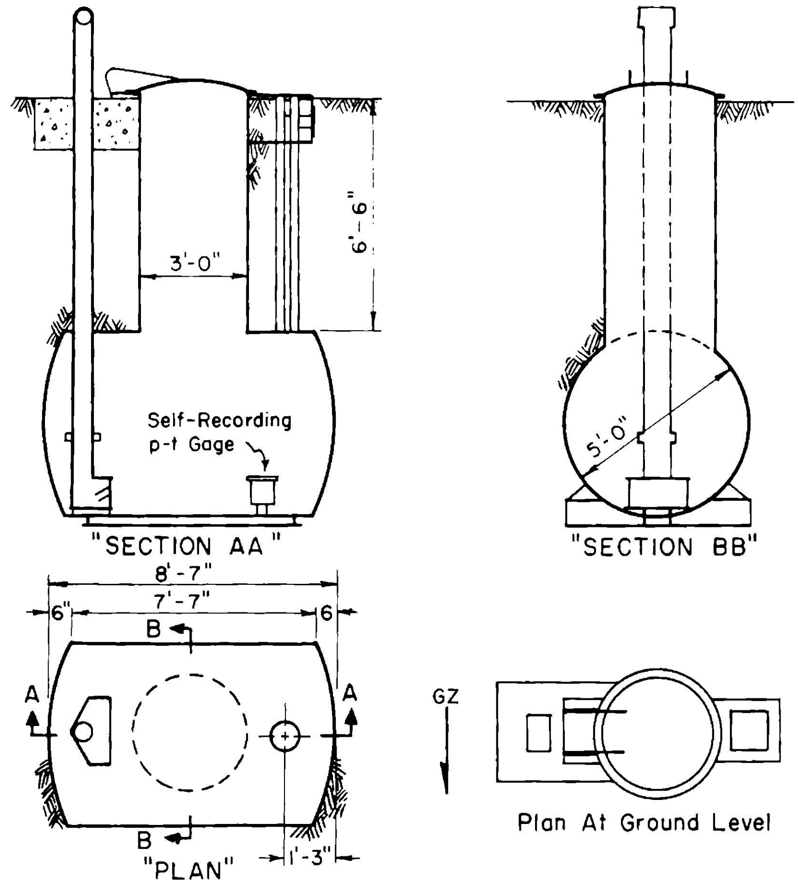

Fig. 9—Pressure plenum for blast closure valve test.

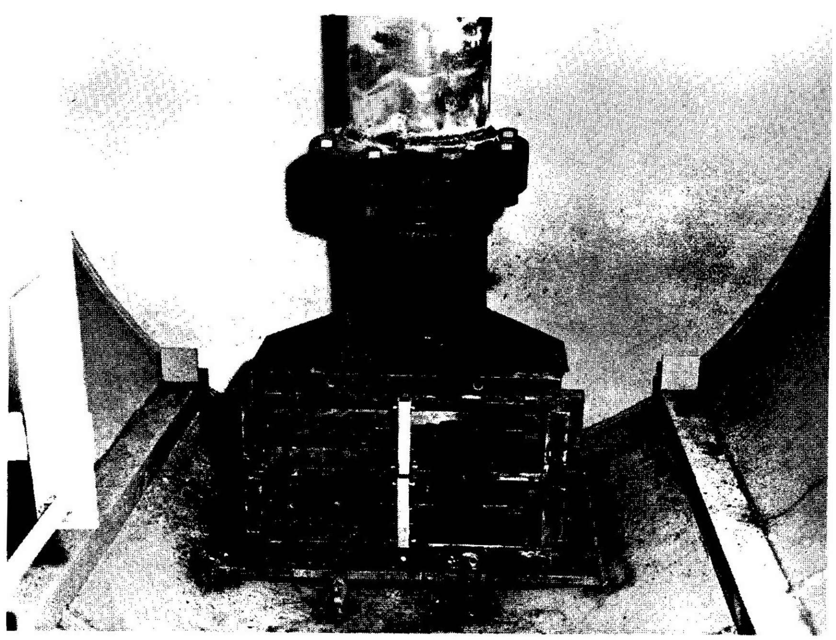

Fig. 10—Blast closure valve installed in test plenum.

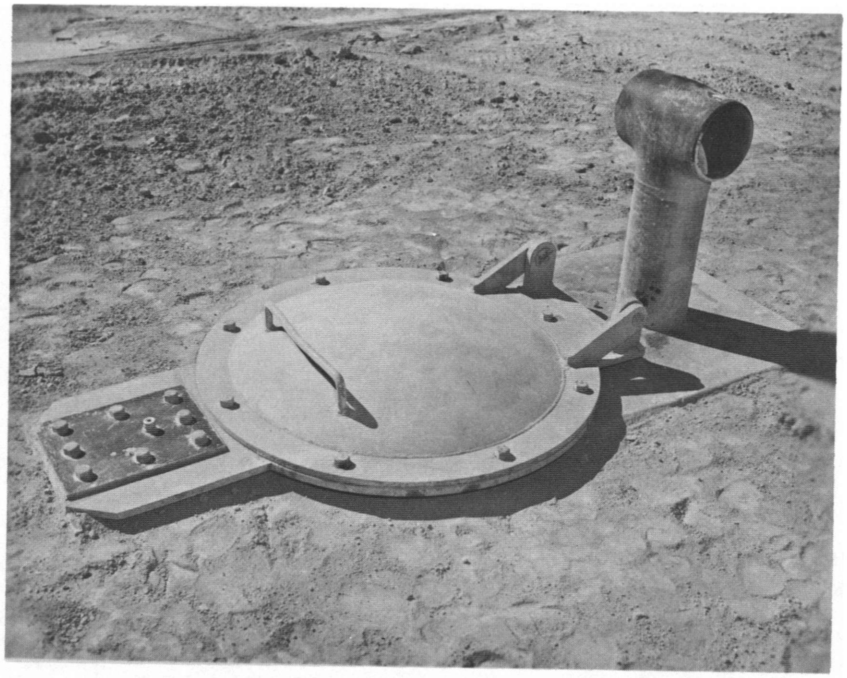

Fig. 11—Blast closure valve test plenum air-intake and access hatch after backfilling.

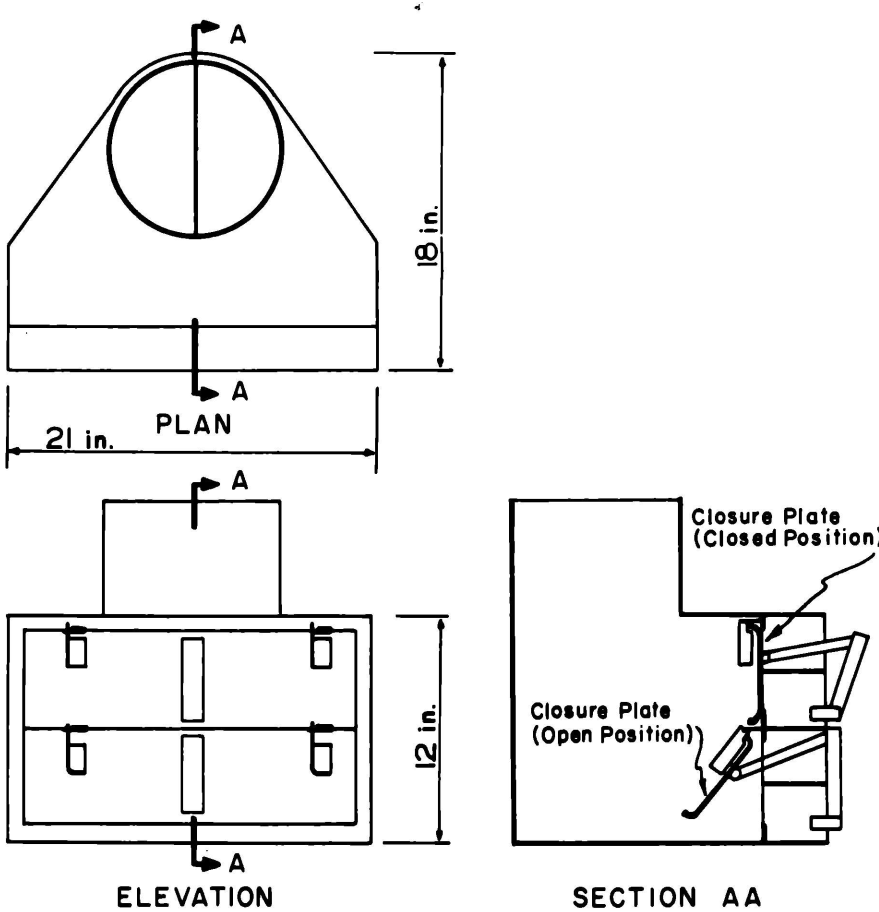

Fig. 12—Schematic representation of blast closure valve.

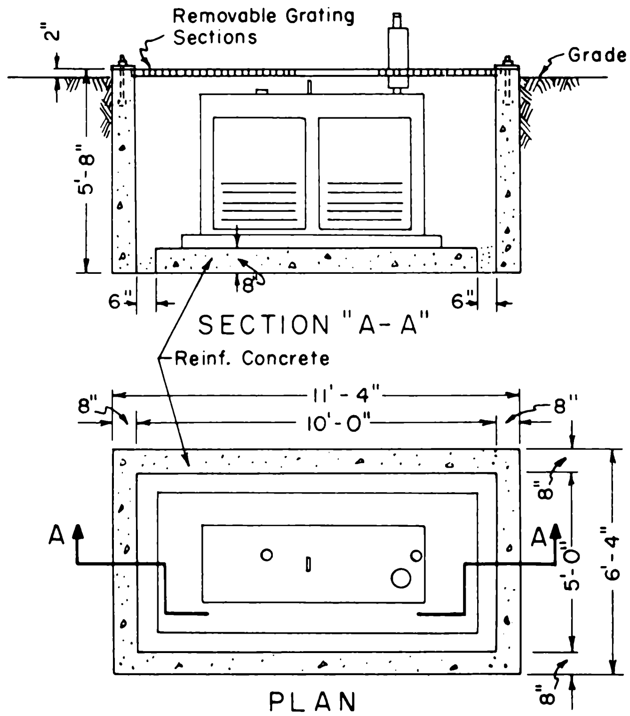

Fig. 13—Test pit, 15-kva generator set.

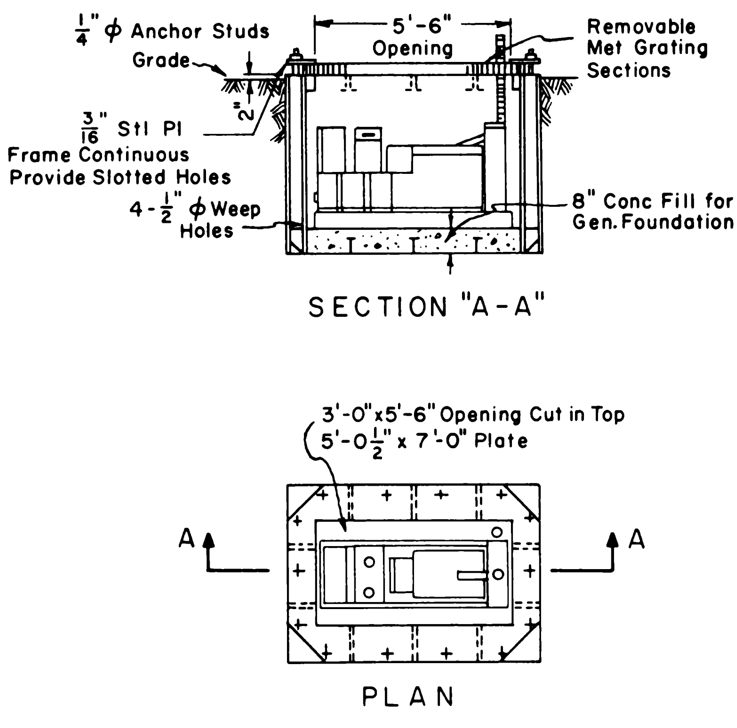

Fig. 14—Test pit, 5-kva generator set.

SUMMARY 18

ISOLATION OF STRUCTURES FROM GROUND SHOCK

(Report WT-1424, Operation Plumbbob, Project 3.5, same title, by R. B. Vaile, Jr., Project Officer, Stanford Research Institute, Menlo Park, Calif., Apr. 22, 1960.)

OBJECTIVES AND SCOPE

The overall objective was to make an initial study of the benefit derived from a special backfill in isolating or protecting underground structures from the violent motions produced by explosions in their vicinity. For this experiment two test structures and a comparison structure were used. One test structure and the comparison structure were placed 750 ft from Ground Zero (GZ) (300-psi predicted peak overpressure; 229-psi actual). The other test structure was placed 1050 ft from GZ (100-psi predicted peak overpressure; 104-psi actual). Figure 1 shows structure locations.

TEST STRUCTURES, INSTRUMENTATION, AND TEST CONDITIONS

Figures 2 and 3 illustrate the structures tested. Each test structure consisted of an inner steel cylinder surrounded by a concrete pipe. The steel cylinder was approximately 2½ ft in diameter and included a 2-ft thick concrete-slab bottom to provide adequate mass. This cylinder was enclosed by a reinforced-concrete pipe approximately 3 ft in outside diameter, 10 ft long, and open at both ends. The steel cylinder was separated from the concrete pipe by a shear barrier consisting of one rubber O ring near the top and two O rings near the bottom of the steel cylinder. The comparison structure consisted of a concrete pipe only. This pipe was identical to those used in the test structures, except that it had a concrete-slab bottom. Each of the three structures was placed with its axis vertical and with its top approximately 2 ft below ground level. The two test structures included a layer of frangible backfill immediately outside the concrete pipe and below the bottom (Figs. 4 and 5).

An octagonal slab was placed flush with the ground surface above each of the structures (Fig. 6). Each slab, designed to protect the structure against direct application of overpressure, included a manhole and a manhole cover. Figure 7 shows in cross section the assembly of the cylinders, concrete slab, and manhole cover.

The excavation for these structures was done with a power auger. For each structure a hole 5½ ft in diameter and 15 ft in depth was augered. The backfill of dry sand was compacted by eccentric vibrators, commonly used in the placement of concrete.

In the design of the special frangible backfill, consideration of various possibilities led to the conclusion that glass bottles would be suitable from the standpoint of stiffness, water imperviousness, and

good aging characteristics. It was further concluded that square shapes, with their better characteristics of frangibility, would be more satisfactory than round ones. It was desired that the frangible elements withstand, without failure, pressure of the order of 20 psi. Complete collapse was avoided by placing the bottles around the outside of the structure so that they covered about 53% of the area. Thus in about 47% of the area, the sand backfill was directly in contact with the structure.

Dynamic recording instrumentation included eight channels for acceleration measurements. In addition to dynamic recording, measurements were made of the permanent displacement, both horizontal and vertical, of each structure. Backup measurements were provided by scratch gauges and cork-and-string gauges.

RESULTS

The results of the experiment are summarized in Table 1, in which the peak values of structure motion are compared with the peak values of free-field motion.

The most significant result of the test was the reduction of the peak value of downward vertical acceleration. From Table 1 it is apparent that the frangible elements (bottles) around the sides of the structure (Fig. 8), together with the sand backfill, reduced the peak downward acceleration of the structures to approximately 25% of that of the free-field earth acceleration at the same depth and distances. The rubber O-ring isolation of the inner cylinder produced a further improvement by a factor of approximately 5.

In Table 1 the figures for horizontal motion indicate that comparison structure 2 moved with essentially the same peak acceleration and velocity as the free field. At the same location test structure 1, the inner cylinder of which was protected by both frangible backfill and rubber O rings, sustained horizontal accelerations only 15% of those sustained by either the free field or the comparison structure.

Of particular significance is the great reduction in the peak acceleration as the wave traveled downward through the soil (Table 1).

Velocity vs. time and displacement vs. time curves were developed by successive integration of the acceleration–time curves.

The relative permanent horizontal displacement of each structure with respect to the slab above it is given in Table 2. The permanent vertical displacements of the slabs, determined by a line of levels run before and after the shot, are listed in Table 3.

Scratch-gauge and cork-and-string gauge measurements are listed in Table 4.

CONCLUSIONS

The broad conclusion derived from this experiment is that special backfills designed to reduce the coupling between underground structures and the surrounding soil have significant promise.

Specific conclusions drawn are:

1. The peak downward acceleration of the outer part of test structure 1 was 26% of the corresponding free-field value at the 10-ft depth. This is the best evidence of the value of the frangible elements and sand.

2. The peak downward acceleration of the inner part of test structure 1 was 21% that of the outer cylinder. This is the best evidence of the value of the rubber O rings as shear barriers. It suggests promise for lubricant-type shear barriers.

3. The horizontal motion of the inner part of test structure 1 was significantly less than that of the free field at the 10-ft depth or of comparison structure 2. Since both the frangible backfill and the O rings acted as compression barriers to horizontal motion, it is impossible to conclude which type of isolation gave the most benefit. The motions were small, and it may well be that the resiliency of the O rings was a major factor.

4. The horizontal motion of comparison structure 2 was approximately the same as that of the free field at the 10-ft depth.

5. The peak downward acceleration of the outer part of test structure 3 was less than 50% of the corresponding free-field value. This demonstrates the value of the frangible elements and sand for this structure.

6. The horizontal motion of the inner part of test structure 3 showed important departures from the motion of the free field at the 10-ft depth. These differences were believed to be due primarily to the effect of the O rings, but the combined effects of the frangible elements and the sand were also included and the two cannot be separated.

7. The benefits of this specific arrangement of frangible backfill and sand were significant at the 104-psi overpressure level and were even more impressive at the 229-psi level.

Table 1—STRUCTURE MOTION COMPARED WITH FREE-FIELD MOTION, PEAK VALUES

	Vertical						Horizontal					
	Accel., g		Vel., fps		Displ., ft		Accel., g		Vel., fps		Displ., ft	
	Down	Up	Down	Up	Down	Gauge	Out	In	Out	In	Out	Gauge
	750-ft ground range						229-psi surface overpressure					
Free-field depth, 1 ft	182	23.9	16.2	4.40	0.747	4VI						
5 ft	54.7	16.4	15.2		0.768	4V5						
10 ft	39.2	14.6	10.9		0.521	4V10	14.3	5.76	1.42	0.166	0.078	4H10
20 ft	46.5	14.3	7.6		0.486	4V20A						
50 ft							5.07	2.88	0.885	0.484	0.014	4H50
Comparison structure 2							11.0	7.08	2.50	0.319	0.098	4HX
Test structure 1												
Outer cylinder	10.0	5.67	6.78	2.09	0.371	4VY1A						
Inner cylinder	1.89	5.14	3.98	2.15	0.400	4VYA	1.73	1.23	0.980	0.271	0.047	4HYA
	1050-ft ground range						104-psi surface overpressure					
Free-field depth, 1 ft	21.3	8.83	6.13	3.31	0.219	6V1						
5 ft	16.8	6.94	6.18		0.307	6V5						
10 ft							1.31	2.80	0.400	0.128	0.008	6H10
20 ft	9.97	2.62	4.06	0.056	0.293	6V20A						
50 ft												
Test structure 3												
Outer cylinder	5.08	3.38	3.65	1.220	0.184	6VY1A						
Inner cylinder							0.798	0.845	0.303	0.238	0.015	6HYA

Table 2—RELATIVE PERMANENT HORIZONTAL DISPLACEMENTS OF STRUCTURES IN INCHES*

Structure	Top of outer cylinder: Toward GZ	Top of outer cylinder: Away from GZ	Top of inner cylinder: Toward GZ	Top of inner cylinder: Away from GZ	Bottom of inner cylinder: Toward GZ	Bottom of inner cylinder: Away from GZ	Bottom of inner cylinder: N	Bottom of inner cylinder: S
Test 1	$\frac{11}{16}$		$\frac{11}{16}$		$\frac{1}{2}$			$\frac{1}{2}$
Comparison 2	$\frac{9}{16}$				$\frac{1}{2}$		$\frac{5}{8}$	
Test 3		$\frac{1}{4}$	$\frac{1}{16}$			$\frac{1}{16}$		$\frac{1}{8}$

*All movements are relative to slab.

Table 3—PERMANENT VERTICAL DISPLACEMENT OF SLABS

Structure	Range, ft	Downward displacement, ft
Test 1	750	0.223
Comparison 2	750	0.161
Test 3	1050	0.025

Table 4—RELATIVE DISPLACEMENTS OF STRUCTURE ELEMENTS IN INCHES AS SHOWN BY SCRATCH GAUGES AND CORK-AND-STRING GAUGES

(Equivalent stylus motions shown by cork-and-string gauges are in parentheses.)

Structure	Element to which stylus is attached	Element to which paper is attached	Maximum fall of stylus below start	Maximum rise of stylus above start	Final stylus position: Vertical: Above start	Final stylus position: Vertical: Below start	Final stylus position: Horizontal: Toward GZ	Final stylus position: Horizontal: Away from GZ
Test 1	Slab	Outer cylinder	4.4	3.6		0.71		0.72
	Outer cylinder	Inner cylinder	2.9 ($2\frac{5}{8}$)	0.5 ($\frac{1}{2}$)	0.09 ($\frac{3}{16}$)			
	Slab	Inner cylinder	($6\frac{7}{8}$)	($3\frac{7}{8}$)		($\frac{11}{16}$)		
Comparison 2	Slab	Outer cylinder	2.5 ($2\frac{1}{4}$)	3.9 ($3\frac{15}{16}$)		0.32 ($\frac{5}{16}$)		0.72
Test 3	Slab	Outer cylinder	1.5 ($1\frac{7}{16}$)	3.1 ($2\frac{7}{8}$)	0.04 ($\frac{1}{16}$)			0.03
	Outer cylinder	Inner cylinder	1.1 ($\frac{15}{16}$)	0.3 ($\frac{3}{8}$)	0.18 ($\frac{1}{4}$)			
	Slab	Inner cylinder	(2)	(3)		($\frac{1}{4}$)		

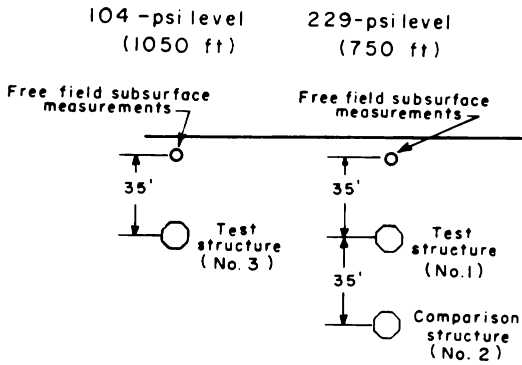

Fig. 1—Structure locations.

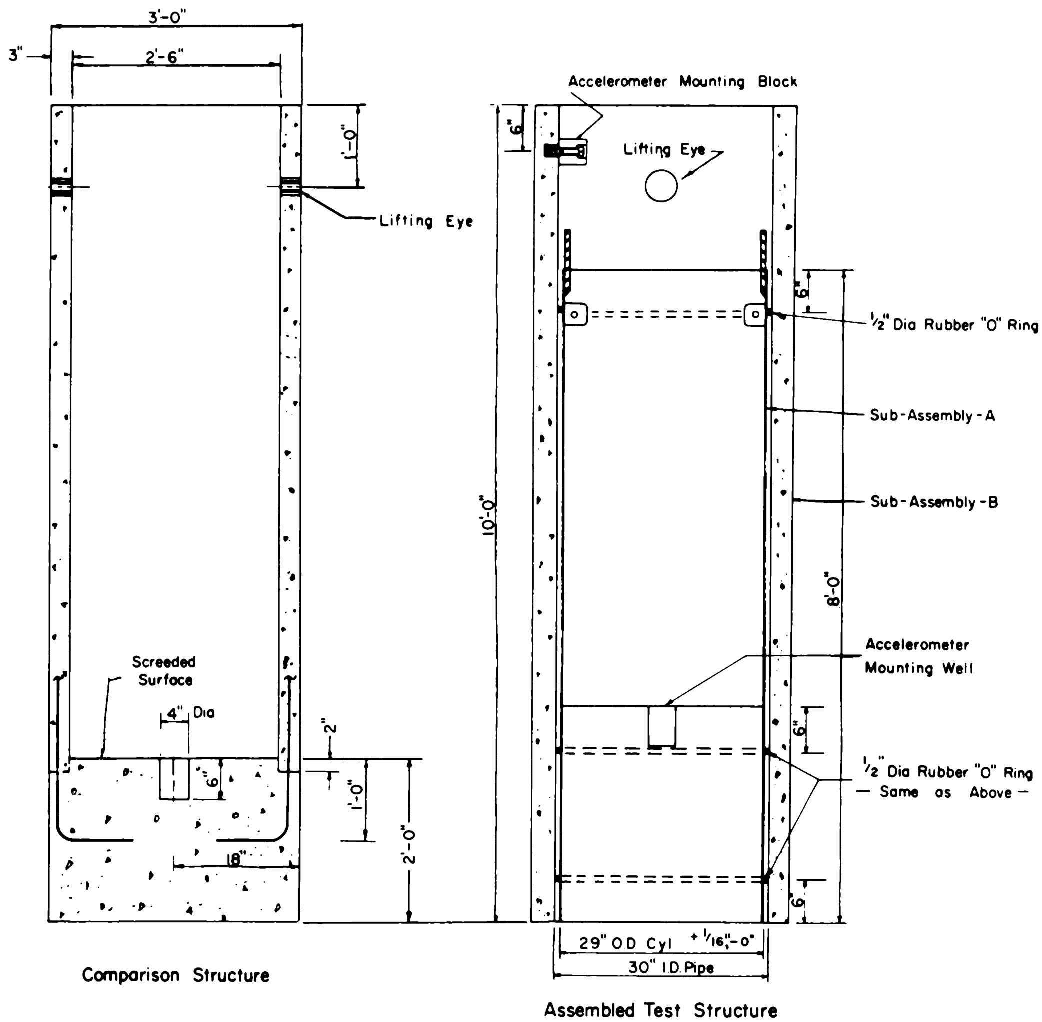

Fig. 2—Comparison structure and test structure.

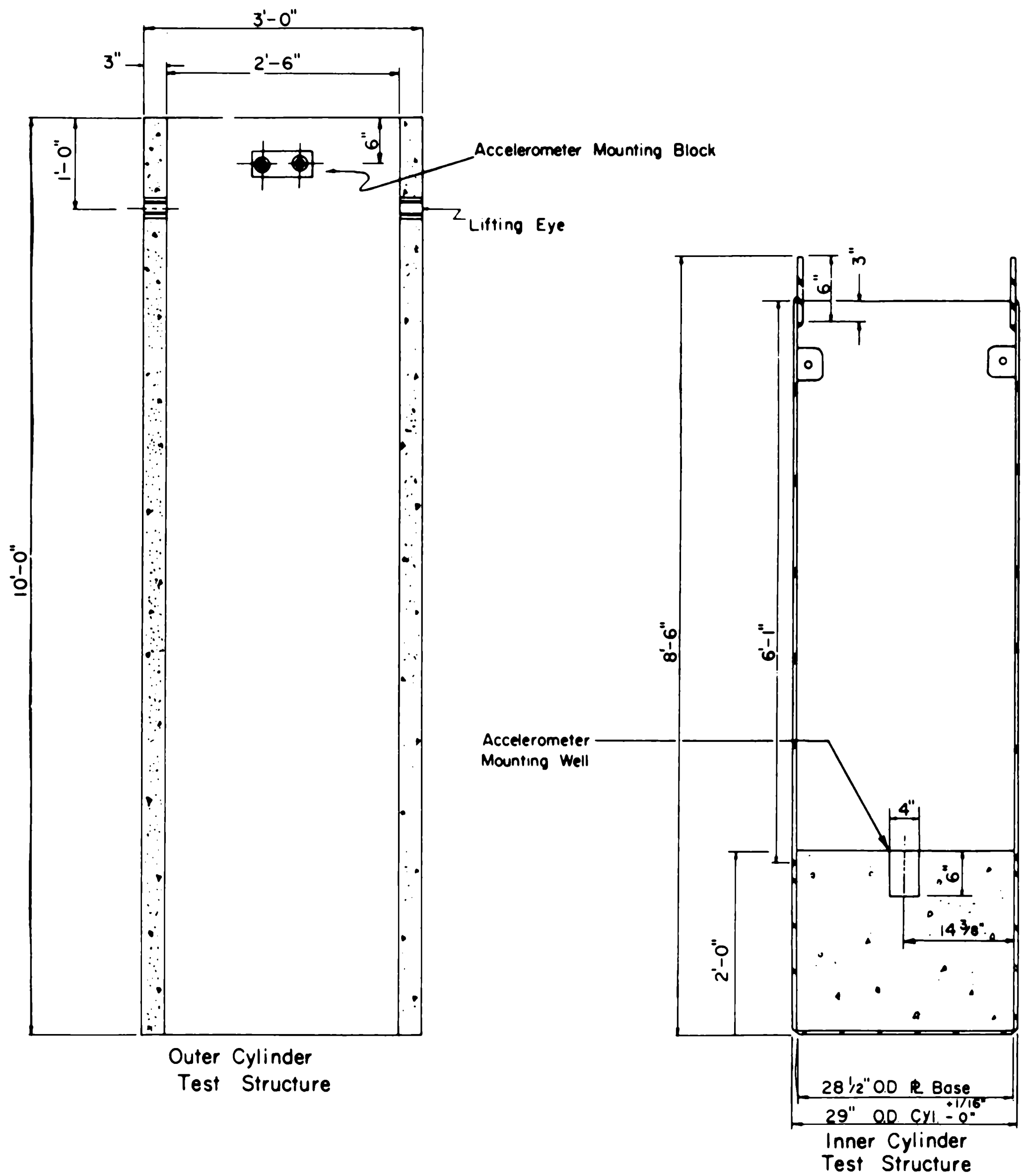

Fig. 3—Cross section of inner and outer cylinders, test structures.

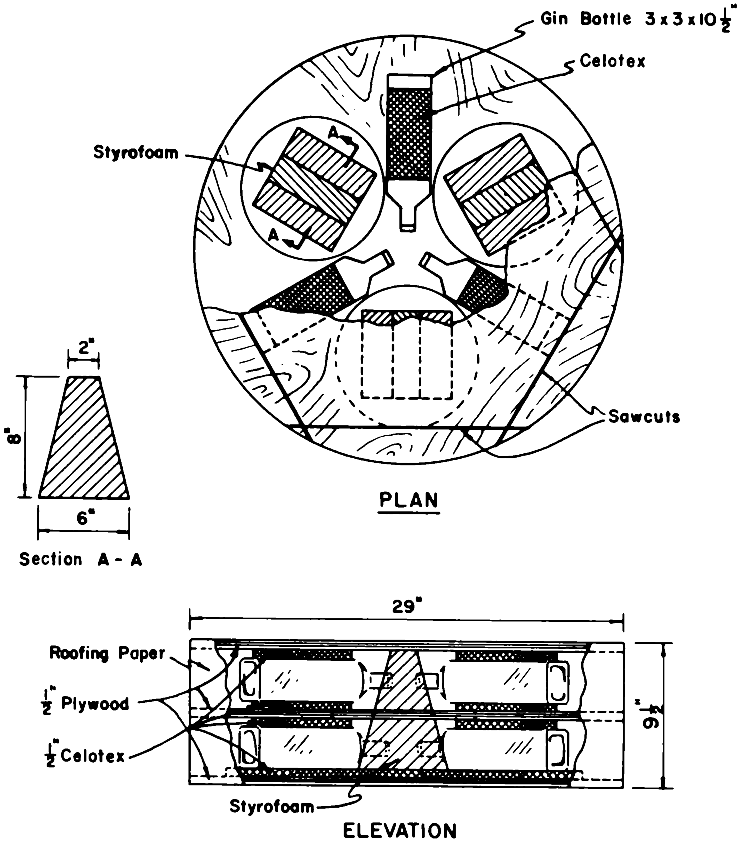

Fig. 4—Plan and elevation of base for inner cylinder.

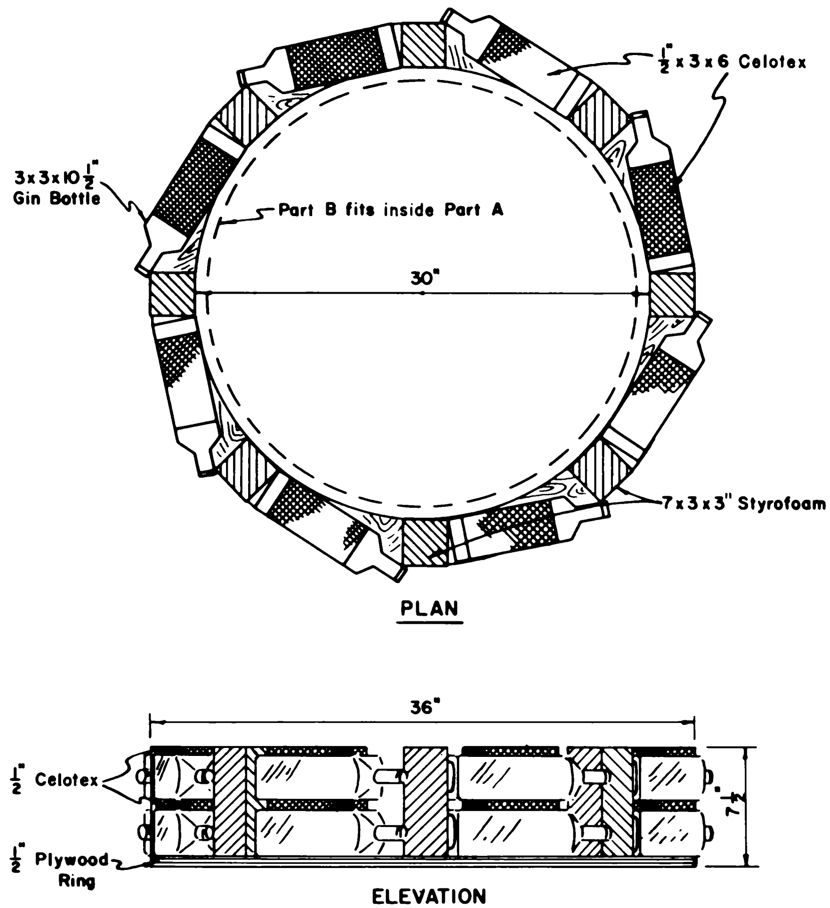

Fig. 5—Plan and elevation of base for outer cylinder.

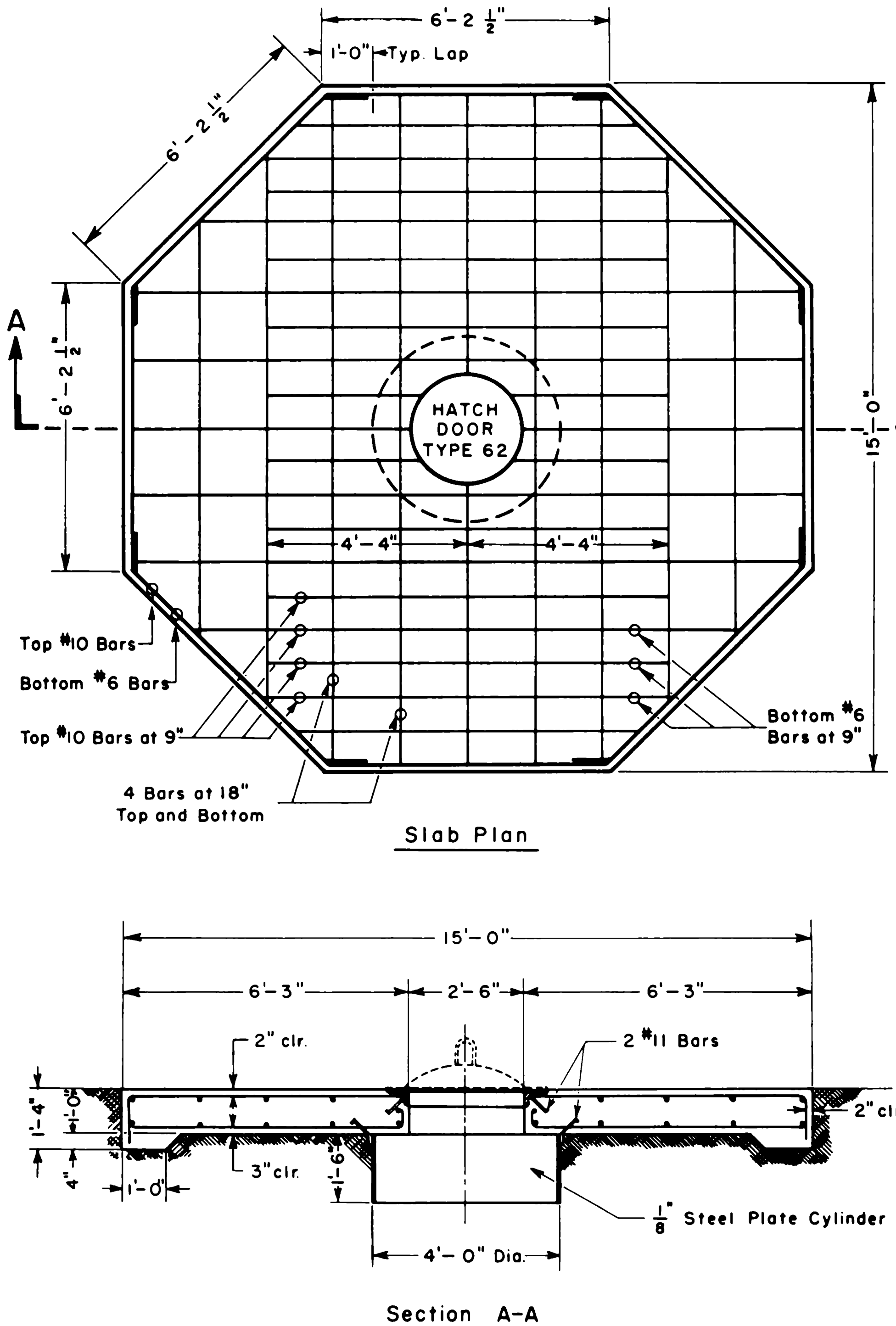

Fig. 6—Concrete slab and hatch cover over buried structure.

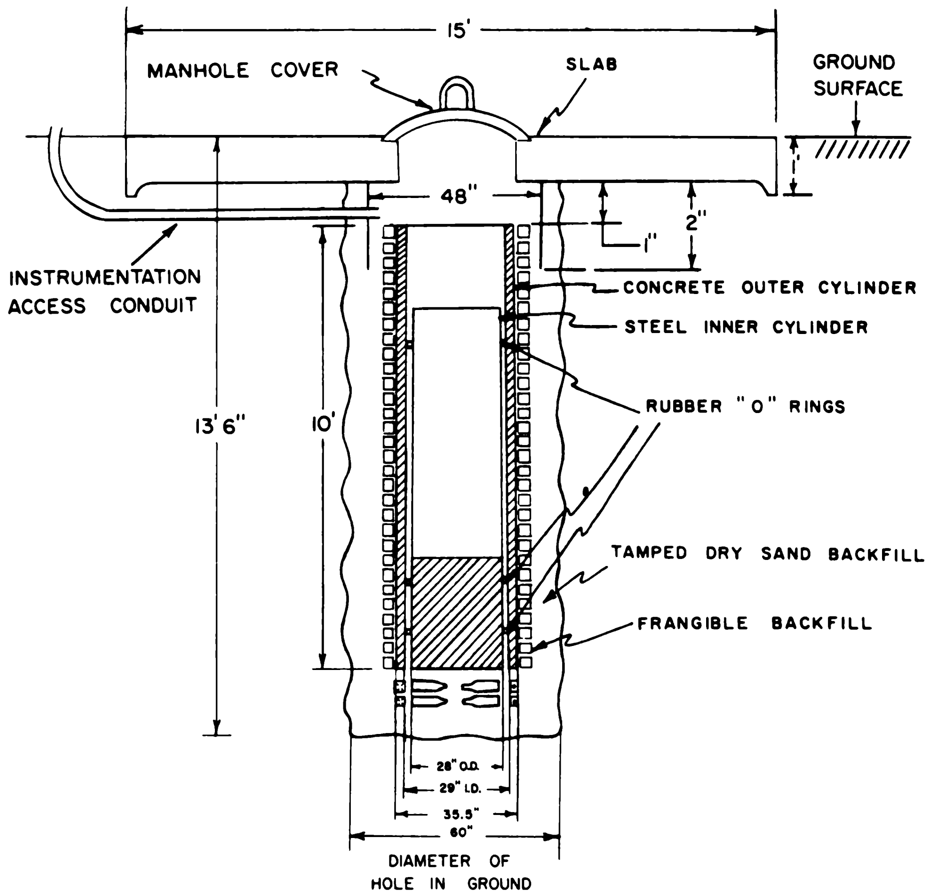

Fig. 7—Cross section of test structure in place.

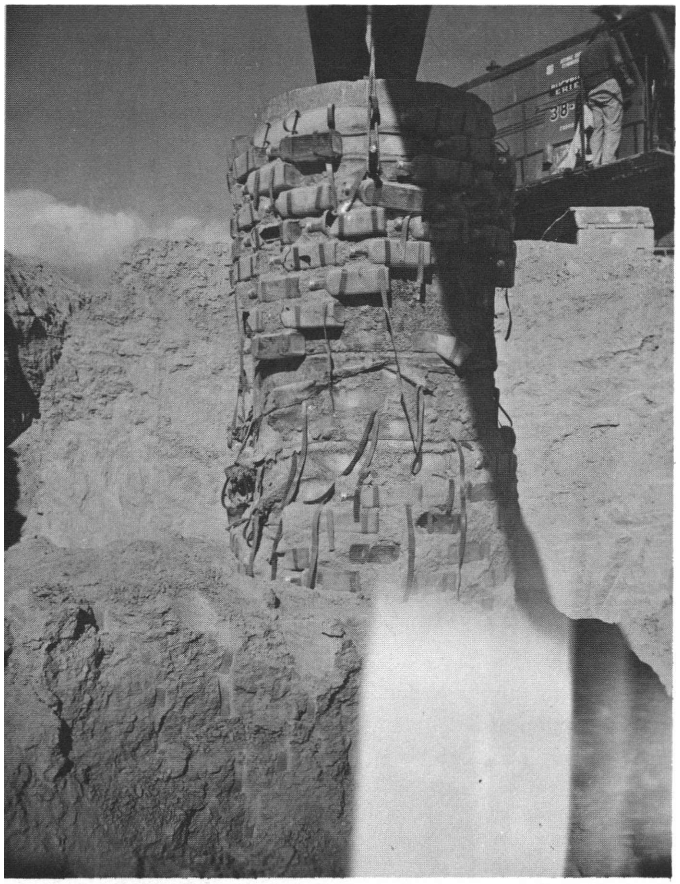

Fig. 8—Frangible elements around outer cylinder of test structure.

SUMMARY 19

FULL-SCALE FIELD TESTS OF DOME AND ARCH STRUCTURES

(Report WT-1425, Operation Plumbbob, Project 3.6, same title, by E. H. Bultmann, Jr., CAPT, USAF, Project Officer, T. G. Morrison, and M. R. Johnson, Mechanics Research Division, American Machine and Foundry Co., Niles, Ill.; and Air Force Special Weapons Center, Kirtland Air Force Base, Albuquerque, N. Mex., Aug. 31, 1960.)

OBJECTIVES AND SCOPE

The primary objectives of the tests were to: (1) determine the blast-wave loading on dome and arch structures, (2) determine the response motions of domes subjected to blast-wave forces, and (3) check the performance of a large blast door after being subjected to blast-wave forces. A secondary objective of the tests was to determine if foundation soil-bearing pressures much higher than those used in conventional practice could be used for carrying the blast loads on a dome structure.

The test structures fell into two general categories: responding structures and nonresponding structures. The responding structures were used primarily to determine the response motions of the structure resulting from the blast load. The nonresponding structures were used principally to measure the distribution of the blast load over the surface of the structure.

Ten structures were used: three 50-ft-diameter, reinforced-concrete, 6-in.-thick responding domes; two 50-ft-diameter, reinforced-concrete, 24-in.-thick nonresponding domes; two 20-ft-diameter responding aluminum domes; two 35-ft-span, 90-ft-long reinforced-concrete nonresponding arches; and one 10 ft 7 in. by 8 ft drawbridge-type door.

The nonresponding structures were instrumented to determine pressure as a function of time, and the responding structures were instrumented to determine pressure and displacement as a function of time. A limited number of shear, strain, and ground-acceleration measurements also were recorded on the responding domes.

The three 50-ft responding domes were identical as far as it was practical to build them. They were placed in the 70-, 35-, and 20-psi regions and were designed to suffer slight damage at the 35-psi level. Both aluminum domes were placed in the 70-psi region. The shell of one was 1 in. thick, the other ½ in. thick. The nonresponding domes and arches were placed, one each, in the expected 70- and 35-psi regions. The nonresponding domes were self-supporting; the nonresponding arches consisted of a 1-ft-thick slab poured on an earth mound. The drawbridge door was placed in the expected 35-psi region.

Actual overpressures developed in the predicted 70- and 20-psi regions were very close to the predicted overpressures. The actual overpressure at the expected 35-psi region was about 40 psi.

Figure 1 shows the location of the test structures with respect to the Ground Zero (GZ) of the blast.

TEST STRUCTURES

Table 1 summarizes the important features of each structure and indicates the sponsoring agency of each.

A generalized cross section of the reinforced-concrete domes is shown in Fig. 2. The placement of the shell reinforcing on the concrete domes is illustrated in Fig. 3; details of the reinforcing are listed in Table 2.

A cross section of the aluminum domes showing the shell and foundation is presented in Fig. 4. Foundation-reinforcing data are listed in Table 2.

Details of two nonresponding arches, identical in construction, are shown in Fig. 5 and Table 2.

Details of the prototype door, which was located at the 35-psi region, are shown in Fig. 6.

The responding concrete domes, as well as the nonresponding arches, were poured on a shotcrete-lined excavation (Figs. 7 and 8).

The aluminum domes were shop-fabricated in two halves. Figure 9 shows an aluminum dome foundation. The two halves of the shell are in the background. They were placed on the foundation and welded together. A completed aluminum dome is shown in Fig. 10.

The completed prototype door is shown in Fig. 11.

RESULTS

The nonresponding concrete arches sustained slight structural damage. Both arches sheared at the end walls, the 70-psi arch shifting about $2\frac{1}{2}$ in. away from GZ at the quarter points of its arc, and the 35-psi arch shifting about 1 in. The 70-psi arch sustained a tension crack just to the leeward of its crown along its full length. Circumferential cracks appeared at the reinforcing bar spacing along the full length of the arc of the 70-psi arch. Typical damage to the arch is shown in Fig. 12.

The nonresponding concrete domes survived the blast with no structural damage. A few hairline cracks appeared in the 70-psi dome and its foundation.

The responding concrete domes suffered various degrees of damage, depending on the pressure range. The dome in the high-pressure region suffered, essentially, total destruction (Fig. 13); the dome in the medium-pressure region was severely damaged (Fig. 14); and the dome in the low-pressure (20-psi) region was undamaged. The steel reinforcing rods from the destroyed regions of both damaged domes were stripped of practically all concrete (Fig. 15), which was remarkable because concrete bonds itself very well to steel. Foundations of all three domes survived without damage, and access doors showed no effects.

Both responding aluminum domes were completely destroyed. The $\frac{1}{2}$-in.-thick dome was dished down into the foundation. The 1-in.-thick shell was crushed against the side of the foundation away from GZ (Fig. 16).

The prototype door survived the test without significant permanent deformation. The locking and hinge mechanisms functioned perfectly after the test.

CONCLUSIONS

Loading: Analysis of the loading data failed to disclose any reflected-pressure effects on the structures because of the lack of a classical type of shock front in the precursor blast wave at each of the structures. Enough loading information was obtained on the nonresponding structures at the 70-psi region to permit the computation of pressure coefficients as a function of time on these structures.

For precursor-type blast waves, where the peak dynamic pressure is significantly greater than that given by the classical theory, dome and arch design should be based on dynamic pressure rather than overpressure.

End effects had a negligible influence on arch loading.

Response: The nonresponding arches responded sufficiently to indicate the validity of the theoretically obtained conclusion that, compared with domes, arches are inefficient structurally in resisting high drag loading.

The cracking at the end walls of nonresponding arches verified the theoretically obtained conclusion that this joint would have to be ruggedly proportioned and highly reinforced to prevent serious cracking.

Ground surface acceleration at overpressure levels of 70 psi and below had negligible influence on dome response.

The foundation design was conservative as predicted, even though the peak and average bearing values were extremely high by conventional standards.

Table 1—SUMMARY OF TEST STRUCTURES

Structure	Type of structure	Primary study	Peak overpressure expected, psi	Construction material	Diameter or span, ft	Length, ft	Height, ft	Shell thickness, in.	Distance from GZ, ft	Midsurface radius, ft
				FCDA Project 30.1						
F-30.1-8001.01	Dome	Responding	70	Reinforced concrete	50		10.7	6	1180	35.75
F-30.1-8001.02	Dome	Responding	35	Reinforced concrete	50		10.7	6	1600	35.75
F-30.1-8001.03	Dome	Responding	20	Reinforced concrete	50		10.7	6	2030	35.75
F-30.1-8008	Prototype door	Responding	35	Structural steel	*		*	*	1600	*
				USAF Project 3.6						
F-3.6-9027.01	Dome	Nonresponding	70	Reinforced concrete	50		11.67	24	1180	36.5
F-3.6-9027.02	Dome	Nonresponding	35	Reinforced concrete	50		11.67	24	1600	36.5
F-3.6-9026.01	Dome	Responding	70	Aluminum	20		4.13	½	1180	14.14
F-3.6-9026.02	Dome	Responding	70	Aluminum	20		4.13	1	1180	14.14
F-3.6-9028.01	Arch	Nonresponding	70	Reinforced concrete	34	90	10.25	12	1180	19.5
F-3.6-9028.02	Arch	Nonresponding	35	Reinforced concrete	34	90	10.25	12	1600	19.5

*Dimensions of the prototype door structure were: 21 ft 3 in. long by 12 ft wide by 9 ft 4 in. high. Dimensions of steel door were: 10 ft 7 in. wide by 8 ft 0 in. high.

Table 2—REINFORCING OF SHELL STRUCTURES (MAIN REINFORCING)

Structure	Shell	Foundations		
		Longitudinal	Stirrups	Dowels
50-ft-diameter responding domes	No. 4 bars at 6-in. centers each face each way	39 No. 6 bars	No. 4 bars at 3-ft centers inclined 45° both ways	No. 4 bars at 6-in. centers inclined 45° both faces both ways
50-ft-diameter non-responding domes	No. 4 bars at 6-in. centers each face each way	39 No. 6 bars	No. 4 bars at 3-ft centers inclined 45° both ways	No. 4 bars at 6-in. centers inclined 45° both faces both ways
34-ft by 90-ft non-responding arches	Transverse: No. 4 bars at 6-in. centers each face	5 No. 8 bars	No. 5 bars at 6-in. centers	No. 6 bars at 12-in. centers both faces
	Longitudinal: No. 4 bars at 12-in. centers each face	16 No. 5 bars		
20-ft-diameter responding domes		18 No. 11 bars 10 No. 6 bars	No. 7 bars at 10-in. centers vertical	

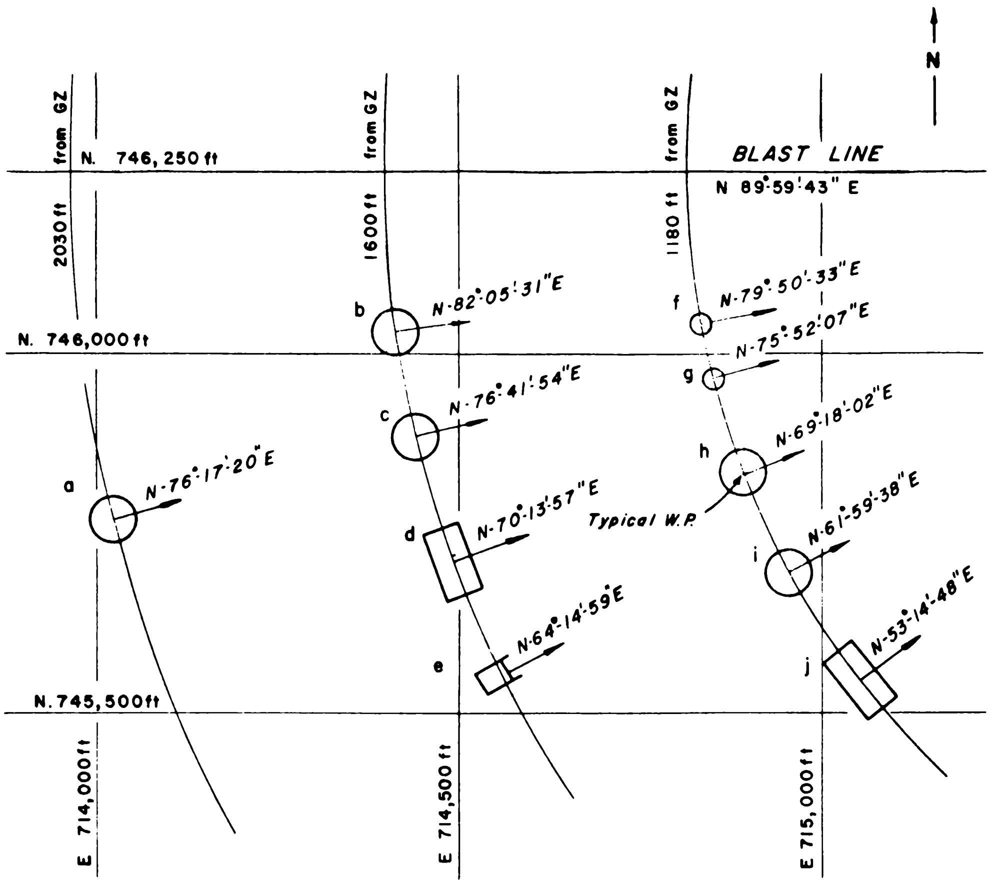

PLOT PLAN

Location of Structure at Work Point

Mark	Project	To Ground Zero	Location		To Blast Line	Structure
		feet	feet		feet	
a	30.1-8001.03	2,030	N-745,768.94	E-714,028.64	481	Concrete Dome
b	30.1-8001.02	1,600	N-746,029.90	E-714.416.90	220	Concrete Dome
c	3.6-9027.02	1,600	N-745,881 .95	E-714,443.61	368	Concrete Dome
d	3.6-9028.02	1,600	N-745,708.02	E-714,494.96	541	Concrete Arch
e	30.1-8008.00	1,600	N-745,555.04	E-714,559.55	695	Prototype Door
f	3.6-9026.01	1,180	N-746,041.93	E-714,839.08	208	Aluminum Dome (1/2-inch)
g	3.6-9026.02	1,180	N-745,961.96	E-714,856.29	288	Aluminum Dome (1-inch)
h	3.6-9027.01	1,180	N-745,833.00	E-714,896.75	417	Concrete Dome
i	30.1-8001.01	1,180	N-745,696.03	E-714,958.74	554	Concrete Dome
j	3.6-9028.01	1,180	N-745,544.08	E-715,055.09	706	Concrete Arch

Fig. 1—Layout of test complex.

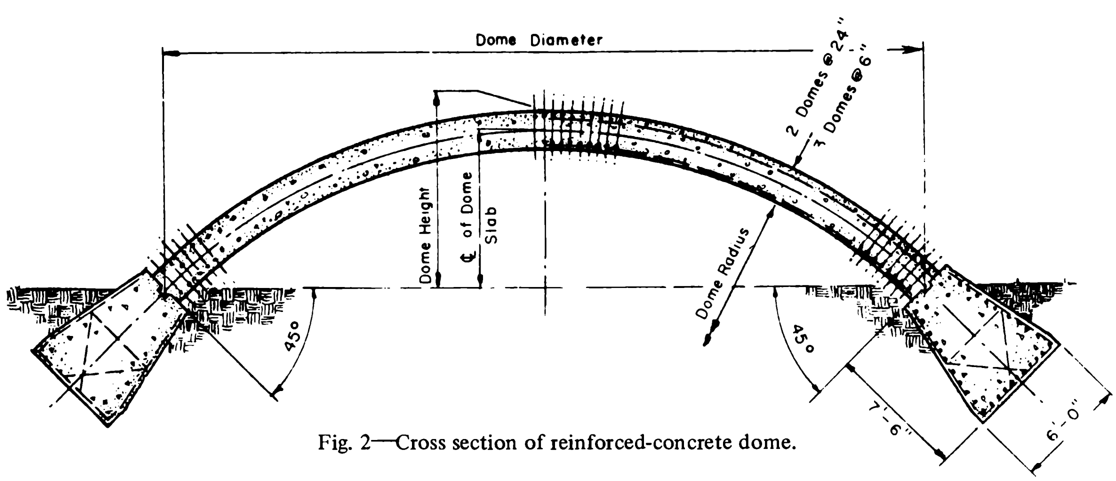

Fig. 2—Cross section of reinforced-concrete dome.

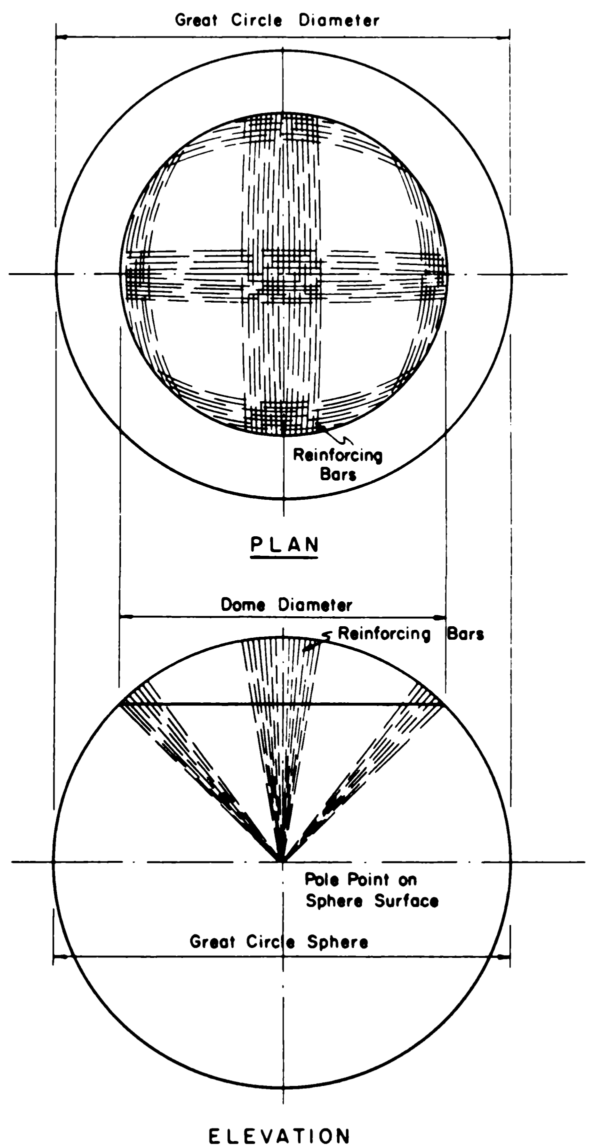

Fig. 3—Reinforcing of concrete dome.

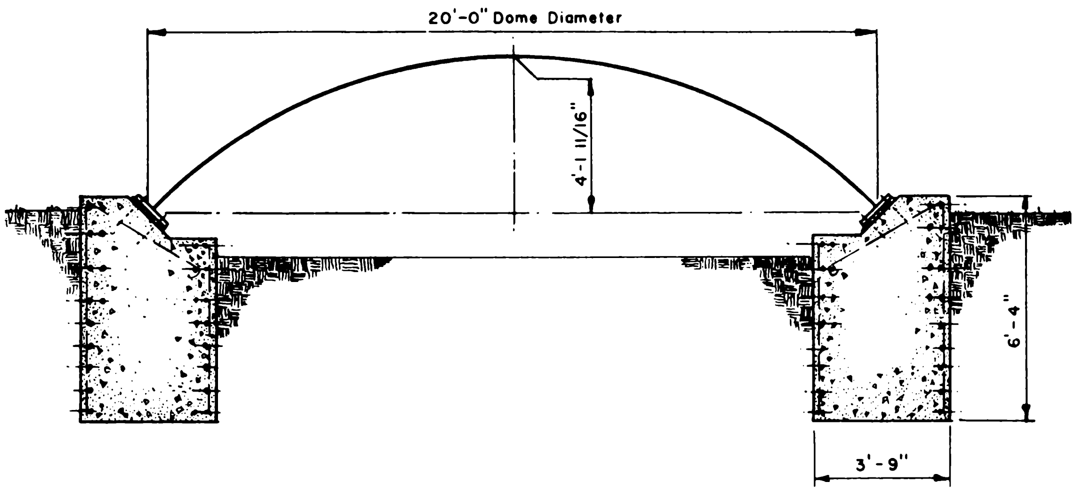

Fig. 4—Cross section through aluminum dome and foundation.

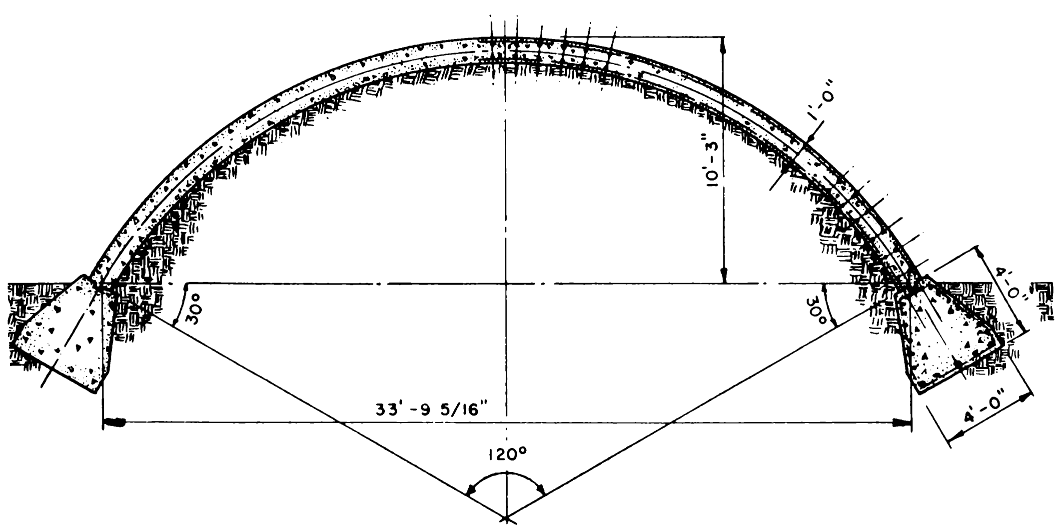

Fig. 5—Cross section through arch and foundation.

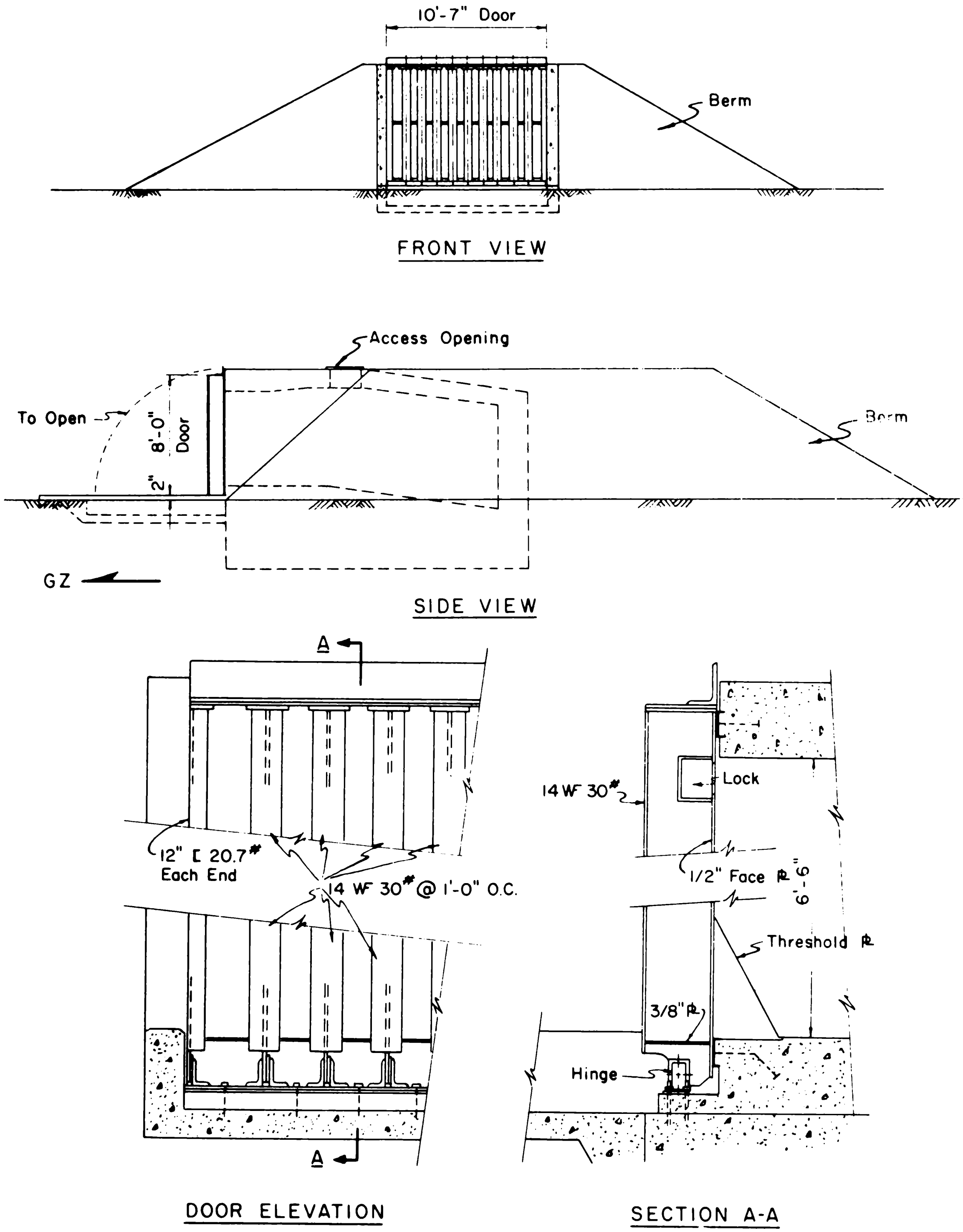

Fig. 6—Prototype door details.

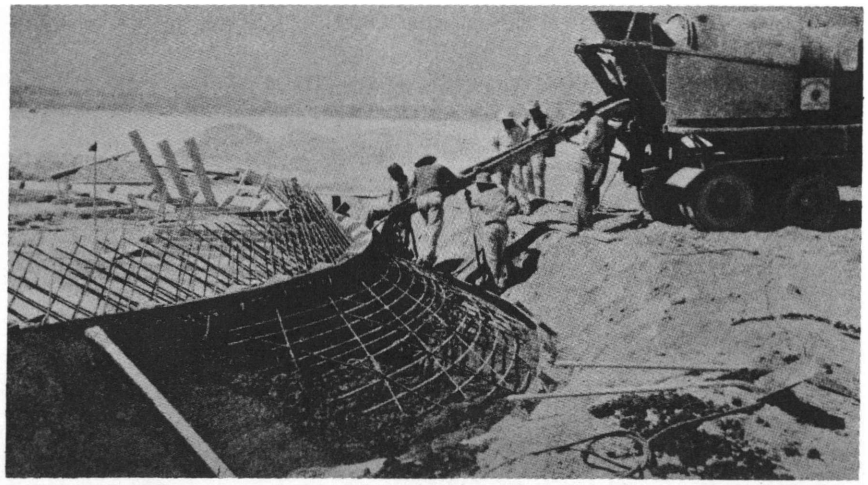

Fig. 7—Construction of foundation for responding concrete dome.

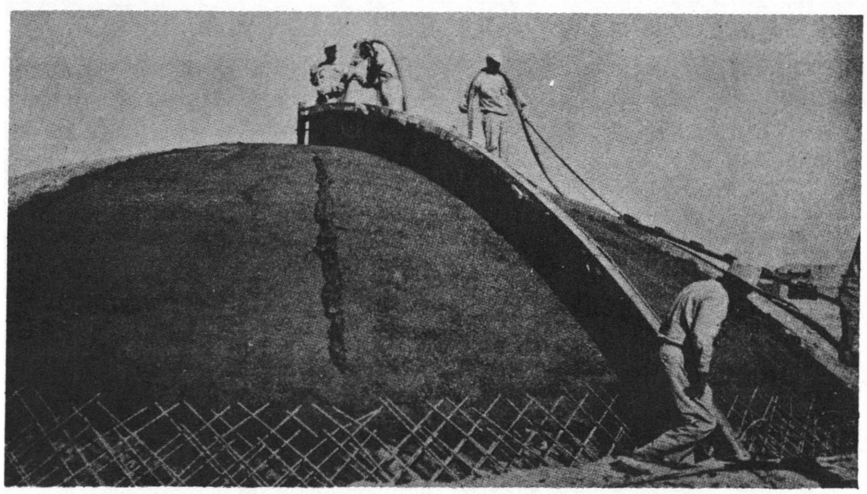

Fig. 8—Shotcreting of earth-berm form for responding concrete dome.

Fig. 9—Foundation for aluminum dome. Two halves of shell are in background.

Fig. 10—Completed aluminum dome.

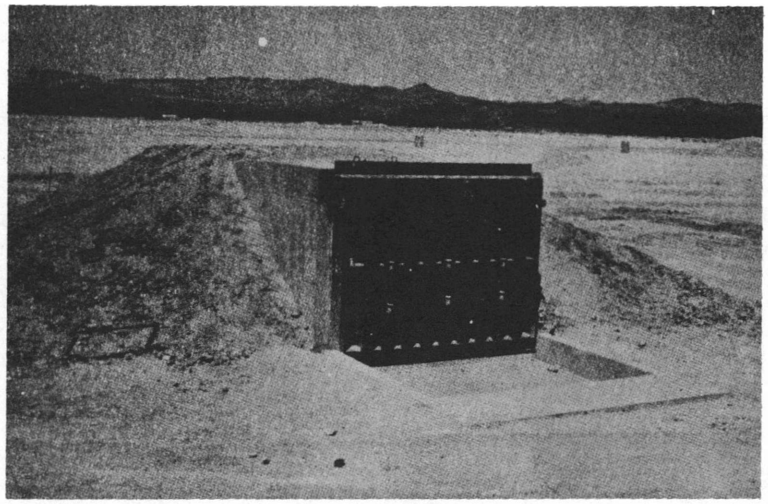

Fig. 11—Completed prototype door.

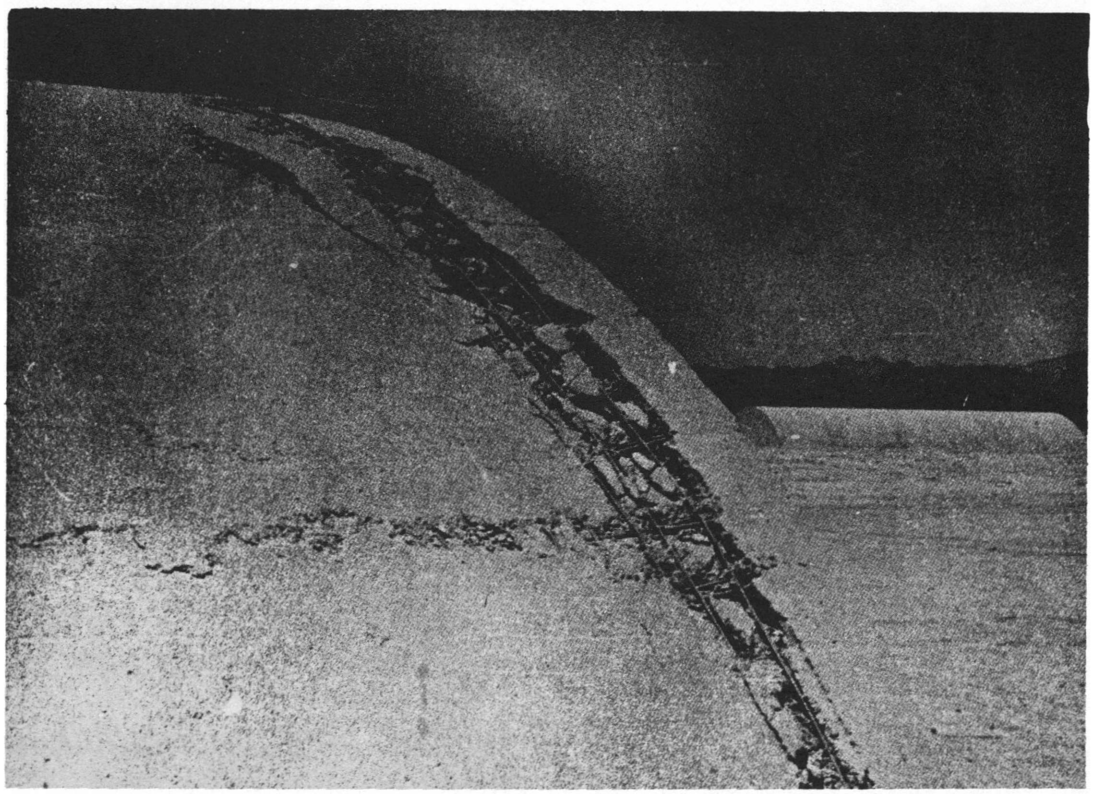

Fig. 12—Damage to side of concrete arch facing GZ at 70-psi overpressure region.

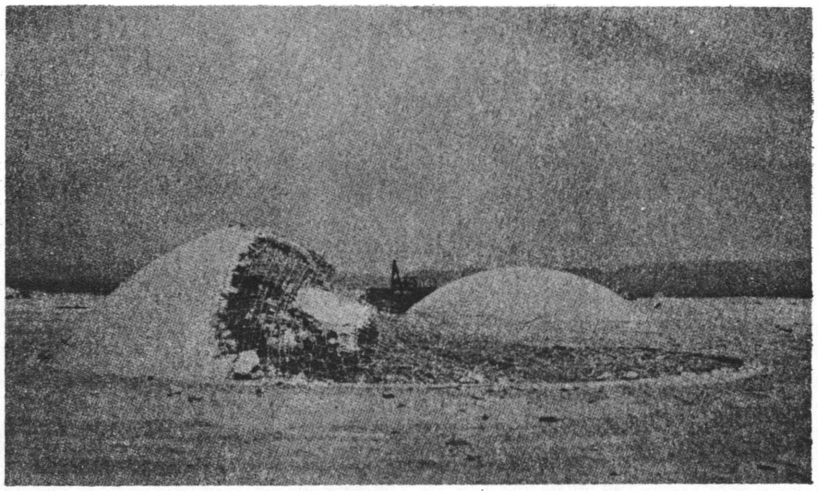

Fig. 13—Left side of responding concrete dome at 70-psi overpressure region.

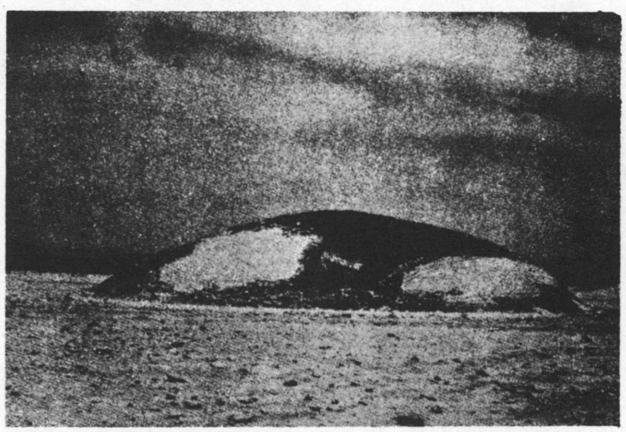

Fig. 14—Damage to responding concrete dome at 35-psi overpressure region, showing side of dome facing GZ.

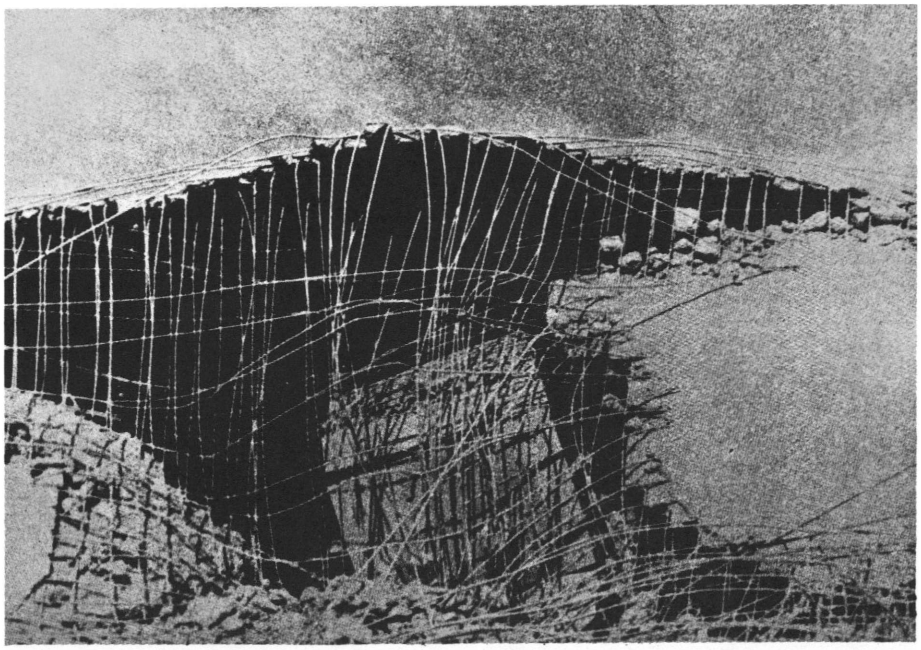

Fig. 15—Responding concrete dome at 35-psi overpressure region.

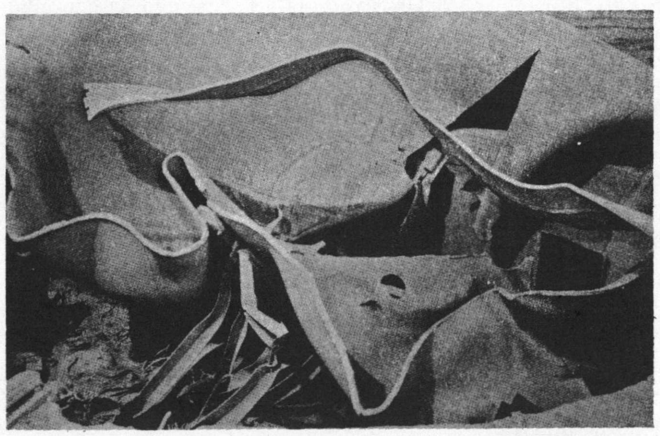

Fig. 16—One-in.-thick aluminum dome, showing side of dome facing GZ.

SUMMARY 20

RESPONSE OF DUAL-PURPOSE REINFORCED-CONCRETE MASS SHELTER

(Report WT-1449, Operation Plumbbob, Project 30.2, same title, by E. Cohen, E. Laing, and A. Bottenhofer, Ammann & Whitney, Consulting Engineers, New York, N. Y., Sept. 15, 1962.)

OBJECTIVES AND SCOPE

The primary objective of Project 30.2 was to evaluate the protection afforded by a reinforced-concrete dual-purpose underground parking garage and personnel shelter against effects of a nuclear detonation. Secondary objectives were to obtain additional information regarding blast load transmitted to underground structures, to obtain information regarding reflected and dynamic pressures in the ramp and on the entrance door, to obtain data on nuclear-radiation attenuation characteristics of the structure, and to check assumptions used in design procedures.

The Office of Civil and Defense Mobilization (OCDM) contracted with Ammann & Whitney, Consulting Engineers, to prepare a preliminary layout for a dual-purpose reinforced-concrete underground parking garage and shelter and to design a structurally representative portion of such a structure to be exposed to nuclear blast for test purposes. The structure was designed with a flat-slab roof system. Figure 3 shows the prototype layout of this construction.

Structure 30.2, a typical full-scale section of the prototype and the largest shelter tested in Operation Plumbbob, was located at the predicted 35-psi peak overpressure level. The shelter was exposed to Priscilla shot, an approximately 37-kt, 700-ft-high balloon burst (ref. ENW, p. 675) at a ground range of 1600 ft. The structure was located with the center line of the ramp radial to Ground Zero (GZ).

Postshot soil borings were made to obtain undisturbed samples for determining soil characteristics.

Preshot and postshot field surveys were made to determine the total lateral and vertical displacement of the structure.

Blast instrumentation consisted of Wiancko pressure gauges, Carlson earth-pressure gauges, dynamic-pressure gauges, and a self-recording pressure gauge. Structural response was recorded by Ballistic Research Laboratories deflection gauges.

Radiation measurements were taken with film dosimeters, gamma-radiation chemical dosimeters, and one gamma-rate telemetering unit.

DESIGN AND CONSTRUCTION

Figure 4 illustrates the below-grade flat-slab test structure. The structure has an interior floor area of 7569 sq ft; a 14-ft vehicular ramp along one side; and a reinforced-concrete rolling door 4-ft 6-in. thick at

the entrance to the shelter area. There is a 3-in.-wide inflatable rubber gasket seal around the door perimeter.

The shelter was designed for dynamic behavior using ultimate-strength theory and theoretical loadings consistent with a peak incident shock of 40 psi for a megaton-range weapon. The roof slab was designed for a 40-psi long-duration load as a flat slab, and the earth-covered walls of the shelter, for a 15-psi long-duration load. The exposed shelter wall and rolling door at the ramp were increased in thickness to provide specified radiation protection.

The strengths of the materials used in the design of the structures, except when increased to account for rapid strain rates, were as follows:

Concrete, 4,000 psi (ultimate)
Reinforcing steel (intermediate grade), 47,500 psi (yield)
Structural steel, 38,000 psi (yield)

The soil encountered was unusual in character and possessed remarkable properties; it consisted of many thinly stratified layers cemented together. The soil was very fine grained and was nonplastic or slightly plastic in character. Pronounced horizontal planes of weakness existed.

RESULTS

The only substantial damage noted in connection with this project was sustained by the retaining wall at the end of the ramp (Fig. 1) where damage was expected because of the orientation of the wall relative to GZ. The damage, however, did not impair the usefulness of the ramp for vehicular use during the immediate postshot period.

The peak average (reflected) pressure on this end wall was 188 psi, considerably higher than the peak side-on pressure of 39 to 40 psi recorded at the ground surface. The damage consisted of complete separation of the top half of the end wall from the bottom, disintegration of the lower portion into loose rubble, separations along the planes of the reinforcement, and failure of the splices without yielding of the steel (Fig. 2). These failures were attributed in part to the poor adhesive quality of the concrete in place.

The absence of cracks in the roof slab and walls indicates that the structure was capable of resisting the blast load without appreciable inelastic deformation. A peak-pressure range of 21 to 42 psi (31 psi av. vs. 39.5 av. on the ground surface) was recorded on the roof surface 3 ft below the ground. The friction angle of the earth adjacent to the structure was approximated at 40°. Consequently, the recorded wall pressures of 2.8 to 5 psi correspond to about a 50% attenuation of the peak surface pressure with depth.

According to the test results, the relative displacement of the foundation with respect to the reference pile was 0.11 in. peak transient and 0.02 in. permanent.

The door withstood the blast without any evidence of shifting or disalignment. Locking bolts in the door were intact and retracted freely. The door wheels were not damaged, and the track was not displaced (Fig. 5). The door and end pilaster were partially blackened by thermal radiation. The pneumatic seal around the doorframe, stripped and torn along its entire length, was forced by the blast pressure toward the interior of the shelter. Despite this failure of the sealing gasket, the rise in pressure in the interior did not exceed 1.0 psi. However, the pneumatic seal around the doorframe should be replaced by a rigid mechanically operated seal.

No damage to the garage interior was observed. Lateral movement of the isolated columns was indicated by a small amount of concrete spalling and by cracking of the floor slab around the perimeter of the column. The cracking occurred at the blast side of the columns, and the spalling occurred at the leeward side.

The peak results from records obtained from the project instrumentation program are summarized in Tables 1, 2, and 3. Figure 6 shows the instrumentation layout. Table 1 lists the peak values for the Wiancko pressure gauges, which were located on the rolling door, the ramp end, and the sidewalls. Results of the Carlson earth-pressure gauges in the shelter roof slab, rolling door, and walls, and in the ramp end and sidewalls are given in Table 2. Table 3 contains the peak values obtained from the deflection gauges placed inside the structure and on the ramp.

All ramp dosimeters were blown away or badly damaged; consequently, data for radiation received on the outside of the shelter are missing. The gamma surface-radiation dose at the structure was estimated at 102,000 r. The average interior dose recorded by the dosimeters in the structure was 1.2 r, which corresponds to an attenuation factor of 1.2×10^{-5}.

The free-field acceleration vs. time ground motions in the horizontal and vertical directions were recorded by accelerometers enclosed in protective canisters buried at various depths below the ground surface. Table 4 lists the peak accelerations recorded to a depth of 60 ft.

CONCLUSIONS AND RECOMMENDATIONS

1. The test structure provided adequate protection from the effects of the test device at the test GZ distance. Despite failure of the door-sealing gasket, the rise in pressure in the interior did not exceed 1.0 psi.

2. The flat-slab roof and supporting structure were more than adequate to resist the 39-psi peak incident test loading.

3. The door design was satisfactory; the pneumatic seal around the doorframe, however, should be replaced by a rigid mechanically operated seal.

4. High pressures that acted on the end retaining wall were the result of the particular orientation of the structure relative to GZ and the site conditions. The damage that occurred under these severe circumstances did not impair the usefulness of the ramp for vehicular use during the immediate postshot period. Moreover, an actual shelter–garage structure would probably have alternate vehicular and personnel entrances and exits. For this reason the design strength of the retaining walls need not be increased. Brittle failure, however, is undesirable, therefore in future designs the details should be modified to produce a more ductile behavior.

5. The blast capacity of the as-built structure was larger than intended; consequently, a prototype design could be placed at a higher pressure level. It is estimated that for a megaton weapon such a structure would be adequate for a peak blast pressure of 50 psi (assuming an allowable displacement equal to approximately three times the peak equivalent elastic value). It is recommended that the concrete strength for the columns and roof slab be made 5000 psi, which was the value of the as-built slab and columns of the test structure.

Table 1—WIANCKO AIR-PRESSURE-GAUGE MEASUREMENTS (PEAK VALUE)

Gauge	Peak pressure, psi	Remarks
P1	109.65	Good record (shift during shot)
P2	266.46	Good record (gauge packed with debris)
P3	104.86	Good record
P4		Record no good (faulty connection)
P5	22.04	Good record

Table 2—CARLSON EARTH-PRESSURE-GAUGE MEASUREMENTS (PEAK VALUE)

Gauge*	Peak pressure, psi	Remarks
$\overline{P}6$	21.27	Good record
$\overline{P}7$	32.11	Good record
$\overline{P}8$	31.05	Good record
$\overline{P}9$	28.17	Good record
$\overline{P}10$		Unreadable (system balance changed before shot)
$\overline{P}11$	41.51	Good record
$\overline{P}12$	3.55	Good record
$\overline{P}13$	2.81	Good record (ground pressure did not return to original zero)
$\overline{P}14$	5.05	Good record
$\overline{P}15$		No record (gauge cable broken)
$\overline{P}16$		Record no good (faulty connection)

*Self-recording.

Table 3—DEFLECTION-GAUGE MEASUREMENTS (PEAK VALUE)

Gauge	Peak wire movement, in.	Peak deflection, in.	Remarks
D1	0.1196	0.25	Good record (center column)
D2	0.2851	0.48	Bad record (column strip)
D3	0.1900	0.32	Good record (column strip)
D4	0.2913	0.49	Good record (column strip)
D5	0.2274	0.38	Good record (column strip)
D6	0.1889	0.31	Good record (column strip)
D7	0.1182	0.20	Good record (column strip)
D8	0.1133	0.19	Good record (column strip)
D9	0.1761	0.29	Good record (column strip)
D10	0.2154	0.46	Good record (center of panel)
D11	0.2723	0.58	Good record (center of panel)
D12	0.2411	0.52	Good record (center of panel)
D13	0.1964	0.42	Good record (center of panel)
D14	−0.0572, +0.0434	−0.16, +0.12	Good record (wall at line 5)
D15			Unreadable (system balance changed before shot)
D16			Gauge destroyed at blast arrival
D17			Gauge destroyed at blast arrival
D18			Unreadable (system balance changed before shot)

Table 4—MEASURED PEAK FREE-FIELD GROUND ACCELERATION

Project 1.4			Project 1.5		
Depth	Vertical	Horizontal	Depth	Vertical	Horizontal
5 ft	9.16 g	No record	Surface	9.1 g	−1.3 g
10 ft	4.84 g	No record	10 ft	5.4 g	2.5 g
Below 10 ft	No record	No record	30 ft	2.2 ft	No record
			60 ft	1.8	−2.4 g

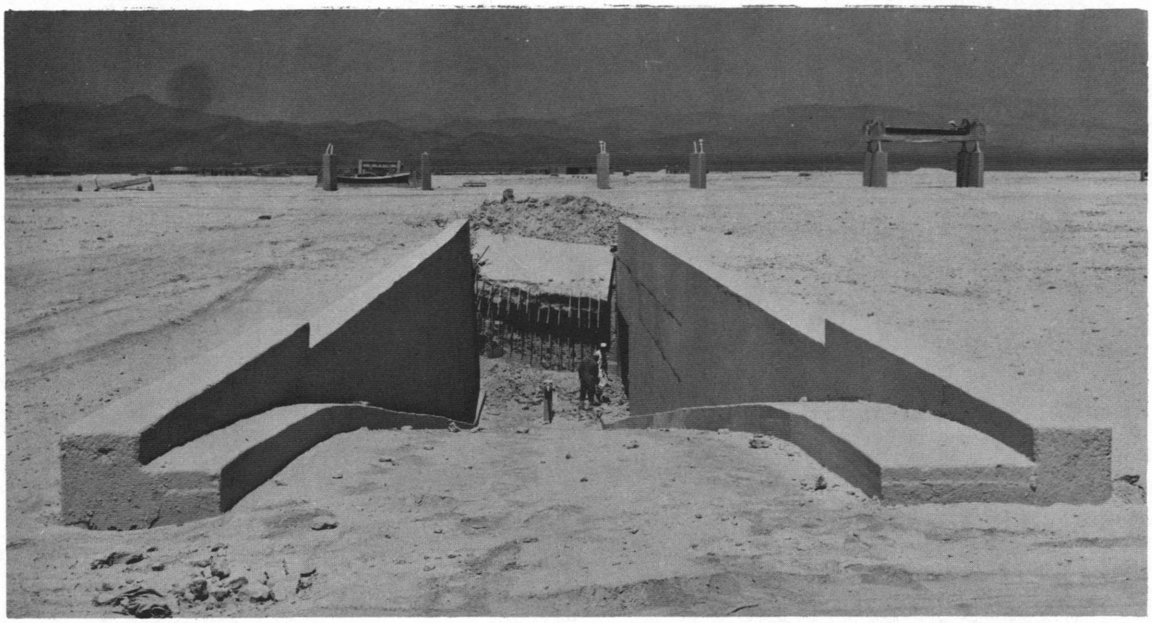

Fig. 1—View of ramp looking toward damaged end wall, postshot.

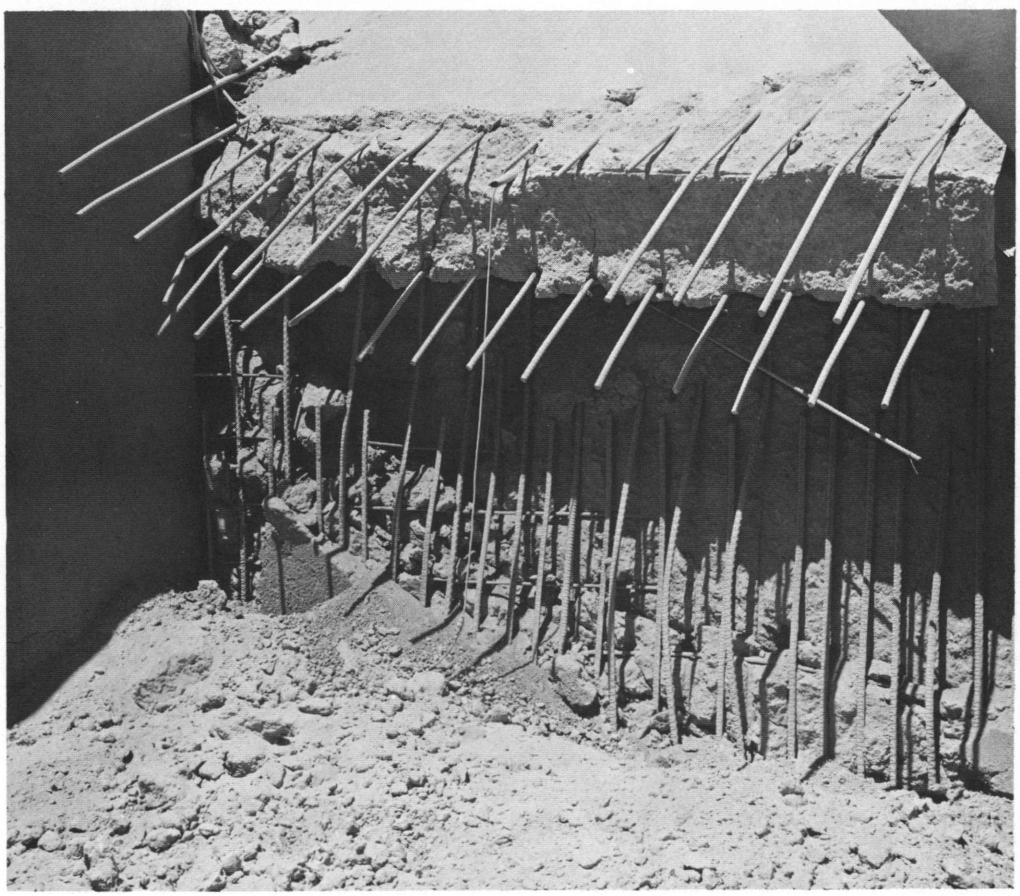

Fig. 2—Detail of failure showing fractured bars, postshot.

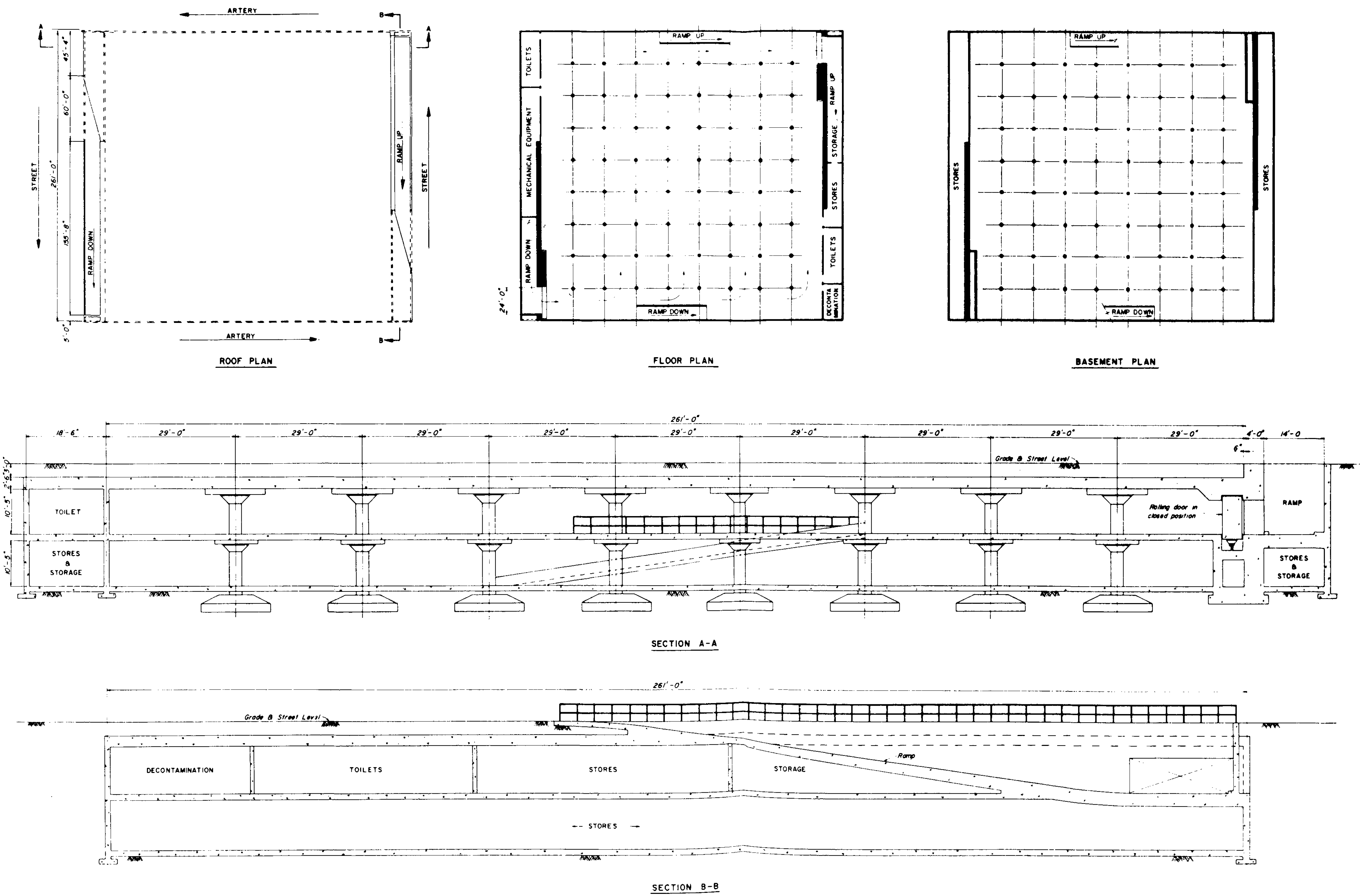

Fig. 3—Preliminary layout of prototype flat-slab structure.

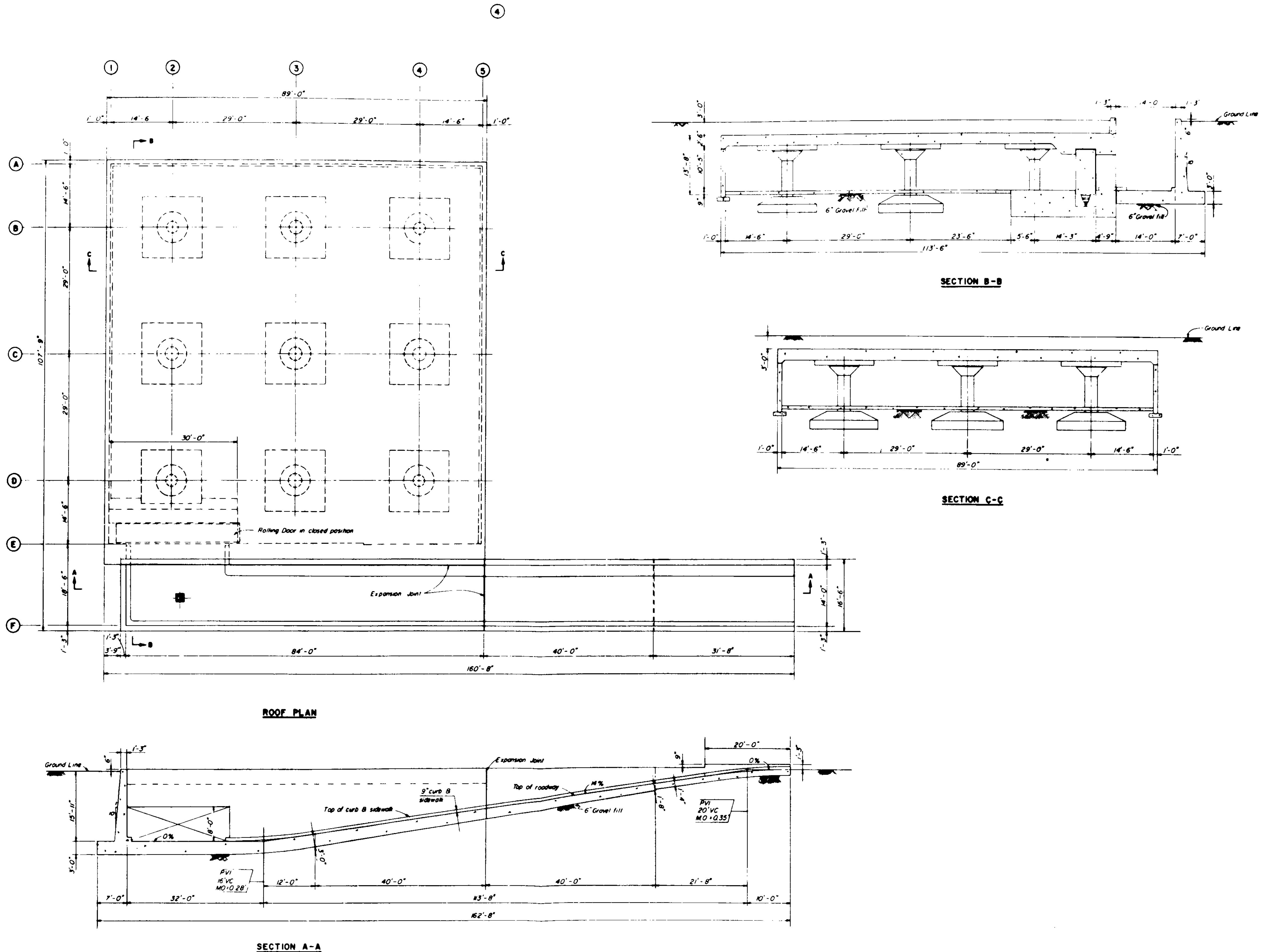

Fig. 4—Parking garage–shelter underground test section.

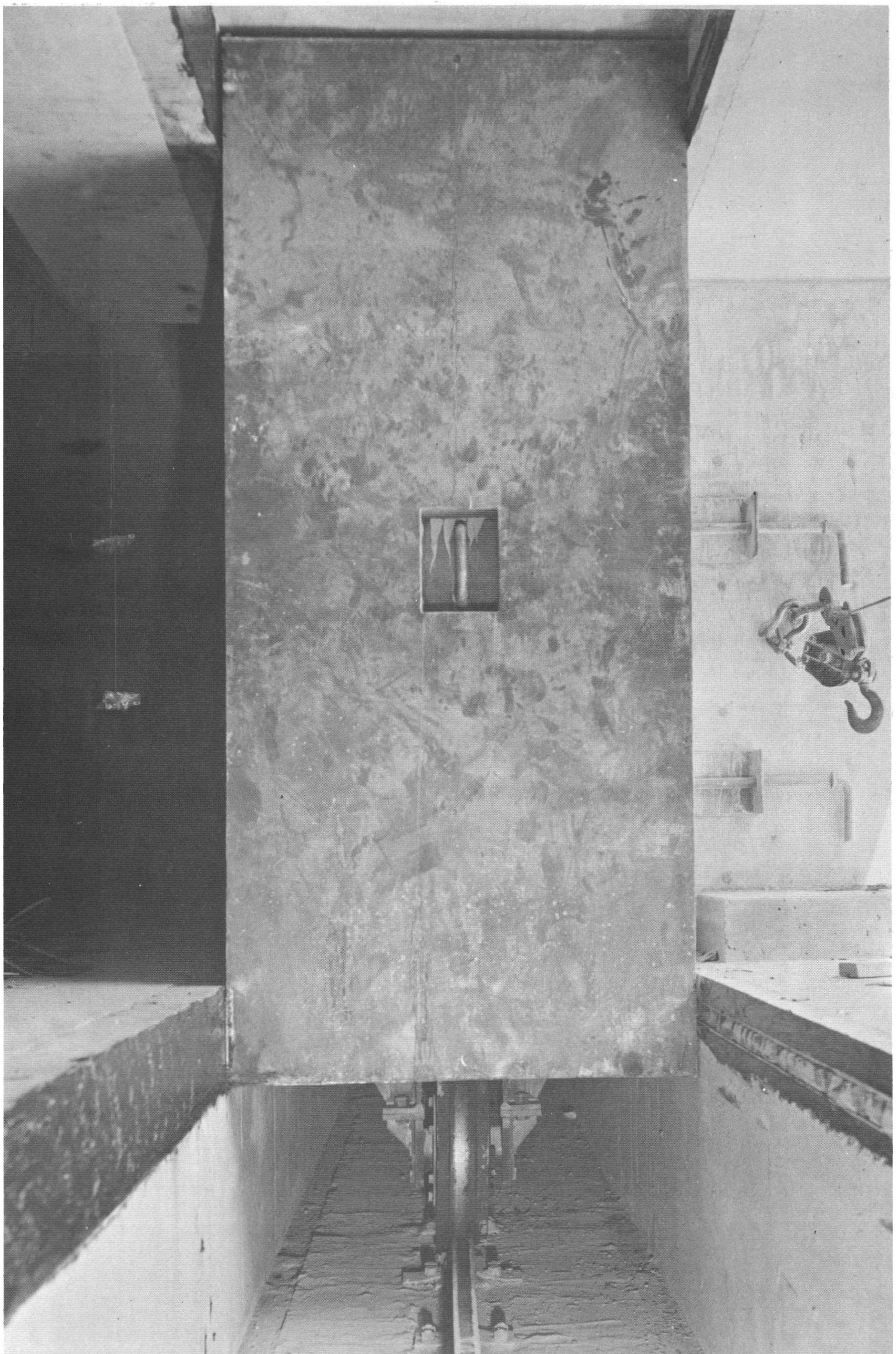

Fig. 5—Wheel assembly and rails, door partly open, postshot.

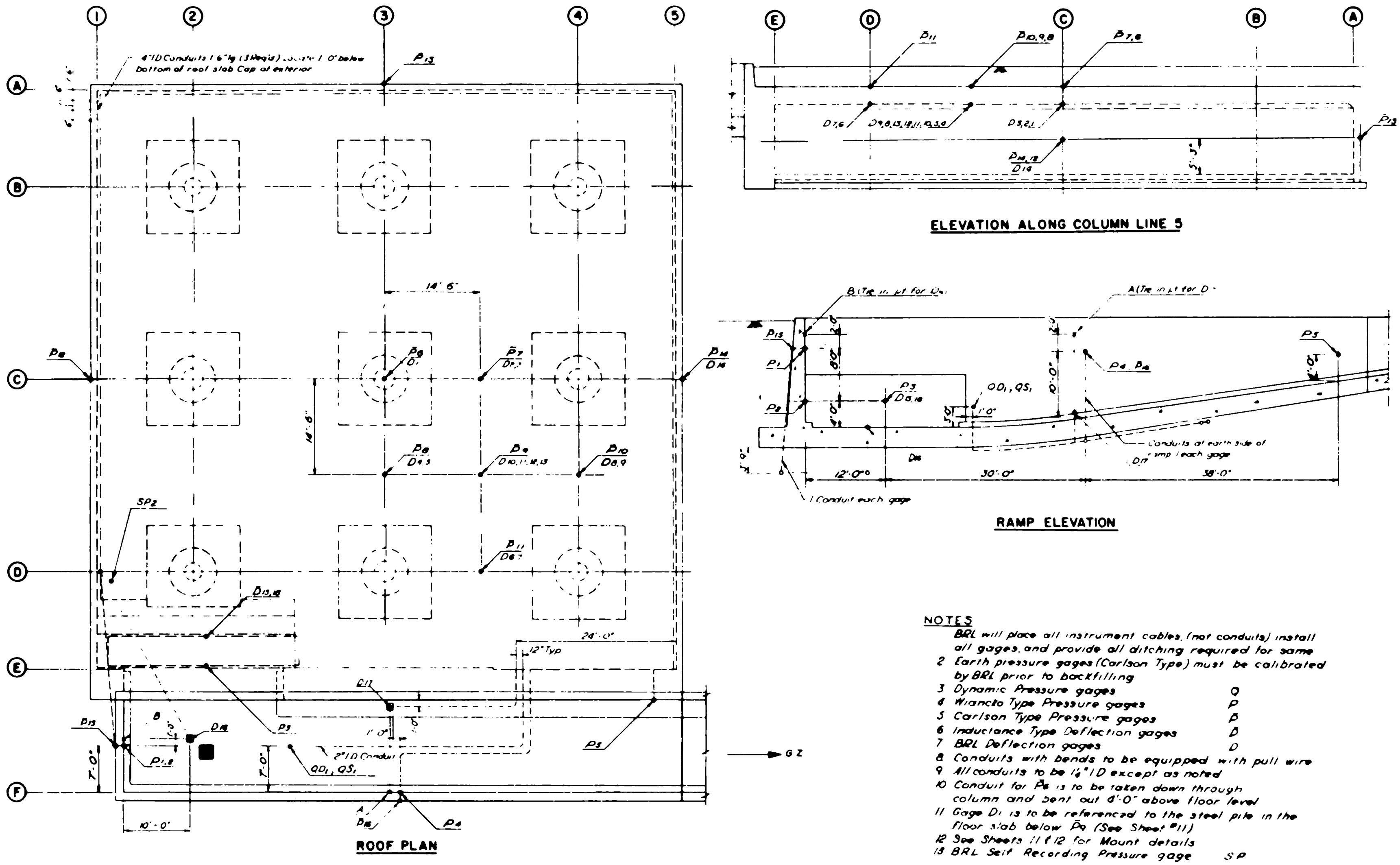

Fig. 6—Instrumentation layout.

SUMMARY 21

EVALUATION OF FCDA FAMILY SHELTER, MARK I, FOR PROTECTION AGAINST NUCLEAR WEAPONS

(Report ITR-1450, Operation Plumbbob, Project 30.3, same title, by Neal FitzSimons, Federal Civil Defense Administration, Nov. 1, 1957.)

OBJECTIVES AND SCOPE

The two primary objectives of this project were to test one of the most recent shelter designs and to collect engineering data to aid in establishing criteria for future designs. Other items of interest were the protective features against initial and fallout radiation and other hazards created by nuclear explosions.

An underground reinforced-concrete family shelter designed for six persons was tested at three anticipated nuclear blast overpressures of 30, 48, and 65 psi. In the design static-load equivalents were assumed and recommended ultimate-strength design procedures were followed. The structures were calculated to sustain a peak incident overpressure of 30 psi.

TEST STRUCTURE AND EQUIPMENT

Figures 1 to 3 show details of the shelter structure. In an effort to simplify the construction problems, only straight reinforcing steel bars or those with 90° hooks were used. This was the reason for selecting the relatively low concrete compressive design strength of 3000 psi (actually 4600 psi, as determined by laboratory tests).

The steel-plate door (Fig. 4) was intentionally over-designed using conventional elastic design methods for an applied normal pressure of about 45 psi. The method used to seal the door was effective and inexpensive. It consisted of a peripheral bar channel seal-welded to the plate. A strip of neoprene was cemented inside this channel. The door was designed so that it could be bolted from the inside against negative pressures but also it could be opened from the outside. Thus, rescue teams could have access if the occupants of the shelter were too badly injured to open the door from the inside.

To ensure the continuous removal of vitiated air so that under sealed conditions the shelter would contain relatively fresh air, an air-driven ventilator was attached to the exhaust pipe (see Fig. 5).

The two criteria established for protection against radiation for the shelter were: (1) an earth-cover equivalent of 6 ft 8 in. over the entire shelter and (2) an entrance corridor with a minimum of two 90° bends.

The horizontal portions of the corrugated-metal escape tube were cast into the end-wall concrete. The inclined section was welded to this after the concrete had cured (Fig. 6).

RESULTS

Measurements of deflections, both permanent and transient, were too small to have significance for structural analysis. There was a permanent deflection in the steel-plate door of the shelter at the 65-psi level. The blast pressures caused a symmetrical concavity in the plate which had a maximum depth of $1\frac{1}{4}$ in. at the center. Despite this distortion, the closure bolts were easily removed, and the door was opened without difficulty.

Damage to the exposed portion of the ventilation pipes was severe. As expected, the air-driven ventilators on the exhaust pipes were blown away, but the welded-steel weather covers on the intake pipes remained undamaged. The vent pipes were bent into an approximately horizontal position (Fig. 7).

The average attenuation factor for gamma radiation varied from 3000 to 4500. Such protection would have been adequate to prevent serious radiation damage to occupants.

CONCLUSIONS

The family shelter would probably sustain peak incident overpressures appreciably greater than 65 psi. The usefulness of the ventilation system was virtually ended by its blast damage.

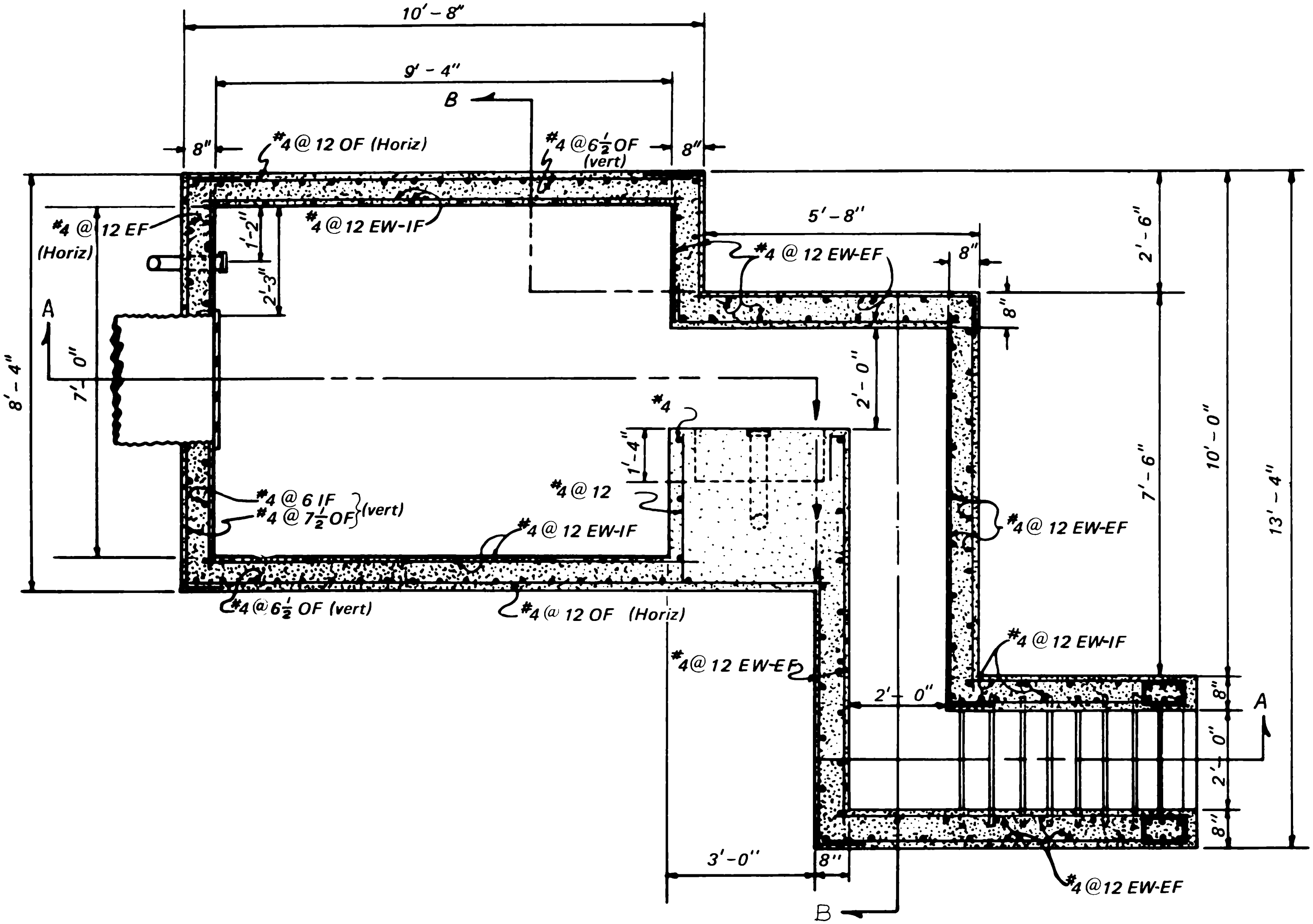

Fig. 1—Floor plan of FCDA family shelter, Mark I.

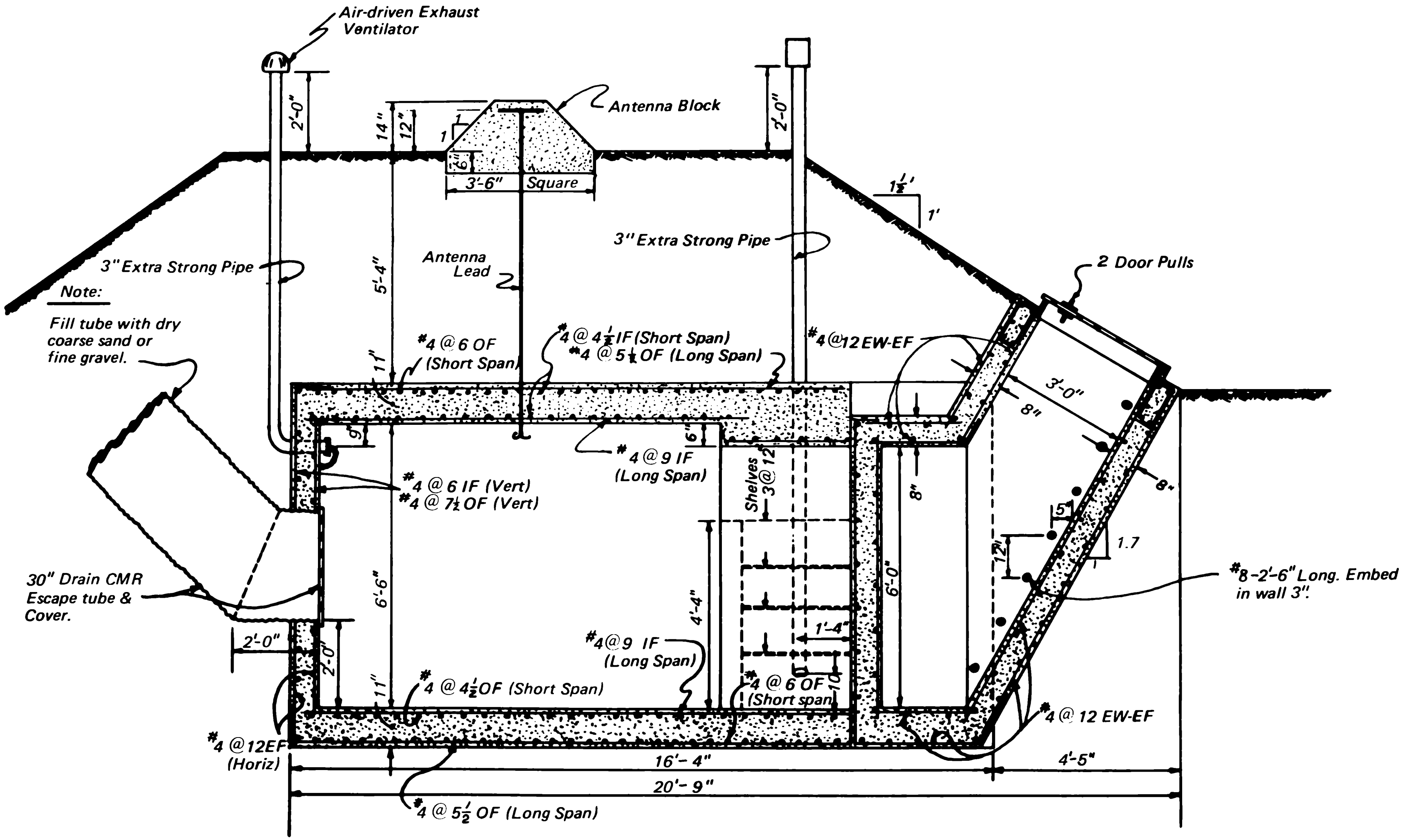

SECTION A-A

Fig. 2—Longitudinal section of FCDA family shelter, Mark I.

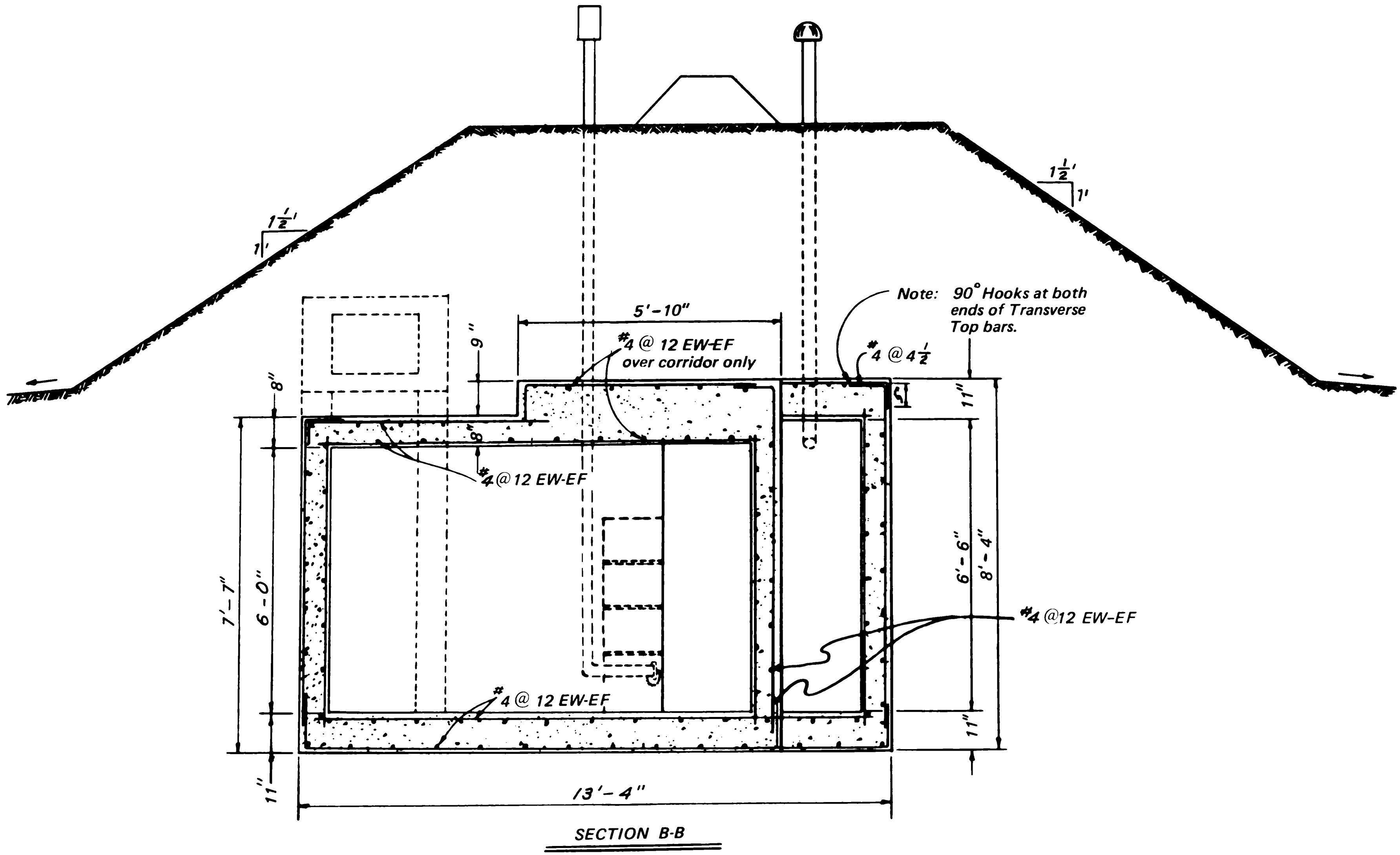

Fig. 3—Transverse section of FCDA family shelter, Mark I.

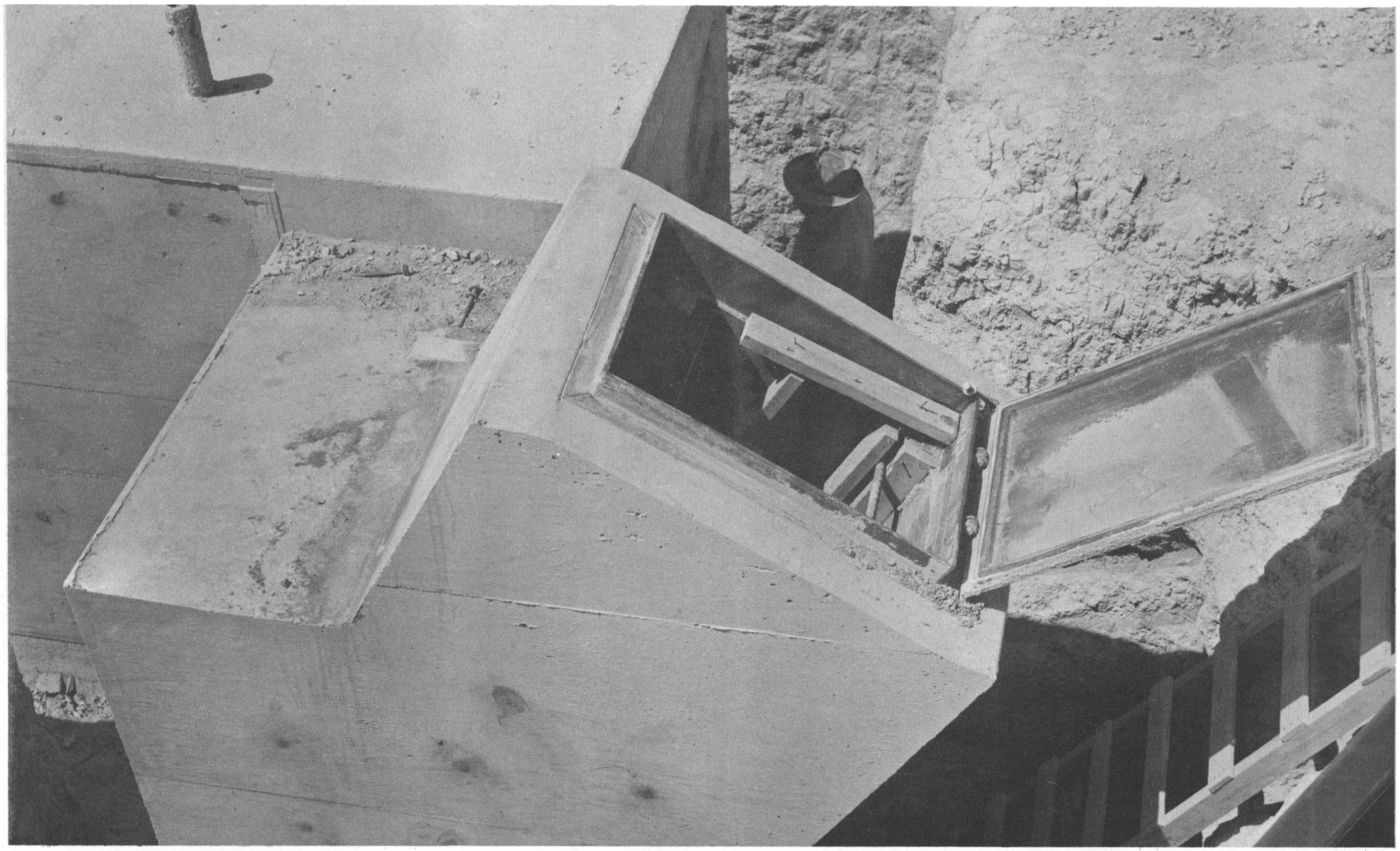

Fig. 4—Shelter entrance corridor before backfill.

Fig. 5—Exhaust pipe with air-driven ventilator; escape hatch with cover in foreground.

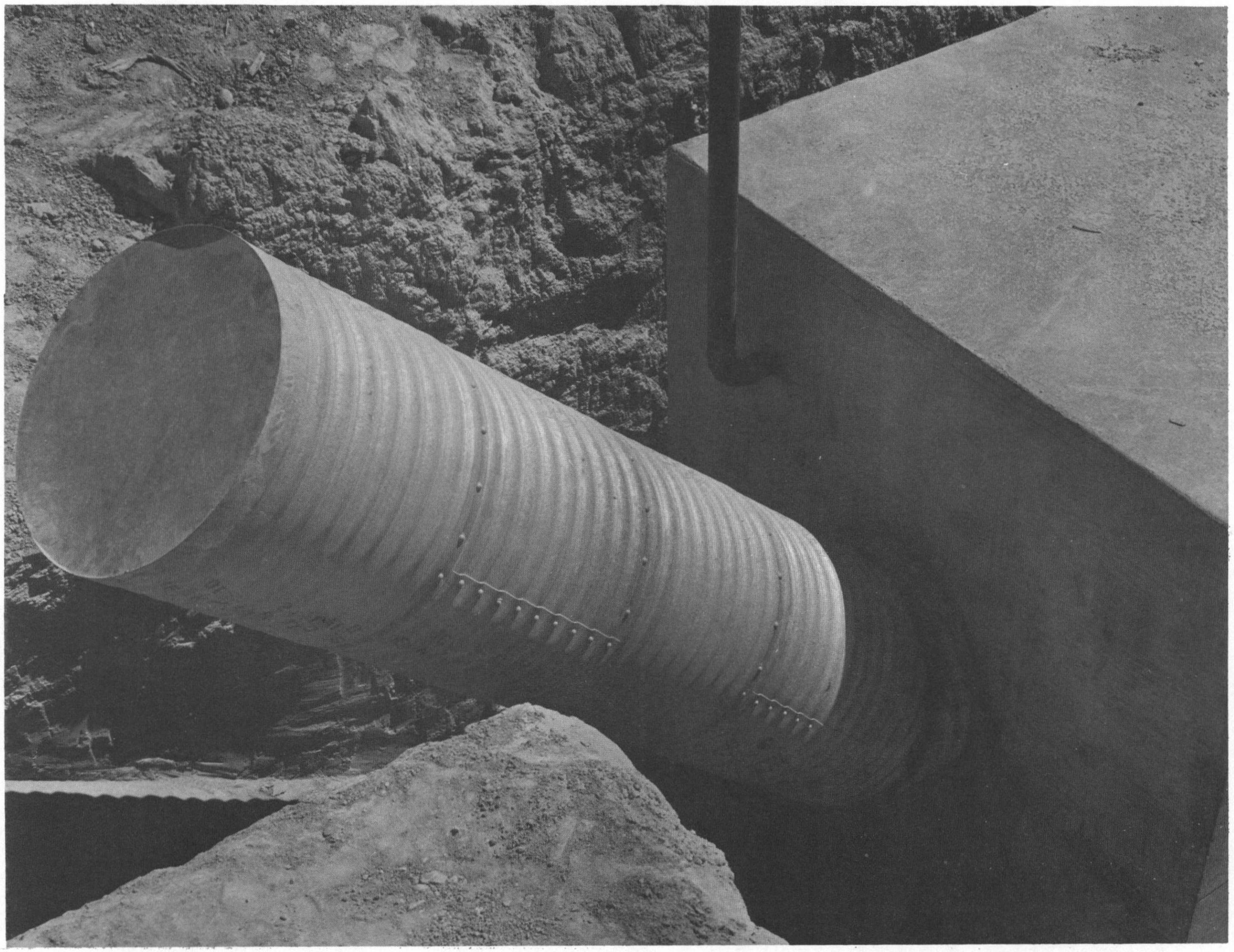

Fig. 6—Corrugated-metal escape tube at rear of shelter before backfill.

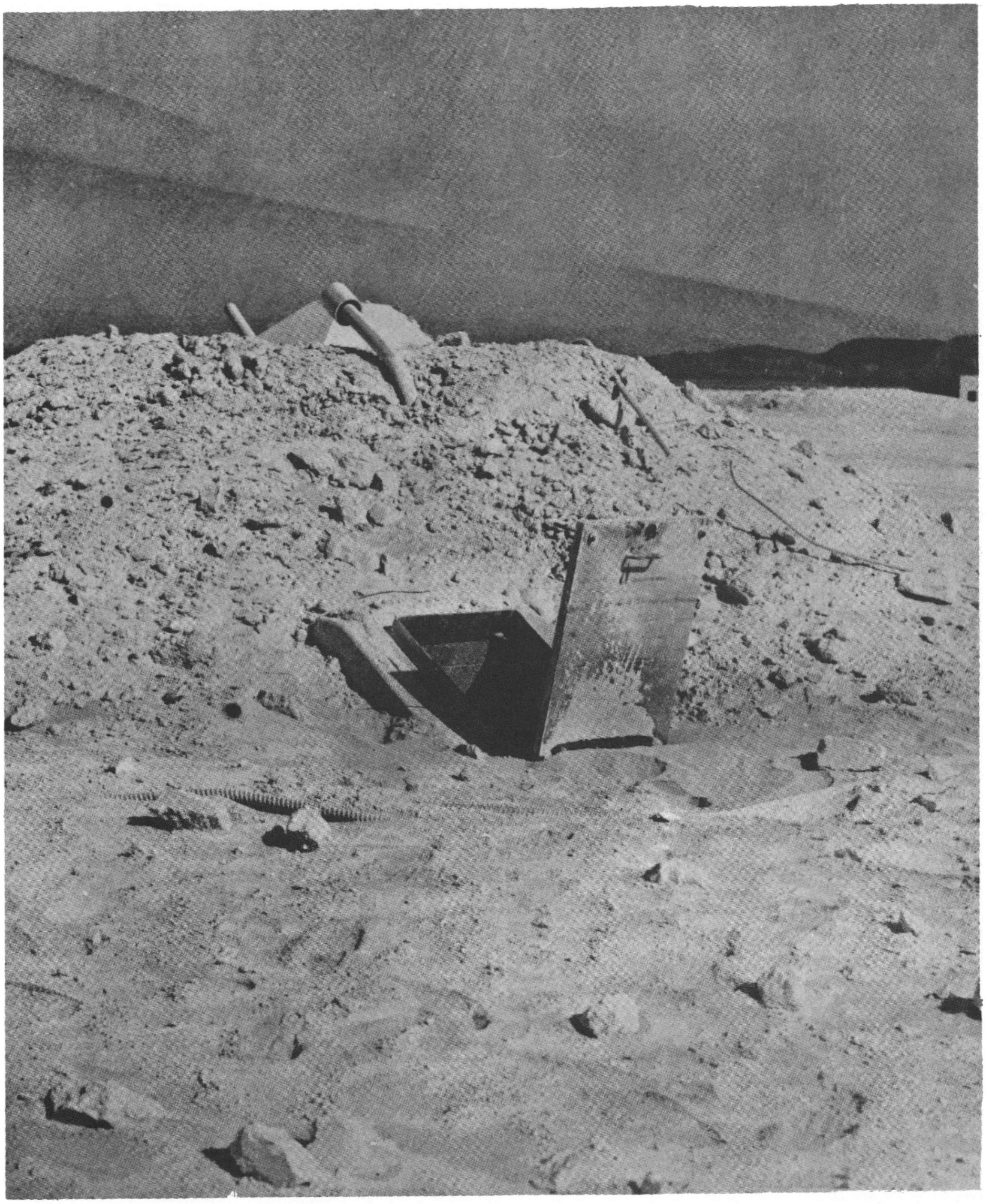

Fig. 7—Family-shelter ventilators bent over by blast.

SUMMARY 22

RESPONSE OF PROTECTIVE VAULTS TO BLAST LOADING

(Report WT-1451, Operation Plumbbob, Project 30.4, same title, by E. Cohen, E. Laing, and A. Bottenhofer, Ammann & Whitney, Consulting Engineers, New York, N. Y., May 28, 1962.)

OBJECTIVE AND SCOPE

The primary objective of this project was to evaluate the effectiveness of a reinforced-concrete steel-plate-lined vault with a steel vault door in providing protection against the effects of a nuclear detonation. Secondary objectives were: (1) to obtain additional information regarding the effects of a nonideal shock wave on blast loading and (2) to verify the assumptions used in design.

The aboveground structure, including the vault door, was exposed to Priscilla shot (about 37 kt, balloon suspended at 700 ft) at the predicted 75-psi peak incident pressure level (1150 ft from Ground Zero, GZ). The structure was oriented with its longitudinal center line radial to GZ (Fig. 1) with the vault door directly facing the blast.

The Mosler Safe Company contracted with Ammann & Whitney to design a selected type vault and to modify a standard vault door for exposure to a nuclear blast in the protective-structure tests sponsored by the Office of Civil Defense and the Office of Civil and Defense Mobilization.

DESIGN AND CONSTRUCTION OF TEST STRUCTURE

The test vault was a rectangular structure with an interior floor area of 102 sq ft. Figure 4 shows details of construction. The walls and roof slab were of 18-in. reinforced concrete, the interior face of which was lined with ½-in.-thick steel plate. The plate and concrete developed composite action by means of shear clips welded to the plate and embedded in the concrete. The vault was anchored into a large mat foundation from 2 to 6 ft thick to prevent it from overturning.

The door was a standard 10-in.-thick vault door modified to resist high-intensity loads. The 7.5-ton door was mounted in a steel-plate box frame weighing 14.5 tons. Figure 5 shows details of the door and doorframe.

The roof slab and the walls of the test vault were designed for dynamic behavior assuming an ideal 100-psi incident shock loading and a megaton-range weapon.

The steel-plate box frame and the vault door were originally designed for dynamic behavior using the theoretical reflected pressures consistent with the reflected pressures consistent with the 100-psi incident shock; the peak reflected pressure was computed to be 495 psi. Because of the nonideal shock and the predicted high dynamic (q) pressures at the test structures, it was decided to locate the vault at the 75-psi

level. The predicted q pressure at the 75-psi level was 300 psi, and the estimated peak front-face pressure was between 320 and 530 psi.

The maximum bearing capacity to be used for the foundation design was specified to be approximately 10 tsf.

The vault was designed by the ultimate-strength theory to utilize the additional strain energy available in the elastoplastic and plastic ranges.

RESULTS

Along the sides of the door box frame, the concrete wall was stripped off, both the inside-face and the outside-face reinforcements were torn out and bent, and the first row of Z clips on the interior plate lining and a small section of the interior plate lining of the vault were partially exposed (Figs. 2 and 3).

One piece of the concrete wall approximately 6 ft by 3 ft 3 in. by 1 ft 6 in. was found 80 ft to the right rear (WNW) of the structure, and a similar piece was found 85 ft to the left rear (WSW) of the structure.

There was no damage to the roof slab or to the rear wall of the vault.

The vault foundation showed no visual evidence of translation or rotation relative to the general ground level. There was a crack approximately ⅛ in. wide across the entire width of the footing slab on a line along the front edge of the door box frame.

The vault door withstood the blast with only minor structural damage. The front face of the vault was partially blackened by thermal radiation (Fig. 3). The light-gauge stainless-steel finish plates were warped and in some cases torn off (Fig. 6). The operating hardware on the surface of the pressure-system box was blown off, apparently in a downward direction. The hardware, except for the cast-iron pressure-system handwheel, which was fractured into several pieces, was found within a 10-ft radius of the door. The housing for the emergency combination dial, which was attached by means of three ½-in.-diameter bolts, was blown off as a unit. The pressure housing, attached to the door by twelve 1-in.-diameter bolts, had a slight downward shift. The top ½-in. plate of the pressure-system housing was deflected.

A visual inspection of the door hinge and doorframe revealed no apparent damage. The original fit was apparently maintained, the door remaining parallel to its frame in all planes, thus indicating a tight fit at the seal between the door and the striker.

The postshot opening of the door presented no major problems; it was opened without difficulty in about 10 min. Figures 8 and 9 show postshot views of the door.

The pressure data from records obtained from the instrumentation for Project 34.1 (WT-1472) are summarized in Table 1. The locations of all gauges on or within the vault are shown in Fig. 7.

The results of the gamma-radiation film dosimeters placed within the structure are given in Table 2 (dosimeter locations b to g, inclusive and j to p, inclusive). Locations a, h, and q were on the outside of the structure, and no recovery was made.

DISCUSSION

The vault door was designed to remain elastic for the theoretical reflected-pressure loading consistent with an ideal (zero rise time) 100-psi incident overpressure. In the test, however, the ratio of rise time to natural period was approximately 3.8; consequently, the response factor was probably only slightly greater than unity.

The separation of the reinforcing steel bars from the concrete and the reduction of the concrete to debris indicated the poor adhesive qualities of the concrete in place.

The extensive damage to the concrete sidewalls demonstrated the value of the interior steel box in providing added protection to the interior of the vault. The instruments and a movie camera in the vault were undamaged by the shock.

The roof slab and rear wall adequately resisted the blast load.

Use of the latest design criteria rather than the methods available at the time of design of the test

structure would not have significantly changed the structure design. The only addition necessary would have been the placement of a blast seal across the intersection of the doorframe and the cantilevered extension of the sidewall. It is probable that the high front pressure seeped into this joint, causing the joint to widen with explosive force, tearing the concrete away from the steel box, and causing major damage to the sidewalls.

Table 1—SUMMARY OF VAULT GAUGE RESULTS

Gauge	Location	Calibration pressure, psi	Time of arrival, msec	First-peak over-pressure, psi	Time of arrival of first peak, msec	Second-peak over-pressure, psi	Time of arrival of second peak, msec	Positive-phase duration, msec	Positive-phase impulse, psi-sec	Remarks
Pressure	Ground baffle	75	222	17	268	87	312	462	8.14	Free field
Pitot-static	3 ft	375	223	518	305					Free field, total pressure
P1	Footing	600	219	277	309					Failed at 333 msec
P2	Front	600	222	410	313				24.0*	Dust filled
P3	Front	600	221	668	300				42.3*	Dust filled
P4	Top	75	225	20	270	66	316	400	5.43	
P5	Top	75	227	15.5	252	60	319	342	4.97	
P6	Back	66	227	18	259	39	345	363	4.36	
P7	Back	66	231	4.6 (21.3)*	250	6.2 (28.8)*	356	334	0.92 (4.32)*	

*Estimated by correction.

Table 2—RESULTS OF GAMMA-RADIATION FILM DOSIMETERS*

Dosimeter	Total dose, r	Dosimeter	Total dose, r
a	No recovery	j	4200
b	4300	k	3100
c	4200	l	3800
d	2800	m	3100
e	4400	n	3200
f	4400	o	3800
g	2600	p	Vials broken
h	No recovery	q	No recovery

*All interior dosimeters were 18 in. from the inside wall.

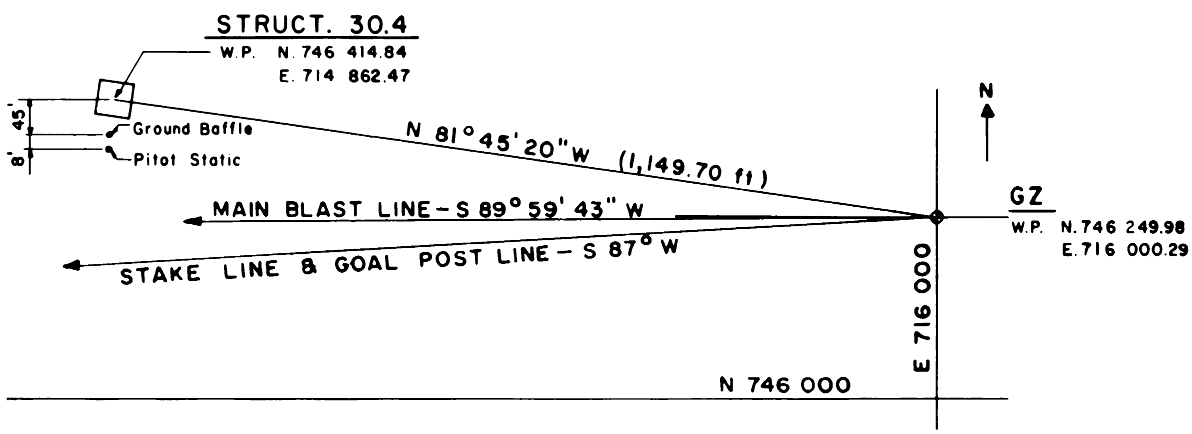

Fig. 1—Orientation of structure 30.4.

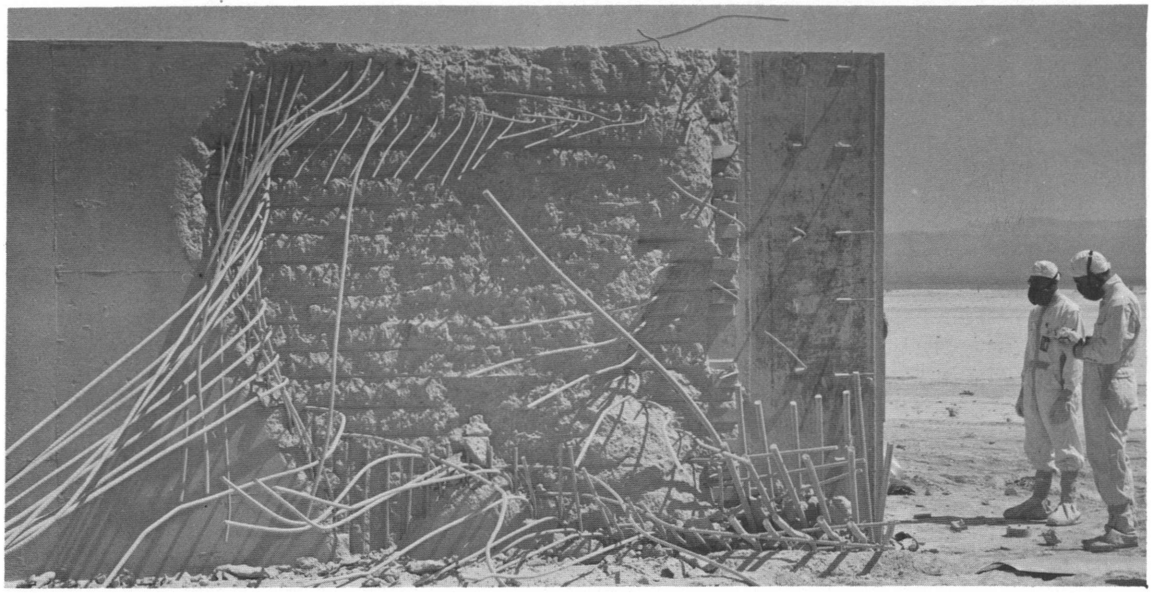

Fig. 2—South face of vault, postshot.

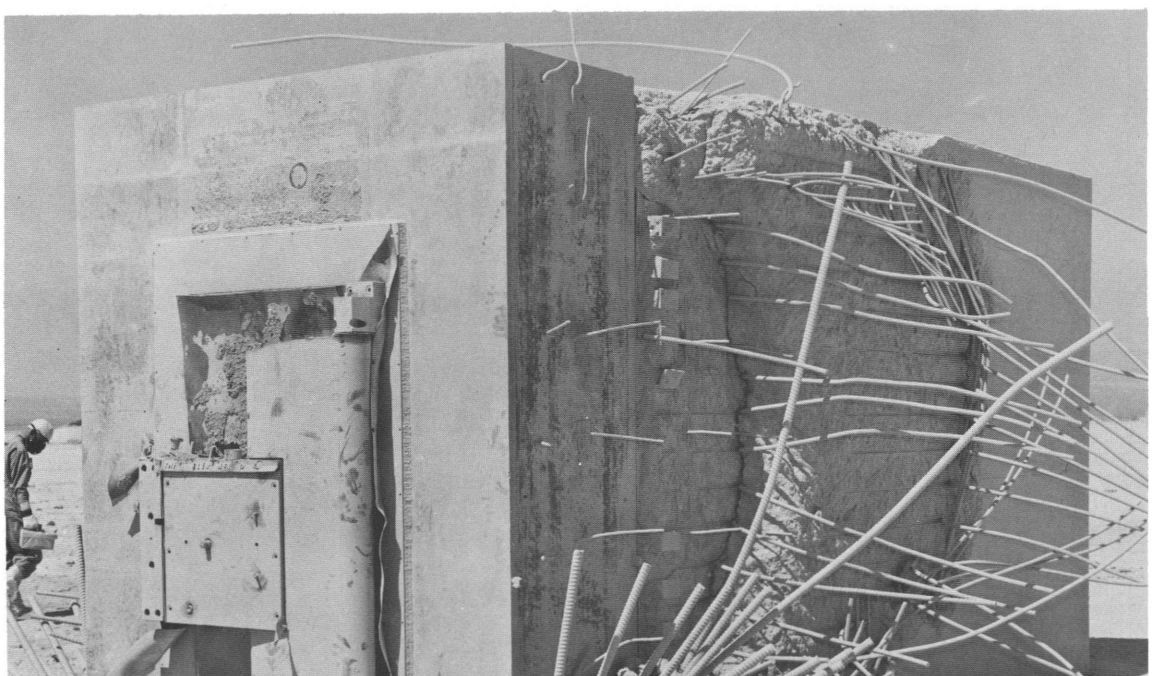

Fig. 3—Front and north faces of vault, postshot.

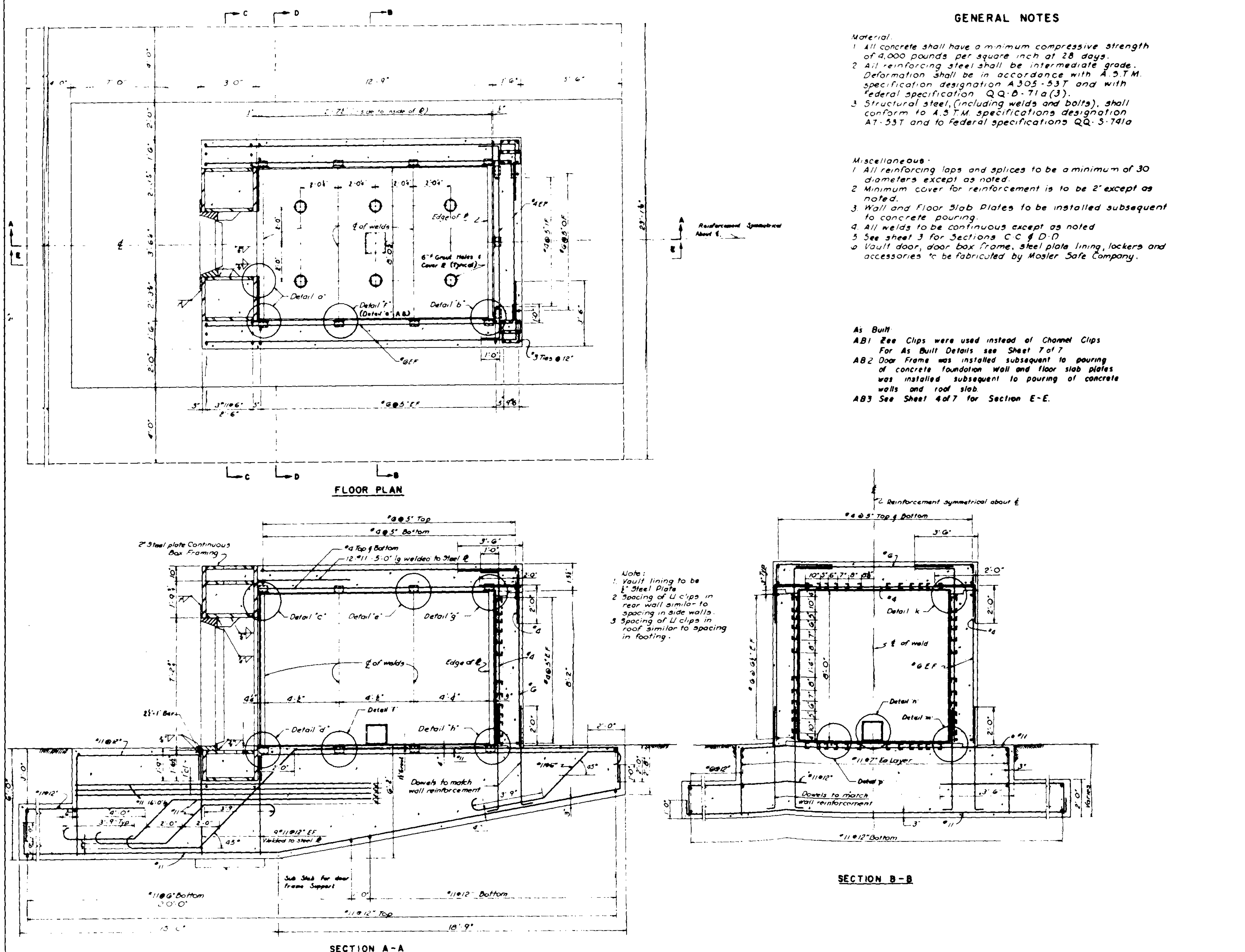

Fig. 4—Floor plan and sections of vault.

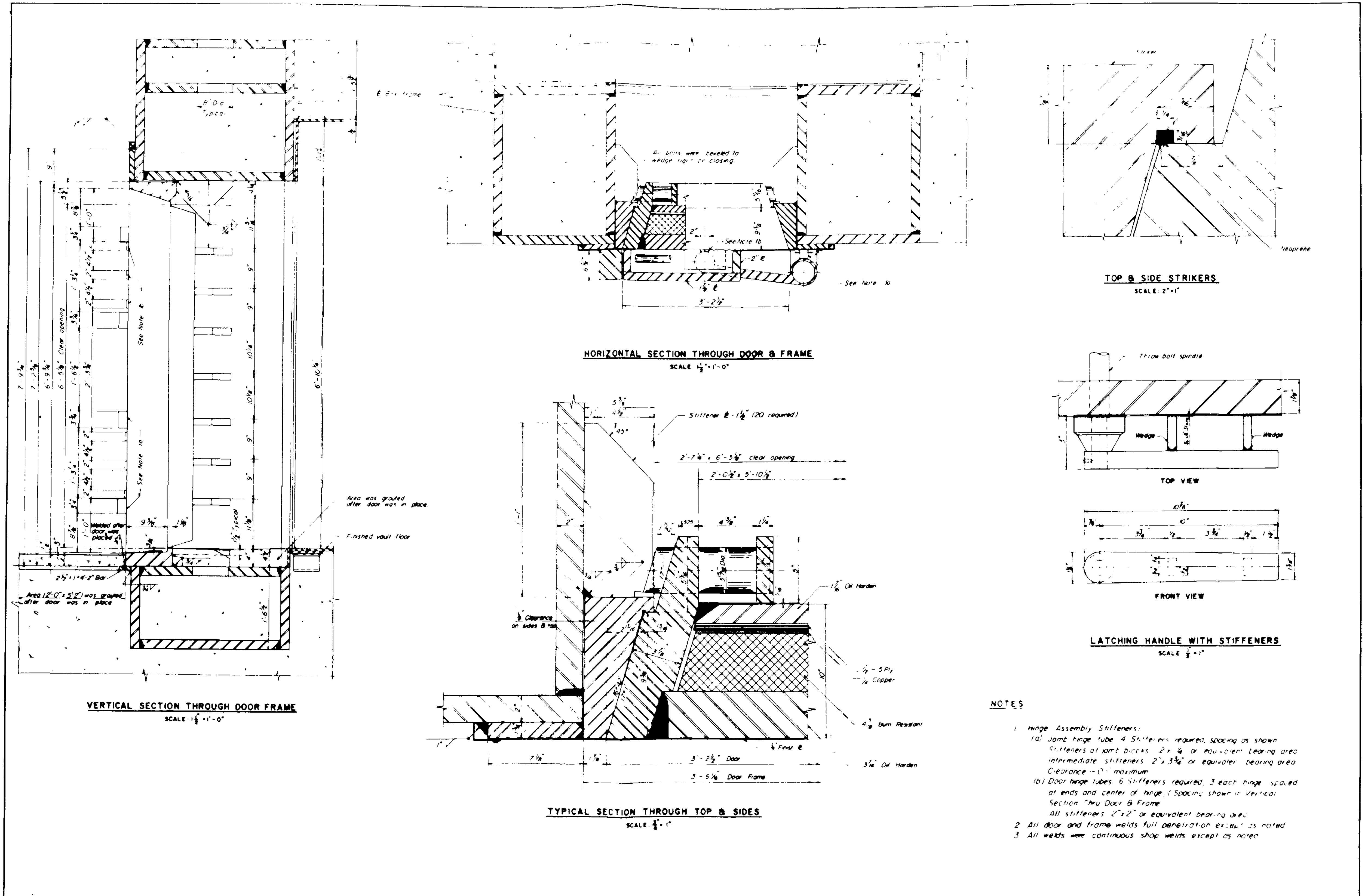

Fig. 5—Modified details for a standard C-10 vault door.

Fig. 6—Close-up view of front face from south showing damage to light-gauge finish plates and hardware, postshot.

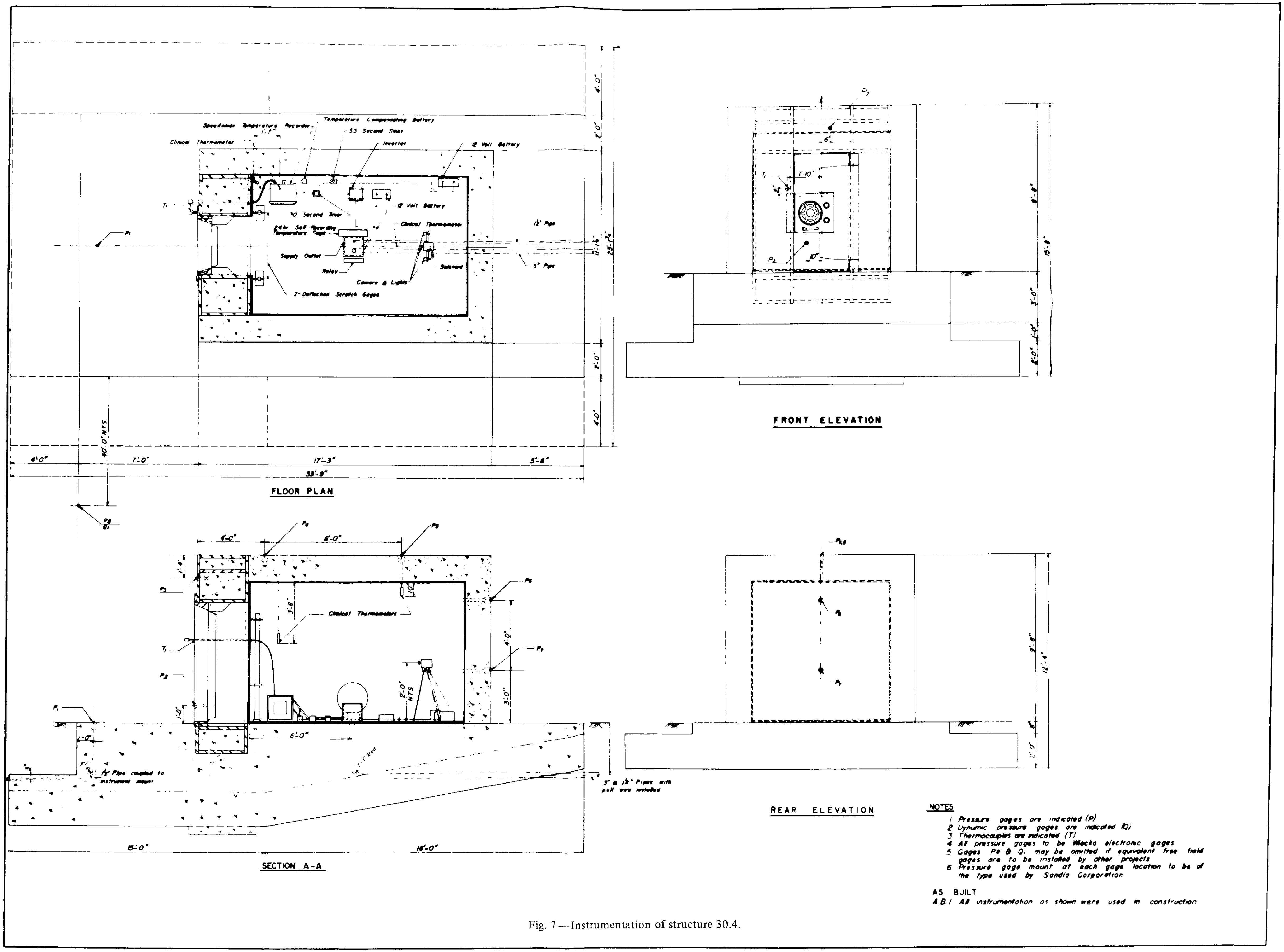

Fig. 7—Instrumentation of structure 30.4.

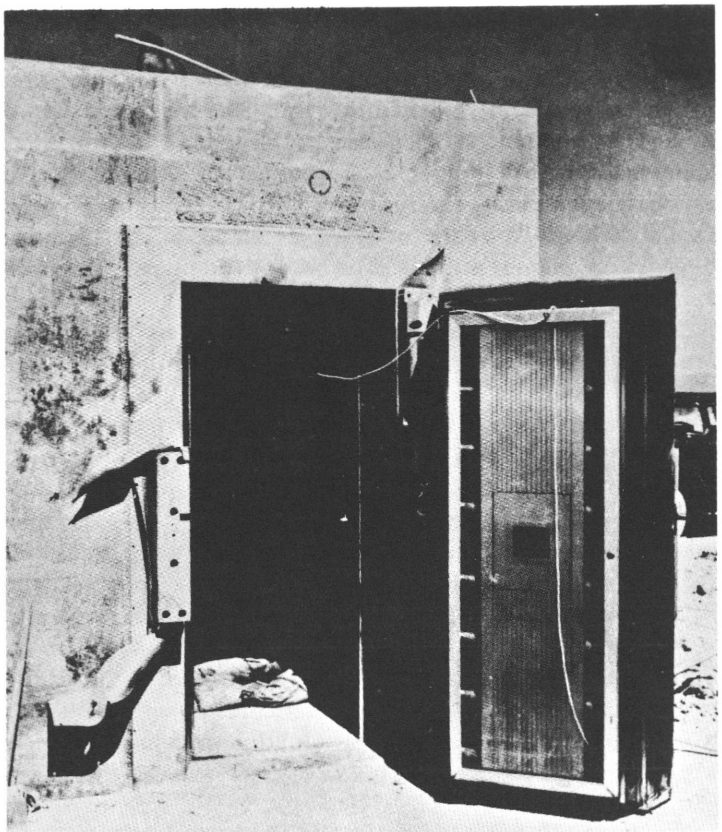

Fig. 8—Front face of vault, door open, postshot.

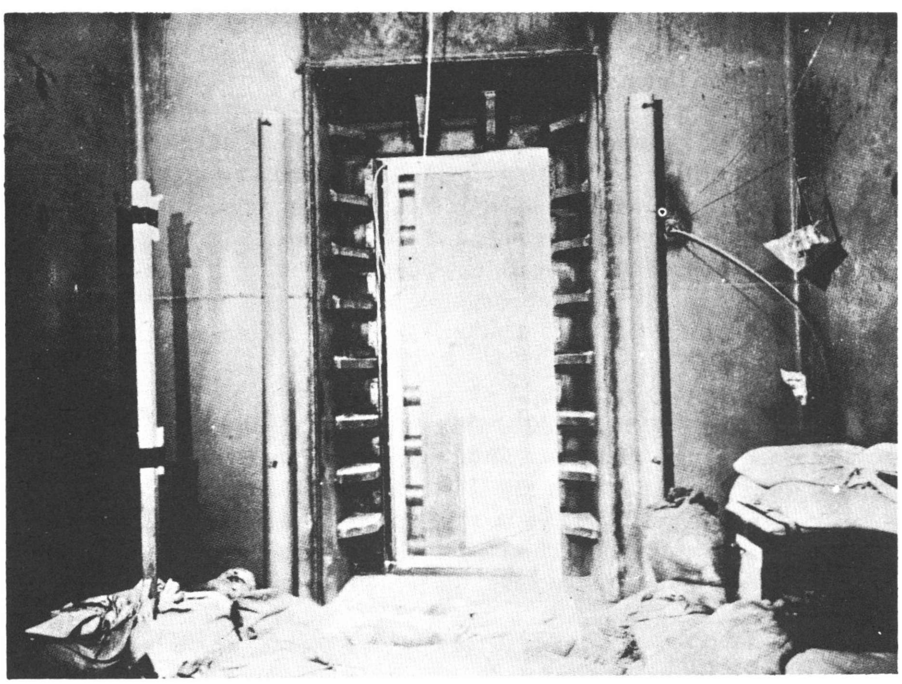

Fig. 9—Interior view looking toward door, postshot.

SUMMARY 23

TEST OF FRENCH UNDERGROUND PERSONNEL SHELTERS

(Report WT-1453, Operation Plumbbob, Project 30.6, same title, by Edward Cohen and Norval Dobbs, Ammann & Whitney, Consulting Engineers, New York, N. Y., June 19, 1962.)

OBJECTIVE AND SCOPE

The objective of this project was to investigate the predicted behavior of French underground personnel shelters, equipment, and instrumentation. Data obtained were to be used for the evaluation and improvement of present designs and for the establishment of design criteria.

Five reinforced-concrete underground structures designed by French engineers were tested: one cast-in-place rectangular structure, one precast circular shelter, and two entranceways at a predicted overpressure of 132 psi, and one entranceway at a predicted overpressure of 118 psi.

Data were to be obtained concerning the characteristics of the blast wave; structural strains; deflections and deformations; soil displacements; and interior and exterior pressures, temperatures, heat, and radioactivity.

Mice were used for biological tests in all five shelters to determine the environmental aspects of the structures when subjected to nuclear blast.

Figure 1 shows the location and orientation of the structures, as well as predicted and maximum recorded overpressures along the blast instrumentation line. All structures, except II-5, were oriented similarly with the entranceways in line with the direction of the blast. This orientation minimized the reflected pressure that would occur on the main blast door. Structure II-5 was oriented at 90° to the other structures, with the entranceway normal to the blast line.

The structures were tested in Smoky shot, a 44-kt nuclear device detonated from a 700-ft steel tower (ref. ENW, p. 675).

STRUCTURES, EQUIPMENT, AND INSTRUMENTATION

Figures 2 to 6 show architectural details of the five test structures, and Figs. 7 and 8 show above- and belowground views, respectively, of interest. The following five structures were exposed:

Structure II-1, rectangular concrete shelter, type 60
Structure II-2, circular shelter, type 50, with precast units
Structure II-3 }
Structure II-4 } entrances and entrance chambers, type 65
Structure II-5 }

Structure II-1 was a complete protective shelter designed to accommodate 50 persons, with 60 cu ft of space provided for each person sheltered. It consisted of the entrance stairs, an antechamber, the main body of the shelter, an emergency-exit tunnel, and an emergency-exit shaft. It was designed for an overpressure of 147 psi with 1-ft 11½-in.-thick main walls and slabs and approximately 0.3% reinforcement.

The main entrance from the landing into the antechamber consisted of an opening 2 ft 3½ in. wide by 4 ft, 10⅞ in. high, which was closed by three doors. On the exterior face of the wall opening was a 1$\frac{9}{16}$-in. structural-steel flat-plate blast door hung on a steel frame that was set before the concrete walls were poured. This door was designed for 147-psi overpressure. On the inside face of the wall opening, a 6$\frac{11}{16}$-in. concrete fire-resistant door and a $\frac{3}{16}$-in. structural-steel gastight door were provided on a single frame.

Radiation attenuation was provided, in addition to the concrete structure, by a minimum 3-ft 11-in. earth cover over the main body of the structure.

Two reinforced-concrete air-exhaust stacks extended 9 ft 3½ in. above grade, and two air-intake stacks extended only 2 ft 8½ in. above ground level. These intake and exhaust stacks were used in the natural-ventilation system and were expendable.

The pipes for these ventilation systems were fitted with an automatic ball-type dual-action antiblast valve, a protective grill at the outer openings to keep small animals out, and a gastight stop flap at the opening inside the shelter.

Normal ventilation was provided by air drawn in from the outside, either directly by gravity through the intake vents or, when the system was operated electrically, through one of the exhaust stacks, through a simple dust filter, and into the chamber. Three quick-acting shutoff valves located between the exhaust stacks and the intake fan controlled the electrically operated system. The output was 15,891.5 cu ft/hr, providing a complete change of air every 30 min.

The superstructure of the shelter, which rose to grade near the entrance, accommodated two pits filled with sand for the filtered-air system. Each filter contained about 35.5 cu ft of clean graded sand in a 2-ft layer over the air-intake apparatus. The system, which had an output of 3178.3 cu ft/hr, drew air in through the two sand filters in parallel; the air was then passed through an activated-carbon filter and aerosol paper into the shelter.

An air-exhaust system consisting of a system of pipe sleeves and vent pipes was provided to prevent a buildup of pressure within the main chamber owing to the mechanical ventilation; the pipe leading to the exterior had a ball-type antiblast valve at its midpoint.

The ventilators could be controlled either electrically from the power for the lighting or manually.

Neither the natural nor the emergency ventilation system of this shelter was in operation during the test since this shelter was highly instrumented. Individual components of this (Nessi) type of ventilation were tested in the less extensively instrumented structures, II-2, II-4, and II-5.

The antechamber had an opening 5 ft 10⅞ in. by 2 ft 3½ in. leading to the main chamber equipped with a 1¼-in. blast door and a $\frac{3}{16}$-in. gastight structural-steel door. The blast door had a steel frame that was placed before the pouring of the concrete walls.

The 13-ft-long emergency-exit tunnel terminated at a vertical shaft 2 ft 7½ in. square, which provided the means of exit to the ground level above. The opening at the top of the shaft was covered by a horizontal ⅜-in. checkered-plate blast door, also designed for an overpressure of 147 psi. The door was so arranged that it could be opened from the inside or the outside of the shaft.

Structure II-2 (cylindrical shelter, type 50) was designed to accommodate a maximum of 32 persons. It consisted of a main entrance shaft, an entrance antechamber, a main precast body, an exit chamber, and an emergency-exit shaft.

The shelter was entered by means of a steel spiral stair in a vertical shaft. The shaft was closed at the top (at grade level) by a horizontally sliding steel-plate blast door 1$\frac{9}{16}$ in. thick. At the bottom of the shaft, another blast door 1¼ in. thick and a gastight door provided access to the antechamber.

Natural ventilation was provided by a system similar in type and design to that used in structure II-1.

A sand-filter pit containing a filtered-air system, which is normally in operation during blast conditions, was located above the antechamber.

The forced ventilation system, which can be either electrically or manually controlled, was in operation during the test.

The main body was composed of 12 circular precast reinforced-concrete elements 8 ft 10½ in. in outside diameter, 10 in. thick, and 1 ft 6½ in. long. These elements were aligned concentrically during construction on a concrete setting bed and were post-tensioned together with eight cables by the Freyssinet method. The 1½-in. joints between precast elements were filled with slow-setting concrete mortar. A bearing stress of 122 psi was obtained on the faces of each element by the tensioning of the cables.

The earth cover above the main structure was 4 ft. 9 in. for this test.

The design of the emergency exit was like that of structure II-1.

Structures II-3, II-4, and II-5 (entrances and entrance chambers) were of poured-in-place reinforced concrete; they were similar in design and size to the entrance and the entrance chamber used for structure II-1. These structures represented entrances for typical shelters (Fig. 9); they consisted only of stairs and one antechamber. The structures were included in the test for comparative evaluation of the adequacy and effectiveness of three different types of doors, as well as added ventilation equipment, which also differed in each entrance chamber.

Structures II-1 and II-2 provided primarily a comparison of effects on shape of structure (rectangular vs. cylindrical) and method of construction (poured-in-place vs. precast elements). Also the effectiveness of the horizontal door of structure II-2 could be compared with that of the vertical door of structure II-1.

All structures were designed by French engineers; the criteria were those for a static loading condition, and the required thickness of concrete and quantity of reinforcement were obtained by an ultimate-strength method of design. The structures were designed to withstand a uniform static overpressure of 147 psi at ultimate stress. A uniform negative pressure of 10 psi was also considered in the design for reversal of static loading.

Initial radiation doses of 2 to 7×10^4 r on the ground surface were assumed to be consistent with design overpressure. It was hoped that an attenuation factor of 1000 would be obtained by using earth covers of 3 ft 11 in. and 4 ft 9 in. above the roofs of the structures.

An extensive instrumentation program was provided. In addition to the equipment furnished from France, U.S. instrumentation was included for comparison purposes. Instruments were provided from France to take the following measurements: pressures, deformations and vibrations, stresses and strains, heat (cal/cm^2) and temperature (°F or °C), nuclear radiation and contamination, and miscellaneous measurements (communications, lighting, etc.).

The U.S. pressure instrumentation equipment consisted of 33 Ballistic Research Laboratories self-recording pressure–time gauges and 2 self-recording very-low-pressure–time gauges. In addition to the instrumentation in the structures, U.S. blast-line pressure data were available for both free-field surface overpressures and the dynamic pressures to which the structures were subjected. The maximum values and the location of the blast-line instrumentation are shown in Fig. 1.

Additional radiation-detection measurements, other than those made with the French instruments, were made with U.S. gamma film dosimeters, gamma-radiation differential chemical dosimeters, and neutron detectors.

Twelve shock gauges and protecting canisters were used in the test. The shock gauge, a completely self-contained mechanical unit, requires no electronic or communication channels. Essentially, it consists of 10 masses attached to cantilever springs mounted on two sides of a vertical plate (Fig. 10). The natural frequencies of the spring–mass system are approximately 3, 10, 20, 40, 80, 120, 160, 200, 250, and 300 cps.

The biological test consisted in placing one sample of 20 mice in each of the five structures. The locations of the test samples for the five shelters are shown in Fig. 11.

RESULTS

Structural Damage—With the exception of structure II-2, all the test structures sustained very slight damage in the shelter areas. Cracking was observed in all structures, but major damage occurred only to those portions exposed to the shock front, such as the entrances and the ventilation projections.

In structure II-2 (cylindrical shelter, type 50), no significant damage was observed in the roof, floors, or walls of either the main entrance or the antechamber. The circular precast rings in the main chamber, however, were extensively damaged but did not collapse. The upper segments of rings 2 through 10 were

displaced downward by varying amounts; the movement downward of ring 10 in relation to ring 11 was approximately ¾ in. In addition, numerous longitudinal and transverse cracks were produced in the rings of the main chamber.

In general, all doors, including blast- and fire-resistant gastight doors, and emergency-exit covers were undamaged. Frames, locking mechanisms, and hinges were in proper operating condition after the test. The only exceptions were the fire door (located past the main blast door) and the gastight door, both in structure II-1; they suffered a moderate degree of damage.

The ventilation systems of the various structures were affected by the blast as follows:

Structure II-1—Inspection of the natural ventilation system showed that the ball-type antiblast valves had operated. The spheres, which were located in the exhaust and intake pipes, had circular indentations that were produced when the blast forced them against the interior vent pipe. The sealing covers, which were located at the interior ends of the pipes, were all blown off and deformed. The three quick-acting shutoff valves, which were in the closed position before the test, were found in good working condition after the test. One of the valves near the dust filter was open; the remaining two valves were in their original closed position after the test.

The aboveground portion of the structure suffered considerable damage. The exhaust and intake stacks were sheared off from 2 ft above to a few inches below grade. Otherwise, the damage consisted of severe chipping and scouring of the concrete.

Structure II-2—The flap-plate cover located at the interior end of the natural intake vent pipe, which was in a closed position during the test, was blown open but remained on the hinge. A circular indentation was present on the antiblast ball valve. The shutoff valves appeared in good operating condition after the test.

The portion of the ventilation system above ground surface was badly damaged by the blast. The weather-protection cover of the vent stack was blown off, as was the overhanging portion of the sandpit roof slab.

Structure II-3—The antiblast flap valve in the exhaust pipe was found in a slightly open position. Of the aboveground portions, the ventilation intake and exhaust stacks were broken off at the ground surface. The dislodged sections were found 10 to 20 yd to the rear of the structure.

Structure II-4—Investigation of the ball-type antiblast valve indicated a circular indentation on the sphere. The aboveground portion suffered only very slight damage.

Structure II-5—The damage was very similar to that experienced at Structure II-3.

The electrical systems within the structures were all in operating condition after the test.

The results of instrumentation measurements are as follows:

External Pressure—As indicated in Fig. 1, the actual incident overpressure at the predicted pressure levels of 132.3 and 118.0 psi was approximately 12% lower than predicted and approximately 20% less than the static design overpressure of 147 psi.

Internal Pressure—In the two full-scale test structures, shelters II-1 and II-2, the maximum recorded internal pressures were 0.4 and 0.7 psi, respectively. Both these structures had the sealing covers on the interior ends of the ventilation pipes blown off by the shock wave. Both maximum internal pressures recorded in shelters II-3 and II-5 were equal to 1.4 psi, even though two basically different types of blast closures were used. Maximum internal pressure recorded in shelter II-4 was 12.0 psi.

Radiation—No readings of the initial radiation were obtained as separate values; however, as can be seen from Fig. 12, the values for the total gamma dose during the first 52 hr after the detonation at various points within the five test structures were within the prescribed allowable for the initial radiation.

Thermal Effects—It was not possible to obtain measurements of thermal effects from the instrumentation provided. Residual thermal effects were not apparent from visual observations.

Ground-shock Spectra—Peak displacement responses to shock of single-degree-of-freedom systems (Reed gauges) of various natural frequencies are presented in Table 1 for shots Smoky, Whitney, Galileo, Charleston, and Stokes (ref. ENW, p. 675). As indicated in this table, peak displacements of Reed gauges of known frequencies were recorded near the surface in the free field and in an underground rectangular structure of Project 30.7 (see Summary 24, "Test of German Underground Personnel Shelters") at the 1005-ft range.

These records show that the horizontal (radial) measurements are generally less than one-half the vertical measurements. The horizontal displacements recorded in the shelter are approximately the same as those for the free-field gauges adjacent to the structure. However, the vertical displacements were considerably less than the free-field measurements, indicating attenuation in the vertical direction. In all cases high accelerations are associated with high frequencies, and high displacements with low frequencies.

Debris and Dust—Deposited debris was comparatively light. A dust layer varied in thickness from approximately $\frac{1}{4}$ in. to a maximum of 2 in. in places where drifting occurred. Some rubble was also present. Interior dust was observed only at the bases of the ventilation ducts.

All vertical or inclined surfaces (ventilation projections, stairs, walls, etc.) facing Ground Zero (GZ) were scoured by sand and debris carried by the blast wave. Aboveground projections that were broken off were deposited from 5 to 100 yd away from their original positions.

Biological Test Results—The immediate mortality of the mice was confined to structure II-2, where 19 of the 20 specimens placed on the top landing of the stairs were found dead upon recovery.

The location, number, time of recovery after the test, and time of death of the mice that had died during the period from their recovery until 20 days after the test are given in Table 2.

Of the control mice left unattended, none had died up until a period of 20 days after the test.

LIMITATIONS IN APPLICATION OF TEST RESULTS

Although the effects (overpressure vs. time, thermal and nuclear radiation, etc.) of small nuclear weapons differ in magnitude from the effects of the large thermonuclear weapons now available and although the physical environment at the Nevada Test Site is not typical of most populated areas, the data obtained from these weapons tests are very useful in estimating response and in evaluating the parameters used in the design. For this reason the records of blast overpressure, ground-shock motions, radiation, and other weapons effects are of prime importance. The results, however, cannot be used directly for proof-test purposes except in special cases.

Table 1 — DISPLACEMENT SHOCK SPECTRA

Radial Direction*				Vertical Direction*			
f	D	f	D	f	D	f	D
cps	in.	cps	in.	cps	in.	cps	in.
Shot Stokes, surface, 33-psi overpressure							
Gauge 1		Gauge 3		Gauge 2		Gauge 4	
2.56		2.66	0.199	2.56	0.710	2.74	0.516
8.82	0.137	8.87	0.0260	8.82	0.569	9.66	0.440
22.0	0.0318	22.2	0.0248	22.0	0.101	20.4	0.165
36.0	0.0451	36.5	0.0093	36.0	0.0498	32.8	0.0633
90.0	0.0231	92.0	0.0074	90.0	0.0385	88.0	0.0560
134	0.0056	132	0.0018	131	0.0128	133	0.0309
184	0.0121	176	0.0017	179	0.0088	185	0.0154
228	0.0027	224	0.0020	209	0.0030	220	0.0066
269	0.0065	279		268	0.0027	265	0.0026
339		312		303	0.0033	293	0.0012
Shot Smoky, inside shelter, 116-psi overpressure							
Gauge 5				Gauge 6			
2.72	2.25			2.54	1.62		
9.37	0.453			8.72	0.906		
22.3	0.113			21.9	0.336		
36.9	0.0451			37.0	0.0744		
95.0	0.0185			92.0	0.0167		
138	0.0101			138	0.0099		
184	0.0099			185	0.0034		
234	0.0041			246	0.0051		
285	0.0022			280	0.0039		
296	0.0031			363	0.0038		
Shot Smoky, surface, 116-psi overpressure							
Gauge 9				Gauge 7		Gauge 8	
2.55	1.95			2.60	5.45	2.53	4.53
9.12	0.359			8.56	1.52	8.82	1.46
22.4	0.189			22.4	0.845	22.6	0.525
33.9	0.131			37.4	0.254	37.1	0.205
93.0	0.0227			91.0	0.132	93.0	0.103
107	0.0149			132	0.0673	137	0.0450
181	0.0107			187	0.0221	180	0.0199
203	0.0042			238	0.0106	236	0.0122
293	0.0055			280	0.0112	294	0.0055
357	0.0027			335	0.0066	328	0.0066
Shot Galileo, surface, 130-psi overpressure							
Gauge 11				Gauge 10		Gauge 12	
2.35	0.653			2.48	4.10	2.47	4.25
8.63	0.377			8.26	0.946	8.23	1.22
22.5	0.164			22.7	0.320	21.0	0.475
36.5	0.0453			37.1	0.314	35.0	0.280
95.0	0.0349			94.0	0.140	94.0	0.121
138	0.0184			138	0.0441	136	0.0267
186	0.0103			187	0.0446	178	0.0442
237	0.0032			234	0.0098	229	0.0161
294	0.0046			272	0.0139	300	0.0121
317	0.0029			365	0.0046	339	0.0053

(Table continued on p. 228.)

Table 1—(Continued)

Radial direction*				Vertical direction*			
f	D	f	D	f	D	f	D
cps	in.	cps	in.	cps	in.	cps	in.
Shot Whitney, surface, 146-psi overpressure							
Gauge 4†				Gauge 3†			
2.74	1.60			2.66	3.10		
9.66	0.260			8.87	1.47		
20.4	0.119			22.2	0.788		
32.8	0.0834			36.5	0.348		
86.0	0.0187			92.0	0.141		
134	0.0118			132	0.0992		
185	0.0088			176	0.0402		
220	0.0064			227	0.0090		
269	0.0026			284	0.0152		
314	0.0054			330	0.0080		
Shot Charleston, surface‡							
Gauge 5 (20-psi overpressure)		Gauge 9 (18-psi overpressure)		Gauge 6 (20-psi overpressure)		Gauge 8 (18-psi overpressure)	
2.72	0.263	2.55	0.265	2.54		2.53	0.728
9.37	0.111	9.12	0.0838	8.72	0.280	8.82	0.368
22.3	0.0900	22.4	0.0691	21.9	0.221	22.6	0.194
36.9	0.0404	33.9		37.0		37.1	0.0828
95.0	0.0190	93.0	0.0096	92.0	0.0246	93.0	0.0208
138	0.0100	107	0.0050	138	0.0093	137	0.0048
184	0.0014	181	0.0023	185	0.0062	180	0.0025
234	0.0030	203	0.0020	246	0.0023	236	0.0015
285	0.0026	293	0.0019	280	0.0023	294	0.0015
296	0.0020	357	0.0009	363	0.0007	328	0.0016
Gauge 11 (15-psi overpressure)				Gauge 10 (15-psi overpressure)		Gauge 12 (12-psi overpressure)	
2.35	0.879			2.48	0.407	2.47	0.492
8.63	0.262			8.26	0.163	8.23	0.177
22.5	0.195			22.7	0.0726	21.0	0.207
36.5	0.0804			37.1	0.0231	35.0	0.0786
95	0.0246			94.0		94.0	0.0193
138	0.0033			138		136	0.0101
186	0.0020			187		178	0.0053
237	0.0019			234		229	0.0005
294	0.0011			272		300	
317	0.0007			365	0.0009	339	0.0006

*f, natural frequency; D, peak displacement.

†Canister tops were about 18 in. below ground level in hard ground. Two other gauges bolted to concrete pads in the same vicinity were knocked loose and data were lost.

‡Tangential direction for gauge 7 (20-psi overpressure): insignificant displacement.

Table 2—MORTALITY RESULTS OF BIOLOGICAL TESTS

Structure No.	Time of recovery after test, days	Number and time of deaths
II-1	2	None
II-2	3	19 before recovery and 1 on day of recovery
II-3	2	1 on 2 days after recovery
II-4	2	1 each on 12 and 17 days after recovery
II-5	2	1 each on 1, 8, 11, and 13 days after recovery

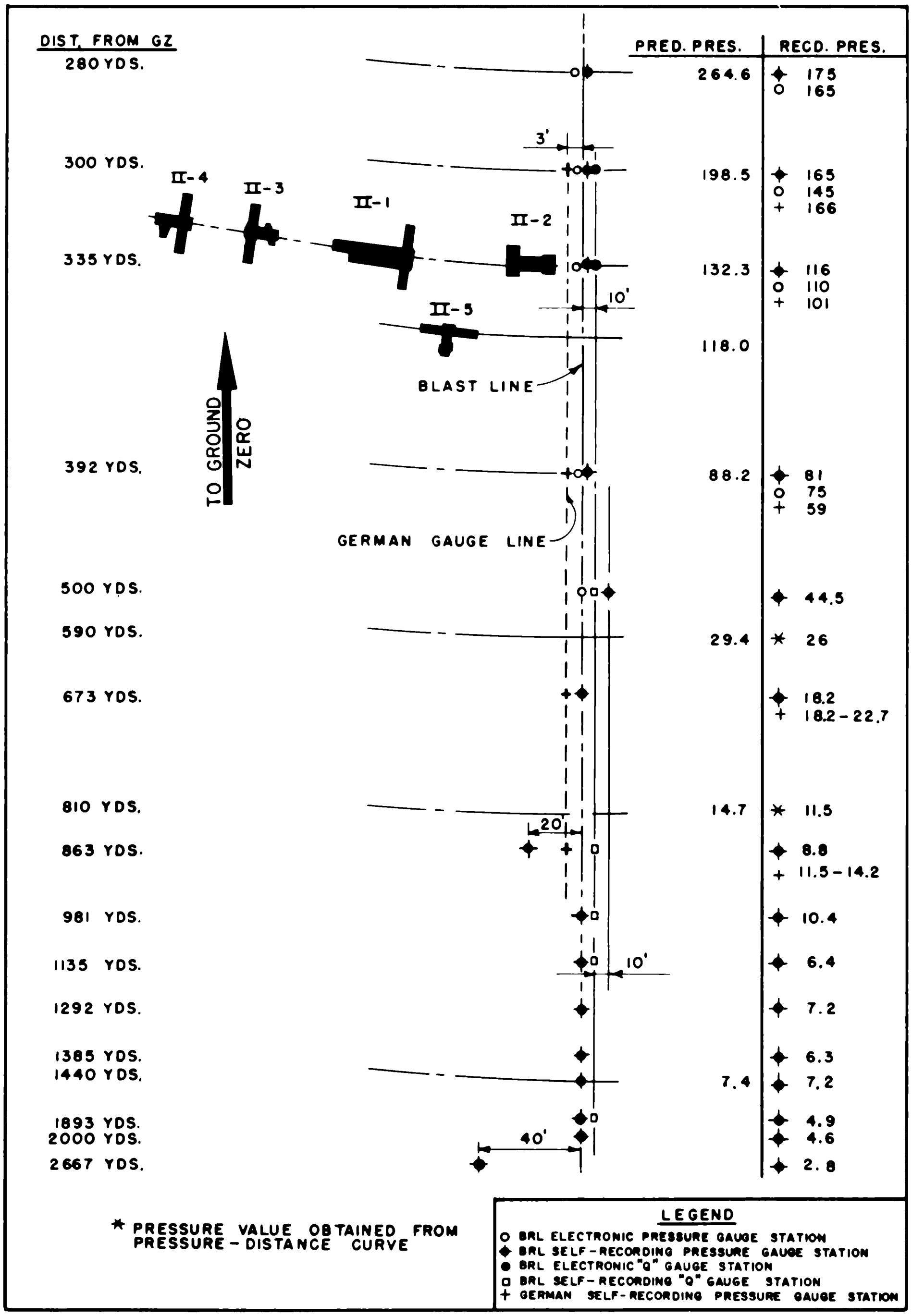

Fig. 1—Location and orientation of structures, Project 30.6.

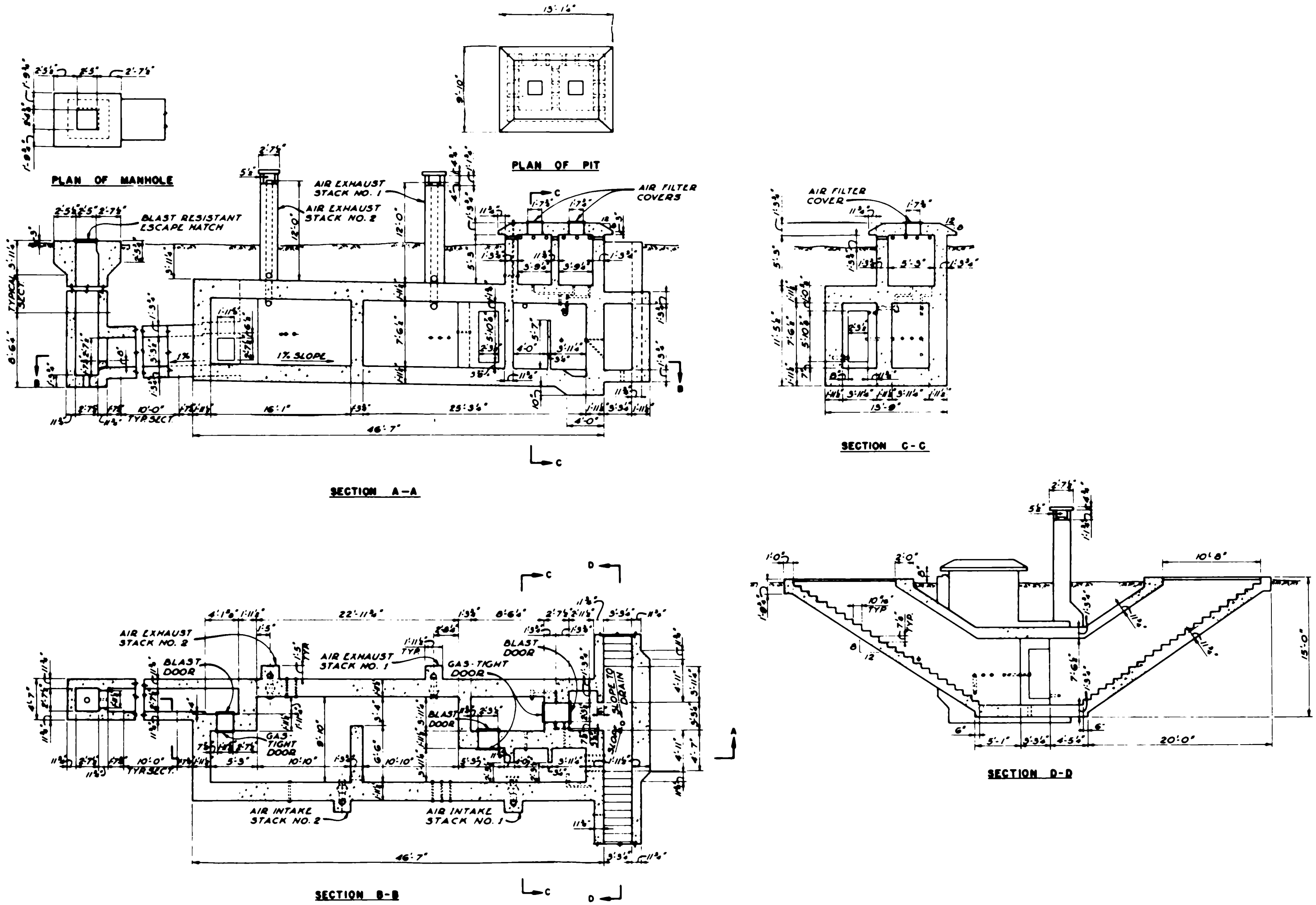

Fig. 2—Rectangular shelter, type 60, structure II-1, architectural layout.

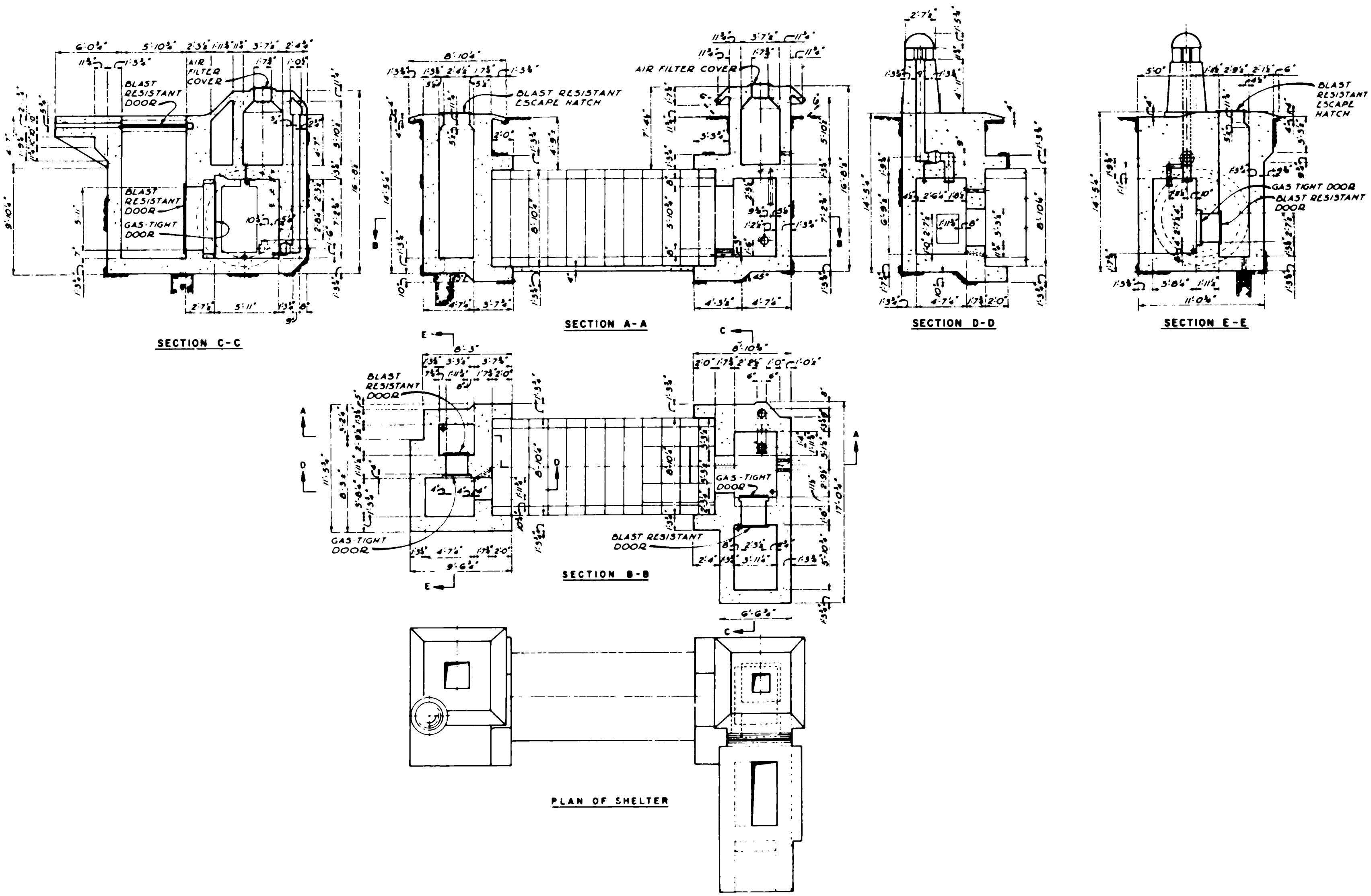

Fig. 3—Circular shelter, type 50, structure II-2, architectural layout.

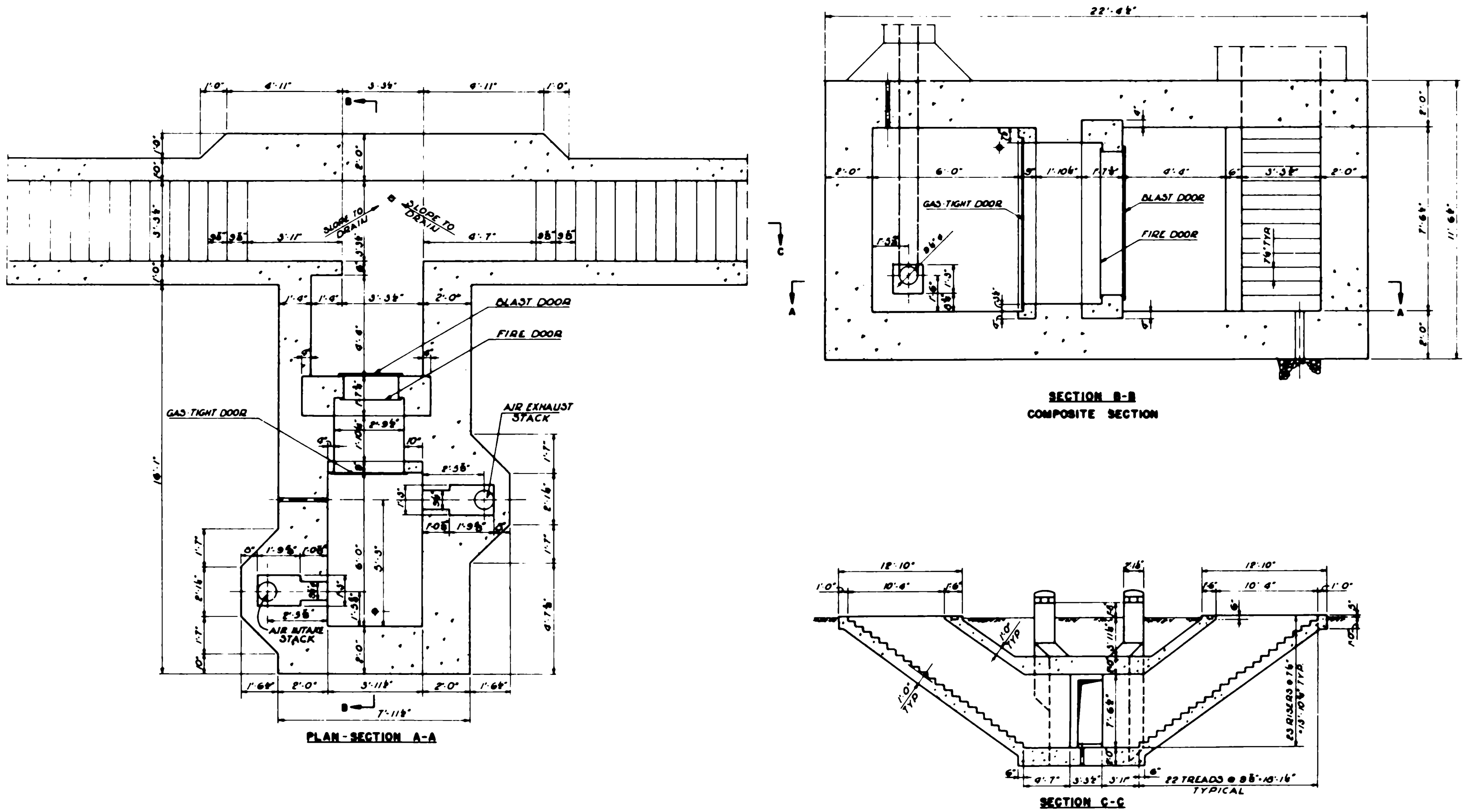

Fig. 4—Entrance and entrance chamber, structure II-3, architectural layout.

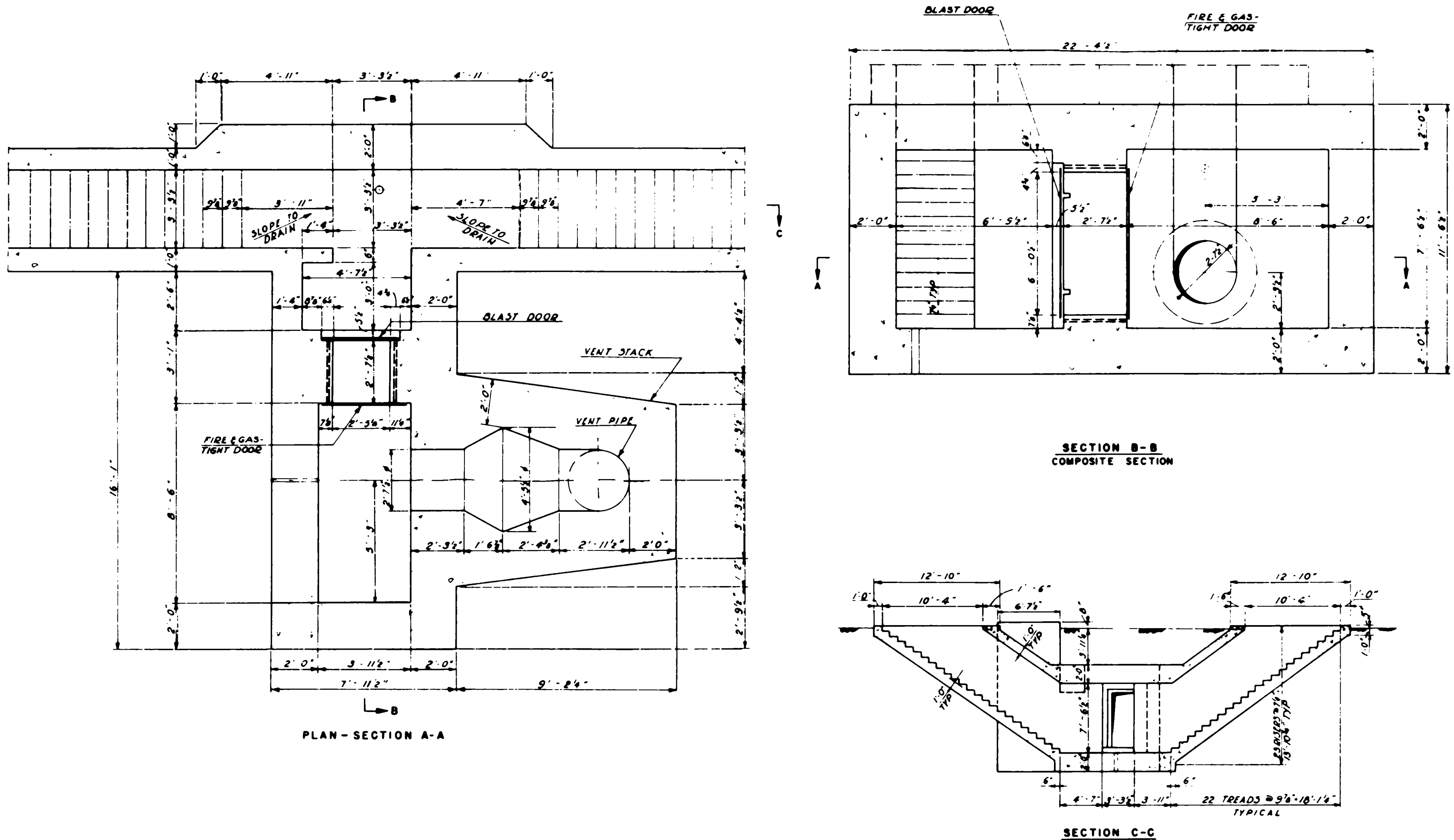

Fig. 5—Entrance and entrance chamber, structure II-4, architectural layout.

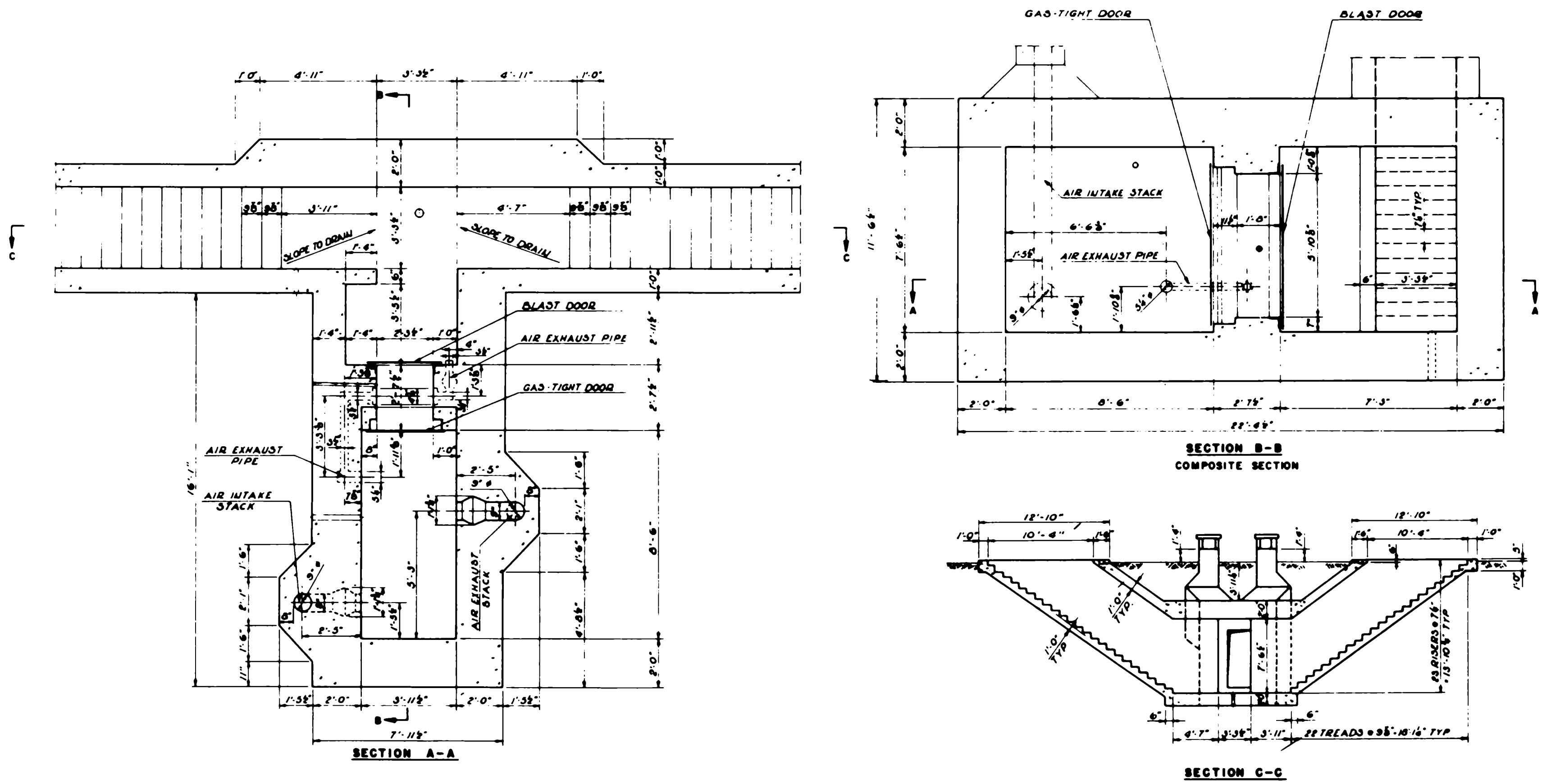

Fig. 6—Entrance and entrance chamber, structure II-5, architectural layout.

Fig. 7—Aboveground view of intake and exhaust stacks.

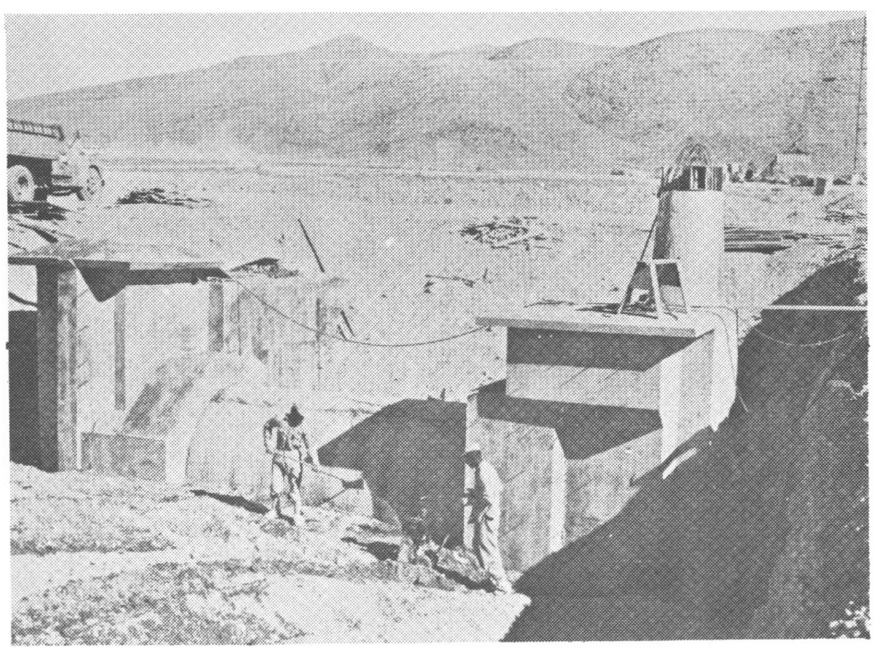

Fig. 8—Exterior view of structure II-2 before backfilling.

Fig. 9—Exterior view of structure II-3.

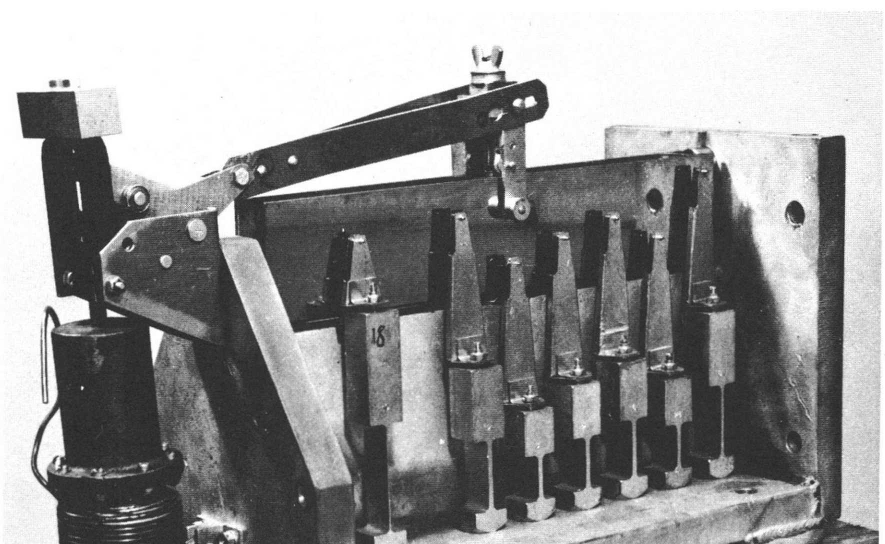

Fig. 10—Shock gauge.

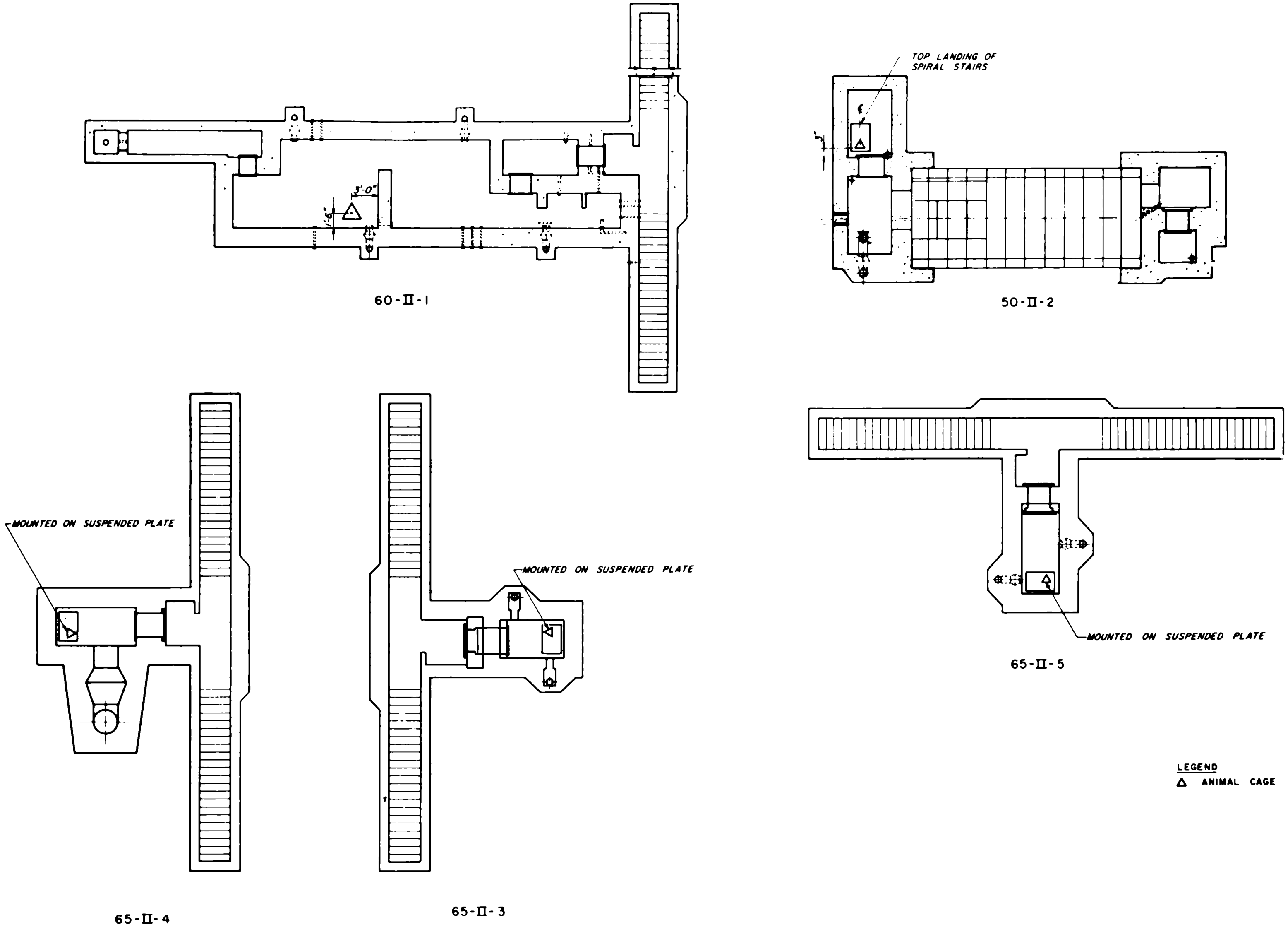

Fig. 11—Locations of biological specimens.

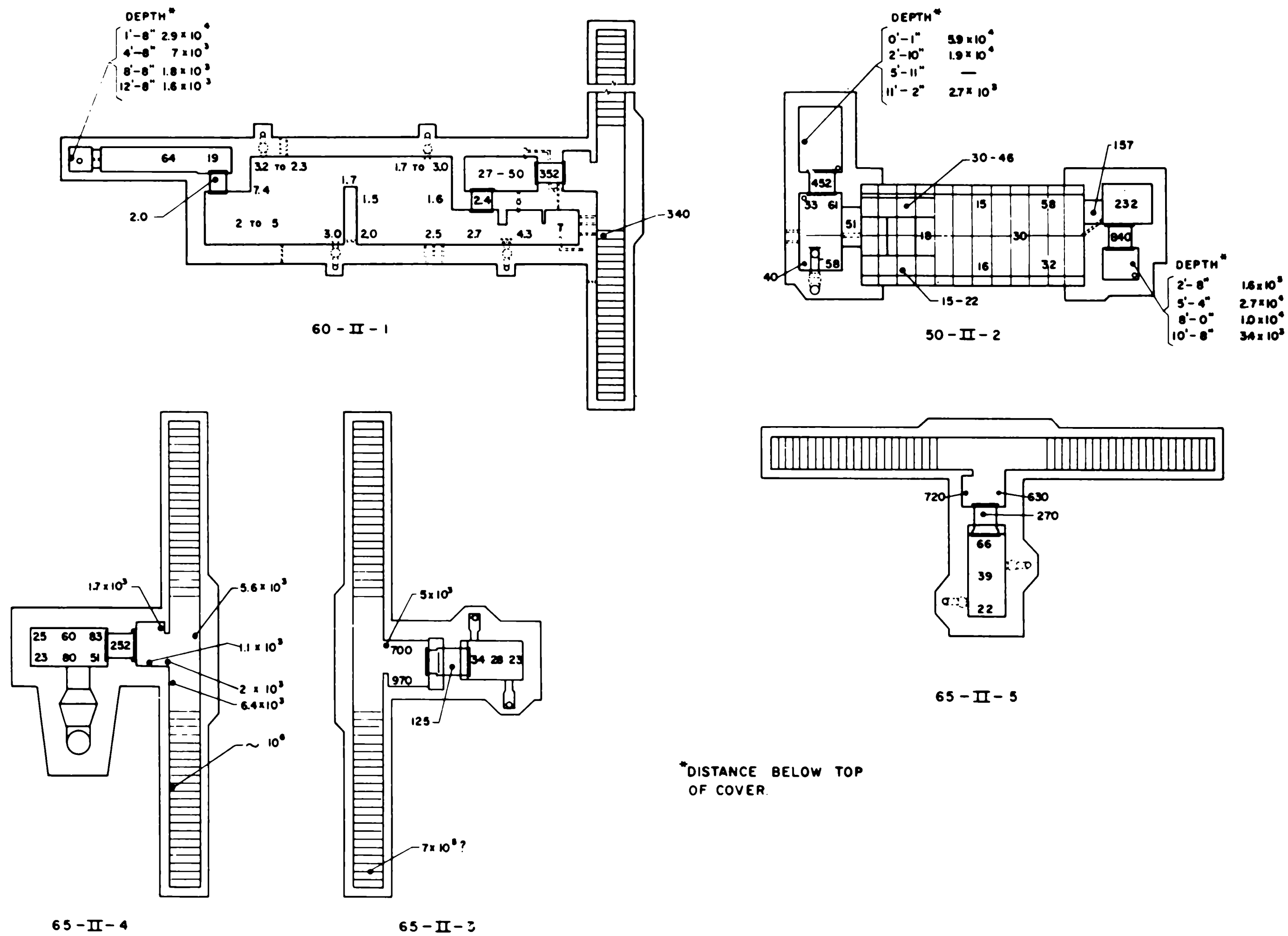

Fig. 12—Approximate total gamma doses during first 52 hr after detonation.

SUMMARY 24

TEST OF GERMAN UNDERGROUND PERSONNEL SHELTERS

(Report WT-1454, Operation Plumbbob, Project 30.7, same title, by Edward Cohen and A. Bottenhofer, Ammann & Whitney, Consulting Engineers, New York, N. Y., June 25, 1962.)

OBJECTIVES AND SCOPE

The main objectives of this project were to observe the behavior under blast conditions of protective shelter structures of German design and, in general, built with German material; to determine the relative efficiency of different types of construction; and to obtain information for the improvement of these structures.

Nine structures were built, consisting of three types of underground cast-in-place concrete personnel shelters: (1) four type-A rectangular shelters designed for an overpressure of 132 psi; (2) two type-A circular shelters also designed for 132 psi; and (3) three type-C rectangular shelters designed for 14.7 psi.

The shelters were constructed at the following predicted blast overpressure levels:

1 type A rectangular	(RAa)	264.6 psi
1 type A rectangular	(RAb)	198.5 psi
1 type A circular	(CAa)	
1 type A rectangular	(RAc)	132.3 psi
1 type A circular	(CAb)	
1 type A rectangular	(RAd)	88.2 psi
1 type C rectangular	(RCa)	29.4 psi
1 type C rectangular	(RCb)	14.7 psi
1 type C rectangular	(RCc)	7.4 psi

Figure 1 shows the location and orientation of the structures, as well as predicted and maximum recorded overpressures. The orientation placed the direction of the entrance stairs radial to Ground Zero (GZ). It was expected that this orientation would provide minimum reflected pressures on the main blast door.

The structures were tested in Smoky shot, a 44-kt nuclear device detonated on a 700-ft steel tower (ref. ENW, p. 675).

Data on strains, deflections and deformations, pressures, soil displacements, and radioactivity were obtained from German instrumentation and from extensive supplemental instrumentation provided by U.S. agencies. Physical characteristics and structural behavior were determined by observation and inspection.

Mice were used as biological specimens in environmental tests in seven of the structures tested. A series of tests was also performed in the nine structures to check for the possible occurrence of dust in the shelters.

An experiment was included to investigate the transmission of ground-shock acceleration to a simulated human body. This test recorded the shock-absorbing characteristics of Ensolite, cellular plastic material in sheet form, a commercial product manufactured by the United States Rubber Company.

Various types of doors and of ventilation systems were also investigated in this test.

TEST STRUCTURES AND EQUIPMENT

Figures 2 to 4 show architectural details of the three types of shelter and Figs. 5 and 6 show interior views. All the shelters were of reinforced-concrete construction and were designed to accommodate 25 persons each. In general, a shelter consisted of the entrance stairs and ramp, a vestibule, the main shelter body, an exit chamber, an emergency-exit tunnel, a vertical exit shaft, and a ventilation shaft.

The ventilation for all three types of shelter was similar. Although the structures were designed to use two systems (natural and filtered air), only the filtered-air system was provided in this test. With this system the air enters four 2-in. pipes passing through the air-intake stack at the ground surface. The air passes down and through a 3-ft 4-in. depth of double-washed coarse sand. The filtered air is then pumped into the main chamber of the structure by a manually or electrically operated air pump. In the type-A shelters, which have a gastight door between the main chamber and antechamber, the foul air is exhausted at the entrance end of the main chamber by a manually operated exhaust valve.

The main blast doors of the structures were of two types. The main entrance doors of both type-A shelters consisted of a steel plate curved inward with tubular members across to act as struts to take the compressive forces when the curved plates of the door were put into tension by the blast loads (Figs. 7 and 8). The second type blast door, used for the main entrance of the type-C shelter, and in a smaller size for the emergency exits of all the structures, is a flat plate with horizontal stiffeners (Fig. 9).

The blast doors for both type-A structures were designed for an overpressure of 220 psi and for type-C structures, 66 psi. The vertical and horizontal emergency-exit blast doors were designed for 147 and 13 psi, respectively.

All doors were made gastight by rubber-tubing gaskets.

The structures were designed for static loading conditions. The equivalent loads assumed were equal to one-third the peak incident overpressure, i.e., 44-psi static load at 132-psi overpressure, and a 5-psi static rebound load. The loads were considered to be uniformly distributed on the exterior walls, roofs, and floor slabs so as to cause maximum working stresses. Minimum allowable design stresses were 1420 psi (4260-psi cube strength) for concrete and 20,000 psi for steel.

The ground-shock experiment with Ensolite was performed in structure RAc at the 132-psi overpressure range. Concrete blocks were cast around concrete-filled rubber boots, the weight of boots and block being approximately equal to that of the average human (Fig. 10). Three pairs of boots were mounted on three different types of flooring: (1) three 1-in.-thick layers of Ensolite cemented together; (2) one 1-in. layer and one ½-in. layer of Ensolite cemented together; and (3) the existing concrete floor of the structure (Fig. 11). The instrumentation included one Wiancko accelerometer mounted on each of the three blocks and two accelerometers on the concrete floor. The instruments on the floor were arranged to measure both vertical and horizontal acceleration of the structure.

The U.S. pressure instruments installed in the structures consisted of Wiancko electronic pressure gauges, Carlson electronic earth-pressure gauges, Ballistic Research Laboratories (BRL) self-recording pressure–time gauges, and BRL electronic and self-recording dynamic-pressure gauges. Five self-recording pressure gauges, supplied by the West German Government, were also used in the test.

Structural response of the structures was recorded by BRL displacement and acceleration gauges and SR-4 strain gauges. Scratch gauges were also used to determine relative deflections of structure RAa.

Twelve shock gauges with protecting canisters were used in the test. The shock gauge is a completely self-contained mechanical unit requiring no electronic or communication channels. Essentially, it consists of 10 masses attached to cantilever springs mounted on two sides of a vertical plate (Figs. 12 and 13).

Radiation measurements were made with U.S. gamma-radiation film dosimeters, gamma-radiation differential chemical dosimeters, and neutron detectors, as well as with gamma-radiation differential chemical dosimeters supplied by the West German Government. Also included for gamma-radiation measurements were two dual-unit telemeters.

Two types of dust collector were used in this study, sticky-tray fallout collectors and motor-driven air samplers.

In general, the biological test consisted of a sample of 20 mice; one sample was placed in each of seven of the nine structures tested. The test objectives were twofold: (1) to place the specimens in the shelters and to follow their mortality rate over a 60-day period postshot, and (2), if possible, in case of death, to relate the cause of death to a specific environmental factor.

RESULTS

Very slight damage was sustained by the test structures. Cracking was observed in all structures, but major damage occurred only to those portions directly exposed to the shock wave, such as the entrances and the type-RA and -CA emergency-exit covers.

A postshot dynamic analysis of the roof slab of shelter RAa was performed using current ultimate-strength theory as well as the recorded incident pressure at the location of the structures. This analysis indicated that only minor cracking could be expected and agreed surprisingly well with the actual damage inflicted on the roof slab.

No residual thermal effects were apparent from visual observation. Instrumentation was not provided for thermal measurements.

The maximum recorded external blast overpressures at the various locations of the structures are shown in Fig. 1, and the blast-line pressure–distance curves for both side-on and dynamic pressures are illustrated in Fig. 14.

The overpressure in the interior of a structure depends to a great extent on the peak and duration of the external pressure, the interior volume of the structure, the size and configuration of the openings leading to the interior, and the type of blast closure employed. In that respect the ventilation systems as tested were just as they would be under actual blast conditions; i.e., the natural ventilation was sealed, and the emergency ventilation with sand filter was open to the atmosphere and to the inside of the main chamber. The maximum overpressure recorded in the ventilation shaft of structure RAc was 14.3 psi, whereas the maximum overpressure in the combination ventilation shaft and emergency exit of structure CAb was 60.0 psi. Results of the special very-low-pressure (VLP) gauges placed in the main chambers of these two structures indicated that the maximum overpressure due to total leakage of the sand filter and overpressure flap valve was approximately 0.2 psi. Gauges in the antechambers recorded maximum overpressures of 3.5 psi in structure RAb, 2.2 psi in RAc, and 0.87 psi in RCa.

The blast results of the structural-response equipment are indicated in Tables 1 to 3. No reliable data were obtained from the deflection gauges. Owing to the small magnitude of the deflections, the gauges themselves produced large errors.

Ground-shock instrumentation records showed that the horizontal (radial) measurements were generally less than one-half the vertical measurements. The horizontal displacements recorded in the shelter were approximately the same as those for the free-field gauges adjacent to the structure. However, the vertical displacements in the shelter were considerably less than the free-field measurements; this indicates attenuation in the vertical direction.

The results of the acceleration test, or Ensolite experiment, which was designed to investigate the transmission of structural acceleration to the concrete blocks, indicated that acceleration was reduced by a maximum factor of about 3. The acceleration data shown in Table 4 illustrate the relative effectiveness of the various thicknesses of Ensolite in reducing ground shock.

No readings of the initial radiation were obtained as separate values, but recorded data indicate the values for the total gamma dose during the first 52 hr after the detonation at various points within all nine test structures. Structure RAc had radiation doses equal to 145 r at the front wall (exposed to the exterior), 47 r by the interior corner of the antechamber, and 22 r at the center of the main chamber. Structure CAb

had interior dose values varying from 9 to 29 r, except directly behind the gastight door where the dose was 140 r. The interior doses in structure RCb varied from a minimum of 36 r at the rear corner to a maximum of 382 r directly inside the main blast door.

According to postshot photographs taken before the entranceways were cleaned, deposited debris was comparatively light. The dust layer varied in thickness from approximately ¼ in. to a maximum of 2 in. at the higher pressure levels in places where drifting occurred. Some rubble was also present. Interior dust was not visibly discernible. It was suggested that dust, as it occurred in the structures studied, would not have been an immediate hazard to shelter occupants.

Of particular interest are the following detailed postshot observations:

1. All doors and about one-half of the emergency-exit hatch covers were essentially undamaged and in operating condition after the test. Three exit-hatch covers were blown down into the exit tunnel.

2. The ventilation systems were, in general, in working condition and had the same settings after the test as before.

3. The entranceways suffered the most severe damage with numerous cracks and separations in walls and floor slabs ranging from $\frac{1}{32}$ in. to several in.

4. No damage was observed in the walls, roof, and floor slabs of the antechambers.

5. In the main chambers the damage was generally limited to extensive hairline cracks in the roof and at the wall haunches.

6. Damage to the exit chambers and exit tunnels and shafts included some slight cracking and spalling of the concrete.

Environmental tests of mice showed that immediate mortality of mice was confined to structure CAb. All 20 mice in that structure were found dead upon recovery. Death was attributed to poisoning by carbon monoxide produced by the gasoline generator that operated the air sampler. The location, number, time of recovery after the test, and time of death of the mice that died in the period from their recovery until 20 days after the test are given in Table 5.

EVALUATION AND DISCUSSION

There was no definite superiority to be found between the two types of construction, i.e., the rectangular vs. the circular shelter design. Some damage, mostly cracks, was experienced in both types at the various locations.

Regarding probable overall exposure to possible shelter occupants, the test results showed a fairly satisfactory balance between structural damage to the shelters, ground-shock effects, blast pressures, and radiation doses as measured inside the main chamber. Thermal effects would be of no concern; however, the death of 20 mice in shelter CAb, attributed to carbon monoxide produced by the gasoline generator, was considered a valuable lesson learned that deserves serious consideration.

Although the effects (overpressure vs. time, and thermal and nuclear radiation) of small nuclear weapons differ in magnitude from the effects of the large thermonuclear weapons now available and although the physical environment at the Nevada Test Site is not typical of most populated areas, the data obtained from this and other similar weapons tests are very useful in estimating response and in evaluating the parameters used in the design. For this reason the records of blast overpressure, ground-shock motions, radiation, and other weapons effects may be considered of prime importance. The results, however, cannot be used directly for proof-test purposes except in special cases.

Table 1—SCRATCH-GAUGE MEASUREMENTS

Gauge*	Member	Angle of gauge to member	Length of scratch, in.	Deflection of member, in.
$\overline{D}$-1	Roof	49°	0.07	0.053
$\overline{D}$-2	Floor	49°	0.10	0.076
$\overline{D}$-3	Wall	69°	0.08	0.075
$\overline{D}$-4	Door	63°	0.46†	

*Self-recording.
†Includes thickness of rubber gasket.

Table 2—ACCELERATION-GAUGE MEASUREMENTS

Structure	Gauge	Peak value, g*	Remarks
RAb	A-1	−14.5	Good record
		+8.5	
CAa	A-1	−11.5	Good record
		+9.5	
RCa	A-1	+1.6	Questionable record

*Upward direction is +.

Table 3—SR-4 STRAIN-GAUGE MEASUREMENTS

Structure	Gauge	Peak value, (in./in.) X 10^{-3}*	Remarks
RAb	S-1	+0.33	Good record
		−0.04	
	S-2	−0.38	Good record
	S-3	−0.80	Good record
	S-4	+1.80	Good record
		−1.50	
CAa	S-1	−0.46	Partial record
RCa	S-1		No record
	S-2		No record
	S-3		Questionable record

*Positive (+) = tension; negative (−) = compression.

Table 4—ENSOLITE EXPERIMENT DATA (STRUCTURE RAc)

Location of gauge	Direction of measurement	Measurement	Gauge	Maximum value*
Boot (3-in. Ensolite)	Vertical	Acceleration	A-1	+3.1 g −2.1 g
Boot (concrete floor)	Vertical	Acceleration	A-2	+9.8 g −2.2 g
Boot (1½-in. Ensolite)	Vertical	Acceleration	A-3	+3.7 g −1.8 g
Concrete floor	Vertical	Acceleration	A-4	−6.6 g +4.8 g
Concrete floor	Horizontal	Acceleration	A-5	+2.8 g −1.8 g
Boot (1½-in. Ensolite)	Vertical	Deflection	D-1	−1.5 in. +0.65 in.

*Horizontal positive (+) acceleration–movement of floor slab toward GZ. Vertical positive (+) acceleration–movement of floor slab upward.

Table 5—MORTALITY RESULTS OF BIOLOGICAL TEST

Structure	Time of recovery, days after the test	Number and time of deaths
RAa	2	1 on 1 day after recovery; 1 on 14 days after recovery
RAc	2	None
RAd	2	None
CAb	2	20 before recovery
RCa	2	None
RCb	2	None
RCc	2	None

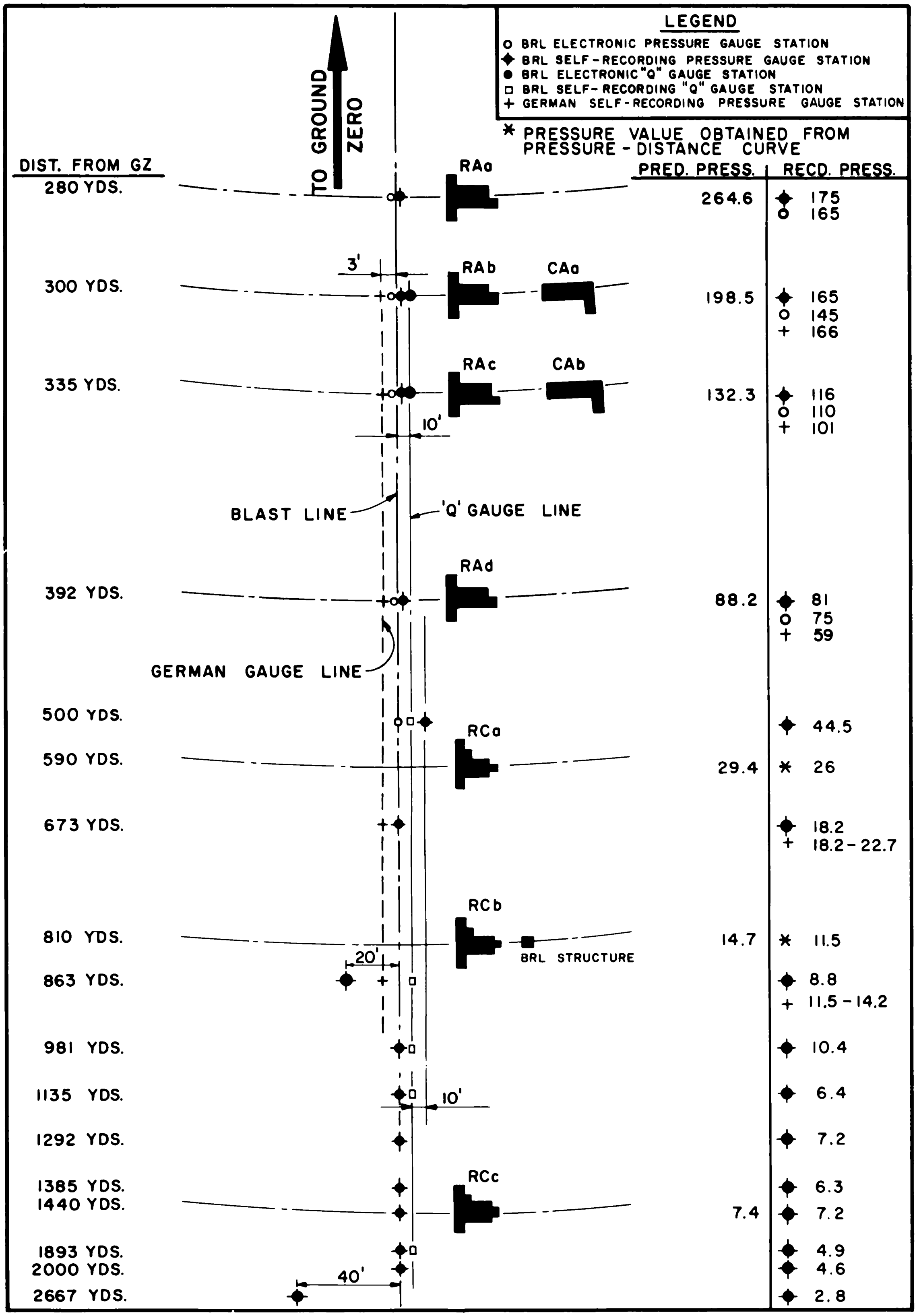

Fig. 1—Location and orientation of structures, Project 30.7.

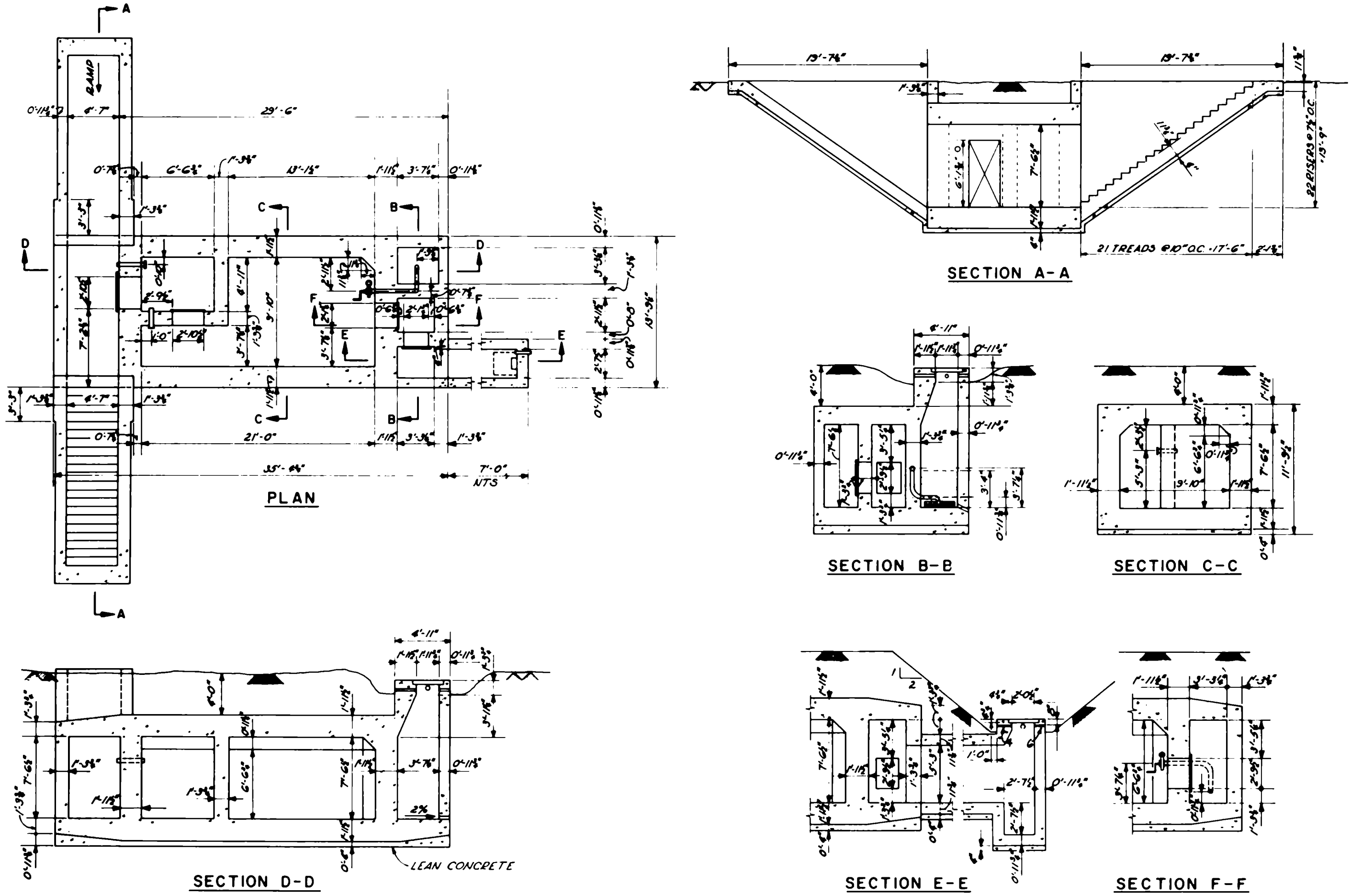

Fig. 2—Architectural layout for type-A rectangular shelter.

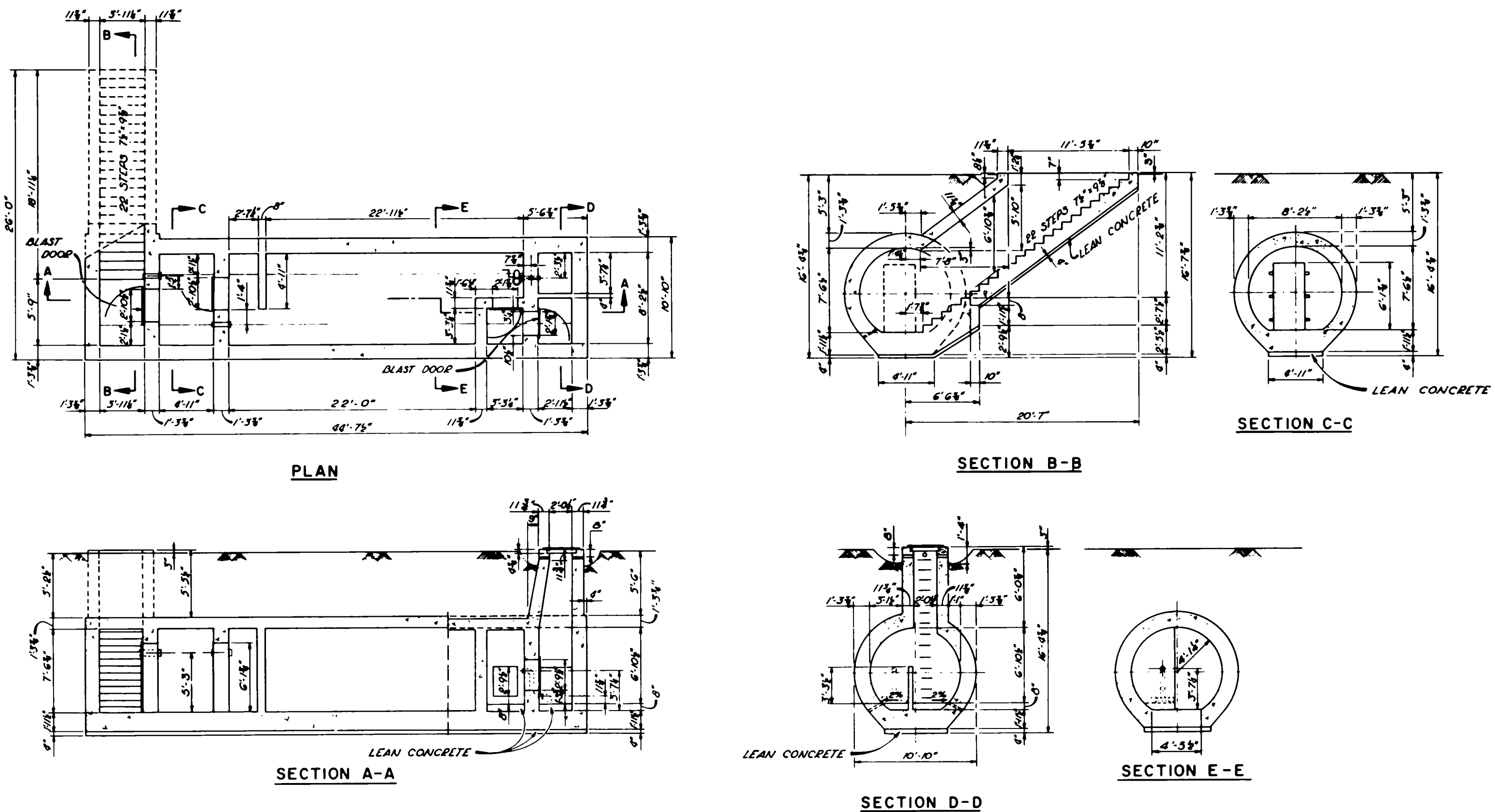

Fig. 3—Architectural layout for type-A circular shelter.

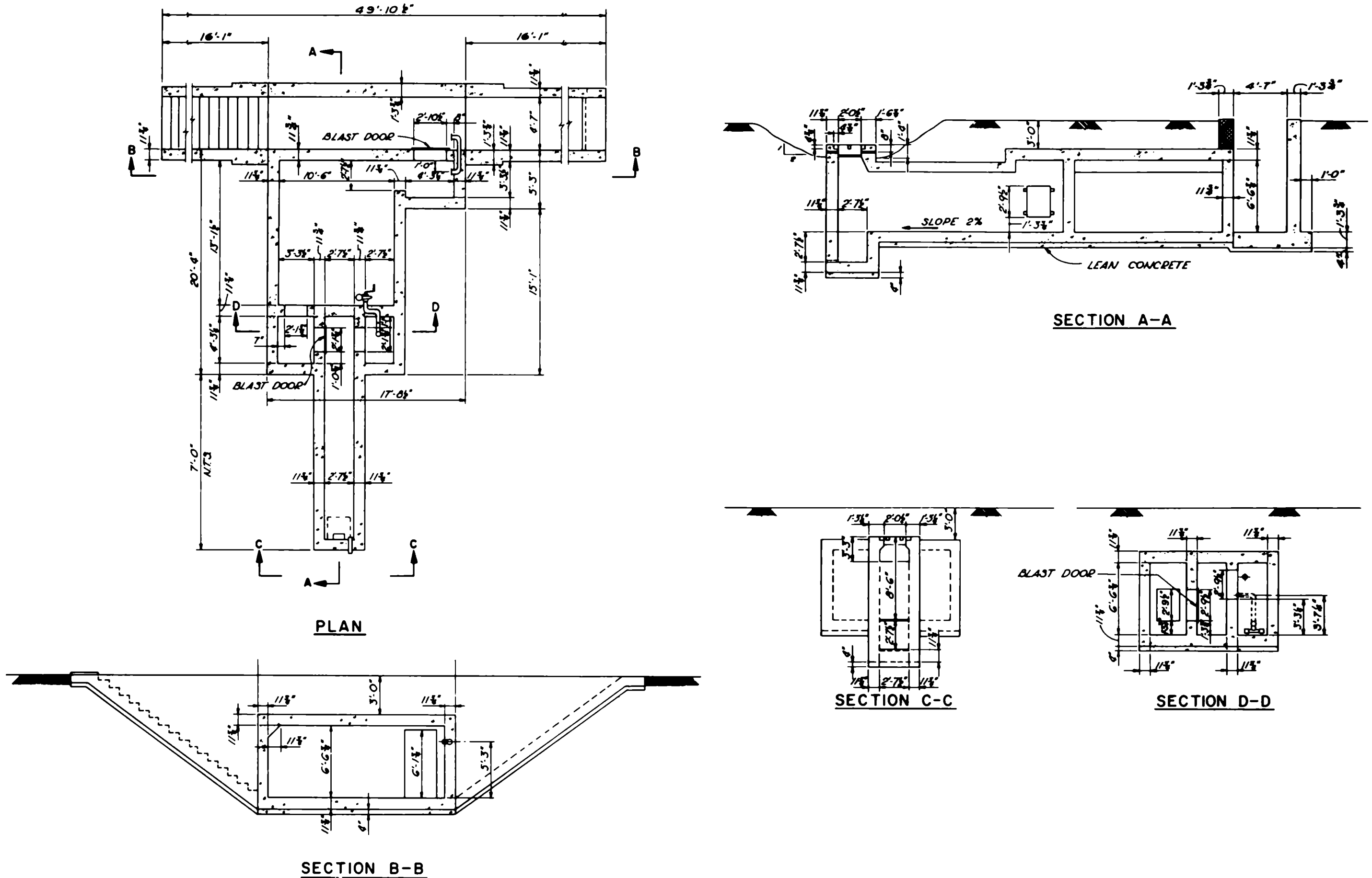

Fig. 4—Architectural layout for type-C rectangular shelter.

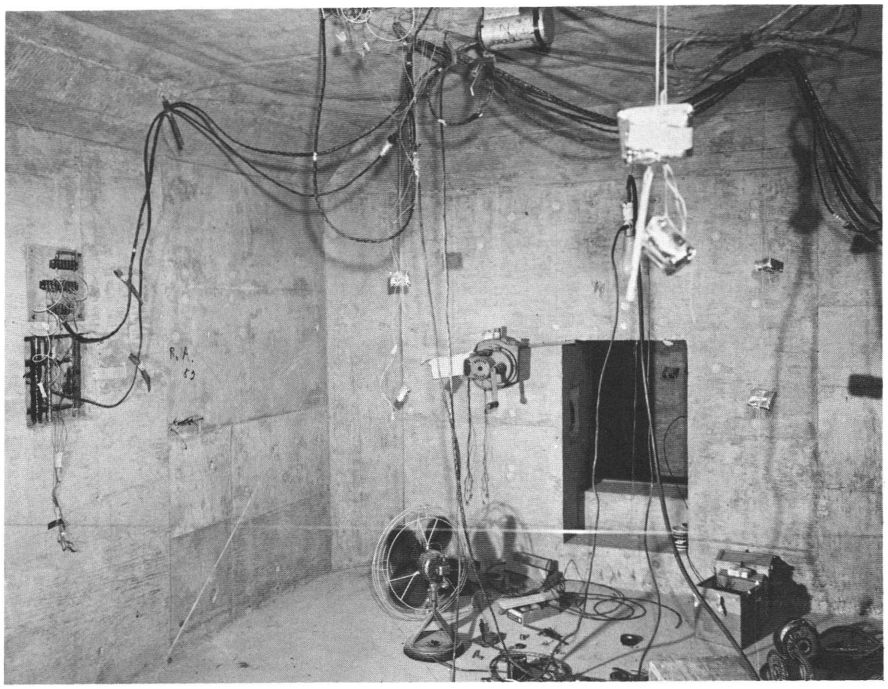

Fig. 5—Main chamber, structure RAb.

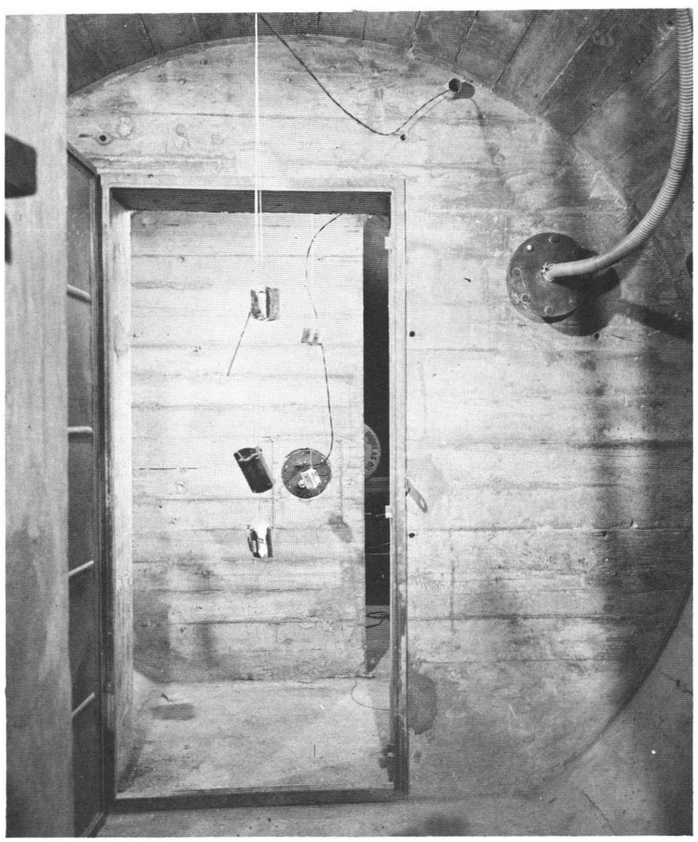

Fig. 6—Looking into main chamber from vestibule, structure CA.

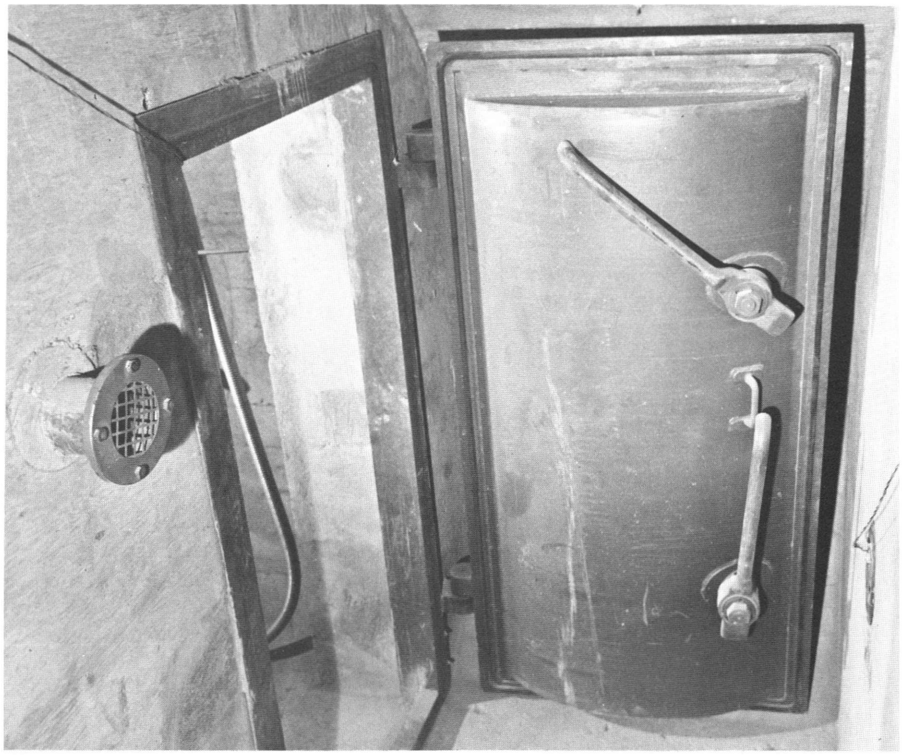

Fig. 7—Interior view of main blast door, structure CA.

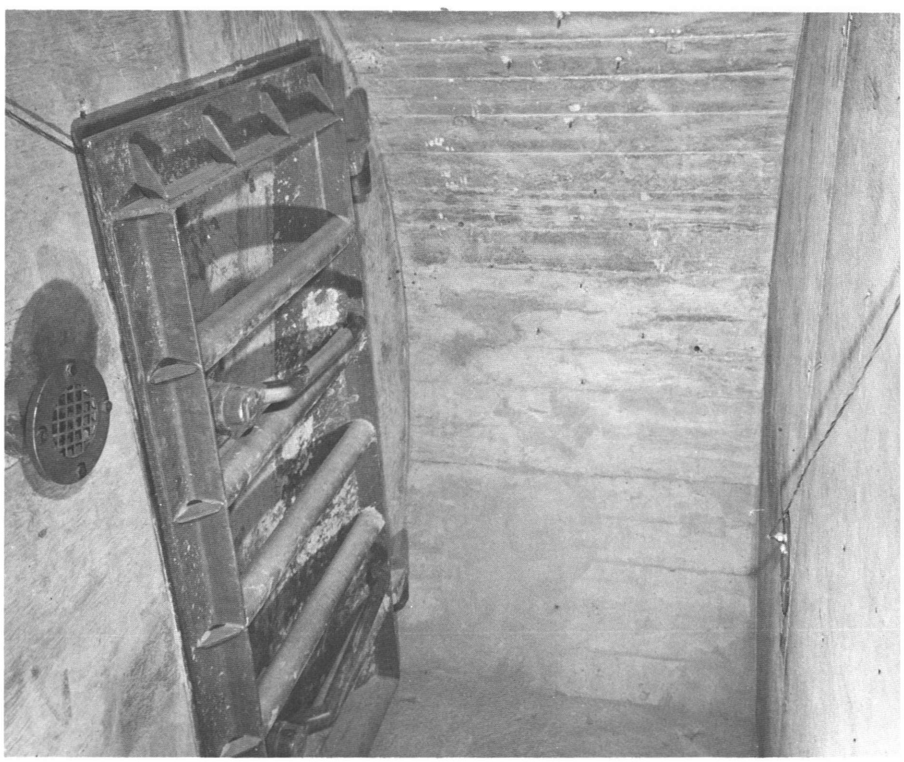

Fig. 8—Exterior view of main blast door, structure CA.

Fig. 9—Emergency-exit blast door, structure RC.

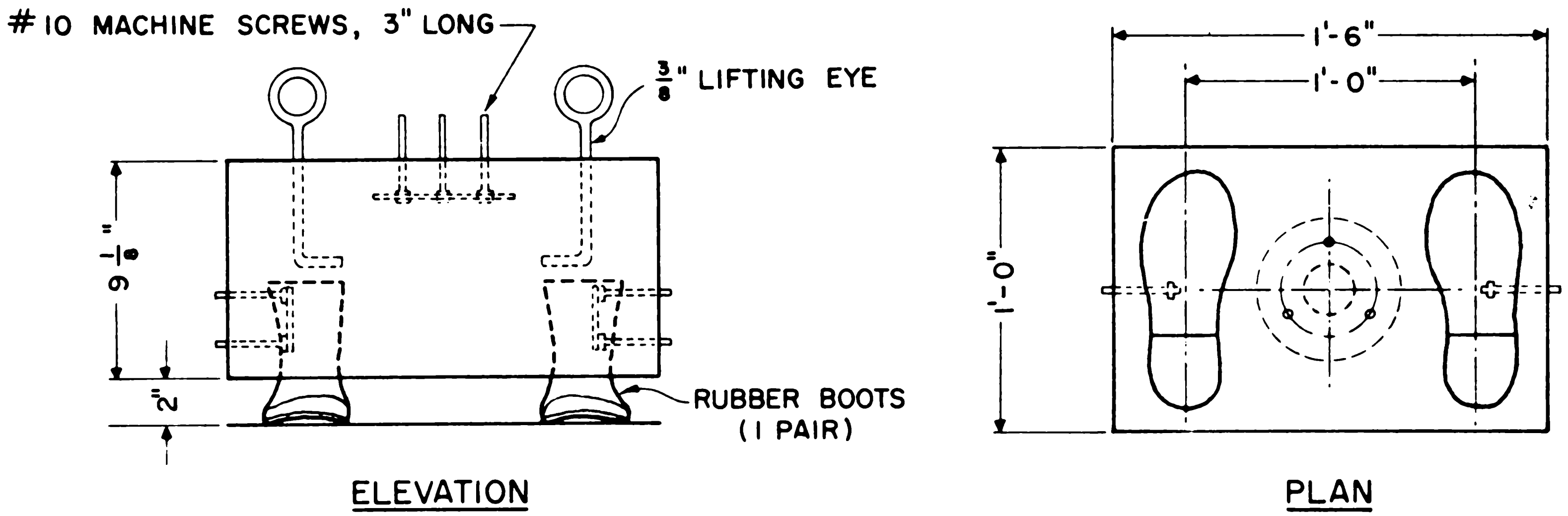

Fig. 10—One hundred and sixty-pound concrete test blocks.

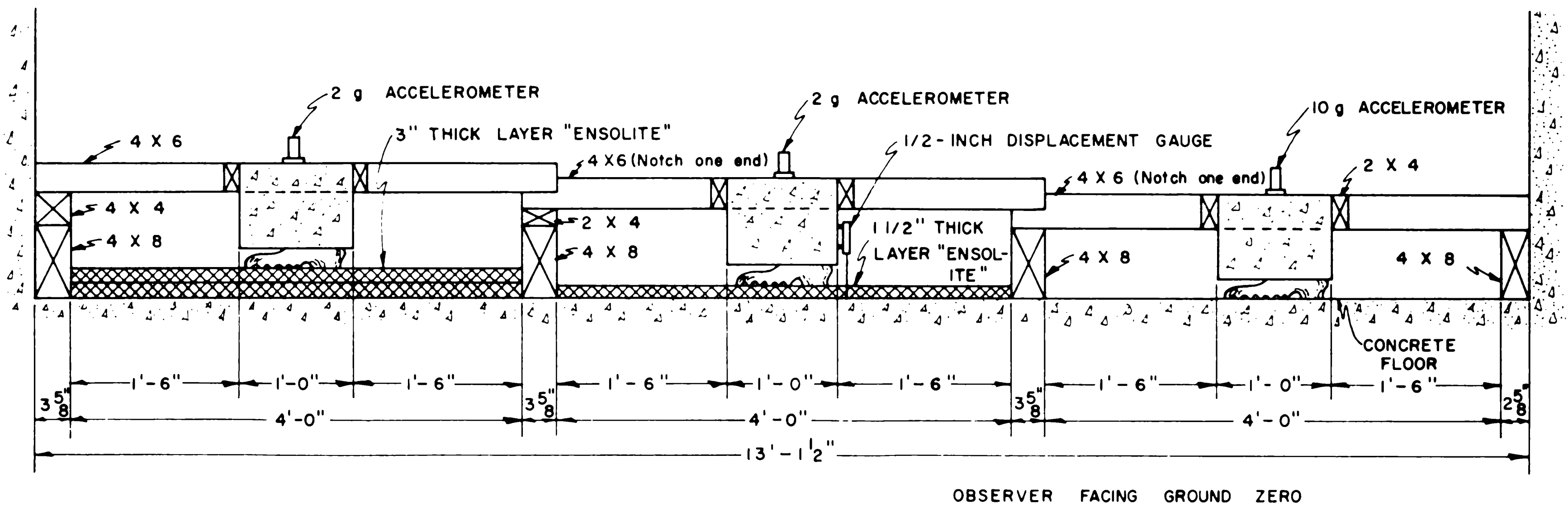

Fig. 11—Cross-sectional view of instrumented test blocks held in wooden frame.

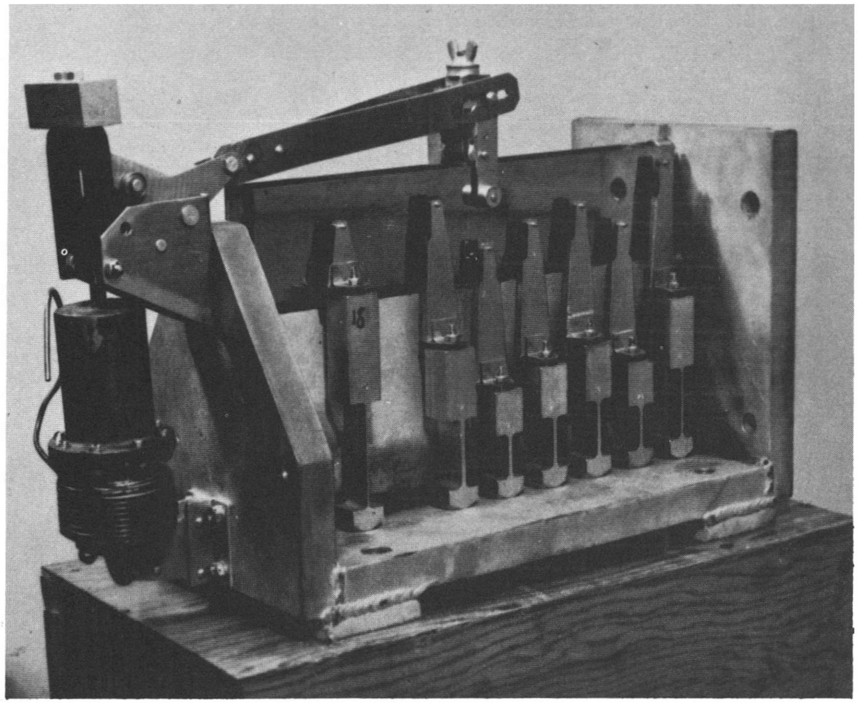

Fig. 12—Shock gauge.

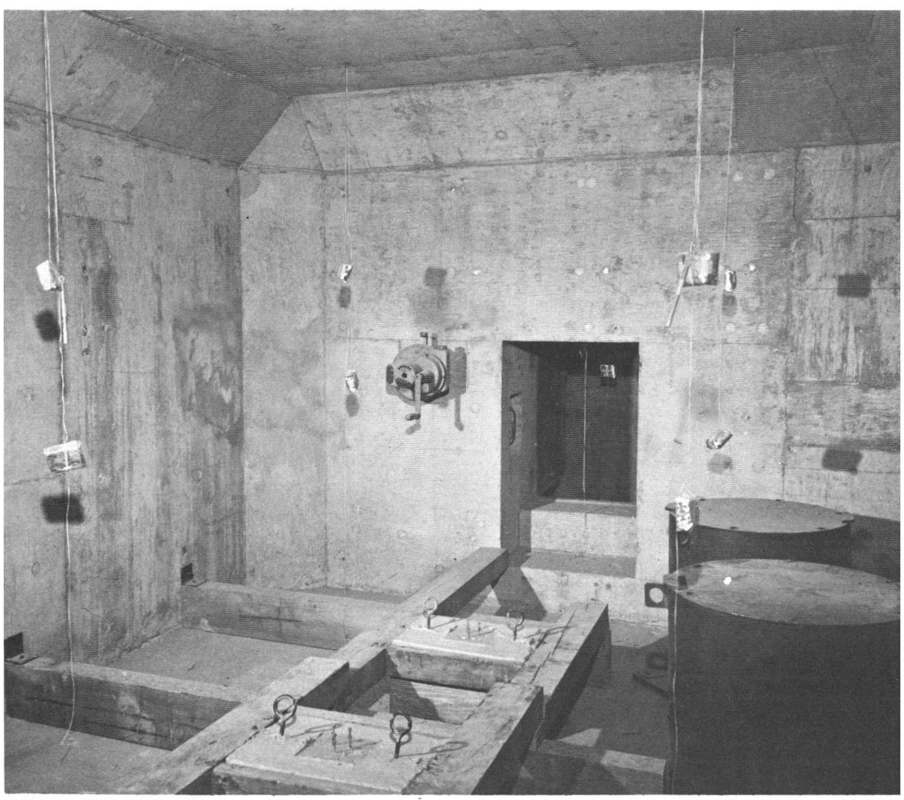

Fig. 13—Shock-gauge canisters and Ensolite test equipment.

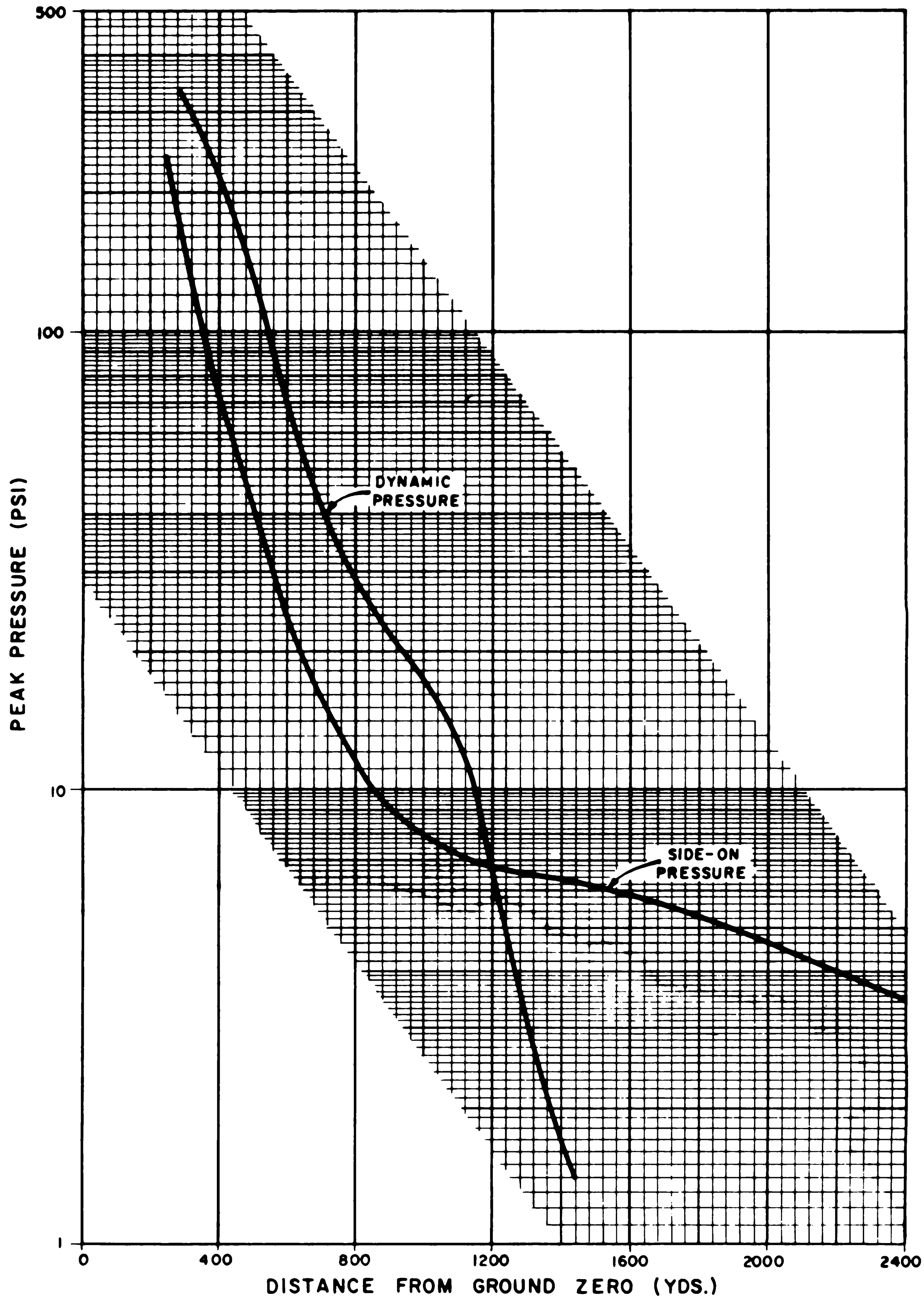

Fig. 14—Blast-line pressure–distance curve.

SUMMARY 25

EVALUATION OF INDUSTRIAL DOORS SUBJECTED TO BLAST LOADING

(Report ITR-1459, Operation Plumbbob, Project 31.4, same title, by Neal FitzSimons, Federal Civil Defense Administration, Washington, D. C., Aug. 22, 1958.)

OBJECTIVES AND SCOPE

The objectives of this project were to test several industrial doors designed for blast resistance to reflected pressures in the range of 3- to 7-psi peak side-on overpressures using commercially available materials and to collect engineering data to establish criteria for future designs.

All doors were designed using recently evolved theories of blast-resistant design. Consideration was given to the ductile properties of the door, its natural period of vibration, and the pressure–time curve of the anticipated blast load in developing the door designs.

Five types of industrial doors were designed and tested under the blast effects of a nuclear device at the Nevada Test Site. One group of doors was tested at 3.5-psi and another group at 7-psi peak incident overpressure. The five basic types of door tested were steel plate, cellular steel, wood plank, hollow plywood, and solid plywood.

TEST STRUCTURES AND INSTRUMENTATION

Figures 1 through 7 show details of the five doors tested, and Fig. 8 illustrates the installation of door units on the exposed wall of one of the simulated motels constructed for a previous test series. These motels consisted of a series of box cell structures of reinforced concrete, with a blank reinforced-concrete wall built at the rear and with framed openings constructed for the doors in the front wall. All doors were wedged shut at their latches to ensure that the deflections measured were purely structural.

All doors were equipped with maximum-deflection scratch gauges, and the steel-plate door at the 7-psi range was instrumented also with a deflection–time recording gauge. The reflected overpressures were measured by three self-recording pressure–time (SR/PT) gauges located on the front walls of the motel at each test range.

RESULTS

A summary of test results is given in Table 1. The peak reflected overpressures were slightly greater than design assumptions. The only door that failed structurally was the hollow-plywood door at the high blast range. Other permanent damage was limited to charring of paint on the wooden doors.

Every door, with the exception of the 2-in. solid-plywood door, was designed for deformations of 1 in. or more at a peak reflected overpressure of 16.2 psi. The reflected pressure at the high-pressure-range motel, as recorded at door midheight, was 17.5 psi.

Deflection data were obtained at both test ranges (Table 1). Only maximum deflections are tabulated because permanent deflections were too small to be ascertained by the methods used. The hollow-plywood door at the high range was almost completely shattered by the blast; the hardware, however, remained intact, though all plywood paneling between the wooden framing was torn free.

CONCLUSIONS

The test successfully demonstrated the structural stability of the four prototype blast-resistant industrial doors under peak reflected overpressures of 17.5 psi (7-psi incident pressure range). Greater structural response at this same pressure range is expected from weapons with larger than the nominal yield of this test shot. It is probable that the much longer peak-overpressure duration of the present-day megaton weapons would create a load pulse of sufficient magnitude to cause considerable damage to these four doors. The complete failure of the hollow-plywood door was partly blamed on faulty construction rather than poor design. It did, however, satisfactorily resist the blast at the low-pressure range.

In general, the test design was considered satisfactory; however, further reduction of the test data will permit refinements in design and should provide useful information for designing similar doors for higher pressures.

Of considerable importance in the design of blast-resistant shelter doors is the strength of the hardware, i.e., the latches and hinges. Normally, a maximum peak negative pressure of 4 psi acting on these hardware items may be considered; however, depending on the flexibility of the door when strained well within its yield range, the "rebound" force may amount to as much as 50% of the positive blast force on the door.

Table 1—SUMMARY OF TEST RESULTS

Door type	Peak reflected overpressure, psi	Positive-phase duration, sec	Maximum positive displacement, in.	Maximum negative displacement, in.	Total amplitude of displacement, in.
2-in. solid plywood	9.0		3/4	1/4	1
Wood plank	9.0		15/64	9/64	3/8
Cellular steel	9.0		7/64	7/64	7/32
Hollow plywood	9.4	0.959	9/32	15/64	33/64
Steel plate	9.4	0.959	1/16	9/16	5/8
3-in. solid plywood	17.6	0.809	37/64	39/64	1 3/16
Wood plank	17.6	0.809	23/32	9/16	1 9/32
Cellular steel	17.6	0.809	3/16	1/4	7/16
Hollow plywood	17.5	0.777	Door failed structurally		
Steel plate	17.5	0.777	19/64	1/8	27/64

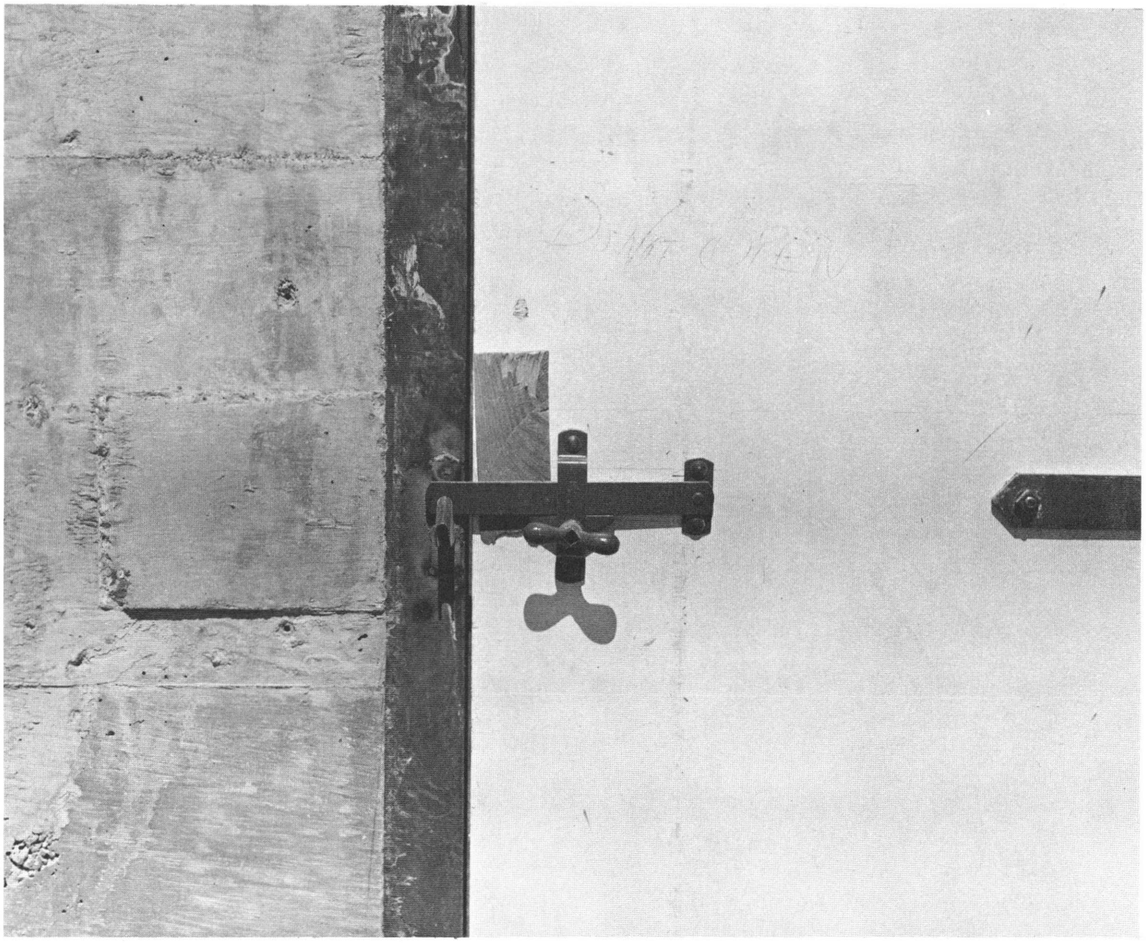

Fig. 1—Steel latch on door and wedge to hold door against stop.

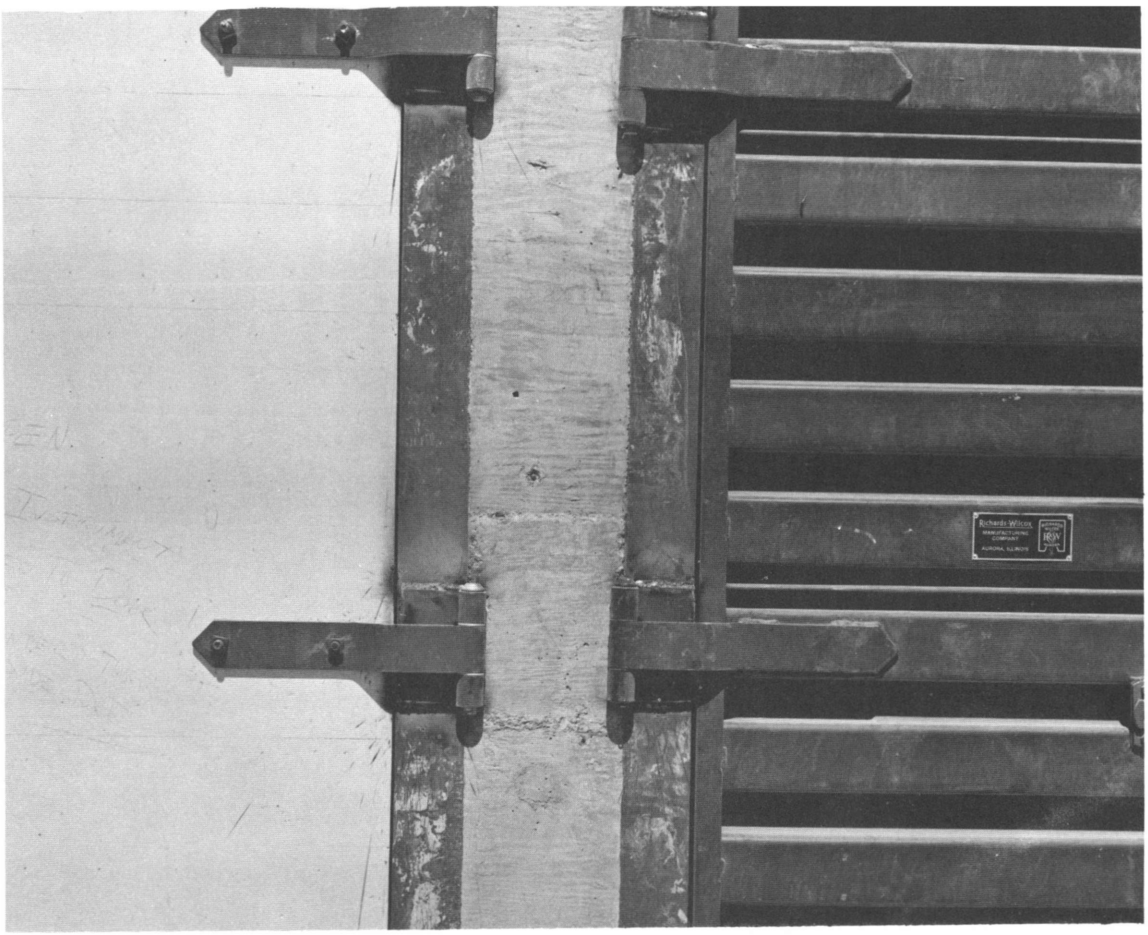

Fig. 2—Steel hinges on doors.

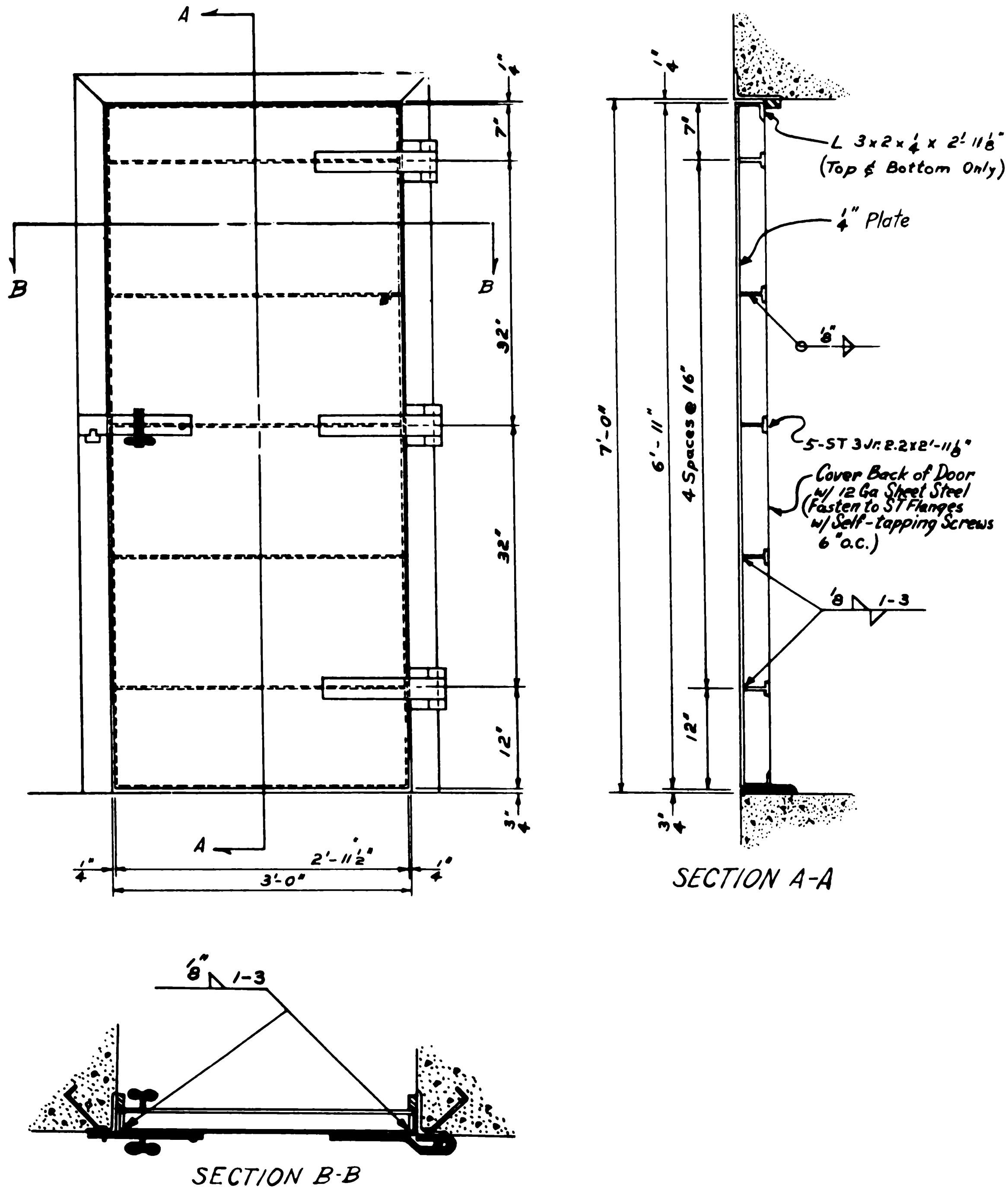

Fig. 3—Detail of steel-plate door.

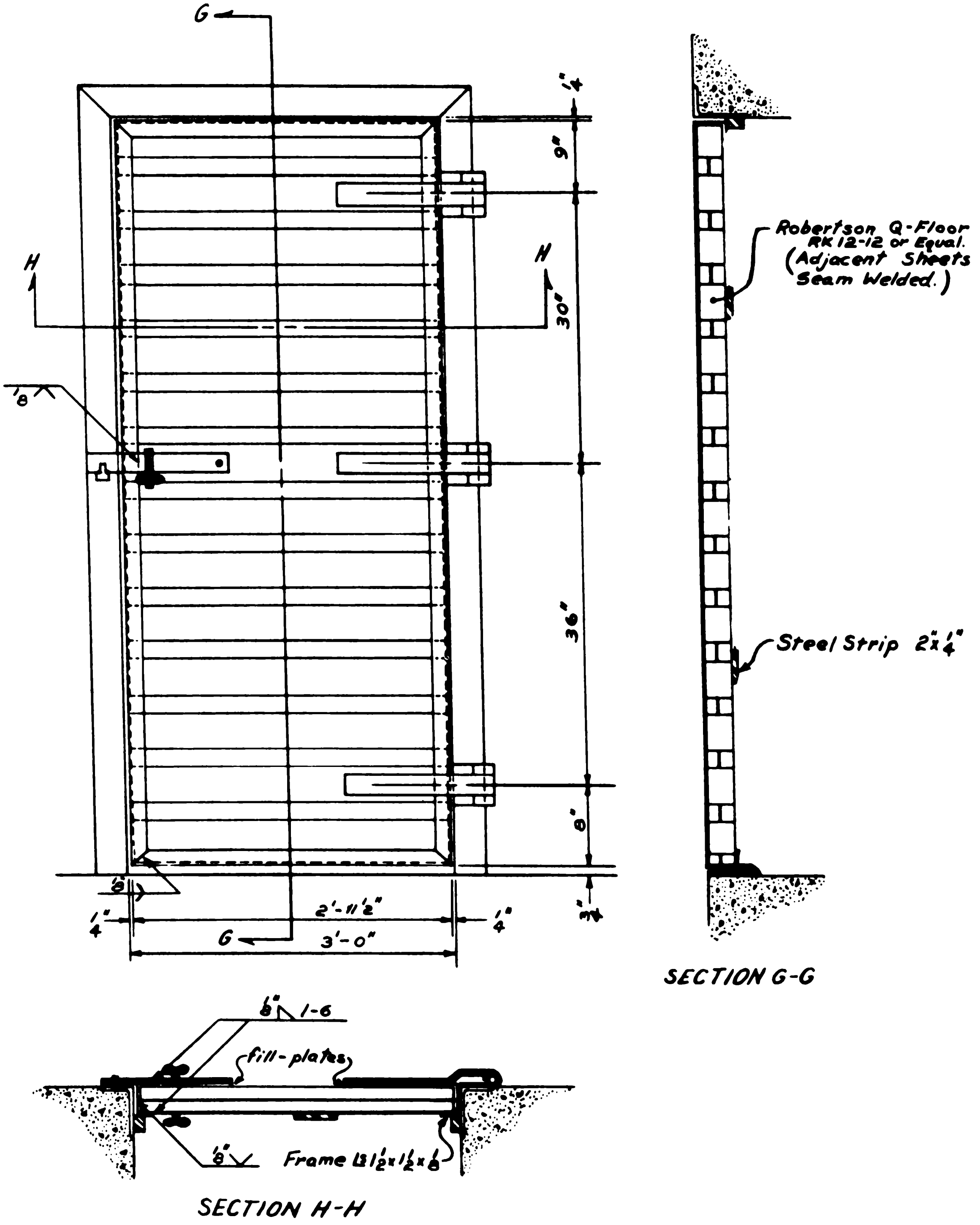

Fig. 4—Cellular-steel door detail.

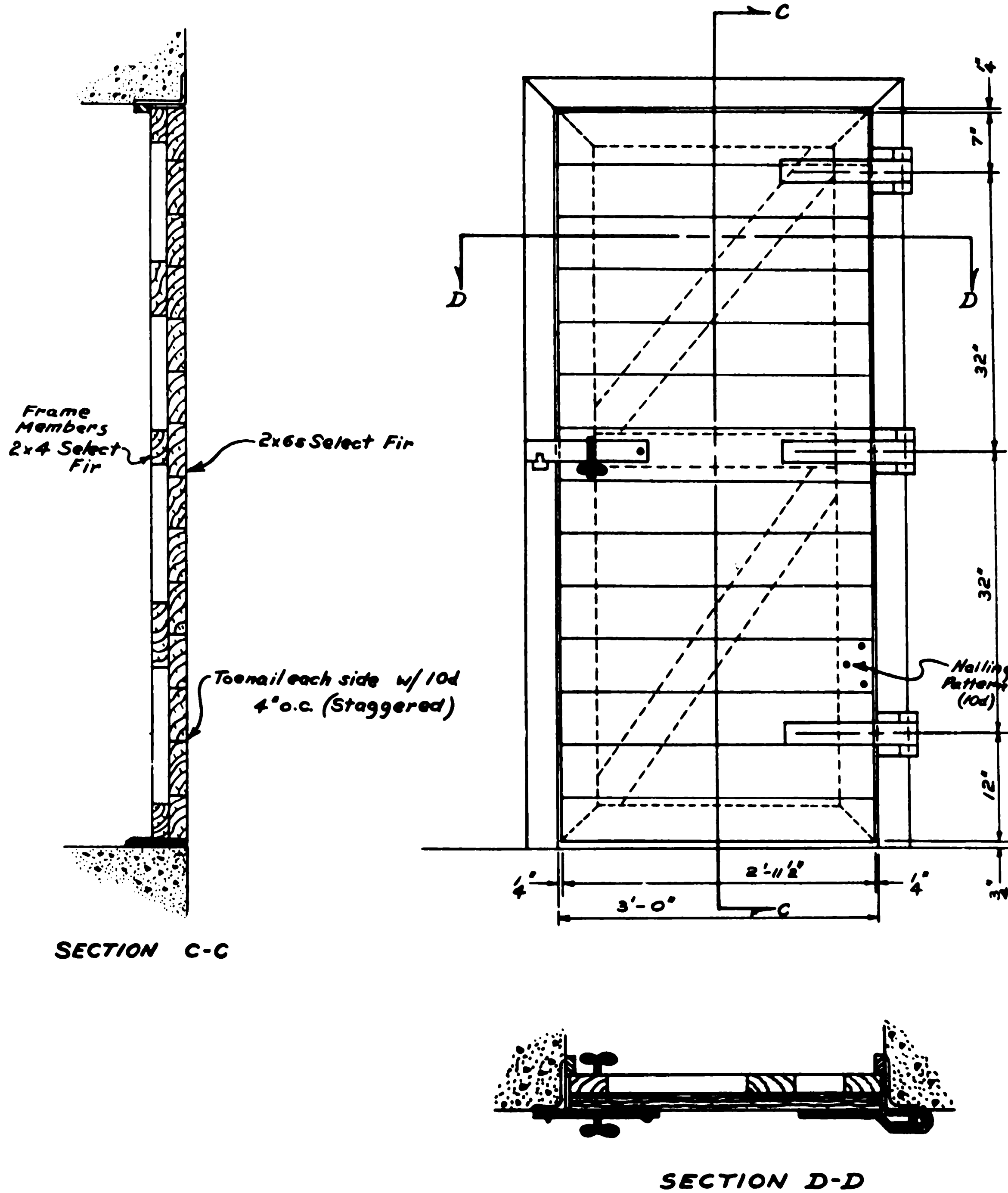

Fig. 5—Wood-plank door detail.

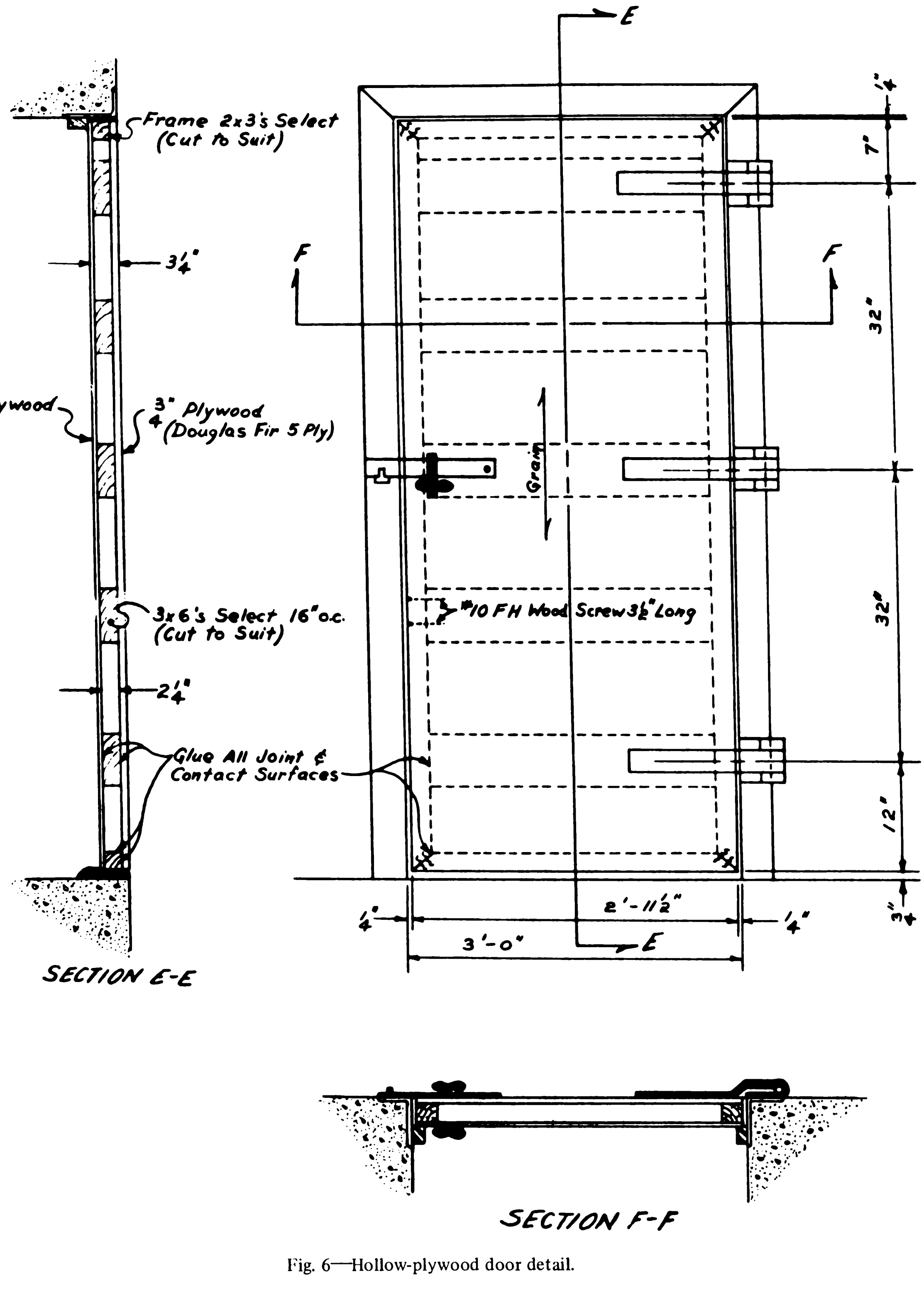

Fig. 6—Hollow-plywood door detail.

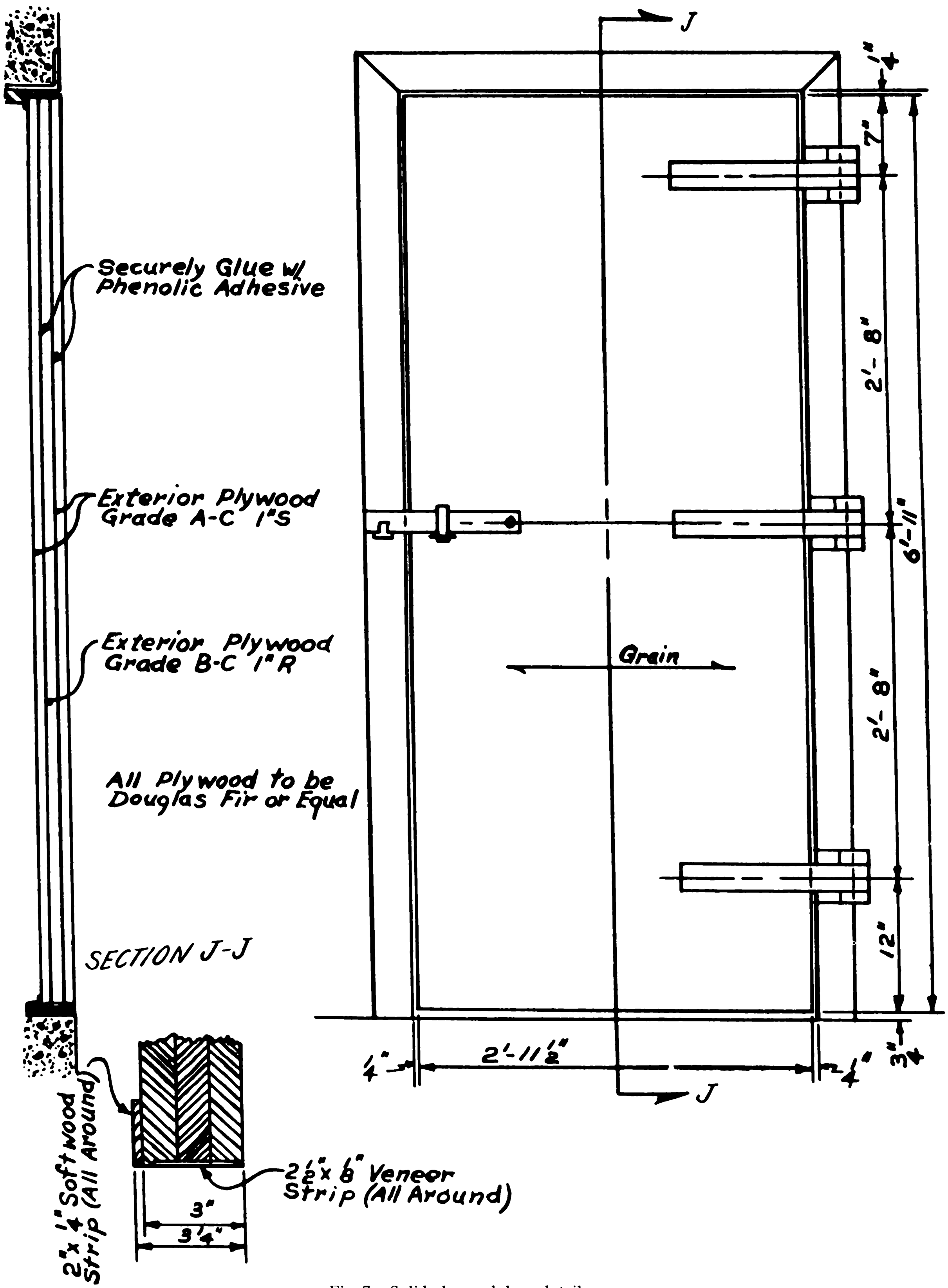

Fig. 7—Solid-plywood door detail.

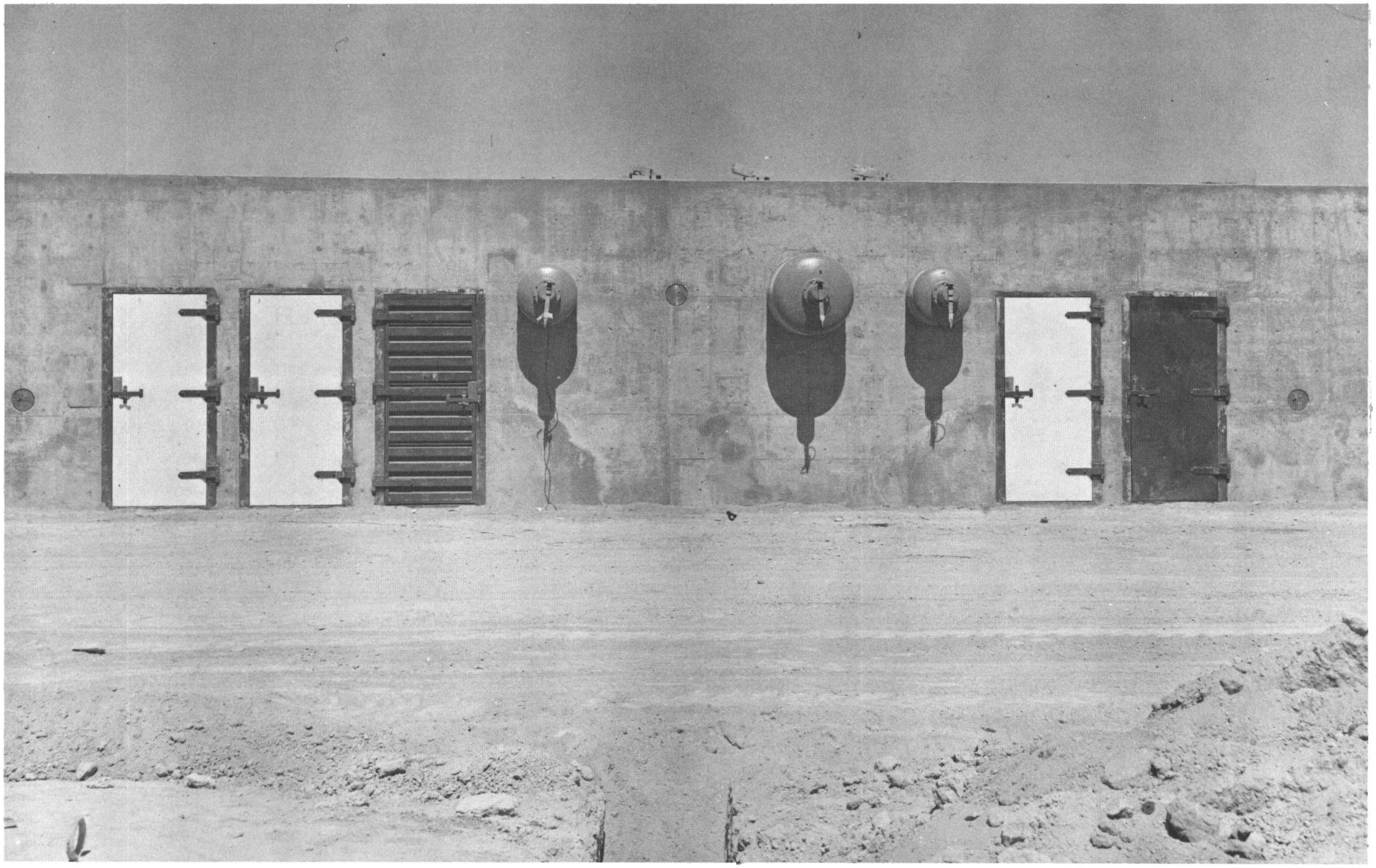

Fig. 8—Typical cell closures. Doors, from left: solid plywood, wood plank, cellular steel, hollow plywood, and steel plate.

SUMMARY 26

TEST AND EVALUATION OF ANTIBLAST VALVES FOR PROTECTIVE VENTILATING SYSTEMS

(Report ITR-1460, Operation Plumbbob, Project 31.5, same title, by F. C. Allen, A. M. Hatch, D. E. Keyt, and D. P. Rohrer, Federal Civil Defense Administration, Washington, D. C., Jan. 20, 1959.)

OBJECTIVES AND SCOPE

Ventilating-air intake and exhaust openings are vulnerable parts of most blast-resistant structures. They must be closed before, or very soon after, the arrival of the shock wave from a destructive explosion if the protective capabilities of the structure are to be realized. Three sizes of poppet-type antiblast valves were designed and fabricated for test purposes by Arthur D. Little, Inc., under contract with the Federal Civil Defense Administration (FCDA). Four 24-in. and five 16-in. valves designed to operate with overpressures up to 50 psi and two 12-in. valves designed to operate with overpressures up to 100 psi were tested.

One objective of this test was to determine the operating characteristics and effectiveness of these prototype antiblast valves when operated under nuclear blast conditions. It was desired to measure the closure times and pressure rises when the valves were closed by shock-wave pressures of 3 to 100 psig. A further objective was to determine the response of a remotely triggered valve system operated by compressed air.

The eleven prototype antiblast valves mounted to simulate shelter protection were installed for test at the Nevada Test Site. The test shot was an above-nominal nuclear weapon detonated on June 24, 1957. The valves were placed in areas of predicted side-on blast pressures as shown in Fig. 1.

TEST VALVES, INSTRUMENTATION, AND TEST PROCEDURE

Design features of the valves are shown in Fig. 2, a cutaway view based upon the proportions of the 16-in. valve. Table 1 lists the salient features of the prototype valves.

Six valves were mounted vertically on the cover slabs of underground pipe cells (Fig. 3): one of each size at the 7.5-psi range, a 16- and a 24-in. valve at the 50-psi range, and a 12-in. valve at the 100-psi range. The other five valves were mounted horizontally on the concrete walls of test cells (Fig. 4): two 16- and one 24-in. at the 7-psi range and one 16- and one 24-in. at the 3.5-psi range. One of the 16-in.valves at the 7-psi range had a pneumatic attachment (Fig. 5) triggered by the light flash from the fireball that closed the valve before the arrival of the shock wave. Each horizontal valve was mounted on one end of a pipe expansion chamber that extended through the wall and projected 10 ft into the test cell (Fig. 6). The pipe expansion

chambers for all horizontal valves, except the 16-in. remotely operated valve, were vented into the test cell through orifice plates.

The valves were instrumented to obtain the pressure–time measurements inside the weatherproof hood and in the test cell and the expansion chamber, as well as a position–time measurement for each valve disk. The reflected pressure–time measurements at the face of each wall upon which the horizontal valves were mounted were also obtained.

RESULTS

All valves closed under blast conditions, reopened after the pressure wave passed, and were in operating condition when inspected after the test. The recorded pressure data are summarized in Table 2.

Peak pressures recorded in the chambers to which the valves were attached were somewhat inconsistent. Peaks in underground pipe cells were under 5 psi except for the 24-in. valve installation at the 50-psi range where 16.9 psi was indicated. Peaks in the horizontal chambers were somewhat higher than expected, and the pressure wave was of short duration, i.e., about 75 msec.

There was no apparent damage to any of the valves other than a partial discoloration and charring of the paint finish caused by thermal radiation. There was no obvious mechanical damage to the valves at the 50- or the 100-psi range except that the expendable insect screens were demolished as predicted.

In some of the valves a slight bounce of the valve disk occurred at closing. In nearly all cases bouncing also occurred on opening. The bouncing was not excessive and had no adverse effect on the operation or integrity of the valve.

The valve that was actuated by light began to close about 90 msec after time zero and was fully closed in 140 msec. The pressure wave reached this valve approximately 1.8 sec after the valve had closed. The pressure in the closed expansion chamber that was connected to this valve showed no rise.

CONCLUSIONS AND RECOMMENDATIONS

The valves provided blast protection generally in accordance with design requirements. They withstood conditions more severe than maximum design conditions and were in operating condition after the test. The light-actuated valve performed satisfactorily; it completely eliminated blast-pressure effects in the chamber to which it was attached.

Antiblast valves of the test prototype design would be suitable for use as components in the ventilating systems of protective structures, provided expansion chambers with sufficient volume to limit the interior pressure rise are used in conjunction with the valves. Valves that close before the arrival of the shock wave are to be recommended if an adequate expansion chamber cannot be provided and might be justifiable in any critical situation. On the basis of the test data, several design modifications should be considered; they are as follows:

1. Decrease the closing time, if practicable, by reducing the mass of moving parts, by providing additional support for a lighter disk in the closed position, or by revising the valve proportions without materially affecting normal flow resistance.
2. Provide a means of holding the valve in the open position which will create less retarding force at closure than an axially loaded coil spring in compression.
3. Design a more compact remotely operating attachment that retains the desirable quality of not interfering with the pressure-sensitive operation of the valve.
4. Delete the instrument housing on top of the valve hood, but retain the central hole for inspection purposes. Provide a cover plate for the opening.
5. Consideration should be given to the design of additional sizes and types of valves, including at least one valve for a lower pressure rating.

Table 1—PHYSICAL DATA ON PROTOTYPE VALVES

Feature	Nominal size valve 12 in.	16 in.	24 in.
Rated capacity, cfm	600	1200	2500
Design overpressure, psi	100	50	50
Diameter of valve body, in.	20.5	23.5	32
Height of valve body and hood above flange face, in.	17.06	21.44	28.56
Projection of stem below flange face, valve closed, in.	10.12	11	18.38
Diameter of disk, in.	13	16	22
Diameter of hub, in.	2.5	2.5	4
Outside diameter of stem, in.	1.5	1.5	2.5
Inside diameter of stem, in.	1	1	1.5
Diameter of seat opening, in.	10.5	13.8	20
Disk travel distance, in.	1.5	2.38	3.63
Diameter of bolt circle, in.	17.75	21.25	29.5
Number of stud bolts	8	8	10
Diameter of stud bolts, in.	1.125	1	1.25
Weight of valve disk, lb	18	26	64
Weight of moving parts, lb	23	31	91
Shipping weight on skids, lb	600	760	1620
Area of screen, sq ft	1.7	2.6	4.9
Minimum spring preload, lb	13	22	26
Minimum throat area, sq in.	52	108	228

Table 2—SUMMARY OF DATA FROM POSITION–TIME AND PRESSURE–TIME RECORDING INSTRUMENTS

Predicted pressure, psig	Actual pressure, psig	Nominal valve size, in.	Mounting position (horizontal or vertical)	Closure time, msec	Total time in operation, msec	Peak pressure in hood, psig	Pressure in chamber, psig
100	112	12	V	*	*	284	*
50	63	16	V	31	1014	118	4.6
50	63	24	V	58	†	122	16.9
7.5	8	12	V	23	847	8.9	2.7
7.5	8	16	V	35	737	5.9	4.4
7.5	8	24	V	53	589	6.8	2.0
7	7.9	16	H	35	749	16.5	8.1
7	7.9	16	H	51	‡	21.8	0
7	7.9	24	H	58	770	16.2	7.2
3.5	3.9	16	H	78	775	4.9	4.6
3.5	3.9	24	H	147	846	8.2	4.4

	7-psi range, psi	3.5-psi range, psi
Peak side-on pressure outside test cell	7.9	3.9
Peak reflected pressure outside test cell	19.2	8.8
Peak overpressure inside test cell	0.49	0.52

*Record lost.

†Opened fully at 264 msec, closed, then reopened at 1044 msec.

‡Remotely operated valve stayed closed.

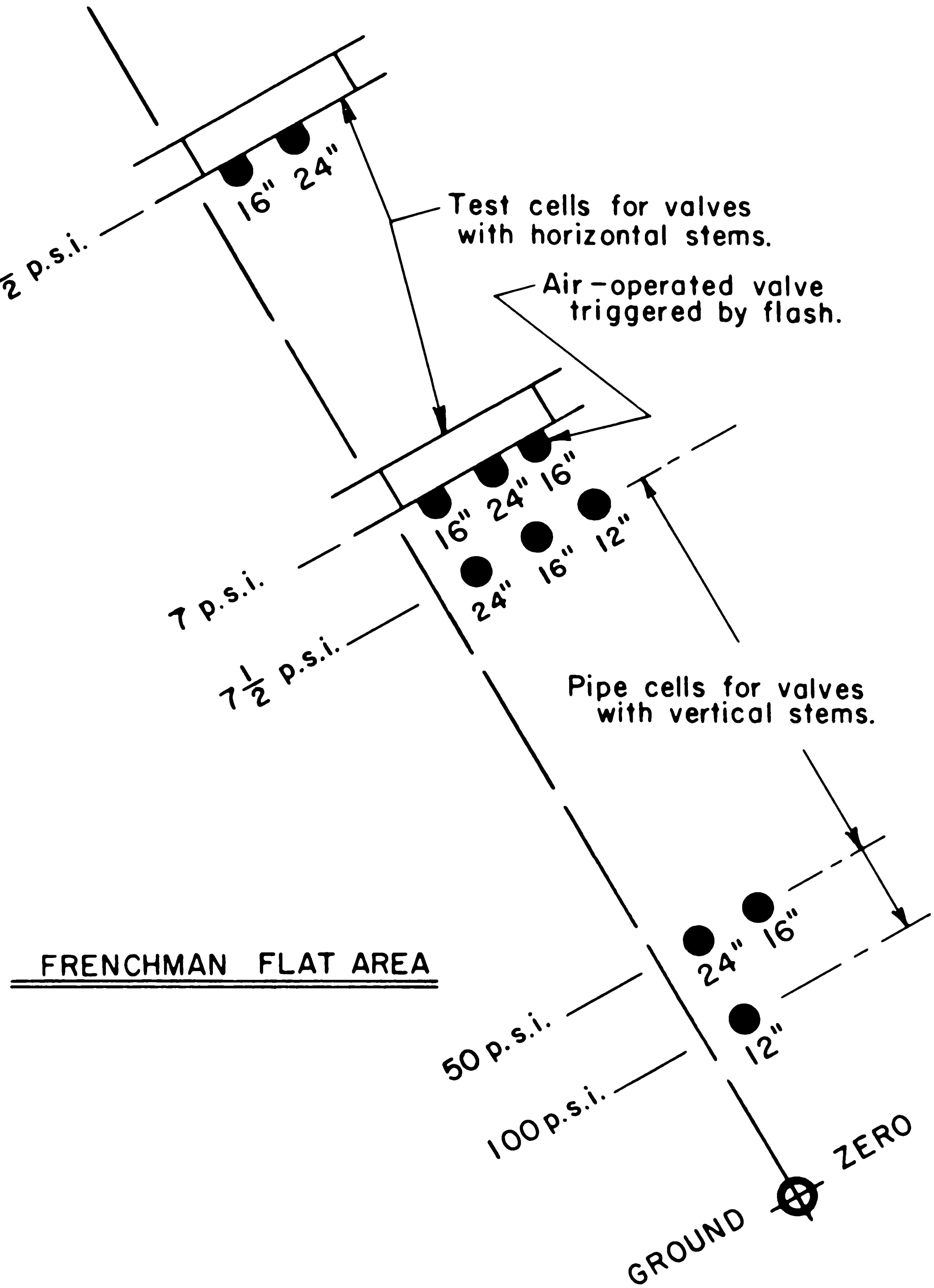

Fig. 1—Diagram showing locations of test valves.

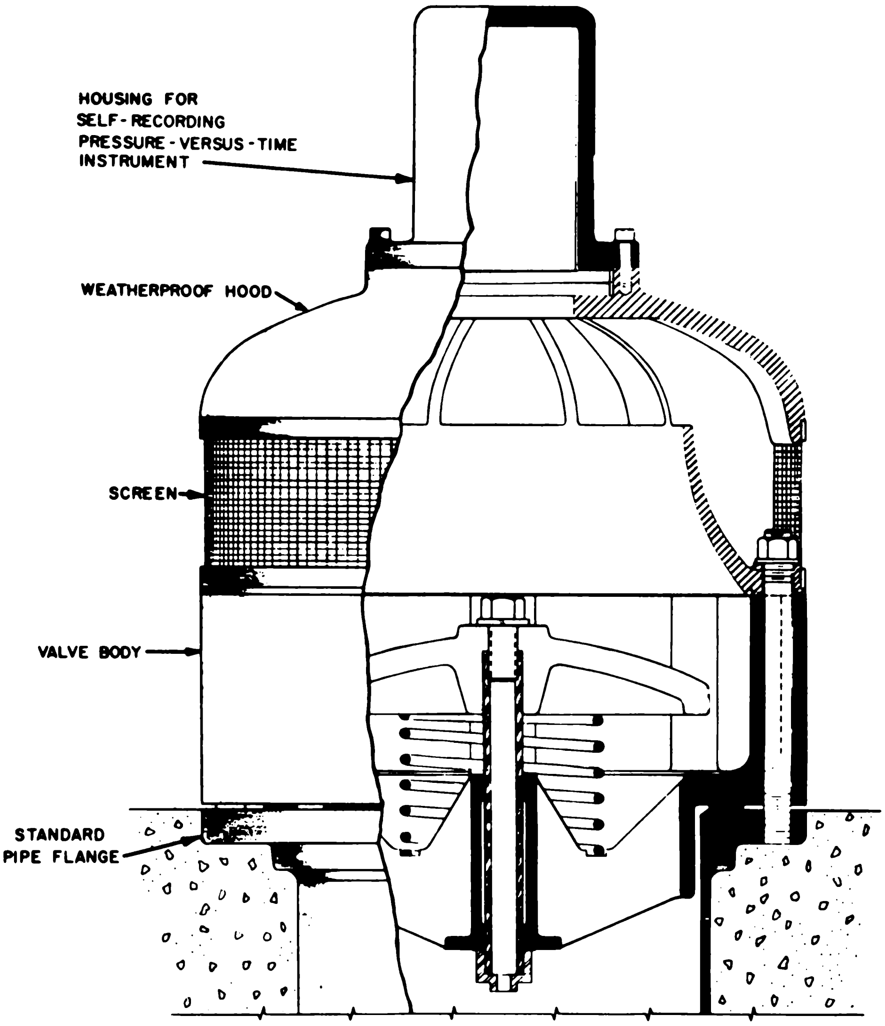

Fig. 2—Cutaway view of prototype antiblast valve.

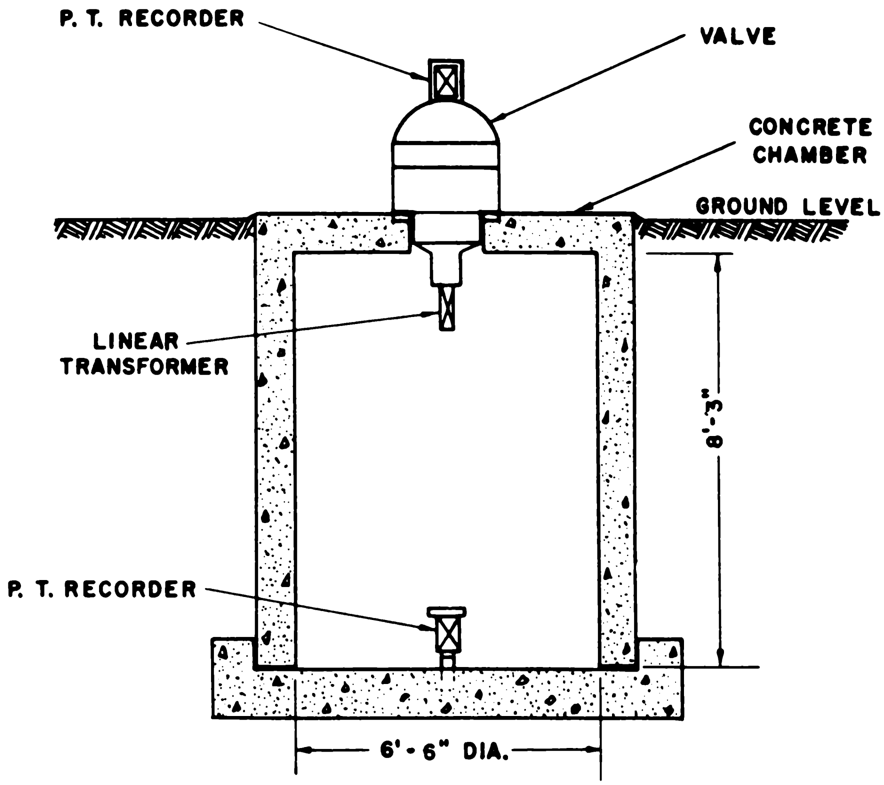

Fig. 3—Mounting of vertical antiblast valves for test.

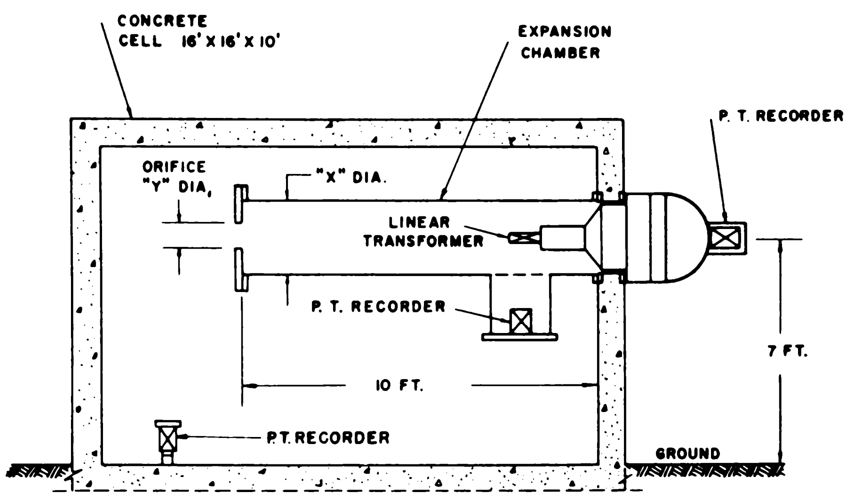

VALVE SIZE	CHAMBER INSIDE DIA. "X"	ORIFICE DIA. "Y"
16"	$15\frac{1}{2}$"	$7\frac{1}{2}$"
24"	$23\frac{1}{2}$"	$11\frac{1}{4}$"

NOTE: FOR THE AIR CYLINDER OPERATED VALVE, THE CHAMBER WAS CLOSED. (NO ORIFICE)

Fig. 4—Mounting of horizontal antiblast valves for test.

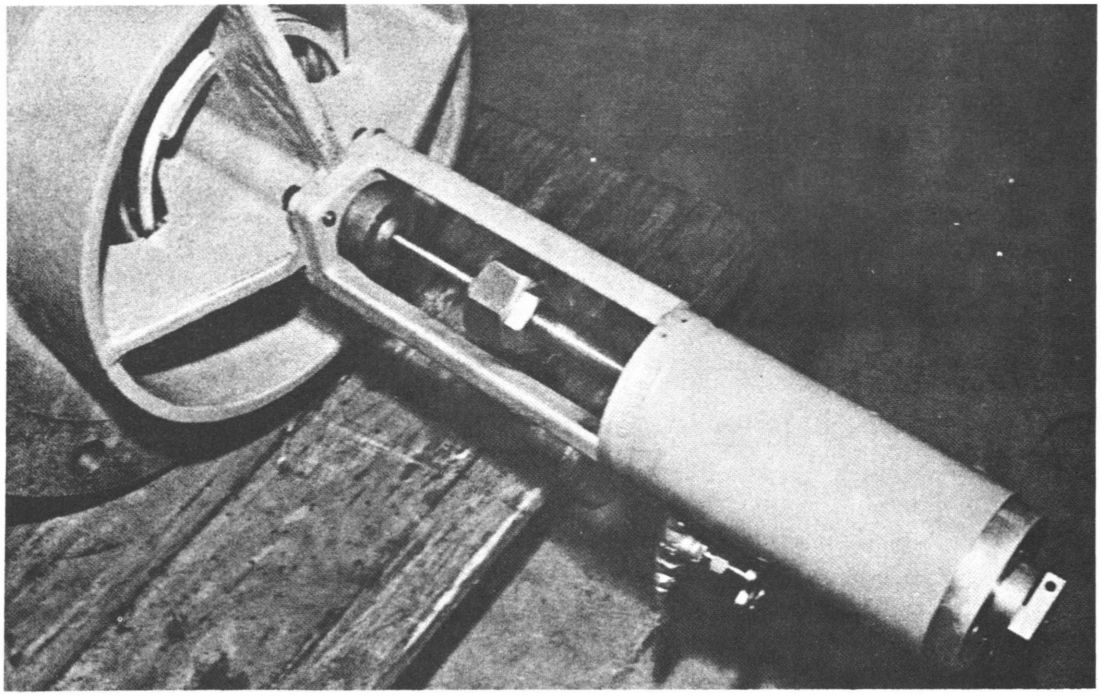

Fig. 5—View of 16-in. prototype valve with pneumatic cylinder attached.

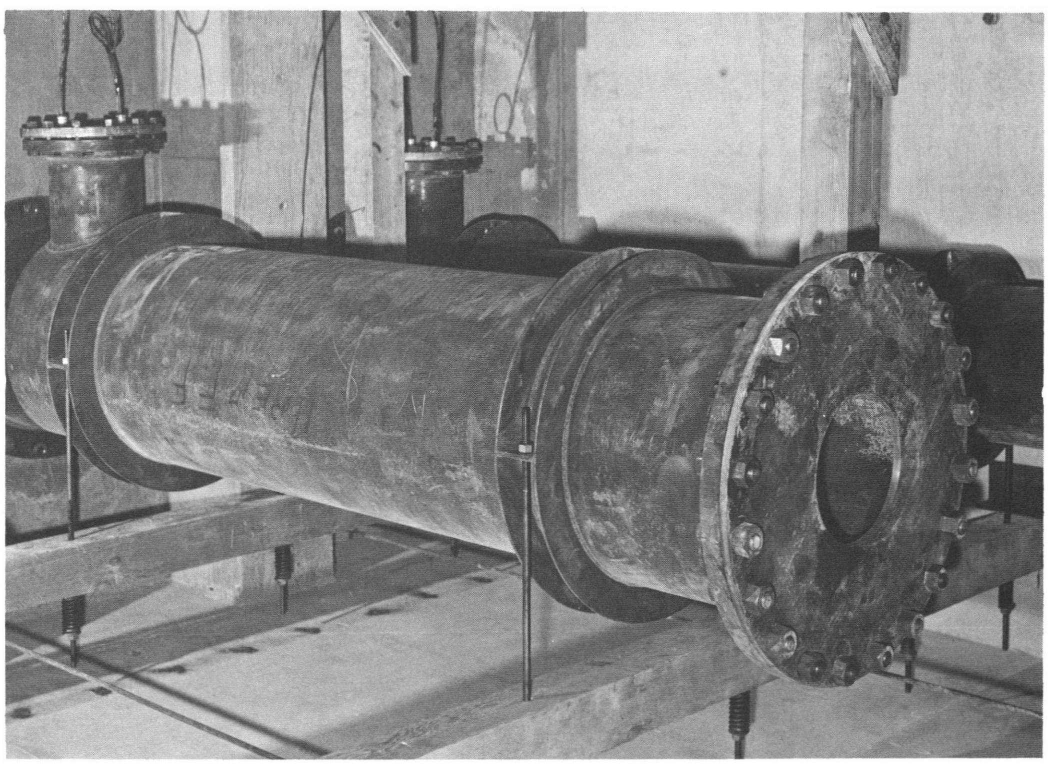

Fig. 6—Expansion chamber for horizontal valves at 7-psi range.

SUMMARY 27

BLAST BIOLOGY – A STUDY OF THE PRIMARY AND TERTIARY EFFECTS OF BLAST IN OPEN UNDERGROUND PROTECTIVE SHELTERS

(Report WT-1467, Operation Plumbbob, Project 33.1; same title, by D. R. Richmond, et al., Lovelace Foundation for Medical Education and Research, Albuquerque, N. Mex., June 30, 1959.)

OBJECTIVE

It was the purpose of Project 33.1 to expose animals to nuclear detonations in open underground shelters with the objective of assessing the total environment within the shelter, i.e., blast, thermal radiation, ionizing radiation, and dust.

SHELTER DESIGN AND EXPERIMENTAL METHOD

The two shelters used in these experiments were of similar construction with the same orientation. Each structure was located at the same distance from Ground Zero (GZ); each, however, was subjected to a different detonation. The structure used in shot 1 was designated 8001 and that used in shot 2, 8002. These two shelters had been used previously in Operation Teapot and were designated 4-34.3b-1 and 1-34.3b-2; design information is contained in Summary 12. Shot 1 (Kepler) was 10 kt and shot 2 (Galileo) was 11 kt (ref. ENW, p. 675).

Each shelter, located 5 ft below the surface, was entered by an L-shaped flight of stairs. Inside were two rooms, each 12 x 12 x 8 ft, separated by a reinforced-concrete partition in which was mounted a heavy steel bulkhead-type door. The outer room with stairwell access was termed a fast-fill chamber since, by virtue of its position and opening to the surface, it would be subjected to the most rapid pressure change following the detonation.

The inner room, which was entered through the partition door, was termed the slow-fill chamber because the blast wave entered through an orifice placed over the open escape hatch. The partition door was tightly sealed during the test.

On shot 1 an aerodynamic mound constructed above the 3-ft-square escape hatch leading into the slow-fill chamber of structure 8001 was evaluated. The inner diameter of the mound, or the effective metering orifice, was 36 in. The orifice consisted of a corrugated-metal pipe 3 ft in diameter welded to a 1-in.-thick steel plate in which a 36-in. orifice had been cut. For shot 2 a similar aerodynamic mound was

constructed over the escape hatch; in addition, a ½-in.-thick sieve plate was bolted over its top. This plate was a composite of four ⅛-in.-thick plates perforated by matching ¼-in.-diameter holes staggered on ½-in. centers. The sieve plate contained 23% open area or 1.63 sq ft.

A plan and section of the shelters and the locations of the various gauges and animals are shown in Figs. 1 to 4. Dogs, pigs, and rabbits were individually harnessed or caged. The guinea-pig and mouse cages held 5 and 20 animals, respectively, compartmentalized to prevent huddling of the animals.

The baffles shown in Figs. 3 and 4 near the entrances were ½-in. steel plate for shot 1 and woven wire screen, gauge 4, with four holes per sq in. for shot 2.

Tables 1 and 2 show the numbering system and the locations of animals for both shots.

RESULTS

The incident overpressure outside the shelter on shot 1 was 42.1 psi with a positive duration of 220 msec; on shot 2 it was 39.2 psi with 255-msec duration.

Overpressure and dynamic-pressure measurements obtained inside the shelters are shown in Table 3, and ionizing radiation measurements are shown in Figs. 5 and 6. Air-temperature measurements were unsuccessful.

In neither shot did the aerodynamic mound attenuate the blast wave any more than was found during past tests in which the same chambers filled through simple inlets of comparable diameter.

The solid baffle protected a dog from a dynamic pressure of 10.5 psi; the other animal at that location, unshielded, was seriously injured from translation. The screen baffle subjected to a dynamic pressure of 2 psi did not adequately shield the animal behind it.

No evidence of radiation injury was observed in the 110 mice and 2 dogs saved for 30 days following their exposure to about 5 r of mixed gamma and neutron radiation on shot 1.

Of the animals saved for radiation effects following shot 2, the mortality observed was as follows: 1/2 swine, 1/14 rabbits, and 16/16 guinea pigs. Only gamma-radiation measurements were successfully taken, and the animal mortality indicated that the total accumulated dose probably was higher than the recorded gamma dose by a factor of 6 or 7.

No symptoms of dust suffocation or accumulations of dust in the respiratory passages were noted following the two shots even though a considerable amount of dust was observed in the air inside the shelters at recovery about 3 hr postshot.

Pathological findings are tabulated in Tables 4 to 7.

DISCUSSION

Blast Effects

For this discussion the biological effects of blast have been divided into three parts:

1. Primary effects, those associated with the application and/or the subsequent release of pressure, or a combination of these, upon an organism.

2. Secondary effects, those resulting as a consequence of the biological target being struck with objects set in motion by or as a consequence of the blast.

3. Tertiary effects, those injuries obtained as a result of the animal being translated by the blast wave.

Primary Blast Effects—In general, the pressure conditions to which animals were exposed in the present study were less severe than the conditions necessary for small-animal mortality. Although the animals were exposed to a wide range of peak pressures, the majority of them were exposed to peak pressures below 30 psi, and few fatalities occurred. Consequently only tolerable conditions to the pressure wave forms encountered were documented, and neither the tolerance limits nor the significant physical parameters are known. Fatal conditions might well be only slightly higher; and, since blast mortality curves have been found to be very steep (a relatively small increase in pressure over threshold conditions covers the range from 0% mortality to 100%), one must be careful not to underestimate the primary blast hazard.

Secondary Blast Effects—Since such precautionary steps as firmly securing all objects that might become potential missiles were taken to prevent these effects within the shelters, none were noted.

Tertiary Blast Effects—The orientation of an animal, its velocity at impact, and the type of impact surface are undoubtedly of primary importance in the pathology encountered in tertiary blast effects. Inside open shelters translation is an important problem, particularly just inside entryways. Aside from eardrum rupture, primary blast effects probably would not be found until conditions were above those where, for unrestrained animals, fatal conditions due to translation exist. This is no doubt particularly true for exposures in the open or inside heavy industrial buildings that might not be completely destroyed by blast.

Thermal Radiation

It was not known from field experiments at the time of the original report the mechanism by which animals inside a shelter, out of the direct line of sight from the explosion, are burned. A later study concluded that hot winds and/or hot wind-borne dust are considered to be the most likely agents.

Table 1—NUMBERING SYSTEM AND LOCATION OF ANIMALS PLACED IN SHELTER 8001, SHOT 1

Species	Location	Number of animals	Animal No.*
Dogs	Wall 1	2	K-1, 2
	Wall 2	2	3, 4
	Wall 3	3	5, 6, 7
	Wall 4	2	8, 9
Rabbits	Wall 2, below bench	4	R-1, 2, 3, 4
	Wall 3, below bench	6	5, 6, 7, 8, 9, 10
	Wall 3, shelf	7	12, 13, 14, 15, 16, 17, 18
	Corner wall 3 and 4, on camera mount	3	11, 19, 20
Guinea pigs	Wall 1	5	GP-1, 1-5
	Wall 2	5	2, 1-5
	Wall 2	5	2a, 1-5
	Wall 3	5	3, 1-5
	Wall 4	5	4, 1-5
	Ceiling 5	5	5, 1-5
	Floor 6	5	6, 1-5
Mice	Wall 1	20	M-1
	Wall 2	20	2
	Wall 3	20	3
	Wall 4	20	4
	Ceiling 5	20	5
	Floor 6	20	6
Dogs	Wall 7	1	K-10
	Wall 8	1	11
	Wall 9	1	12
	Wall 10	1	13
	On bench, center of room	1	14
Rabbits	None		
Guinea pigs	Wall 7	5	GP-7, 1-5
	Wall 8	5	8, 1-5
	Wall 9	5	9, 1-5
	Wall 10	5	10, 1-5
	Ceiling 11	5	11, 1-5
Mice	Wall 7	20	M-7
	Wall 8	20	8
	Wall 9	20	9
	Wall 10	20	10
	Ceiling 11	20	11

*Mice are not individually numbered.

Table 2—NUMBERING SYSTEM AND LOCATION OF ANIMALS PLACED IN SHELTER 8002, SHOT 2

Species	Location	Number of animals	Animal No.*
Dogs	Wall 1	2	G-1, 2
	Wall 2	1	3
	Wall 3	3	4, 5, 6
	Wall 4	2	7, 8
Rabbits	Wall 3, shelf	10	R-1, 2, 3, 4, 5, 6, 7, 8, 9, 10
Guinea pigs	Wall 1	5	GP-1, 1-5
	Wall 2	5	2, 1-5
	Wall 3	5	3, 1-5
	Wall 4	5	4, 1-5
Mice	Wall 1	20	M-1
	Wall 2	20	2
	Wall 3	20	3
	Wall 4	20	4
Dogs	Wall 8	1	G-9
	Wall 10	1	10
Rabbits	Wall 8, shelf	10	R-11, 12, 13, 14, 15, 16 17, 18, 19, 20
	On bench, center of room	10	21, 22, 23, 24, 25, 26, 27, 28, 29, 30
Guinea pigs	Wall 7	5	GP-7, 1-5
	Wall 8	5	8, 1-5
	Wall 9	5	9, 1-5
	Wall 10	5	10, 1-5
Mice	Wall 7	20	M-7
	Wall 8	20	8
	Wall 9	20	9
	Wall 10	20	10

*Mice are not individually numbered.

Table 3—PARAMETERS OF THE BLAST WAVE INSIDE SHELTERS 8001 and 8002

Gauge location	Peak over-pressure, psi	Time to peak pressure, msec	Duration of positive phase, msec	Peak negative pressure, psi	Time to peak negative pressure, msec	Duration of entire wave, sec
			Structure 8001			
Fast-fill						
Wall 1	25.7	51	292	−3.4	406	2.32
Wall 2	27.0	45	240	−3.5	354	2.71
Wall 3	23.8	50	245	−6.3	399	2.66
Wall 4	25.6	66	297	−3.2	420	2.60
Average	25.5	53	269	−4.09	394	2.58
Q_1*†	10.5					
Slow-fill						
Wall 8	9.0	119	330	−3.01	472	2.95
Wall 10†	10.0					
Average	9.5					
			Structure 8002			
Fast-fill						
Wall 1	30.4	68	305	−3.5	464	3.44
Wall 2‡	30.2	59				
Wall 3	30.5	68	294	−3.3	403	
Wall 4†	30.0					
Average	30.3	65	300			
Q_2§	2.0					
Slow-fill						
Wall 8	4.1	194	517	−2.3	1097	3.42
Wall 10	4.1	212	506	−2.3	1254	3.19
Average	4.1	203	512	−2.3	1176	3.31

*Located 5 ft from main doorway, 5 ft above floor, and 2 ft from wall 1 (parallel with wall).
†Peak pressure only.
‡Peak pressure and time only.
§Located 7 ft from main doorway, 5 ft above floor, and 2 ft from wall 1 (parallel with wall).

Table 4—PATHOLOGICAL FINDINGS FOR SHELTER 8001: DOGS, RABBITS, AND GUINEA PIGS

Animal No.	Body weight*	Lung hemorrhage	Lung weight, % of body weight	Eardrum rupture† Right	Eardrum rupture† Left	Remarks
			Dogs			
Fast-fill						
K-1	15.4	Slight†	1.01	x	x	Translated and violently impacted; sustained a fractured lumbar vertebra and associated severed spinal cord; ruptured spleen and liver (massive hemoperitoneum); disrupted lining of urinary bladder; laceration of the anterior wall of I. V. septum with hemopericardium
K-2	17.3	None		–	–	
K-3	17.7	Slight‡		NR	NR	Two hemorrhagic areas in lung—measured 1½ X 1½ cm
K-4	20.4	None		–	x	
K-5	16.8	None‡		x	x	Hemorrhagic right frontal sinus
K-6	14.1	None‡	1.11	x	–	
K-7	15.4	None	0.82	x	x	
K-8	17.7			–	–	Not sacrificed for immediate blast effects
K-9	16.8	None	1.11	–	–	A few petechiae found microscopically in lung parenchyma
	16.8 ± 0.6§		1.01 ±0.07§			
Slow-fill						
K-10	16.8	None	1.15	–	–	
K-11	13.2	None	1.04	–	–	
K-12	14.1	None	1.06	–	–	
K-13	15.9	None	1.13	–	–	
K-14	16.8			–	–	Not sacrificed for immediate blast effects
	15.4 ± 0.7§		1.10 ±0.03§			
			Rabbits			
Fast-fill						
R-1	2243	Slight	0.49	x	x	
R-2	2238	Slight	0.45	x	x	
R-3	2420	None	0.45	x	x	
R-4	2758	None	0.47	x	x	
R-5	2450	None‡	0.45	x	x	
R-6	2117	None	0.47	x	x	
R-7	2473	None‡	0.48	x	x	
R-8	1788	None	0.53	x	x	
R-9	2439	None	0.47	x	x	
R-10	1847	None‡	0.60	x	x	Slight emphysema
R-11	2253	None	0.44	x	x	
R-12	2123	None	0.52	x	x	
R-13	2151	Slight‡	0.46	x	x	Emphysema
R-14	2524	Slight	0.52	x	x	
R-15	2415	Slight	0.62	x	x	
R-16	2300	None	0.43	x	x	
R-17	3870	None	0.28	x	x	

(Table continued on p. 280.)

Table 4—(Continued)

Animal No.	Body weight*	Lung hemorrhage	Lung weight, % of body weight	Eardrum rupture† Right	Left	Remarks
R-18	2321	None	0.43	x	x	
R-19	2149	None	0.70	x	x	
R-20	2192	None	0.46	x	–	
	2354 ± 94.1 §		0.49 ± 0.02 §			
			Guinea Pigs			
Fast-fill						
GP-1-1	380	None	0.89	x	x	Pneumonitis
2	416	None‡	1.47	x	x	Pneumonitis‡
3	527	None	0.70	x	x	Petechial hemorrhage and emphysema
4	385	None‡	1.01	NR	NR	Pneumonitis‡
5	437	None	1.97	x	x	Pneumonitis
GP-2-1	487	None	0.86	x	x	Pneumonitis
2	455	Slight	1.60	x	x	
3	505	Slight‡	1.46	NR	NR	Pneumonitis and bronchitis
4	472	None	0.70	x	x	Pneumonitis
5	471	None	0.83	x	x	Pneumonitis
GP-2a-1	441	None	0.86	x	x	
2	448	None	0.85	x	x	
3	396	None	0.93	x	x	
4	545	None	0.82	x	x	
5	461	Moderate	1.21	x	x	
GP-3-1	396	Moderate‡	2.68	x	x	Dead on recovery; ruptured stomach and bronchitis
2	470	None	0.91	x	x	
3	448	Slight	1.63	x	x	Pneumonitis
4	413	Slight	0.97	NR	NR	
5	420	None	0.98	NR	NR	
GP-4-1	319	None	1.00	x	x	Pneumonitis
2	606	None	0.89	NR	NR	Pneumonitis
3	494	None	1.07	NR	NR	Pneumonitis
4	510	None	1.08	x	x	Pneumonitis
5	586	None	0.63	x	x	
GP-5-1	403	None	0.64	x	x	
2	423	None‡	0.80	x	x	
3	386	None‡	0.88	x	x	
4	338	None‡	1.15	x	x	Pneumonitis
5	328	None‡	1.92	x	x	
GP-6-1	623	None	0.83	x	x	
2	586	None	1.02	NR	NR	Pneumonitis
3	314	None	1.59	x	x	Dead on recovery
4	513	None	0.88	NR	NR	
5	452	None	1.15	NR	NR	
	453 ± 13 §		1.11 ± 0.07 §			
Slow-fill						
GP-7-1	382	None	1.12	x	x	Pneumonitis
2	439	None	0.86	x	x	Pneumonitis
3	508	None	1.10	–	–	
4	500	None‡	0.90	x	x	
5	590	None	0.85	–	x	

Table 4—(Continued)

Animal No.	Body weight*	Lung hemorrhage	Lung weight, % of body weight	Eardrum rupture† Right	Left	Remarks
GP-8-1	434	None	0.83	x	x	
2	418	None	1.44	x	x	
3	497	None‡	0.86	–	–	Bronchitis‡
4	608	None‡	0.76	x	x	
5	541	None	0.92	x	x	
GP-9-1	509	None	1.16	x	x	Pneumonitis
2	382	None	1.10	x	x	
3	497	None	0.66	NR	x	
4	464	None	1.79	x	x	Pneumonitis
5	437	None	1.17	x	x	
GP-10-1	557	None‡	0.65	NR	NR	
2	547	None	0.73	x	x	
3	466	None	0.79	x	x	
4	624	None	0.90	NR	NR	
5	403	None‡	1.24	x	x	
GP-11-1	370	None	2.24	–	x	
2	398	None	1.00	x	x	
3	340	None	1.47	x	x	Pneumonitis
4	354	Questionable	1.47	x	x	Pneumonitis
5	461	None	1.50	x	NR	
	469 ±16§		1.10 ±0.08§			

*Body weights are in kilograms for dogs and in grams for rabbits and guinea pigs.
†x, –, and NR indicate that the eardrums were ruptured, intact, or not readable, respectively.
‡Findings verified histologically.
§Mean and standard error of the mean.

Table 5—PATHOLOGICAL FINDINGS FOR SHELTER 8001: MICE*

Cage No.	Mortality	Lung hemorrhage
	Fast-fill	
1†	1/10	0/10
2	2/10	10/10
3	0/10	0/10
4	0/10	2/10
5	0/10	4/10
6	0/10	0/10
	Slow-fill	
7	0/10	0/10
8	0/10	0/10
9	0/10	0/10
10	0/10	0/10
11	0/10	0/10

*No thermal effects were noted in any of the mice from shelter 8001.

†Saved 10 mice from each cage of 20 for the observation of radiation effects.

Table 6—PATHOLOGICAL FINDINGS FOR SHELTER 8002: DOGS, SWINE, RABBITS, AND GUINEA PIGS

Animal No.	Body weight*	Thermal effects	Lung hemorrhage	Lung weight, % of body weight	Eardrum rupture† Right	Left	Remarks
			Dogs				
Fast-fill							
G-1	20.4	First-degree burns over scrotum, inner thigh, under both axillae, and about the mouth; extensive singeing	None	0.91	x	x	Translated from shelf without injurious impact
G-2	19.5	Areas of erythema and singeing of hair over hindquarters	None	1.07	x	x	
G-3	20.9	None	None	1.23	x	x	
G-4	22.3	None	None (?)	1.03	x	–	Slight degree of hemorrhage nasal sinus; bilateral and petechial hemorrhage in lung found histologically
G-5	23.2	Slight singeing over entire body	None	0.98	x	–	
G-6	16.8	None	None	1.00	x	x	
G-7	21.4	None	None	1.02	x	x	
G-8	17.7	None	None	1.02	–	–	
	20.3 ± 0.8‡			1.04 ± 0.03‡			
Slow-fill							
G-9	19.5	None	None	0.92	x	–	
G-10	16.4	None	None	1.04	–	–	
	18.0 ± 1.55‡			0.98 ± 0.06‡			
			Swine				
Fast-fill							
P-1		None	None		x	–	Small area of contusion lining of small intestine
P-3		None	Slight		x	x	
P-5		Carbonized and first-degree burns on forehead and ears; hair singed over shoulders and front area of legs	Moderate		x	x	
Fast-fill							
P-7		First-degree burns; singed	Massive		x	x	Dead at recovery; hemothorax, fractured right ribs 6 to 8, punctured

Table 6—(Continued)

Animal No.	Body weight*	Thermal effects	Lung hemorrhage	Lung weight, % of body weight	Eardrum rupture† Right	Left	Remarks
							lungs, petechial hemorrhages in pancreas, adrenal fat, and small intestine; subcapsular hemorrhage in spleen
P-8		None	None		NR	NR	
Slow-fill							
P-4		None	None §		–	–	
P-6		None	None §		–	–	
P-9		None	None §		–	–	Died of radiation sickness on D+14
			Rabbits				
Fast-fill							
R-1	2950		None	0.47	–	x	
R-2	2962		None	0.68	x	–	
R-4	2700		None	0.48	x	x	
R-6	2860		None	0.42	NR	NR	
R-8	2500		Slight	0.44	–	–	
R-10	2800		Slight	0.39	x	x	
	2795 ± 71‡			0.48 ± 0.04‡			
Slow-fill							
R-12	2750		None	0.40	–	–	
R-14	2558		None	0.39	x	NR	
R-16	1626		None	0.80	–	x	
R-18	2652		None	0.45	–	–	
R-20	2805		None	0.46	–	–	
R-22	3245		None	0.34	–	–	
R-24	2723		None	0.40	–	–	
R-26	2497		None	0.44	–	–	
R-28	2918		None	0.48	–	–	
R-30	2741		None	0.55	–	–	
	2652 ± 132‡			0.47 ± 0.04‡			
			Guinea Pigs¶				
Fast-fill							
GP-1-1	464	Singed	None	0.73	x	x	
2	328	Singed	None	2.65	x	x	
3	472	Singed	None	0.80	x	x	
GP-2-1	453	Slight singeing	Slight	0.95	x	x	
2	383	Slight singeing	Slight	1.17	x	x	
3	434	Slight singeing	Slight	1.06	x	x	
GP-3-1	418	None	Slight	0.96	x	x	
2	438	None	None	0.96	x	x	
3	514	None	Slight	0.88	x	x	

(Table continued on p. 284.)

Table 6—(Continued)

Animal No.	Body weight*	Thermal effects	Lung hemorrhage	Lung weight, % of body weight	Eardrum rupture† Right	Left	Remarks
GP-4-1	497	None	Slight	0.88	x	x	
2	494	None	Slight	0.85	x	x	
3	470	None	Slight	0.98	x	x	
	447 ± 15‡			1.07 ± 0.15‡			
Slow-fill							
GP-7-1	378	None	None	1.32	–	–	
2	448	None	None	0.94	–	–	
3	451	None	None	0.93	–	–	
GP-8-1	453	None	None	0.93	–	–	
2	471	None	None	0.85	–	–	
3	460	None	None	1.00	–	–	
GP-9-1	456	None	None	1.03	–	–	
2	430	None	None	0.91	–	–	
3	483	None	None	0.72	–	–	
GP-10-1	492	None	None	0.85	–	–	
2	463	None	None	0.86	–	–	
3	437	None	None	1.12	–	–	
	452 ± 8‡			0.86 ± 0.05‡			

*Body weights are in kilograms for dogs and in grams for guinea pigs and rabbits.
†x, –, and NR indicate that the eardrums were ruptured, intact, or not readable, respectively.
‡Mean and standard error of the mean.
§Saved for observation of radiation effects.
¶There were 2 animals each saved from cages 4 and 5 for observation of radiation effects.

Table 7—PATHOLOGICAL FINDINGS FOR SHELTER 8002: MICE

Cage No.*	Mortality	Thermal effects	Lung hemorrhage
		Fast-fill	
1	14/20	20/20 burned and singed	18/20
2	1/20	9/20 singed; 2/20 burned	7/20
4	0/20	0/20	1/20
		Slow-fill	
8	0/20	0/20	0/20
10	0/20	0/20	0/20

*Saved all 20 mice from cages 3, 7, and 9 for radiation effects.

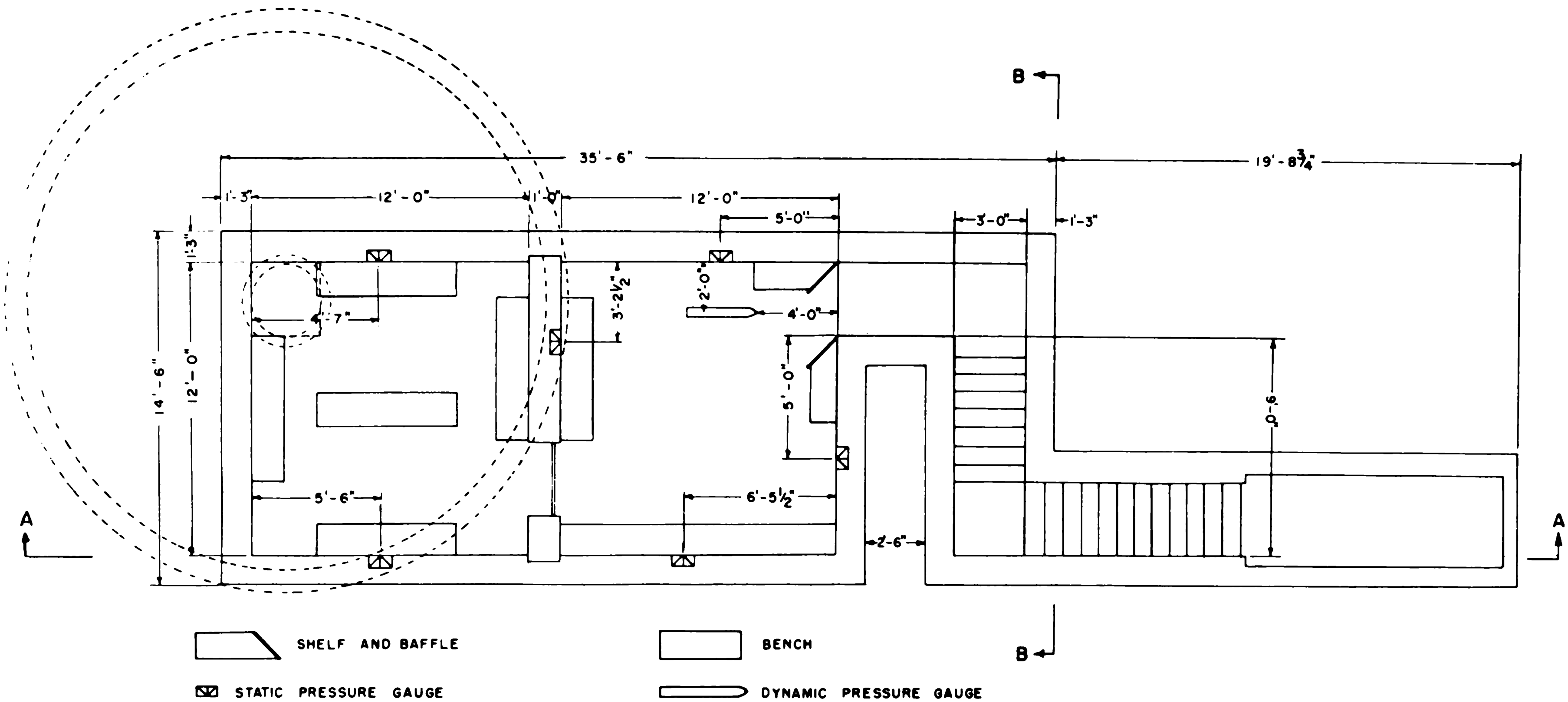

Fig. 1—Plan of underground shelter 8001.

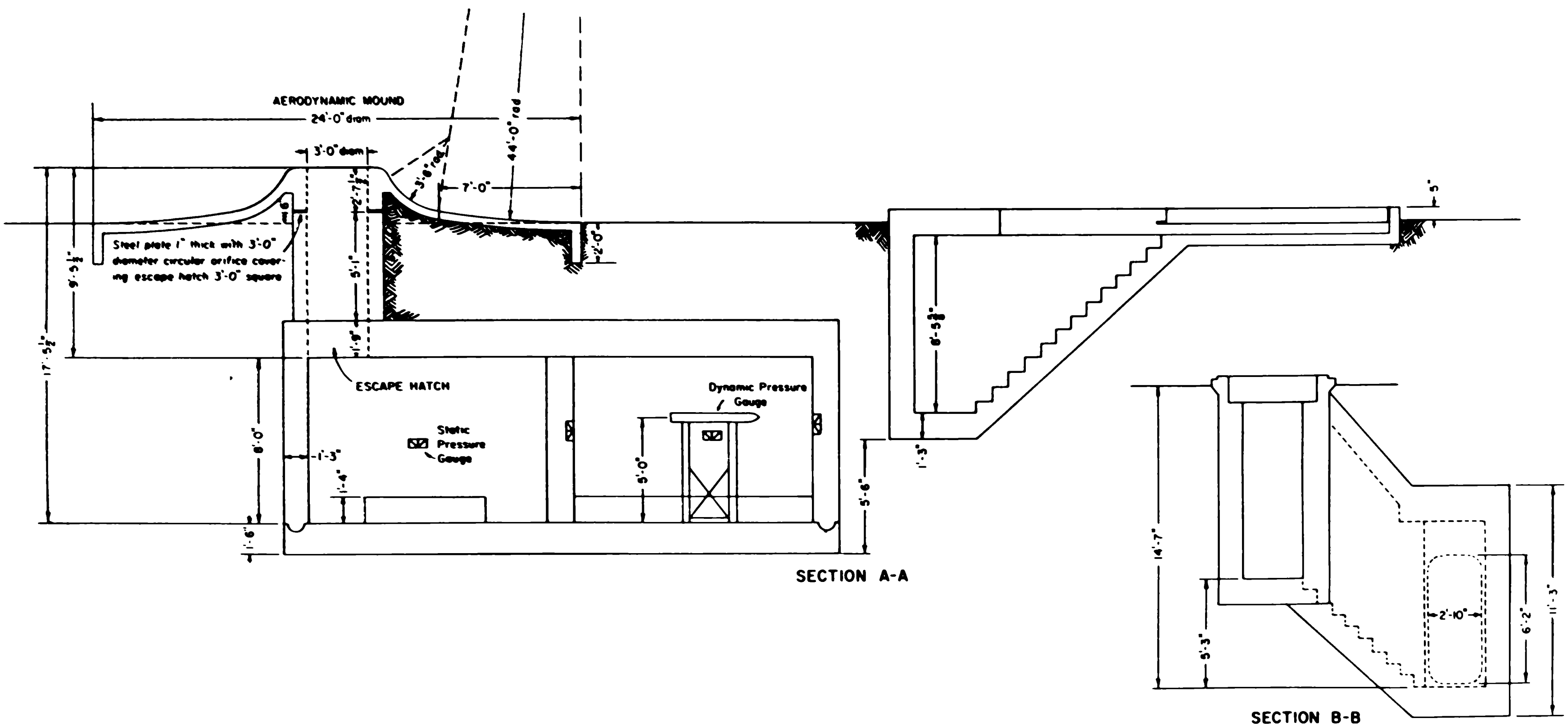

Fig. 2—Section of underground shelter 8001.

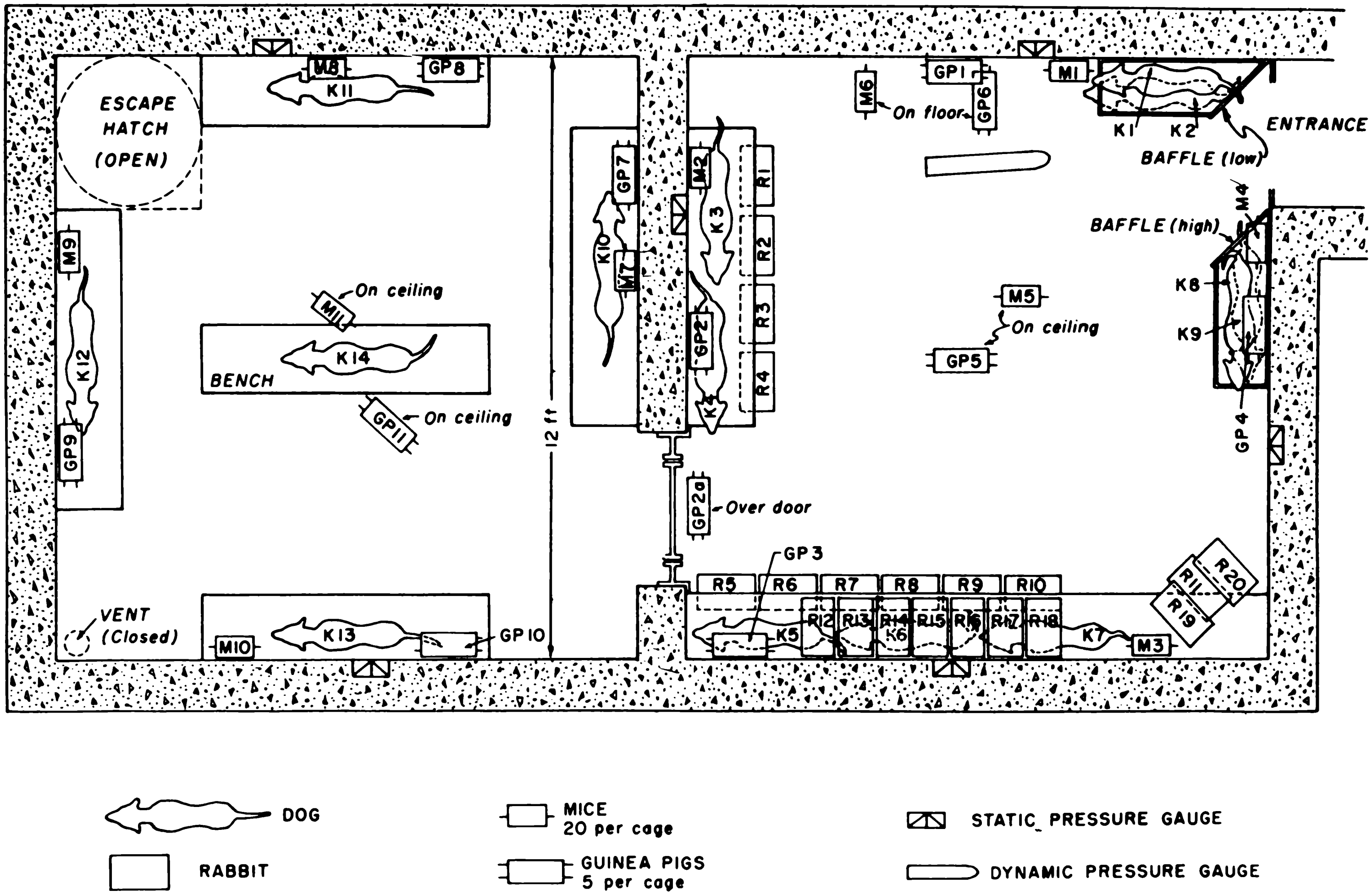

Fig. 3—Locations of animals and instruments in shelter 8001.

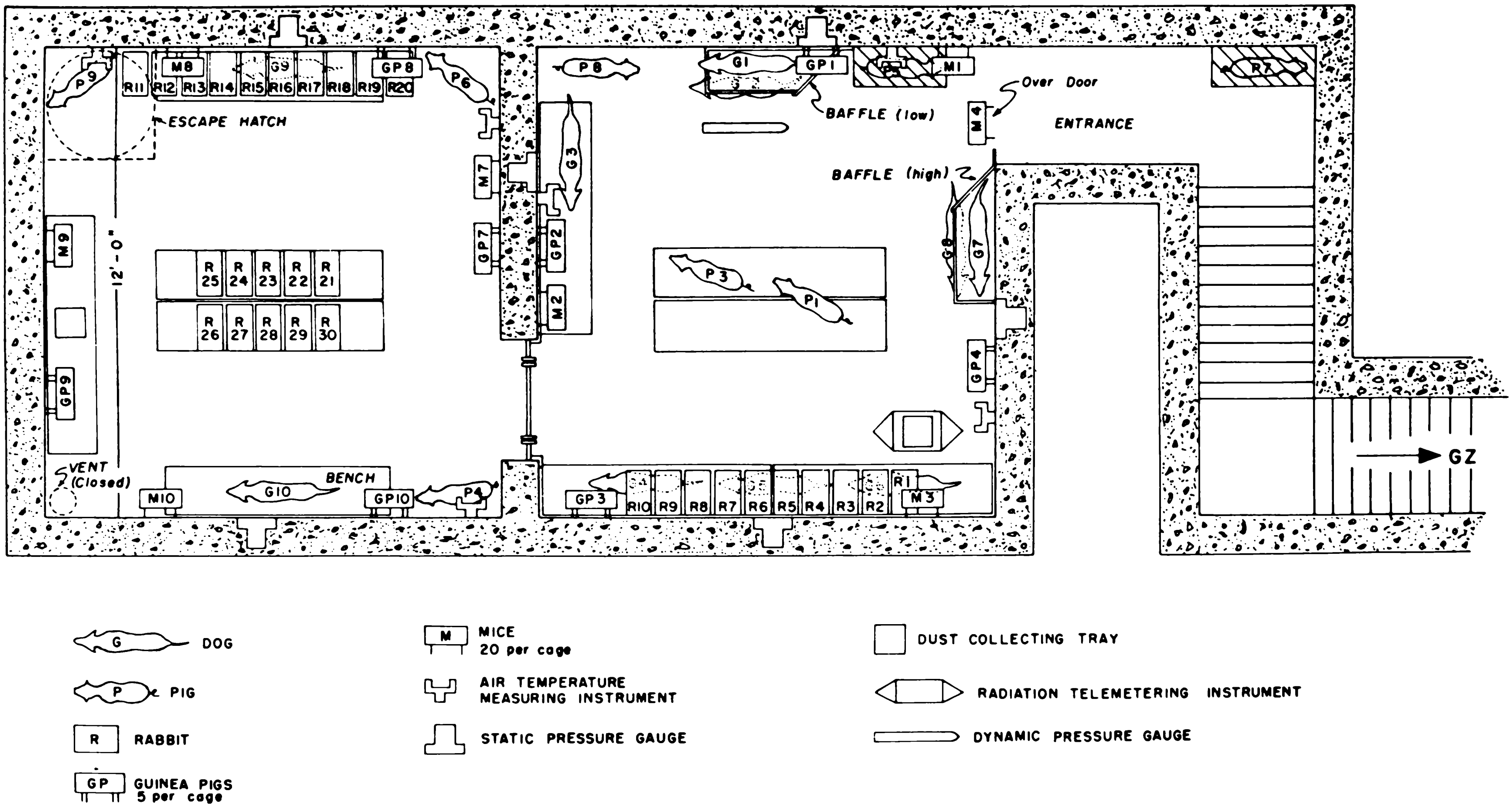

Fig. 4—Locations of animals and instruments in shelter 8002.

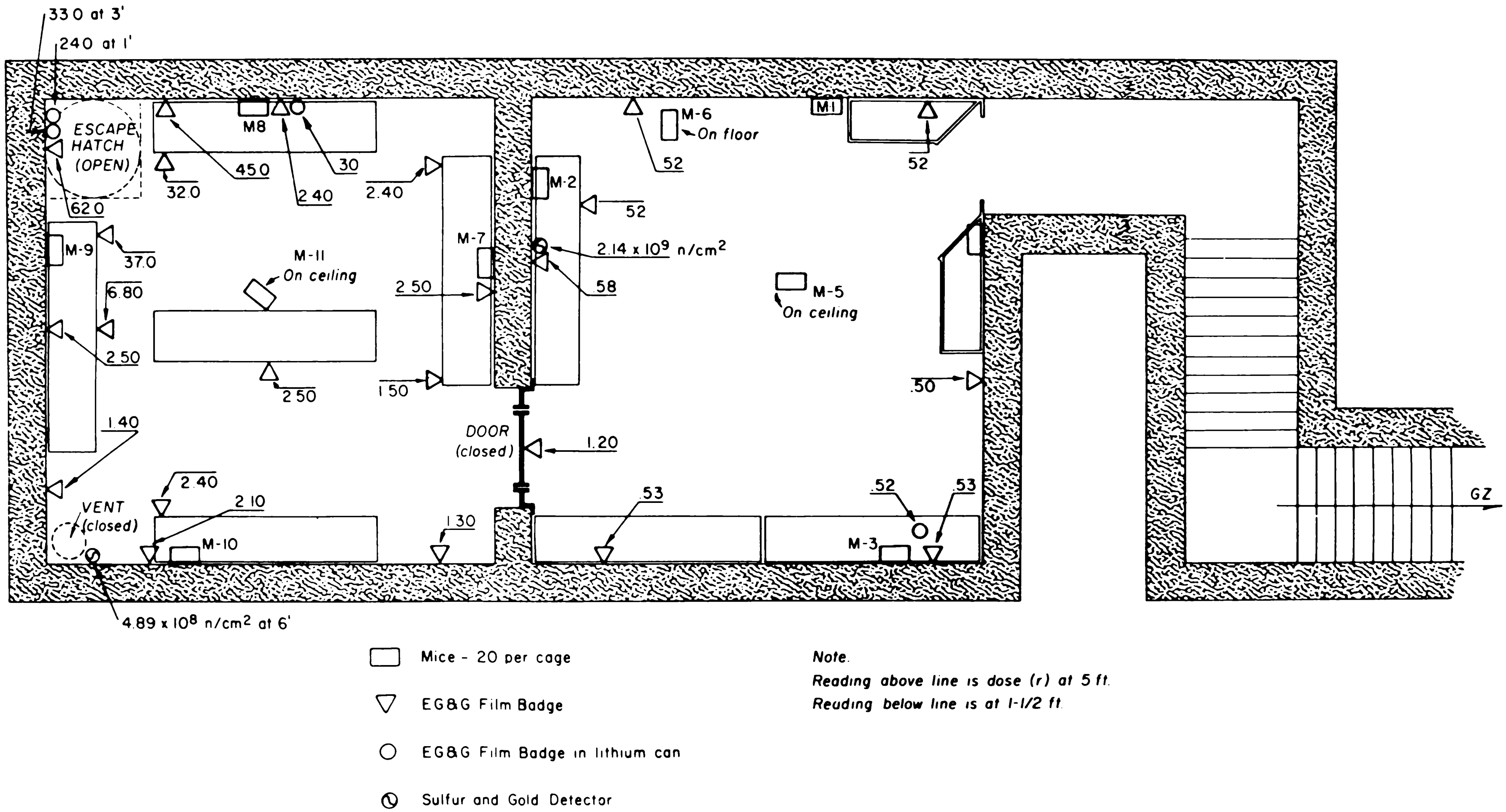

Fig. 5—Locations and types of measurements recorded by various radiation dosimeters inside shelter 8001.

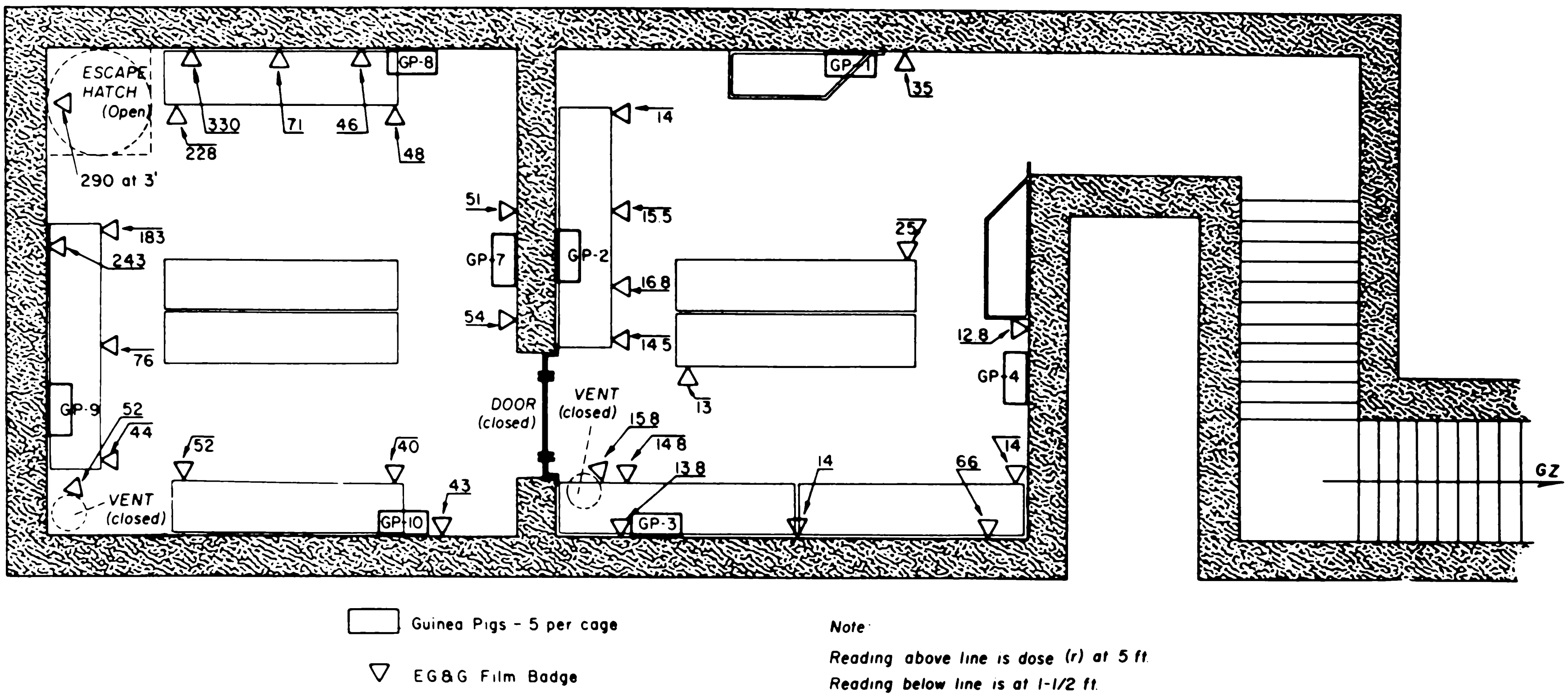

Fig. 6—Locations and types of measurements recorded by various radiation dosimeters inside shelter 8002.

SUMMARY 28

COMPARISON TEST OF REINFORCING STEELS

(Report WT-1473, Operation Plumbbob, Project 34.2, same title, by R. H. Carlson and J. P. Murtha, Sandia Corporation, Albuquerque, N. Mex., Sept. 27, 1960.)

OBJECTIVE AND SCOPE

The primary objective of this project was to determine the relative merits of hard-grade reinforcing steel and intermediate-grade reinforcing steel in resisting blast loading.

Slab pairs were placed at ground level over deflection chambers (Figs. 1 and 2) and loaded with the incident pressure pulse from a nuclear device. Two station locations (Fig. 3) were chosen so that the loadings were approximately 7- and 5-psi peak overpressure. The slabs comprising each pair were identical except for the grade of reinforcement in each. Slab strengths were varied, and two test stations were used to increase the probability of realizing the response necessary to emphasize the advantages of each steel grade.

Measurements were made of the dynamic midspan slab deflections and the transient loading pulse (Fig. 3). A thorough posttest survey was conducted to determine the severity of the damage to the concrete slabs.

Smoky shot of Operation Plumbbob, Aug. 31, 1957 (ref. ENW, p. 675), was chosen for this project because its yield (43 kt) and height of burst would give an ideal pressure wave of sufficient magnitude in a region where the project could be located.

TEST STRUCTURES AND DESIGN CONSIDERATIONS

The actual project drawing of the test beams is shown in Fig. 4 and properties of the beams are summarized in Tables 1, 2, and 3.

The experiment was designed to permit dynamic failure of several beam pairs. It was felt that, if the pretest predictions were evidenced, it would be possible to determine the advantages of the respective grades of steel when evaluated from a blast-resistant standpoint. In all cases the beam pairs tested were as nearly identical as was possible, except for the grade of steel reinforcement.

Because of the interest that had been focused on rail steel (ASTM designation A 16-54T), it was used to represent hard-grade reinforcement. Intermediate-grade billet-steel bars (ASTM A 15-54T) were selected as low-yield-point steel because of their extensive use in construction.

RESULTS

General

All slabs remained intact on their respective supports. Practically no spalling or concrete breakage away from the steel reinforcement occurred under any of the slabs. In all cases clean tension cracks opened in the tension zone of each slab. Figure 5 is a closeup photograph of the tension cracks in slab IW3A, the weakest slab tested. No shear failures were apparent. In the forward station all beams reinforced with intermediate-grade steel exhibited top-surface concrete crushing; whereas only the weakest rail-steel beam showed this damage. In the rear stations only one intermediate-grade reinforced slab, IW1B, exhibited compression-zone crushing. Figure 6 shows relative permanent deflection and tension crack pattern for slabs IW1A and RW1A.

Instrumentation

All self-recording deflection gauges produced clear and legible records. Tables 4 and 5 show permanent and dynamic slab deflections, respectively; see also Table 6.

All four electronic strain records were lost because of instrumentation failure. The loss prohibits any determination of dynamic increase in the properties of the reinforcing steel. One tension reinforcing bar in each slab was marked to permit permanent strain measurements with an extensometer. Table 7 shows maximum permanent strains recorded in each slab.

The three electronic pressure records are satisfactory. Table 8 gives peak pressure, duration, and impulse for the predicted and observed Smoky shot pressure pulse at both forward and rear stations. Slab responses calculated before the test and summarized in Table 9 are based on the predicted pressure data in Table 8.

CONCLUSIONS

1. The following observations are apparent for every slab pair tested in Project 34.2:
   a. Midspan dynamic deflection of the intermediate-grade slab was at least one and one-half times as great as the deflection of the rail slab.
   b. Permanent midspan displacement exhibited by the intermediate-grade slab was at least twice that of the rail slab.
   c. Permanent strain measured over a 10-in. gauge length on the tension reinforcing steel of the intermediate-grade slab was at least twice as great as that measured in the rail slab.
2. Comparison of certain rail and intermediate-grade slabs indicated that:
   a. When rail and intermediate-grade slabs having equal static yield strengths are subjected to loading pulses with the same peak pressures but different durations, the slab with the shorter load-duration-to-natural-period ratio will absorb a lesser impulse in producing the same response as will the slab with the greater duration-period ratio.
   b. When rail and intermediate-grade slabs are reinforced with identical amounts of tension steel and subjected to identical loading pulses, the rail-steel slab displays the more desirable response within the limits of these tests.

3. In a reinforced-concrete structural member, the reinforcement index, the steel ratio, and whether or not there is compression steel all limit the maximum strain that can accrue in the tension reinforcing steel. In all cases, concrete crushing occurred when the tension steel reached a strain of about 3.4%.

4. Deflection-vs.-time characteristics for the slabs of a pair are similar until the intermediate-grade slab yields.

5. The apparent dynamic increase calculated for the increase in strength of the rail-steel slabs was as high as 25%, with an average of 10%. The intermediate-grade steel strength varied from 10 to 40%, with an average of 25%.

6. Dynamic response of all test slabs was inversely proportional to their static strength.

7. Prediction procedures for structural response provide the necessary accuracy for design purposes when the blast loading can be determined. It should be noted that the uncertainty of predicting response

for a given set of conditions in the plastic state is far greater than that of determining the strength required for a given loading.

8. Within the limits of the Project 34.2 experiment, no evidence of brittle failure of rail steel was observed.

RECOMMENDATIONS

Several questions undoubtedly remain to be answered before the rail-steel controversy can be resolved. It was felt that, if the following recommendations were carried out, the resulting data would fill the gaps in current knowledge:

1. That a comparative experiment be conducted wherein the ratio of fundamental natural period to load duration is 0.3 or less. Such an experiment could be conducted on a reduced scale using high explosives.

2. That structural members reinforced with rail steel be tested under blast loading for various types of end conditions. End fixity and two-way slabs should be considered for future testing.

3. That a statistical survey be run to determine variability in the strength of rail steel currently being manufactured. Mill reports from several mills and several heats at a given mill should be included in the survey.

Table 1—PROPERTIES OF THE TEST SECTIONS*

Beam designation	Steel type	Bottom bars	Top bars	Area of tension steel (A_S), sq in.	Area of compression steel (A'_S), sq in.	Percent of tension steel (p), %	Percent of compression steel (p′), %	A'_S/A_S
RCA RCB	Rail	7 No. 5	6 No. 4	2.17	1.20	1.29	0.71	0.55
ICA ICB	Intermediate	7 No. 5	6 No. 4	2.17	1.20	1.29	0.71	0.55
RW1A RW1B	Rail	6 No. 5	5 No. 4	1.86	1.00	1.11	0.59	0.54
IW1A IW1B	Intermediate	6 No. 5	5 No. 4	1.86	1.00	1.11	0.59	0.54
RW2A RW2B	Rail	5 No. 5	4 No. 4	1.55	0.80	0.92	0.48	0.52
IW2A IW2B	Intermediate	5 No. 5	4 No. 4	1.55	0.80	0.92	0.48	0.52
RW3A	Rail	4 No. 5	3 No. 4	1.24	0.60	0.74	0.36	0.48
IW3A	Intermediate	4 No. 5	3 No. 4	1.24	0.60	0.74	0.36	0.48

*All beams have the following dimensions in common: D = 9 in.; d = 7 in.; b = 24 in.; L = 228 in.; $k''d$ = 1 in. All ties are No. 2, intermediate-grade steel, spaced each end: 12 sets at $3\frac{1}{2}$ in.; 7 sets at 10 in.

Table 2—CONCRETE TEST DATA*

Cylinder No.	Batch No. 1 (IW1A, ICA, RCB) Ultimate strength, psi	Batch No. 1 Ultimate strain, in./in.	Batch No. 2 (IW1B, RW2B, RCA, ICB) Ultimate strength, psi	Batch No. 2 Ultimate strain, in./in.	Batch No. 3 (RW1A, RW2A, IW2A, IW2B) Ultimate strength, psi	Batch No. 3 Ultimate strain, in./in.	Batch No. 4 (RW3A, RW1B, IW3A) Ultimate strength, psi	Batch No. 4 Ultimate strain, in./in.
1	4146	0.0033	4358	0.0033	5827	0.0036	5358	0.0038
2	5014	0.0014	4638	0.0030	5094	0.0037	4972	0.0042
3	4718	0.0021	4591	0.0026	4733	†	4583	†
4	4801	0.0013	4011	0.0044	5245	0.0031	5317	0.0029
5	4532	0.0023	3981	0.0029	5237	0.0026	4829	0.0031
6	3623	†	3756	†	6150	0.0031	4791	0.0021
Average‡	4643	0.0021	4316	0.0032	5511	0.0032	5053	0.0032

*Tests conducted on D + 9 and D + 10 days.
†Bad break.
‡All average values are average of 5 tests.

Table 3—AVERAGE YIELD AND ULTIMATE STRENGTH OF TENSION REINFORCING STEEL AS DETERMINED BY STANDARD TENSILE COUPON TESTS

Slab	Yield strength, psi	Ultimate strength, psi
ICA	49,256	79,708
RCA	73,269	124,083
IW1A	50,609	81,189
RW1A	79,056	123,541
IW2A	48,011	77,787
RW2A	64,387	118,274
IW3A	44,348	71,420
RW3A	77,296	129,879
ICB	49,759	80,101
RCB	70,500	118,759
IW1B	46,904	75,687
RW1B	66,440	119,547
IW2B	51,494	81,314
RW2B	71,732	123,975

Table 4—RELATIVE PERMANENT DEFLECTIONS OF SLABS AT MIDSPAN

Slab	Permanent deflection, in.	Ratio*
RCA	3.8	3.29
ICA	12.5	
RW1A	6.5	2.49
IW1A	16.2	
RW2A	8.2	2.37
IW2A	19.4	
RW3A	9.3	2.69
IW3A	25.0	
RCB	1.7	2.88
ICB	4.9	
RW1B	3.3	2.94
IW1B	9.7	
RW2B	4.4	2.25
IW2B	9.9	

*Ratio of permanent intermediate-grade deflection to permanent rail-grade deflection.

Table 5—MAXIMUM DYNAMIC SLAB DEFLECTIONS

Beam pair	Maximum observed deflection, in.	Ratio* of max. deflection	Predicted max. deflection, in.	Ratio of observed to predicted deflection
ICA	15.1	1.98	11.6	1.30
RCA	7.6		5.7	1.33
IW1A	19.1	1.75	15.6	1.22
RW1A	10.9		7.9	1.38
IW2A	22.2	1.66	20.2	1.10
RW2A	13.4		11.4	1.18
IW3A	>25.0†	>1.61	>22.0	
RW3A	15.5		16.1	0.96
ICB	7.2	1.53	4.6	1.57
RCB	4.7		3.5	1.34
IW1B	11.9	1.89	6.6	1.80
RW1B	6.3		4.1	1.54
IW2B	11.4†	1.63	9.4	1.21
RW2B	7.0†		5.2	1.35

*Ratio of intermediate to rail maximum deflections.

†Values taken from questionable deflection-time records. For IW3A, however, displacement of slab was greater than capacity of gauge.

Table 6—SUMMARY OF OBSERVED AND PREDICTED SLAB DEFLECTIONS

Slab	Observed: Permanent deflection, in.	Observed: Time of max. defl., msec	Observed: Dynamic deflection, in.	Pretest prediction: Time of max. defl. Msec	Pretest prediction: Time of max. defl. Ratio*	Pretest prediction: Max. defl. In.	Pretest prediction: Max. defl. Ratio*	Posttest analysis (no increase assumed for concrete strength): Calculated Y max., in.	Ratio*	t_m, msec	Ratio*	Assumed increase factor in steel strength	Posttest analysis (15% increase assumed for concrete strength): Calculated Y max., in.	Ratio*	t_m, msec	Ratio*	Assumed increase factor in steel strength
RCA	3.8	120	7.6	97	0.81	5.7	0.75	7.2	0.95	112	0.92	1.10	7.6	1.00	121	1.01	1.05
ICA	12.5	190	15.1	166	0.87	11.6	0.77	14.9	0.99	202	1.06	1.20	15.7	1.04	208	1.09	1.20
RW1A	6.5	150	10.9	122	0.81	7.9	0.72	10.9	1.00	153	1.02	1.00	9.0	0.83	139	0.93	1.00
IW1A	16.2	210	19.1	187	0.89	15.6	0.82	9.3	1.01	222	1.06	1.25	19.9	1.04	228	1.09	1.20
RW2A	8.2	160	13.4	157	0.98	11.4	0.85	13.7	1.02	168	1.05	1.30	14.1	1.05	174	1.09	1.25
IW2A	19.4	210	22.2	202	0.96	20.2	0.91	23.3	1.05	237	1.13	1.40	20.3	0.91	221	1.05	1.40
RW3A	9.3	160	15.5	183	1.14	16.1	1.04	15.8	1.02	167	1.04	1.25	15.4	0.99	163	1.02	1.25
IW3A	25.0	>140	>25.0	>200		>22		30.4		239		1.45	31.0		241		1.40
RCB	1.7	100	4.7	77	0.77	3.5	0.74	4.6	0.98	97	0.97	1.00	4.1	0.87	92	0.92	1.00
ICB	4.9	140	7.2	109	0.78	4.6	0.64	6.9	0.96	146	1.04	1.10	6.34	0.88	135	0.96	1.15
RW1B	3.3	125	6.3	88	0.70	4.1	0.65	6.6	1.05	136	1.09	1.00	6.4	1.02	130	1.04	1.00
IW1B	9.7	180	11.9	142	0.79	6.6	0.55	11.1	0.93	196	1.09	1.15	11.1	0.93	196	1.09	1.15
RW2B	4.4	125	7.0	108	0.86	5.2	0.74	6.88	0.98	132	1.05	1.10	6.9	0.99	132	1.06	1.10
IW2B	9.9	>130	11.4	172		9.4	0.82	12.4	1.09	205		1.20	11.2	0.98	200		1.20

*All ratios are determined by comparing value of interest to the observed value.

Table 7—MAXIMUM PERMANENT STRAINS IN TENSION REINFORCEMENT

Beam pair	Maximum strain, %	Ratio*
ICA†	2.74	3.38
RCA	0.81	
IW1A†	4.08	3.09
RW1A	1.32	
IW2A†	3.70	2.15
RW2A†	1.72	
IW3A†	5.95	3.10
RW3A	1.92	
ICB	1.44	2.82
RCB	0.51	
IW1B†	2.63	2.74
RW1B	0.96	
IW2B	2.32	2.04
RW2B	1.14	

*Ratio of maximum strains of intermediate-grade slab to maximum strains of rail-grade slab.

†Slabs exhibiting concrete crushing in compression zone.

Table 8—PRESSURE, DURATION, AND IMPULSE FOR OBSERVED AND PREDICTED LOADING PULSE AT EACH STATION

	Predicted		Recorded	
	Forward station	Rear station	Forward station	Rear station
Peak pressure, psi	6.75	4.75	6.60	4.72
Duration, msec	1000	1090	768	966
Impulse, psi-msec	2636	2164	2461	2124

Table 9—SUMMARY OF PREDICTIONS OF SLAB RESPONSE

Slab	40 kt Time of yield, msec	40 kt Yield deflection, in.	40 kt Time of max. defl., msec	40 kt Max. deflection, in.	45 kt Time of yield, msec	45 kt Yield deflection, in.	45 kt Time of max. defl., msec	45 kt Max. deflection, in.	50 kt Time of yield, msec	50 kt Yield deflection, in.	50 kt Time of max. defl., msec	50 kt Max. deflection, in.
RCA	47	3.27	97	5.74	47	3.27	97	5.71	46	3.32	101	6.19
ICA	36	2.20	162	11.21	36	2.21	166	11.55	35	2.20	169	12.78
RC1A	45	3.19	122	7.76	45	3.20	122	7.89	44	3.23	127	8.52
IW1A	35	2.15	184	15.40	35	2.15	187	15.57	34	2.14	188	17.21
RW2A	43	3.08	154	11.32	43	3.08	157	11.40	42	3.10	160	12.59
IW2A	34	2.09	198	19.98	34	2.09	202	20.19	33	2.07	180	21.52
RW3A	42	3.06	180	15.92	42	3.06	183	16.11	41	3.07	183	17.48
IW3A	33	2.02	>200	>20.0	33	2.02	>200	>22.0	33	2.02	>200	>24.0
RCB	77	3.31	77	3.31	66	3.31	77	3.49	61	3.31	79	3.72
ICB	46	2.16	104	4.16	45	2.20	109	4.56	43	2.18	120	5.37
RW1B	62	3.23	86	3.82	59	3.23	88	4.09	56	3.22	92	4.46
IW1B	44	2.10	136	5.91	43	2.13	142	6.60	41	2.09	158	8.12
RW2B	57	3.12	103	4.77	55	3.14	108	5.20	53	3.16	114	5.80
IW2B	43	2.09	167	8.45	42	2.12	172	9.40	38	2.10	182	10.59

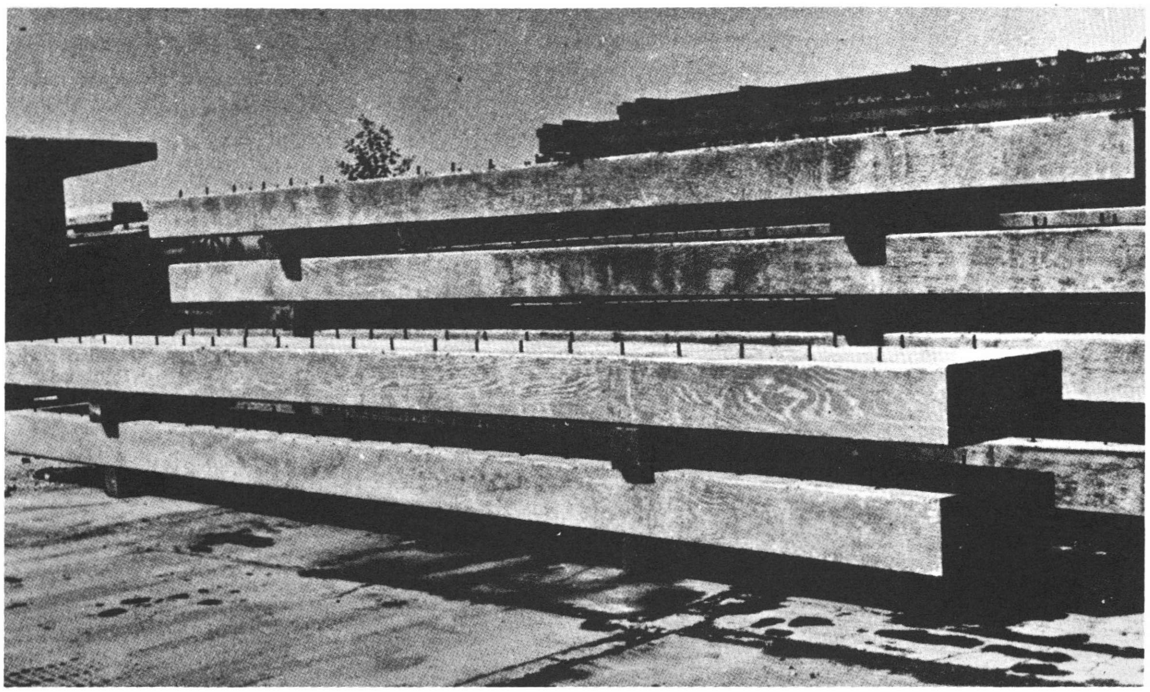

Fig. 1—Slabs stacked in yard for curing.

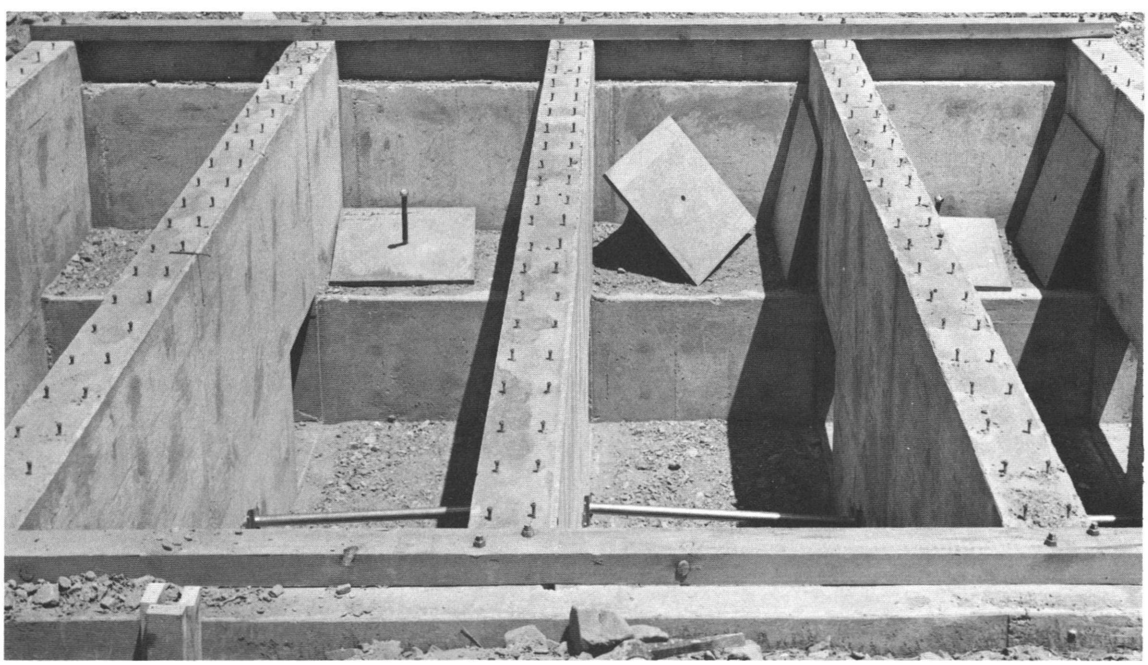

Fig. 2—Completed forward station, slabs not in place.

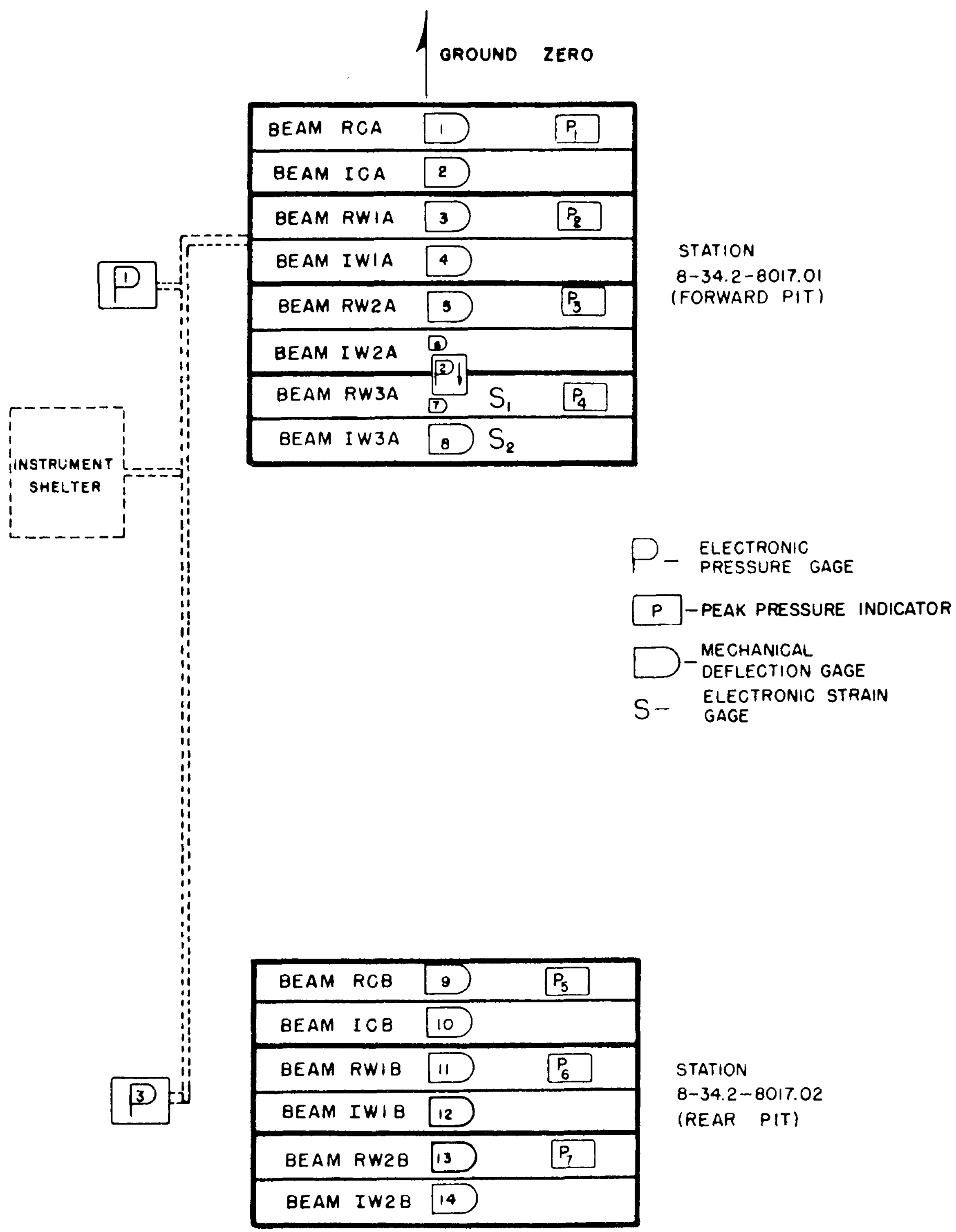

Fig. 3—Schematic diagram of slab and instrument layout.

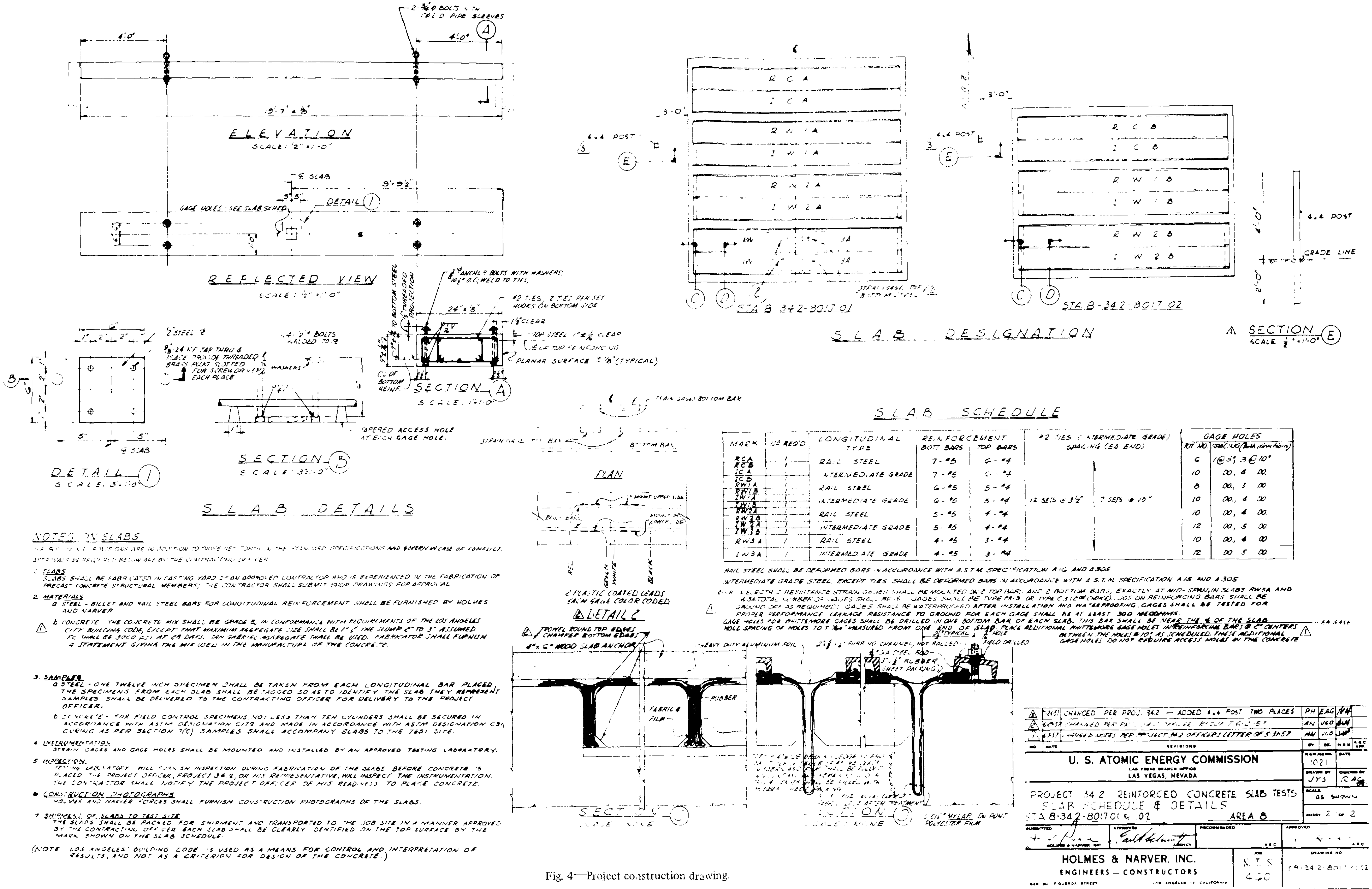

Fig. 4—Project construction drawing.

Fig. 5—Photograph showing tension cracks beneath slab IW3A.

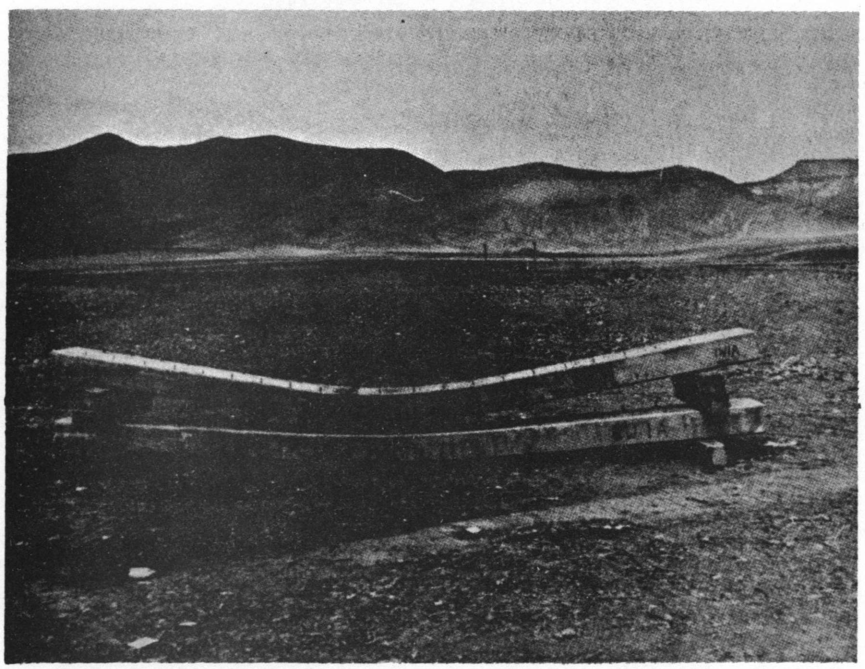

Fig. 6—Slabs IW1A and RW1A, showing relative permanent displacement and tension crack pattern (IW1A on top).

SUMMARY 29

TEST OF BURIED STRUCTURAL-PLATE PIPES SUBJECTED TO BLAST LOADING

(Report WT-1474, Operation Plumbbob, Project 34.3, same title, by R. A. Williamson and P. H. Huff, Holmes & Narver, Inc., Architect-Engineers, Los Angeles, Calif., July 28, 1961.)

OBJECTIVES AND SCOPE

The general purpose of the test was to determine the resistance of buried structural-plate pipe to high surface overpressures resulting from air-burst. This information was to be used primarily to evaluate the suitability of structural-plate pipe as a partial substitute for heavy concrete tunnel sections in the construction of scientific stations located at ranges close to nuclear detonations.

"Structural plate" (or the trade name Multi-Plate used by Armco Steel Corp.) pipe is constructed of curved sectional corrugated-metal plates having longitudinal and circumferential bolted seams. Corrugations are nominally 2 in. deep and spaced 6 in. apart.

Multi-Plate pipe is classed in the general category of flexible metal pipe. When it is supporting earth cover, Multi-Plate pipe is capable of deflections large enough to cause a favorable redistribution of external soil pressure before it fails. This redistribution increases its ability to resist static loads and largely invalidates theoretical attempts to determine stresses or collapsing loads. Similarly, reliance on empirical data is necessary in determining the resistance of buried flexible pipe to blast overpressure acting on the ground surface. These data may then be accomplished only by the use of tests, observation, and experience.

The project consisted in the testing of two 20-ft lengths of pipe buried under 10 ft of earth cover. Test stations 1 and 2, located at ranges 825 and 900 ft, respectively, from the Ground Zero (GZ) of the Smoky event (ref. ENW, p. 675), were expected to be subjected to overpressures of 265 and 195 psi, respectively.

TEST STRUCTURES AND PROCEDURE

Details of the test structures are given in Fig. 1. Figure 2 shows an interior view of pipe at station 1.

The pipe used was 7-ft-diameter, 10-gauge galvanized Multi-Plate, which was furnished by Armco. The pipe material was copper-bearing iron, with a minimum tensile yield strength of 27 kips/sq in. Joint strength more nearly consistent with the strength of the pipe walls was provided, using eight bolts per foot in longitudinal seams instead of the usual four bolts per foot.

The timber end walls, shown in Figs. 1 and 3, incorporated features that were intended to minimize end effects due to blast loading. One feature was the use of several thicknesses of asphalt-impregnated fiberboard on the face against the end of the pipe to provide, as far as feasible, free movement of the pipe wall. A second feature consisted in extending the timbers several feet outside the pipe walls to engage a

large amount of earth fill. The purpose of this was an attempt to resist dynamic earth pressure against the ends of the pipe without causing high axial stresses in the pipe.

The unusual soil conditions indigenous to the Nevada Test Site were encountered at the location selected; the results of the test may, therefore, not be applicable to other locations. Beneath a thin surface layer of soil was a hard stratum of conglomeritic gravel particles about 1 in. maximum in size bound by a natural cementitious material into a matrix several feet thick. Blasting was necessary to penetrate this stratum. Below it was a deposit of dense, fairly well cemented sand and gravel that was excavated with a backhoe. Material that met specification requirements for backfill was obtained from a site about 1.4 miles away. Compaction was by machine tamping. The average field density of the backfill material was about 114 lb/cu ft, and the average compaction attained was about 93% of maximum. Shear tests indicated an internal coefficient of friction of 1.42 and 0.875 at stations 1 and 2, respectively.

The principal measurements taken of each pipe were the transient changes in horizontal and vertical diameters vs. time, vertical and horizontal accelerations of the pipe invert, and the maximum interior overpressure. Supplementary data were the preshot and postshot measurements of horizontal and vertical diameters, joint slip, distances between end bulkheads, and elevations of the ground surface. Soil properties obtained included density, percentage of compaction, gradation, and the coefficient of internal friction.

RESULTS

Maximum surface overpressures were 245 and 190 psi at stations 1 and 2, respectively.

None of the peak-overpressure diaphragms ruptured, which indicated that the maximum interior overpressure at both stations was less than 0.5 psi.

Peak transient and residual diameter changes, obtained by the self-recording deflection gauges, are summarized in Table 1.

No usable postshot elevations were obtained because the absolute preshot elevation of the reference point was not determined.

The trace of the accelerometer records is shown in Fig. 4. Figures 5 and 6 show the horizontal and vertical invert velocities and displacements, respectively, obtained by successive integration of the acceleration-vs.-time records.

Table 2 summarizes preshot and postshot measurements of horizontal and vertical pipe diameters, as well as average distances between end bulkheads.

The motion of the pipe may be explained qualitatively as a flattening of the ring section caused by the downward movement of the earth mass over the pipe and displacement of the earth at the sides of the pipe.

CONCLUSIONS

The principal conclusions follow:

1. Under conditions similar to those of this test, Multi-Plate pipe could be substituted for reinforced-concrete sections.

2. The portion of the blast load carried by the pipe was less than the total load acting on the ground surface. The major portion of the load was apparently carried by the fill above the pipe.

3. Friction forces between fill and trench walls were fully mobilized, as indicated by subsidence of surface monuments.

4. The small deformations of the pipe and the lack of slip in the bolted joints indicate that the peak load on the pipe was a small percentage of the load required to produce failure. Under soil conditions and depth of burial comparable to those that existed in these tests, a much higher overpressure of comparable duration would be required to cause pipe failure. This overpressure would probably be not less than that required to cause large general permanent subsidence of the ground surface.

5. In general, transient and residual pipe-diameter deformations were not proportional to the peak overpressure at the ground surface.

6. Residual deformations were a large percentage of the transient deformations, although the latter were small. Because of this it is possible that repeated blast loadings would cause further residual deformations. Such a tendency to creep under repeated loads would be an important factor when deformations are large.

7. The peak transient horizontal force acting on the bulkheads was apparently a small fraction of the peak overpressure at the ground surface.

8. The buried pipe, under the conditions of this test, provided adequate protection to contents against nuclear radiation. The average accumulated doses in the 1½-month period between zero time and time of recovery were 1.4 and 0.7 r at stations 1 and 2, respectively.

Table 1—PEAK TRANSIENT AND RESIDUAL DIAMETER CHANGES FROM SELF-RECORDING GAUGES

Location	Vertical*	Horizontal*
	Station 1	
Peak:		
Feet	−0.074	+0.032
Inches	−0.89	+0.39
Residual:		
Feet	−0.057	+0.019
Inches	−0.68	+0.23
	Station 2	
Peak		
Feet	−0.028	+0.035
Inches	−0.34	+0.41
Residual:		
Feet	−0.0025	+0.016
Inches	−0.03	+0.19

*Increases are indicated by +; decreases by −.

Table 2—SUMMARY OF PRINCIPAL DATA*

	Vertical and horizontal diameters †			
	Station 1		Station 2	
	Vertical	Horizontal	Vertical	Horizontal
Preshot diameter, ft	6.919	6.954	6.953	6.815
Postshot diameter, ft	6.904	6.959	6.940	6.855
Residual change, ft	−0.015	+0.005	−0.013	+0.040
Residual change from gauge, ft	−0.057	+0.019	−0.0025	+0.016
Discrepancy:				
Feet	+0.042	−0.014	−0.0105	+0.024
Inches	+0.50	−0.17	−0.12	+0.29
Transient change from gauge:				
Feet	−0.074	+0.032	−0.028	+0.035
Inches	−0.89	+0.39	−0.34	+0.41
	Slant diameters†			
	Station 1		Station 2	
	A	B	A	B
Preshot diameter, ft	6.735	6.773	6.813	6.756
Postshot diameter, ft	6.714	6.789	6.837	6.694
Residual change:				
Feet	−0.021	+0.016	+0.024	−0.062
Inches	−0.25	+0.19	+0.29	−0.74
	Average distance between end bulkheads			
	Station 1		Station 2	
Preshot	20 ft 2 11/16 in.		20 ft 2 7/8 in.	
Postshot	20 ft 2 7/16 in.		20 ft 3 7/16 in.	
Change	−1/4 in.		+9/16 in.	
	Joint slip			
	Station 1		Station 2	
Longitudinal	None		None	
Circumferential	None		None	

*Increases are indicated by +; decreases by −.

†Slant diameter A is inclined nominally at 45° to the horizontal with the lower end nearer GZ. Diameter B is nominally at 90° to diameter A. Measurements are taken between marks on projecting bolt heads.

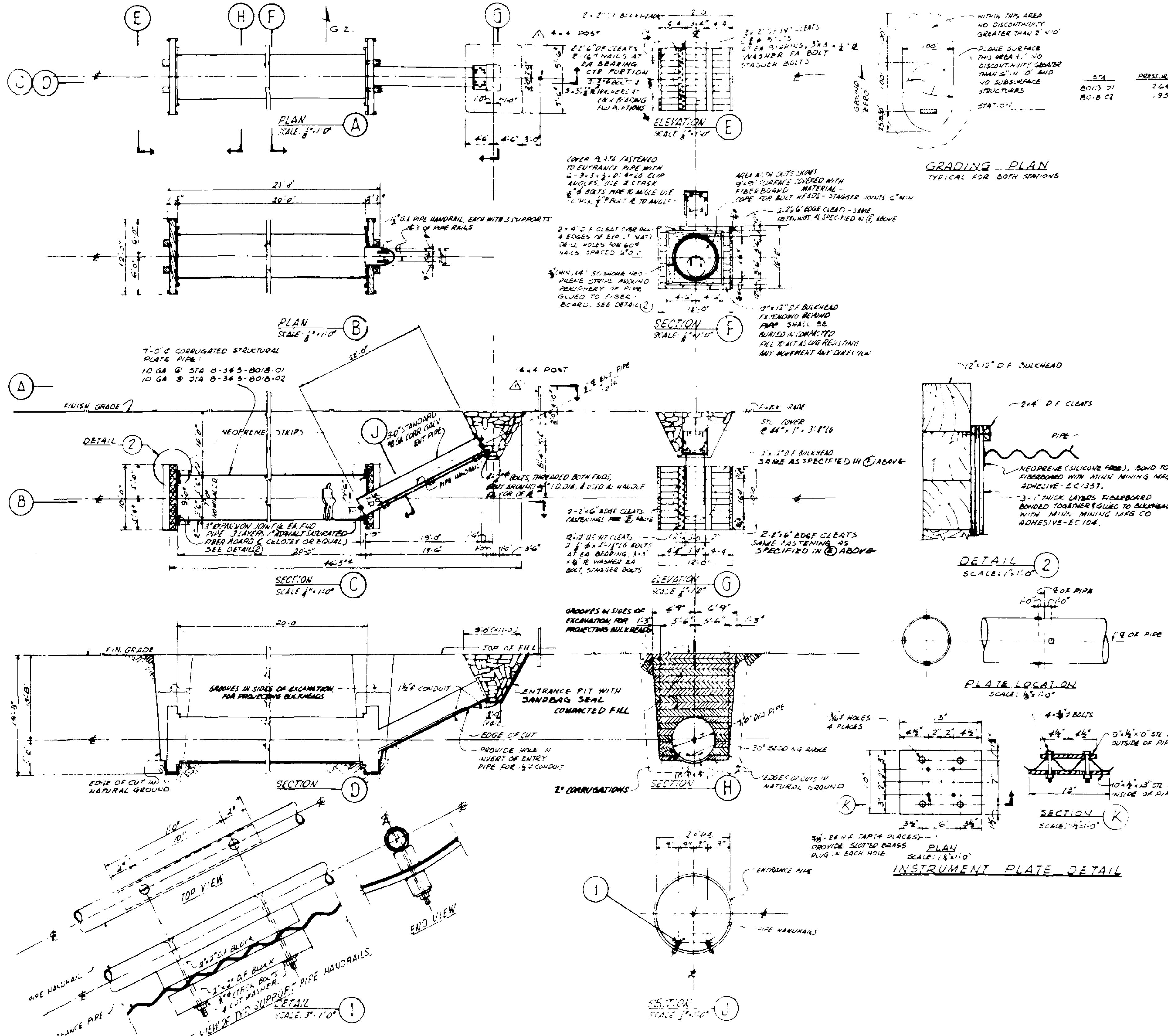

PIPE MATERIALS

1. Pipe shall be furnished in conformance with requirements of Division 4, Section 19, of the standard specification for highway bridges of AASHO, 6th ed., and the additional requirements here specified.

2. Minimum guaranteed tensile yield strength and ultimate tensile strength of the pipe material shall be specified by the manufacturer.

3. Bolts shall be high strength bolts of not less than ¾" diameter. Bolt and nut materials shall conform to the requirements of the current edition of ASTM A-325. Calibrated power or torque wrenches shall be used for tightening bolts. Bolts shall be tightened to a tension of not less than 29,000 lb or torque of not less than 320 ft-lb. Shaped bolt heads and nuts shall be used, or standard type bolts and nuts with shaped washers shall be used in lieu thereof.

4. Longitudinal seams shall have not less than 8 bolts per foot.

WOOD

1. Lumber shall be 1500F Douglas fir grade marked, conforming to WCLA grading rules #15.

STRUCTURAL STEEL

1. All structural steel shall conform to the current edition of ASTM A-7.

PLACEMENT OF PIPE

1. The pipe shall be installed so that longitudinal seams are located symmetrically with respect to the vertical diameter of the pipe. Longitudinal seams shall not occur at the horizontal or vertical diameters in the midlength portion of the pipe.

EXCAVATION AND BACKFILL

1. Backfill material shall be free from large rocks and large lumps or clods larger than 3" in diameter. Backfill material used shall be subject to the approval of the project representative before placement. Fill shall be compacted to 90% optimum density, as determined in accordance with AASHO Standard Method T-99.

2. Fill material shall be compacted in 6" layers and placed alternately on both sides of pipe. Fill above top of pipe shall not be placed until after field measurements are made by Holmes & Narver field forces.

3. If feasible, fill material against each face of wood bulkheads shall be placed and compacted so as to prevent undue penetration of the fiberboard material by the end of the pipe.

REQUIRED SOIL TESTS

1. The following data shall be obtained relative to the compacted fill material below the level of the top of the pipe at both stations prior to the event: (1) percentage of compaction, (2) unit weight, (3) coefficient of internal friction, and (4) soil classification. Results shall be presented in report form.

2. The same information is required for the fill material above the top of the pipe. After the event, the percentage of compaction and unit weight of the fill material above the top of the pipe shall be rechecked.

FIELD MEASUREMENTS

1. The following data shall be obtained by Holmes & Narver field forces at both stations. Measurements of inside vertical and horizontal diameters at the midlength of the pipe: (1) prior to backfilling, (2) with backfill at the top of pipe, (3) with backfill completed, (4) within a few days of the event, and (5) after the event. Measurements shall be taken to the nearest 0.001 ft between clearly marked points on the corrugations.

2. Invert elevations to the nearest 0.01 ft, at ends and midlength of the pipe, obtained when diameters are measured.

3. Average width of excavation in the middle third of the pipe length measured at the top of the pipe.

4. Elevation of buried monuments located in a vertical plane at the midlength of the pipe, normal to the pipe axis. Monuments shall be located about 1 ft below finished grade. One directly over the pipe axis and two on each side of the pipe axis, one just within and one just beyond the limits of the excavation. Elevations shall be recorded before and after the event.

CONSTRUCTION PHOTOGRAPHS

1. Holmes & Narver field forces shall furnish construction photographs when: (1) excavation is completed and pipe is in place, (2) end bulkheads and entrance pipe are installed, and (3) fill is completed and before sandbags are placed.

Fig 1—Plans, sections, and details of Project 34.3 buried-pipe tests.

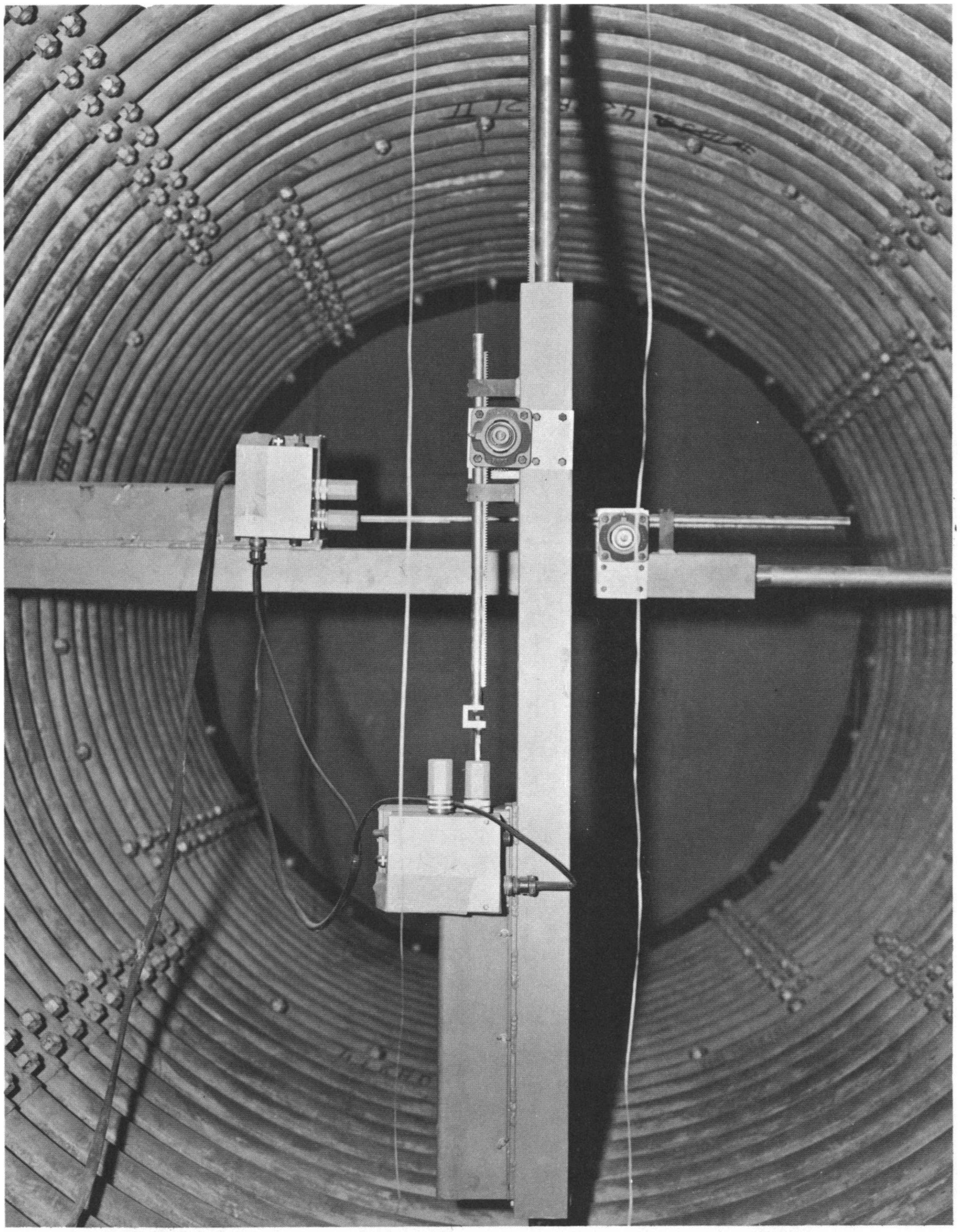

Fig. 2—Deflection gauges and film badges installed in pipe.

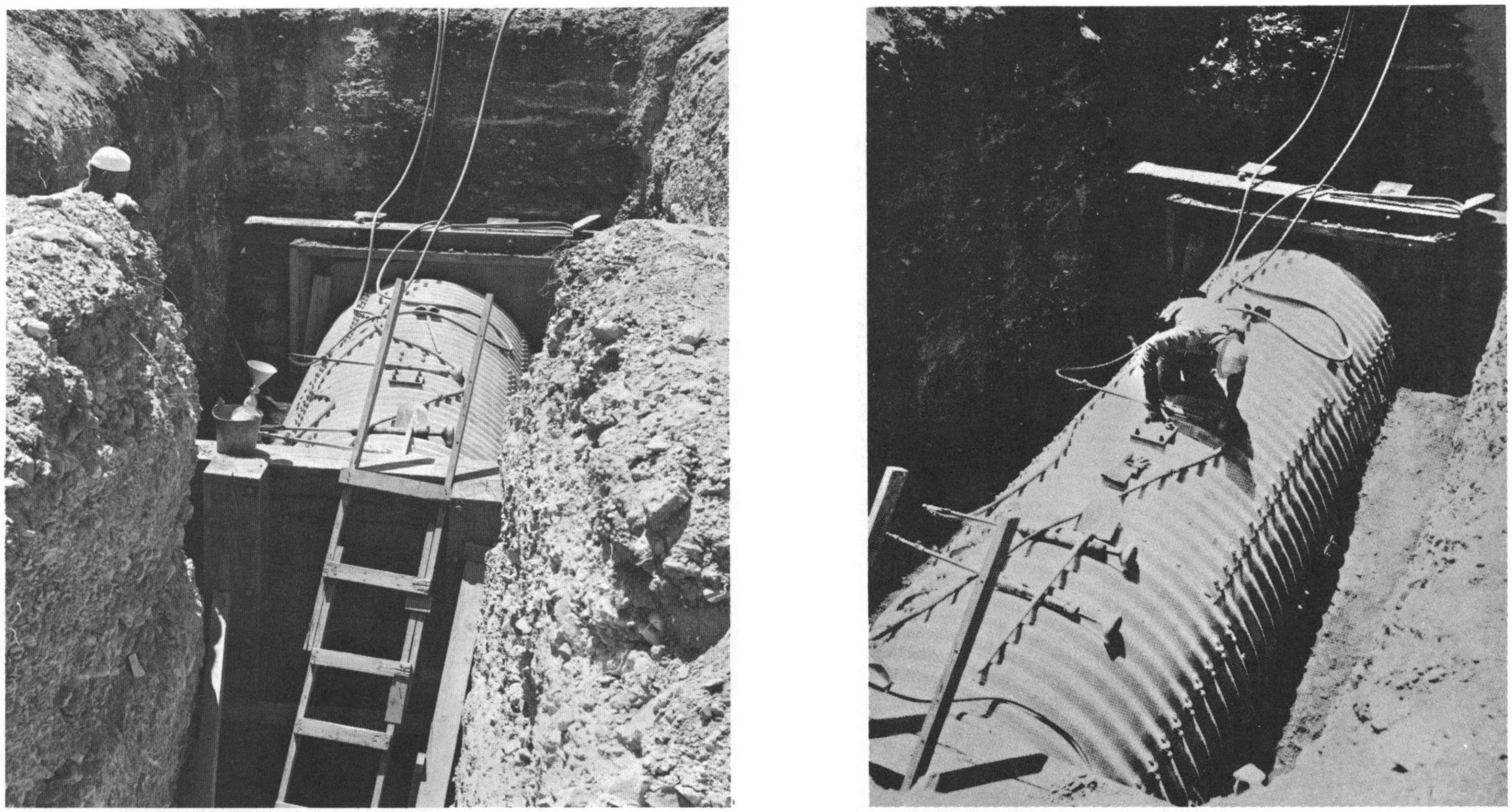

Fig. 3—Exterior views of pipe in place before placing backfill.

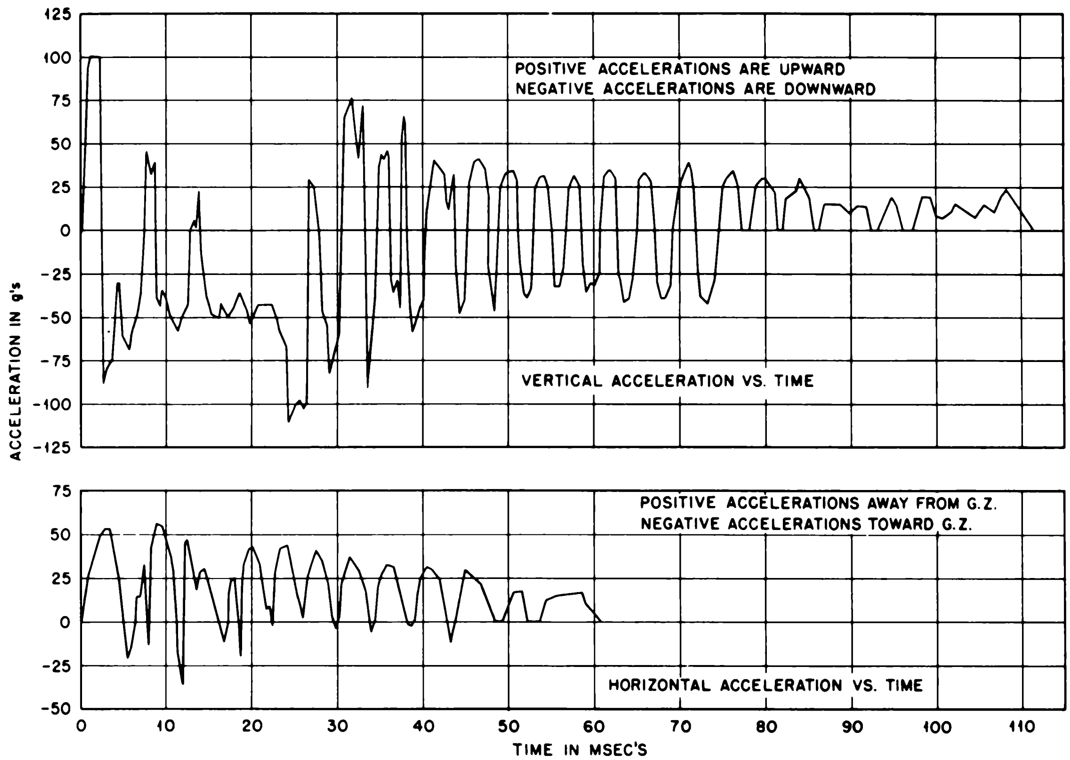

Fig. 4—Invert accelerations, station 1.

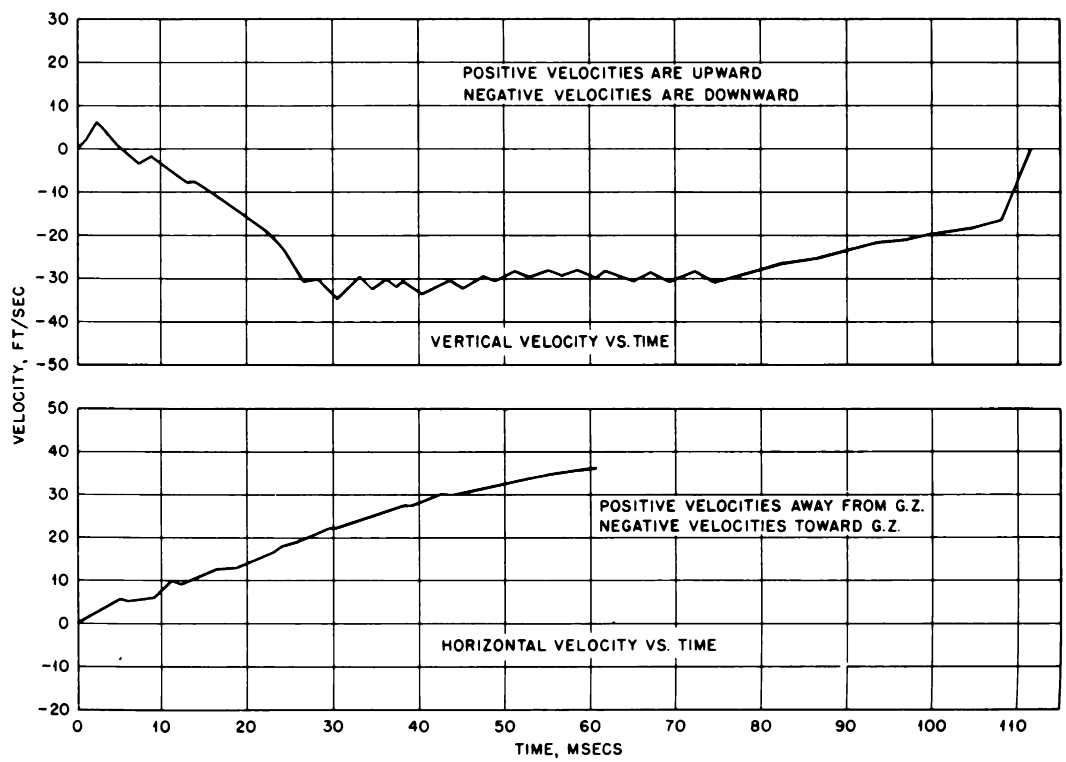

Fig. 5—Invert velocities, station 1.

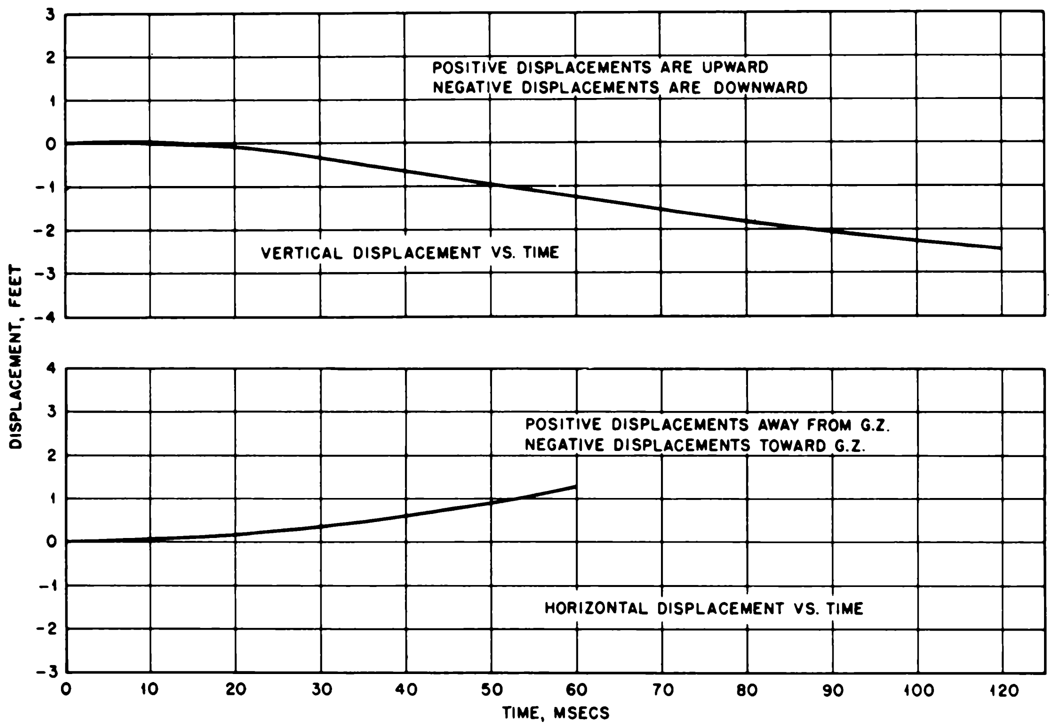

Fig. 6—Invert displacements, station 1.

SUMMARY 30

BLAST EFFECTS ON AN AIR-CLEANING SYSTEM

(Report WT-1475, Operation Plumbbob, Project 34.4, same title, by Richard Dennis, Charles E. Billings, and Leslie Silverman, Harvard University Air Cleaning Laboratory, Boston, Mass., Oct. 22, 1962.)

OBJECTIVES AND SCOPE

At the request of the Division of Reactor Development, U. S. Atomic Energy Commission, a study of the effect of shock waves on various types of air-cleaning equipment, such as are used in plant process and laboratory areas, was undertaken by the Harvard University Air Cleaning Laboratory. Although this investigation was specifically concerned with shock waves generated by nuclear or high-explosive blasts that impact upon air-cleaning devices in a direction opposite to that of normal airflow, the test results are considered of similar interest in connection with ventilation systems for blast shelters, with or without blast-valve protection.

Objectives of this project were: (1) to determine the effects of blasts on filtration devices and typical air-cleaning systems in the 3- and 1-psi overpressure range; (2) to measure dust dislodged by blast from AEC filters and dry plates and reentrained in reverse-flow air; (3) to determine the pressure attenuation and dust-recovery characteristics of typical wire-mesh viscous filters and dry Fiberglas filters; (4) to determine the natural damping effect of ductwork and stacks; and (5) to compare field and laboratory data to determine if present and future laboratory tests can be extrapolated to predict field conditions.

Preliminary laboratory shock-tube tests had provided a convenient and economical means of establishing damage-causing pressure levels and of estimating the amount of dust reentrainment. Typical results of this study are summarized in Table 1.

Field tests were conducted in a chemical-plant control room and in a concrete house, located in Area T-1 on Galileo shot (ref. ENW, p. 675). Overpressures in these locations were expected to be about 3 and 1 psi, respectively.

VENTILATION SYSTEMS

Identical systems were constructed for the chemical-plant control room and the concrete residence. Figures 1 and 2 show plan views of this equipment in relation to building orientation.

The air-cleaning system in each building simulated stack, duct, and hood configurations commonly used by the AEC. The systems are illustrated in Figs. 3 to 5.

The maximum filtering capacity of each air-cleaning system was predicted to be approximately 4500 cu ft/min.

Filtration devices placed in each of the six hoods (the rectangular wooden duct sections) are indicated in Table 2 according to their positions relative to normal airflow. The AEC filters (Fig. 6) referred to are cellulose–asbestos or all-glass media pleated within wooden frames 24 in. square and 6 or 12 in. deep. These filters are designed for high-efficiency collection (>99.9%) of fine (>1μ in diameter) particles.

Dust-Stop prefilters (Fig. 7) used in hoods 1, 3, and 6 were standard roughing filters designed to remove coarse (5 μ) particles from the gas stream. Their primary function is to extend the service life of high-efficiency filters.

The Far-Air filter (Fig. 8) is an adhesive-coated metal screen. Dimensions and filtration characteristics of this device are about the same as those of the Dust-Stop filters.

A collecting-stage section constructed to dimensions of a standard low-voltage electrostatic precipitator (Fig. 9) was installed in hood 6. The unit was composed of 34 parallel aluminum plates coated with a thin layer of calcium carbonate.

RESULTS

Postshot Condition of Chemical Plant and Equipment (Exterior Peak Pressure of 4 Psig)

Building Damage—No significant structural damage to the exterior or interior of the chemical-plant room was observed. All temporary window and door closures installed for these tests appeared to be unaffected by the blast.

Exhaust Ventilation and Air-cleaning Equipment—No visible signs of damage or displacement of steel and wood duct systems were detected. Preliminary inspection of AEC filters and the Far-Air unit showed no visible signs of damage. Dust-Stop prefilters in hoods 1 and 3 (Fig. 10) were intact with but a slight bowing-out of the center metal supporting strip. The Dust-Stop filter located in the supply-air opening in the entrance door and subjected to side-on pressure was completely destroyed (Fig. 11).

Dust Dislodgement and Degree of Dispersion—Floor areas opposite hoods containing loaded filters were coated with dust. The hoods themselves were completely coated, and significant dust deposits ranging from 20 to 200 g appeared on the bottom sections (Fig. 12). Dust-Stop prefilters and the Far-Air filter (Figs. 10 and 13) were saturated with dust. Dust was deposited on the filter-supporting screens in streamlined wedge-shaped projections, indicating that it had impacted at high velocities. A thin dust film on the outside faces of the filters showed that airflow had reversed during the negative phase of the shock condition.

Postshot Condition of Concrete Residence (Exterior Peak Pressure of 1.9 Psig)

Building and Equipment Damage—No signs of physical damage were noted in the concrete house or in the ventilation and the air-cleaning systems. This was expected since the building was in a zone of comparatively low overpressure. However, the supply-air Dust-Stop filter placed in the exit door and subjected to side-on pressure was blown into the building and completely destroyed.

Dust Dislodgement and Degree of Dispersion—In comparison with the chemical plant, no differences were detected in unloading patterns of AEC filters or in dust recovery by prefilters located in hoods 1, 2, 3, and 6. Qualitatively, however, there appeared to be less dust dissemination in this building. Very little dust was deposited in hood 4, which contained a Far-Air filter in front of the loaded AEC filter, indicating that afterfilters may be an effective means of reducing dust dislodgement. The Dust-Stop and Far-Air prefilters in hoods 1, 2, and 3 showed evidence of large dust holdings. A slight bowing-out of the Dust-Stop filter center supporting strip was observed.

Inspection of the electrostatic-precipitator unit in hood 6 indicated negligible removal of dust from the lubricated plates and nearly complete removal from the dry plates.

Pressure

Maximum overpressures of 4.0 and 1.9 psig were recorded within less than 5 msec for outside (roof) pressures in both test locations. Table 3 indicates that peak pressures recorded in the stack and breeching of

each system were approximately 70% of outside pressures. Pressures in front of the hoods attached to the two branches of the main plenum ducts were about half as large as those in the stack and breeching and about 30% of the outside peak pressure. Upstream hood pressures varied from 1.0 to 1.6 psig for the chemical plant and from 0.5 to 0.8 psig for the concrete house. No significant differences were noted between peak pressures recorded in front of and behind the AEC filters and the Far-Air filters.

Maximum room pressures in both buildings at equilibrium were about the same as those within the ventilating system (1.1 psig for the chemical plant and 0.6 psig for the concrete house).

Dust Losses from Air-cleaning and Recovery by Hood and Prefilter Systems

Relevant data are summarized in Table 4.

CONCLUSIONS

The following conclusions are based on the limited experimental data obtained in this study. General extrapolation to structures differing widely in closure details and in position and size of air-entry ports (exhaust and supply-air openings) does not appear warranted.

1. No apparent damage to AEC filters housed in prototype ventilation systems occurred at outside peak pressure levels less than 4.0 psig.

2. Complete destruction of Dust-Stop filters occurred at pressure levels greater than 2.0 psig. Minor damage occurred at overpressures greater than 0.4 to 1.4 psig.

3. Reentrainment losses from AEC filters housed in two different structures ranged from 53 to 86% of the initial filter holdings in the 4.0-psig area and from 41 to 64% in the 1.9-psig area.

4. Reentrainment losses varied directly with the initial filter dust load.

5. Reentrainment losses from 6-in. AEC filters were significantly higher than those determined for the 12-in. models.

6. Reentrainment of dust from dry electrostatic-precipitator plates in the 1.9-psig area was high, showing greater than 90% loss.

7. Reentrainment losses from adhesive-coated plates, on the basis of visual inspection, appeared much lower than those from dry plates.

8. Dust-Stop and Far-Air prefilters were effective in collecting dust dislodged from AEC filters. Results averaged 33% recovery in the 4.0-psig area and 50% in the 1.9-psig area.

9. Large percentages of the dust dislodged from AEC filters were deposited in the hoods immediately in front of the filters. Observed values were 26 and 40% in the 4.0- and 1.9-psig areas, respectively.

10. A considerable amount of dust escaped the hood-filter systems and was discharged into the room atmosphere. The observed amounts were 41% of the preshot loading in the 4.0-psig area and 22% in the 1.9-psig area.

11. The use of Far-Air afterfilters as shock attenuators to minimize reentrainment from loaded AEC filters reduced the dust dislodgement by a factor of greater than 10 (4.5% dust loss in comparison with an average value of 53% for other filters in the 1.9-psig area).

12. Experimental results reported for Dust-Stop filters apply equally well to similar low resistance, low strength, mineral fiber prefilters. Data obtained for Far-Air units also apply to similar steel frame, wire screen, heavy-duty prefilters.

13. Stack and ductwork systems normally located downstream of air-cleaning equipment caused significant attenuation in peak shock pressures. For the structures involved in this study approximately 70% attenuation took place.

14. Analyses of test results indicate sufficient similarity to previous laboratory shock-tube tests to verify that laboratory-scale experiments can yield predictable and reliable results for field applications.

Table 1—SUMMARY OF SHOCK-TUBE FILTER TESTS

Filter type*	Shock pressure, psi	Duration of positive phase,† msec	Total impulse,‡ psi-msec	Initial filter loading, g	Dust loss, g	Calculated equivalent nuclear explosion§ Distance, ft	Calculated equivalent nuclear explosion§ Yield, kt	Effects
D	0.5							Moderate damage
D	1.5							Complete failure
AEC-6	2.1	720	605			4800	3.5	No damage
AEC-6	3.1	860	1070			5600	14	Partial failure
AEC-6	6.0	860	2060			5200	30	Complete failure
AEC-6	1.7	660	430	155	152	6500	7	98% dust removal
AEC-6	1.9	850	650	26	8	7600	13	32% dust removal
AEC-12	2.5	790	790	429	359	6800	13	84% dust removal
AEC-12	2.4	760	730	39	20	5350	8	51% dust removal

*D is a Dust-Stop Fiberglas filter (20 by 20 by 2 in., 800 cu ft/min rated capacity); AEC-6 is a pleated-paper filter (24 by 24 by 6 in., 500 cu ft/min rated capacity); and AEC-12 is a pleated-paper filter (24 by 24 by 12 in., 1000 cu ft/min rated capacity).

†No negative-pressure phase observed.

‡Summation of area under pressure–time curve.

§Based upon unpublished data of Sandia Corporation.

Table 2—FILTRATION DEVICES AND LOCATIONS IN SIMULATED VENTILATION SYSTEMS

Hood	Prefilter	Final filter	Blowoff afterfilter
1	Dust-Stop* (20 X 20 X 2 in.)	12-in. AEC†	
2	Far-Air‡ (20 X 20 X 2 in.)	6-in. AEC†	
3	Dust-Stop* (20 X 20 X 2 in.)	12-in. AEC†	
4		12-in. AEC†	Far-Air§,¶
5		6-in. AEC†	
6	Dust stop*,¶ (20 X 20 X 2 in.; electrostatic-precipitator plates)	12-in. AEC*	

*Clean.

†Loaded.

‡Oiled, clean.

§Dry, clean.

¶Not installed in chemical plant.

Table 3—PEAK-PRESSURE MEASUREMENTS IN TEST BUILDINGS

	Chemical-plant control room			Concrete house		
Location*	Gauge	Peak pressure, psig	Percentage of peak pressure, %	Gauge	Peak pressure, psig	Percentage of peak pressure, %
Roof	P-1	4.0	100	P-15	1.9	100
Stack	P-2	⟵ No record ⟶		P-16	1.2†	63
Breeching	P-3	2.9	72	P-17	1.3	68
Room	P-4	1.1†	27	P-18	0.59	31
Hood 1U	P-5	1.4†	35	P-19	0.57	30
Hood 1D	P-6	1.2	30	P-20	0.55	29
Hood 2U	P-7	1.2	30	P-21	0.55	29
Hood 3U	P-8	1.2	30	P-22	0.54†	28
Hood 3D	P-9	1.2	30	P-23	0.63	33
Hood 4U‡	P-10	1.0	25	P-24	0.51	27
Hood 4D	P-11	1.4†	35	P-25	0.60	32
Hood 5U	P-12	1.6	40	P-26	0.54	28
Hood 6U	P-13	1.1	27	P-27	0.67	35
Hood 6D	P-14	1.3	32	P-28	0.54	28

*U refers to upstream of AEC filter and D refers to downstream of AEC filter (relative to shock front).

†Peak pressure only; no pressure–time trace.

‡Peak pressure upstream and downstream of Far-Air afterfilter.

Table 4—DUST LOSSES FROM AIR-CLEANING EQUIPMENT AND RECOVERY BY HOOD AND PREFILTER SYSTEMS

		AEC filters					Hood dust recovery		Prefilter dust recovery				Dust loss to building, %	
			Preshot dust load		Dust loss									
Hood	Peak pressure upstream, psi*	Size†	Total grams	Grams per sq ft surface	Grams	Preshot load, %	Total grams	AEC filter loss, %	Type	Grams	AEC filter loss, %	Filter efficiency, %	Preshot loading	Dislodged material
						Chemical-plant control room								
1	1.4	12	744	3.7	557	75	145	26	D‡	109	20	26	41	54
2	1.2	6A	357	3.6	306	86	57	19	F§	90	29	36	45	52
3	1.2	12	575	2.9	331	58	140	42	D	75	23	39	20	35
4	1.0	12	554	2.8	294	53	89	30					37	70
5	1.55	6	213	2.1	155	73	20	13					63	87
6	1.4	No data, equipment not installed												
							Concrete house							
1	0.64	12	548	2.7	224	41	77	34	D	73	33	50	14	33
2	0.64	6	212	2.1	110	52	34	31	F	47	43	62	14	26
3	0.54	12A	826	4.1	460	56	169	37	D	116	25	40	21	38
4¶	0.64	12	585	2.9	26	4.5	15	58					2	42
5	0.67	6A	275	2.8	177	64	73	41					38	59
		Electrostatic-precipitator dust load												
			Total grams	Grams/plate										
6	0.76	Dry	1.25	0.073	1.18	94	Not measurable		D	Not valid**				
6	0.76	Oiled	3.74	0.22	0	0††								

*Indicates peak pressure immediately in front of AEC filter.

†6 and 12 refer to 500 and 1000 cu ft/min capacity filters, respectively; A indicates all-glass media.

‡D refers to Dust-Stop prefilter.

§F refers to lubricated Far-Air prefilter.

¶Far-Air afterfilter located 9 in. in front of 12-in. AEC filter.

**Weight gain, 3 g, exceeded electrostatic-precipitator weight loss. Actual gain due to backflow of dusty room air.

††Laboratory analyses indicated weight gain. Attributed to backflow of dusty air from room.

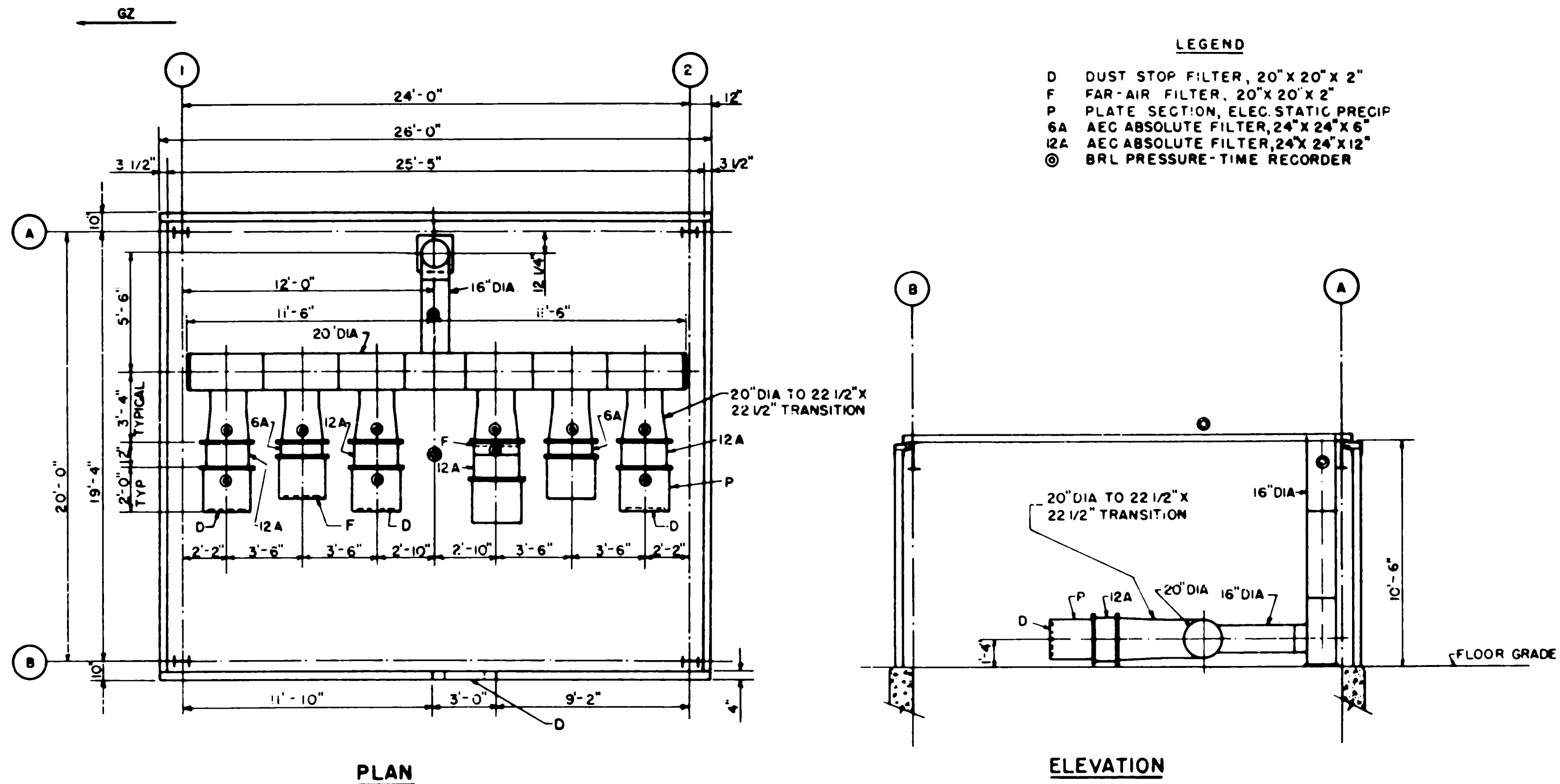

Fig. 1—Schematic diagram of ventilation system in chemical plant.

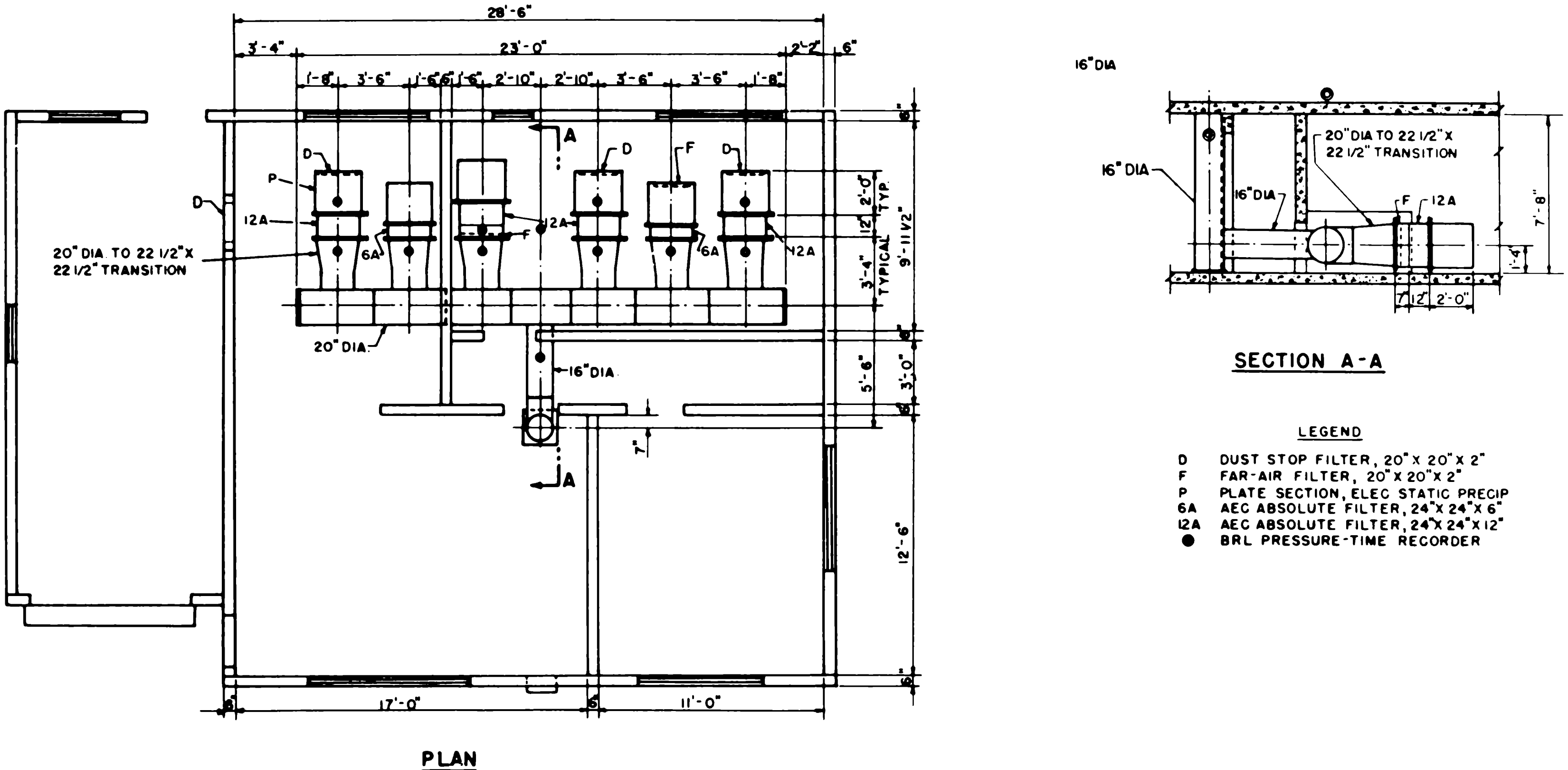

Fig. 2—Schematic diagram of ventilation system in concrete house.

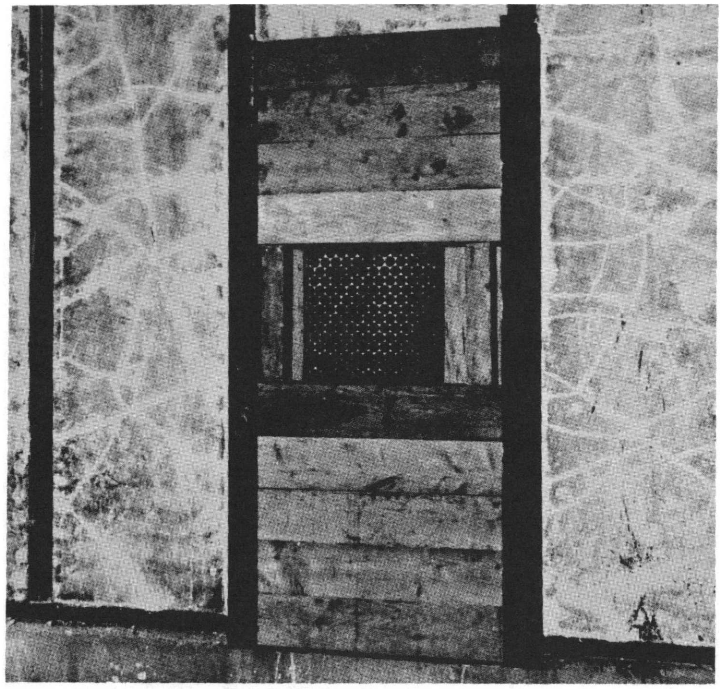

Fig. 3—Door closure and Dust-Stop filter in control room of chemical plant.

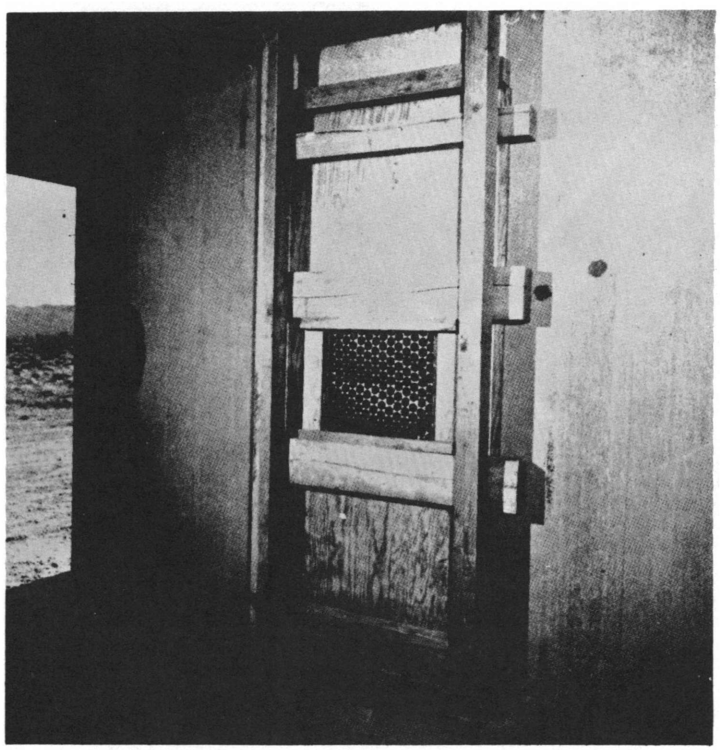

Fig. 4—Door closure and Dust-Stop filter in concrete house.

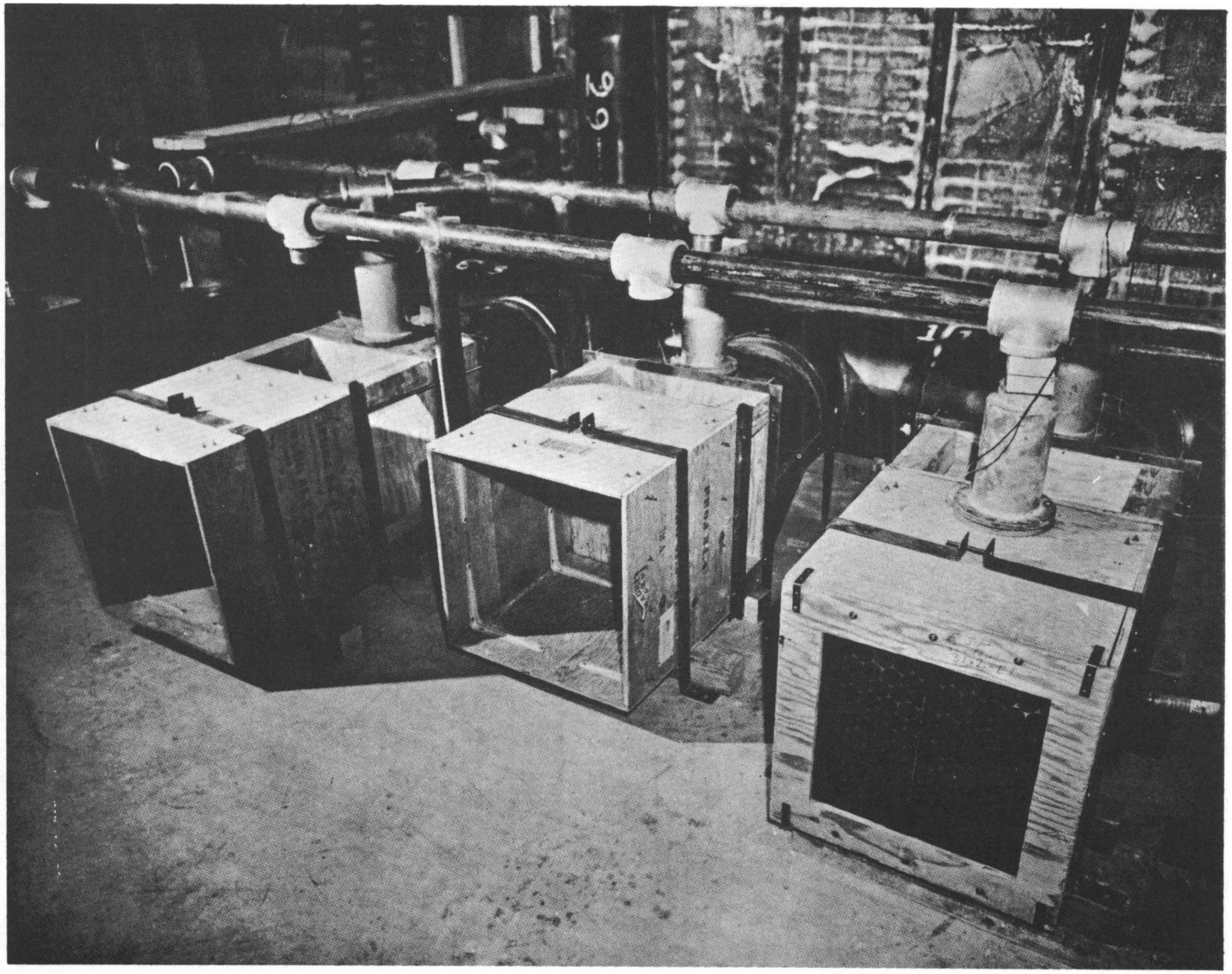

Fig. 5—Ventilation system in chemical plant, preshot.

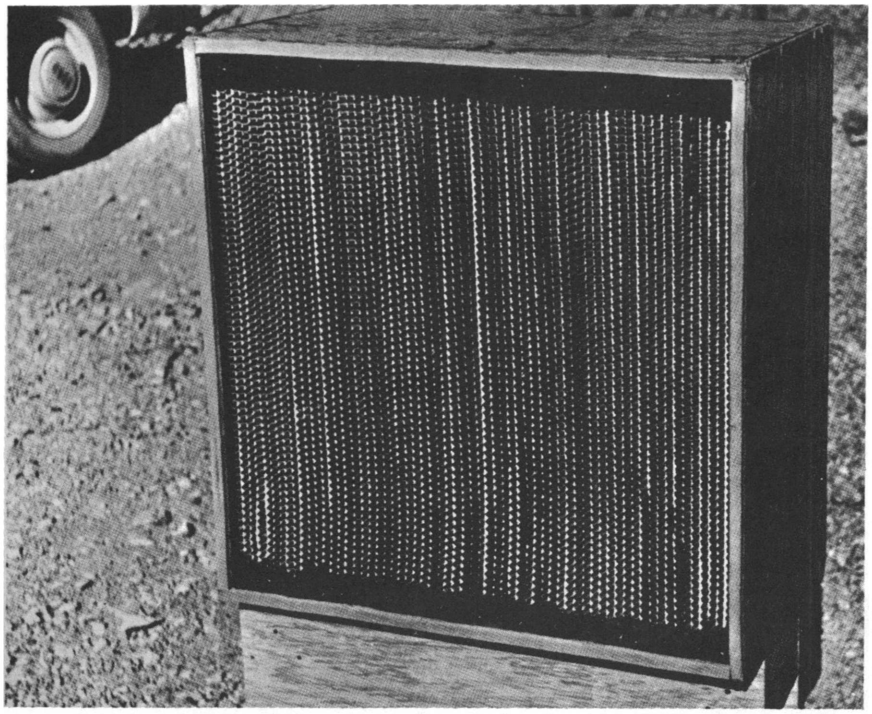

Fig. 6—AEC filter.

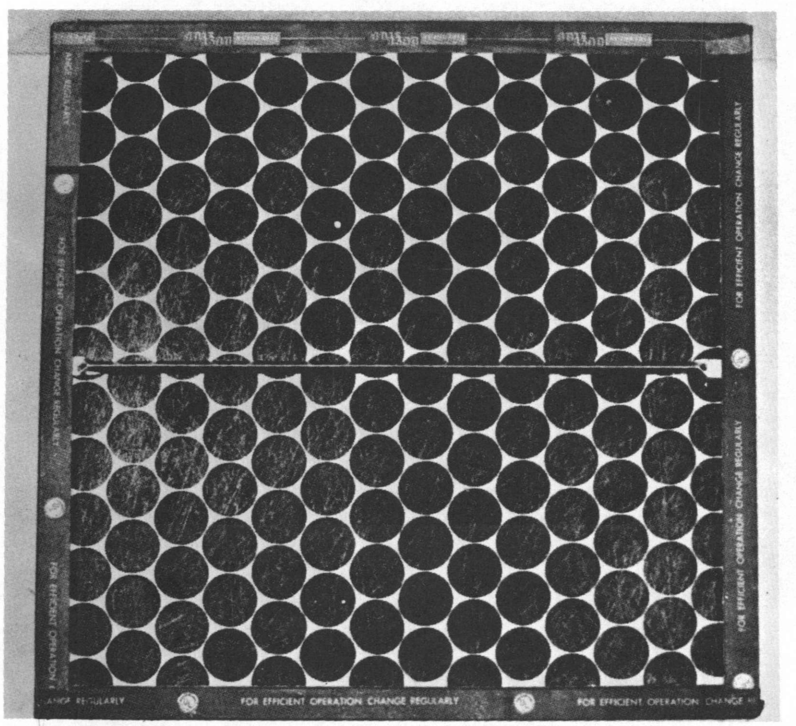

Fig. 7—Dust-Stop prefilter.

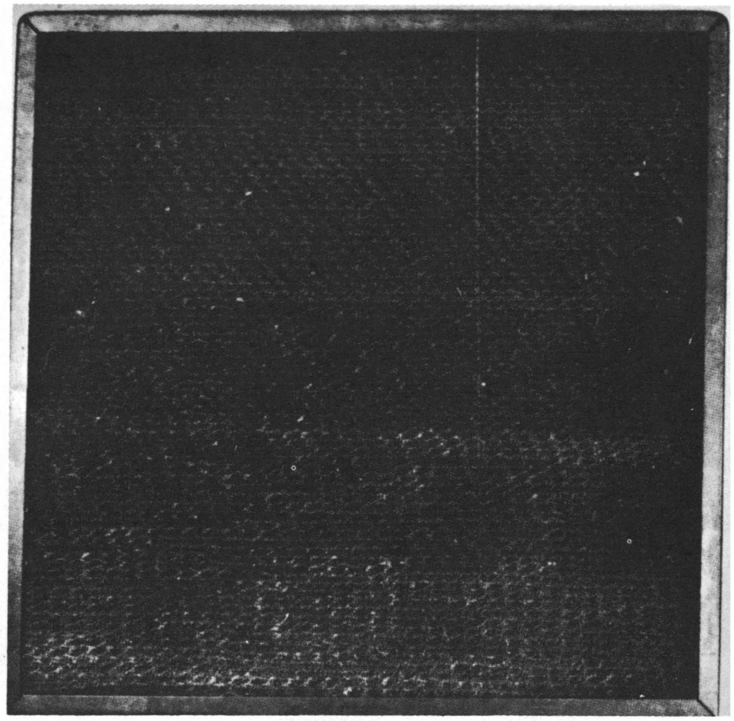

Fig. 8—Far-Air filter.

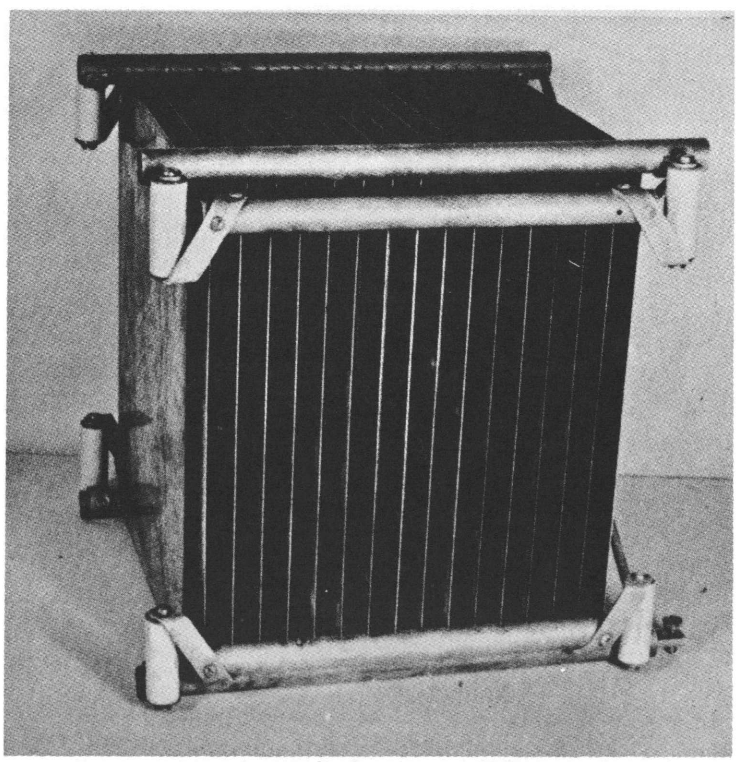

Fig. 9—Electrostatic-precipitator collecting stage.

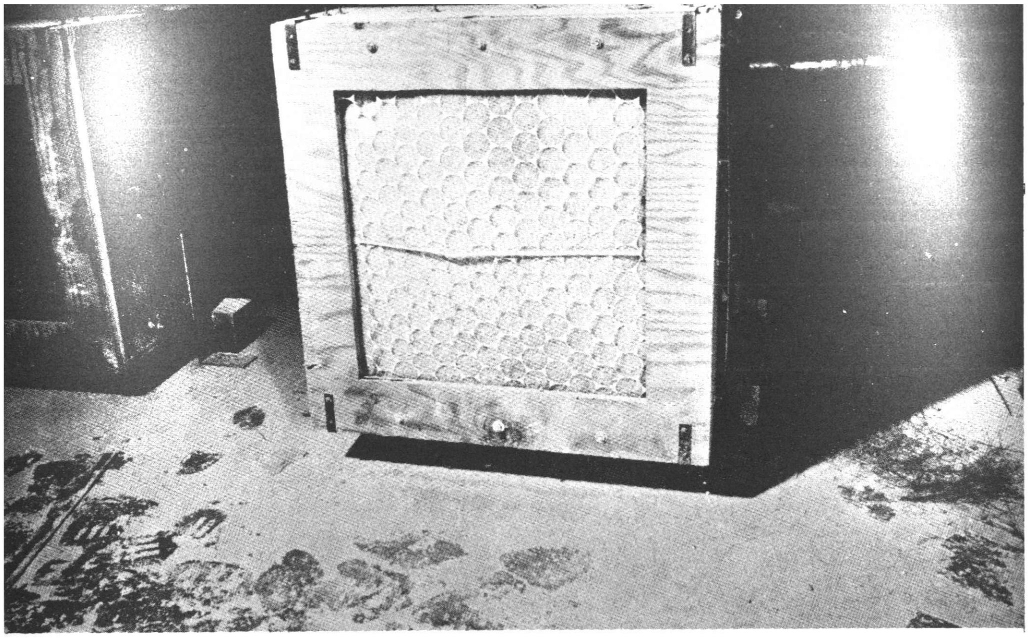

Fig. 10—Dust-Stop filter in hood 3 in chemical plant, postshot.

Fig. 11—Dust-Stop filter debris in chemical plant, postshot.

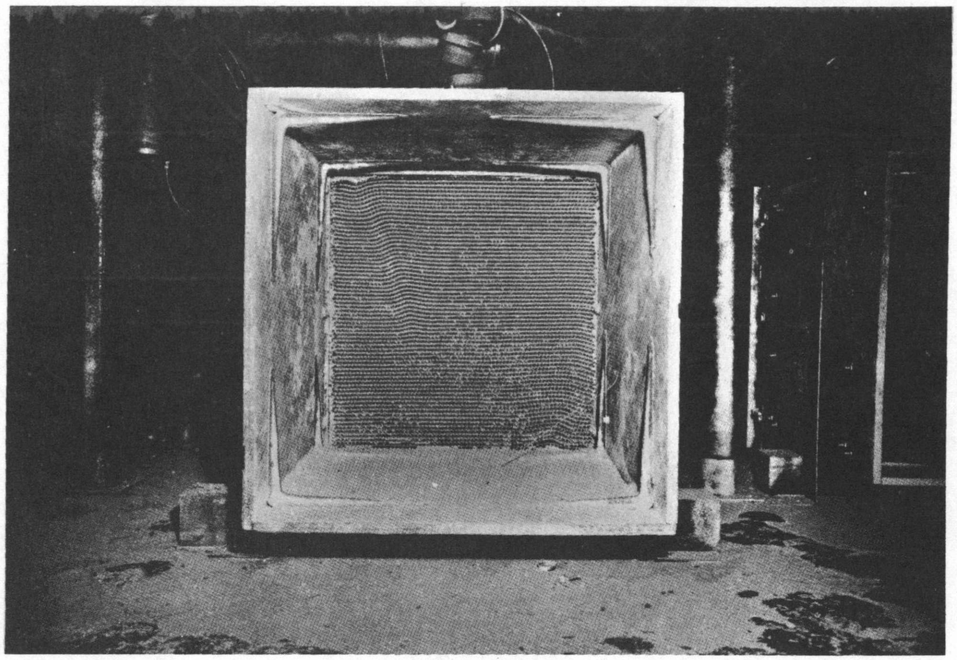

Fig. 12—Dust loss from 12-in. AEC filter in hood 4 in chemical plant, postshot.

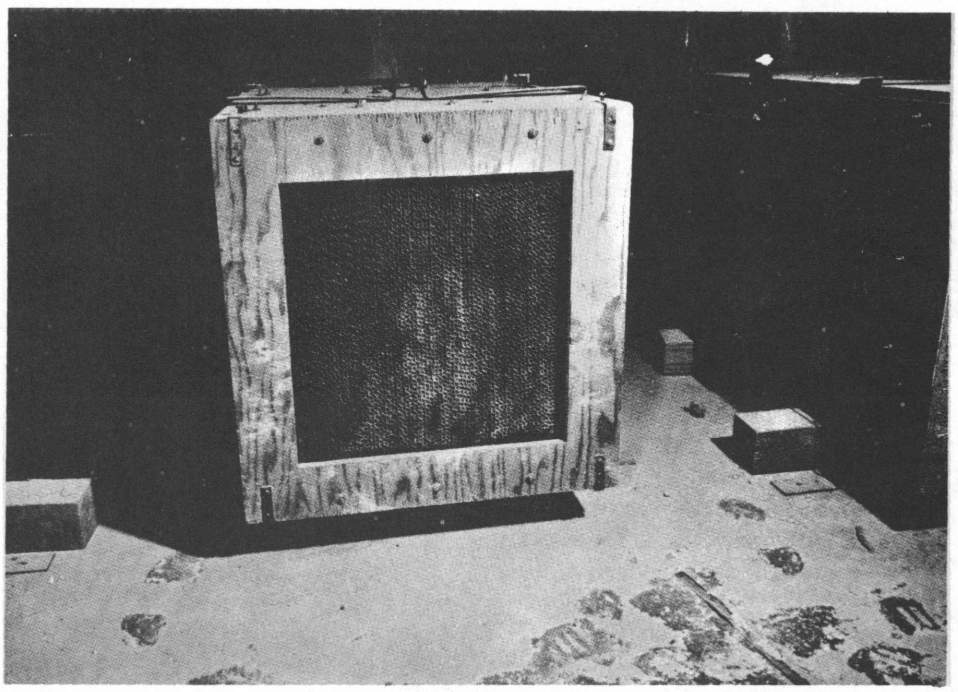

Fig. 13—Far-Air filter in hood 2 in chemical plant, postshot.

SUMMARY 31

RESPONSE OF EARTH-CONFINED FLEXIBLE-ARCH STRUCTURES IN HIGH-OVERPRESSURE REGIONS

(Report WT-1626, Operation Hardtack, Project 3.2, same title, by J. C. LeDoux, LCDR, CEC, USN, Project Officer, and P. J. Rush, U. S. Naval Civil Engineering Laboratory, Port Hueneme, Calif., Jan. 22, 1961.)

OBJECTIVES AND SCOPE

An objective of this project was to determine structural responses and failure criteria of earth-confined corrugated-steel flexible arches subjected to high-overpressure blast loadings from nuclear detonations. A flexible arch is considered here to be an arch structure whose ultimate supporting capacity is dependent upon confinement within a surrounding earth configuration.

A collateral objective was to determine the radiation-shielding effectiveness of such structures with a minimum cover of 5 ft of coral sand.

Because the soil and groundwater conditions at the Eniwetok Proving Ground (EPG) did not permit the steel arches to be placed below natural grade level, the structures were confined within massive non-drag-sensitive earthwork configurations of coral sand. Empirical determinations were made of the responses of (1) three earth-confined prefabricated corrugated-steel flexible arches when subjected to long-duration blast loadings from Koa shot, a megaton-range detonation (ref. ENW, p. 675), and (2) one similar earth-confined flexible arch when subjected to blast loadings of relatively short duration from a kiloton-range detonation, Cactus shot (ref. ENW, p. 675).

Figures 1 and 2 show test layouts for Cactus and Koa shots, respectively.

The effectiveness of corrugated-steel arches of commercially available design within various earthwork configurations when subjected to short-duration blast loads of up to about 60 psi had been determined during Operations Upshot-Knothole (Summary 6, WT-729), Teapot (Summary 11, WT-1128), and Plumbbob (Summary 17, WT-1422). Previous test results are summarized in Table 1.

TEST STRUCTURES AND PROCEDURE

Three of the structures (3.2a, 3.2b, and 3.2c) consisted basically of corrugated-steel, arch-type Navy stock ammunition-storage magazines, of 25-ft span and 48 ft length with certain modifications. The arch configurations of these structures consisted of bolted 10-gauge curved corrugated-steel panels of the properties listed in Table 2. No ribs or other framing members were used. Design details of a typical 25-ft-span test structure are shown in Figs. 3 and 4; Figs. 5 and 6 are photographs of the test structures.

Structure 3.2d consisted of a specially fabricated corrugated-steel arch approximately 38 ft in span and 40 ft long (Fig. 7). Entrance tunnel arrangements for the structure were the same as those used for structures 3.2a, 3.2b, and 3.2c.

Coral sand obtained from the excavations and additional coral sand from other areas of the same island sites were used for the earthworks (Figs. 8 and 9). These coral sands had an average density of only 78 lb/cu ft, contained quantities of tiny seashells, and were generally lacking in useful structural qualities; but no other types of soil were available. Most of the earthwork was placed in 1-ft lifts; each lift was soaked with seawater and compacted with bulldozers.

RESULTS

Table 3 is a summary of important blast and structural data related to all four of the test structures.

Short-pulse Blast Loading, Structure 3.2a, Cactus Shot

Structure 3.2a on site Yvonne was subjected to a short-pulse (0.440-sec) blast loading of 85-psi overpressure generated by Cactus shot. Notable information obtained from the recovery excavation of structure 3.2a follows:

1. An extensive transverse rupture at a bolted seam of the arch shell (Fig. 10) had occurred 8 ft rearward of the midlength (midpoint) and 16 ft forward of the rear end wall. This rupture extended from the floor, on the side away from Ground Zero (GZ), vertically to a point that had originally been 3 ft from the arch crown on the GZ side.
2. A large amount of sand entering the structure through this extensive rupture had formed a cone-shaped pile approximately 9 ft high and 15 ft in diameter at the base.
3. The arch had separated from the front wall for a distance of approximately 2 ft. Sand entered at this point to form a pile 2 ft high and 4 ft wide at the base.
4. Scratch-gauge records indicated that the initial translation of the arch was almost directly forward at the crown for a distance of 8 to 9 in., whereas points at 45° on both sides of the arch moved almost directly downward for 4 to 5 in.
5. The footing on the GZ side had moved downward 3½ in. The movement of the footing away from GZ could not be determined.
6. Most panels in the bottom row, on the side away from GZ, had torn loose from the next higher panels but were still attached to bottom channel members, which remained bolted to the concrete footing. The bottom panels had rotated inward around their bottom anchorage, and some panels were lying on the deck.
7. Corrugations in some panels were partially flattened, but most corrugations were not badly deformed.

Long-pulse Blast Loadings, Structures 3.2b, 3.2c, and 3.2d, Koa Shot

Structure 3.2b was subjected to a 78-psi overpressure loading of 1.50 sec positive-phase duration. Reconnaissance made within 7 days after the detonation indicated that complete and apparently symmetrical collapse of the corrugated-steel arch had occurred, and a large quantity of sand had entered the building (Figs. 11 and 12). The dome-shaped steel hatch cover was not damaged, and fastening dogs were loosened without difficulty. The concrete hatch enclosure was not damaged, and the 4-ft-diameter corrugated-steel-pipe entrance tunnel was not noticeably deformed.

Structure 3.2c was subjected to a 180-psi overpressure loading of at least 2.24 sec duration. Reconnaissance made within 7 days after the detonation showed that complete and apparently symmetrical collapse of the steel arch had occurred (Fig. 13). Previous reconnaissance showed that the earthwork configuration had been washed with a water wave, and a large depression had formed over the projected area of the structure. The entrance hatch, when cleared of some 2 ft of sand, was found undamaged. The 4-ft-diameter entrance tube had collapsed to a vertical height of 1½ ft at the point of joining to the arch

structure. The axial load on the vertical end-wall sections from the edge of the arch shell apparently caused this tunnel collapse.

The steel arch had completely collapsed symmetrically about the crown and most generally at the center, with a lesser degree of deformation close to both end walls (Fig. 13). These end walls were still in a generally vertical condition, although the panels of the walls had separated and were bent.

Structure 3.2d (38-ft span) was subjected to 83-psi overpressure forces with a positive-phase duration of 1.40 sec. Deformation had occurred symmetrically about the crown (Figs. 14 and 15). The front and rear end walls had apparently failed before the steel arch had collapsed. A large quantity of the backfill sand had flowed into the structure through the end-wall openings (Fig. 15); this interior sand may have in some degree restricted the collapse of the steel arch. There was no failure of any horizontal or vertical bolted seams in the arch structure. All the anchor bolts holding the bottom channel members of the arch to the concrete foundation footing had sheared and pulled out of the footing; so the arch was in effect free of any restraint except the passive resistance of the surrounding soil. The concrete foundation footings had been displaced and were cracked and broken.

The hatch was covered with approximately 6 ft of sand, which was removed by bulldozer and hand shovels, but no damage to hatch, hatch structure, or entrance tunnel was noted.

Conclusions

Smaller Steel Arches

The 25- by 48-ft 10-gauge corrugated-steel arch structure (3.2a), confined within a non-drag-sensitive earthwork of coral sand, collapsed on the side away from GZ when subjected to an 85-psi overpressure loading of 0.440 sec duration generated by an 18-kt surface detonation. Based on localized but extensive damage, it can be estimated that 100% personnel casualties and 25% equipment casualties probably would have resulted if the structure had been used as a blast- and radiological-effects shelter.

An identical earth-confined steel-arch structure (3.2b) completely collapsed when subjected for a duration of 1.50 sec to a 78-psi overpressure loading generated by a 1.31-Mt surface detonation. Another identical earth-confined steel-arch structure (3.2c) completely collapsed when subjected to 180-psi overpressure loadings for a duration of 2.24 sec. Both of the above structures suffered extensive separations at the bolted joints of their component panels; the geometries of the arches were completely flattened. If these two structures had been used as blast and radiological shelters, it is estimated that 100% personnel and equipment casualties would have resulted.

All three of the above-described corrugated-steel arches had experienced loadings that caused responses in the compression mode. At some period during the loading phases, the arches suffered loss of integrity caused by failure of the component steel panels at the horizontal bolted joints. The degree of collapse damage appeared to be a function of the duration of loading.

Larger Steel Arch

The specially designed and fabricated 1-gauge corrugated-steel arch structure of 38-ft span and 40-ft length (3.2d), confined within a non-drag-sensitive earthwork of coral sand, was subjected for a duration of 1.40 sec to an 83-psi blast overpressure generated by a 1.31-Mt surface detonation. The arch suffered complete deformation in the form of reversals of curvature on both sides of the crown. If this structure had been used as a blast- and radiological-effects shelter, it is estimated that 100% personnel casualties and 75% equipment casualties would have been suffered.

Direction of Forces

The deflection records obtained and the damaged condition of all four steel arches indicated that the principal loading forces were downward in the vertical direction. No evidence of important horizontal forces upon the structures was found. Thus, it may be concluded that the shapes and dimensions of the confining earthworks were such as to attenuate in large degree the drag dynamic forces generated by the detonations.

Confining Soil

The coral beach sand used in constructing the confining earthworks was greatly deficient in density, cohesion, shear strength, and compactability, all qualities contributing to an efficient soil structure. This material, however, had to be used for lack of anything better.

Foundation Footings

The concrete foundation footings of all four steel-arch structures were damaged by cracking and spalling in varying degrees. All had displaced downward as they had been designed to do, and all had been tilted outward. It was concluded that the foundations came closer to resisting applied loads than did the steel-arch structures they supported.

Table 1—TESTS OF CORRUGATED-STEEL FLEXIBLE STRUCTURES

Operation and shot	Structure	Exposure condition	Overpressure, psi	Dynamic pressure, psi	Damage
Upshot-Knothole Shot 9	Upshot-Knothole 3.15	Surface structure; 3-ft earth cover on sides of arch (lake-bed silt)	10.8	*	Elastic response; door projected into structure
Upshot-Knothole Shot 10	Upshot-Knothole 3.15	Surface structure; 3-ft earth cover on sides of arch (lake-bed silt)	8.1	*	Elastic response; no significant damage
Teapot Shot 12	Upshot-Knothole 3.15	Surface structure; 3-ft earth cover on sides of arch (lake-bed silt); crown exposed flush with surface of earth cover	13.0	33.0	No significant damage
Teapot Shot 12	Teapot 3.6	Surface structure; 3-ft earth cover (granular material); moderately wide earth berm	30.0	150.0	Side of arch toward GZ collapsed; not operational; 50 to 100% personnel casualties estimated
Plumbbob Priscilla shot	Plumbbob 3.3a	Semi-buried; equal cut-and-cover–5-ft	100	*	No significant damage
	Plumbbob 3.3b	earth cover over crown (gravelly,	58	*	No significant damage
	Plumbbob 3.3c	silty sand)	56	*	No significant damage

*Not recorded.

Table 2—PROPERTIES OF CORRUGATED-STEEL PLATES

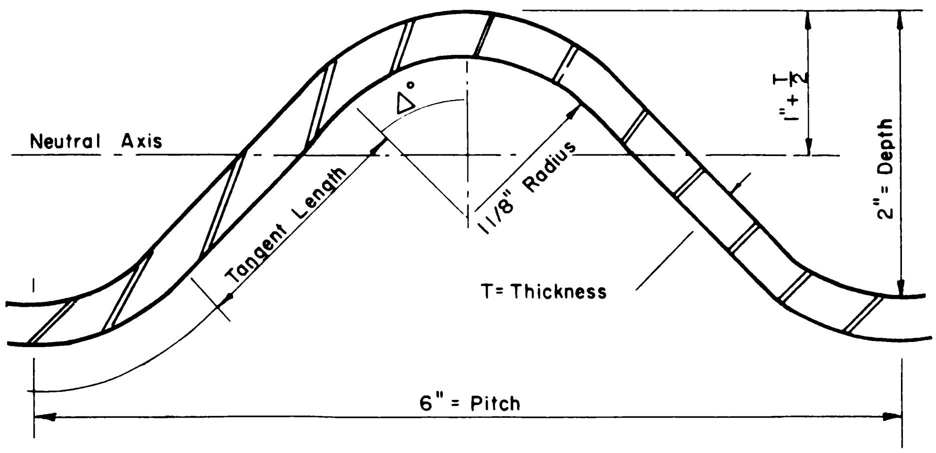

	10-gauge	8-gauge	1-gauge
Thickness, in.	0.1345	0.1644	0.2758
Tangent length, in.	1.8606	1.8283	1.7019
Angle, degrees and minutes	44°00′	45°00′	46°05′
Moment of inertia, in.^{4}*	0.0781	0.0961	0.1659
Area of section, sq in.*	2.003	2.415	4.120
Section modulus, cu. in.^{3}*	0.0732	0.0888	0.1458
Radius of gyration, in.	0.684	0.686	0.695

*Per foot of horizontal length of structure.

Table 3—SUMMARY OF STRUCTURAL TEST RESULTS

	Structure 3.2a Station (322.01)	Structure 3.2b Station (322.02)	Structure 3.2c Station (322.03)	Structure 3.2d Station (322.04)
Span of structure, ft	25	25	25	38
Gauge of steel arch sections	10	10	10	1
Gauge of end walls	8	8	8	3
Earth over crown of structure, ft	5	5	5	5
Code name of shot	Cactus	Koa	Koa	Koa
Site of device	Yvonne	Gene	Gene	Gene
Site of structure	Yvonne	Irene	Helen	Irene
Yield predicted	13 to 17 kt	1.25 to 2.25 Mt	1.25 to 2.25 Mt	1.25 to 2.25 Mt
Approximate yield reported	18 kt	1.31 Mt	1.31 Mt	1.31 Mt
Distance from GZ, ft	980	4470	3200	3950
Overpressure predicted, psi	75*	75†	200†	100†
Overpressure measured, psi	85	78	180	83
Duration positive phase, sec	0.440	1.51	2.24	1.4
Arrival time, sec	0.141	0.86	0.20	0.635
Dynamic pressure, psi	‡	‡	‡	‡
Maximum internal pressure, psi	2.9	23.0	34.5	5.2
Maximum vertical acceleration of floor slab, g§	+7.0 −3.19	‡	‡	‡
Maximum horizontal acceleration of floor slab, g¶	+3.6 −1.76	‡	‡	‡
General postshot conditions	Collapse on side away from GZ	Complete (symmetrical) collapse with separation of panels at bolted joints	Complete (symmetrical) collapse with separation of panels at bolted joints	Collapse (symmetrical) to severely deformed shape

*On basis of 15-kt yield.
†On basis of 1.5-Mt yield.
‡Not available.
§ + indicates upward acceleration; – indicates downward acceleration.
¶ + indicates direction away from GZ; – indicates direction toward GZ.

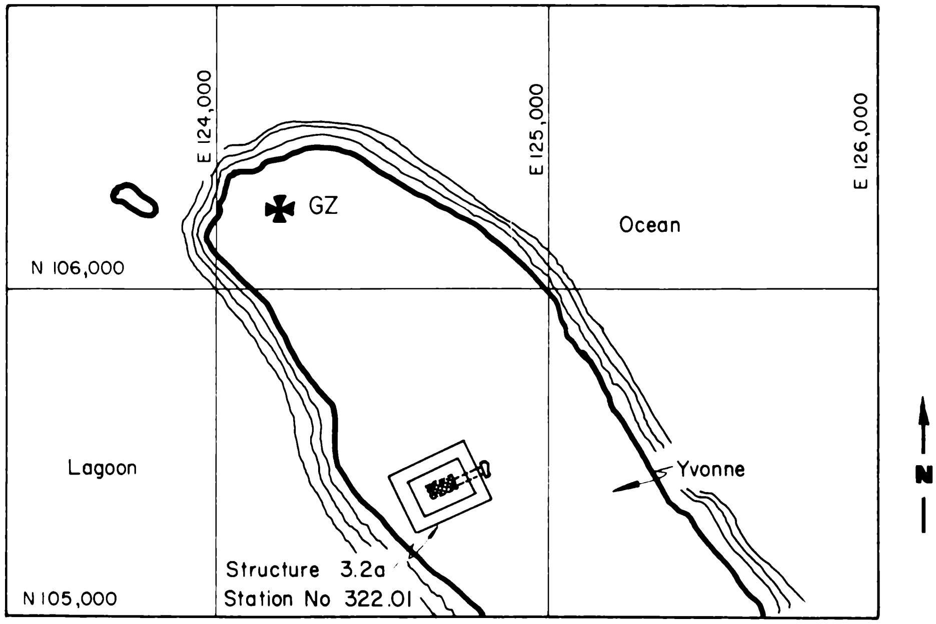

Fig. 1—Plot plan for Cactus shot.

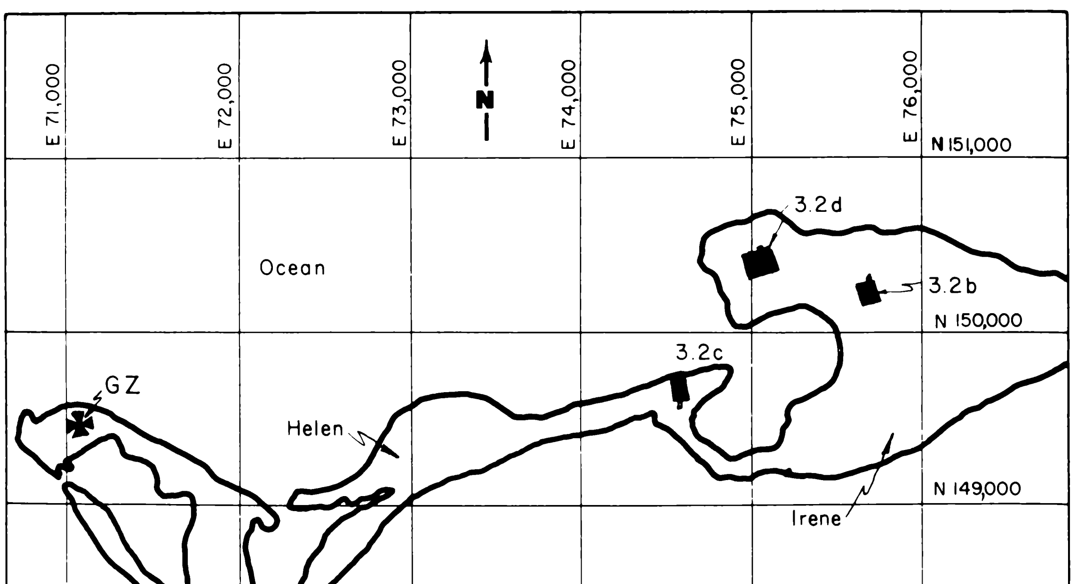

Fig. 2—Plot plan for Koa shot.

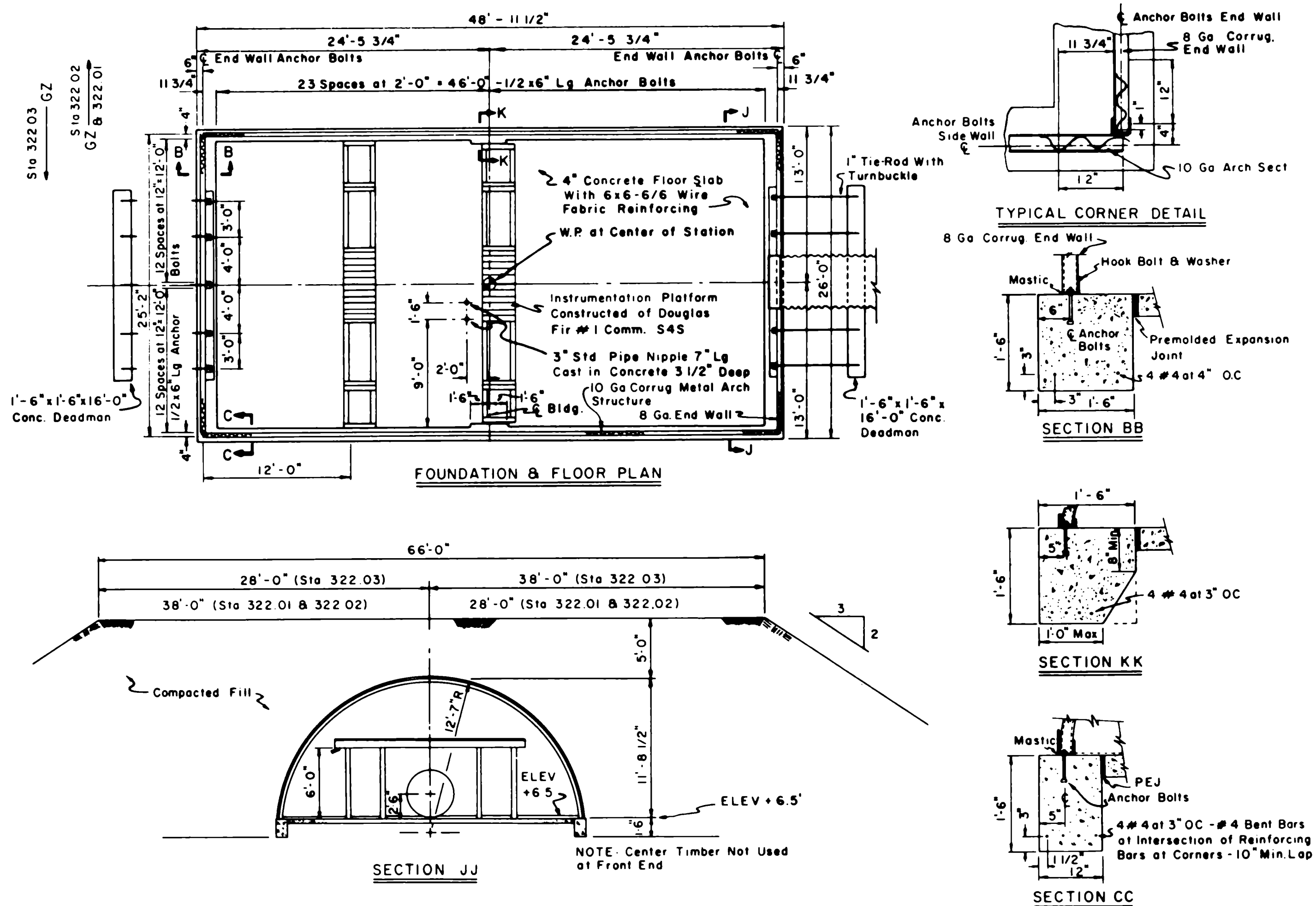

Fig. 3—Plan and details of typical 25-ft-span test structure.

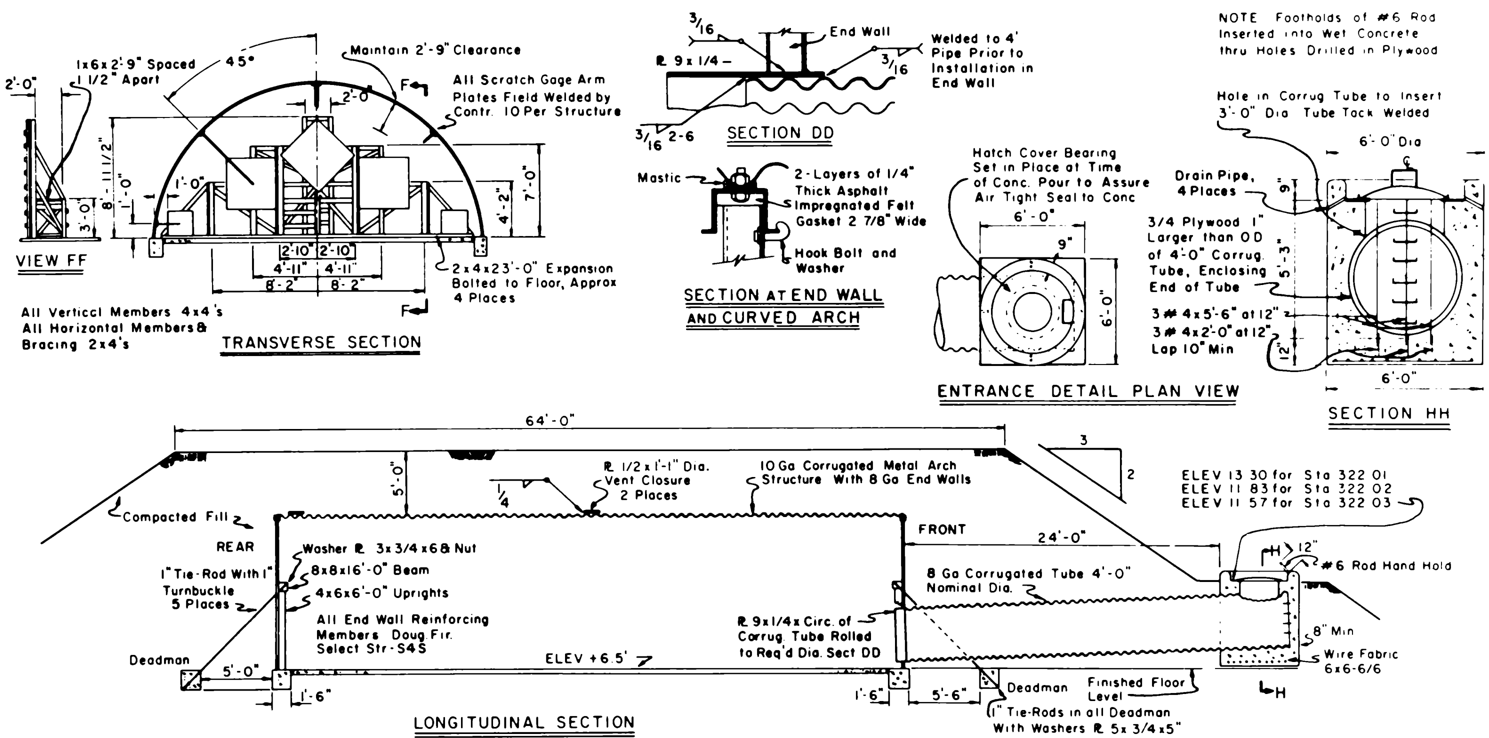

Fig. 4—Section and details of typical 25-ft-span test structure.

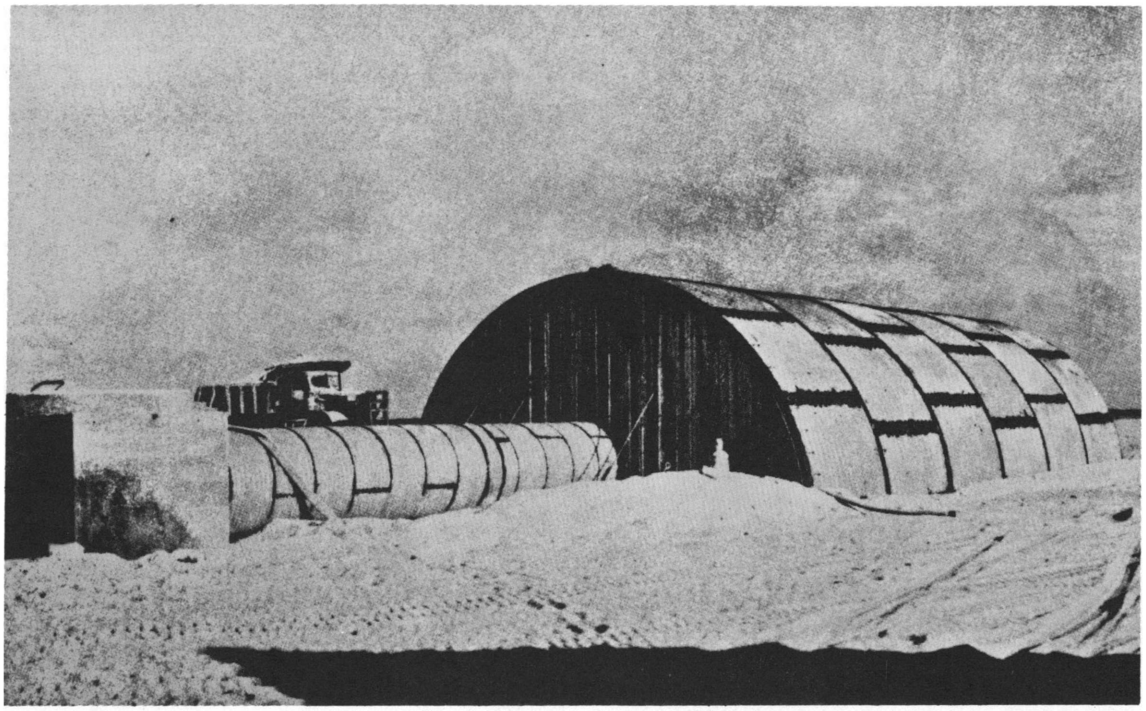

Fig. 5—Entrance-tunnel arrangement, structure 3.2c.

Fig. 6—Typical entrance to test structure. This was intended to furnish access for purposes of the test operation; it was not designed for all protective purposes.

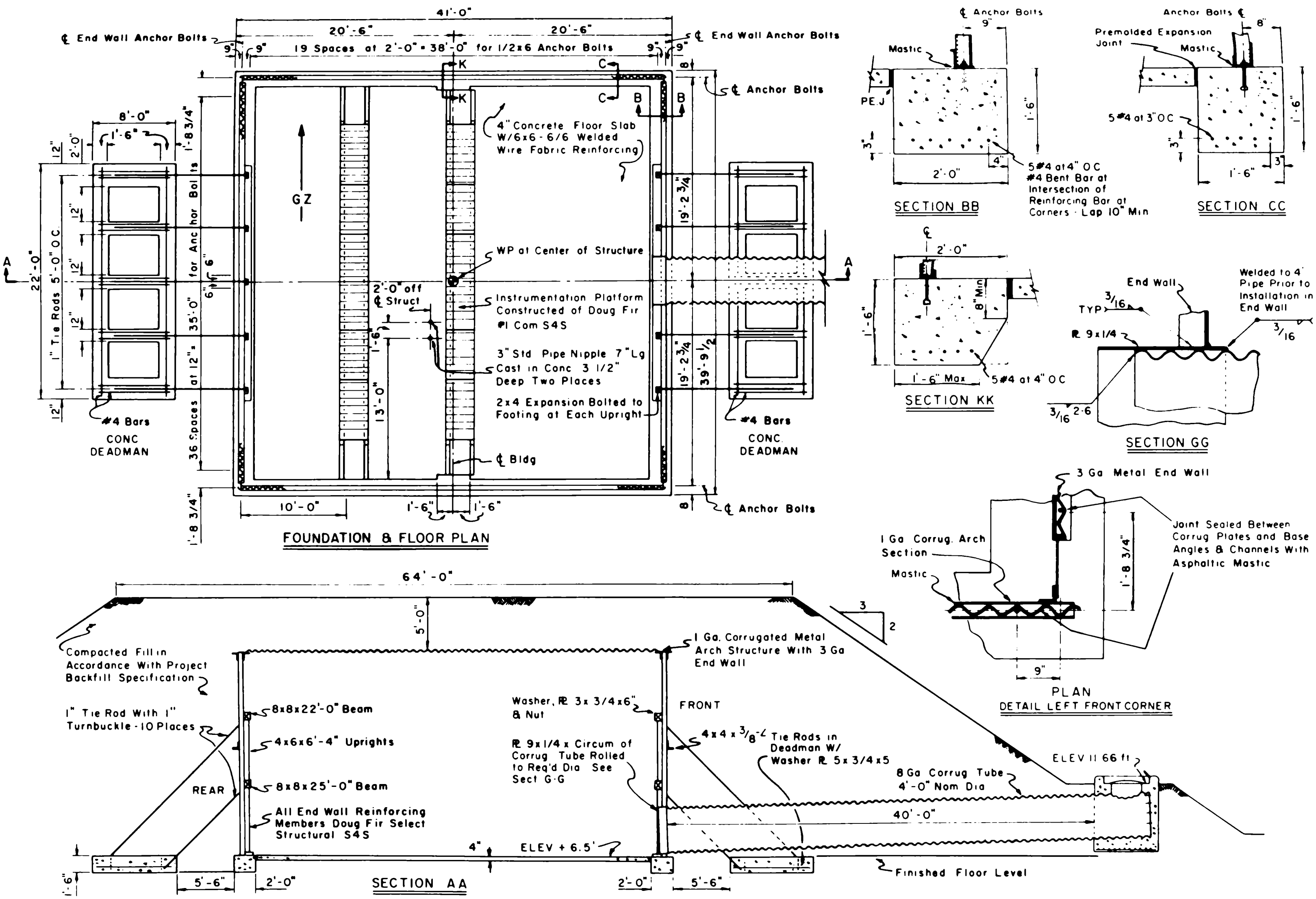

Fig. 7—Plan and section of 38-ft-span test structure.

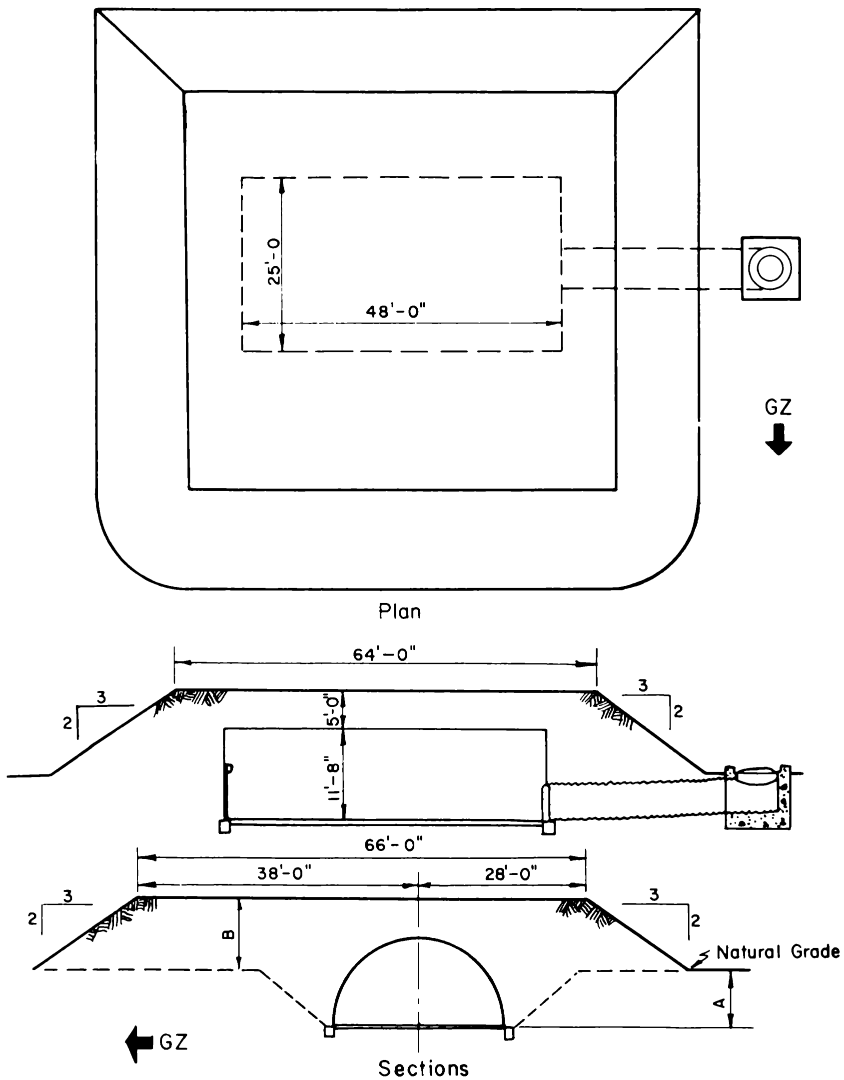

Fig. 8—Earth configuration, 25-ft-span structure. For structure 3.2a, A = 5.0 ft, B = 12 ft; for 3.2b, A = 3.0 ft, B = 14 ft; and for 3.2c, A = 1.5 ft, B = 15.5 ft.

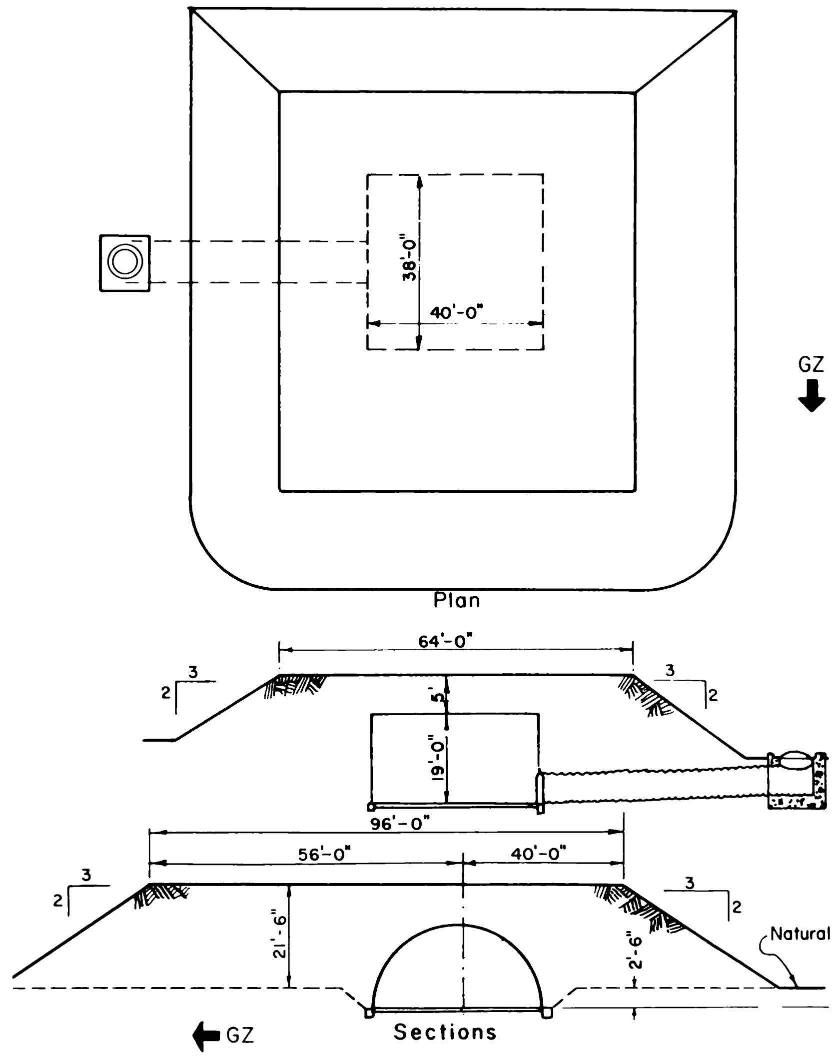

Fig. 9—Earth configuration, 38-ft-span structure.

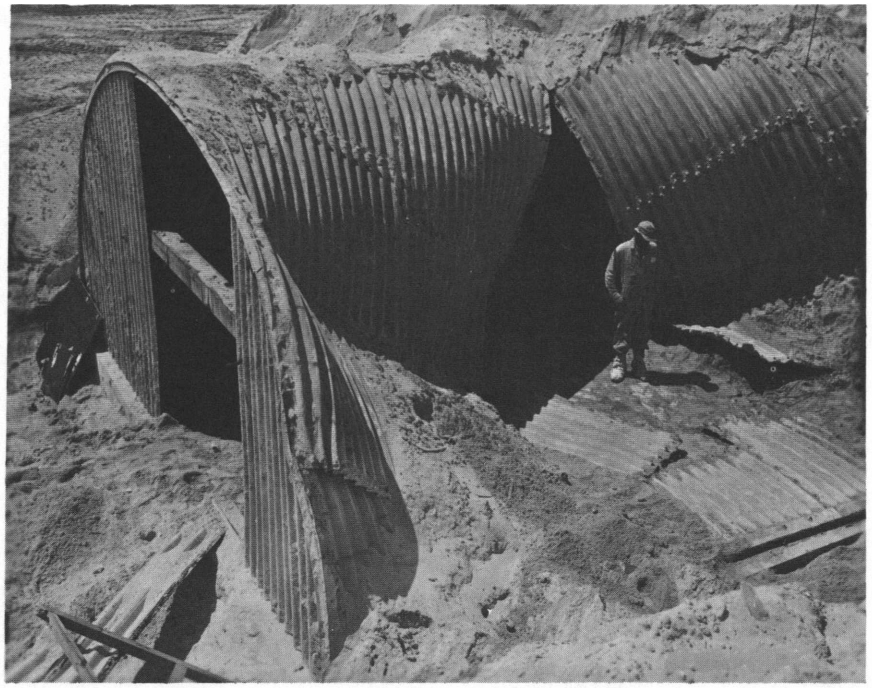

Fig. 10—Structure 3.2a, postshot, showing deformed section of structure on side away from GZ after excavation for examination. End-wall sections had been removed so that sand could be removed from within the structure more easily.

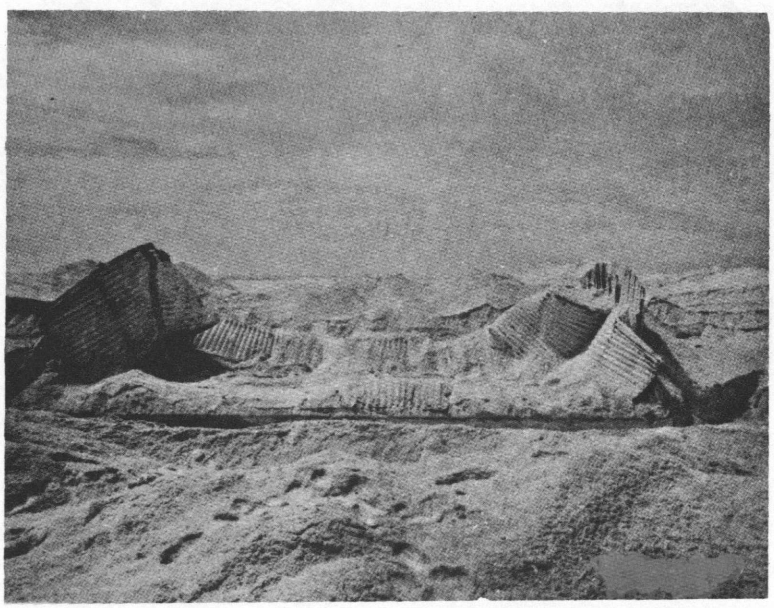

Fig. 11—Structure 3.2b, side view, looking toward GZ.

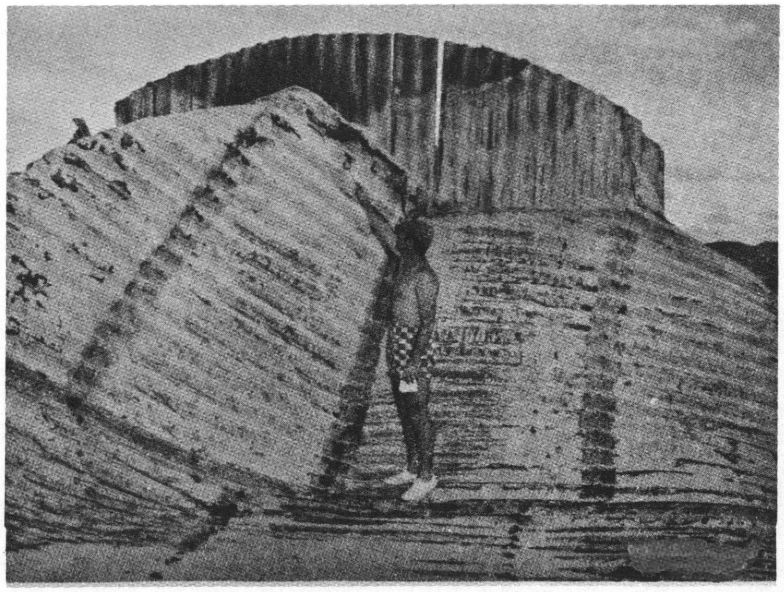

Fig. 12—Structure 3.2b, position of original crown of arch shell after collapse; end wall remained upright; GZ to left.

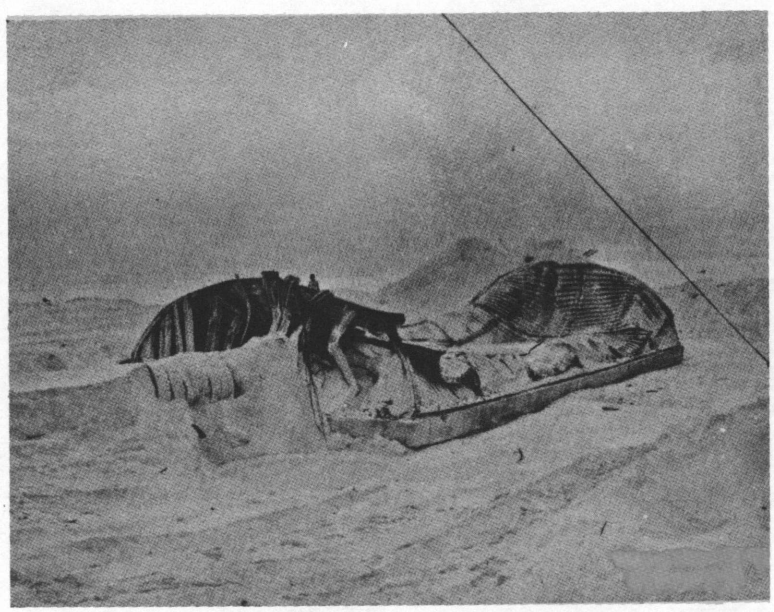

Fig. 13—Structure 3.2c, damaged end walls; GZ to left.

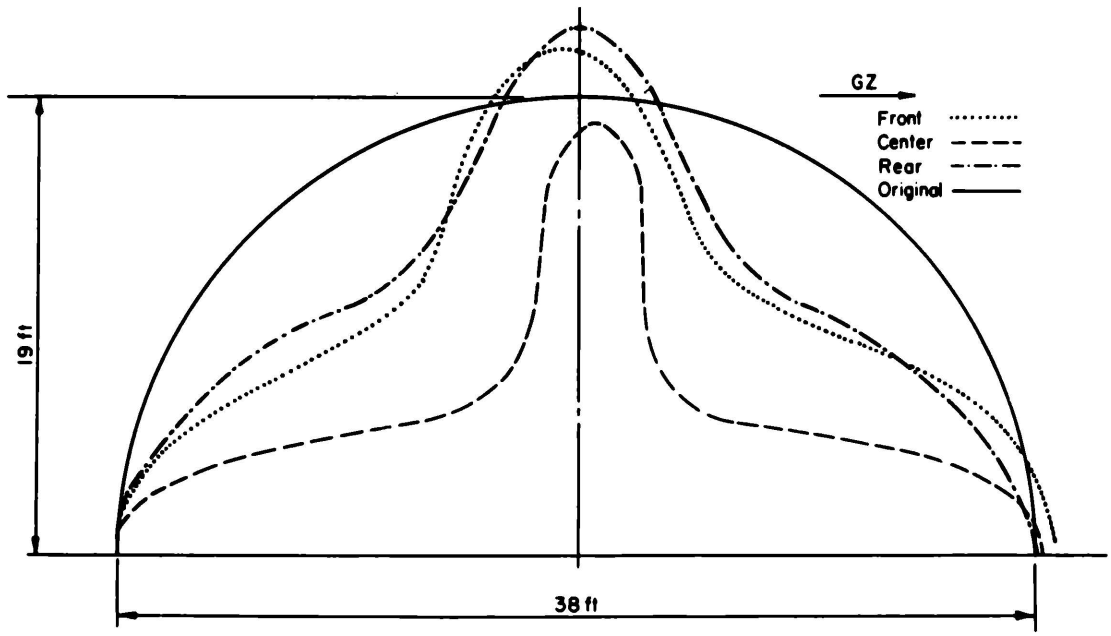

Fig. 14—Structure 3.2d, profiles of deformed arch shell at front, center, and rear.

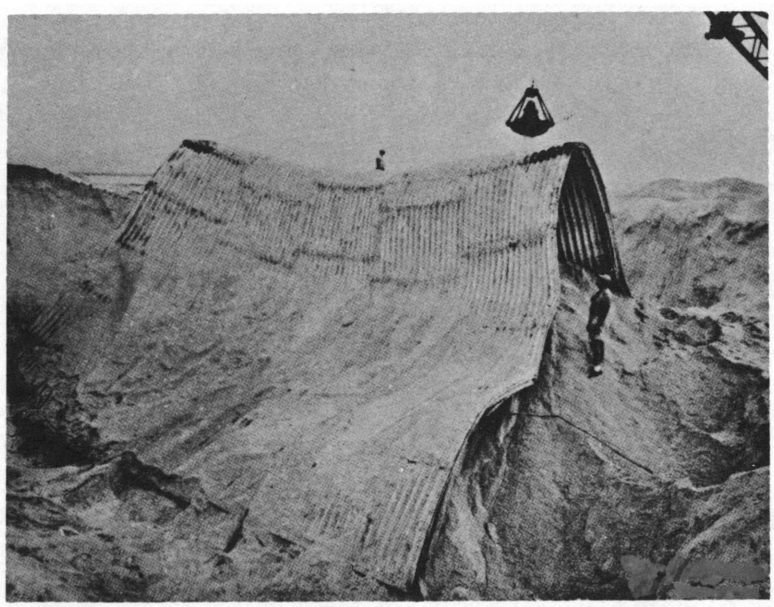

Fig. 15—Structure 3.2d, infiltration of sand after end-wall failure; looking toward GZ.

SUMMARY 32

BEHAVIOR OF DEEP REINFORCED-CONCRETE SLABS IN HIGH-OVERPRESSURE REGIONS

(Report WT-1630, Operation Hardtack, Project 3.6, same title, by E. H. Bultmann, Jr., CAPT, USAF, Project Officer, J. D. Haltiwanger, R. N. Wright III, and J. T. Hanley, University of Illinois, Urbana, Ill., June 30, 1961.)

OBJECTIVES AND SCOPE

The primary objective of the test was to determine the dynamic behavior of deep reinforced-concrete slabs in the overpressure region of 200 to 600 psi and thereby to provide a basis for establishing design criteria for reinforced-concrete structures under blast loads.

Both one-way and two-way slabs placed flush with the ground surface were tested. The ratios of effective span to depth varied from 1.43 to 7.0. It was expected that for slabs of these proportions shearing strength would prove to be the controlling design parameter. Consequently, the test specimens were designed particularly for the study of the shear strength of slabs both with and without shear reinforcement. Flexural strength, however, was also considered.

The slabs were tested during Koa shot, and the weapon yield was 1.31 Mt (ref. ENW, p. 675).

TEST STRUCTURES AND PROCEDURE

Slabs of both the one-way and the two-way types were designed with spans of 6.0 ft with their tops flush with the ground surface so that only the overpressure would act on them.

Because the instrumentation in this project was extremely limited, the information gained from the tests depended primarily upon the differences between the slabs that failed and those that did not. For such information, one specimen in each series had to be so weak that it was almost certain to fail, even at the lowest probable pressure, and one other specimen had to be so strong that it would not fail even at the highest probable pressure. Between these extremes, the strengths of the specimens were varied as uniformly as possible by varying depth, flexural reinforcement, and shear reinforcement.

The one-way slabs (for details see Tables 1 and 2, and Figs. 1 through 4) were designed for peak overpressure levels of 600 and 175 psi, which were originally predicted on the basis of a nuclear-device yield of 1.5 Mt to occur at ranges of 1830 ft (station 360.01) and 3100 ft (station 360.02), respectively, from Ground Zero (GZ). At each of the locations, 15 such slabs were tested. At the predicted 600-psi location, the slabs had effective depths varying from 20 to 56 in., and, at the predicted 175-psi location, from 11 to 31 in.

At each of the two predicted overpressure levels, the slabs were tested in groups having a common depth. The diagonal tensile strength within any given depth group was varied by using different percentages of flexural and web steel. Though most of these one-way slabs were proportioned so that failures should occur as a result of weakness in diagonal tension, it was expected that some of the failures might be of a flexural or pure-shear nature, since the basis for ultimate strength computations, particularly under dynamic loads, was admittedly rather uncertain.

Ten two-way slabs (for details see Tables 3 and 4, and Figs. 5 and 6) were designed for test under the higher pressure level of 600-psi. As in the case of the one-way slabs, they were designed so that their strengths appeared to be dependent primarily upon the diagonal strength of the slabs. The parameters that influence the strength of the one-way slabs apply equally well to two-way slabs.

The simple instrumentation system used consisted of (1) free-field overpressure measurements at each of the two sites with self-recording pressure–time gauges; (2) six self-recording accelerometers, two placed on the supporting structure of each of the three groups of slabs; and (3) permanent deflection measurements, primarily for determining the response of each slab to the applied loading.

RESULTS

The test results are summarized in Tables 5 through 7. The most significant damage was observed in the one-way slabs at the range of 1830 ft. Of the 15 test specimens, 9 exhibited definite evidence of permanent damage. As would be expected on the basis of the predicted failure overpressures listed in Tables 6 and 7, most of the damage occurred in the form of vertical flexural cracking and diagonal cracking in the slabs. However, the extent of damage observed was still small compared with that which would have been predicted on the basis of the measured overpressure of 1100 psi (Figs. 7 and 8).

The one-way slabs at a range of 3100 ft showed only very slight damage. Since the one-way slabs at a range of 1830 ft sustained no heavier damage than they did when subjected to a pressure of almost twice the nominal design value, it is not surprising that those at a range of 3100 ft were virtually undamaged when loaded with approximately their design nominal pressure.

The two-way slabs at a range of 1830 ft sustained very severe damage. The evidence available, however, indicates that this damage resulted from foundation distortions and breakage rather than from applied surface loads. As indicated in Figs. 9 and 10, this entire series of specimens appears to have been subjected to severe fissuring of the supporting subsoil. This contention is supported by the data in Table 7 where it is noted that the limited amount of damage to individual slabs which was in evidence occurred not on the weakest slabs but rather on those three that were in the area of most severe foundation damage. It is inconceivable that, except as influenced by the foundation distortions just mentioned, slabs 20-3, 20-4, and 25-1 could have been damaged when slabs 15-1, 15-2, 20-1, and 20-2 were not.

CONCLUSIONS

In terms of the original objectives of this project, the results were, at least for the one-way slabs, partially successful. Despite differences between predicted and observed response, the results obtained from this project are in relative agreement with those obtained in static tests of deep beams, as covered in the report, "An Investigation of the Behavior of Deep Members of Reinforced Concrete and Steel," by W. J. Austin and others, University of Illinois, February 1959, (Contract AF 29 (601)-468). The results of these tests were not available at the time of the preliminary design and analysis of the slabs tested under Project 3.6.

In particular, the data from laboratory tests mentioned above indicate that the present criteria for anchorage-bond and pure-shear failures are very conservative. An analysis of relevant data indicates that a diagonal-tension failure is not possible for a uniformly loaded, simply supported one-way slab or beam. None of the slabs tested under Project 3.6 failed in anchorage bond, pure shear, or diagonal tension.

The effect of web reinforcement on the behavior of the one-way slabs tested under Project 3.6 was qualitatively the same as that obtained in static tests of deep beams. Specifically, comparing the response of slab 28-1 with that of 28-2 and 28-3 and the response of 36-1 with 36-2, it is apparent that web

reinforcement inhibits the development of major inclined cracks even in very deep members under dynamic loads. It is concluded, therefore, that web reinforcement should be provided to ensure failure in flexure rather than in some more brittle mode.

None of the test slabs were reinforced in compression, although those with web reinforcement had very small bars at the top to which the web reinforcement was tied. A large number of slabs developed vertical cracks from top to bottom in the vicinity of midspan. It is believed that the only logical explanation for these cracks is that tensile stresses were developed at the top surface during rebound. It is concluded, therefore, that wherever support conditions are such that significant tensile stresses can be developed in the top of the slab, longitudinal reinforcement for resistance against rebound should be provided. This reinforcement will result in more ductile flexural response in the direction of the applied load.

Table 1—PROPERTIES OF ONE-WAY SLABS

Slab*	ϕ,† %	ϕ_w,‡ %	Design predictions of failure overpressures §: Pure shear, psi	Flexure, psi	Diagonal tension, psi	Ultimate concrete strength,¶ psi	Revised predictions of failure overpressures**: Pure shear, psi	Flexure, psi	Diagonal tension, psi
			Station 360.01, Ground Range 1830 ft, Predicted Pressure 600 psi						
20-1	1.5	1.5	375	400	450 to 600	5410	505	520	650 to 870
28-1	1.0	0	525	550	300 to 400	6679	875	680	400 to 535
28-2	1.0	0.5	525	550	450 to 600	6900	905	680	665 to 885
28-3	1.0	1.0	525	550	600 to 800	6571	860	680	900 to 1200
36-1	1.0	0	660	880	495 to 660	6845	1130	1130	670 to 895
36-2	1.0	0.5	660	880	750 to 1000	7020	1160	1130	1110 to 1480
36-3	0.75	0	660	660	420 to 560	6832	1130	850	580 to 775
36-4	1.5	0	660	1320	600 to 800	6180	1120	1700	780 to 1040
36-5	0.5	0.5	660	450	540 to 720	6328	1045	570	745 to 995
44-1	1.0	0	800	1350	750 to 1000	6310	1260	1690	960 to 1280
44-2	0.75	1.0	800	1010	1330 to 1770	6208	1240	1270	1880 to 2500
44-3	0.5	0	800	670	525 to 700	6744	1345	840	705 to 940
44-4	0.25	0.2	800	340	450 to 600	6238	1250	420	600 to 800
56-1	0.5	1.2	1100	1100	1950 to 2600	6614	1820	1370	2850 to 3810
56-2	0.5	0	1100	1100	800 to 1067	6586	1810	1370	1130 to 1510
			Station 360.02, Ground Range 3100 ft, Predicted Pressure 175 psi						
11-1	1.5	1.5	200	130	150 to 200	5628	280	160	200 to 270
16-1	1.0	0.5	300	170	150 to 200	5443	410	225	190 to 255
16-2	1.5	0	300	260	130 to 170	5609	420	335	145 to 195
16-3	1.5	0.5	300	260	190 to 250	5535	415	335	235 to 315
21-1	1.0	0	390	300	170 to 230	6882	670	385	230 to 305
21-2	1.0	0.5	390	300	260 to 350	6117	595	385	350 to 470
21-3	0.5	0.5	390	150	170 to 230	6587	640	195	260 to 345
21-4	0.5	0	390	150	110 to 150	6273	610	195	155 to 205
21-5	1.5	0	390	460	190 to 250	5821	570	580	260 to 345
21-6	0.75	0.25	390	230	190 to 250	5654	550	290	235 to 315
26-1	0.75	1.0	480	330	480 to 640	6688	805	440	675 to 900
26-2	0.5	0	480	230	190 to 250	5932	710	295	230 to 305
26-3	1.0	0	480	480	260 to 350	5203	625	590	305 to 405
31-1	0.5	1.0	570	330	530 to 700	5917	840	420	740 to 985
31-2	0.5	0	570	330	240 to 320	6692	955	420	345 to 460

*Each slab is designated first by its effective depth and then by its code number at that depth.
†ϕ = the percentage of flexural reinforcement.
‡ϕ_W = the percentage of web steel (assumed constant over the length of the beam).
§Based on concrete strength of 4000 psi and dynamic yield of 50 ksi for reinforcing steel.
¶From cylinders tested on shot date.
**Based on shot-date cylinder strengths and dynamic-yield value of 63 ksi for reinforcing steel.

Table 2—DIMENSIONS OF ONE-WAY SLABS

		Reinforcing steel									
		Longitudinal						Vertical			
Slab	h,* in.	d_1,* in.	No. of bars	d_2,* in.	No. of bars	d_3,* in.	No. of bars	Type	Bar size	h',* in.	Spacing, in.
Station 360.01											
20-1	22½	21	8	19	8			B	5	21	5¼
28-1	30½	29	8	27	7						
28-2	30½	29	8	27	7			A	5	29	10¼
28-3	30½	29	8	27	7			B	5	29	7¾
36-1	39½	37	10	35	10						
36-2	39½	37	10	35	10			A	5	37	10¼
36-3	39½	37	8	35	7						
36-4	39½	38	10	36	10	34	9				
36-5	39½	36	10					A	5	36	10¼
44-1	47½	46	8	44	8	42	8				
44-2	47½	45	9	43	9			A	5	45	5¼
44-3	47½	45	6	43	6						
44-4	47½	44	6					A	3	44	9¼
56-1	58½	57	8	55	7			B	5	57	6½
56-2	58½	57	8	55	7						
Station 360.02											
11-1	12½	11	9					A	5	11	3½
16-1	18½	16	9					A	4	16	6¾
16-2	18½	17	7	15	6						
16-3	18½	17	7	15	6			A	4	17	6¾
21-1	23½	22	6	20	5						
21-2	23½	22	6	20	5			A	4	22	6¾
21-3	23½	21	6					A	4	21	6¾
21-4	23½	21	6								
21-5	23½	22	9	20	8						
21-6	23½	21	9					A	3	21	7¼
26-1	28½	27	6	25	5			B	5	27	7¾
26-2	28½	26	7								
26-3	28½	27	7	25	7						
31-1	32½	31	8					B	5	31	7¾
31-2	32½	31	8								

*See Fig. 1 for guide to dimensions.

Table 3—PROPERTIES OF TWO-WAY SLABS

(Station 360.01, Ground Range 1830 ft, Predicted Pressure 600 psi)

			Design predictions of failure overpressures†				Revised predictions of failure overpressures §		
Slab*	ϕ, %	ϕ_w, %	Pure shear, psi	Flexure, psi	Diagonal tension, psi	Ultimate concrete strength,‡ psi	Pure shear, psi	Flexure, psi	Diagonal tension, psi
10-1	1.5	0	370	300	95 to 130	5151	475	394	110 to 145
15-1	1.2	1.3	550	600	450 to 600	6421	885	706	650 to 870
15-2	1.2	0	550	600	170 to 230	5249	720	706	225 to 300
20-1	0.6	0	740	500	220 to 300	6485	1200	630	310 to 415
20-2	0.6	1.0	740	500	470 to 630	6368	1180	630	700 to 930
20-3	0.9	0	740	800	300 to 400	6437	1190	945	380 to 510
20-4	0.9	1.0	740	800	600 to 800	6236	1150	945	850 to 1130
25-1	0.5	0	930	800	300 to 400	6946	1610	825	460 to 615
25-2	0.5	0.8	930	800	660 to 800	5609	1305	825	840 to 1110
30-1	1.0	1.5	1110	2000	1800 to 2400	6752	1870	2370	2680 to 3580

*Each slab is designated first by its effective depth and then by its code number at that depth.
†Based on concrete strength of 4000 psi and dynamic yield of 50 ksi for reinforcing steel.
‡From cylinders tested on shot date.
§Based on shot-date cylinder strengths and dynamic-yield value of 63 ksi for reinforcing steel.

Table 4—DIMENSIONS OF TWO-WAY SLABS

		Reinforcing steel								
		Longitudinal*				Vertical				
Slab	h,* in.	d_1,* in.	s,† in.	d_2,* in.	s,† in.	Bar size	h′,* in.	a,* in.	L,* in.	b,* in.
10-1	12	3								
15-1	17	15½	2½			5	15½	10	80	5
15-2	17	15½	2½							
20-1	22	20½	3¾							
20-2	22	20½	3¾			5	20½	7½	75	7½
20-3	22	20½	2½							
20-4	22	20½	2½			4	20½	5	75	7½
25-1	27	25½	3½							
25-2	27	25½	3½			5	25½	7	77	10½
30-1	32½	31¼	3	29½	3	5	29½	6	78	6

*See Fig. 5 for guide to dimensions.
†Both ways.

Table 5—DISPLACEMENTS OF ONE-WAY SLAB FOUNDATIONS

Reference-point elevations									
Station 360.01, Ground Range 1830 ft					Station 360.02, Ground Range 3100 ft				
Slab	Stud*	Pretest	Posttest	Change	Slab	Stud*	Pretest	Posttest	Change
20-1	1	11.046	4.633	−6.413	11-1	1	8.978	8.479	−0.499
	5	11.033	4.546	−6.487		5	8.976	8.467	−0.509
28-1	1	11.031	4.599	−6.432	16-1	1	8.990	8.497	−0.493
	5	11.023	4.508	−6.515		5	8.983	8.479	−0.504
28-2	1	11.028	4.554	−6.474	16-2	1	8.986	8.501	−0.485
	5	11.023	4.446	−6.577		5	8.996	8.499	−0.497
28-3	1	11.031	4.518	−6.513	16-3	1	8.973	8.489	−0.484
	5	11.033	4.444	−6.589		5	8.988	8.492	−0.496
36-1	1	11.028	4.464	−6.564	21-1	1	8.983	8.501	−0.482
	5	11.031	4.398	−6.633		5	8.995	8.504	−0.491
36-2	1	11.030	4.444	−6.586	21-2	1	8.983	8.506	−0.477
	5	11.020	4.321	−6.699		5	8.990	8.501	−0.489
36-3	1	11.033	4.416	−6.617	21-3	1	8.985	8.512	−0.473
	5	11.031	4.303	−6.728		5	8.995	8.507	−0.488
36-4	1	11.045	4.385	−6.660	21-4	1	8.983	8.512	−0.471
	5	11.031	4.229	−6.802		5	8.975	8.492	−0.483
36-5	1	11.025	4.324	−6.701	21-5	1	8.978	8.512	−0.466
	5	11.033	4.263	−6.770		5	8.980	8.499	−0.481
44-1	1	11.028	4.276	−6.752	21-6	1	8.973	8.511	−0.462
	5	11.018	4.139	−6.879		5	8.975	8.497	−0.478
44-2	1	11.020	4.224	−6.796	26-1	1	8.983	8.522	−0.461
	5	11.043	4.108	−6.935		5	8.991	8.514	−0.477
44-3	1	11.020	4.186	−6.834	26-2	1	8.991	8.532	−0.459
	5	11.020	4.083	−6.937		5	9.000	8.527	−0.473
44-4	1	11.030	4.150	−6.880	26-3	1	8.978	8.522	−0.456
	5	11.033	4.084	−6.949		5	8.983	8.509	−0.474
56-1	1	11.025	4.103	−6.922	31-1	1	8.976	8.522	−0.454
	5	11.030	3.998	−7.032		5	8.983	8.516	−0.467
56-2	1	11.057	4.066	−6.991	31-2	1	8.983	8.529	−0.454
	5	11.063	3.941	−7.122		5	8.988	8.521	−0.467

*Slab reference studs 1 and 5 are located over the edges of the foundations; therefore, the elevation changes are due principally to foundation displacement. Stud 1 is on the GZ end of the slab; stud 5 is on the end away from GZ. All measurements indicated in feet.

Table 6—SUMMARY OF TEST RESULTS ON ONE-WAY SLABS

Slab	Revised predicted failure overpressures* Pure shear, psi	Flexure, psi	Diagonal tension, psi	Observed response	Permanent center deflection,† in.
			Station 360.01, Ground Range 1830 ft, Effective Peak Pressure 1100 psi		
20-1	505	520	650 to 870	Extensive midspan vertical cracking	+0.24
28-1	875	680	400 to 535	Failure, possibly in shear-anchorage, central and lower portion broken out	−0.20
28-2	905	680	665 to 885	Midspan vertical cracking, diagonal cracking near supports	+0.10
28-3	860	680	900 to 1200	Midspan vertical cracking, diagonal cracking near supports	+0.11
36-1	1130	1130	670 to 895	Long curved crack from support region to midspan, vertical crack near support	+0.04
36-2	1160	1130	1110 to 1480	None	0
36-3	1130	850	580 to 775	Long curved crack from support region to midspan	+0.03
36-4	1120	1700	780 to 1040	None	+0.01
36-5	1045	570	745 to 995	Midspan vertical cracking; diagonal cracking near supports	+0.12
44-1	1260	1690	960 to 1280	None	−0.04
44-2	1240	1270	1880 to 2500	None	−0.02
44-3	1345	840	705 to 940	Midspan vertical cracking	+0.02
44-4	1250	420	600 to 800	Midspan vertical cracking; diagonal cracking near supports	+0.07
56-1	1820	1370	2850 to 3810	None	0
56-2	1810	1370	1130 to 2510	None	−0.03
			Station 360.02, Ground Range 3100 ft, Effective Peak Pressure 210 psi		
11-1	280	160	200 to 270	Light midspan vertical crack	+0.02
16-1	410	225	190 to 255	None	−0.01
16-2	420	335	145 to 195	None	+0.07
16-3	415	335	235 to 315	Light midspan vertical crack	+0.03
21-1	670	385	230 to 305	Light vertical cracks at midspan and quarter point	−0.01
21-2	595	385	350 to 470	None	+0.01
21-3	640	195	260 to 345	Light vertical cracks at midspan and quarter point	+0.03
21-4	610	195	155 to 205	Light vertical cracks at midspan and quarter point	+0.03
21-5	570	580	260 to 345	Light vertical crack at midspan on one side only	+0.01
21-6	550	290	235 to 315	Light vertical crack at midspan on one side only	0
26-1	805	440	675 to 900	None	+0.02
26-2	710	295	230 to 305	None	0
26-3	625	590	305 to 405	None	+0.02
31-1	840	420	740 to 985	Possible vertical crack at midspan on one side only	0
31-2	955	420	345 to 460	None	0

*Refer to Table 1.

†Measure relative to line between supports. Positive deflections are downward.

Table 7—SUMMARY OF TEST RESULTS ON TWO-WAY SLABS
(Station 360.01, Ground Range 1830 feet, Effective Peak Pressure, 1100 psi)

	Revised predicted failure overpressures*				
Slab	Pure shear, psi	Flexure, psi	Diagonal tension, psi	Permanent center deflection,† in.	Observed damage
10-1	475	394	110 to 145		Slab could not be found
15-1	8885	706	650 to 870	0	None
15-2	720	706	225 to 300	5/32	None
20-1	1200	630	310 to 415	1/32	None
20-2	1180	630	700 to 930	1/16	None
20-3	1190	945	380 to 510		Roughly circular crack pattern on bottom
20-4	1150	945	850 to 1130		Straight-line cracks running in both principal directions visible on bottom
25-1	1610	825	460 to 615		Cracks visible in bottom near supports; curved cracks near one corner on sides
25-2	1305	825	840 to 1110	1/32	None
30-1	1870	2370	2680 to 3580	1/16	None

*Refer to Table 3.

†Permanent deflections relative to line between supports. Data from initial reentry straightedge measurements. Positive deflections are downward.

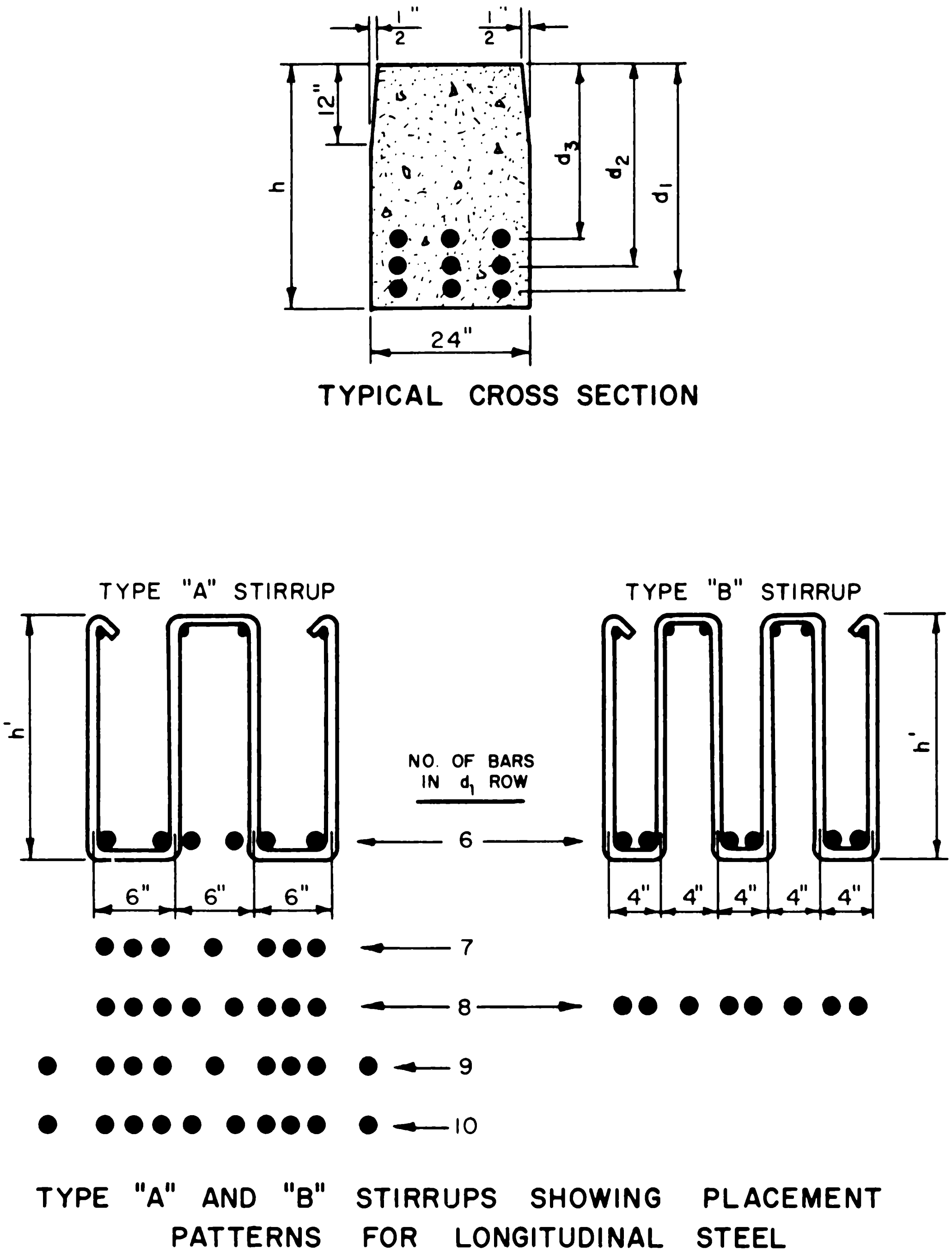

Fig. 1—One-way slab details.

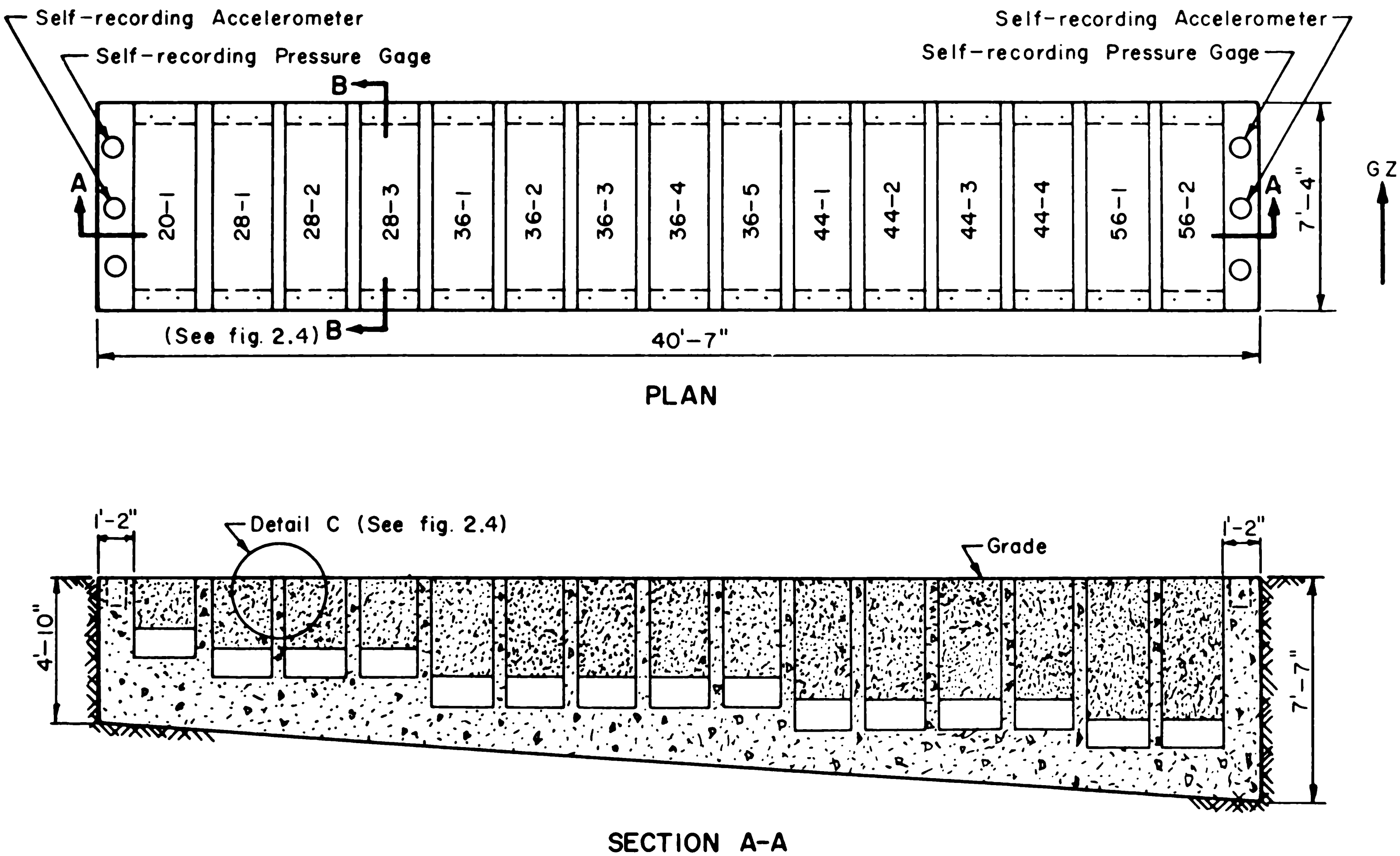

Fig. 2—One-way slab supports at station 360.01.

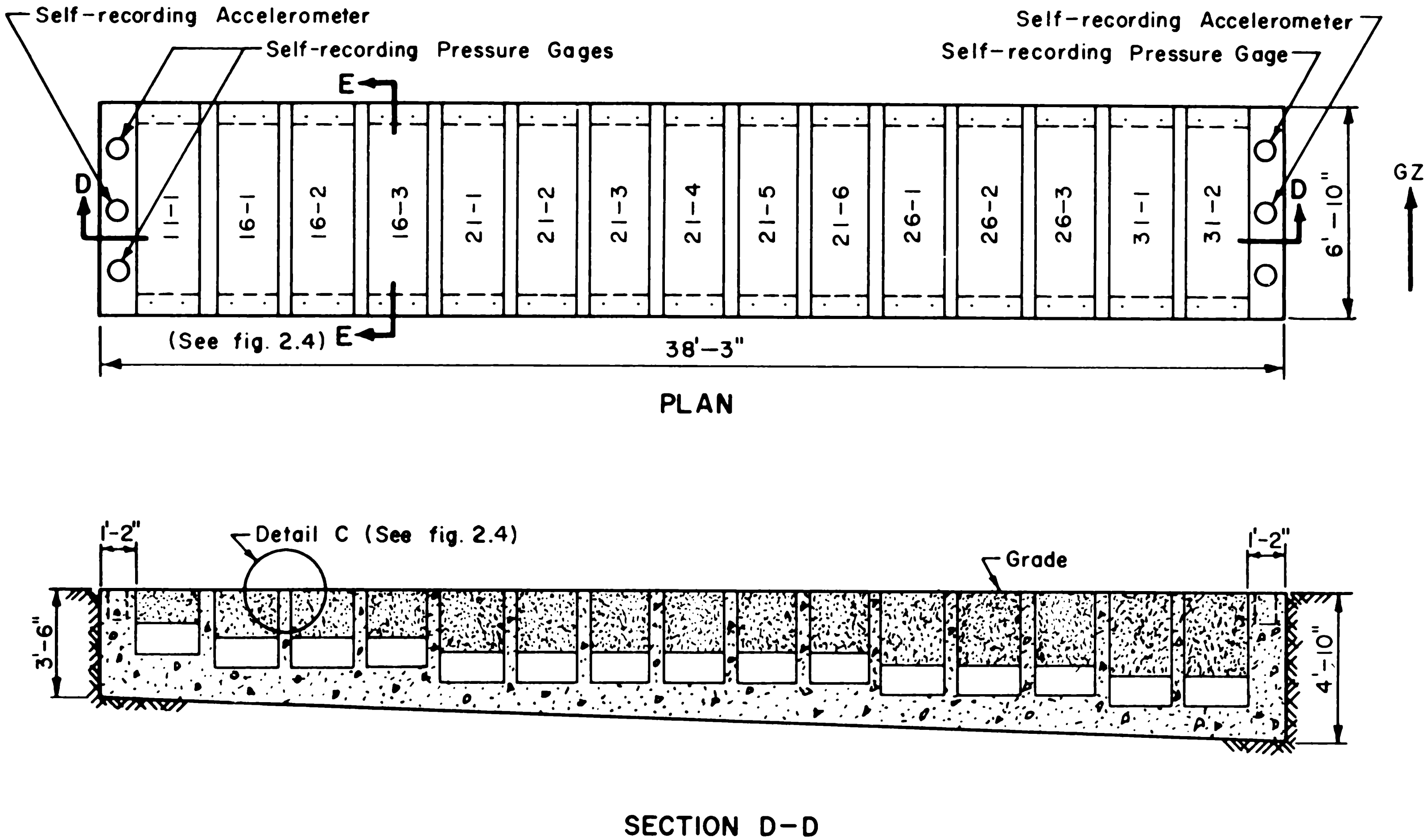

Fig. 3—One-way slab supports at station 360.02.

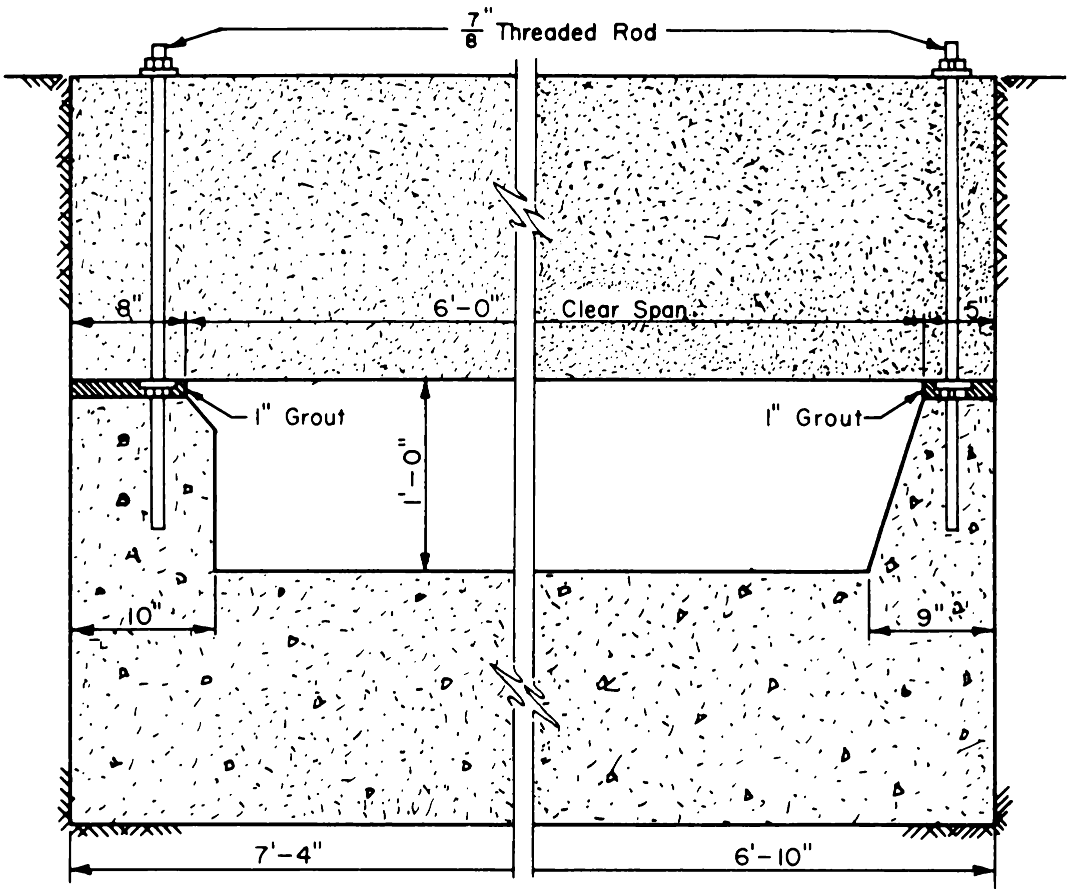

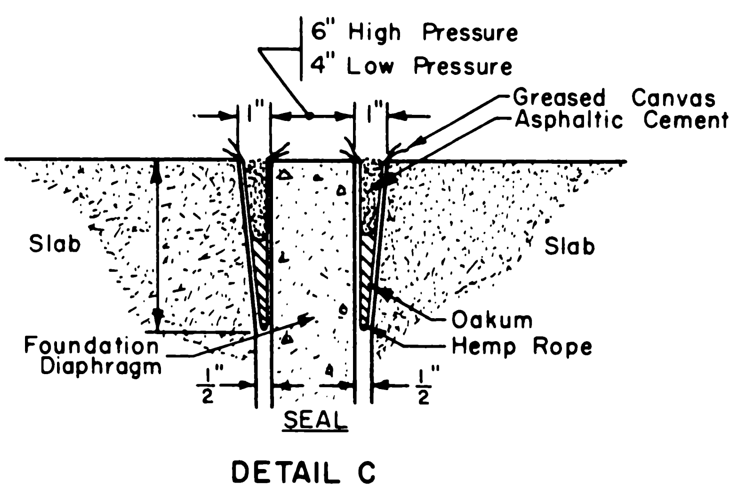

Fig. 4—One-way slab support details.

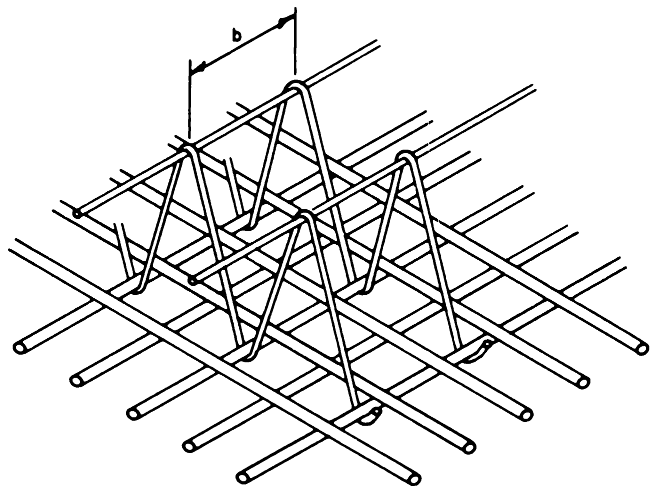

TYPICAL REINFORCEMENT DETAIL

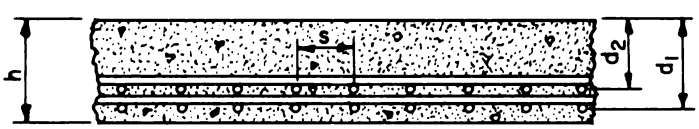

Note: Reinforcement at depth d_2 occurs only on slab 30-1.

TYPICAL CROSS SECTION

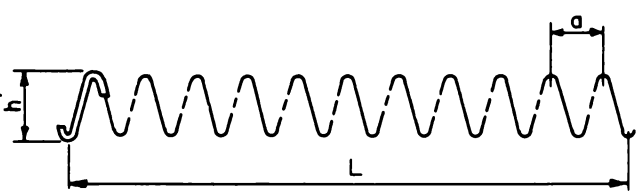

TYPICAL STIRRUP

Fig. 5—Two-way slab details.

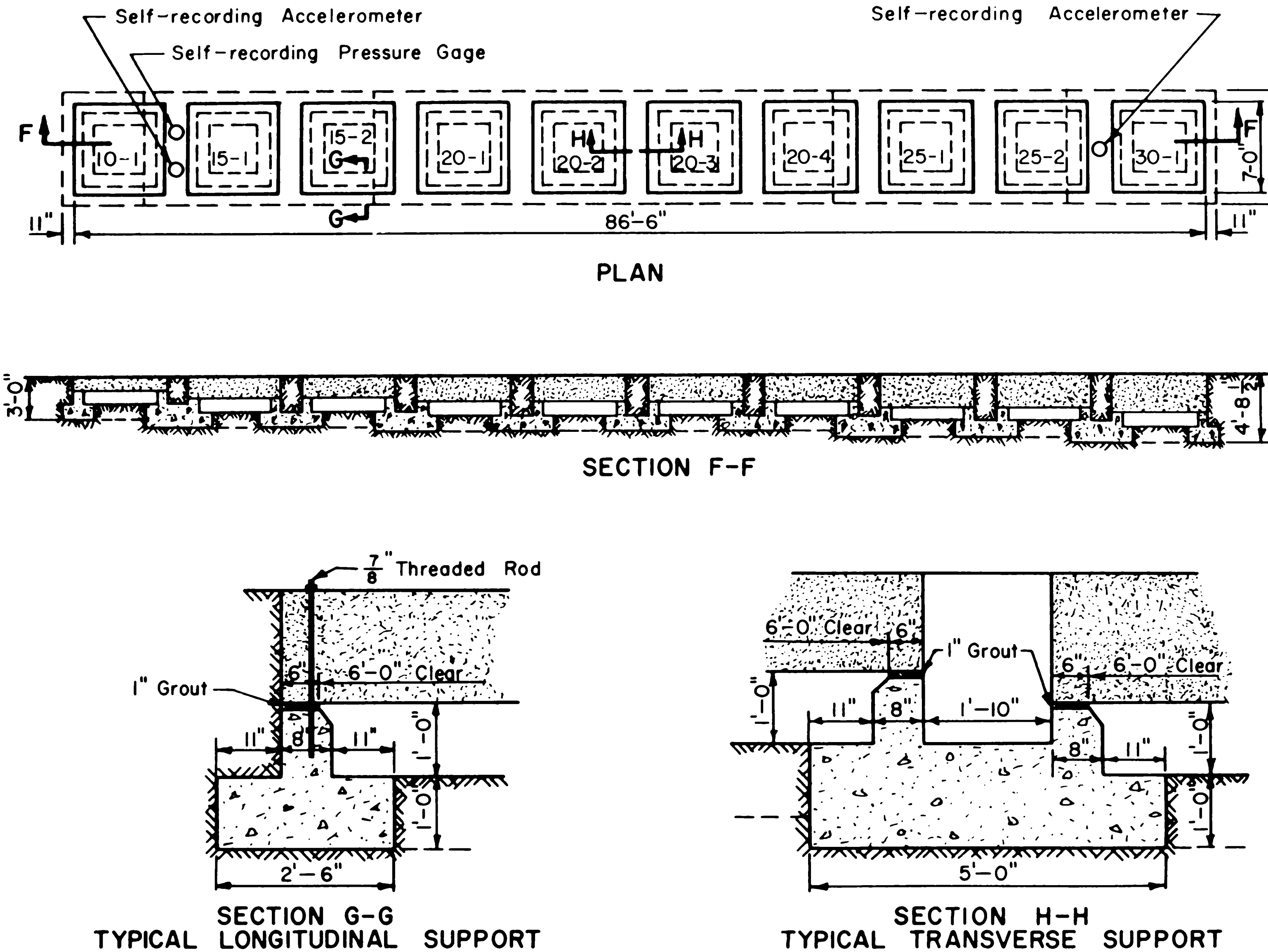

Fig. 6—Two-way slab supports at station 360.01.

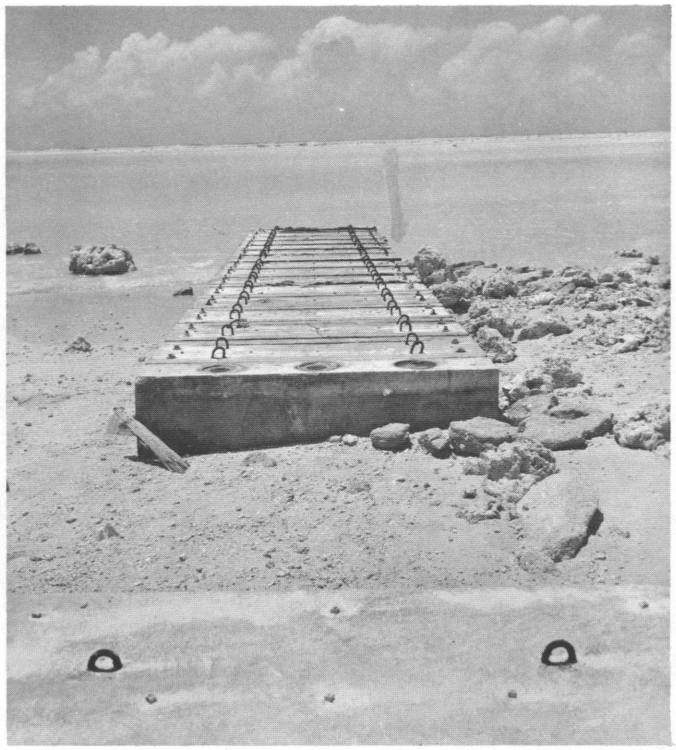

Fig. 7—Posttest view of one-way slabs at station 360.01, range 1830 ft. Ground Zero is to the left.

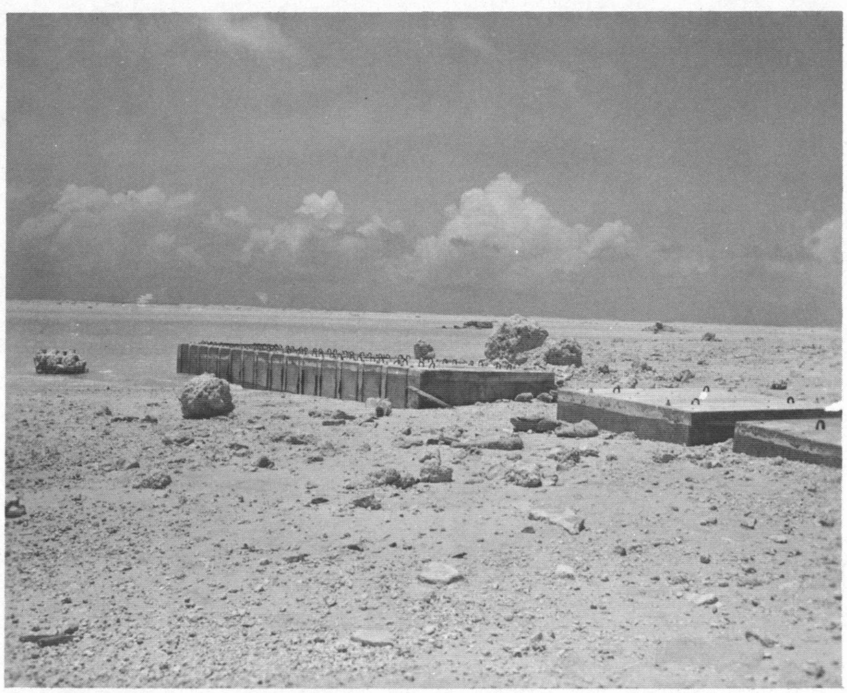

Fig. 8—Posttest view of one-way slabs at station 360.01, range 1830 ft, looking at GZ side of slabs.

Fig. 9—Posttest overall view of slabs at station 360.01, range 1830 ft. Note edge of crater adjacent to one-way slabs in rear. Ground Zero is to the left.

Fig. 10—Posttest view of two-way slabs at station 360.01, range 1830 ft, looking away from GZ, showing evidence of foundation failure.

SUMMARY 33

PHYSICAL DAMAGE SURVEY OF AEC TEST STRUCTURES

(Report WT-1701, Operation Hardtack, Project 34.1, same title, by R. A. Cameron, Jr., and P. H. Huff, Holmes & Narver, Inc., Architect–Engineers, Los Angeles, Calif., May 29, 1962.)

OBJECTIVE AND SCOPE

The objective of Project 34.1 was to record and evaluate damage sustained by selected Atomic Energy Commission test structures as a result of air blast and thermal radiation. Although emphasis was placed on the study of structures exposed to high levels of overpressures and thermal radiation, some data pertaining to damage resulting from lower overpressures were also included in the project. The structures located in the lower overpressures included wood-frame houses. The tests of these wood-frame structures will, however, not be covered in this summary.

Damage-survey efforts were concentrated on the base structure of tower T-7c used in the Quay shot of Operation Hardtack, Phase II (ref. ENW, p. 676). The tower base consisted of a massive reinforced-concrete base house and a connecting tunnel 200 ft long. It had suffered only minor damage when it was originally used in the Boltzmann event of Operation Plumbbob (ref. ENW, p. 675). After some modification and repair, it was reused in the Quay event.

Figure 1 illustrates earth-cover requirements for a fully buried structure.

TEST STRUCTURE AND PROCEDURE

Figure 2 shows a plot plan and a section of the base structure of tower T-7c. A concrete plug (Fig. 3) was placed in the circular opening that had been occupied by a cylindrical steel tank during the Boltzmann event. The lower 5 ft 10¾-in. section of the concrete plug was poured two weeks before the shot, and the remainder was poured one week before the shot. The plug was expected to protect instruments mounted on a recoverable sled in the tunnel. Design load on the plug was a static 1200 psi, and it was designed for "punching" shear on the cylindrical surface.

Additional blast protection for the instruments was provided by a structural-steel blast door at the tunnel entrance, 200 ft from Ground Zero (GZ) (Figs. 2 to 5). The door, which weighed approximately 1800 lb, was designed for overpressures of 35 and 6 psi on the exterior and interior, respectively.

RESULTS

The explosion demolished the concrete plug as well as much of the surrounding base and caused failure of the blast door. Lack of dynamic shear strength in the young concrete was a possible factor in plug failure. The instrument sled could not be recovered because large amounts of debris blocked its removal. Although the fireball just touched the surface of the base, a conspicuous jet preceded it down the tower pipe. Thermal radiation was estimated to be 320 cal/cm^2 at the surface of the plug.

The blast-pressure vs. time measurements were only partially successful since only peak values, rather than overpressure-time records, were obtained. The gauge located on top of the base house, 17 ft from GZ, recorded a peak of 580 psi, and the gauge on the surface of the ground 70 ft south of GZ indicated a maximum of 280 psi.

On the basis of the recommended yield estimate of 79 tons, blast loadings at GZ, 83 ft below the point of detonation, and at the entrance of the tunnel 200 ft from GZ were estimated as follows:

	GZ	Tunnel entrance
Side-on overpressure, psi	254*	24
Positive-phase duration, sec	0.05	0.06
Reflected pressure, psi	1600*	

*Computed by assuming a spherical shock front emanating from a spherical source of energy. Jetting (Fig. 6) probably caused much higher local pressures.

Accelerometers failed to yield any information because one could not be recovered and the other suffered extensive missile damage. (See Summary 37.)

The visible fireball as it reached maximum size touched the surface of the mounded earth surrounding the base (Fig. 6).

The surface of the base immediately beneath the tower was damaged extensively, and the massive reinforced-concrete walls of the upper part of the base were demolished (Fig. 7). One corner of the structure and the surrounding earth-fill were blown out (Fig. 8). The concrete plug was completely destroyed, and the resulting debris fell into the tunnel below (Fig. 9).

Both the tunnel and the lower part of the tower base sustained minor damage. The tunnel roof adjacent to the plug cracked slightly and sagged. A vertical crack, approximately ¼ in. wide and extending from floor to ceiling, formed in each wall of the tunnel about 16 ft from the plug.

The blast door covering the entrance of the tunnel was blown outward and came to rest about 66 ft from its installed position. Although this door was not extensively damaged, there was a slight horizontal bend across its center. Failure of the blast door was probably caused by reflected pressure acting on the inside of the door as a result of failure of the plug.

CONCLUSIONS

1. Damage to base structure of tower T-7c

a. The base was loaded by a jet that traveled along the pipe connecting the nuclear device to the base.

b. Resistance of the plug to dynamic loading was not as high as expected, and/or loading was much higher than expected.

c. Since failure of the blast door was caused primarily by failure of the plug, no conclusions could be drawn concerning adequacy of its design.

2. Damage to close-in structures

a. Reinforced-concrete structures that were buried and those with a cover of loosely mounded earth survived overpressures of 1100 and 1050 psi, respectively, without damage.

b. Earth cover was effective in reducing the severity of loading on structures.

c. Earth-mounded or buried structures designed for a static load equal to the peak anticipated overpressure on the surface survived without damage.

d. Reinforced-concrete members did not appear to be affected structurally after exposure to thermal-radiation doses as high as 2000 cal/cm^2, although minor spalling on some structures was observed.

e. No conclusions were drawn concerning thermal-radiation effects on the strength of steel members. Members exposed to 2000 cal/cm^2 were badly distorted and suffered surface scaling and discoloration. It was impossible to ascertain how much of that distortion was due to heating of the material before arrival of the shock front and how much was caused by overpressure. Thermal radiation of this intensity could cause pronounced reduction in the strength of steel.

f. Unpainted wood surfaces were moderately charred by exposure to 30 cal/cm^2.

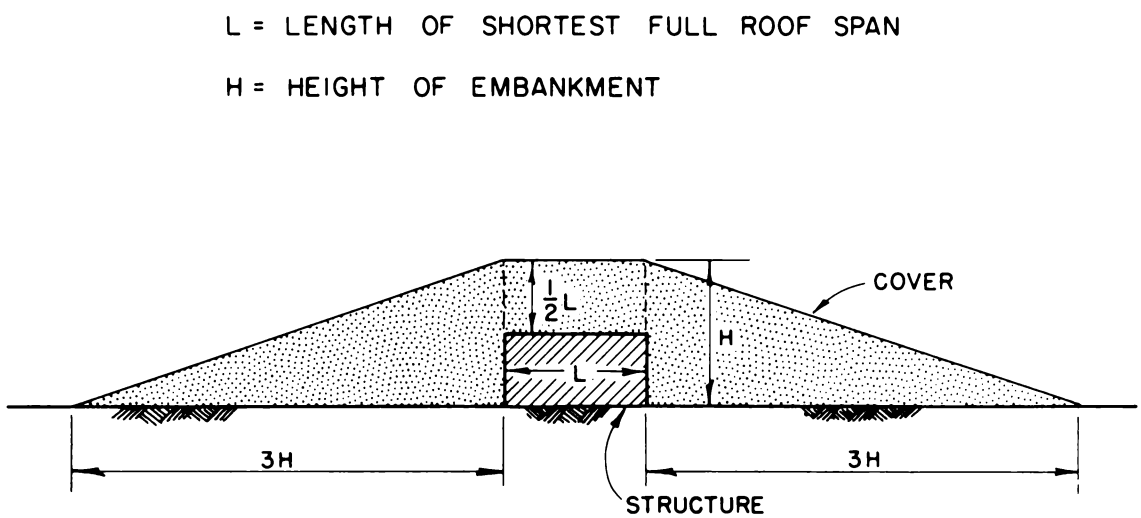

Fig. 1—Earth-cover requirements for fully buried structure.

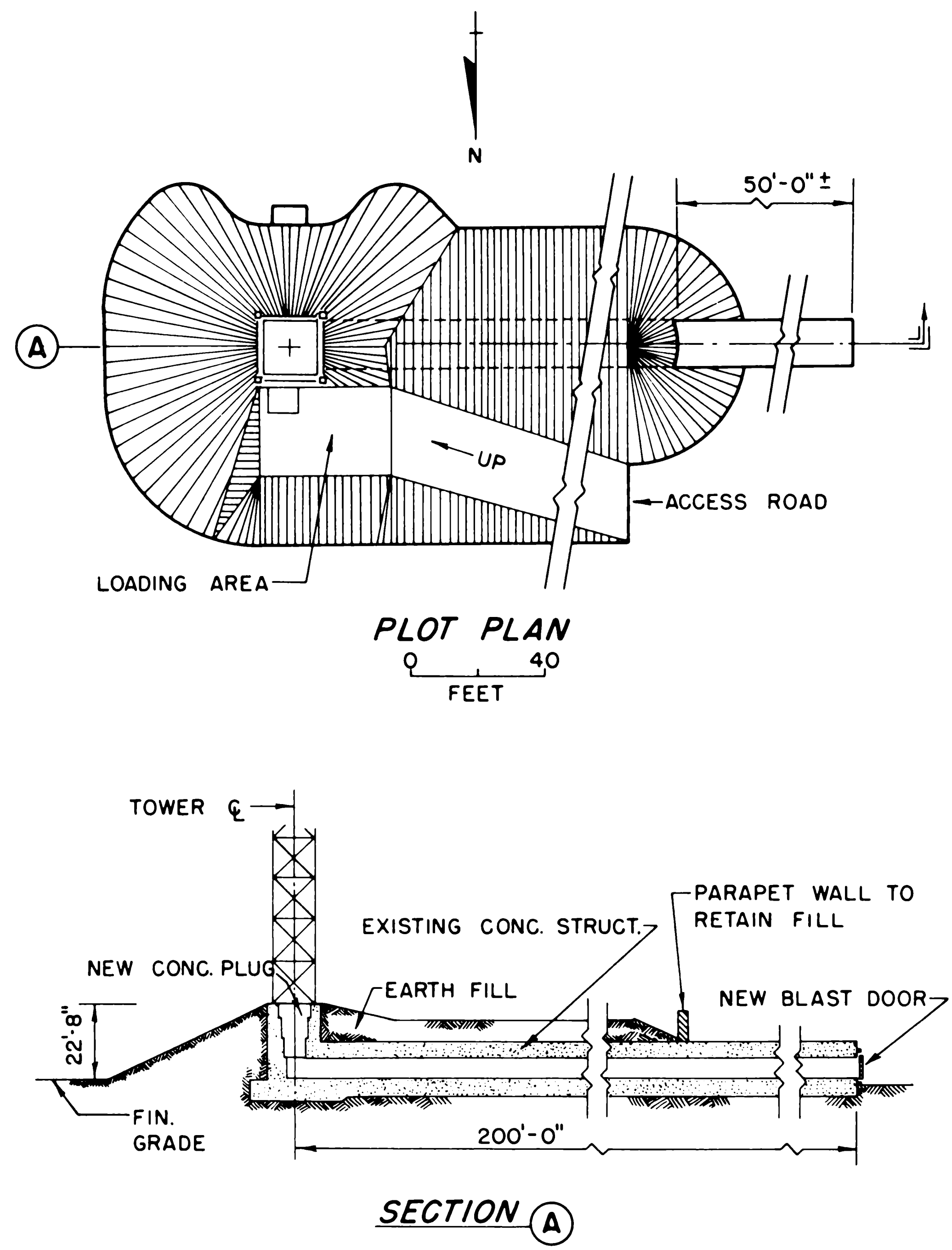

Fig. 2—Plot plan and section of base structure of tower T-7c.

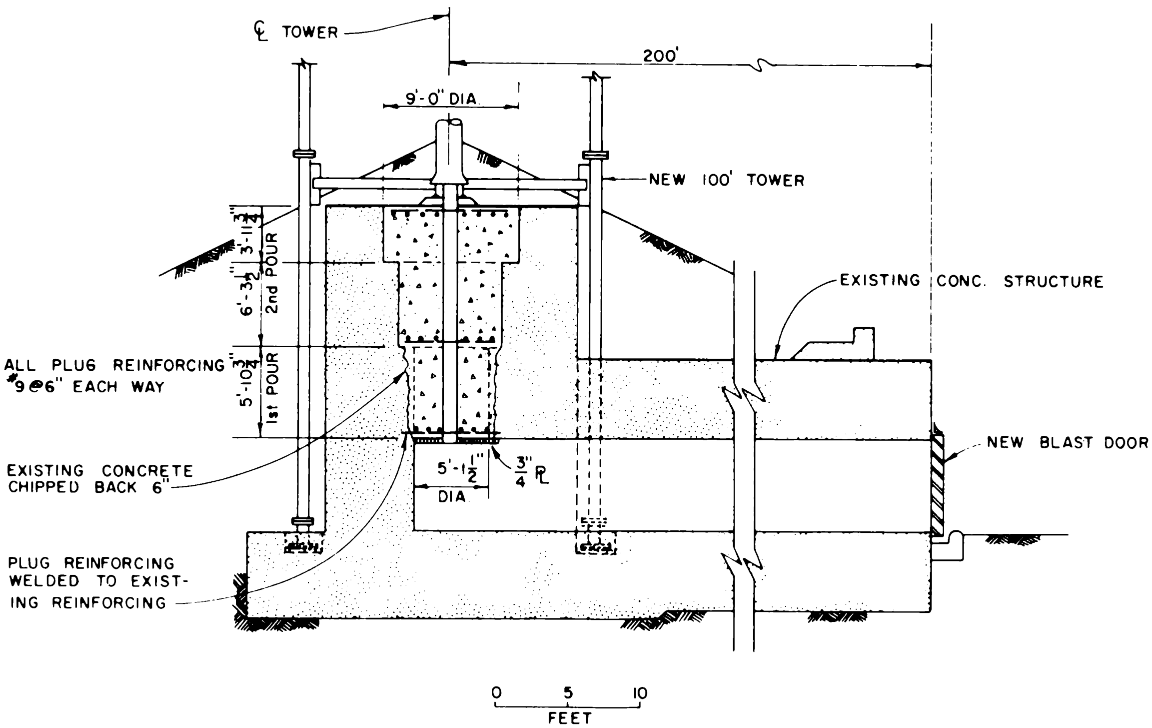

Fig. 3—Section through new concrete plug.

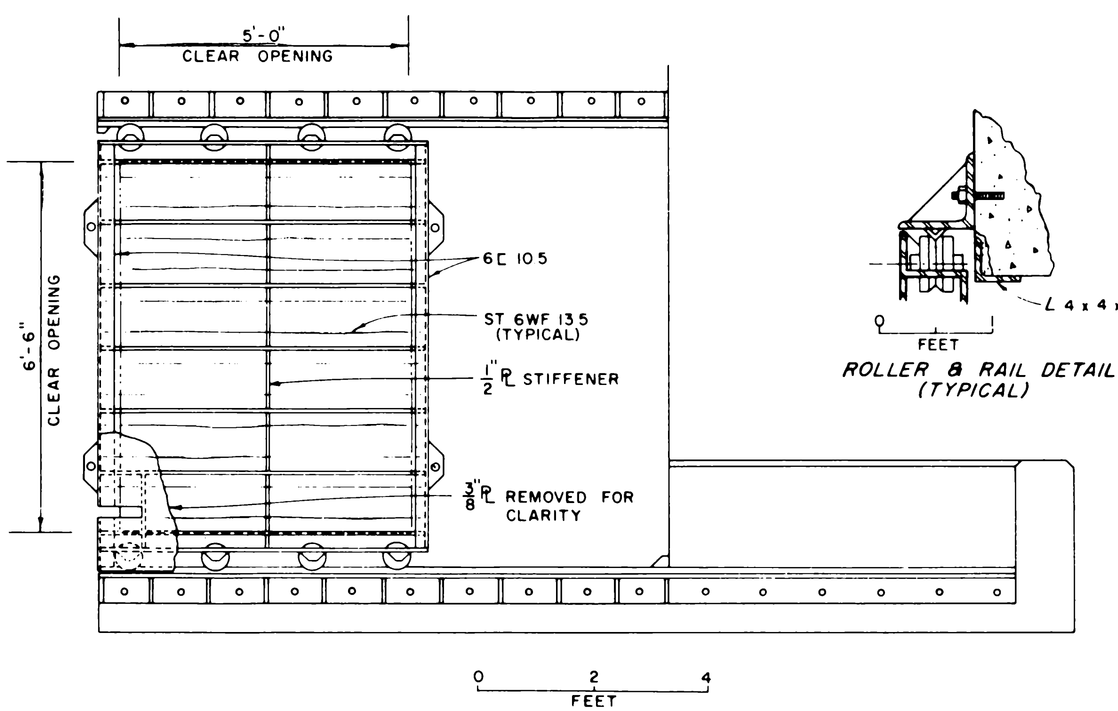

Fig. 4—Exterior elevation of blast door.

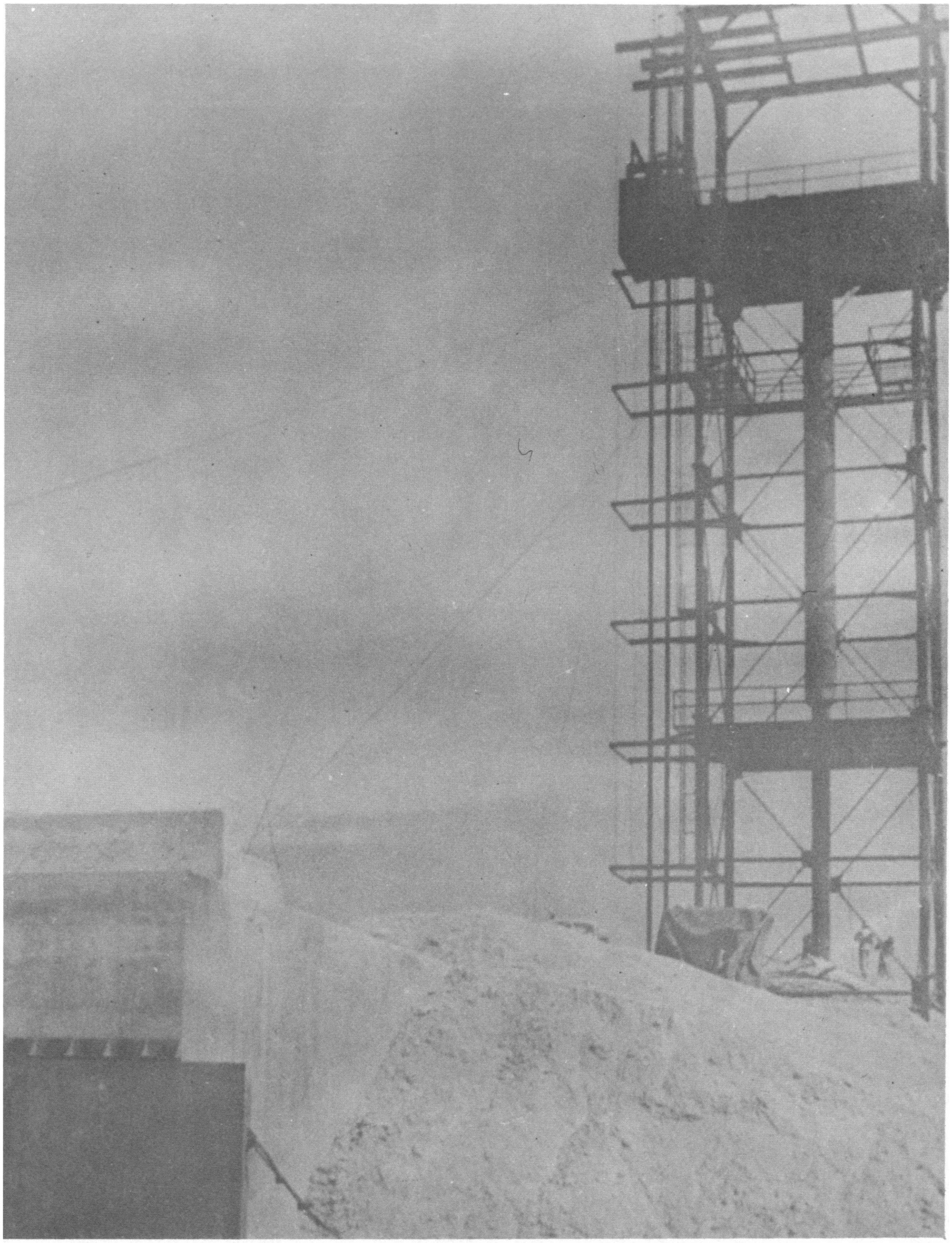

Fig. 5—View from end of tunnel toward GZ, pre-Quay event.

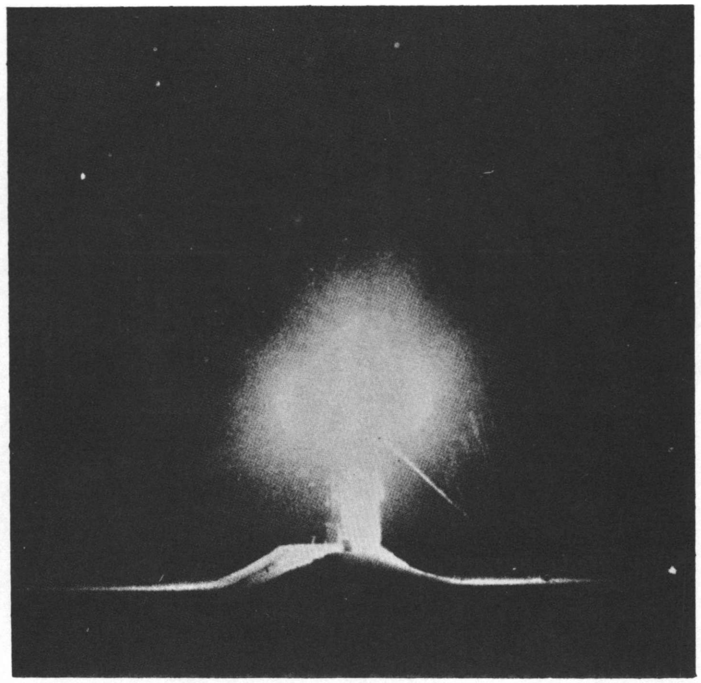

Fig. 6—Quay event fireball.

Fig. 7—Post-Quay event damage to tower base.

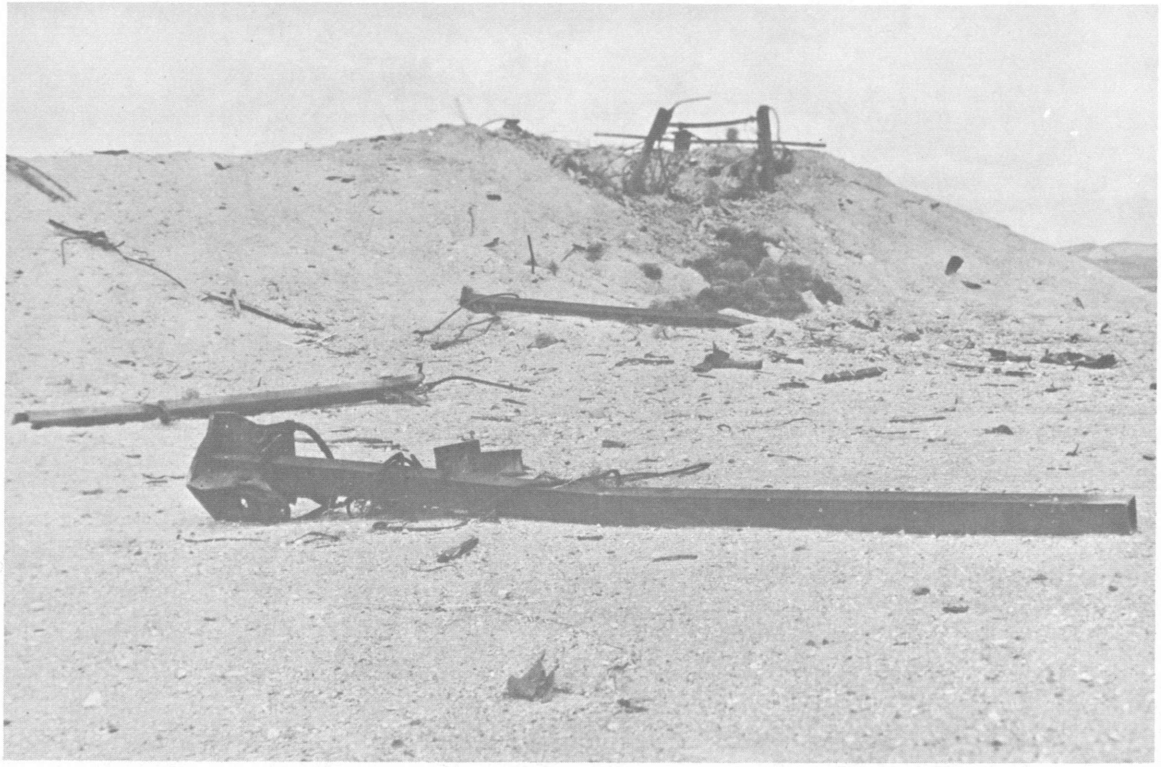

Fig. 8—Post-Quay event damage, horizontal view of tower-base area.

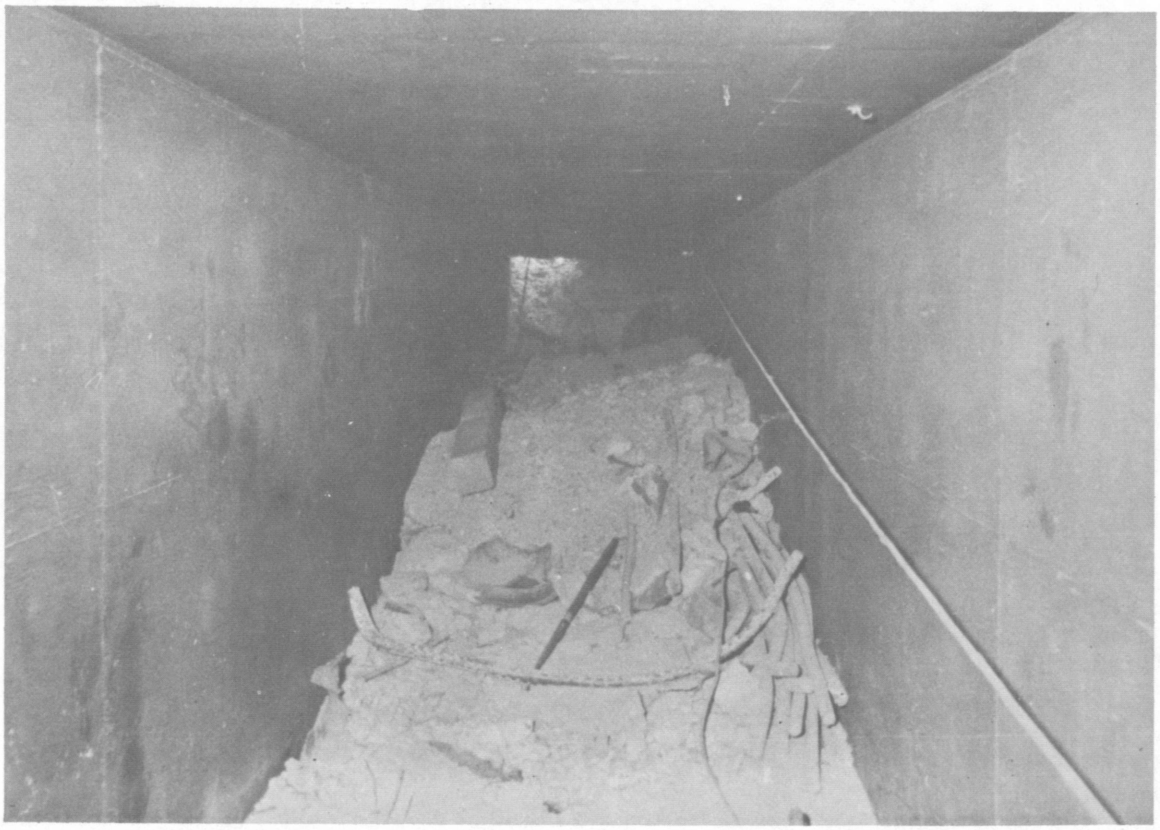

Fig. 9—Post-Quay event damage to tower-base tunnel.

SUMMARY 34

EVALUATION OF BLAST AND SHOCK EFFECTS ON TUNNEL SUPPORT STRUCTURES

(Report ITR-1714, Operation Hardtack, Project 26.13, same title, by A. A. Lee, Project Officer, and E. Y. Wong, Holmes & Narver, Inc., Architect–Engineers, Los Angeles, Calif., Nov. 5, 1959.)

OBJECTIVES AND SCOPE

This project was initiated to obtain test information on the effects of underground nuclear detonations on tunnel linings. The objective was to be attained by gathering qualitative and quantitative information on the quantities and velocities of rock broken from the periphery of the tunnels and on the dynamic response of tunnel linings exposed to these loads. Evaluation of this information should contribute to improvement in the design of tunnel linings.

Project participation included four shots located as follows (ref. ENW, pp. 676 and 677): Tamalpais, U12b.02; Evans, U12b.04; Logan, U12e.02; and Blanca, U12e.05.

Layouts of the various drifts are shown in Fig. 1. Measurements were made before, during, and after these shots by such methods as normal surveying, still and high-speed photography, and deflection gauge instrumentation (Figs. 2 to 4).

BACKGROUND

Following the completion of Operation Plumbbob, which included an underground nuclear explosion identified as Rainier, the Atomic Energy Commission and participating agencies began advance planning for a series of nuclear tests of tunnels at the Nevada Test Site. It was decided that reentry into areas close to the zero point would be necessary to recover desired data and samples. Holmes & Narver, Inc., architect–engineers for AEC, were responsible for the design of tunnel linings for these reentries.

Although the tunnel-damage data from Rainier were limited, extensive data were available from previous underground high-explosive tests conducted by the Corps of Engineers in both sandstone and granite. These tests had been made at several scaled charge weights against tunnels of corresponding scale size.

The full scale for these tests was 320,000 lb of TNT and a tunnel diameter of 30 ft. The high-explosive charge of 320,000 lb against the full-scale test model is equivalent to a ⅕-scale test of a 20-kt

device. assuming that all the energy of the nuclear device is blast energy, i.e.,

$$(40{,}000{,}000)\,(1/5)^3 = 320{,}000\ \text{lb}$$

A comparison of damage between the underground high-explosive tests and the Rainier event indicated that the nuclear explosion produced considerably less effect than is obtained by an equivalent total-energy TNT explosion. Although an exact correlation has not yet been established because of the limited data, it was considered possible to relate damage-distance data from the high-explosive tests with the data from the Rainier shot to obtain an approximate correlation for damage distance in volcanic tuff. From this correlation on damage-distance relations, tentative design criteria for the tunnel linings were developed.

Holmes & Narver proposed this project so that the design criteria on tunnel linings might be improved.

Rock Breakage

The mechanism of damage in rock from an underground explosion is described as follows: A deep explosion creates a camouflet, a roughly spherical cavity, in the rock. In a spherical zone around the camouflet the rock is crushed by the high pressures exerted, and the limit of crushing is related to the compressive strength of the rock. Beyond the limit of crushing, a compressive stress pulse travels out through the rock at the seismic velocity characteristic of the rock. The shape of the pulse is influenced to some degree by the type of explosive, the charge density, and the degree of confinement.

The wavelength of the pulse induced by the detonation of a high-explosive charge is equal to approximately one-half the distance to the explosion. The pulse length induced by a nuclear detonation is somewhat longer. In either case, the intensity of the stress pulse is reduced and the wave shape is changed as the stress pulse moves through the rock.

When the compressive stress pulse reaches an extensive free face, two reflected pulses are generated: a reflected shear pulse and a reflected tensile pulse. The proportion of energy going into each of these reflected pulses is largely dependent on the angle of incidence. Since rock is stronger in shear than in tension and the tensile pulse travels faster than the shear pulse, the reflected tensile pulse tends to break the rock as it moves back into it. If the magnitude of the reflected tensile pulse is sufficient to break the rock, the broken rock moves forward with a velocity that is a function of a number of factors, such as the density of the rock and the amount of energy imparted to the rock. Reference 1 provides a detailed discussion of the reflection theory of rock breakage.

The distance from the free face at which rock breakage occurs is influenced by the wavelength of the stress pulse. Since the wavelength from a nuclear explosion is longer than the wavelength from a high-explosive charge, tension failure occurs farther back from the free face. Regardless of the direction of the impinging wave, the material will tend to fail in a plane roughly parallel to the surface in a phenomenon known as "slabbing." After one slab has been detached, another free face is presented. This may result in successive failures of the same type.

The same breakage mechanism applies to tunnel damage from an adjacent explosion except that other complicating factors must be considered. With a large explosion in relation to a given tunnel size, the stress field approaches that developed by a static load. The stress wave diffracts around the opening, and the tendency of the rock to slab off and move into the tunnel is resisted by arching action.

Damage Zones

Tunnel damage in the underground explosion test series has been classified by the Corps of Engineers into four successive degrees of damage, and the four areas fitting these descriptions were identified by zone numbers. The same zoning classification is used in this project. Tunnel damage resulting from an adjacent detonation is shown schematically in Fig. 5 and is described as follows:

Zone 1: Complete Damage. The rock is completely crushed out to a point defined by the compressive strength of the rock. Beyond the area of complete crushing, the rock is propelled from all sides

of the tunnel, completely closing the tunnel. In this zone a damage profile does not exist. The outer limit of Zone 1 is that point where the damage profile begins. Indications from limited test observations with motion picture photography show that fly rock may have a maximum velocity of about 100 ft/sec, with lower velocities for the larger masses of rock.

Zone 2: Block Breakage. The rock breakage is continuous and increases in thickness nearer the explosion. The breakage extends far around the tunnel; sizable amounts of rock are broken, and the pieces are large and block-like. The general shape of the damage profile is a line distinctly inclined to the original tunnel surface. The outer limit of Zone 2 is that point where the general shape of the damage profile changes from a line distinctly inclined to the original tunnel surface to a line nearly parallel with the original tunnel surface. The damaged area varies from 30 to 80% of the original cross-sectional area of the tunnel. The maximum fly-rock velocity ranges from 30 to 60 ft/sec.

Zone 3: Continuous Slabbing. The rock breakage is continuous and relatively uniform in thickness; it is principally on the side toward the explosion. The outer limit of Zone 3 is that point at which rock breakage and the damage profile become discontinuous. The damaged area varies from 5 to 30% of the original tunnel cross-sectional area. The maximum fly-rock velocity is about 20 to 30 ft/sec, and the heavier spalls are believed to fall almost vertically.

Zone 4: Discontinuous Damage. The rock breakage is irregular and intermittent; breakage may include the dislodging of material previously loosened by tunnel driving. The damage profile is discontinuous in this zone. The outer limit of Zone 4 is that point beyond which no significant rock breakage occurs. The damaged area increases the cross-sectional area of the tunnel from zero to 5%. Maximum fly-rock velocity is about 2 ft/sec. Available evidence indicates that spalls drop vertically.

Damage-distance Criteria

The underground nuclear detonation test of Operation Hardtack, Phase II, took place in the same area and in the same material, volcanic tuff, as the Rainier event in Operation Plumbbob. Rainier data were correlated with high-explosive test information to develop tentative tunnel-lining design standards appropriate for use in volcanic tuff. At the Rainier site the outer limit of damage was 500 ft, and complete closure occurred at a distance of 200 ft from the explosion. When reduced by cube-root scaling of the 1.7-kt for Rainier, these distances become 420 and 168 ft, respectively, for a 1-kt yield.

It was decided to relate the outer limit of Zone 4 from the high-explosive tests to the corresponding zone from the Rainier event, both scaled to 1 kt. On this basis, the radial distances from the zero point to the outer limits of the various damage zones of a 1-kt device are as follows: Zone 1, 116 ft; Zone 2, 230 ft (tunnel closure in this zone); Zone 3, 312 ft; and Zone 4, 420 ft. Distances for corresponding damage for other yields were obtained by multiplying the above distances by the cube root of the given yield.

Design Loading

The design loads on the linings in tunnels U12b and U12e were computed from the maximum weight of rock and the kinetic energies per foot of tunnel measured along the center line. These computations are based on the procedures and data given in Reference 2, and the results are tabulated in Table 1.

RESULTS

Owing to reentry and instrumentation-recovery problems, most of the data obtained were static measurements from surveying and from still photography. The high-speed cameras installed to determine fly-rock velocity and set deflection had not been recovered at the time of writing, but no record was expected because the film probably had been fogged by radioactivity. Some quantitative information was obtained by deflection gauges mounted on the tunnel lining; however, the gauges presently recovered failed to give an adequate deflection–time trace to permit a transient-response study.

Documentary Photographs

Documentary photographs illustrate the following for the four test shots:

Tamalpais. Figure 6 shows the closure of tunnel U12b.02 at a distance of 65 ft beyond the blast door. Note the rapid reduction of damage from the point of closure outward toward the blast door. Some damage occurred in alcove 1, as seen in Fig. 7. At this distance from the explosion the damage is slight, but there is definitely more damage when the tunnel is at right angles to the zero point.

Logan. Figure 8 shows a typical damaged section along the U12e.05 drift from the Logan event. It also shows a marked similarity to the type of damage found in tunneling operations in "squeezing" ground. Since we know that damage in squeezing ground results from radial loading, it is reasonable to assume an analogous situation here.

Evans. No postshot documentary photographic coverage has as yet been possible in U12b.04.

Blanca. The point of closure of tunnel U12e at station 16+70 is shown in Fig. 9. Note the massive size of the broken blocks of rock. Figure 10 shows the situation at station 19+29 at the time of redriving the drift. The elevation of the cylindrical mass of cable, pipe, lagging, and sets is approximately the same as the center of the original drift. The mass, however, is approximately 7 ft to the left of the original center line. Hand specimens of rock from the face show no cracks when inspected with a 10-power mineral hand lens.

Cross-section Measurements

Postshot cross-section measurements were taken in U12b.02 and U12e. A typical example of the data obtained is shown in Fig. 11.

CONCLUSIONS

Tentative conclusions based on the limited data available are:

1. The stress field produced by an underground nuclear detonation in tuff acts essentially as a hydrostatic load around the tunnel, which would permit the use of simplified design loading for tunnel linings.
2. The configuration of the tunnel at the zero point influences the damage-distance relations to a large degree; the straight-end configurations produced greater damage than the hooked-end configuration (Table 2).
   a. The damage-distance relations based on a previous test (Rainier event. See reference 3) for determining the point of closure ($168\ W^{1/3}$) and the point of no damage ($420\ W^{1/3}$) are in close agreement with results obtained from a test in a tunnel with similar hooked-end configuration.
   b. Though the damage-distance factor for straight-end tunnels is much larger, there is also a large difference in this factor between the two events that took place in tunnels with this configuration; hence, no firm damage-distance criteria have been developed for tunnels with a straight-end configuration.

REFERENCES

1. W. I. Duvall and T. C. Atchison, *Rock Breakage by Explosives,* U. S. Department of the Interior, Bureau of Mines, Report of Investigations 5356, September 1957.
2. *An Engineering Manual on Design of Underground Installations in Rock,* U. S. Department of the Interior, Bureau of Mines, March 1957.
3. G. W. Johnson and C. E. Violet, *Phenomenology of Contained Nuclear Explosions,* USAEC Report UCRL-5124(Rev. 1), Lawrence Radiation Laboratory, University of California, December 1958.

Table 1—WEIGHT AND KINETIC ENERGY OF ROCK BY ZONE

Zone	Max. damage area, % original cross section	Max. wt. of broken rock per ft of tunnel, lb		Max. kinetic energy per ft of tunnel, ft-lb	
		U12b	U12e	U12b	U12e
4	5	350	850	3	7
3	30	2,100	5,080	1,470	3,540
2	80	5,600	13,500	7,800	18,800

Table 2—CLOSURE, SCALED DISTANCES

Event and tunnel	Tunnel configu-ration	Distance, zero point to closure, ft	Angle of incidence, zero point to closure, deg	Yield, kt	Distance to point of closure, scaled to 1 kt, ft	Outer limit zone 4, scaled to 1 kt, ft
Rainier,* U12b	Hooked	200	14	1.7	168	420
Tamalpais, U12b.02	Hooked	80	28	0.09	179	~420
Logan, U12e.02	Straight	820	35	4.5	496	~1190
Evans, U12b.04	Hooked	Unknown		0.045	Unknown	Unknown
Blanca, U12e.05	Straight†	870	16	23	306	~690

*Information from Operation Plumbbob, included for comparison.

†With venting to the unusable portion of the drift beyond the zero point.

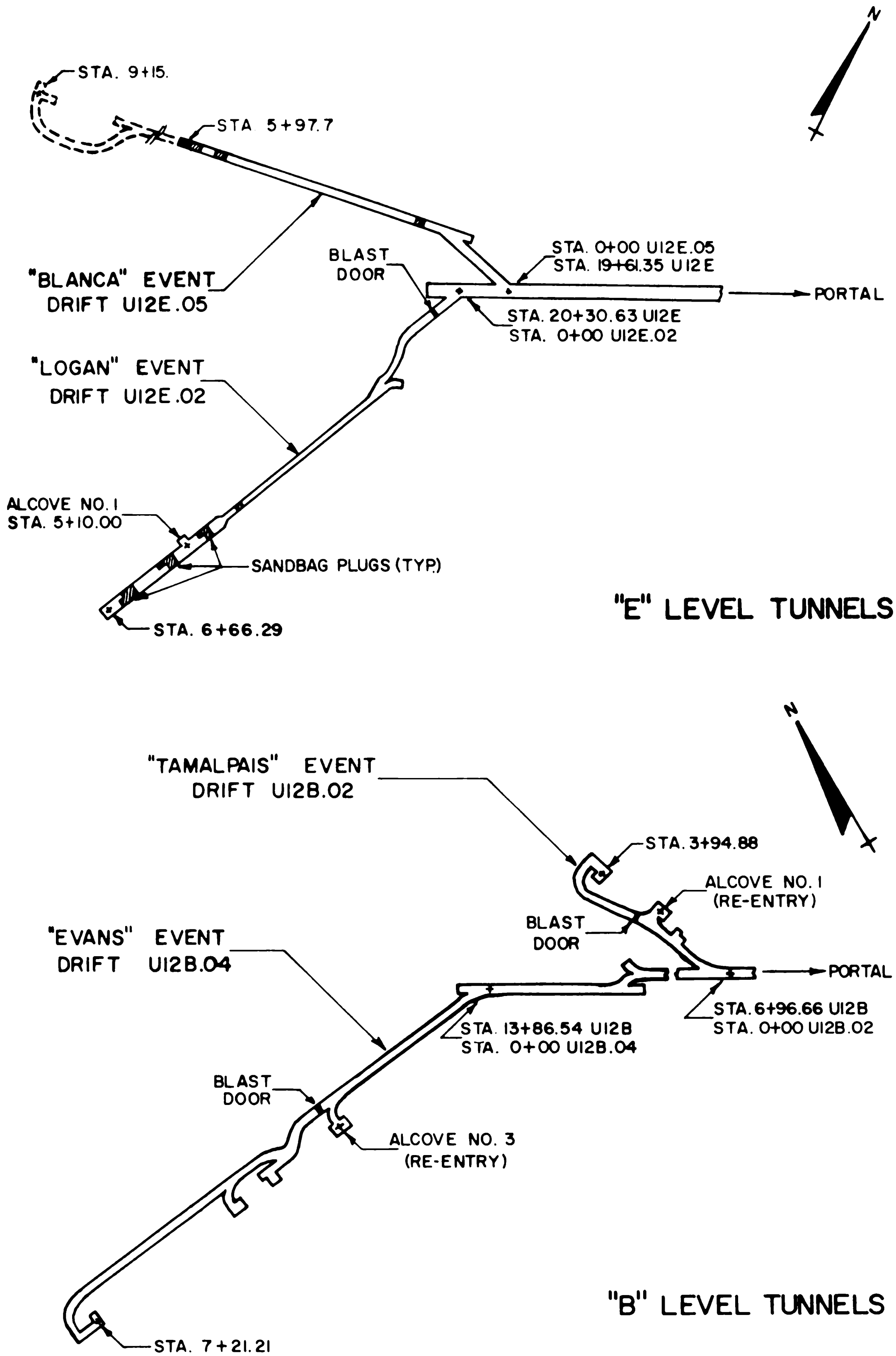

Fig. 1—General layout, B and E level tunnels.

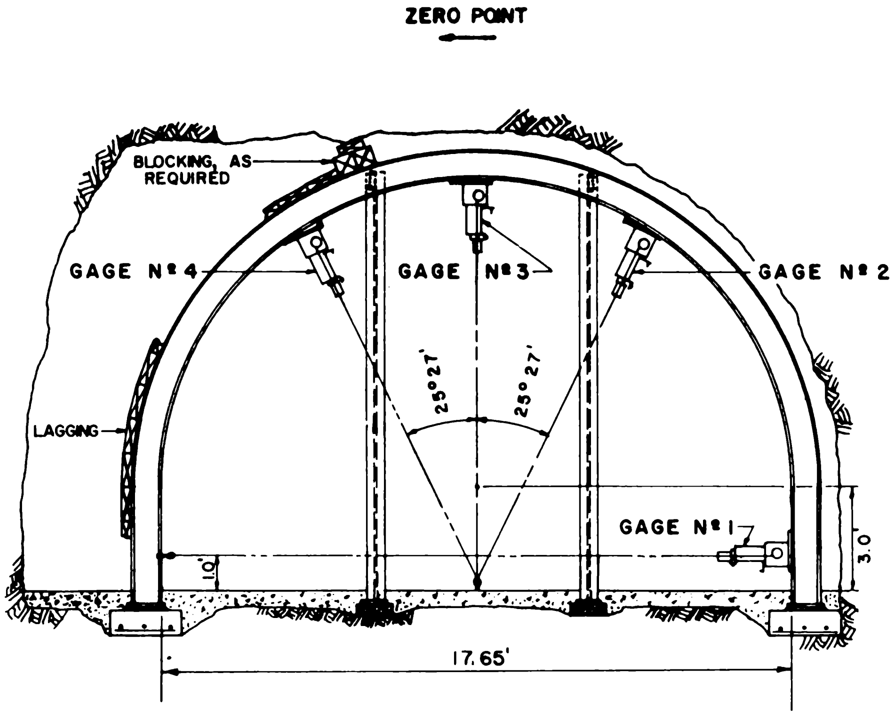

Fig. 2—Gauge setup in alcove 1, drift U12b.02, Tamalpais event.

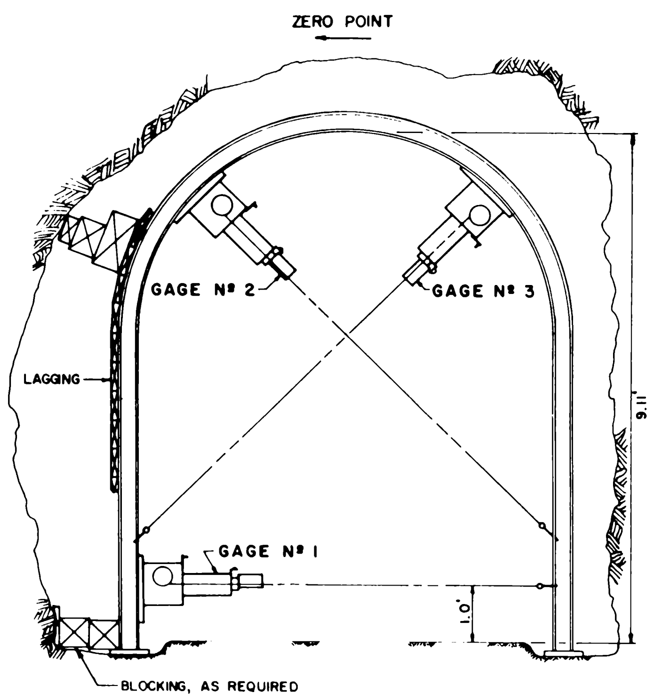

Fig. 3—Gauge setup in station 2+85, drift U12e.05, Logan event.

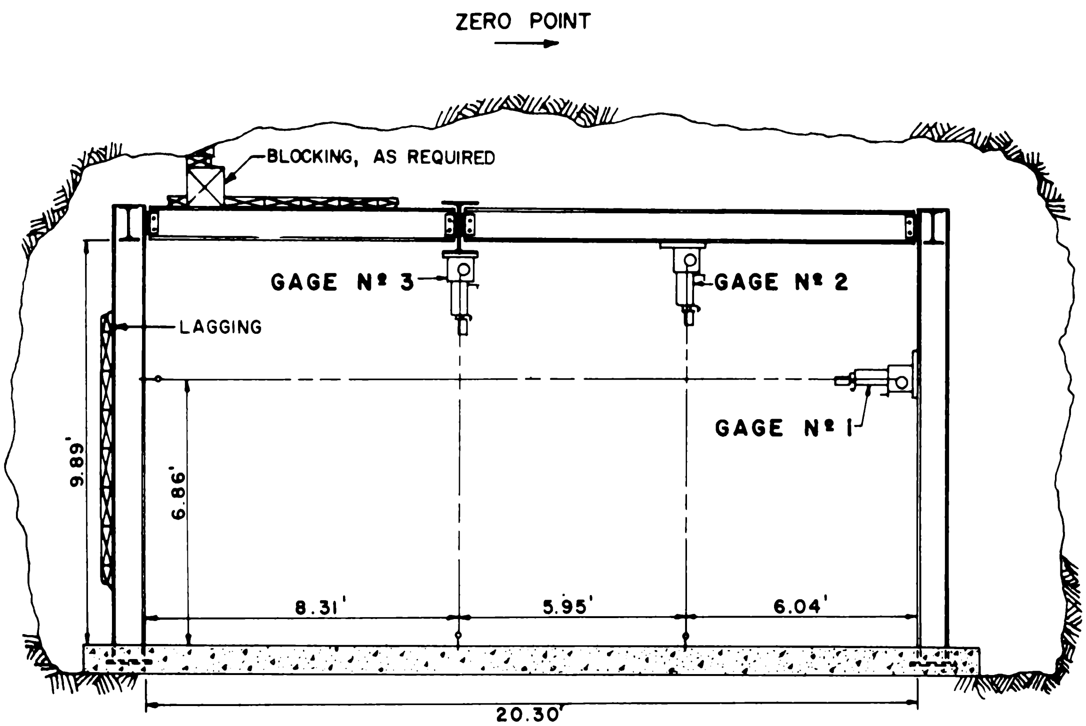

Fig. 4—Gauge setup in alcove 3, drift U12b.04, Evans event.

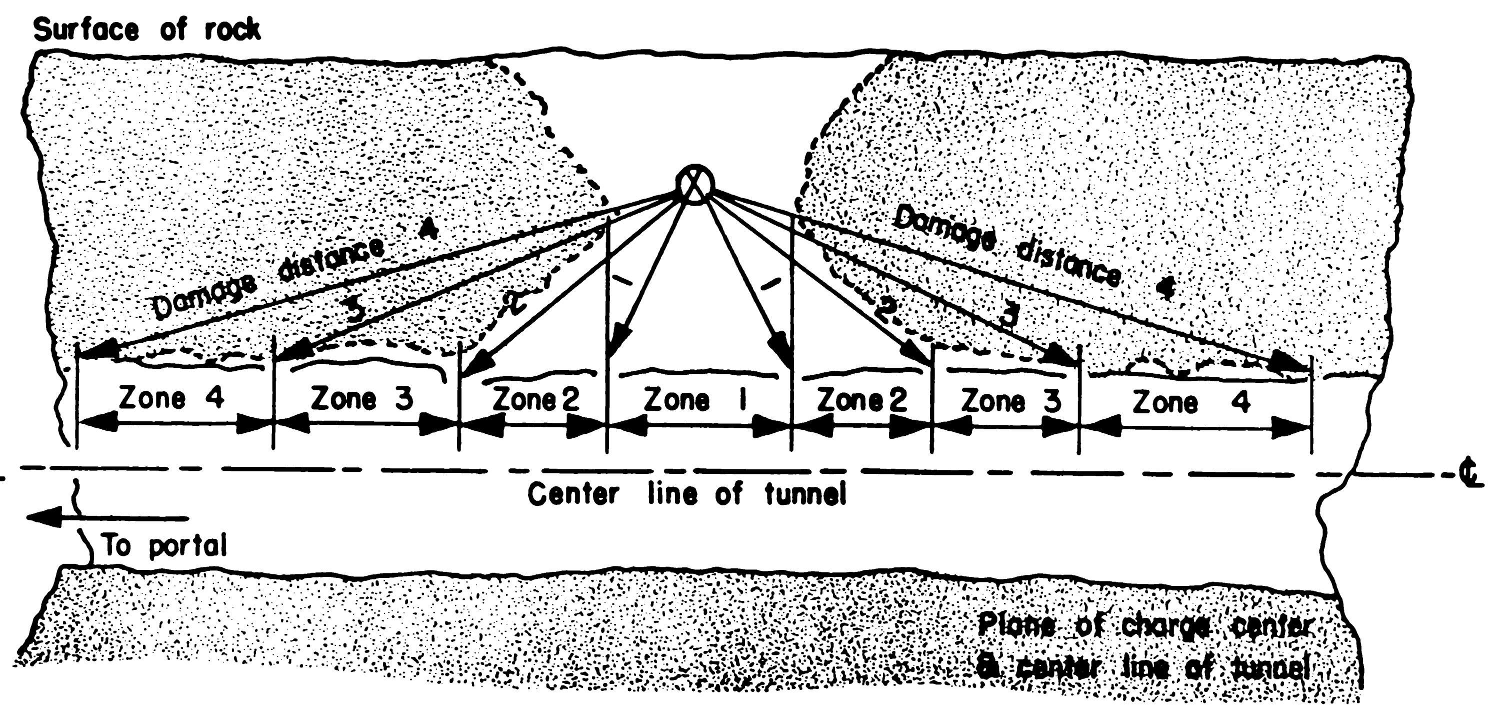

Fig. 5—Schematic diagram shows damage-distance notation and zones of damage.

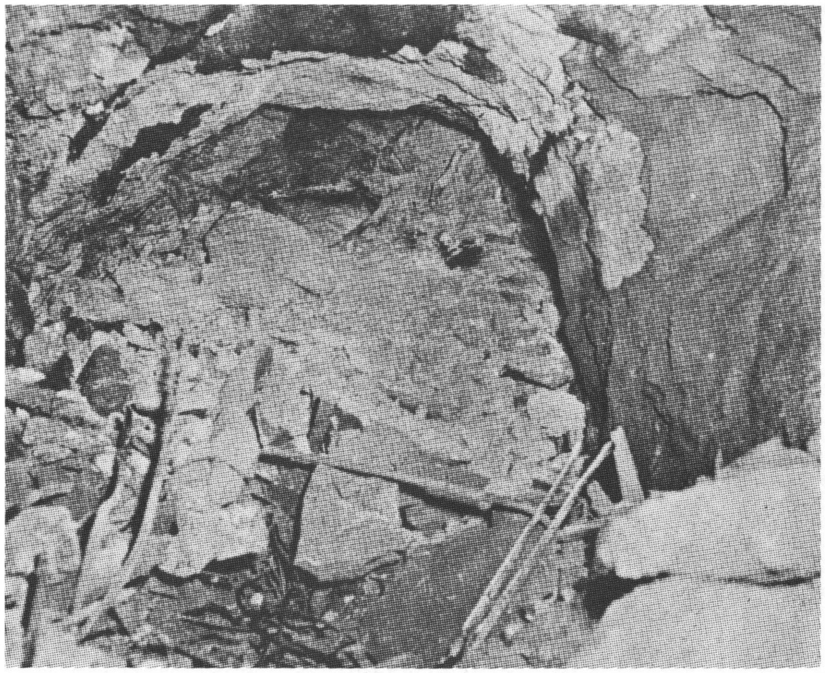

Fig. 6—Point of closure, drift U12b.02, Tamalpais event.

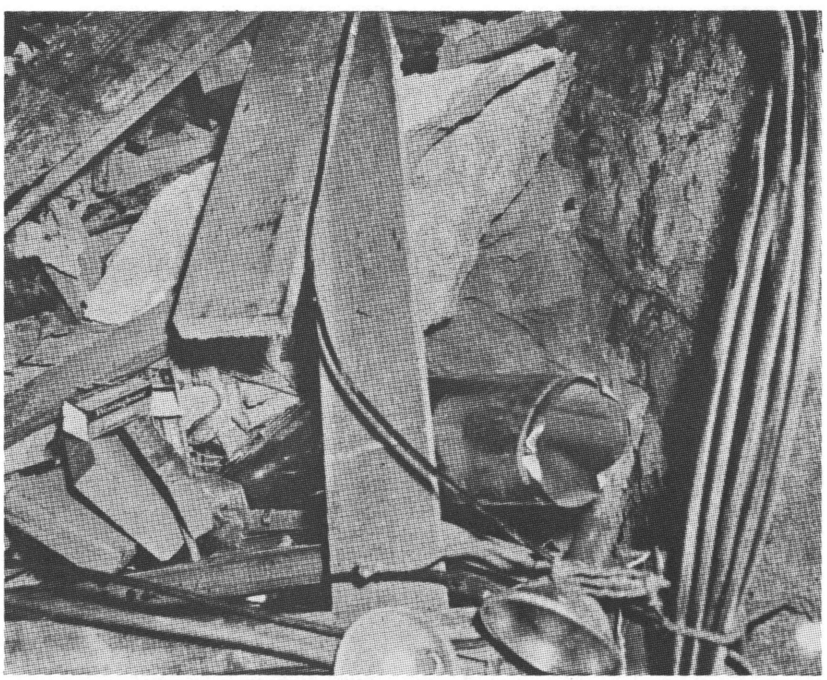

Fig. 7—Damage to alcove 1, drift U12b.02, Tamalpais event.

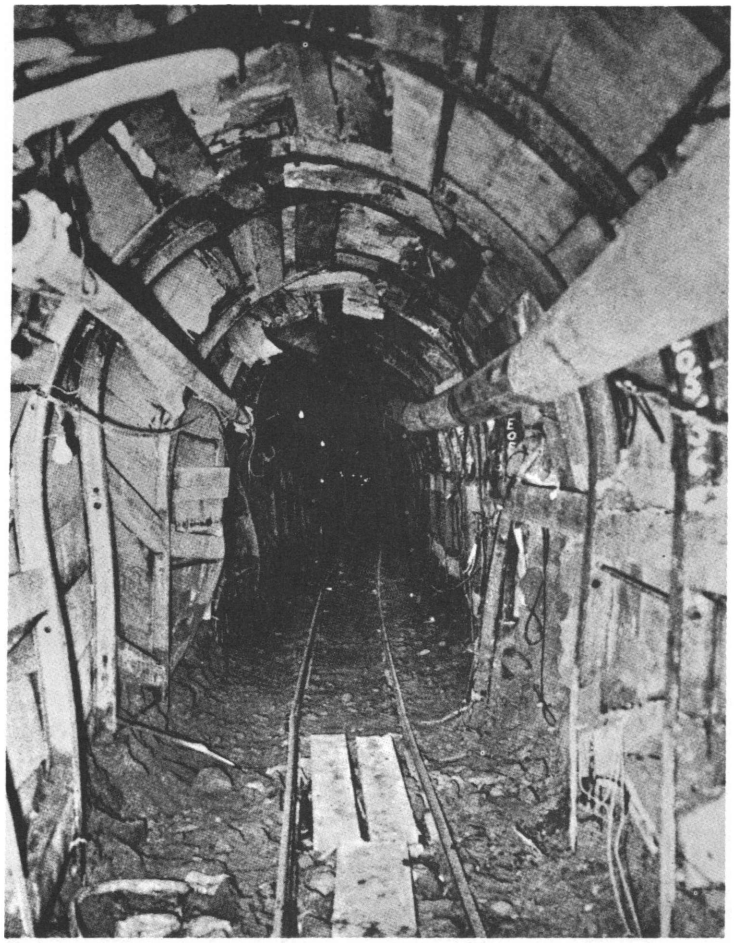

Fig. 8—Typical damaged section, drift U12e.05, Logan event.

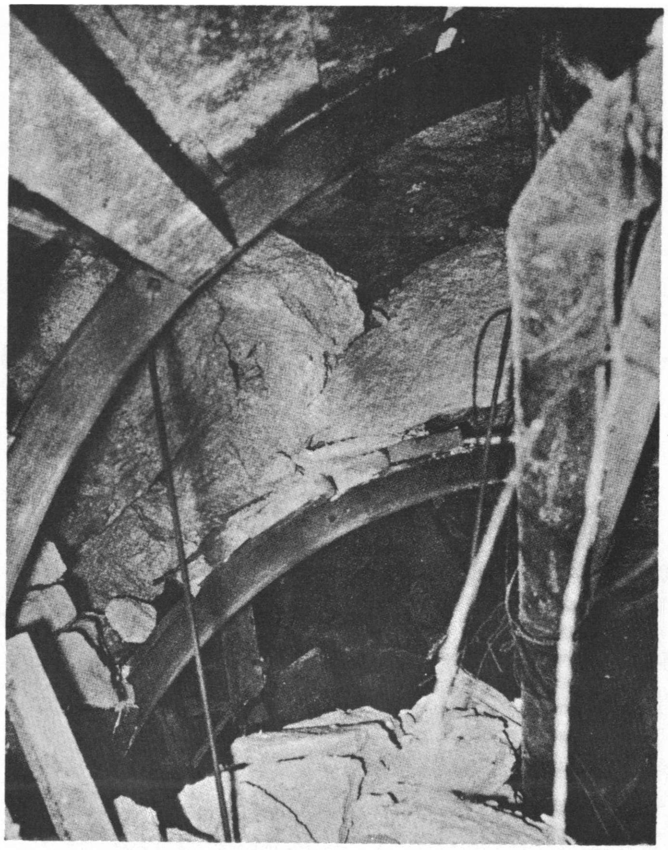

Fig. 9—Point of closure, station 16+70, tunnel U12e, Blanca event.

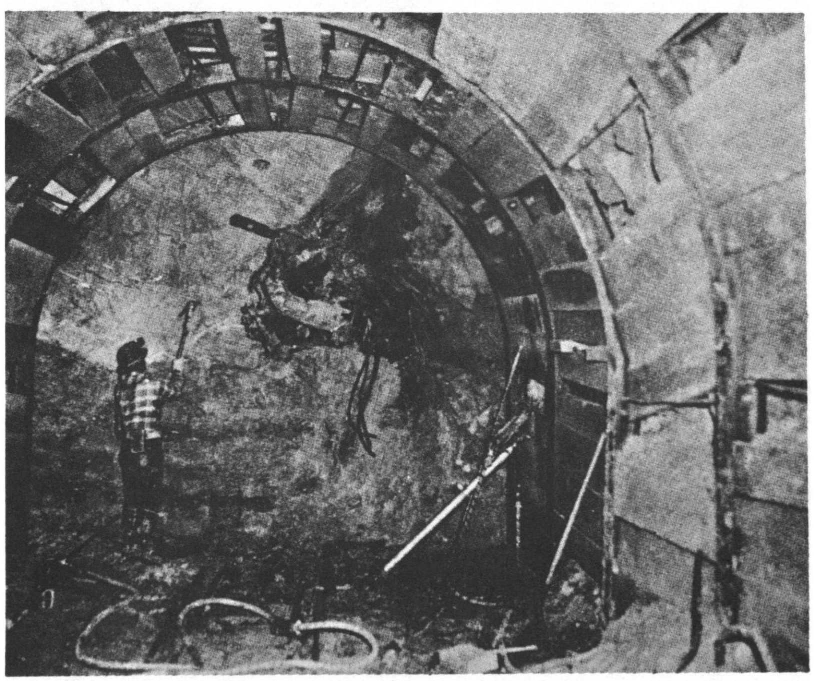

Fig. 10—View at station 19+29, post-Blanca.

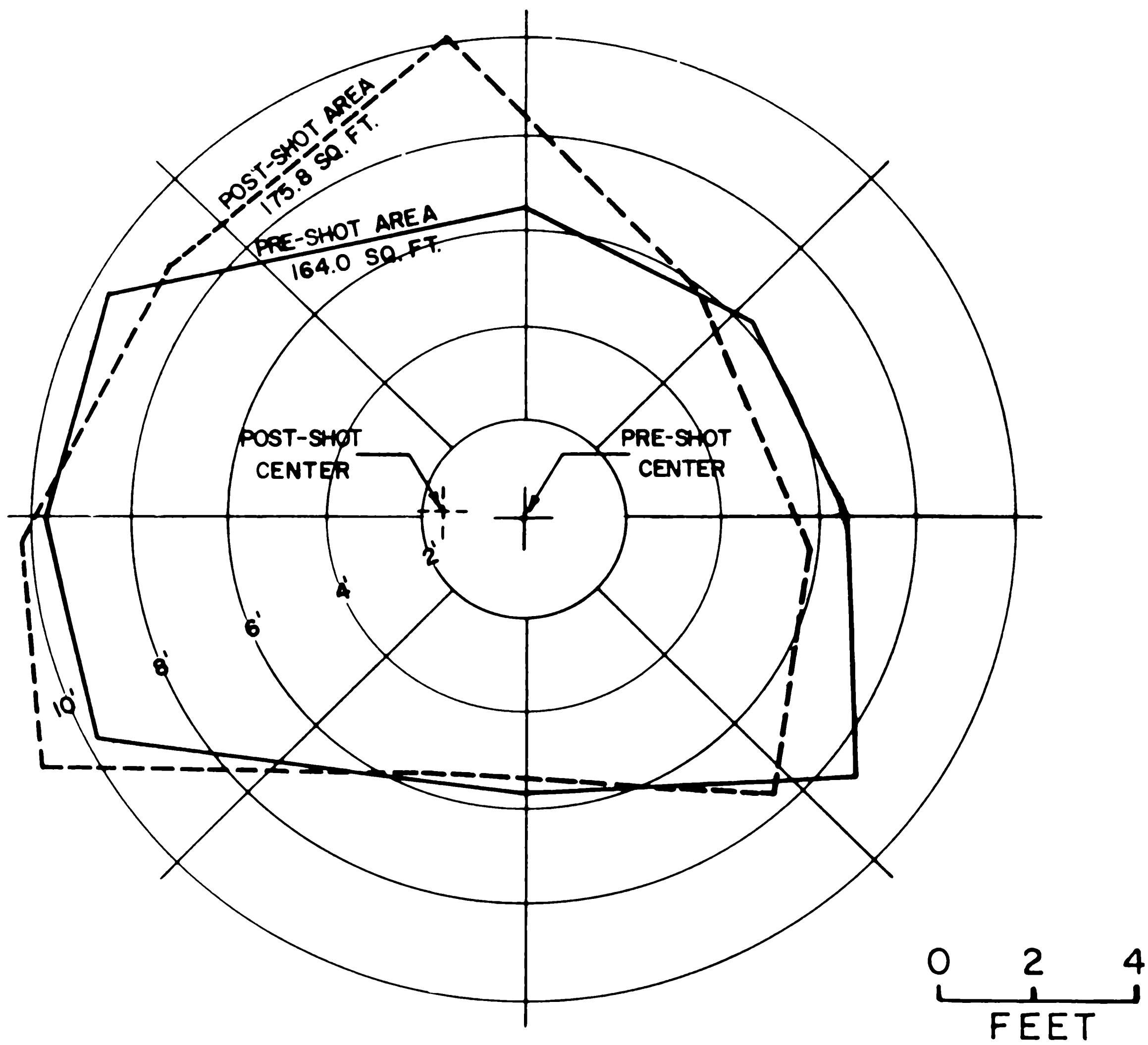

Fig. 11—Preshot and postshot cross sections, drift U12e, station 11+20.

SUMMARY 35

RETEST AND EVALUATION OF ANTIBLAST VALVES

(Report ITR-1717, Operation Hardtack, Project 70.3, same title, by James E. Roembke, Office of Civil and Defense Mobilization, Mar. 27, 1959.)

OBJECTIVES AND SCOPE

The objectives of this test were to determine operating characteristics and effectiveness of three sizes of antiblast valves when operated under nuclear blast conditions at overpressures predicted to damage or destroy the valves. It was desired to determine the closure times and pressure rises within the test chambers when the valves were closed by shock-wave pressures in excess of 100 psi. A further objective was to obtain information to supplement data obtained in Operation Plumbbob (see Summary 26). The FCDA had contracted with Arthur D. Little, Inc., to develop the prototype antiblast valves that were tested satisfactorily in Operation Plumbbob. (Fig. 2, Summary 26).

Analysis of the damage to the valves would make it possible to refine the design by using components of equal structural strength, thereby reducing the weight and cost and at the same time increasing the speed of closure, and improving the valves' protective capability. The expendable insect screens that were destroyed in the previous test were omitted in this test. Three valves, one each of the 12-, 16-, and 24-in. sizes, were tested at maximum predicted 175-, 150-, and 125-psi overpressures, respectively, from a very small yield device. The valves were mounted vertically on cover slabs of underground-pipe cells. They were instrumented to obtain: (1) pressure–time measurements inside the weatherproof hood; (2) pressure–time measurements in the pipe expansion chamber; and (3) position–time measurements for each valve disk.

Because all instrumentation data were lost for the 12-in. valve tested at 100 psi in Operation Plumbbob, this test at higher overpressures was considered important even if the valves sustained no physical damage.

The reinforced-concrete underground-pipe cells, including their 5½-ton concrete covers, were located on a common base slab. Figure 1 shows the three test cells in position, and Fig. 2 shows the same test cells from an elevation approximating the angle of blast to the structures. The valves that were located at the higher overpressure ranges in Operation Plumbbob were used for this test. Each valve was disassembled, cleaned, and lubricated to ensure its operability before transportation to the site for mounting. All valves were vertically mounted on the cover slabs, as shown in Fig. 3. As in Operation Plumbbob, each valve contained a self-recording pressure–time (SR/PT) instrument inside the valve hood, and there was a similar instrument inside each pipe test cell. Figure 4 illustrates the placement of one of the SR/PT gauges.

RESULTS

The 12- and 16-in. valves closed in approximately 20 and 66 msec, respectively, after the blast wave entered the valve chamber; they opened after the pressure wave subsided. The valves were in operating condition when inspected after the test. The 24-in. valve traveled approximately one-third of its required distance to close and then returned to its normally open position. Peak pressures recorded in the chambers to which the valves were attached required a detailed analysis and evaluation. There was no obvious mechanical damage to any of the valves, and the repainted surfaces were unscorched after the blast. The results, in general, were consistent with the results of the test in Operation Plumbbob.

One of the major objectives, i.e., to damage or destroy the valves to determine points of failure, was not accomplished because the nuclear device to which they were subjected failed to yield its anticipated overpressures.

Peak pressures inside the valve hoods were somewhat less than the measured peak incident overpressure value of approximately 20 psi. Peak pressures inside the pipe test cells were less than 2 psi.

CONCLUSIONS

Owing to the short duration of the pressure wave from the particular nuclear device to which they were subjected, the peak-pressure effects in the expansion chambers or underground pipe cells were less than those recorded in Operation Plumbbob at lower overpressure ranges. It is probable that, owing to the heavier mass of the moving parts of the 24-in. valve, the peak incident overpressure was of insufficient duration to completely close the disk. In other words, the pressure wave subsided before overcoming the inertia and the spring load of the 24-in. valve. The weight of moving parts of the 12-in. valve is 23 lb; of the 16-in. valve, 21 lb; and of the 24-in. valve, 91 lb. Even though the 24-in. valve did not completely close, the pressure inside the expansion chamber did not exceed 2 psi. Although the test did not result in the high overpressures anticipated, it did produce data for an overpressure range that was different from that of the previous test and for a shorter duration weapon. These data will be valuable in a redesign of the valves.

It was recommended that the data from Operation Plumbbob and from this test be thoroughly evaluated by the designers to ascertain what modifications should be made in redesign to speed up closing time and to reduce the mass of the valve. A latching device should be developed to retain the disk in a closed position where negative pressures could damage equipment or collapse ductwork.

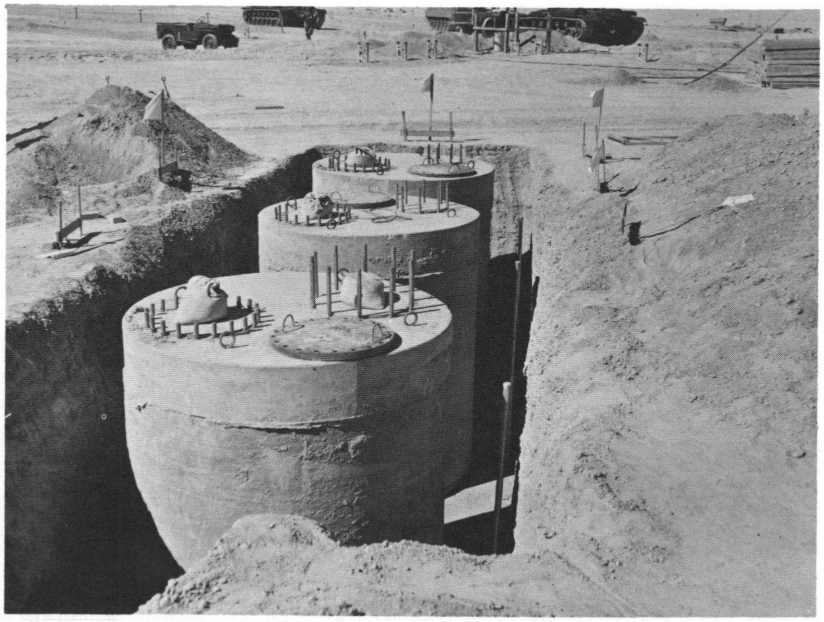

Fig. 1—Test cells in place before backfilling.

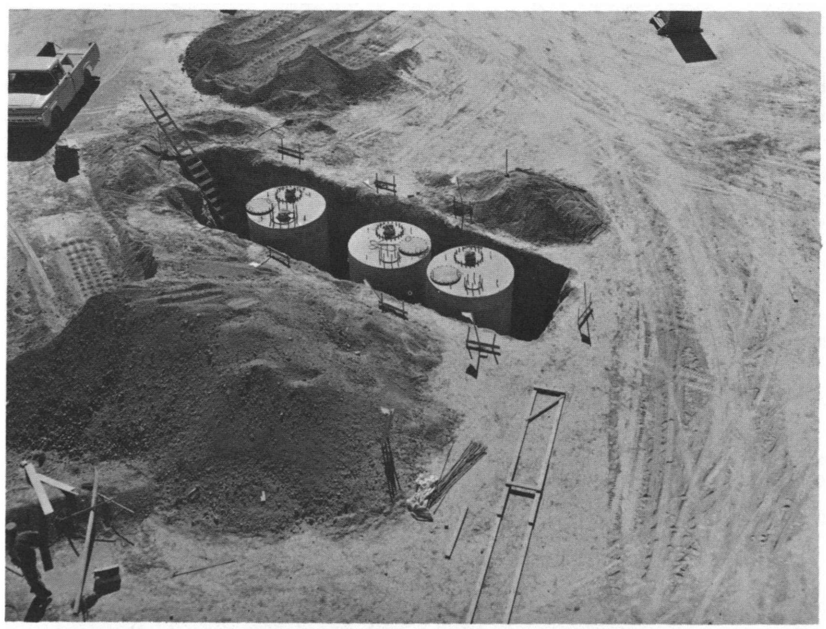

Fig. 2—Cells before backfilling and placing valves.

Fig. 3—Valves mounted at predicted 175-, 150-, and 125-psi overpressure ranges.

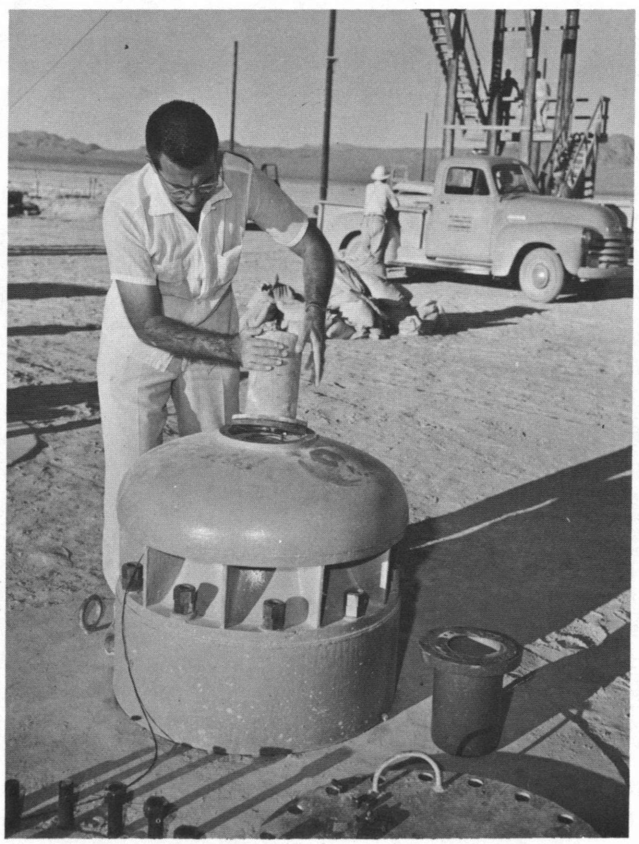

Fig. 4—Placing SR/PT gauge on top of blast valve.

SUMMARY 36

EFFECT OF NUCLEAR WEAPONS ON OCDM FAMILY FALLOUT SHELTER

(Report ITR-1718, Operation Hardtack, Project 70.4, same title, by James E. Roembke, Office of Civil and Defense Mobilization, Mar. 27, 1959.)

OBJECTIVES AND SCOPE

The primary objective of this project was to evaluate the capabilities of a conventionally designed underground family fallout shelter to resist the blast effects of a nuclear detonation and to determine the degree of protection from nuclear radiation. Secondary objectives were to test a standard 3-in. vertical check valve as an antiblast valve and to test the blast resistance of the sensing element for a remote-reading-station radiation-monitoring device, CD V-711.

In the Vesta event (ref. ENW, p. 678), the three shelter structures, located one mile from Ground Zero (GZ), were subjected to considerable fallout but rather insignificant blast. The subsequent Rushmore event (ref. ENW, p. 677) subjected the structures to short-duration blast overpressures on the order of 1.5 to 13.5 psi and to initial radiation.

STRUCTURES AND EQUIPMENT

The criteria for the design of the shelter were to develop a simple, easy-to-build, box-like structure that would provide adequate protection from fallout radiation. Complex and elaborate entranceways were to be avoided as were special hard-to-form curved or diagonal sections.

Figures 1 and 2 show design details of the shelter structure. The top and bottom slabs were designed as one-way slabs, with supports on two sides, rather than two-way slabs with supports on all four sides. This permits extending the length of the structure indefinitely to vary its capacity. Reinforcing rods in the 8-in. walls meet only the minimum code requirements for shrinkage and temperature.

Vent stacks were placed and capped before backfilling. A standard 3-in. vertical check valve (Fig. 3) was placed on the intake stack at each of the three overpressure levels to determine its suitability as a small antiblast valve.

A blast line was established using self-recording pressure–time gauges at the ground line near each shelter. One gauge was also mounted inside each structure to assist in determining the effectiveness of the 3-in. check valve, referred to above, by measuring pressure rise, if any, inside the shelter.

Deflections of walls, ceiling, and floor were to be measured by simple scratch gauges.

Radiation instrumentation was placed to determine the gamma dose inside and outside the shelter.

The shelter was oriented to provide the least protection from initial radiation which, owing to the height of the burst, could penetrate the ½-in. steel-plate hatch cover and enter the shelter without completing two full 90° turns.

Film badges were placed at heights of 1, 3, and 5 ft from the floor. Chemical dosimeters were strategically located adjacent to some of the film badges.

RESULTS

A summary of results is given in Table 1.

There was no apparent blast damage to any of the structures. Deflection gauges indicated that the structures did not respond; i.e., no measurable permanent or even transient deflections were experienced.

The 3-in. vertical check valve appeared to operate satisfactorily as an antiblast valve. No physical damage was apparent. As indicated in Table 1, pressures inside the structures were well below the range for physical injury to occupants or mechanical damage to equipment.

Film badge and chemical dosimeter data obtained in the tests were not published in the subject report. Various complications, including unusual dust conditions caused by high winds, were blamed for the loss of some of the radiation data.

DISCUSSION

Lack of structural response to the blast pressures at the 13.5-psi range does not necessarily indicate that the basic underground family fallout shelter will sustain similar peak incident overpressures from larger weapons. It is probable that the duration of the peak overpressure was not long enough to create a load pulse of sufficient magnitude to cause the structure to respond. Even though the natural period of the structural elements is short, the actual blast load was, relatively, of such extremely short duration that it appears improbable that an extrapolation or prediction of response to the effects of larger yield nuclear weapons (of much longer positive blast duration) can be made on the basis of this test. Nevertheless, it may be concluded, with assurance, that the shelter is capable of resisting the blast effects of a nuclear weapon at an overpressure range of 5 to 10 psi, as was predicted.

Table 1—SUMMARY OF PRELIMINARY DATA

Station No.	Original predicted over-pressure, psi	Actual over-pressure (approx.), psi	Duration (approx.), msec	Over-pressure in shelter, psi	3-in. vertical check valve	Apparent structural damage	Station monitor sensing element
904.01	20	13.5	133	0.2	Closed	None	No apparent damage
904.02	10	3.2		0.1	Closed	None	None installed
904.03	5	1.2		0.06	Remained open	None	None installed

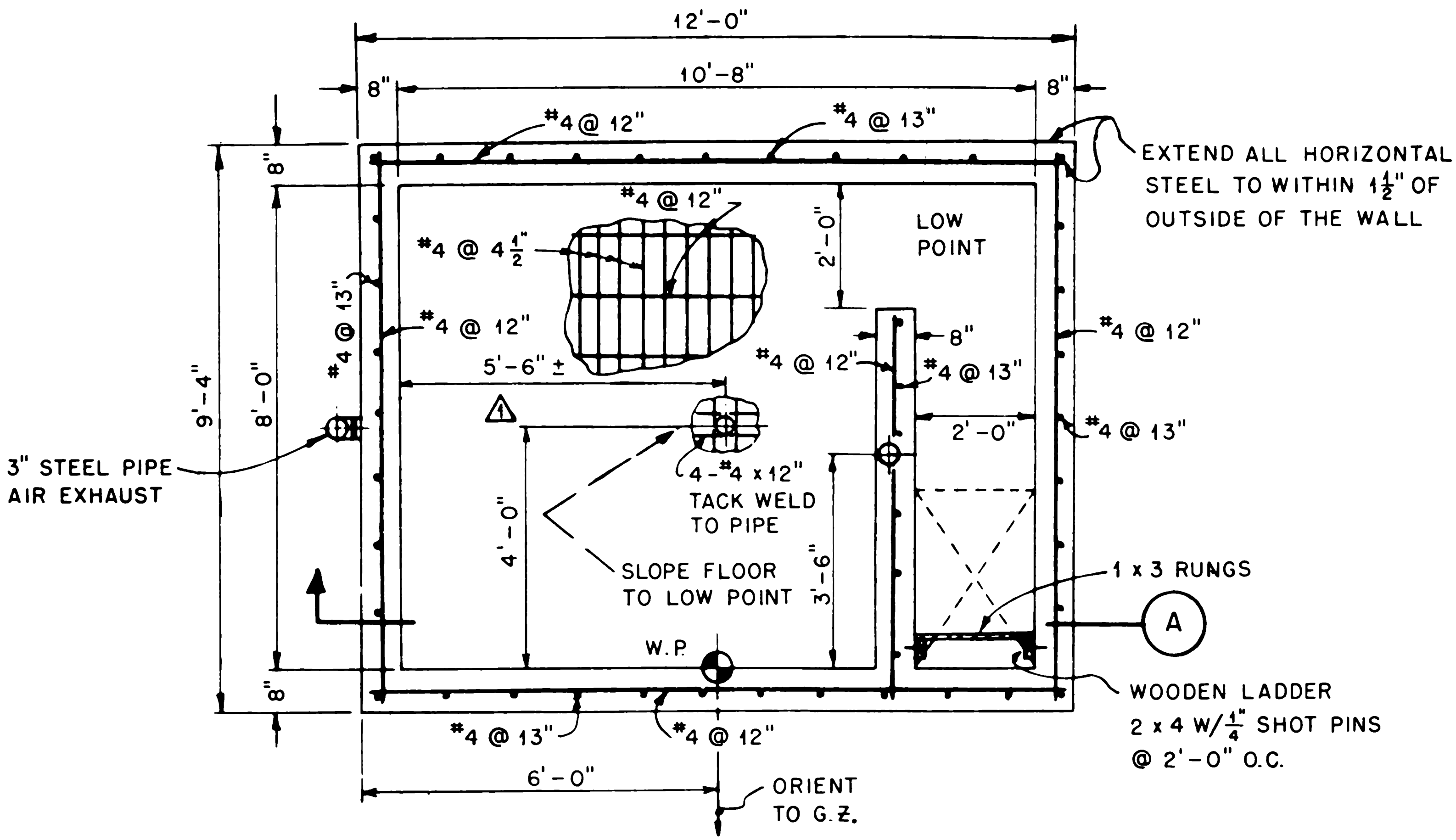

Fig. 1—Basic underground family fallout shelter, plan.

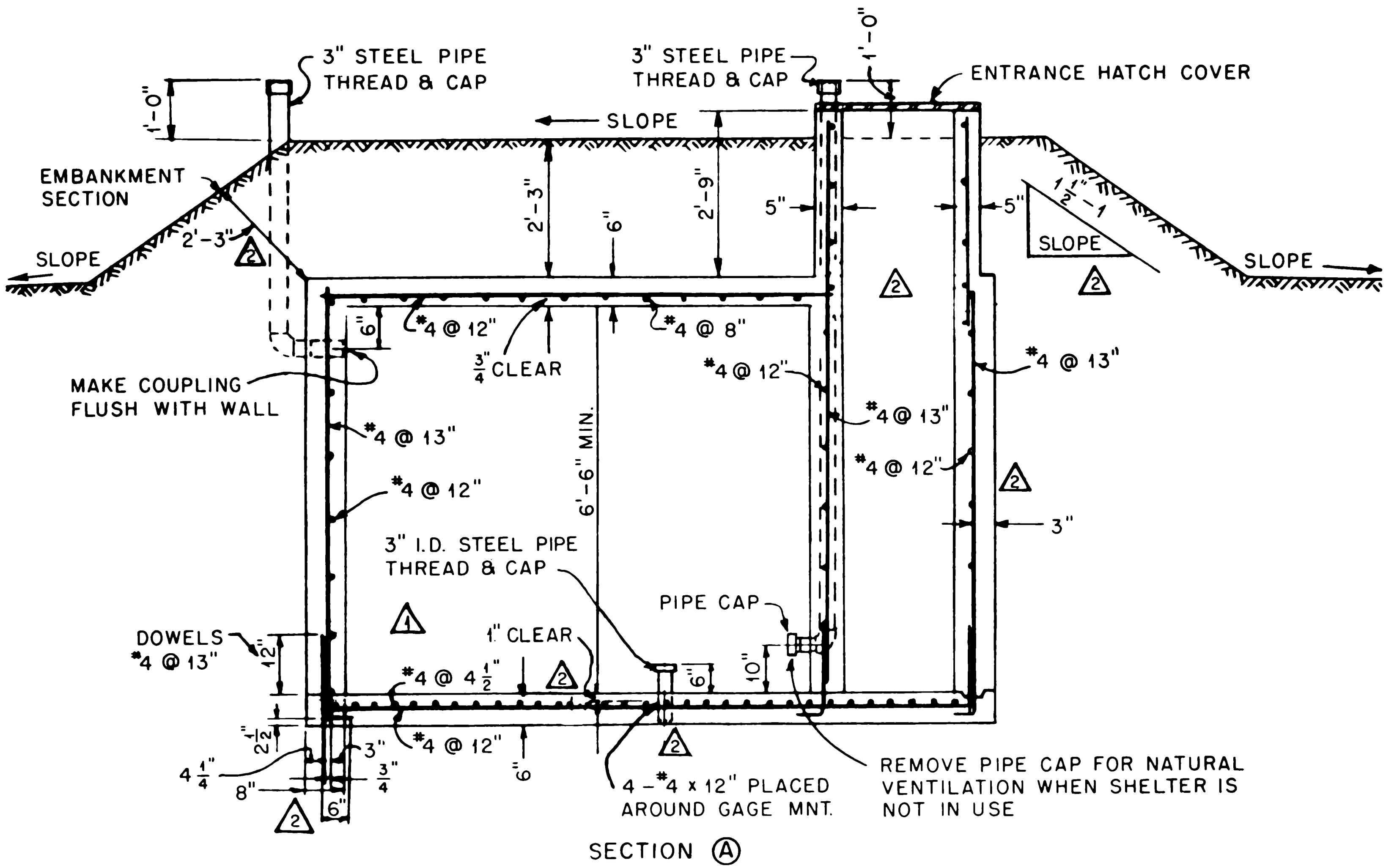

Fig. 2—Basic underground family fallout shelter, longitudinal section.

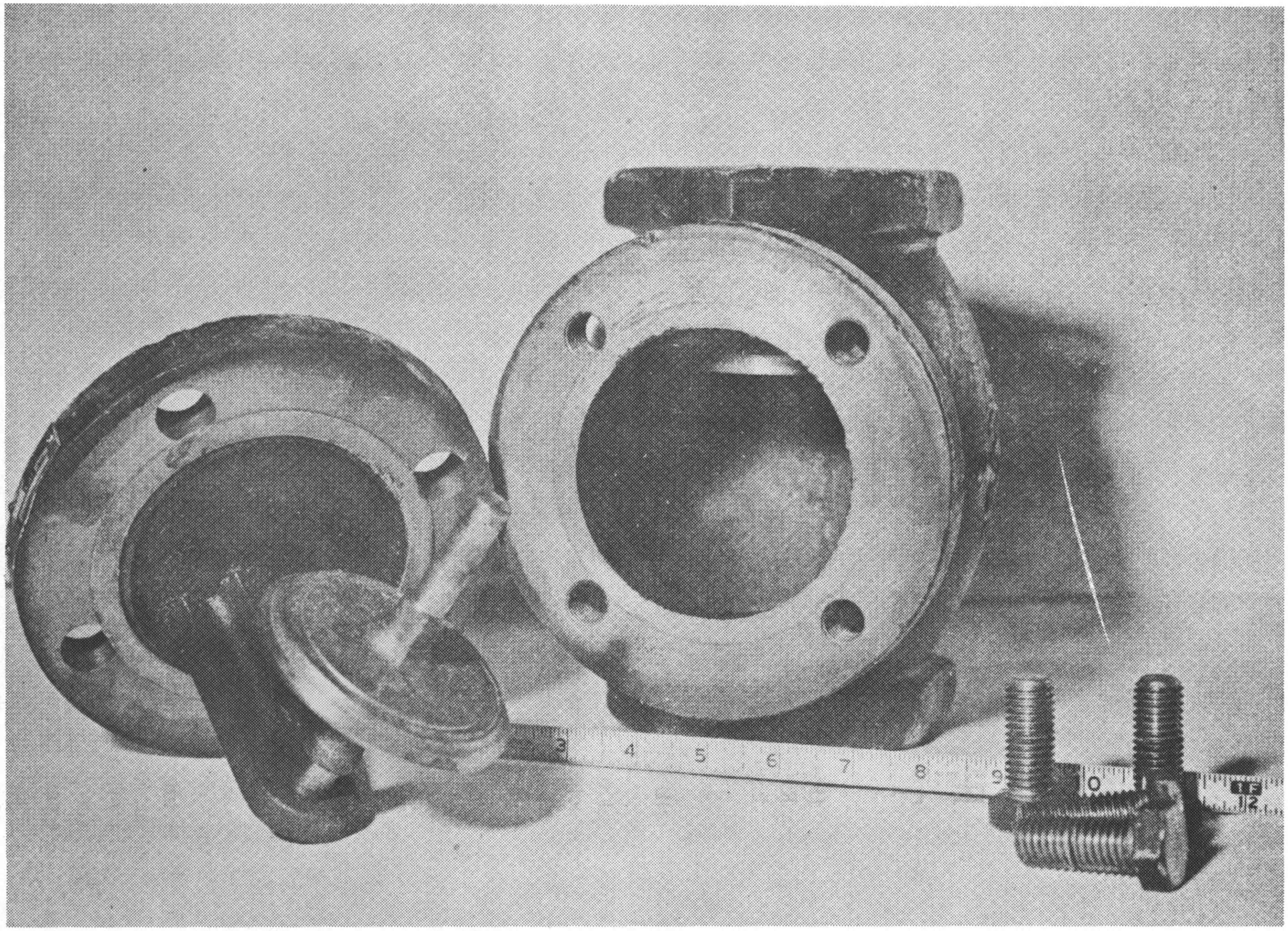

Fig. 3—Disassembled 3-in. standard vertical check valve.

SUMMARY 37

RADIATION SHIELDING AND RESPONSE STUDIES OF AEC TEST STRUCTURES

(Report WT-1723, Operation Hardtack, Project 34.2, same title, by R. A. Cameron, Jr., and P. H. Huff, Holmes & Narver, Inc., Architect–Engineers, Los Angeles, Calif., Dec. 10, 1963.)

OBJECTIVES AND SCOPE

The general objective of this project was to study the effects of airburst nuclear explosions on underground structures. The specific objectives were: (1) to determine initial gamma-radiation doses in different positions inside four small shallow-buried reinforced-concrete test structures and (2) to compare the accelerations inside two of these structures with the accelerations in the adjacent free field.

Film badges, chemical dosimeters, and energy-dependent film badges were placed throughout all four of the structures. The two types of dosimeter (chemical and film badges) were provided by Edgerton, Germeshausen & Grier, Inc. The self-recording pressure–time and acceleration–time gauges under this project were provided by Ballistic Research Laboratories (BRL) under Project 34.3.

The two phases of experiments, namely, the radiation shielding (phase I) and the structural response (phase II), are covered separately in the following:

Phase I. RADIATION SHIELDING

Procedure

The four structures used in this experiment were located in Areas 7 and 9 of Yucca Flat at the Nevada Test Site. Stations 7-24, 7-53, and 7-302.01 were located in Area 7, and station 9-22-6001 was located in Area 9 (Figs. 1 and 2). Each of the structures was of typical blast-resistant reinforced-concrete construction, and each had been used during Operation Plumbbob in 1957 for housing scientific and operational equipment. Structural details and shielding features of these test structures are illustrated in Figs. 3 to 6.

Entrance to each of the three shelters located in Area 7 was through the roof of the structure. Steel hatch covers provided blast protection. Since there were no locking mechanisms to prevent the covers from being blown off by the blast, the hatchways of the two close-in stations were covered with several layers of sandbags (approximately 1 ft in total thickness).

The shelter in Area 9 had a personnel entrance located at the south end of the structure. At the time of the detonation this entrance was protected by a heavy (1½-in. plate) steel blast door and sandbags.

In Area 7 this project participated in three events—Mora, Lea, and Socorro (ref. ENW, pp. 676 and 677). In Area 9 the participation was in the Vesta event (ref. ENW, p. 678) and in the Rushmore event (ref. ENW, p. 677).

Results

Energy-dependent Film Badges. The tin- and lead-shielded film badges, which were located in stations 7-24, 7-53, and 7-302.01 for the Socorro event only, were uniformly darkened by the radiation, and no energy-spectra information was obtained. The uniform darkening of these badges indicates a roughly isotropic angular distribution at the location of the badges.

Film Badges and Chemical Dosimeters. The results obtained from these badges and dosimeters are tabulated and the instrument-station locations indicated in Figs. 7 to 10. The general reduction of dose with increased distance from the roof and from the hatch openings was apparent at all stations.

Discussion and Conclusions

It is apparent that the gamma dose was underestimated in all the shelters. Particularly evident is the failure of the solid-angle method to consistently predict the dose to within even an order of magnitude.

Any prediction method relies heavily on accurate prediction of the surface gamma and neutron doses. This dose determination is particularly difficult for close-in locations such as those considered in this report.

All the shelters observed in this project received large neutron doses. When the neutrons penetrate the concrete, they produce gamma photons; no information has been available, however, concerning the partition of the emerging neutrons and gammas as a function of concrete thickness. Greater thicknesses result in a net decrease of dose, but this decrease is by smaller factors than might be expected.

Radiation backscattered from the shelter walls probably added to the doses at all detectors.

Clearly, then, interior gamma doses that are predicted by considering only the attenuation of exterior gamma doses will be low, regardless of the method of prediction.

Conclusions

The conclusions that can be drawn from the results of this phase of the project are as follows:

1. Increased distance from a hatch or area of reduced mass thickness resulted in a marked decrease of initial gamma dose, even in the smallest of the shelters.
2. The gamma radiation was roughly isotropic in angular distribution near the floors of the shelters.
3. The path-of-least-resistance method of predicting average interior gamma dose was consistently low in its predictions, usually by a factor of 3.
4. Solid-angle calculations, as described in the original report, were not satisfactory for predicting dose variations inside a shelter.

Phase II. GROUND MOTION AND STRUCTURAL RESPONSE

Procedure

The three structures used in this part of the project were located in Area 7 of Yucca Flat at NTS. Station 7-313, which was the base structure of Tower T-7c (Fig. 11), is described in considerable detail in the summary of Report WT-1701 (Summary 33). Report WT-1701 covers the structural damage to the base structure; this report examines the instrumentation data recorded at this structure in the same event (Quay).

Underground stations 7-24 and 7-53 were exposed to three events, Mora, Lea, and Socorro (ref. ENW, pp. 676 and 677). Project participation at station 7-313 was only in the Quay event (ref. ENW, p. 676).

Instrumentation

Area 7. The vertical and horizontal acceleration components of stations 7-24 and 7-53 were measured by an accelerometer installed in one corner of the floor of each station. Installation details are shown in Fig. 12. The free-field ground accelerations (Fig. 12), both vertical and horizontal radial components, were measured by two accelerometers installed approximately 20 ft south of the two structures.

The accelerometers and two pressure–time gauges were installed in an array as shown in Fig. 13.

Area T-7c. Two BRL self-recording pressure–time gauges were installed in the vicinity. One BRL accelerometer was bolted to the floor inside the base house. The free-field accelerometer was placed adjacent to a pressure gauge 70 ft south of Ground Zero (GZ).

The gauges in Area T-7c were peak gauges only since timing signals were not available.

Results

All data presented here were reduced by BRL personnel.

Overpressures. Table 1 summarizes the peak pressure–time data obtained in the events at the various stations.

Accelerations. Peak accelerations recorded in Area 7 are shown in Table 2. Peaks only are shown because, in general, the positive duration was short and the acceleration was small.

In the T-7c area no accelerometer readings were obtained. The base house was filled with debris, and the instrument could not be recovered; the other accelerometer, located adjacent to the pressure–time gauge 70 ft south of GZ, suffered extensive missile damage.

Discussion

A comparison of the recorded and predicted peak pressures is shown in Table 3. The agreement is seen to be quite good except for the readings from the gauges in Area T-7c.

An inspection of Tables 2 and 4 indicates that, although considerable variation exists, the peak values of downward and upward accelerations are about equal, particularly in the case of free-field measurements. A similar correspondence is seen between the horizontal peaks in directions away from and toward GZ.

In general, the peak horizontal and vertical accelerations were about equal. This tends to confirm the conclusions and design recommendations of the American Society of Civil Engineers Publication No. 42, which recommends that horizontal maximum accelerations be assumed equal to the vertical maximums.

A comparison of the free-field and structure accelerations shows that, except for one instance, the peak accelerations in the structures were higher by an average of about 50% than the vertical free-field maximums, and by about 25% than the horizontal peaks.

Conclusions and Recommendations

On the basis of the rather limited information obtained in this test, it is tentatively concluded that peak accelerations inside shallow-buried rigid structures can be expected to be higher than the corresponding peak accelerations in the adjacent free field.

Until further information is available, it is recommended that the predicted free-field displacements and velocities, as well as accelerations (both vertical and horizontal), be increased by a factor of 1.5 if they are intended to describe the peak motions of a shallow-buried blast-resistant concrete structure.

Table 1—PEAK PRESSURE–TIME DATA

Event and yield	Gauge number	Ground range, ft	Slant range, ft	Maximum pressure, psi	Remarks
Mora	709.01	201	1513	11	Good record
2.0 ± 0.2 kt	709.02	207	1514	10	Good record
Lea	709.02	207	1514	9	Good record
1.4 ± 0.1 kt					
Socorro	709.02	207	1465	22	Good record
6 ± 1 kt					
Quay		17	85	580	Peak pressure only
79 tons					
		70	108	280	Peak pressure only

Table 2—MAXIMUM ACCELEROMETER READINGS

Event and yield	Station	Gauge number	Direction of acceleration	Maximum acceleration, g	
				Positive*	Negative
Mora	7-24	708.01	Vertical	13	6
2.0 ± 0.2 kt	7-24	708.01	Horizontal	8	16
	7-53	708.02	Vertical	No record	
	7-53	708.02	Horizontal	No record	
	Array	708.03	Vertical	6	9
	Array	708.03	Horizontal	7	5
	Array	708.04	Vertical	19	20
	Array	708.04	Horizontal	No record	
Lea	7-24	708.01	Vertical	14	14
1.4 ± 0.1 kt	7-24	708.01	Horizontal	20	17
	7-53	708.02	Vertical	18	18
	7-53	708.02	Horizontal	6	6
	Array	708.03	Vertical	9	9
	Array	708.03	Horizontal	10	15
Socorro	7-24	708.01	Vertical	34	24
6 ± 1 kt	7-24	708.01	Horizontal	19	7
	7-53	708.02	Vertical	15	18
	7-53	708.02	Horizontal	33	11
	Array	708.03	Vertical	15	15
	Array	708.03	Horizontal	15	16

*Positive vertical acceleration is up; positive horizontal acceleration is away from GZ.

Table 3—COMPARISON OF RECORDED AND PREDICTED AIR PRESSURES

Event	Slant range, ft	Maximum recorded pressure, psi	Maximum predicted pressure: Height-of-burst curves	Maximum predicted pressure: Reflected free air
Mora	1513	11	10	10
	1514	10	10	10
Lea	1514	9	8	8
Socorro	1465	22	24	23
Quay	85	580		1400
	122	280		490

Table 4—AVERAGE ACCELERATIONS

		Average of peak accelerations in Stations 7-24 and 7-53, g	Average of peak free-field accelerations, g
Vertical motion:			
Mora	Up	13	6
	Down	6	9
	Average	9.5	7.5
Lea	Up	16	9
	Down	16	9
	Average	16	9
Socorro	Up	25	15
	Down	21	15
	Average	23	15
Horizontal motion:			
Mora	Away from GZ	8	7
	Toward GZ	16	5
	Average	12	6
Lea	Away from GZ	13	15
	Toward GZ	12	16
	Average	12.5	15.5
Socorro	Away from GZ	26	15
	Toward GZ	9	16
	Average	17.5	15.5

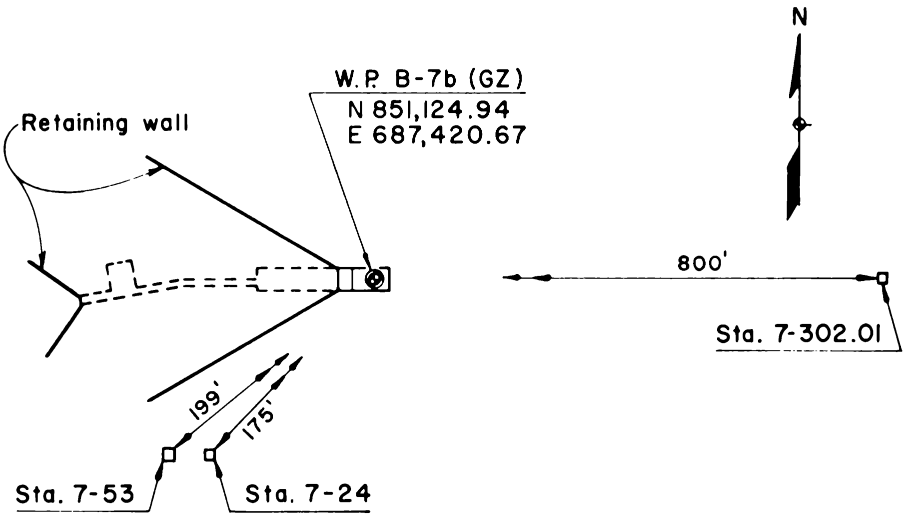

Fig. 1—Plan, Area 7 vicinity.

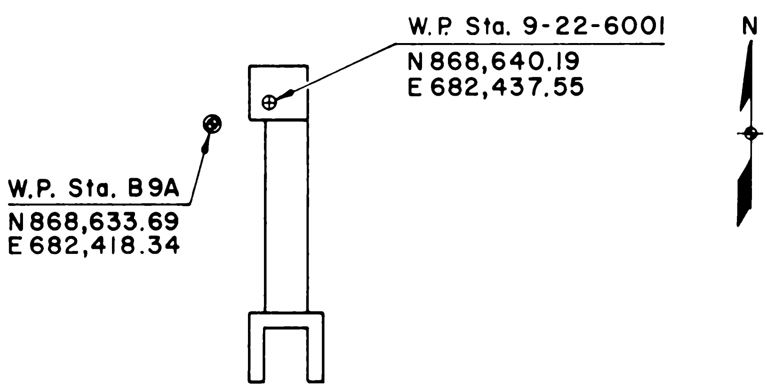

Fig. 2—Plan, Area 9 structure.

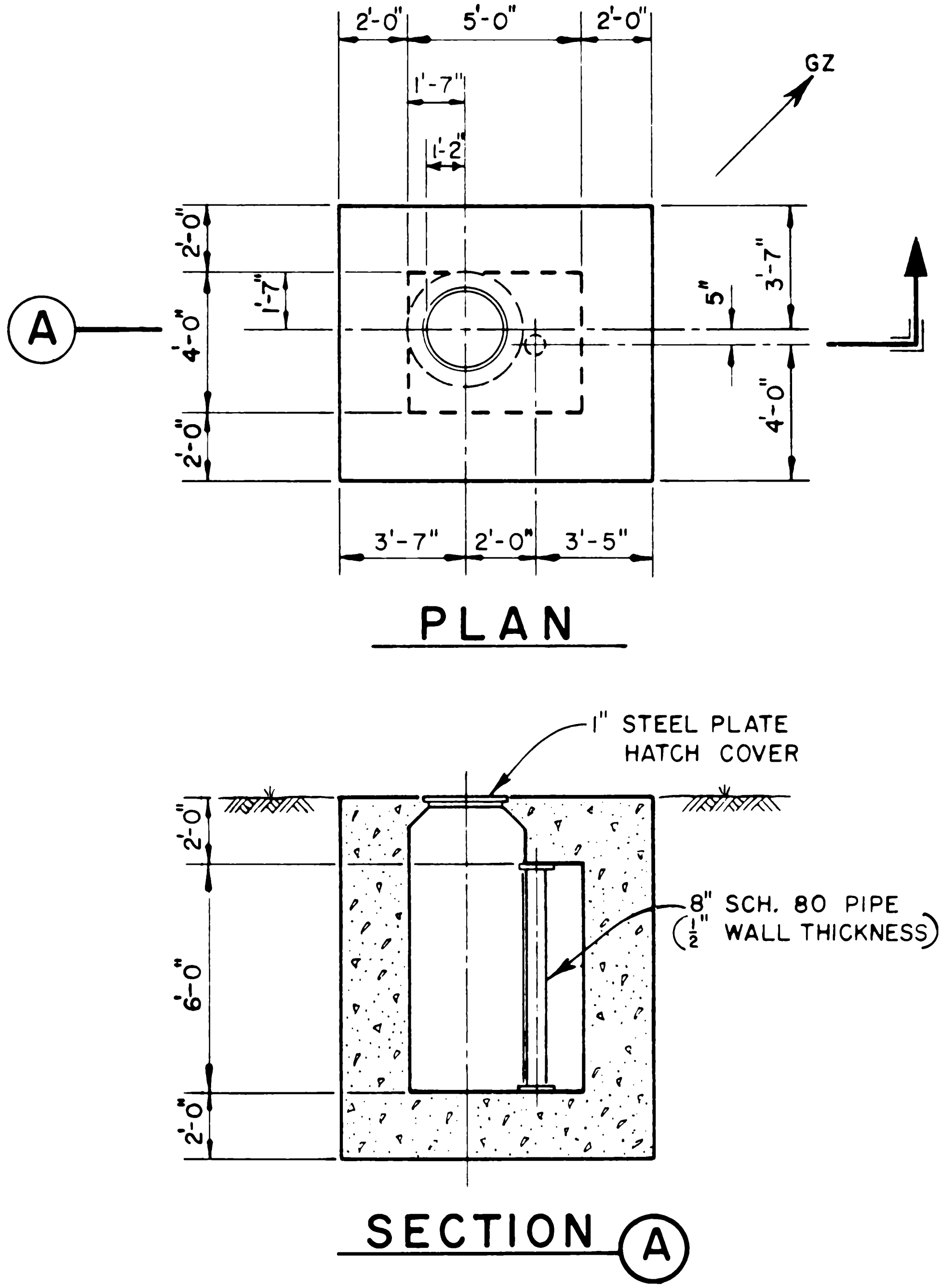

Fig. 3—Station 7-24, plan and section.

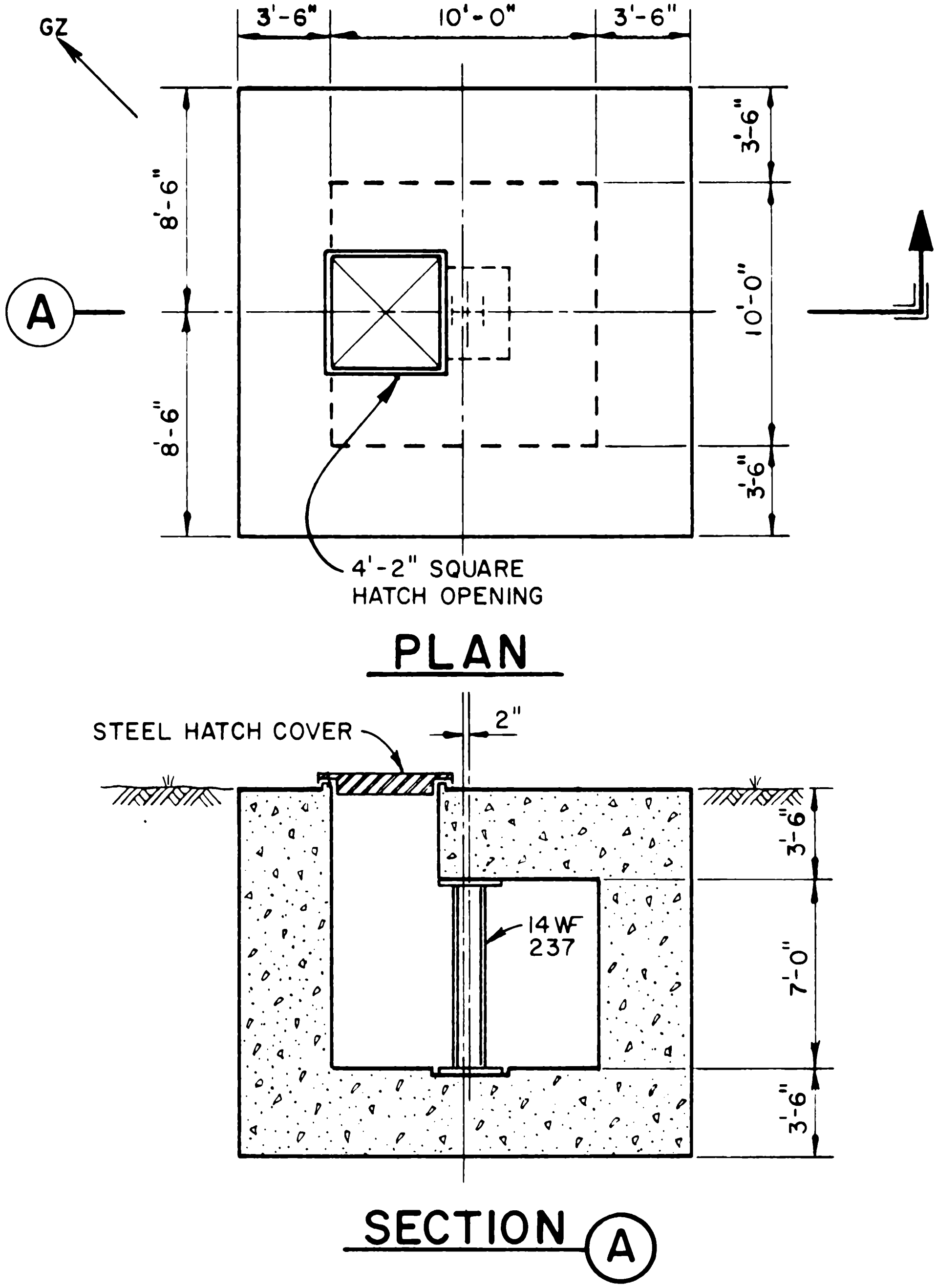

Fig. 4—Station 7-53, plan and section.

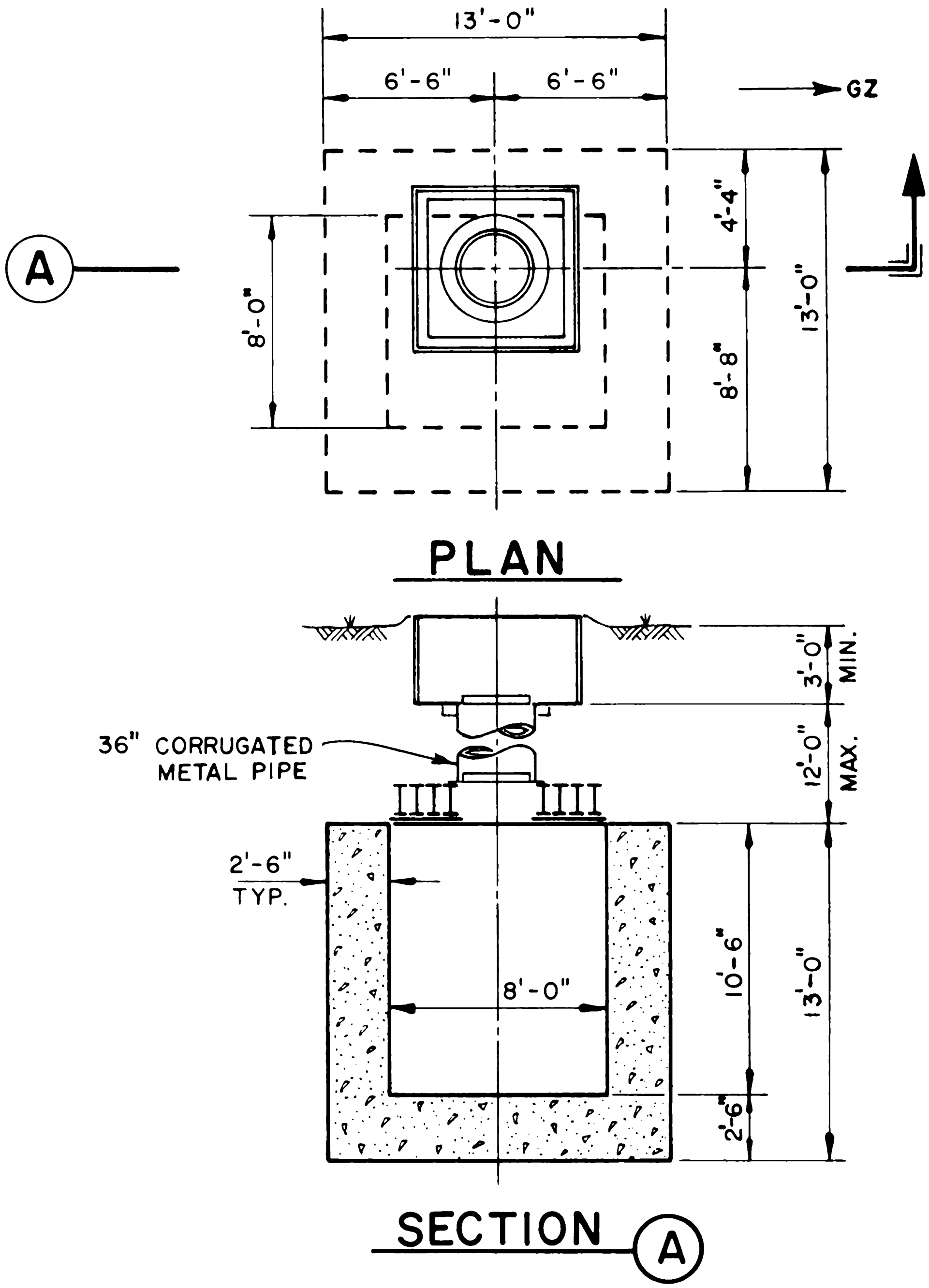

Fig. 5—Station 7-302.01, plan and section.

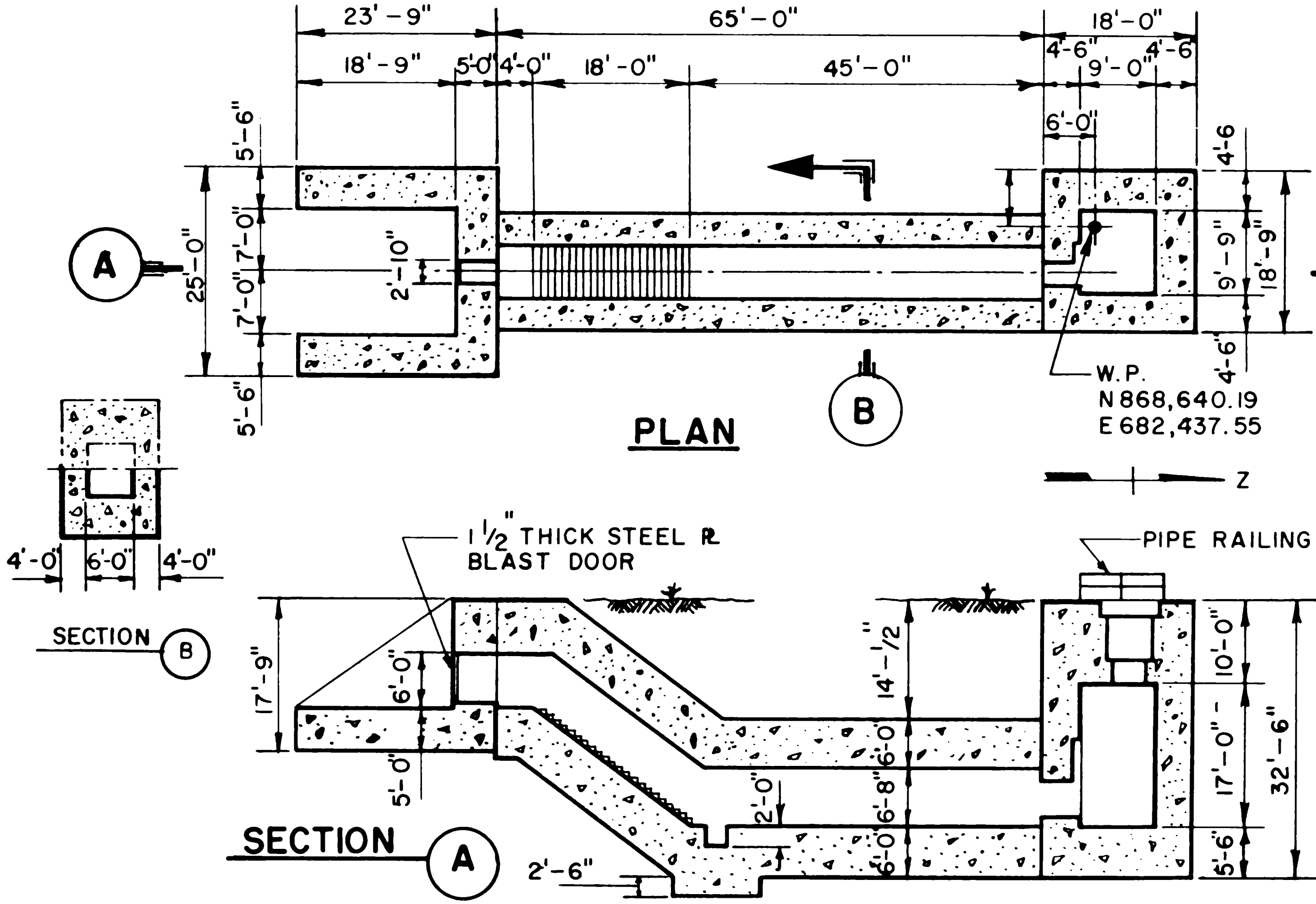

Fig. 6—Station 9-22-6001, plan and sections.

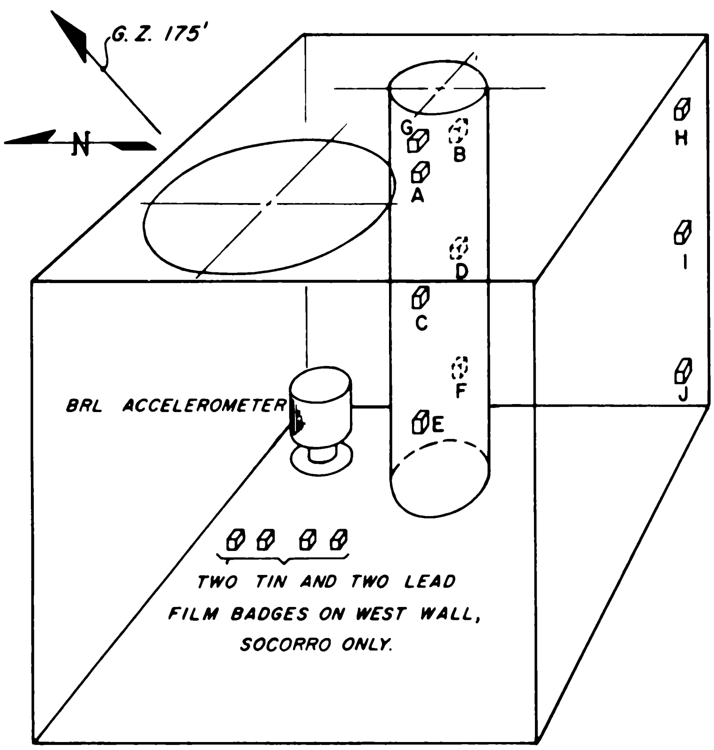

FILM BADGE DOSIMETERS

DOSES IN ROENTGENS

BADGE	EVENT		
	Mora	Lea	Socorro
A	425		1380
B	125	No results. All films damaged in development.	375
C	230		800
D	89		300
E	145		610
F	64		225
G	218		740
H	69		205
I	75		260
J	62		225
AVERAGE:	150		512
MEDIAN:	89		300

NOTES:

1. NO CHEMICAL DOSIMETERS LOCATED IN THIS STATION
2. FOR STRUCTURE DIMENSIONS, SEE FIGURE 2.3
3. BADGE G IS ON CEILING

Fig. 7—Station 7-24, badge locations and readings.

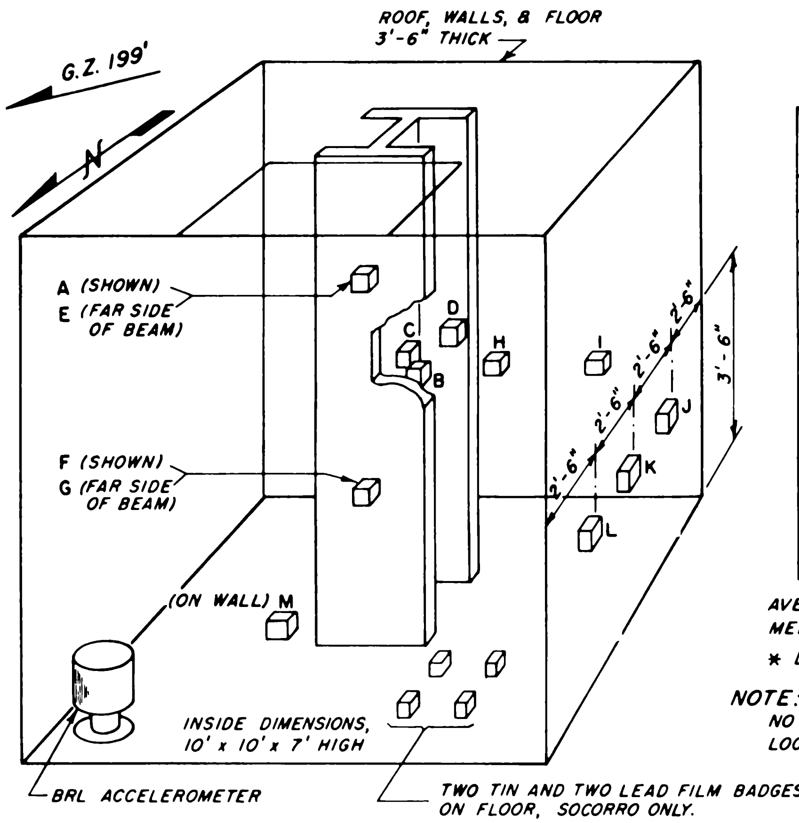

FILM BADGE DOSIMETERS

DOSES IN ROENTGENS

BADGE	EVENT		
	Mora	*Lea*	*Socorro*
A	415	1370	1280
B	75	145	255
C	71	110	250
D	76	160	280
E	29	97	150
F	310	670	930
G	31	82	146
H	37	100	150
I	*	99	160
J	*	83	165
K	*	167	710
L	*	168	395
M	*	440	825
AVERAGE:		*284*	*438*
MEDIAN:		*145*	*255*

* *Damaged in Development*

NOTE:
NO CHEMICAL DOSIMETERS WERE LOCATED IN THIS SHELTER

Fig. 8—Station 7-53, badge locations and readings.

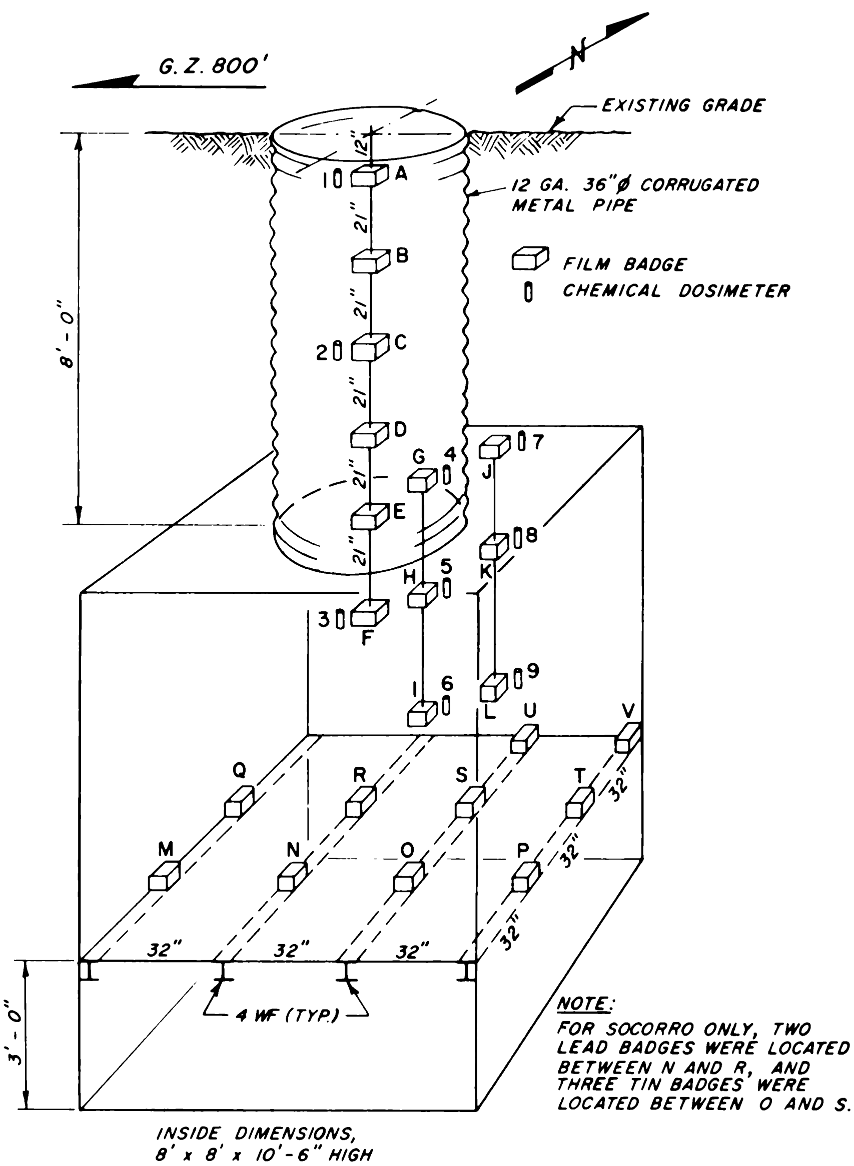

FILM BADGE DOSIMETERS
DOSES IN ROENTGENS
STA. 7-302.01

BADGE	EVENT		
	Mora	Lea	Socorro
A	*	4000	12000
B		27.5	6000
C		31.5	2900
D		23	1050
E		26	2020
F		26.5	280
G		*	125
H		80	960
I		48	165
J		*	700
K		*	380
L		*	245
M		11.5	670
N		20.1	235
O		6.4	275
P		9.5	130
Q		10.2	118
R		18.5	165
S		10.5	160
T		9.2	110
U		13	105
V		6.7	82

* Damaged in development

CHEMICAL DOSIMETERS
DOSES IN ROENTGENS
STA. 7-302.01

Dosimeter Number	EVENTS Lea & Donna Ann
1	12,400
2	78
3	65
4	180
5	110
6	32
7	**
8	25
9	51

** Less than 25R

Fig. 9—Station 7-302.01, badge and dosimeter locations and dosimeter readings.

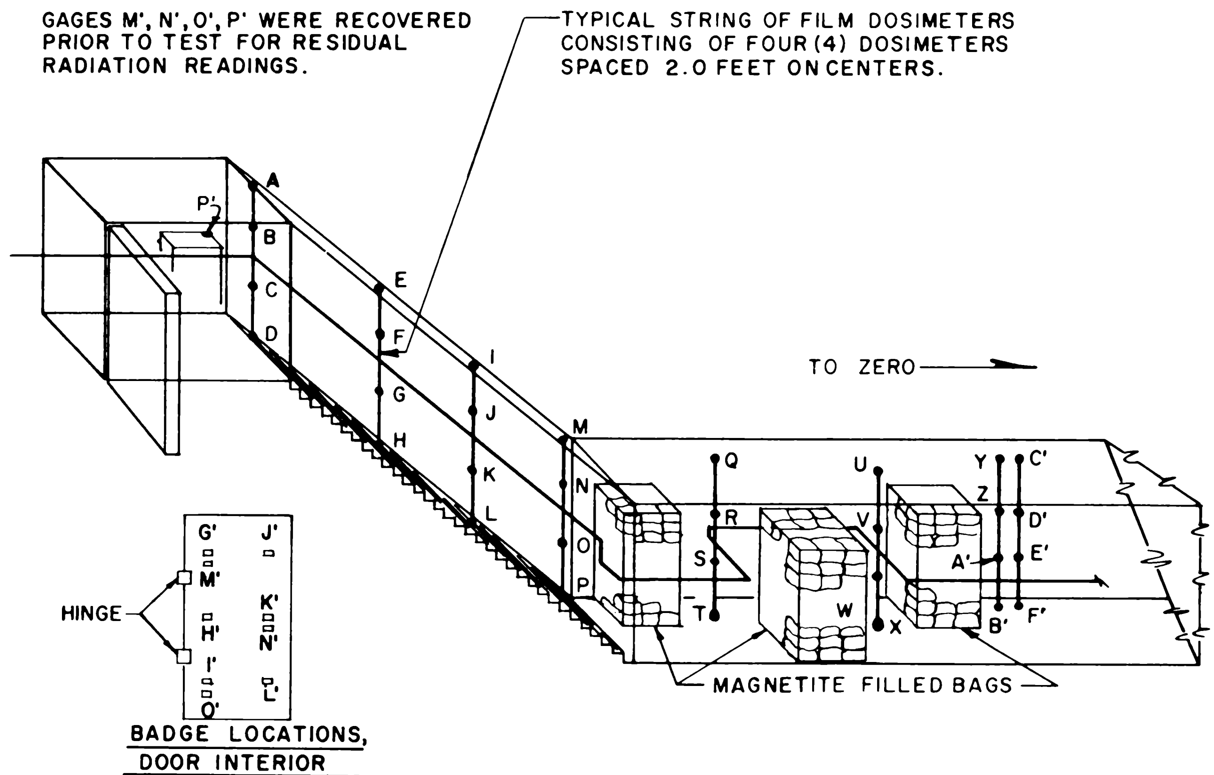

FILM BADGE DOSIMETERS

DOSES IN ROENTGENS

STA. 9-22-6001

BADGE	Rushmore Event	BADGE	Rushmore Event
A	6.9	V	*
B	6.8	W	
C	5.8	X	
D	4.8	Y	
E	3.2	Z	
F	3.1	A'	
G	2.4	B'	2.2
H	1.9	C'	*
I	1.9	D'	*
J	1.7	E'	*
K	1.3	F'	*
L	1.2	G'	145
M	0.9	H'	33
N	0.7	I'	11.5
O	0.8	J'	195
P	0.5	K'	50
Q	*	L'	14
R		M'	*
S		N'	
T		O'	
U		P'	

* Less than 0.1R

Chemical dosimeters 10 thru 25 all recorded less than 25 R.

Fig. 10—Station 9-22-6001, dosimeter locations and readings.

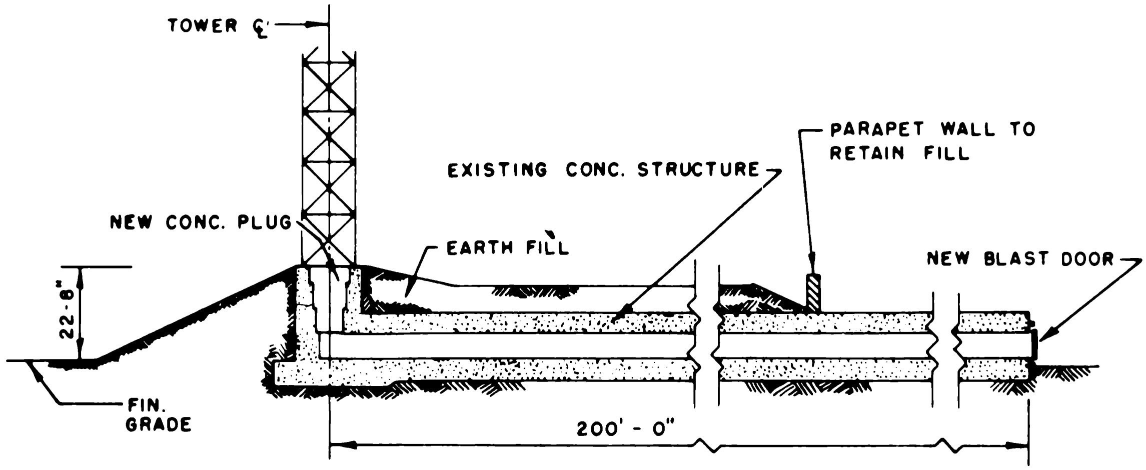

SECTIONAL SIDE ELEVATION

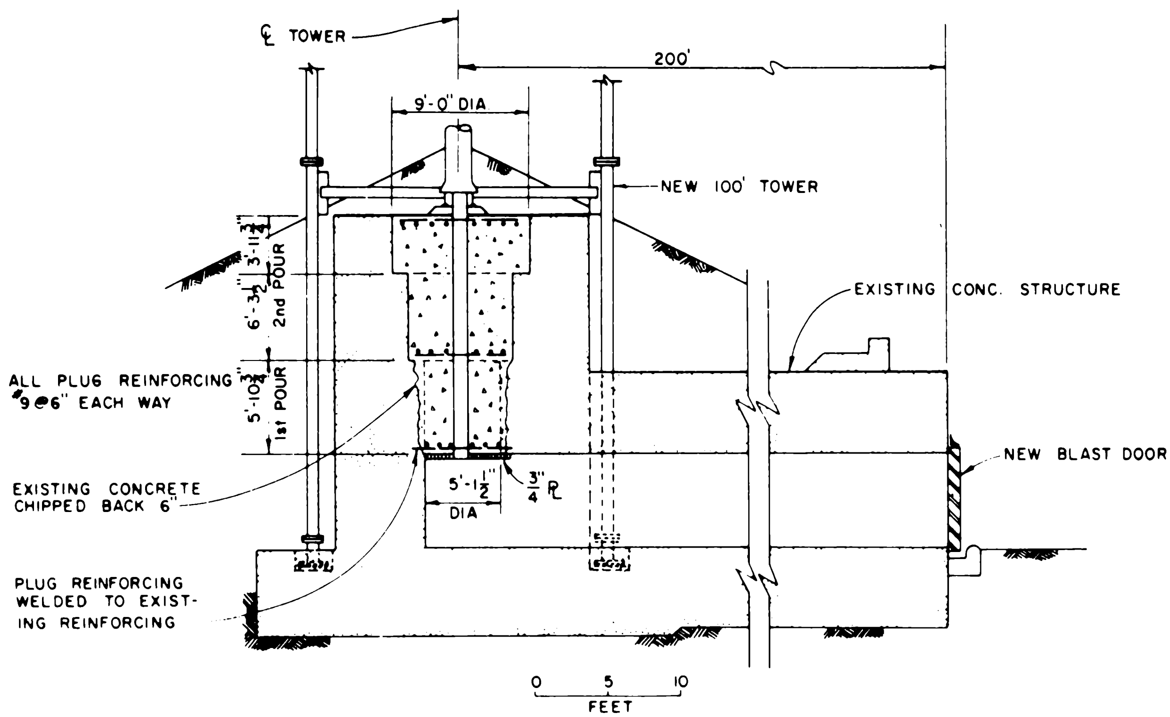

DETAIL

Fig. 11—Base structure, Tower T-7c.

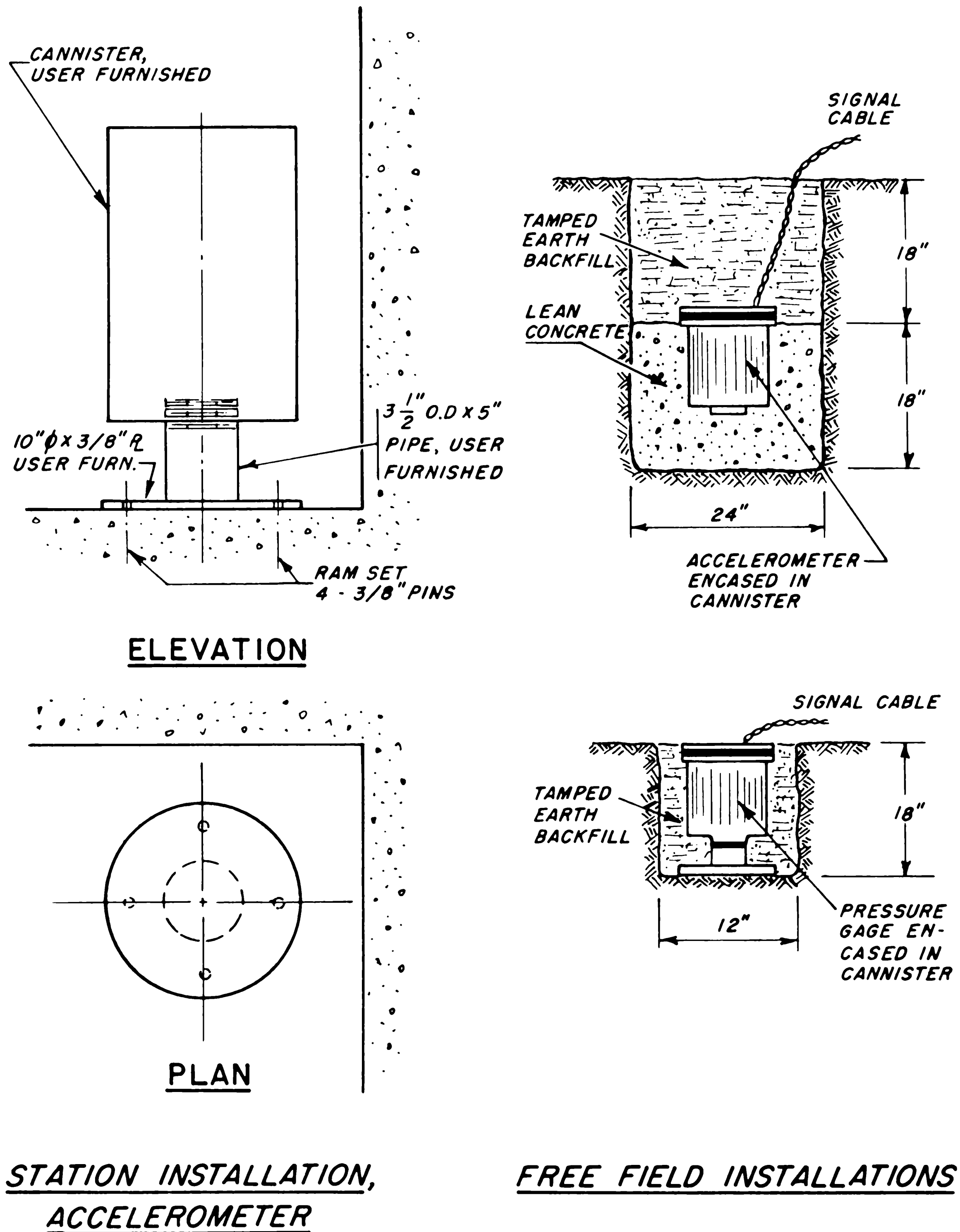

Fig. 12—Gauge-installation details.

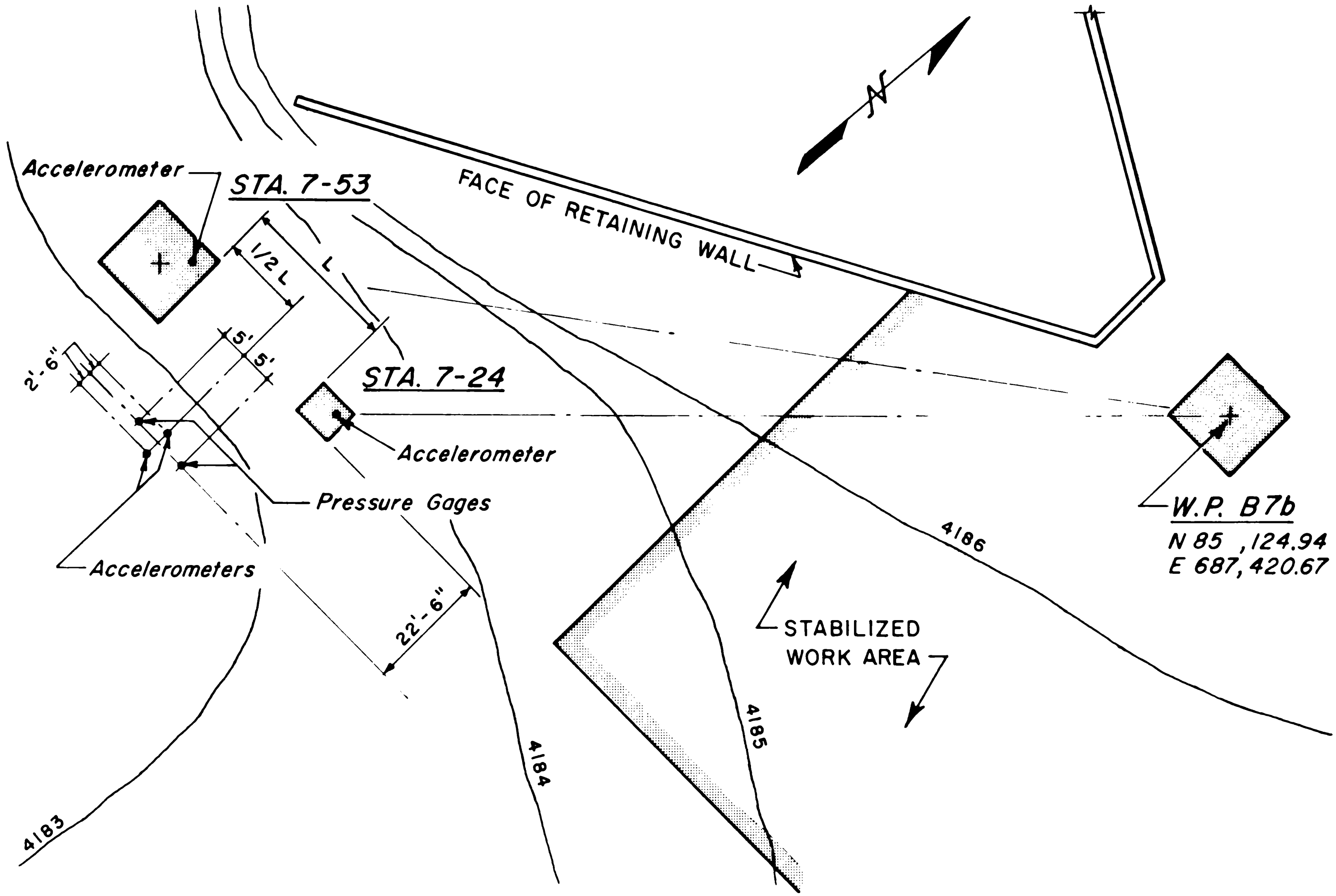

Fig. 13—Area 7 plan, showing gauge array in relation to stations.

DISCUSSION, EVALUATION, AND RECOMMENDATIONS

GENERAL

In the summaries greatest coverage is given to the structural integrity of items necessary for the protection of occupants of various types of shelter against the principal effects associated with the detonation of nuclear weapons, namely, air blast, ionizing and thermal radiation, and ground shock. It is important in any blast shelter design to attain a reasonably balanced protection for the occupants against all expected effects. Other factors to consider include cost, availability of materials, site conditions, and the various architectural and mechanical facilities required for the reasonable comfort of the shelter occupants.

KILOTON VS. MEGATON

Most of the tests covered in the summaries involved yields in the low-kiloton range; however, in a few cases shelters of the same design were subjected to comparable peak overpressures from both a low- and a high-yield weapon, and useful knowledge was gained. Owing to the much longer duration of the positive-pressure pulse, a megaton weapon burst would, particularly for structures sensitive to so-called drag loading (ductile rather than brittle type structures), cause greater damage at the same pressure level than a low-yield kiloton weapon burst. This should be kept in mind when interpreting or applying the results of the tests. The subject is discussed in great detail in Chap. IV of *The Effects of Nuclear Weapons* (ENW) and in other publications listed in the Bibliography.

BIOLOGICAL HAZARDS

Most biological experiments, using live animals and dummies as test specimens, were conducted in open, i.e., doorless, shelters. Valuable data were obtained on the biological effects. In a few instances, for example, in the higher pressure range, data on ground-shock acceleration effects on both open and closed shelters are of interest. Special attention is called to the publication CEX-65.4, *Biological Tolerance to Air Blast and Related Biomedical Criteria* (see Ref. 27 of Bibliography), which greatly supplements the data given in the summaries and furnishes further medical analysis of the test data.

Earlier tests had pointed up the inadequate protection offered occupants of open type shelters, both from primary and secondary blast effects and from the initial ionizing- and thermal-radiation effects. Such shelters would be justified only in an emergency when trench and simple home-basement shelters could be hurriedly constructed for rather limited protective features.

ENTRANCEWAYS AND DOORS

The configuration of shelter entranceways should be designed with an eye toward minimizing the reflection of the blast pressure on the entrance door yet offering relatively easy access. Results of recent

studies referred to in the Bibliography offer valuable cost and detailed design data. A cost study may often favor extra strengthening of an entrance door to make it capable of resisting a greater reflected blast pressure rather than suggesting a more elaborate but costly design and configuration of the entranceway. The orientation of the door relative to the shelter interior and the exposure of the occupants, in the event of an excessive blast force and subsequent failure of the door, must also be considered. A concrete wall inside the shelter and opposite the door could be conveniently constructed in connection with a vestibule.

Most of the many doors tested successfully withstood the blast in the predicted pressure range, although a greater structural response could be expected at the same pressure range from a high-yield weapon. Equally resistant were the hardware items, such as latches and hinges, which were subjected to an assumed maximum peak negative pressure of 4 psi, and/or, depending on the ductility of the door design, to a rebound force which might, conservatively, amount to as much as 50 percent of the positive blast force on the door.

Test results bear out the importance of a satisfactory seal around the blast door or the provision of a gastight second door of low blast resistance inside the main blast-resistant door to minimize the interior blast pressure.

MAIN SHELTER STRUCTURE

It is evident that the fully buried or partly buried earth-covered shelters offer the most satisfactory design concept for balanced protection against both blast and radiation effects. In the higher pressure range, effectiveness, as far as structural integrity is concerned, is gained by the curved and the short-span rectangular designs. In some soils, such as well-stabilized clayey types, a certain arching effect of the earth cover, which reduces the blast load on a deeply buried, short-span shelter structure, can be expected. On the other hand, the tests indicated only an insignificant reduction in the peak overpressure with depth of soil.

In spite of its greater ductility, the arch-shaped structural-plate steel construction exhibited a more favorable design against collapse from excessive blast loads than the less ductile reinforced-concrete construction. The steel shelter to a great extent benefitted from the passive soil pressure in resisting excessive deformation of the arch structure.

Tests indicated certain advantages in separating the footings for a shelter structure from the main floor slab, which then could be made much thinner and more flexible. Particularly in the high-pressure region, this would (1) reduce the ground-shock effect on the floor slab, especially for a metal arch, and (2) improve the overall flexibility of the structure. Also, with partly buried shelters, considerable reduction in the effects of the blast pressures on the structure may be gained by widening and streamlining the earth berm over the shelter.

Of the test projects covered in the summaries, only two involved the effects of an underground nuclear explosion on buried shelters, namely, on reinforced-concrete four-walled structures and on rock-tunnel linings. It was learned that, because of the apparent lack of relative motion between the structure and the surrounding soil, even close to the edge of the crater only slight structural damage may be expected. At greater distances, problems not connected with the strength of the shelter structure itself are likely to predominate, such as damage to utility pipes and conduits entering the structure, owing to the greater relative motion than exists at closer range. This effect can be greatly reduced by the use of flexible couplings and by ensuring that there is sufficient flexibility in the lines at the structure. In general, it may be concluded that, comparatively, the overall effects from an underground burst may be assumed to be considerably less damaging than those from an air burst of the same yield and at the same distance from Ground Zero.

On the basis of the test results described in the summaries, the following rating is suggested to illustrate the comparative effectiveness of typical shelter structures for overall tolerable protection of occupants against nuclear weapons effects. In parentheses are given the related maximum peak blast overpressures at ground level at the shelter location.

1. Tunnels in rock and deep underground, heavily reinforced concrete-pipe shelters (200 psi)
2. Buried, or partly buried, earth-covered shelters
   a. *Corrugated steel:* pipe and cattle pass (100 psi), and arch shape (75 psi)

b. *Reinforced concrete:* pipe and cattle pass (100 psi), short-span rectangular and arch (75 psi), long-span rectangular (e.g., garage type mass shelter) (50 psi), and dome shape (25 psi)

c. *Aluminum:* dome shape (25 psi)

3. Surface shelters*: vault type (50 psi)
4. Dwellings—family type shelters

a. *Earth-covered* reinforced-concrete basement exit (25 psi), and wood-covered trench and metal arch (10 psi)

b. *Indoor** basement lean-to and corner room, and utility type (up to 5 psi)

In most instances a reduction must be considered in the pressures indicated above to account for greater blast effects at the same pressure level from a high-yield weapon than from the low-yield weapons employed in the Nevada tests. This is particularly true of the more flexible, so-called drag type structures. Other conditions to consider include the site differences, e.g., soil conditions. The physical environment at the Nevada Test Site may be assumed not typical of most urban areas.

VENTILATION

Severe damage to the exposed portions of air-intake pipes was experienced in several of the test projects, although the other parts of the shelter assembly sustained only minor damage. Of the many types and shapes of exposed ventilating ducts tested, only the rock grille escaped without damage. Compared with the other ventilating ducts, however, the rock grille proved to be a rather inefficient throttling device. Efforts to improve the various air intake designs for greater strength and efficiency should be pursued.

Of the methods developed to reduce or completely prevent the blast pressure from entering the shelter through ventilation openings, the blast closure valve method is undoubtedly the most effective. A variety of valve designs were tested, and useful information was gathered. Later studies, including shock-tube tests, have added further to the knowledge necessary to develop effective and economical types of fast-acting closure devices. (See Ref. 14 of the Bibliography.)

Typical air-cleaning systems were tested to study their resistance to blast and to analyze the problems connected with severe dust conditions. The 6- and 12-in.-deep high-resistance AEC type filters suffered no apparent damage at peak pressure levels of less than 4 psig. Damage to Dust-Stop filters ranged from only minor at 1.4 psig to complete destruction at overpressures greater than 2 psig. Interesting data were accumulated on dust problems in regard to loss of effectiveness of the filters; however, those problems may be assumed to be peculiar to the Nevada Test Site; they may be expected to be of relatively minor importance at more typical locations.

SUGGESTED APPLICATION OF SHELTER DATA

The test data originally published in the Weapons Tests (WT) Reports have undoubtedly been of value in arriving at more rational criteria for designs of various types of blast shelters. It is hoped that this publication, too, will be helpful in that respect and also of more direct benefit to the individual designer because of its compact coverage of applicable test data and its ready availability to the general public.

As a follow-up of these summarized test results, it is suggested that a Government-sponsored project be started at an early date to produce a consolidated catalog of recommended designs of blast shelters. Admittedly, there is a wealth of data available on the subject, including fairly complete design details on a number of special shelter types. However, these data are scattered in numerous reports and publications; therefore each design case would require extensive search and research for applicable information. The proposed document, by assembling and to a large extent supplementing available information, would greatly benefit designers, such as the engineer or architect, or homeowners confronted with the task of designing satisfactory shelters suitable for the special conditions at hand.

The preparation of such a shelter publication might be considered a rather elaborate project; it would require considerable professional talent to present complete and up-to-date design details, such as could be

*Satisfactory blast protection but, generally, inadequate radiation protection can be expected.

necessary for construction purposes, and preferably would include estimated cost data and materials listing. It is, however, generally agreed that such data are long overdue, particularly in consideration of a possible impending national emergency.

It is suggested that the document present a wide variety of designs that offer reasonably balanced protection for the shelter occupants against, at a wide range of blast overpressures, the various effects resulting from nuclear weapon bursts. The designs would include: family, group, and communal type shelters; hasty type up to more permanent dual-purpose types; surface, semi-buried, and fully buried types; of different materials, such as wood, concrete, steel, and possibly other materials found reasonably suitable and more readily available; and featuring competitive shapes, such as rectangular, cylindrical, and arch shapes.

Standardization of structural items as well as mechanical equipment should be encouraged to reduce design and construction efforts as much as possible.

Efforts should also be made to simplify the problems of blast-resistant design analyses. Attention is invited to the particular case that, because of the relatively long blast-pressure pulse of the megaton weapons, the structural design may in most cases be greatly simplified if the dynamic load is considered practically as a static load. Usually a fairly accurate yet conservative design is possible, if the static load is based on the peak side-on overpressure, with all pertinent parameters reasonably well related to this quantity. This simplified method is generally not recommended in design against low weapon yields when the impulse of a dynamic loading becomes much more important. In most instances the designer is then confronted with a rather complicated dynamic analysis involving consideration of the response of the structural elements, when measured by their transient and permanent deflections. For the simplified method, see Ref. 18 of the Bibliography.

Considerable interest has been directed toward the use of subway tunnels and large-sized underground utility pipes as shelters, for large-city populations. The results of recent shelter studies (see referenced publications in the Bibliography) emphasize the effectiveness and economy of such dual-purpose and similar types of mass shelters.

BIBLIOGRAPHY

1. American Society of Civil Engineers, *Design of Structures to Resist Nuclear Weapons Effects,* Manual of Engineering Practice No. 42, American Society of Civil Engineers, New York, N. Y., 1961.
2. American Society of Heating, Refrigerating, and Air-Conditioning Engineers, *Survival Shelters, Guide and Data Book, 1964—Applications, Chap. 30,* American Society of Heating, Refrigerating, and Air-Conditioning Engineers, New York, N. Y., 1964.
3.*Bechtel Corporation, Protective Blast Shelter System Analysis, Detroit, Michigan, Final Report, Bechtel Corporation, for the Office of Civil Defense, June 1968.
4. Boegly, W. J., Jr., W. L. Griffith, and K. P. Nelson, Conceptual Design of a Dual-Use Utility Tunnel Blast Shelter for White Plains, New York, USAEC Report ORNL-4362, Oak Ridge National Laboratory, March 1969.
5.*Bogardus, H. F., et al., Studies of the Naval Facilities Engineering Command Protective Shelter. II. Summer Trials, Report NRL-6656, Naval Research Laboratory, Mar. 29, 1968.
6.*Breck, R. S., Shelter Air Conditioning Unit, Report AD659428, Carrier Air Conditioning Company, February 1967.
7.*Condit, R. I., Area-wide Shelter Systems, Report AD635931, Stanford Research Institute, December 1965.
8.*Corps of Engineers, U. S. Army, Design of Structures to Resist the Effects of Atomic Weapons, Reports EM-1110-345-413 through 421, Superintendent of Documents, U. S. Government Printing Office, Washington, D. C., 1959.
9.*Curione, C., Construction Resources Availability in Support of Blast Shelter Programs, Final Report, Stanford Research Institute, for the Office of Civil Defense, May 1968.
10.*Curione, C., Summary of Cost Trends of Mass Production as Applied to 5 to 10 Psi Shelters, Final Report, Stanford Research Institute, for the Office of Civil Defense, February 1967. (USAEC file number NP-16804.)
11. Glasstone, S. (Ed.), *The Effects of Nuclear Weapons,* revised ed., Superintendent of Documents, U. S. Government Printing Office, Washington, D. C., 1964.
12.*Holmes & Narver, Inc., AEC Group Shelter, USAEC Report CEX-58.7, 1960.
13.*Illinois Institute of Technology Research Institute, Civil Defense Shelter Options for Fallout and Blast Protection (Single Purpose), Final Report, Project J6115, Illinois Institute of Technology Research Institute, for the Office of Civil Defense, June 1968.
14.*Kiang, R., Blast-Actuated Closure Valves for Personnel-Type Shelters, Final Report—Phase II, Report AD661648, Stanford Research Institute, February 1967.
15.*Longinow, A., Civil Defense Shelter Options for Fallout and Blast Protection (Dual Purpose) Project M6101, Final Report, Report IITRI-M-6101, Illinois Institute of Technology Research Institute, May 1967.
16.*Mitchell, J. H. (Comp.), Nuclear Explosion Effects on Structures and Protective Construction—A Selected Bibliography, USAEC Report TID-3092, April 1961.

*Available from Clearinghouse for Federal Scientific and Technical Information, Springfield, Va. 22151. Price: printed copy, $3.00; microfiche $0.65.

17. National Academy of Sciences–National Research Council, Civil Defense–Project Harbor Summary Report, Publication 1237, National Academy of Sciences, Washington, D. C.
18. Newmark, N. M., Recommended Specifications for Blast-Resistant Design, Civil Defense Technical Manual TR-11, University of Illinois, January 1958 (reprinted March 1962).
19. Newmark, N. M., and J. D. Haltiwanger, Principles and Practices for Design of Hardened Structures, Report AFSWC-TDR-62-138, University of Illinois, December 1962. (Available to Civil Defense-certified architects and engineers in protective construction.)
20. Norris, C. H., et al., *Structural Design for Dynamic Loading,* Civil Engineering Series, McGraw-Hill Book Company, Inc., New York, 1959.
21. Office of Civil Defense, Publications Index, MP-20 (latest issue). [Publications issued by Office of Civil Defense are furnished free upon request; inquiries or requests should be sent to the state or local civil defense offices.]
22. Office of Civil Defense, Shelter Design and Analysis, Vol. 1; Fallout Radiation Shielding, TR-20 (Vol. 1), Department of Defense, June 1968. (Available to architects and engineers qualified in fallout shelter analysis.)
23.*Stevenson, J. D., and J. A. Havers, Entranceways and Exits for Blast-Resistant Fully-Buried Personnel Shelters, Project M6064, Final Report, Report AD636048, Illinois Institute of Technology Research Institute, September 1965.
24.*Svaeri, O. W., and N. I. Stein, Air Distribution Studies in Multi-Room Shelters, Final Report, Report PSDC TR-21/22, for the Office of Civil Defense, The Protective Structures Development Center, Fort Belvoir, Va., March 1967.
25.*URS Corporation, Development and Evaluation of a Shock Tunnel Facility for Conducting Full-Scale Tests of Loading, Response, and Debris Characteristics of Structural Elements, Summary Report, Report URS 680-2, for Stanford Research Institute and the Office of Civil Defense, December 1967.
26.*Vortman, L. J., A Risk-Oriented Approach to Protection From Nuclear Weapons, USAEC Report SC-4689(RR), Sandia Corporation, September 1962.
27.*White, C. S., I. Gerald Bowen, and Donald R. Richmond, Biological Tolerance to Air Blast and Related Biomedical Criteria, USAEC Report CEX-65.4, Lovelace Foundation for Medical Education and Research, Oct. 18, 1965.
28.*Wiehle, Carl K., Shelter Entranceways and Openings, Final Report, Report AD662749, Stanford Research Institute, September 1967.

*Available from Clearinghouse for Federal Scientific and Technical Information, Springfield, Va. 22151. Price: printed copy, $3.00; microfiche $0.65.

INDEX

The numbers in the index are summary numbers.